Bull. Min. Res. Exp. (2015) 151: 1-46

Bulletin of the
Mineral Research and Exploration

http://bulletin.mta.gov.tr

THE LATE QUATERNARY TECTONO-STRATIGRAPHIC EVOLUTION OF THE LAKE VAN, TURKEY

Naci GÖRÜR[a*], M. Namık ÇAĞATAY[a], Cengiz ZABCI[a], Mehmet SAKINÇ[a], Remzi AKKÖK[a], Hande ŞİLE[a] and Sefer ÖRÇEN[b]

[a] *Istanbul Technical University, Faculty of Mines, Department of Geology, 34469 Maslak, Istanbul, Turkey*
[b] *Yüzüncü Yıl University, Faculty of Engineering and Architecture, Department of Geology, 65080, Campus, Van, Turkey*

Keywords:
Lake Van, Tectono-Stratigraphy, Lake Level Fluctuations, Climate

ABSTRACT

Many of the terraces around the Lake Van record a relatively short period of the much longer geological history of the Lake Van Basin. Their deposition took place during the last ca. 125 ka BP. They accumulated in a large array of shallow lake and lake margin environments, such as alluvial fan/braided river, beach, Gilbert-type delta, nearshore lake and offshore lake. Variability of their lithofacies provides evidence for climatic and tectonic controls of their depositional conditions. During their deposition high relief areas in the watershed delivered abundant detritus to the coastal areas of the lake. The sedimentation was therefore dominated by terrigenous clastic deposits. The highest concentrations of the coarse clastic sediments were at the mouths of the major streams where they formed Gilbert-type deltas. These river-dominated lacustrine deltas formed during rising lake levels and are relatively more abundant and thicker in the eastern margin of the lake, indicating that this margin mostly had a low-energy coast sheltered from the prevailing westerly winds. However, some areas of the same margin adjacent to deltas were also supplied with sediments by waves and storm-induced longshore currents to form beaches. Storms and storm-generated traction currents were perhaps active agents along the shores of the Lake Paleo-Van as suggested by the presence of the coarse-grained material in its nearshore facies. Somehow, during times of lake highstands, turbidity currents seem not to have played an important role in the sediment transportation along the lake margin, because the nearshore sediments hardly show any evidence of turbidite depositon, such as graded bedding and sole-marks. The offshore lake was relatively quite standing water, depositing laterally persistent, thinly-bedded to varved and fine-grained sandstones and mudstones in part with hydroplastic disruptions, such as slumps and convolute beddings. Because of the lack of sufficient datings of the terrace sequences around Lake Van, we cannot correlate them unequivocally. However, the absence of large-scale cyclicity within a given terrace sequence in each locality suggests that deposition of each terrace occurred during a separate lake level fluctuation each reaching to higher level than the modern lake level followed by a regression. The available age data suggest that high lake levels, reaching up to 1760 m asl, occurred during the last interglacial (MIS 5; 123-71 ka BP), 26-24 ka BP, 22-21 ka BP and 10-6 ka BP. The younging of the terrace deposits along with the decrease in elevation suggests either a gradual decline of lake level with time, or the effect of the cumulative uplift with time or both. The fluctuating lake level was probably due to a combination of climatic, volcanic and tectonic processes. Considering the hydrologically closed nature of the lake, climate probably played more important role than the others. Since the formation of the youngest terrace sediments of 6 ka BP, perhaps the climate in the basin has been mostly relatively more arid and evaporative. During the entire history of the lake (last 600 ka), geology of the area has been characterized by the neotectonic régime of Turkey with active dip- and strike-slip faults, resulting in the offshore lake the characteristic slump structures and convolute beddings, and eruptions of mainly the Nemrut Volcano.

* *Corresponding author: Naci Görür, gorur@itu.edu.tr*

1. Introduction

Lake Van is situated in eastern Anatolia. It is a 3522 m^2 basin with a maximum water depth of 455 m (Degens and Kurtman, 1978). It is the largest soda lake in the world (alkalinity =153 meq l^{-1}, pH=9.81) (Reimer et al., 2009). It also ranks the fourth-lake on Earth by volume (576 km^3). It has a closed drainage system with several perennial streams (e.g., Zilan, Ala Çay, Karasu, Dönemeç and Kotum), flowing down into the lake from the surrounding high mountains (Süphan and Nemrut volcanoes in north and west, Bitlis Massif in south, Eastern Van Mountains in east). These streams transport large amounts of sediments that have been accumulating in the lake basin during its 600 ka history (Litt et al., 2009; Stockhecke et al., 2014). Owing to the lake level changes due to climate, local tectonics and volcanism, these sediments were deposited at various elevations on the basin margins.

Up to now, some studies were carried out on the terraces to enlighten stratigraphic, tectonic and climatic evolutions of the Lake Van Basin. Most of them dealt with the determination of the different shoreline elevations and their ages in order to evaluate the lake-level changes and the regional climate events during or after the last glacial period (Valeton, 1978; Kempe et al., 2002; Kuzucuoğlu et al., 2010). In addition, studies on the varve record, bacterial diversity, palynology, geochemistry, bathymetry and volcano-seismicity of the lake itself also exist (Degens and Kurtman, 1978; Kempe and Degens, 1978; Wong and Finckh, 1978; Wong and degens, 1978; Degens et al., 1984; Kempe et al., 1991; Landmann, 1996; Landmann et al., 1996*a, b*; Kadıoğlu, 1997*a,b*; Wick et al., 2003; Şengör et al., 2003; Landmann and Kempe, 2005; Lopez-Garcia et al., 2005; Kaden et al., 2005; Utkucu, 2006; Horasan and Boztepe-Güney, 2007; Kuzucuoğlu, 2010; Kaden et al., 2010; Çukur et al., 2013; Sumita and Schmincke, 2013*a, b*; Stockhecke et al., 2014; Çağatay et al., 2014). Little work has been done on the sedimentology of the elevated lake terrace sediments, in spite of their spectacular outcrops in the relatively recently dissected lacustrine basin.

The purpose of this work is to discuss the tectono-stratigraphic evolution of the Lake Van Basin based on the study of the lacustrine terraces and their depositional environments in space and time. To achive this objective, we first summarize the geological and seismo-tectonic settings of the basin, then describe the terrace sediments in detail, and finally, by interpreting their depositional environments, we discuss the temporal evolution of the Lake Van Basin.

2. Setting

2.1 General Geology

The Lake Van Basin has a heterogeneous stratigraphic basement that crops out on the lake margins. Northern and western margins are underlain mostly by Neogene to Quaternary volcanic rocks and in part by Miocene clastic and carbonate sediments (Figure 1). The eastern margin is dominated by Upper Cretaceous to Oligocene ophiolitic mélange and flysch, forming the East Anatolian Accretionary Complex. The southern margin is represented mostly by Palaeozoic metamorphic rocks of the Bitlis Massif (Figure 1). All these rocks have acted as sources for the 700 m-thick sediments accumulated in the Lake Van since its formation about 600 ka BP (Litt et al., 2009; Stockhecke et al., 2014).

Mainly faults and folds characterize the geological structures in the Lake Van Basin (Şaroğlu and Güner, 1981; Güner, 1984; Şengör et al., 1985; Yılmaz et al., 1998; Toker and Şengör, 2011; Şengör et al., 2008; Çukur et al., 2013). Faults are represented predominantly by short and discontinuous strike-slip faults with an irregular distribution. They are common in the north and the east of the lake, striking NW-SE, NE-SW and E-W. The NW-SE- and E-W-striking faults are mostly dextral, whereas the NE-SW-striking ones are generally sinistral (Figure 1). Most of the strike-slip faults appear to be active and dominate the seismo-tectonics of the region. Beside them, a small number of active thrusts and normal faults are also observed in the close vicinity of the Lake Van. The thrust faults, which ruptured during the October 2011 Van Earthquake (M=7.1), also characterize the eastern margin between the Lakes Van and the Erçek (Akyüz et al., 2011; Erdik et al., 2012; Doğan and Karakaş, 2013; Fielding et al., 2013). Normal faults are seen in the area in association with the strike-slip faults. They mostly form where the strike-slip faults make releasing step-overs (i.e. the faults bounding the Northern Ridge in western part of Lake Van). Folds occur mostly in the east of the Lake Van, affecting the ophiolitic mélange and the associated formations. They are generally local, discontinuous and broad anticlines and synclines with a general NE-SW trend (Figure 11 in Şengör et al., 2008).

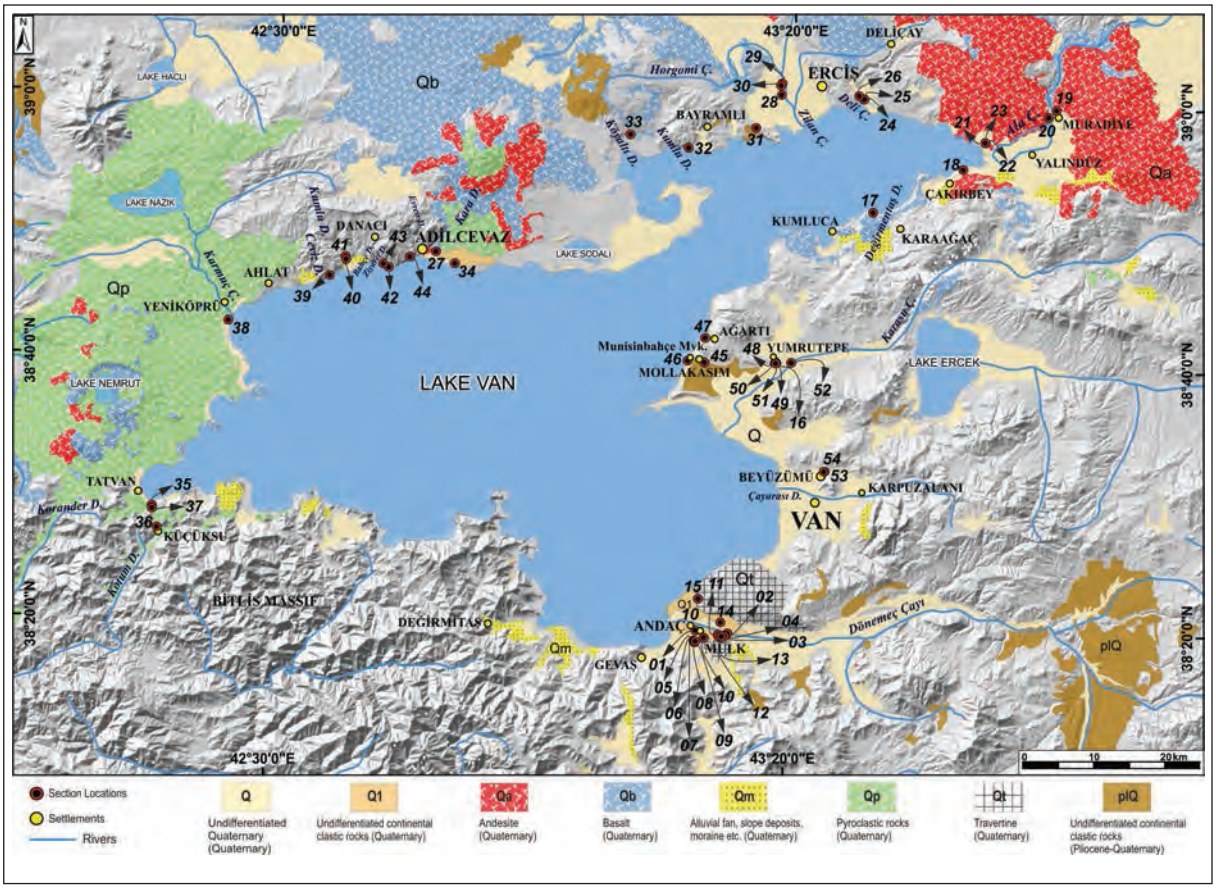

Figure 1- Geological map (compiled from Şenel and Ercan, 2002) of the Lake Van watershed, showing the locations of sites where terraces were studied.

The geology of the Lake Van Basin has been shaped mainly after the closure of the Bitlis Ocean in the medial Miocene (Şengör and Yılmaz, 1981; Şengör et al., 1985; Görür, 1992). This closure resulted from the collision of the Arabian and Eurasian plates and created the eastern Anatolian high plateau. The plateau is formed mainly from the East Anatolian Accretionary Complex, which developed south of the Rhodope-Pontide magmatic arc. It has a massive dome structure in part with smaller and local domes. The Lake Van Basin is located on such a local dome (the Lake Van dome, Şengör et al., 2008). It developed as part of the paleo-valley system of the River Euphrates in the E-W-trending Muş-Van Basin (Erinç, 1953; Wong and Degens, 1978; Degens et al., 1978; Şaroğlu and Güner, 1981; Güner, 1984; Şengör et al., 1985; Yılmaz et al., 1998; Şengör et al., 2008; Kuzucuoğlu et al., 2010; Çukur et al., 2013). The Muş and Van basins were separated by the eruption of the Nemrut Volcano about 600 ka BP (Yılmaz et al., 1998; Kuzucuoğlu et al., 2010; Litt et al., 2012).

2.2. Seismotectonics

The eastern Anatolian high plateau is still rising and undergoing an active deformation (Şengör et al., 2008). This is indicated in the Lake Van region by the occurrence of earthquakes of various intensities during the historical and instrumental periods. During the historical period, 13 earthquakes with epicentral intensities, ranging from VI to IX were recorded in the area. These events occurred in AD 1110, 1245, 1276, 1441, 1582, 1647, 1648, 1701, 1704, 1715, 1879, 1871 and 1881, causing a great damage in the settlements around the lake (Ergin et al., 1967). During the instrumental period (between 1930 and 2011), 87 earthquakes of magnitudes more than 4.0 occurred in the region (Horasan and Boztepe-Güney, 2007). Three of them were very destructive and large events, having magnitudes greater than 7.0. They were 1930, M=7.6 Iran, 1976, M=7.3 Çaldıran and 2011, M=7.2 Van earthquakes (Figure 2). Focal mechanism analysis indicates that most of these earthquakes resulted from the ruptures

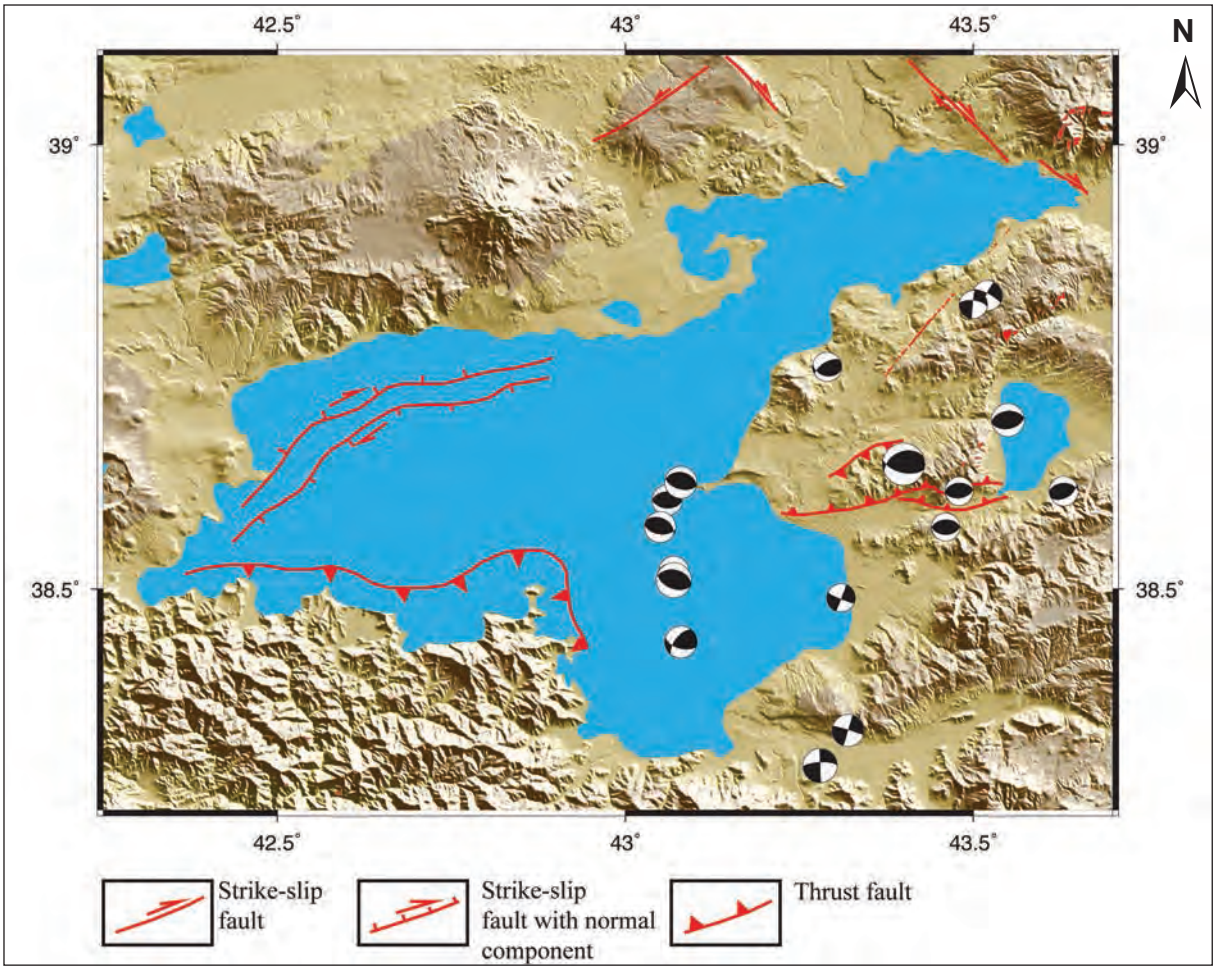

Figure 2- Seismotectonic map of the Lake Van and the surrounding region. Active faults are compiled from Emre et al. (2013) and Çukur et al. (2013), and focal mechanism solutions are from Harvard CMT catalogue (Ekström et al., 2012).

of the strike-slip faults, particularly those of the dextral ones. This is an expected result, because the dextral strike-slip faults outnumber both the sinistral strike-slip faults and the thrusts in the region. Thrust-related events mostly occur in the south and the east of the Lake Van in conformity with the distribution of these faults in the basin (Wong and Finckh, 1978; Şengör et al., 1985; Örgülü et al., 2003; Tan, 2004; Horasan and Boztepe-Güney, 2007). Majority of the earthquakes are shallow events generated predominantly in the upper 10 km of the crust.

3. Chronology, Sedimentology and Depositional Environments of the Terrace Sediments

3.1. Age of the Terrace Sediments

Terrace sediments crop out in the lake margins at various elevations, ranging from 1656 m to 1754 m (Figure 1). They are mostly confined to valleys and coastal areas where they display packages of ca. 3 m-to 25 m-thick offshore lake to marginal lake (nearshore lake, delta, beach and alluvial fan) facies with well-preserved sedimentary features, providing important clues to their depositional environments. Their available ages are compiled in Table 1. They are dated in Güzelsu (Dönemeç Çayı Valley), Beyüzümü (Çayarası Valley), Yumrutepe (Karasu Valley), Karahan Village, Adilcevaz (Kara Dere valley) and Kotum Dere Valley (Figure 1). The dating was made by previous studies using radiocarbon and $^{234}Th/^{238}U$ methods (Kempe et al., 2002; Kuzucuoğlu et al., 2010) and by us using Optically Stimulated Luminescence (OSL) method (Kuzucuoğlu et al., 2010; this study) (Table 1).

In the Dönemeç Çayı Valley (Güzelsu), mainly offshore lake sediments crop out at an elevation of 1705 metres above sea level (masl) and yield an age, ranging between 20.9 and 20.7 ^{14}C calib. ka BP

Table 1- The dates of terraces around the Lake Van. The compiled data are from Kuzuoğlu et al. (2010), Kempe et al. (2002), Mouralis et al. (2010), and this study.

Site	Name	LON (°E)	LAT (°N)	Age	Horizon	Material	Method	Reference
Yumrutepe (YUM 4)	Van 05-49	43.311	38.673	>34000 BP	Shells at beach level	$CaCO_3$	Radiocarbon	Kuzucuoğlu et al. (2010)
Beyüzümü	Van 05-51	43.392	38.537	>31000 BP	Shells on top layer (above peat)	$CaCO_3$	Radiocarbon	Kuzucuoğlu et al. (2010)
Beyüzümü	Van 06-BT 10-15	43.392	38.537	>34000 BP	Top of 2.5 m peat sequence	Organic	Radiocarbon	Kuzucuoğlu et al. (2010)
Beyüzümü	Van 06-01	43.392	38.537	>30000 BP	Peat Layer 7b within (top) sequence	Organic	Radiocarbon	Kuzucuoğlu et al. (2010)
Beyüzümü	Van 06-67	43.393	38.537	n.d.	Paleosol in channel fill	Organic	Radiocarbon	Kuzucuoğlu et al. (2010)
Yumrutepe (YUM 1)	Van 06-61	43.311	38.673	n.d.	Paleosol buried below flood silts	Organic	Radiocarbon	Kuzucuoğlu et al. (2010)
Zeve 1 (Lower Karasu)	Van 07-1	43.227	38.592	n.d.	Paleosol in buried T4" alluvial terrace	Organic	Radiocarbon	Kuzucuoğlu et al. (2010)
Orene (Lower Zilan)	Van 07-13	43.314	39.012	n.d.	Paleosol in buried T4" alluvial terrace	Organic	Radiocarbon	Kuzucuoğlu et al. (2010)
Kırklar	Van 05-36b	43.607	38.968	24900±800 cal. BP	Black layer below tephra (sup.)	Organic	Radiocarbon	Kuzucuoğlu et al. (2010)
Kırklar	Van 05-36a	43.580	38.982	25700±600 cal. BP	Black layer below tephra (inc.)	Organic	Radiocarbon	Kuzucuoğlu et al. (2010)
Adilcevaz	Van 06-76a	42.748	38.806	5940-6185 cal. BP	Charcoal associated with ceramics	Charcoal	Radiocarbon	Kuzucuoğlu et al. (2010)
Adilcevaz	Van 06-76b	42.753	38.806	9470-9550 cal. BP	Charcoal in aceramic layers (base)	Charcoal	Radiocarbon	Kuzucuoğlu et al. (2010)
Güzeldere (Apricots)		43.220	38.336	20700±300 cal. BP	Organic matter (upper level)	Organic	Radiocarbon	Kempe et al. (2002)

Table 1- *continue*

Site	Name	LON (°E)	LAT (°N)	Age	Horizon	Material	Method	Reference
Kotum	06-33 sup.	42.309399	38.472325	102.2 +3.8/ -3.7 BP	Low travertine		U/Th	Kuzucuoğlu et al. (2010)
Kotum	06-33 inf.	42.309520	38.472297	102.1 +8.1/ -7.5 BP	Low travertine		U/Th	Kuzucuoğluet al. (2010)
Yumrutepe	OSL16	43.311347	38.673269	12±1.8 ka	Nearshore lake sediments (?)	Polymineral	OSL	This study
Kotum-Küçüksu Valley	VAN 021	42,314185	38,478190	117±5.2 ka	Pyroclastics (pumice fall)	Mineral	Ar/Ar	Mouralis et al. (2010)
Yumrutepe	OSL48-1	43.310298	38.674525	10±1 ka (n=9), 15±1 ka (n=25), 20±1 ka (n=9)	Nearshore lake sediments (?)	Quartz	OSL	This study
Adilcevaz	OSL27-1	42.757291	38.805548	10.3±1.1 ka	Nearshore lake sediments (lower level)	Polymineral	OSL	This study
Adilcevaz	OSL27-2	42.757291	38.805548	6.14±0.7 ka	Nearshore lake sediments (middle level)	Polymineral		
Adilcevaz	OSL27-3	42.757291	38.805548	8.2±0.92 ka	Nearshore lake sediments (upperlevel)	Polymineral	OSL	This study
Beyüzümü	OSL54	43.391304	38.537251	15±1 ka	Nearshore lake sediments	Quartz	OSL	This study

(Kempe et al., 2002) (Figure 1). In the Çayarası Valley (Beyüzümü) southeast of Van City, nearshore laminated lake sediments located at 1754-1761 masl elevations were dated ? 30-34 ^{14}C calib. ka BP using radiocarbon method (Kuzucuoğlu et al., 2010) and 15.1 ka using OSL method (this study). In Yumru Tepe in the Karasu Valley, beach and Gilbert-type delta deposits located at 1736 and 1712 masl elevations, respectively have 30-34 ^{14}C calib. ka BP, same as the age of the nearshore lake sediments in the Çayarası Valley (Kuzucuoğlu et al., 2010) (Table 1; Figure 1). Our OSL age for the same sequence at a higher elevation ranges from 10 to 20 ka BP with the most frequent ages occurring at 15.1 ka BP, whereas the age at the lower elevation is 12 ± 1.8 ka BP. Around the Karahan Village, another Gilbert-type delta sequence is exposed at 1690 masl elevation, for which Kuzucuoğlu et al. (2010) found ages varying between 24.9 and 25.7 ^{14}C calib. ka BP (Table 1). In the northern margin, around Adilcevaz (in the Kara Dere Valley), nearshore lake sediment located at an elevation of 1697 masl are dated between 6.1 and 10.3 ka BP by OSL method (this study). Kuzucuoğlu et al. (2010), however, report the formation of only up to 13 m high terraces above the present lake level near the river mouths during the early Holocene, between 5.9 and 9.7 ^{14}C calib. ka BP

So far the oldest dated terraces are found in the Kotum Dere Valley. According to Kuzucuoğlu et al (2010), the oldest terrace is dated to be older than 105 ka BP. This terrace reaches 1755 masl, about 110 m above the present lake level and 20 m above the present lake threshold, and was deposited during a period when pyroclastic deposits dammed the lake's outlet in the Kotum Valley. Another terrace in the lower Kotum Dere Valley (our Sections KOD1 GPS-035 and KOD$_2$, GPS-037; Fig 1) reach 1730-1735 m, and is dated sometime between 100-35 ka, according to the ^{39}Ar/^{40}Ar and U/Th ages of the travertine and pumice units disconformably underlying the laminated terrace sediments (Kuzucuoğlu et al., 2010; Mouralis et al., 2010).

The dating of the terraces revealed that their age generally increases with their elevations. Older terraces commonly occur at high elevations in most part of the Lake Van Basin, except the terrace in the Kara Dere Valley in the Adilcevaz region, which yields younger age despite its high elevation (1697 masl; 50 m above the present lake level). However, the most previously published age data presented here on the terraces should be evaluated and used with caution, because the stratigraphic position, lithology, facies association, stratigraphic relations and depositional environment of the dated samples are not unequivocaly documented. Consequently, the terraces cannot be correlated facies by facies throughout the basin on the basis of the available ages. It is therefore difficult to discuss temporal and spatial evolution of their depositional conditions with the available age data. However, we consider that it would be reasonable to think that the terraces reflect the natural history of the Lake Van Basin over the last ~125 ka BP, the age of the so far known oldest dated terrace sediments.

In the following paragraphs, we describe the terraces first and than interpret their environments of deposition. Based on this interpretation we than reconstruct the depositional environmental conditions and discuss the tectono-stratigraphic evolution of the Lake Van Basin during the last ~125 ka BP.

The terraces were examined at 22 locations, including Dönemeç Çayı Valley (Güzelsu), Çayarası Valley Beyüzümü), Karasu Valley (Yumrutepe and Mollakasım), Munisinbahçe Mevkii, Boğaz Dere Valley, Hasan Dere Valley, Değirmentaş Dere Valley, around Village Çakırbey, Alaçay Valley, Village Karahan, Deliçay Valley, Zilan Valley, around Kaş Burnu, Kumlu Dere Valley, Çayır Mahallesi, Karadere Valley (Adilcevaz), Evren Deresi valley, Ziyaret dere valley, Kumlu Deere valley at Village Soğanlı, Ceviz Dere Valley, Karmuç Çayı Valley and Kotum Dere Valley (Figures 1, 33, 34 and 35).

3.2. Stratigraphic Sections studied in the Dönemeç Çayı Valley

3.2.1. Section-DÖN$_1$ (GPS-001, lat: 38.3332°, long: 43.1891°, elev: 1687 masl)

Description: This section was studied at the southern slope of the Dönemeç Çayı Valley, between the Villages of Andaç and Mülk (Figure 1). It is a 5 m-thick clastic and laterally persistent sequence, consisting mainly of very fine-grained and well-sorted sandstone with minor amounts of siltstone and claystone. The sandstone displays fine parallel lamination, micro cross-lamination and small-scale trough cross-stratification both in the lower and the upper parts of the section. In the middle part, it contains distinctive convolute lamination and flame structures (Figure 3).

Figure 3- Terrace section $DÖN_1$ in Dönemeç Çayı Valley, showing fine scale ripple lamination, trough cross-stratification, convolute lamination and flame structures. For location see figure 1.

Interpretation: These sediments were probably deposited in the offshore environment of the Paleo-Lake Van as suggested by such features as the lateral persistency, very fine grain size, lamination, small-scale cross-stratification, convolute lamination, and flame structures. These soft-sedimentation deformation structures are interpreted to form due to the seismic shocks, triggering liquefaction and/or fluidisaton of unconsolidated sediments (Üner, 2014). The absence of any fresh-water organisms in these sediments may have been due to the inhospitable soda water of the Paleo-Lake Van. The convolute laminations probably formed when the sediments were water saturated and perhaps subjected to earthquake shocks.

3.2.2. Section-$DÖN_2$ (GPS-002), lat: 38.3299°, lon: 43.2409°, elev: 1708 masl)

Description: This section is located in the southern flank of the Dönemeç Çayı Valley, 4.7 km east of the Section-$DÖN_1$ (Figure 1). It is made up of 7 m-thick yellowish green and upward-coarsening sandstone unit with various sedimentary structures. At the base of the section, sandstone is fine-grained,

poorly-cemented and planar laminated that gradually passes upward into a fine to medium-grained and well-sorted sandstone with common bioturbation and bidirectional trough-shaped cross-stratification (up to 40 cm) (Figure 4). This cross-bedded and burrowed sandstone is followed by 30 cm-thick, whitish and thinly-bedded clayey carbonate or marl with an erosional contact. The section then continues towards the top with a well-sorted and medium-to coarse-grained sandstone, becoming pebbly at the top.

Interpretation: The upward-coarsening sequence of predominantly well-sorted sandstone with well-developed laminations, burrowings and bidirectional cross-stratifications seem to be representative of many of the features observed in the shoreface of a beach environment. The complex hydraulic conditions of this environment permit the accumulation of a wide range of sediments from fine sand to gravel with common burrowing structures and multidirectional trough cross-bed sets. The bidirectional trough cross-beds probably indicative of deposition under strong longshore current conditions. The erosion of these beds and the burrow tops indicate that this environment was subjected to modification by storm-generated waves. The clayey carbonates overlying the truncation surface perhaps represents the suspended sediments deposited as the storm wanes (Hayes, 1967; Howard, 1972; Reineck and Singh, 1972; Kumar and Sanders, 1976; Davidson-Arnott and Greenwood, 1976).

3.2.3. Section-DÖN$_3$ (GPS-003-004, lat: 38.3271°/3268, lon: 43.2359°/2356, elev: 1713/1715 masl)

Description: This section is exposed at the southern slope of the Dönemeç Çayı Valley, 600 m from Section-DÖN$_2$ described above (Figure 1). It starts at the base with 20 cm-thick brown, fine- to medium-grained sandstone overlain by up to 60 cm reddish to yellowish green mudstone with no internal structure, except some burrows and few discoidal pebbles in its lower parts. Above the mudstone is interbedded sandstone and 30 to 40 cm-thick green shale succeeded by 40 cm-thick and well-bedded sandstone with scoured-loaded basal contact. This sandstone and the underlying units are cut by a low-angle erosional surface, probably representing a basal glide plain at the base of a relatively small-scale slump or slide deposits . The section then continues upward with up to 2 m-thick poorly-sorted, ungraded

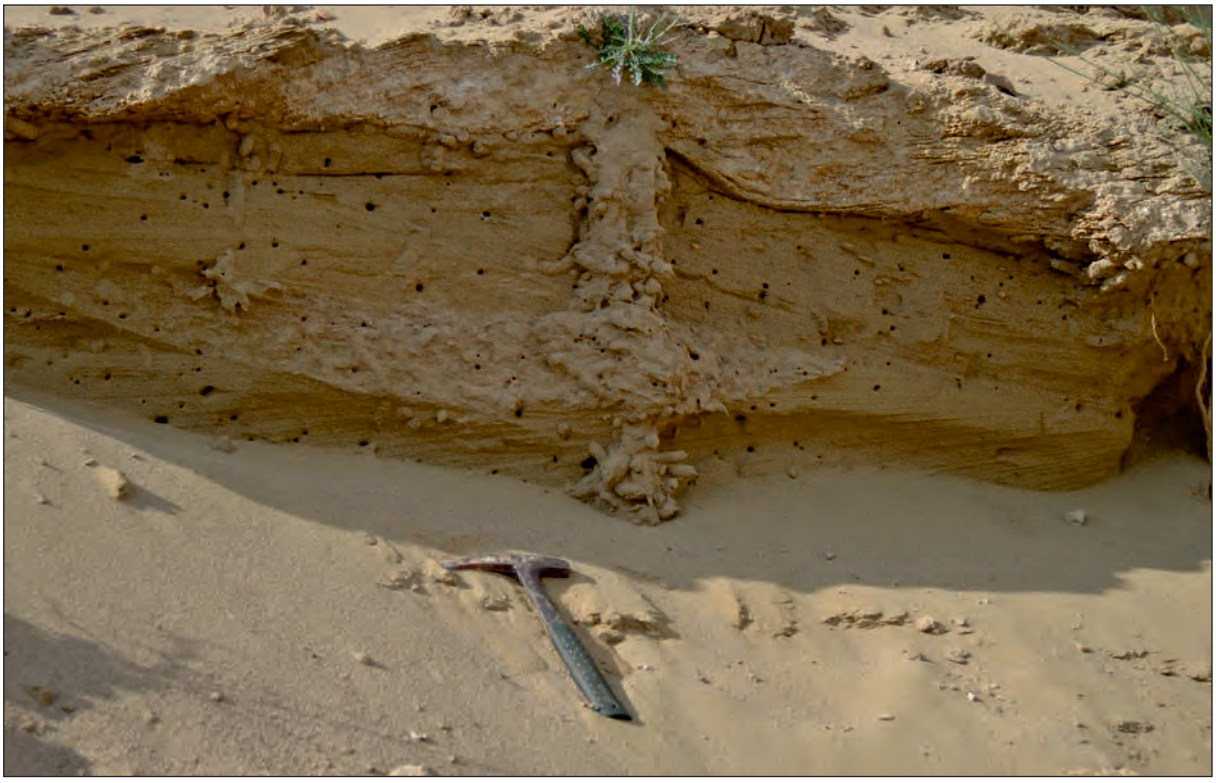

Figure 4- The sandstones in the terrace section-DÖN$_2$ show bidirectional planar cross-beddings and common bioturbation. For location see figure 1.

and monogenic conglomerate. It forms a mainly clast-supported and poorly- to moderately-sorted pebble assemblage. Pebbles are commonly angular to subrounded and mostly have platy or discoidal shape. They are composed predominantly of travertines derived from a nearby bedrock slope (Figure 1). The conglomerate commonly displays a lenticular geometry with erosional bases, characterizing different episodes of channeling into the underlying sediments. Toward the NE, this flat-lying conglomerate and the underlying sandstone sit on top of steeply NE-dipping interbedded sandstone and conglomerate and thus form a three-part structure, similar to that of a delta (Figure 5).

Interpretation: This section displays the features of a Gilbert- type delta. The burrowed mud and the interbedded shale and sandstone in the lower part of the section probably accumulated as prodelta sediments (bottomset) in the Lake Paleo-Van, whereas the overlying horizontal conglomerate and sandstone were deposited in the delta platform (topset). The steeply dipping interbedded sandstone and conglomerate were deposited as delta slope sediments (foreset). The Paleo-Lake Van was probably abutting a steep slope of an adjacent high where travertine deposits were exposed like today's elevated travertine highs in the section area. The high provided limited detritus to the lake from a short distance as indicated by the coarse grain size of the topset deposits and the angularity of the clasts in the conglomerate. However, the sediment supply was persistent enough to build a small Gilbert-type delta in the lake's margin. The erosional surface, cutting the delta platform may indicate channel erosion or a slide, occuring in the delta front.

3.2.4. Section-DÖN$_4$ (GPS-014, lat: 38.3732°, lon: 43.1925°, elev: 1705 masl)

Description: This section is located at the northern flank of the Dönemeç Çay Valley, 300 m south of the Dönemeç Village (Figure 1). It is about 10 m-thick sedimentary sequence that is essentially composed of yellowish green very fine- to fine-grained sandstones with various types of sedimentary structures (Figure 6). It starts at the base with 70 cm-thick laminated sandstone in part with cross-bedding. It is overlain

Figure 5- Section DÖN$_3$, showing steeply NE-dipping foreset beds of a Gilbert-type delta. The foreset beds are underlain by bottom-set beds of mudstone and fine-grained sandstone and overlain by conglomeratic topset beds. For location see figure 1.

with a rather sharp contact by about 30-40 cm-thick, thinly-bedded rippled sandstone sandwiched between two 10 cm-thick horizontal sandstone beds. This unit passes upward into another 1 m-thick sandstone package that consists predominantly of thin (5-10 cm) wave rippled sandstone beds separated by thin shale beds. The wave ripples appear to decrease in length and amplitude upward. The rippled sandstone package is succeeded by a 1.0-1.2 m-thick massive to faintly laminated and very fine-grained sandstone to clayey sandstone unit. Within this unit, a 10 cm-thick horizontal sandstone and a very-thinly-bedded and folded slump deposit are recognized (Figure 6). The unit is than followed by about 80 cm-thick sandstone package, containing three sandstone beds of 25 to 35 cm thickness. The sandstone beds with erosional bases are interbedded with very thin mudstone beds. Above the sandstone package, a 1.3 m-thick white sediment occurs. This sediment appears to be laminites with alternating millimetric laminae of microcrystalline carbonate and clastic material in various proportions. At the base of the laminites, few short water-escape structures, i.e. burst-through structures, are observed. The laminites pass upward into very fine sandstone of 1.5 m thick that seems thinly-bedded at the base and massive at the top (Figure 6).

Interpretation: The abundance of laminated to very finely-bedded sandstones throughout the sections suggests that these sediments originated in a low energy offshore environment of the Paleo-Van. However, the presence of small-scale wave rippled and cross-bedded sandstones indicate intermittent higher energy conditions and they were probably deposited by low velocity traction currents. The slump sheet and the overlying sandstones with erosional bases show some characteristic features of soft sediment deformation and turbidites, respectively. The former probably formed as a result of liquidization of unconsolidated sediments, whereas the latter accumulated by turbidity currents. Considering the high seismic activity of the Lake Van region, both processes were probably triggered by earthquake shocks. The carbonate-rich laminites most probably represent varves, resulting from seasonal sedimentation under relatively deep water (high lake level) conditions. High carbonate contents were

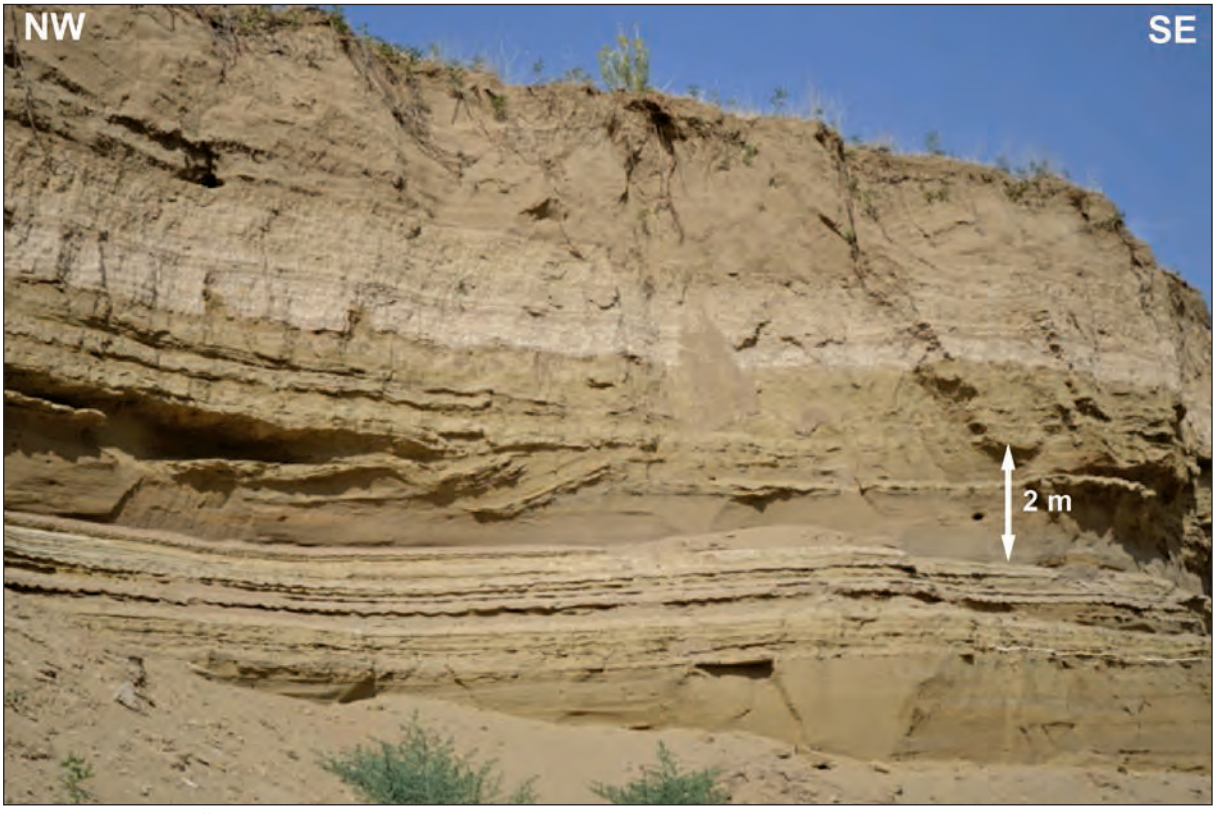

Figure 6- Section-DÖN$_4$ located on the northern flank of the Dönemeç Çay Valley, 300 m south of the Dönemeç Village (Figure 1). The section consists essentially of yellowish green, very fine-to fine-grained sandstones with laminites. The sequence shows slump and water escape structures. For location see figure 1.

probably induced by input of calcium-rich waters (Litt et al., 2009; Stockhecke et al., 2014; Çağatay et al., 2014).

3.3. Stratigraphic Section Examined in the Çayarası Valley, Beyüzümü District

3.3.1. Section-CV_1 (GPS-053-054, lat: 38.5373°/5372, lon: 43.3923°/3913, elev: 1761-1754 masl)

Description: This section is located about 1 km to the northeast of the Beyüzümü district of Van City (Figure 1). It is characterized, as a whole, by 25 m of sandstones, becoming more conglomeratic in upper parts (Figure 7). The sandstones are generally yellowish brown to beige in color and show various textures and sedimentary structures throughout the section. At the base of the section, there is horizontally-stratified sandstone with small pebbles, containing common and well-preserved fresh water bivalves (*Dreissena* sp). Above these fossiliferous coarse clastics is 1.5 m of gray, fine- to medium-grained sandstone with faint and discontinuous ripple marks. It passes upward across a sharp contact into a 50 cm-thick and massive clayey sandstone overlain by a 1.5 m-thick, white to beige and laminated mudstone (Figure 7). From this mudstone upward, the sequence continues with yellowish green to brown, locally fossiliferous, wave rippled sandstone, grading upward into brown laminated to massive sandstone alternating in part with rippled sandstone beds. To the top of the section, the sandstones are gradually overlain by about 5 m-thick, carbonate cemented and generally planar cross-bedded conglomerates in part with yellow sandstone interbeds, similar to the sandstones in the lower parts of the section.

All four radiocarbon dates from the Section-CV_1 terrace are indefinite and older than 30 ka BP (Kuzucuoğlu et al., 2010) (Table 1). Our single OSL age from the yellow laminated sand in the part of the section at 1754 m elevation is 15±1 ka BP, which is considerably younger than the radiocarbon ages of Kuzucuoğlu et al. (2010).

Interpretation: The widespread fine-to medium-grained sandstones of this section probably accumulated in a nearshore lake environment of the Paleo-Van rather than deeper water offshore

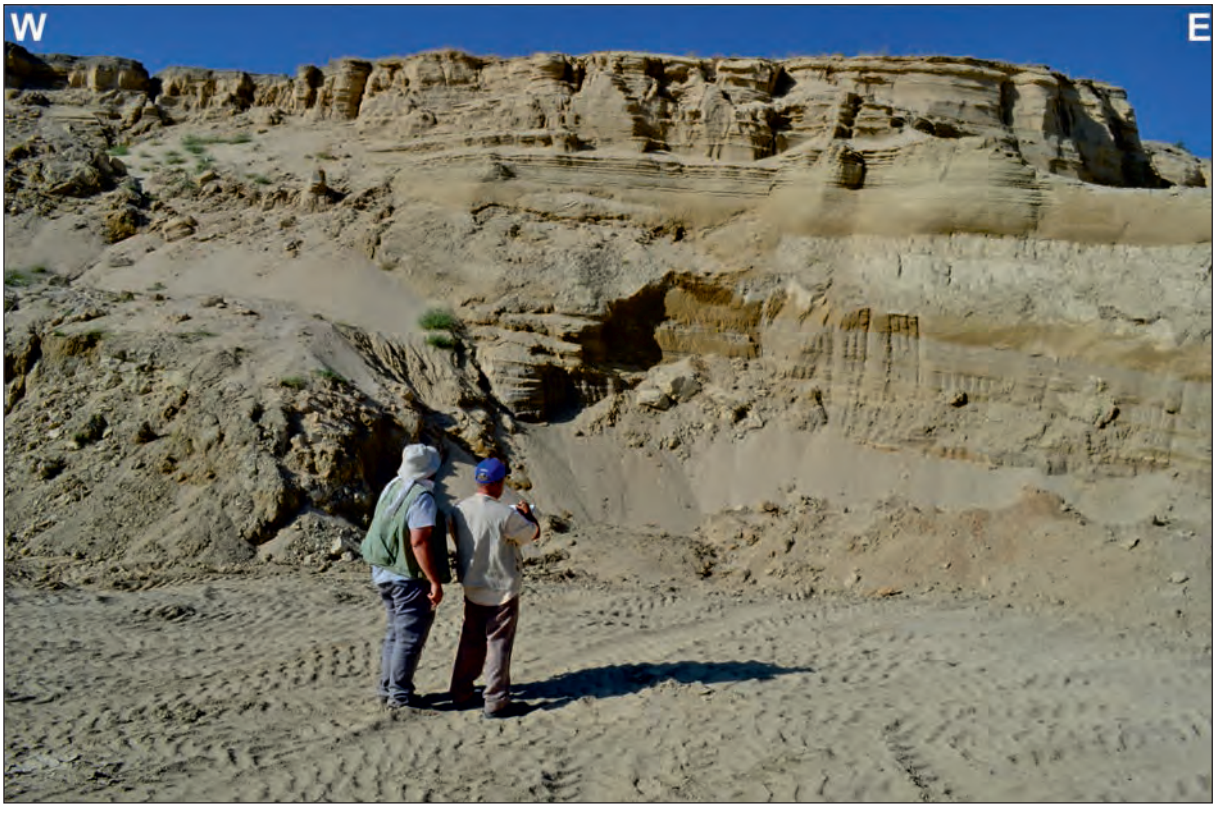

Figure 7- Section CV_1 in Çayarası Valley in Beyüzümü district, South of Van City. This 25 m-thick section consists mainly of sandstones with conglomerates in the upper parts. For location see figure 1.

environment, because they contain no evidence of turbidite, slump or varve deposition. Therefore, it is believed that most of the sand-sized material in this section was contributed by river inflow, leading to the deposition in nearshore environments under the influence of the shoreline processes, including current or wave activity (Sly, 1978; Piccard and High, 1981). Such processes could account for most of the features observed in the sandstones of this section. The presence of *Dreissena* sp. suggests that alkalinity and salinity of the lake water was low, possibly due to the proximity of the depositional site to the river mouth. The overlying cross-bedded coarse clastics indicate that the nearshore lake deposits graded upward into alluvial fan-fluvial facies, owing to either a drop in lake-level or an increase in sediment supply or both.

3.4. Stratigraphic Section in Yumrutepe in the Karasu Valley

In this valley, lake-related Quaternary sediments crop out about 1 km south of the Yumrutepe Village (Figure 1). They are composed mainly of interfingering coarse clastic deposits with various facies characteristics, indicating that they were deposited in different neighboring depositional environments. In order to show their lateral and vertical facies changes, these sediments are described below from three sections, located at different elevations.

3.4.1. Section-KV$_1$ (GPS-048-049-050, lat: 38.6748°, lon: 43.3096°, elev: 1733 masl)

Description: This section is a 3.5 m-thick sequence, commencing at the base with 1.0 m of greenish gray and massive pebbly mudstone overlain with a sharp and erosional contact by a 1.0 m-thick, brownish gray conglomerate (Figure 8). The conglomerate is composed of moderately sorted, subrounded to rounded small pebbles (<4 cm) with an orientation parallel to the bedding surfaces. The beds are thin (≤10 cm) with well-defined sharp basal boundaries. This conglomerate is succeeded by a red, grain-supported conglomerate unit without any bedding. The clasts of the red conglomerate are commonly rounded pebbles, showing normal

Figure 8- Section-KV1 in Yumrutepe, Karasu River Valley at 1733 masl. This sequence consists of greenish gray and massive pebbly mudstone in the lower part and brownish gray and red conglomerates in the upper part. For location see figure 1.

grading. The pebble size varies between 2 and 25 cm with an average of 4 cm.

Interpretation: The horizontally stratified conglomerate may be interpreted as deposits of a powerful stream. Its well-defined beds with nonerosive and erosive bases, moderate sorting, abundant rounded clasts with normal grading and absence of fossils support this interpretation. The tractional activity of turbulent streamflows was perhaps important in its deposition. This deposit compares closely to streamflood deposits and probably occupied a distal alluvial fan environment (Bluck, 1967; Steel, 1974; Steel and Wilson, 1975; Heward, 1978; Nilsen, 1982). The overlying unstratified red conglomerate with erosional base and normal grading probably represents a braided river channel.

3.4.2. Section-KV_2 (GPS-048-049-050, lat: 38.6733°, lon: 43.3095°, elev: 1736 masl)

Description: This section, located about 90 m above the present lake level, represents the highest part of the terrace section in Yumrutepe locality (Figure 1). Toward the south, the Section-KV_1 passes laterally into 7 m-thick Section-KV_2 that exhibits close stratigraphic and sedimentologic similarities to the former. It also contains brownish gray and red conglomerates in the same order as observed in the Section-KV_1 (Figure 9). At the base it consists of 1.5 m thick brownish gray conglomerate with some local sand lenses (Figure 9). The basal unit is overlain by thinly (10-15 cm) bedded, weakly cemented yellow sandsone, which is followed upwards across a truncation surface by SE-dipping beds of coarse sandstone with some conglomerate interbeds. These dipping beds are overlain by a flat lying and *Dreissena* sp. bearing coarse pebble conglomerate above a second truncation surface. This conglomerate unit is overlain by a 0.3-0.7 m-thick loosely cemented green fine sandstone. The overlying unit above the green sandstone and below the soil zone at the top of the section is the red conglomerate as observed in the Section- KV_1. It is generally unstratified or crudely stratified with abundant poorly-sorted sand or granule matrix. Large pebbles are generally subrounded to rounded pebbles with subordinate amount of boulders derived from a local source.

Interpretation: The moderately - to well - sorted fabric of the brownish gray conglomerate suggests tractive transport or reworking of the deposit. The planar and non-erosive bases of its beds in the upper and lower parts of the section exclude channelised, turbulent currents. Its size, shape, sorting, segregation into well-stratified layers and fossil content may indicate a beach face depositional environment for this sediment (Bluck, 1967; Clifton, 1973). These characteristic features probably resulted from reworking and winnowing by waves and storms in the backshore to foreshore sub-environments of a beach along the Paleo-Lake Van. The intervening sandstone with planar cross-bedding may support this interpretation. The presence of freshwater bivalves near the top of the sequence indicates considerably lower lake water salinity and alkalinity than those of the present-day lake waters.

The geographic positions and the stratigraphic relations of the Sections-KV_1 and KV_2 may indicate that the alluvial fan recognized in the former extended to the shore of the Paleo-Lake Van where its deposits were reworked to form the beach deposits of the latter.

Figure 9- Section-KV_2 in Yumrutepe, Karasu River valley at 1736 masl. It consists mainly of brownish gray and red conglomerates with some sandstone interbeds. Note the SE-dipping sandstone and conglomerate beds in the middle part of the section. See figure 1 for location.

The coarseness, poor sorting and granular matrix of the red conglomerate on top may suggest high water discharge, sediment supply and rapid deposition in the depositional area. The red color, erosional base and unfossiliferous nature of the conglomerate may indicate that this depositional area was a braided river.

3.4.3. Section-KV_3 (GPS-016, lat: 38.6732°, lon: 43.3113°, elev: 1712 masl)

Description: This section is a more than 10 m-thick sedimentary succession with horizontally- and steeply inclined-bedded units towards SE (Figure 10). The inclined-bedded unit is composed mainly of conglomerate and sandstone, dipping at 35-40 toward the east. Bed contacts are commonly sharp and their thickness avarages 30 cm with a range of 20-80 cm. Conglomerate is gray, clast-supported, moderately- to well-sorted and seems common in the lower parts of the unit. Sandstone is yellowish gray and thinly-laminated in part with wavy bedding.

The horizontally-bedded unit overlies the inclined-bedded unit with a sharp and planar contact. However, in places, pinch-outs between these units are also observed. The horizontally-bedded units start at the base with 40 cm of gray conglomerate and continue upward with yellowish gray sandstone. The conglomerate is clast-supported and moderately-sorted with subangular to rounded gravels, showing no channel structures. The overlying sandstone is fine- to medium-grained, thinly-laminated with common wavy and lenticular bedding. It also shows in places some soft sediment deformational structures, such as sedimentary dikes (Figure 11).

Age of terraces at Yumrutepe: OSL dating of quartz in the green sandstone unit in the upper part of section KV_2 at around 1735 masl provided an age of 15±1 ka BP (n=25) (Figure 9, Table 1). The other less reliable OSL ages from the same unit are 10±1 ka BP (n=9) and 20±1 ka BP (n=9). The poorly cemented, fine- to medium-grained, laminated yellow sandstone unit with horizontal beds above topset beds in Section-KV_3 at Yumrutepe at 1712 masl has an OSL age of 12±1.4 ka BP (Figure 11, Table 1).

Our OSL ages are considerably younger than radiocarbon ages of Kuzucuoğlu et al. (2010) for the

Figure 10- Section-KV_3 at Yumrutepe locality, showing SE-dipping foreset sandstone beds and horizontal conglomerate topset beds of a Gilbert-type delta complex. For location see figure 1.

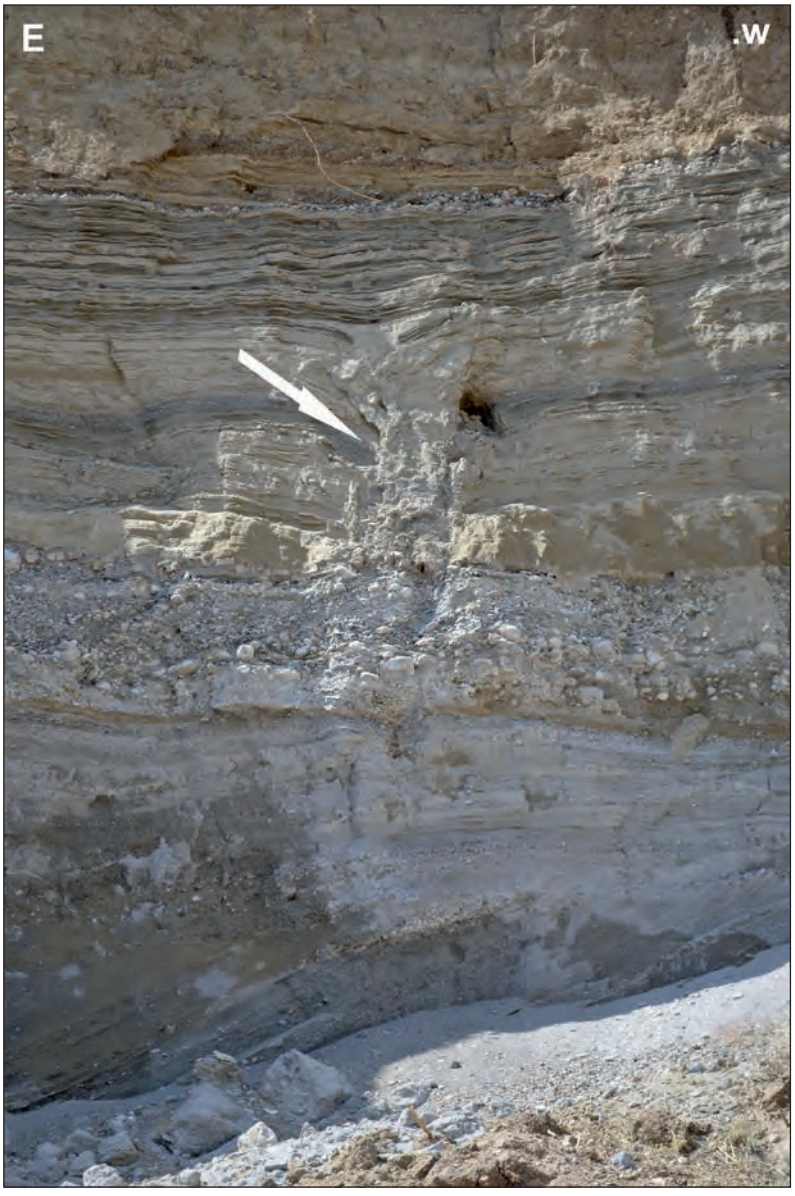

Figure 11- The upper part of Section-KV_3 at Yumrutepe locality above the conglomeratic topset beds of Gilbert-type delta, showing soft sediment structures, such as water escape structures (arrow), in the fine to medium grained yellow sandstone. For location see figure 1.

same terrace sequences. These authors obtained a radiocarbon age greater than 34 ka BP from shells of *Dreissena* sp. around a 1735 masl in the Section KV_2. They concluded that this terrace (their C1'' transgressive series), located at 1730-1735 masl, formed sometime between100 ka BP and 34 ka BP. Located at ~1700 masl in the Yumrutepe locality, Kuzucuoğlu et al. (2010) defined yet another older transgressive fan delta series (C1') with its bottom set having an age older than 105 ka BP. This age is inferred from the age of Kotum ignimbrite that blocked the Kotum Valley (outlet of the Lake Paleo-Van) and resulted in a high lake level during, the Marine Isotope Stage-5 (MIS-5).

Interpretation: The section represents a Gilbert-type delta. The horizontally-bedded unit forms the topset, whereas the steeply-bedded unit forms the foreset deposits of the delta. The foreset deposits probably accumulated in response to bedload deposition and grain avalanching on a steep slope (Allen, 1984; Dunne and Hempton, 1984). The dike structures in the topset beds may indicate that pore-water pressure temporarily exceeded the lithostatic

pressure in these sediments, leading to liquefaction. This condition was probably caused by a seismo-tectonic event, such as an earthquake shock.

3.5. Stratigraphic Section in the Munisinbahçe Locality

This section is located at the eastern coast of the Lake Van in the Munisinbahçe locality, 2 km west of the Village Mollakasım (Figure 1).

3.5.1. Section-MB$_1$ (GPS-046, lat: 38.6741°, lon: 43.1681°, elev: 1684 masl)

Description: This is about 6 m-thick succession of coarse clastic sediments, consisting of conglomerate, pebbly granulestone, pebbly sandstone and sandstone (Figure 12). Pebbly granulestone forms, at the base of the section, a light gray, 1m-thick, moderately to well-sorted and sub-rounded to rounded unit. This unit displays both a normal gradation (an upward grain size decrease) and a faint, NNW-dipping low-angle planar cross-bedding. The cross-bedding is highlighted by a foreset-parallel alignment of the small pebbles (Figure 12). The granulestone is overlain with a sharp and planar contact by a greenish gray and horizontally-stratified conglomerate. Normal grading is also apparent in this facies. Moderately- to well-sorted and well-rounded small pebbles (≤4 cm) grade upward into coarse sand. The thickness of the conglomerate slightly varies along the section; it is 1.0 m in the east and thins toward the west. This conglomerate passes upward across a sharp and planar surface into a 60 cm of moderately-sorted, rounded and clast-supported conglomerate with an overall lenticular geometry. In contrast with the underlying conglomerate, this unit shows reverse grading; i.e. finer clasts occur at the base and the relatively coarser clasts at the top. A 50 cm-thick pebbly coarse sandstone sits on this conglomerate above a sharp and probably erosional contact. This sandstone exhibits well-developed very fine horizontal stratification with the larger grains with their long axis parallel to the bedding surface. This well-bedded sandstone is succeeded by a 1.5 m-thick conglomerate that forms a mainly clast-supported,

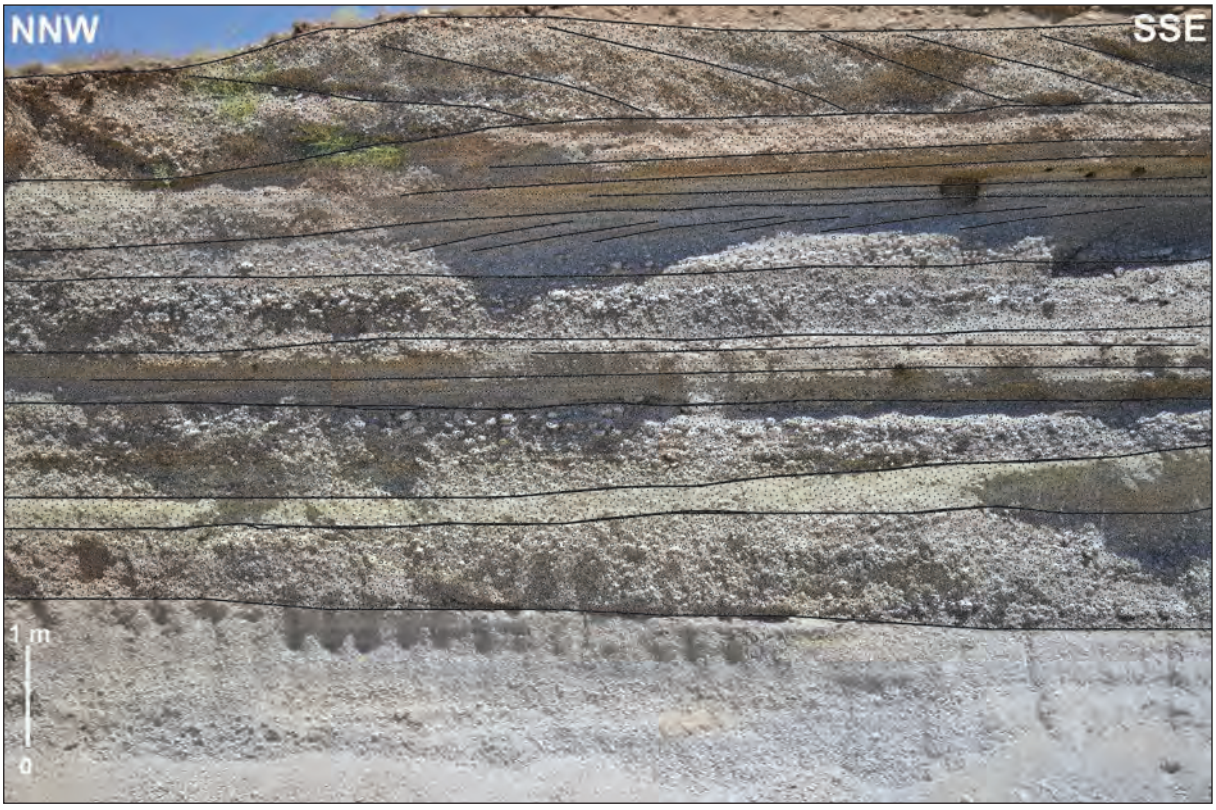

Figure 12- Section-MB$_1$ (GPS-046). This 6 m-thick succession consists of conglomerate, pebbly granulestone, pebbly sandstone and sandstone. Note the SSE-dipping cross-bedding in the top red conglomerate unit, which contrasts with the NNW-dipping cross-stratifications of the light gray conglomerate unit in the lower part. See figure 1 for location.

moderately-to poorly-sorted and generally well-rounded pebble (≤ 5 cm) assemblage. The base of the conglomerate body is sharp and probably erosive with a tabular surface. The upper boundary is gradational with an irregular and convex-up surface marking a transition into a 50 to 60 cm of light gray sandstone. This sandstone shows NNW-dipping planar cross-bedding and wedging out in the dip direction. Above this unit is 40-cm thick, red and pebbly coarse sandstone to granulstone with a sharp and erosional tabular base. It passes upward in turn into a 1 m-thick red conglomerate across a sharp and erosional surface. This red conglomerate is generally without grading, clast-supported and composed of a pebble and occasional cobble assemblage, showing a rather variable degree of sorting. It displays relatively a large-scale cross-bedding, usually only possible to identify from some distance. The inclined foreset strata are tabular and are composed of moderate-to well-sorted and mainly well rounded small pebbles. The cross-bedding in this red unit has SSE-dipping, contrasting with the NNW-dipping cross-stratifications of the lower light gray to greenish gray conglomerate (Figure 12).

Interpretation: The horizontal stratification in most of the light gray to greenish gray conglomerate beds of the Section-MB_1 reflects varying discharge and discontinuous accretion during deposition. The coarseness and the clast-supported texture suggest high water discharge and sediment concentrations in the depositional flows. Tractive transport and reworking (or recycling) are reflected by the abundance of the rounded clasts. Occurrence of the planar cross-beddings in the sandstone beds within these conglomerates indicates that turbulent flows were also important in their deposition. The NNW-dipping of these cross-beddings in the lower part suggests a southwesterly sediment transport direction. From the light of all these evidence the light gray to greenish gray conglomerates and the associated sandstones are interpreted to represent accretion and migration of channel bars in a braided stream or an alluvial fan environment (Rust, 1972; Bull, 1972; Nemec and Steel, 1984).

The red clastics in the upper part of the section probably represent a different episode of a braided river or alluvial fan deposition as suggested by their colour, erosional base and the cross-bedding with a dip opposite to that of the lower unit. The SSE-dipping planar cross-bedding in the red conglomerate indicates a northwesterly sediment transport direction during its deposition. The change of sediment source area may indicate a topographic differentiation in the region as a response to local tectonism.

3.6. Section studied in Mollakasım Village in the Boğaz Dere Valley

This section was studied on the western margin of the Boğaz Dere Valley, 700 m SE of the Mollakasım Village (Figure 1).

3.6.1. Section-BD_1 (GPS-045, lat: 38.6722°, lon: 43.1952°, elev: 1733 masl)

Description: This section is represented mainly by 10 m of light gray sandstone with variable sedimentary textures and structures throughout the section. Generally light gray, medium-to coarse-grained, well-sorted and rounded sandstone predominates with minor amounts of yellowish gray granulestone and conglomerate. The sandstone contains low-angle plane bedding, sub-horizontal plane lamination, ripple cross-lamination, bidirectional (N- and S-dipping) planar cross-bedding and trough cross-bedding (Figures. 13 and 14). The granulestone and very fine-grained conglomerates contain large amount of lithic carbonate grains and occur either in continuous beds (15 to 40 cm thick) in trough cross-beds or in small channels (Figure 14). When they form continuous beds, they have sharp upper and lower contacts and show in places normal or reverse grading.

Interpretation: The complex sequence of multidirectional sedimentary structures and variable sediment textures of the deposits in the Section-BD_1 suggest that these deposits probably accumulated in complex hydraulic conditions, such as the shoreface part of a beach environment. The trough cross-bedded facies were probably deposited in the surf zone by multidirectional current flow, whereas the bidirectional planar cross-bedded sediments were laid down in the upper shoreface by strong longshore currents. The coarser–grained deposits with graded bedding may have been resulted from storm-generated turbidity currents. The presence of small-scale channels and sharp truncation surfaces between the laminated bed sets indicate that high amplitude waves were periodically scouring the bottom of the depositional environment. The absence of large pebbles and cobbles in this beach may suggest that this area of the Lake Paleo-Van was either beyond the reach of the coarse clastics or such sediments were not available in this area and its close vicinity.

Figure 13- The sandstone unit in Section-BD_1 shows low-angle plane bedding, sub-horizontal plane lamination, bidirectional planar cross-bedding. The sediments represent a beach environment. See figure 1 for location.

Figure 14- Section-BD_1 (GPS-045). The granulestone and very fine-grained conglomerates containing abundant lithic carbonate grains show trough cross-bedding and small channel structures. See figure 1 for location.

3.7. Stratigraphic Section Measured around the Hasan Dere Valley

This section is located on the Lake Van shore, 200 m south of the mouth of the Hasan Dere Valley (Figure 1).

3.7.1. Section-HD_1 (GPS-047, lat: 38.7034°, lon: 43.1960°, elev: 1656 masl)

Description: This section is exposed in a ~15 m high coastal cliff located 1.3 km west of the Village Ağartı (Figure 1). It is represented by a gray conglomerate alternating with brown sandstone toward the top of the section. The conglomerate forms two thick intervals (5 and 4 m, respectively) in the lower half of the section and is composed of well-rounded, moderately- to poorly-sorted polygenic clasts with a grain-supported texture. Although its clasts range in size from 1 to10 cm, the average clast size is about 3 to 5 cm. The conglomerate is massive and disorganized without any internal structures. However, a bed-parallel alignment of relatively coarser clasts is seen along its contact with the each brown sandstone interbeds. The brown sandstone dominates the upper half of the section and is characterized by well-developed horizontal lamination and banded texture. Bands probably consist of couplets formed by materials of different color, size and composition. The section is ended with a matrix-supported and fine-grained conglomerate unconformably overlying the lithologies descibed.

Interpretation: On the basis of its ungraded nature, lack of internal structure, disorganized fabric and clast-supported texture, the gray conglomerate may be interpreted as debris flows deposited rapidly by high concentration and viscosity flows (Johnson, 1970; Lowe, 1979 and 1982; Gloppen and Steel, 1981; Nemec and Steel, 1984). Its interbedded occurrence with the brown sandstone may indicate that the depositional site was a nearshore lake environment of the Paleo-Van as discussed below.

The fine lamination and varve-like banding in the brown sandstone may be suggestive criteria of lacustrine sedimentation. However, the alternation of this unit with the coarse gray conglomerate facies indicates that the depositional environment was intermittently high energy one, probably a transitional environment between the offshore and the shoreline, rather than a deep-water environment. The occurrence of the sand-sized material nearly exclusively in shoreline or nearshore settings of the modern lakes may support this interpretation (Sly, 1978; Picard and High, 1981). The coarse and fine clastic materials of the gray conglomerate and the brown sandstone were perhaps contributed by a river inflow or an alluvial fan into the lake where they were handled and reworked by shoreline processes and finally deposited as debris- and sheet-flow sediments. The alternation of the gray conglomerate and the brown sandstone may suggest either a series of changes in lake-level or a periodic increase in sediment contribution throughout their deposition.

3.8. Stratigraphic Section Studied Around the Değirmentaş Dere Valley

This section is measured on the coast of the lake Van, 500 m west of the Değirmentaş Dere valley (Figure 1).

3.8.1. Section-DT_1 (GPS-017, lat: 38.8662°, lon: 43.4640°, elev: 1675 masl)

Description: This section represents 5 m of lacustrine sediments, comprising a 2 m-thick yellowish gray sandstone unit sandwiched between two 1.5 m-thick gray conglomerate units (Figure 15). The conglomerates are generally poorly-sorted and composed of pebbles and occasionally cobbles and boulders. Each conglomerate unit displays a rather disorganized fabric. However an overall vertical corsening in clast size and a faint bed-parallel clast orientation are observed. The contacts of the conglomerate units with the sandstone unit appear to be sharp and nonerosional.

The yellowish gray sandstone is a fine-grained, well-laminated, banded and occasionally rippled facies, displaying an intra-formational angular unconformity along the whole length of the outcrop. The surface of the unconformity is sharp, tabular and shows no sign of erosion. With the horizontal and inclined beds above and below, it looks like a large-scale, low-angle planar cross-stratification.

Interpretation: The sediments of this section show stratigraphic and sedimentological resemblances to the sediments of the Section-HD_1 around the Hasan Dere Valley. Therefore, they may have been deposited under similar depositional conditions. The yellowish gray sandstone and gray conglomerate probably accumulated also as debris- and sheet-flow sediments in a nearshore lacustrine environment, forming a transitional zone between the offshore and

Figure 15- Section-DT_1 consists of a 2 m-thick yellowish gray sandstone unit sandwiched between two 1.5 m-thick gray conglomerate units. See figure 1 for location.

shoreline environments of the Paleo-Van. The intra-formational angular unconformity within the yellowish gray sandstone was perhaps cut by a slide (or channel erosion?) and rapidly filled by a prograding unit, leading to the large-scale horizontal to cross-stratified deposits observed.

3.9. Stratigraphic Section Measured Around the Village Çakırbey

3.9.1. Section-CB_1 (GPS-18, lat: 38.9219°, lon: 43.6089°, elev: 1676 masl)

Description: This section is located at the coast of the Lake Van, 2.6 km northeast of the Village Çakırbey (Figure 1). It is represented mainly by 20 m-thick, gravelly granulestone to coarse sandstone deposits, dipping steeply toward the west, i.e. toward the Lake Van (Figure 16). These sediments form two distinct sequences separated by a sharp erosional surface. The lower sequence consists mainly of 10 to 50 cm-thick and well-developed gravelly coarse sandstone beds with a dip of 40°. These beds are separated in places by conglomerate channels or interbeds. Conglomerate channels are up to 40 cm-thick and appear to be common in the upper slope of the dipping beds. The conglomerate interbeds are poorly- to moderately-sorted and usually clast-supported but have in places a considerable amount of sand matrix. Clasts are dominantly well-rounded to subangular and range from cobbles to small pebbles, with most averaging 2.5-3 cm in diameter. Clasts, particularly the larger and platy ones, seem to be imbricated parallel to the bedding.

The upper sequence starts at the base with a 3 m-thick, poorly-sorted and matrix-supported conglomerate and continues upward with a gravelly granulestone to coarse sandstone facies, similar to that of the lower sequence. The basal conglomerate has a sharp and erosional base and pinches out in the up-slope direction. In conformity with this pinching, the stratification in the upper sequence as a whole shows a marked down-slope divergence of bedding. The upper sequence beds have a dip angle smaller than that of the lower sequence, which results in the whole section appearing to be a large-scale single planar cross-bedding (Figure 16).

Interpretation: The facies association, facies characteristics, sedimentary structures and depositional dip (primary dipping) of the sediments in

Figure 16- Section-CB_1 is 20 m-thick and consists of gravelly granulestone to coarse sandstone, dipping steeply toward the west, i.e. toward the Lake Van, See figure 1 for location.

the Section-CB_1 indicate that they were deposited as foreset beds on the slope of a Gilbert-type fan delta developed in the Paleo-Van. The conglomerates were transported here probably by sediment gravity flows, including grain flows, debris flows or density currents. The erosional surface between the lower and the upper sequences was perhaps generated in the delta slope by a gravity-induced slump or a slide. This surface was than rapidly filled with the sediments of the prograding upper sequence units (Lewis, 1980; Lowe, 1982; Nemec and Steele, 1985; Todd, 1989; Nemec, 1990; Dorsey et al., 1995; Falk and Dorsey, 1998; Sohn, 2000; McConnico and Bassett, 2003, 2007).

3.10. Stratigraphic Section in the Ala Çay Valley

Two stratigraphic sections were measured in the Ala Çay Valley, around the Village Muradiye; one is located 870 m NW and the other one is situated 1475 m SW of the village (Figure 1).

3.10.1.Section-AC_1 (GPS-019, lat: 38.9987°, lon: 43.7593°, elev: 1706 masl)

Description: The section comprises 3.5 m of soft, friable, laminated and rippled sandstones without conglomerate. At the base, it consists of 40 cm-thick, beige to light brown and thinly-bedded to laminated coarse sandstone passing upward, through a 15 cm of rippled sandstone, into 80 cm-thick interbeded fine-grained and laminated sandstone and mudstone. Above this sandstone is a fine-grained sandstone of 80 cm thickness with common well-developed lamination and micro-cross-lamination. Then the section continues with a 70 cm of relatively darker brown cyclic deposit. This deposit is characterized by alternating 6-to 8-cm-thick layers of laminated fine sandstone and carbonate. The section ends up with 60 cm-thick sandstone with no discernable internal structure.

Interpretation: An offshore lacustrine origin for these sediments is interpreted primarily from stratigraphic, lithologic and structural considerations. Their thin-stratification, varve-like bedding, lamination, ripple-stratification, fine-grain size and the absence of pebbles may indicate deposition in the offshore lake environment of the Paleo-Van, because such depositional structures are common in central lake deposits (Picard and High, 1972).

3.10.2. Section-AC_2 (GPS-20, lat: 38.9897°, lon: 43.7467°, elev: 1681 masl)

Description: This section consists mainly of 4.5 m-thick interbedded sandstone, clayey sandstone and mudstone (Figure 17). The sandstone is generally beige to light brown and medium- to coarse-grained and forms mostly horizontal beds of 20 cm thickness. It also displays ripple structures towards the upper part of the section. The clayey sandstone is brown in color and shows a horizontal stratification with beds ranging in thickness from 15 cm to 50 cm. The mudstone is brown, laminated and contains in part thin and light-colored carbonate bands.

Interpretation: The Section-AC_2 is about 1420 m away from the Section-AC_1 to which it displays lithological similarities. The sediments exposed in the Section-AC_2 were also deposited in the offshore lake environment of the Paleo-Lake Van. The existence of appreciable amounts of mudstone in this section may further indicate that their depositional site was deeper than that of the Section AC_1.

3.11. Stratigraphic Section Measured Around the Karahan Village

3.11.1. Section-KAR_1 (GPS-021-022-023, lat: 38.9563°, lon: 43.6444°, elev: 1690 masl)

Description: This section is represented by a 4 m-thick sedimentary sequence with a flat-lying upper and inclined lower units (Figures 18 and 19). The contact between them is a sharp and erosive planar surface. The upper unit consists mainly of interbedded sandstone and conglomerate beds. Sand beds are 15 to 40 cm-thick, beige to yellowish brown, medium to coarse-grained, and moderately- to well-sorted with rare random pebbles scattered throughout the beds at the base of the section. Conglomerate beds are approximately 30 cm-thick, locally cross-bedded, well-sorted and mainly clast-supported with sub-rounded to rounded clasts. These sediments include well-preserved fresh water gastropods and mammalian bone fragments. The former is found in the sandstone beds, whereas the latter in the conglomerate beds.

The inclined lower unit is characterized mainly by 20 to 30 cm-thick and well-developed planar beds of gray granulestone to coarse sandstone, dipping at 30°-35° toward the SW, i.e. toward the Lake Van. These beds are often iron-stained and contain very small pebbles concentrated mostly on the bedding planes (Figure 19).

Interpretation: The facies associations described in this section indicate a Gilbert-type fan delta environment. The flat-lying sediments probably form subaerial to shallow-marine topset sediments. The presence of the mammalian bone fragments in the conglomerate and the well-preserved gastropods in the sandstone may be cited as evidence for this

Figure 17- Section-AC_2 consists of 4.5 m-thick interbedded sandstone, clayey sandstone and mudstone with ligh coloured, thin carbonate beds. See figure 1 for location.

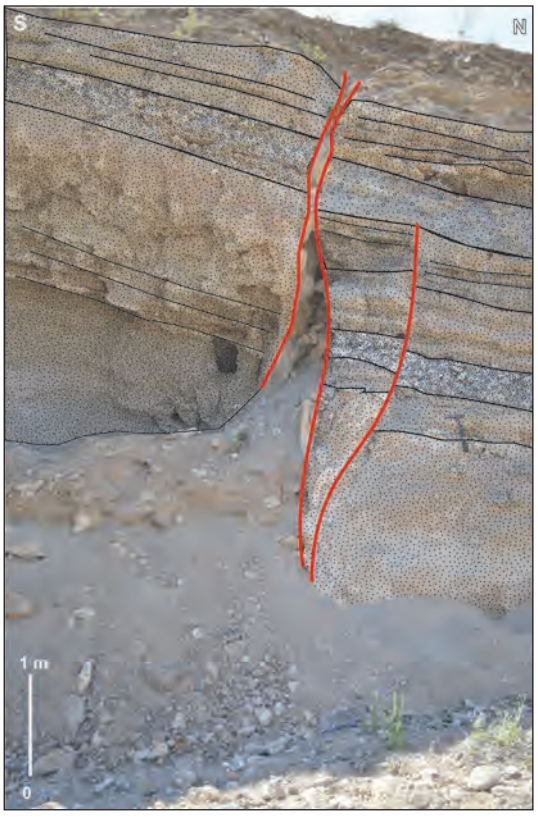

Figure 18- Section-KAR_1 is a 4 m-thick sequence consisting of a flat-lying upper unit of interbedded sandstone and conglomerate. See figure 1 for location.

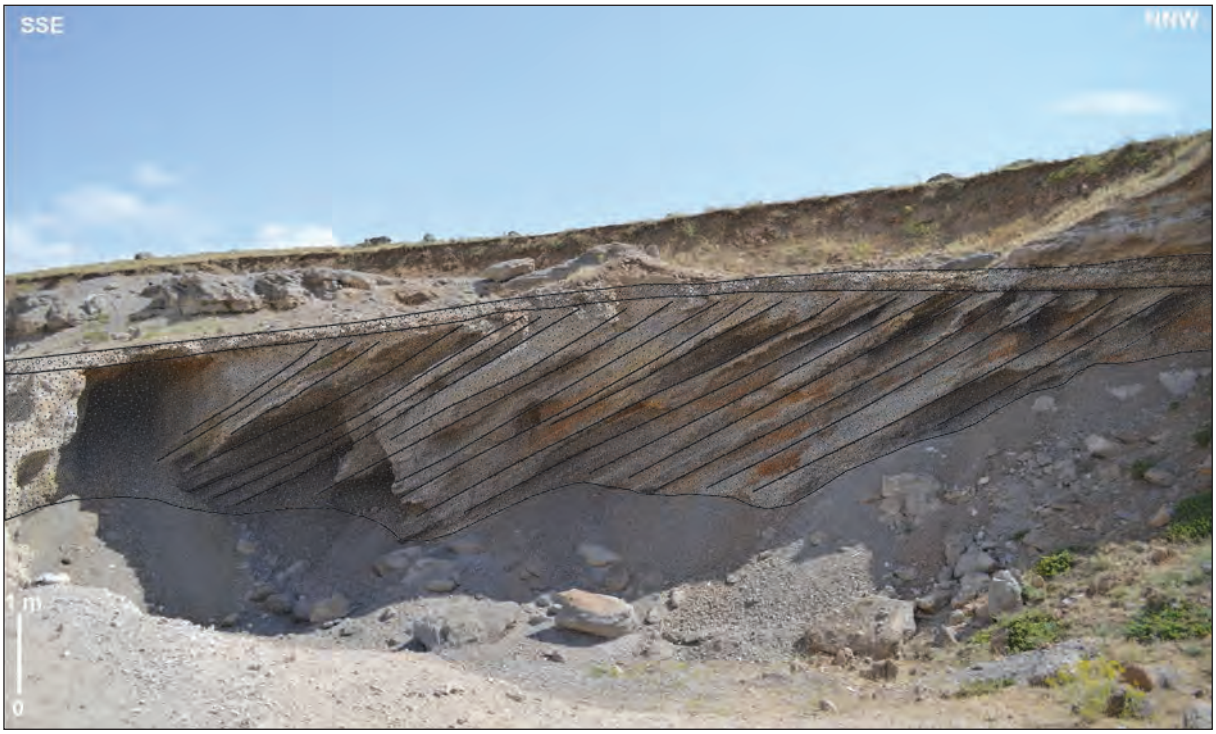

Figure 19- Inclined lower unit in Section-KAR_1, consisting of 20 to 30 cm-thick and well-developed planar beds of gray granulestone to coarse sandstone. The beds dip toward the SW, i.e. toward the Lake Van and represent the foresets of a Gilbert type delta.

interpretation. The textural properties and sedimentary structures of the conglomerate may indicate that they were deposited by a braided river and perhaps reworked later by wave processes. The underlying inclined sediments perhaps developed as the foreset beds of the delta as a result of a grain-flow process (Nemec, 1990; Nichols, 2009). The stratigraphic relation of the flat-lying and the inclined sediments suggest that the delta was prograding into the lake as a result of either a drop in lake-level or an increase in the rate of sediment supply.

Age of the Karahan Village Terrace deposits: The Gilbert fan delta sequence was dated to be between 25.7 and 24.9 ka BP in the area (in Kırklar) by Kuzucuoğlu et al. (2010), using radiocarbon analysis of organic matter (Table 1). The level of this dated terrace is 1693 m, about 45 m above the present lake level.

3.12. Stratigraphic Section Measured in the Deliçay Valley

3.12.1. Section-DV$_1$ (GPS-24-25, lat: 39.0095°, lon: 43.4467°, elev: 1678 masl)

Description: The section displays throughout its 5 m thickness a yellowish brown, very finely-bedded to laminated very fine-to fine-grained sandstone in part with common symmetrical wave-ripple cross-lamination (Figure 20). In the lower part of the section, the sandstone is interbedded with white siltstone beds (10 cm), rich in microcrystalline carbonate. In the upper part of the section, there is a syndepositional deformation zone marked by convoluted and deformed sandstone laminations, varying in thickness from 30 cm to 90 cm.

Interpretation: The association of the following characteristics indicates that these sediments were deposited in the offshore of the Lake Paleo-Van: very fine bedding, lamination, fine texture, symmetrical wave-ripple cross-lamination, convolute-bedding and deformed laminations. Very fine bedding, lamination and fine grain size may suggest accumulation in a quiet standing water, below the wave-base. The common symmetrical wave-ripple cross-lamination may indicate that oscillatory flows existed in the environment. The convoluted and disturbed sandstone layers probably originated from soft-sediment deformation that may have been induced by seismic liquefaction and/or fluidization (Seilacher, 1969; Moretti et al., 2002).

Figure 20- Section-DV$_1$ includes 5 m thick yellowish brown, very finely-bedded to laminated, very fine-to fine-grained sandstone with symmetrical wave-ripple cross-lamination. For location see figure 1.

3.12.2. Section-DV_2 (GPS-026, lat: 39.0139°, lon: 43.4383°, elev: 1705 masl)

Description: This section is represented by ca. 5 m-thick yellow to yellowish brown very fine-grained to fine-grained sandstone with rare brown mudstone interbeds. Bed thickness is variable, ranging from 10 to 20 cm. Bed contacts are sharp. The beds display internal horizontal lamination, wavy lamination and micro cross-lamination. The sandstone displays in various levels, some soft-sediment deformational structures. Individual horizons are 25-30 cm-thick and laterally continuous for tens of metres. They are overlain and underlain by undeformed horizontal beds. The deformational structures in these flat-lying beds mostly include overturned folds (Figure 21).

Interpretation: This section probably represents the offshore lacustrine environment of the Paleo-Van. These sediments were deposited from suspension of fine-grained sediments with minor bedload influence. The occurrence of the soft-sediment deformational structures may be attributed to liquefaction and fludization induced by earthquake shock in the seismically active Lake Paleo-Van Basin.

3.13. Stratigraphic Section Measured in the Zilan Valley

3.13.1. Section-ZV_1 (GPS-028, lat: 39.0135°, lon: 43.3124°, elev: 1667 masl)

Description: This section represents a sedimentary succession, comprising 15 m thick mudstone in the lower and 10 m thick sandstone in the upper part. The mudstone is mainly dark greenish gray in color and displays well-developed horizontal lamination formed from greenish gray and brown silt- or claystone laminae.

The sandstone overlies the mudstone with a sharp and erosional contact. It is beige to brown, thinly- to medium-bedded, locally rippled and medium- to coarse-grained with some large-scale lenticular cross-bedding, dipping to the S.

Interpretation: The laminated mudstone indicates deposition in a low energy subaqueous depositional environment. It was perhaps deposited rhythmically from suspension due to absence of wave activity. It accumulated most probably in the relatively deep offshore environment of the Paleo-Van.

Figure 21- 31 Section-DV_2 (GPS-026) locally shows soft-sediment deformational structures, which also include overturned folds. See figure 1 for location.

Stratigraphic and sedimentological features of the sandstone may suggest that it was perhaps a distal distributary mouth bar formed near the lakeward limit of a deltaic distributary channel. The large-scale lenticular beddings in this facies may be interpreted as channelizing and scouring events. The progradation of the delta across the lake-floor of the Paleo-Van resulted probably in this coarsening-up section.

3.13.2. Section-ZV_2 (GPS-29-30, lat: 39.0253°, lon: 43.3111°, elev: 1694 masl)

Description: The section starts at the base with gray, thinly-bedded to laminated, coarse- to medium-grained and well-sorted sandstone and pebbly sandstone with a primary dipping of 30° to 40° toward the east (Figure 22). These sandstones are about 8 m-thick and pass upward abruptly into 3 m-thick, horizontally-bedded to laminated gray to brown sandstone, including thin (10-15 cm) interbeds of fine conglomerate. However, towards the top of the section, the thickness of the conglomerate beds increases (up to 60 cm). Both the inclined and the horizontal sandstone and conglomerate beds are cut by a large- scale slide or a channel filled with large-scale horizontal to cross-stratified gray sandstone, displaying internal lamination (Figure 22). The slide or channel deposits are also overlain by the horizontal beds.

Interpretation: This section is a typical succession of a Gilbert-type delta. The inclined sandstones represent foreset beds, whereas the horizontally layered sandstone and interbedded conglomerate may characterize the topset beds. The presence of large-scale channel or slide deposits toward the top of this section suggests that subaqueous slumping and downslope mass movement of sediments were taking place in the delta front environment. The slide surface appears to have been filled by the prograding deltaic sediments.

3.14. Stratigraphic Section Measured in the western part of the Kaş Burnu

3.14.1. Section-KB_1 (GPS-031, lat: 38.9710°, lon: 43.2719°, elev: 1727 masl)

Description: This section is of 7 m thick, consisting of pumice and sandstones (Figure 23). Pumice is seen in the lower part of the section and is

Figure 22- Section-ZV_2 in Zilan Valley, consisting of 8 m thick, gray, thinly bedded and laminated sandstone with eastward dips of 30° to 40° at the base, 3 m thick horizontally bedded and laminated sandstones in the middle, and large scale slide and channel sandstone and conglomerates on top, which are themselves covered by horizontally bedded sandstones. See figure 1 for location.

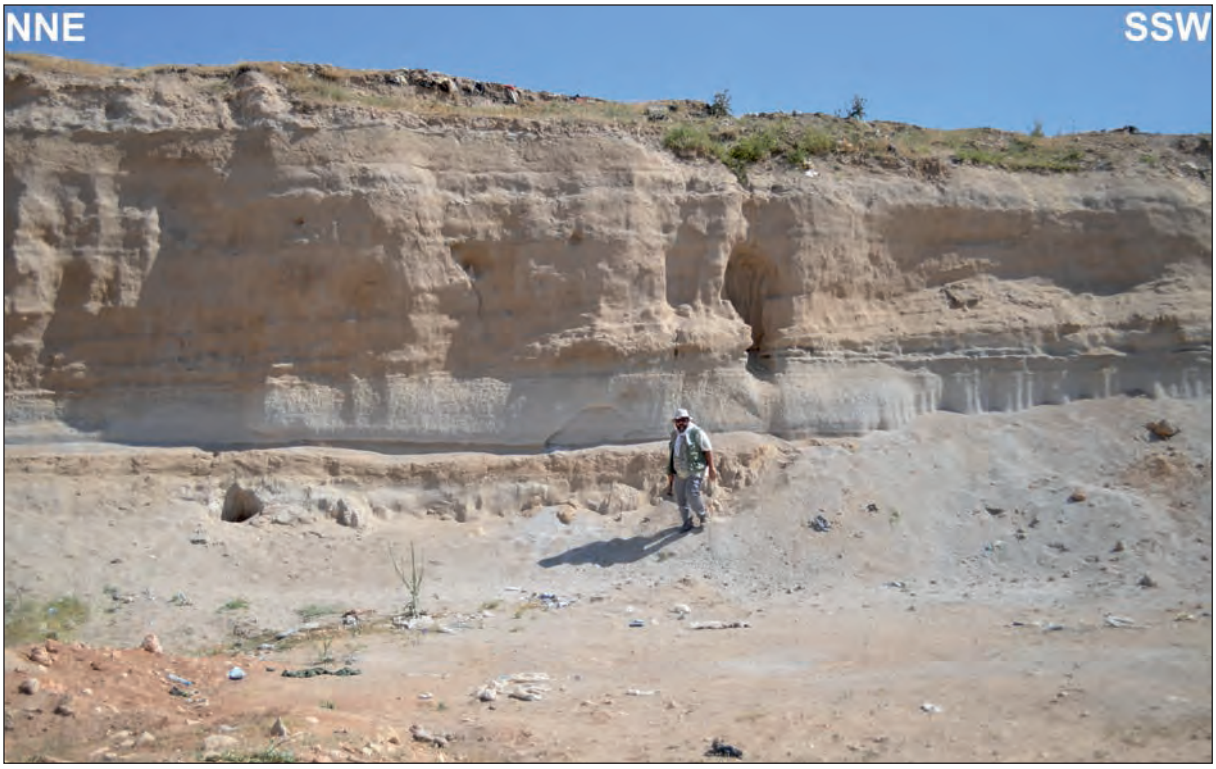

Figure 23- Section-KB_1 consisting of 2 m-thick pumice in the lower and 5 m-thick horizontally bedded sandstones in the upper part. See figure 1 for location.

characterized by highly vesicular texture without any apparent phenocrysts. It displays alternating white and dark gray laminae and bands. This 2 m-thick pumice is overlain conformably by 5 m-thick, light brown to beige and coarse-grained sandstone, passing upward into relatively finer-grained sandstone.

Interpretation: The finely banded and laminated texture of the pumice and the conformably overlying sandstones may indicate that they accumulated perhaps in a low-energy subaqueaous lake environment of the Paleo-Van. This major pumice deposit may probably correspond to the Nemrut Formation dated between 33.7 and 28.6 ka BP by Sumita and Schmincke et al. (2013*a*, *b*).

3.15. Stratigraphic Section Measured in the Kumlu Dere Valley

This section is located at the coast of the Lake Van, 500 m west of the Kumlu Dere Valley.

3.15.1. Section-KD_1 (GPS-032, lat: 38.9442°, lon: 43.1628°, elev: 1667 masl)

Description: This 15 m-thick section displays an intricately intermingled white to beige conglomerate and sandstone that are cut in places by low-angle erosional surfaces. The conglomerate is clast-supported with coarse, well-rounded and poorly-sorted clasts derived probably from a single source, namely the Adilcevaz Limestone forming the basement rock in the area. The sandstone is fine- to medium-grained and thinly-bedded to laminated. It forms a number of levels in the section either interfingering or alternating with the conglomerate with various thicknesses.

Interpretation: The poorly-sorted but clast-supported texture of the conglomerate with relatively well-rounded pebbles and boulders indicate that this sediment was deposited by currents of high water discharge and sediment concentration. The well-rounded clasts suggest that the transportation in these currents was mainly in traction mode. Thin bedding and lamination of the sandstone may indicate a relatively low energy depositional environment for this fine clastic rock. This environment seems to be a distal part of an alluvial fan extending into the lake. However, their complex contact relation suggests that both lithological units were deposited in an area adjacent to a steep relief from where streams flowed down the steep slopes, transporting the coarse conglomerate onto an alluvial fan that prograde into the Lake Paleo-Van.

3.16. Stratigraphic Section Measured around the Çayır Mahallesi, Adilcevaz

3.16.1. Section-CM_1 (GPS-034, lat: 38.7911°, lon: 42.7881°, elev: 1676 masl)

Description: The section is located on the coast of the lake, 2 km east of the Çayır Mahallesi. It commences with 2 m of gray pumice, passing upward, through a 40 cm-thick brown mudstone, into a 4 m-thick white travertine. In the mudstone, a faint lamination is observable. The travertine is coarsely crystalline limestone displaying abundant cavities of various sizes.

Interpretation: This gray pumice originated by eruption of most probably the Nemrut Volcano and deposited as airfall deposit in the Paleo-Lake Van. Deposition of this tephra unit was followed by the laminated brown mudstone. The travertine may have formed around a spring at the lake margin.

3.17. Stratigraphic Section Measured in the Easten Margin of the Kara Dere Valley

3.17.1. Section-KRD_1 (GPS-027, lat: 38.8055°, lon: 42.7571°, elev: 1697 masl)

Description: This section is about 20 m-thick, comprising in its lower half gray pebbly sandstone, showing very fine horizontal bedding and lamination (Figure 24). The pebbles are commonly small and rounded. Toward the top of the section, the gray pebbly sandstone starts to alternate with brown sandstone that dominates the upper half of the sequence together with interbedded light-gray, well-rounded pebble and cobble conglomerate and pebbly sandstone. The brown sandstone is hard, wave-rippled and forms protruding horizontal beds with sharp boundaries. Wave ripple-marks commonly occur in this sediment. The interbedded conglomerate and pebbly sandstone occur as continuous and discontinuous units of 0.1 m to 1.5 m thick with horizontal and planar cross-bedding. The dip of cross-beds is towards SSW. The sequence often displays in its various levels several large-scale erosional surfaces marked by iron oxide staining.

Interpretation: These sediments probably belonged to a nearshore setting of the Paleo-Van. Sheet flow currents, operating in the shoreface to nearshore environments, perhaps deposited the gray, horizontally layered pebbly sandstone and conglomerate. The brown sandstone was probably deposited in relatively in the deeper waters of the lake as indicated by its texture, lamination and wave ripples. The large-scale erosional surfaces or scars were perhaps made by slides and slumps caused by high sedimentation loading or storm.

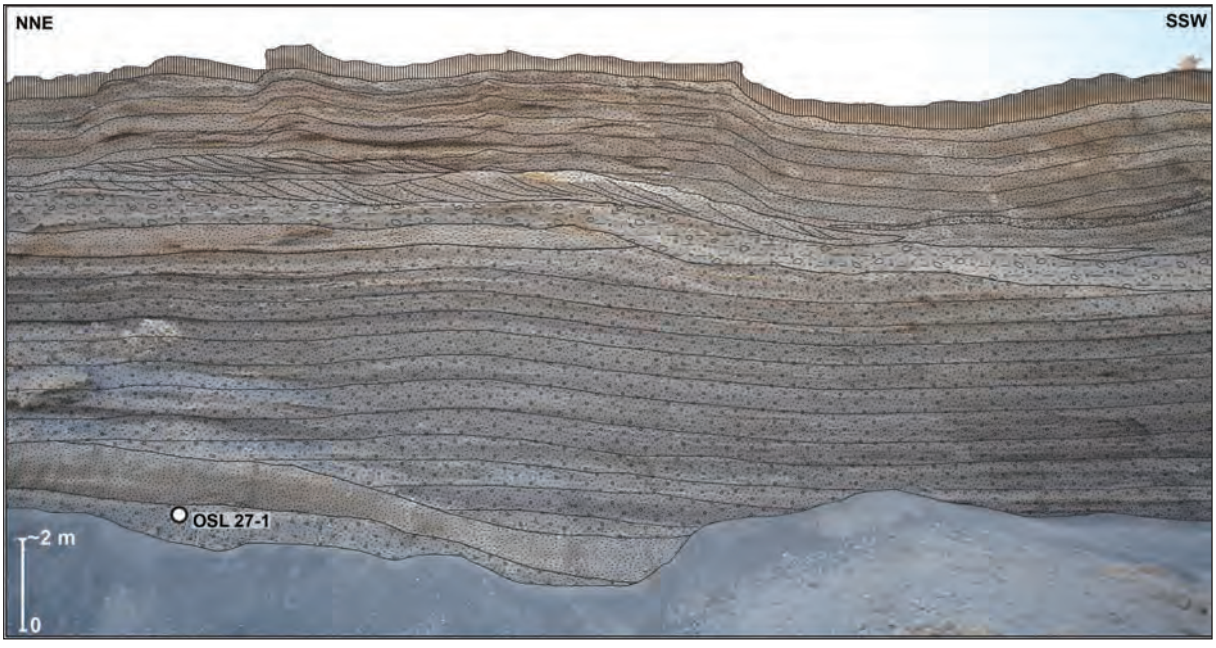

Figure 24- The 20 m thick section-KRD_1 (GPS-027) in Kara Dere consists of horizontal bedded and laminated pebbly sandstone in the lower part and interbedded brown pebbly sandstone and conglomerate in the upper part. See figure 1 for location.

3.18. Stratigraphic Section Measured in the Evren Deresi Valley

3.18.1. Section-ED_1 (GPS-044, lat: 38.7981°, lon: 42.715°1, elev: 1683 masl)

Description: This section consists of 2 m thick sandstone in its lower and 3 m thick conglomerate in its upper part (Figure 25). The contact between these lithological units is sharp and planar. The sandstone is gray and medium- grained with thin horizontal bedding and lamination. These sedimentary structures are well-marked by their colours, displaying different shades of gray. The overlying conglomerate is brownish red in colour and show horizontal bedding. It consists of poorly to moderately sorted pebbles and local cobbles. Individual conglomerate beds mostly display a disorganized fabric, although some of them locally show bedding plane-parallel clast orientation.

Interpretation: The gray sandstone, with its thin horizontal bedding and lamination, may represent the relatively deep part of Paleo-Lake Van. The unconformably overlaying conglomerate may be interpreted as indicative of fluvial deposition. This conglomerate is certainly a product of a powerful stream. Its poor to moderate sorting lack of fossils and sheet-like or tabular beds with sharp, planar and non-erosional base support this interpretation. It probably represents accretion and migration of longitudinal bars of a braided stream (Rust, 1972), flowing into the lake.

3.19. Stratigraphic Sections Measured Around the Ziyaret Dere Valley

Two sections were measured in this area. First one (ZD_1) is 1 km to the east of the valley, whereas the second one (ZD_2) is 500 m to the west of the walley.

3.19.1. Section-ZD_1 (GPS-042, lat: 38.7846°, lon: 42.6814°, elev: 1673 masl)

Description: The section is characterized by a 20 m-thick succession of conglomerates and sandstones; the former predominate over the latter. Conglomerates occur in both the lower and the upper parts of the succession. The lower conglomerate is more than 10 m-thick, massive to poorly-bedded,

Figure 25- Section-ED_1 (GPS-044) in Evren Deresi Valley consists of 2 m thick sandstone in its lower and 3 m thick conglomerate in its upper part. Note the sharp and lanar contact between these units.

generally poorly-sorted and devoid of fossils (Figure 26). It is clast-supported and does not display any noticeable sedimentary structures. Its clasts are angular to subrounded and dominantly in pebble size. In the SE end of the section, it passes upward across a sharp and planar contact into 3.5 m-thick, gray, fine-to medium-grained and thinly-bedded to laminated sandstone (Figure 26). Toward the NE end of the section, this sandstone changes in colour to brown with similar lithological features. The brown sandstone forms here a large-scale channel structure (Figure 27). It is then succeeded by a conglomerate unit, forming the upper part of the section. This upper conglomerate is 3 m-thick, comperatively finer-grained and matrix-supported with inclined primary strata terminating on the horizontal beds of the brown sandstone, thus forming a downlap contact with this unit (Figure 27).

Interpretation: The lower conglomerate was probably deposited in an alluvial fan environment. Poor sorting, clast shapes and absence of fossil and bedding are all features of such depositional environment. The finely-bedded to laminated brown and gray sandstones probably represent the bottomset beds of a fan delta. The foreset beds are represented by the upper conglomerate, which were built out over the brown sandstone as the delta prograded. The deposition of the upper conglomerate perhaps occurred by debris flows as suggested by its poorly-sorted gravel in a sandy matrix (Namec, 1990). The sharp contact between the lower conglomerate and the overlying sediment is a disconformity, indicating that the delta setting developed over the alluvial fan when the lake level rose and lake waters inundated the marginal areas of the basin where alluvial fans were forming.

3.19.2. Section-ZD_2 (GPS-043, lat: 38.7885°, lon: 42.6724°, elev: 1666 masl)

Description: The section is composed mainly of 3.5 m-thick brown sandstone in the lower half and about 1.5 m-thick yellow and clayey sandstone in the upper half of the section. The brown sandstone is generally fine-grained and silty in part, containing thin (less than 15 cm) interbeds of conglomerate and coarse sandstone. It is characterized by well-developed horizontal laminae. The upper yellow sandstone conformably overlies the brown sandstone and displays striking syndepositional deformational

Figure 26- Section-ZD_1 (GPS-042) in Ziyaret Dere Valley consists of 20 m-thick succession of conglomerates and sandstones. Conglomerates occur in both the lower and the upper parts of the succession. See figure 1 for location.

Figure 27- 3 m thick upper conglomerate beds in upper part of Section-ZD_1 (GPS-042) in Ziyaret Dere forming a downlap contact with brown sandstone unit. See figure 1 for location.

structures, such as convolute lamination and flame structures.

Interpretation: The well-laminated brown sandstone facies may have accumulated on the lake-floor environment of the Paleo-Lake Van, not far away from the shoreline. The presence of conglomerate and coarse sandstone interbeds between this sandstone may indicate that this part of the lake was occasionally being fed by currents carrying coarse sediments from the shoreline. The yellow sandstone was also offshore lake sediment, which was most probably disturbed and deformed by seismic shaking.

3.20. Stratigraphic sections measured in the Kumlu Dere Valley at Soğanlı Village

3.20.1. Section-KDS_1 (GPS-040-41, lat: 38.7931°, lon: 42.6120°, elev: 1693 masl)

Description: This section is very similar to the Section-ZD_2 both in composition and stratigraphy. Its lower part consists of about 20 m of brown and coarse sandstone, in part with conglomerate and pebbly sandstone. The sandstone shows well-developed and laterally continuous lamination. It is overlain by 3 m-thick brownish sandstone, showing a large-scale convolute-bedding (Figure 28).

Interpretation: As stated in the interpretation of the previous section ZD_2, the laminated brown sandstone accumulated in the low-energy environment of the Paleo-Lake Van-floor and was severely deformed probably by seismic waves.

3.21. Stratigraphic Section Measured Around Ceviz Dere Valley

3.21.1. Section-CZ_1 (GPS-039, lat: 38.7724°, lon: 42.5861°, elev: 1663 m)

Description: This section was studied on the shoreline of the Lake Van, 150 m west of the Ceviz Dere. It is a 4 m-thick section, commencing with planar cross-bedded coarse sandstone overlain by a thin conglomerate bed. Above comes 2.5 m-thick, horizontally- bedded and dominantly brown mudstone to muddy sandstone, passing upward into coarse and pebbly sandstone.

Interpretation: The facies association of this section indicates that these sediments probably

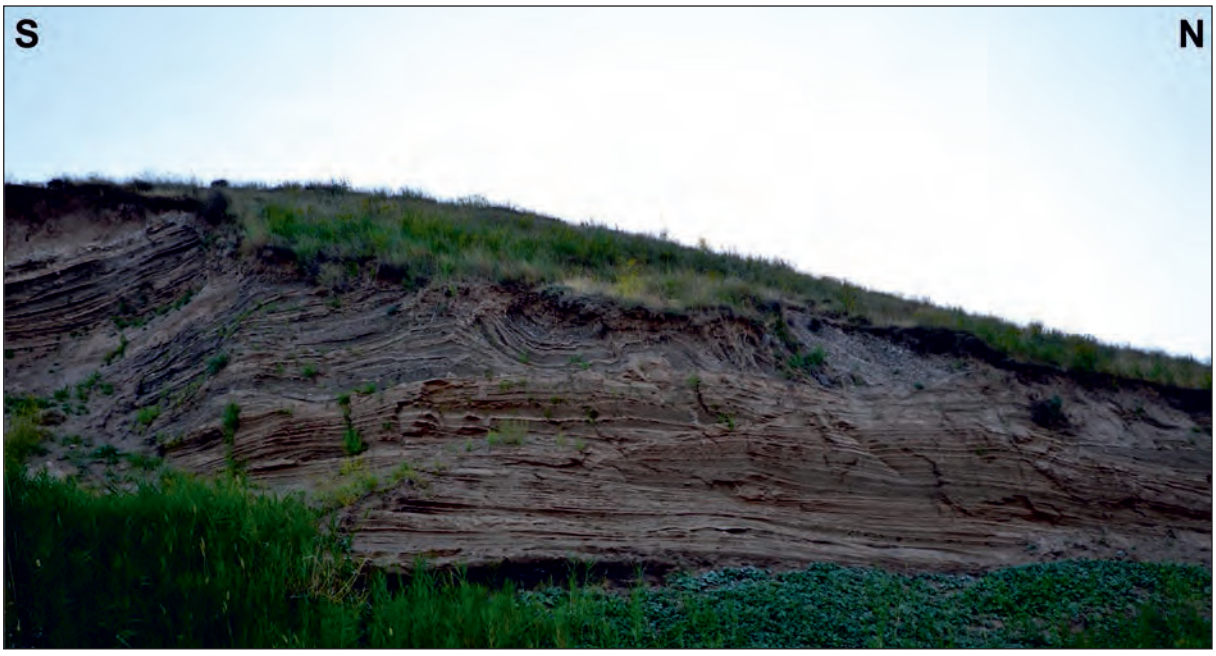

Figure 28- Section-KDS$_1$ (GPS-040-41) in Kumlu Dere Valley, Soğanlı Village, showing a large-scale convolute-bedding in brown sandstone. For location see figure 1.

accumulated in the nearshore environment of the Paleo-Lake Van. The cross-bedded sandstone and the overlyin conglomerate probably represent the foreshore to shoreface environments of a beach along the lake. The overlying brown mudstone and muddy sandstone were deposited nearshore environment during a rise in the water level of oscillating Lake Van.

3.22. Stratigraphic Section Measured Around Karmuç Çayı Valley

3.22.1. Section-KC$_1$ (GPS-038, lat: 38.7122°, lon: 42.4242°, elev: 1660 masl)

Description: This section is measured near the shore of the Lake Van, 850 m west of the Karmuç Valley. It is of 17 m thick and characterized by yellowish gray sandstone, including interbeds of conglomerate in various levels. The sandstone is fine-grained, horizontally-laminated and wave-rippled in part with low-angle large-scale cross-stratification. It forms a thick and distinct unit in the upper part of the section. The interbedded conglomerates are planar cross-stratified, with well-rounded pebble size grains and commonly erosional basis.

Interpretation: These sediments were probably deposited in the nearshore environment, forming a transitional zone between the offshore and the shoreline of the Paleo-Lake Van. Their low-angle cross-stratification and wave ripple-marks suggest wave-agitation in this environment. The cross-bedded conglomerates with erosional basis may indicate coarse-grained sediment influx by various currents from the shoreline. The thick occurrence of the laminated sandstone towards the top of the section suggest deepening of the lake.

3.23. Stratigraphic Section Measured in the Kotum Dere Valley

3.23.1. Section-KOD$_1$ (GPS-035, lat: 38.4757°, lon: 42.3091°, elev: 1656 masl)

Description: The section is made up of 8 m-thick, yellow and thinly-bedded to laminated travertine in its lower part and a succession of yellowish gray siliciclastic sediments in its upper part. The contact between these two facies associations is sharp and marked by a thin (15 cm) basal conglomerate. The siliciclastic sediments are characterized by finely-bedded to laminated and locally cross-bedded sandstone in part with conglomerate interbeds (Figure 29). The cross-beds dip to the NE, i.e. toward the modern Lake Van.

Interpretation: The travertine constitutes the stratigraphic basement in the area. The laterally continuous layering and lamination of this unit may indicate that it formed in the littoral environment of

Figure 29- Section-KOD_1 (GPS-035) in lower Kotum Dere Valley consists of 8 m-thick, yellow and thinly-bedded to laminated travertine in its lower part and yellow gray, finely-bedded to laminated sandstone with conglomerate interbeds in the upper part. A 15 cm thick basal conglomerate marks the base of the sandstone unit above the travertine. For location see figure 1.

the paleo-lake where the subaqueous vegetation favoured the precipitation of the travertine. Regional considerations and sedimentary structures of the upper clastic succession suggest a nearshore lake environment for these sediments.

3.23.2. Section-KOD_2 (GPS-037, lat: 38.4721°, lon: 42.3095°, elev: 1670 masl)

Description: The section comprises various sandstone facies, sitting on a travertine above a disconformity. The sandstone at the base is 1.5 m-thick, silty and fine-grained. It is followed upwards by a 1 m-thick polygenic conglomerate with an erosional base. The conglomerate forms a lensoidal horizon, parallel to the bedding above and below. It is overlain by 3.5 m thick brown and medium-bedded to laminated sandstone, with local slump structures or convolute beddings sandwiched between horizontally-bedded to laminated sediments (Figure 30). Large-scale slide surfaces are also seen in the section.

Interpretation: Facies characteristics and their comparison with the similar facies of the sections described elsewhere around the Lake Van suggest that these sandstones and the associated conglomerate accumulated in a nearshore lake environment of the Paleo-Van. Horizontal thin bedding, lamination and convolute bedding within the sandstone all support this interpretation. The conglomerate was perhaps transported into the lake by traction currents from the shore. The large-scale sliding surfaces indicate rapidly prograding sediments on an unstable slope.

Age of Kotum Vallley terraces: The travertine underlying the terraces in the Kotum Valley have been dated at 102 ka BP by Kuzucuoğlu et al. (2010), using $^{230}Th/^{234}U$ method (Table 1), Elsewhere in the Kotum Valley the terraces are underlain by 4 m thick pumice fall, in which feldspars yielded an age of 117±5.2 ka BP, using $^{39}Ar/^{40}Ar$ method (Mouralis et al., 2010) (Table 1). Therefore, the two terrace sections described in the lower Kotum Valley in this study are younger than about 100 ka BP. According to Kuzucuoğlu et al. (2010), these terraces reach levels of 1730-1735 masl (ca. 85 m above the present lake level).

Figure 30- Section-KOD_2 (GPS-037) in the upper Kotum Dere Valley, showing slump structures and convolute beddings sandwiched between horizontally-bedded to laminated sandstone in the upper part of the section. For location see figure 1.

4. Discussion

4.1. Reconstruction of Depositional Environments: Tectono-Stratigraphic Evolution of the Lake Van Basin

Before reconstructing the interpreted depositonal environments and their paleogeographic distribution in the Lake Van Basin, we list the features common to all the studied terrace sections below:

Sections are commonly thin, ranging in thickness between 3 and 25 m. Relatively thick sections (i.e. more than 15 m) are found in the valleys situated to the north and west of Lake Van. They are generally regressive in nature, showing upward shallowing and coarsening sequences.

The sections do not show a distinct large-scale cyclicity characterized by packages of alternating well-developed upward-fining and –coarsening sequences separated by erosional contacts. Instead, relatively small-scale lateral and vertical facies changes or interfingerings are observed in the marginal lake sediments.

Terrace sediments consist predominantly of terrigenous clastic material with limited lithological diversity. Sandstone and conglomerate are the predominant lithologies throughout the sections. Distinct carbonate units exist as travertine or tufa in a few sections and mostly constituting the stratigraphic basement of the terrace sections where observed. No evaporites or other chemical sediments are found in the study area.

Terrace sediments hardly contain any biota. The fauna occasionally found in these deposits includes usually fresh-water gastropods and bivalves (*Dreissena* sp.).

The terraces around the Lake Van are mostly made up of clastic sediments accumulated in various lake-related depositional environments, including alluvial fan/braided river, beach, delta, nearshore and offshore. These depositional environments are characterized by distinct physical, chemical and biological conditions, including the fauna and flora, geology, geomorphology, climate, and, for subaqueous environments, the depth, temperature, salinity, and current and wave regimes. Therefore, if

the variability of the depositional environments of the terrace sediments, based on facies changes, are discussed with emphasis on these conditions, it may be possible to enlighten, to a certain extent, the local tectonics and the climate prevailed in the Paleo-Lake Van basin during its geological history. In the following paragraphs, we make such an attempt to deal mainly with the depositional conditions of the sedimentary environments in the Paleo-Lake Van basin.

4.1.1. Alluvial Fan/Braided River Environment

The alluvial fan/braided river sediments are recognized in the Sections-KV_1, KV_2, MB_1, KD_1, ED_1 and ZD_1. Although they are not significant in the basin in terms of volume, they are important because their deposition is sensitive to tectonic and climatic controls. They imply vertical tectonic activity during or immediately prior to their deposition. The sections-KV1, KV2 and MB1 are measured in the Karasu Valley and Munisinbahçe locality (around Mollakasım) (Figure 1). These areas are located just to the N and NW of the Çomaklıbaba Mountain that is bounded from north and south by active thrust faults. It is quite possible that these faults uplifted the Çomaklıbaba mountainous area that provided debris and increased stream competence to accumulate the terrace deposits. Of course, these alluvial fans/braided rivers may have also developed due to base-level lowering, as in the case where the River Karasu has eroded its floor at a more rapid rate than its tributary streams have (Carryer, 1966; Bull, 1972). The other three sections (KD_1, ED_1 and ZD_1) are situated in the northern margin of the Lake Van where the NE-SW striking strike-slip faults occur in the adjacent high areas (Figure 1). These faults may have created uplift in the catchment areas which provided sediments to the alluvial fans/braided rivers, reaching to the Lake Paleo-Van. This interpretation is supported by the geology of the region as discussed in Section 2.1. This basin lies in the center of a dome structure underlain by the thinnest crust in the eastern Turkey. It has been rising since the closure of the Bitlis Ocean in the medial Miocene with the development of significant strike- and dip-slip faults, resulting in a topographic differentiation in the region (Şengör et al., 1985, 2008).

Most of the modern alluvial fans occur in arid or semi-arid regions (Bull, 1972; Blair and McPherson 1994). Perhaps, the Lake Paleo-Van also had arid climate during the formation of the alluvial fans/braided rivers recognized in the terraces. However, the well-bedded and clast-supported coarse conglomerates of the alluvial fans in the area studied indicate that they were deposited by sheet flood processes under wet conditions (Harvey et al., 2005). This may suggest that there was enough water supply in the Lake Paleo-Van Basin to the mainstream channels leading towards the fans. The water source may be the rainfall over the entire basin or snowmelt runoff from all or part of the basin during the warm and wet interstadials.

4.1.2. Beach Environment

The beach deposits are best seen in the Dönemeç Çayı (Section-$DÖN_2$), Karasu (Section-KV_2) and Boğaz Dere (Section-BD_1) Valleys that are bounded by high terains with many distributary streams, extending down to the main valleys. The existence of the beach deposits in these areas indicates that these valleys were once invaded by the Lake Paleo-Van and the water level of the lake was 60 to 85 m higher than the present lake level (1648 m asl). It seems that the Streams Dönemeç Çayı, Boğaz Dere, Karasu and their distributary creeks transported abundant detritus to the lake where they were handled and reworked by shoreline processes in some parts of the valleys. The beaches developed along the skirts of the adjacent highs and therefore they were probably narrow and limited in spatial distribution. The narrowness of the beaches and their rapid sideward or upward passages into finer-grained nearshore lake or coarser-grained alluvial fan/braided river sediments may have been resulted from the reduced wave activity and lack of tidal effects in the Paleo-Lake Van. However, the wave energy on the beaches was high enough to rework and accumulate the well-sorted, –rounded and cross-rippled sandstones in part with conglomerates in these environments. These sediments were perhaps shaped under the effects of wave swash-backwash along the beaches.

The beach deposits clarly mark lake level and therefore their occurrence at various elevations, such as 1708 m asl (Section-$DÖN_2$), 1733 m asl (Section-BD_1) and 1736 m asl (Section-KV_2) indicates that the lake-level was much higher and variable in the past. The absence of large-scale cyclicity in the studied terraces suggest that the lake level changes do not appear to represent great fluctuations in water depth of the Lake Van. It rather show a an apparent gradual drop in water level from 1755 masl at ~125 ka BP to its modern level at 1647 m, as suggested by the younging ages of the shoreline facies with decreasing elevation. However, considering the closed nature of

the Lake Van, the intensive late Quaternary volcanism and active tectonics of the area, it is most likely that Lake Van has been subjected to significant lake level fluctuations under the influence of climatic, tectonic and volcanic processes (e.g., see Sumita and Schmincke, 2013*a, b*). The effect of the climate on the lake-level was through evaporation-precipitation balance. The Lake Van level was generally higher during interglacial and interstadials than that during glacial and stadials, according to the sedimentological, palynological and isotopic evidence from the sediments cored within the lake (Çağatay et al., 2014, Stockhecke et al., 2104; Litt et al., 2014). As discussed in Section 2.1, the Lake Van Basin and the surrounding areas have been subjected to convergent tectonics since the medial Miocene. Owing to this tectonics, the marginal lake facies or terraces may have been uplifted gradually to upper elevations. During the formation of the marginal lake facies, the climate was probably drier, providing suitable conditions for excessive evaporation. These circumstances during the stadials may have resulted in a gradual fall in the water level, leading to the contraction of the lake. As the lake shoreline shifted towards the basin center, its margins were exposed gradually to subaerial conditons where the weathering and erosional processes modified the sediments. This development increased the sediment supply and the sediments thus provided were deposited at the margins as beach and delta deposits during the fall in water level.

4.1.3. Delta Environment

Gilbert-type delta deposits mostly occur in the eastern margin of the Paleo-Van and they are best observed in the Dönemeç Valley (Sections-$DÖN_3$), Karasu Valley (Section-KV_3), Çakırbey Village (Section-CB_1), Karahan Village (Section-KAR_1), Zilan Valley (Section- ZV_2) and the Ziyaret Dere Valley (Section-ZD_1). Their concentration along this gradually rising margin is not surprising, because this type of coarse-grained deltas usually form where high sediment supply, high water flux and steep basin margin are available (Postma, 1990; Çukur et al., 2013). As mentioned in the discussion of the beach environment above, the uplift of the eastern margin created steep topography to supply coarse-grained sediments, while the dropping lake-level caused the marginal streams to downcut to new base levels and carried the detritus to deposit the prograding Gilbert-type deltas. During this time, with high erosion rates due to low vegetation cover, the climate was perhaps the major factor enhancing the sediment supply and runoff, despite the glacial conditions prevailed in the area as suggested by the ages of these sediments. Glaciers probably played an important role in streamflow régimes with the release of their meltwaters perhaps during the interstadials of Late Glacial period. Recent studies on borehole stratigraphic secions recovered by the PaleoVan project of the International Continental Drilling Program (ICDP) shows that increased snow precipitation and meltwater delivery to Lake Van during the Late Glacial (Çağatay et al., 2014; Kwiecien et al., 2014).

A Gilbert-type delta environment usually has low energy with limited water agitation. In this environment, fluvial processes predominate over the wind-induced wave and currents. Therefore, the distribution of the Gilbert-type deltas in the Lake Paleo-Van Basin may suggest that the eastern margin of this lake was a low-energy coast sheltered from winds. Probably the prevailing wind was perhaps blowing either from the north or south and thus not affecting much the eastern shore. The Gilbert-type deltas may also provide evidence for the depth of the Lake Paleo-Van, because the lake water level determined the heights of the foreset. Considering the heights of the foresets, its depth perhaps did not exceed few tens of metres where the deltas formed.

4.1.4. Nearshore Lake Environment

This environment was recognized in the Sections-CV_1, -HD_1, -DT_1, -KRD_1, –KC_1 and KOD. It formed a transitional zone between the beach and the offshore lake environments. Sandstones with subordinate conglomerates are the dominant facies. The presence of these sediments requires a physical mechanism capable of transporting them to the environment, because transitional zone environments are generally below the wave-base and mostly accumulate finer-grained sediments. The existence of coarser-grained sediments in this environment is mostly resulted from deposition during heavy storms. In the stormy weathers, much coarse-grained sediments are eroded from beaches and are brought to transitional zones. This was perhaps the case along the Plaeo-Lake Van shores where storms were apparently active during the deposition of the nearshore sediments. The relatively coarse-grained sediments of the aluvial fans, beaches and the Gilbert-type deltas along the lake coast acted during storms as sources for these sediments. The subordinate conglomerates were laid down in the vicinity of the

stream mouths, whereas the sandstones and minor amounts of mudstones with wave ripples and very fine parallel laminations may have been spread out farther to the deeper waters where relatively finer grains could accumulate. These sediments were perhaps transported to these depositional sites by storm-generated traction currents or river-inflow currents deflected along the lake margin. Turbidity currents seem not to have played an important role in the sediment transportation, because the Paleo-Van nearshore sediments show no evidence of turbidite depositon, such as graded bedding and sole-marks. The existence of large-scale slump scars in the nearshore sediments indicates gravitational instabilities in this environment. The environment was perhaps often subjected to shocks from storms, earthquakes or sudden adition of more sediment (Dyskstra, 2004; van Rensbergen et al., 1999; Schnellmann et al., 2002, 2005; Chapron et al., 2006; Volland, et al., 2007; Toker et al., 2007).

4.1.5. Offshore Lake Environment

Offshore lake sediments are best exposed in the Sections-$DÖN_1$, -$DÖN_4$, -AC_1, -AC_2, -DV_1, -DV_2, -ZV_1, KB, -CM_1 -ZD_2 and -KDS_1. Deposition of these sediments in quiet, standing water is suggested by the laterally persistent facies, thin-stratification, varves, fine grain size and hydroplastic disruptions, such as slumps and convolute beddings. The processes thought to be responsible for their deposition were perhaps downslope directed tractional currents near the shore and settling from suspension furthest out in the lake. The varve sedimentation in this lake seems to be a characteristic process and certainly represent seasonal settling from suspension in deep waters (Kempe, 1977; Stockhecke et al., 2012). Oxygen isotopes, Mg/Ca ratios in carbonates, and pollen and charcoal data from these annually laminated sediments revealed that there was an arid climate event with low lake levels in the Paleo- Lake Van Basin with treeless steppe vegetation during the Late Glacial (ca. 14 ka varve years; Landmann et al., 1996*a, b*, 2011; Çağatay et al., 2014); wet climatic conditions were established in the basin during the Holocene time (Wick et al., 2003; Çağatay et al., 2014). The well preservation of the varve sediments in the Paleo-Van lake environment suggests that the lake floor was inhospitable for the benthic life. This hostility was perhaps due to its extreme chemical water composition with high alkalinity and salinity at the time (Gessner, 1957; Danulat and Selçuk, 1992; Landmann, 1996*a, b*). The high salinity (22 ‰) and sodium and bicarbonate rich waters was resulted from the weathering of the volcanic rocks in drainage basin and evaporation in a closed basin. The lake occasionaly deposited tufa in the Section-CM_1 and microbiolites in the shallow offshore areas, indicating involvement of blue-green algae and bacteria in carbonate deposition in the lake (Kempe et al., 1991; Lopez-Garcia et al., 2005).

The convolute beds and fluid escape structures are mostly restricted to single layers bounded by undisturbed beds above and below. These structures in the terrace sedimentary sequences may be interpreted to have been triggered by paleo-earthquakes, considering the seismically active nature of the (Ambraseys, 1988; McCalpin and Nelson, 1996; Türkelli et al., 2003; Litt et al., 2009). Their occurrence at different elevations ($DÖN_4$: 1700 asl, KDS_1: 1693 m asl, $DÖN_1$: 1687 m asl, DV_1: 1678 m asl and ZD_2: 1666 m asl) suggests that these seismic events recurred at least five times during the last 34 ^{14}C ka BP. Unfortunately the exact time of the earthquakes cannot be given, because the individual convolute beds could not be dated in this study. These events may have been generated in the area either by ground shaking by eaertquakes or by the eruption of the Süphan or Nemrut Volcanos. Among the sections studied, only two sections (KB1 and CM1) between Erciş and Adilcevaz contain volcanic material associated with the offshore lake sediments. The sections occur at two different elevations of 1676 m asl and 1727 m asl. If the difference in the elevations was not caused by tectonics, the Süphan or Nemrut Volcanos must have been erupted twice during 9.7-5.9 ka BP interval according to the age of the nearby Section-KRD_1 in Karadere Valley in Adilcevaz.

4.2. Terraces and lake level changes

Presence of old lake terraces at various elevations around the Lake Van Basin suggest significant lake level changes over the last ~125 ka. This is also supported by the presence of lowstand deltas and onlap sequences in the subaqueous seismic reflection profiles (Damcı et al., 2012; Çukur et al., 2013 and 2014). The lake terraces observed around Lake Van are believed to represent relatively high water level periods of Paleo-Lake Van relative to its present lake level, even though tectonic uplift can account for some of their elevation.

As pointed out in Section 3.1, the age data on the various terraces around the Lake Van are insufficient

for their basin wide stratigraphic correlation, and thus for reaching sound conclusions about the lake level changes and the role of tectonic uplift in their present elevation. However, some preliminary conclusions can be reached concerning the general long-term lake level oscillations. The following assumptions are used when discussing the lake level changes of the Paleo-Lake Van, using the old lake terraces:

The Gilbert-type deltas observed in the valleys around Lake Van were deposited during rising lake level.

The parallel finely bedded and laminated clayey silt and sandstone facies were deposited in relatively deep water (e.g.,Landmann et al., 1996*a, b*; Kempe et al., 2002; Stockhecke et al., 2013; Çağatay et al., 2014).

The hydrological system in the watershed of Lake Van and the lake level follow a general wet and high-stand interglacial versus dry and low-stand glacial pattern (Stockhecke et al., 2014; Çağatay et al., 2014). However, there are exceptions to this general trend, as evidenced by some terraces dated between 26 and 21 ka BP (Kuzucuoğlu et al., 2010), which may be associated with snow melting during interstadials periods of Late Glacial (Çağatay et al., 2014)..

With the above considerations, considering its >100 ka age (Kuzucuoğlu et al., 2010), the highest terraces reaching 1761 masl in the Beyüzümü district (Çayarası Valley) and 1755 m in the Kotum Valley was likely deposited during marine isotope stage 5e (Eemean), as corroborated by the organic carbon-rich, finely laminated sediments of this stage analyzed in the ICDP PaleoVan cores (Stockechke et al., 2013, 2014). The deposition of this terrace, located at 110 m above the present lake level and 20 m above the present lake's threshold, is associated with pyroclastic deposits damming the lake's outlet in the Kotum Valley. Another terrace in the lower Kotum Dere Valley, close to the river mouth, represented by our Sections KOD1, GPS-035 and KOD_2 GPS-037) (Figure 1), reaches up to 1730-1735 masl (Kuzucuoğlu et al., 2010) and was probably deposited during a later substage of the last interglacial (i.e., MIS 5a). This conclusion is supported by high lake levels evidenced by the multiproxy analyses of ICDP cores recovered from Lake Van (Çağatay et al., 2014), and the presence of peat (swamp) deposits under the ~80 ka BP old İncekaya basaltic hyaloclastite unit located at 1777 masl elevation (Sumita and Schmincke, 2013*a*). Such a high elevation (41 m above the present lake level and 40 m above the sill in Kotum) of the peat representing the lake level at the time is most likely partly due to tectonic uplift.

In the absence of age data, another alternative for the age of the delta in the the lower reaches of the Kotum Valley is 30-34 ka BP during which dramatic changes are recorded in the total organic and inorganic carbon contents and stable oxygen and carbon isotope values of sediments in the ICDP stratigraphic section (Çağatay et al., 2014) and an onlapping sequence in seismic sections occurs (Çukur et al., 2014). All these evidence indicate a rapid lake level rise. This rapid increase in the lake level was most probably the result of melt water delivery with low ‰^{18}O and ‰^{13}C values, caused by the D-O event following H4 (ca 35 ka BP; Wolff et al, 2010; Blockley et al., 2012). This transgression also corresponds in time with the Nemrut volcano activity leading to the deposition of the Nemrut formation, which was associated with the caldera forming eruption of 10 km^3 of magma (Sumita and Schmincke, 2013*a*).

The Gilbert fan delta observed at 1690 m in Karahan Village (GPS-021, 022, 023; Kırklar) near the northern shore of Lake Van was deposited during 26-24 ka according to the radiocarbon dating of Kuzucuoğlu et al. (2010) (Table 1). This suggests that the lake level reached an altitude of at least 45 m above the present level during that time. Even though there are no supporting ages, Kuzucuoğlu et al. (2010) suggests that co-eval terrace sediments are also present in Yumrutepe in the Karasu Valley in the east and in the Engil River Valley in the southeast of the lake. The same authors also state that the coastal cliff terrace at Mollakasim (GPS-047) represents abrasion type terrace formed during a regression after the lake level transgression during 26-24 ka BP.

Most of the terraces deposited in the valleys close to the river mouths are dated to two periods: 22-21 ka BP and 10-6 ka BP. The terraces are in the form of Gilbert type delta sequences. Those belonging to the first period were dated in Güzelsu in Engil River valley by Kempe et al. (2002). Terraces of similar age are also found in Mollakasım (GPS-045) in Karasu and in Kotum, Zilan, Karasu, and Bendimahi river valleys. These terraces reach up to 1700 m elevation.

The transgressive episode during 22-21 ka BP was followed by a drastic lake level fall, reaching to

minimum levels durig 16-14 ka BP (Landmann et al., 1996*a, b*; 2011). This lakel level fall is also supported by deposition of dolomite, low TOC and increased rate of mass flow events in the ICDP borehole sections (Çağatay et al., 2014; Stockhecke et al., 2013), and subaqueous prograding deltas at ca -200 m in the seismic sections in the Northern and Tatvan basins (Damcı et al., 2012; Çukur et al., 2014).

The last period of coastal terrace deposition occurred during the early Holocene. The most representative of these young terraces is the one near Adilcevaz in the Karadere valley, which has been dated between 10 and 6 ka BP (Table 1). During this time, the lake level reached 1676 masl (~30 m above the present lake level). These terraces were deposited during a transgression following the major regression at 16-15 ka BP and a somewhat smaller scale regression during the Younger Dryas (Landmann et al., 1996*a, b*, 2011; Çukur et al., 2014; Çağatay et al., 2014).

5. Conclusions

On the basis of the preceding discussions, the following summary and conclusions may be given:

1. The terraces studied around the Lake Van record the last ca. 125 ka of the 500-ka-long geological history of the Lake Van Basin as suggested by the oldest terrace sediments dated in the Çayarası Valley (Beyüzümü) and Kotum Dere Valley at 1754-1761 masl elevations.
2. The terrace sediments formed from clastic sediments accumulated in a large array of relatively shallow lacustrine environments, such as offshore lake, nearshore lake, Gilbert-type delta, beach and alluvial fan/braided river.
3. The terraces deposited in the form of Gilbert type fan deltas around Lake Van represent deposition during transgressive episodes. Such episodes are observed during MIS5, 34-30 ka, 26-24 ka BP, 22-21 ka BP and 10-6 ka BP.
4. The level was controlled by climate, tectonism and volcanism. The interglacial and interstadial periods were generally characterized by high lake levels with the sediments supplied mostly by running waters as wet conditions were established in the area. During the during interstadial periods of the Last Glacial meltwaters from snow and ice contributed water and sediment to the lake. Volcanism contributed tephra, volcanoclastic sediments and may have caused changes in the elevation of the lake's outlet, thereby influencing the lake levels. Tectonic uplift or warping associated with the dip-slip and/or strike-slip faults also affected the lake level and increased the sediment input.
5. Variability of shoreline and delta facies provides evidence for the distribution of wave energy and the effects of paleowinds. Higher wave energy existed along the northern margin and in some parts of the eastern margin of the Paleo-Lake Van where the beach and the nearshore lake sediments were strongly affected by lake processes. The relatively coarse grain size of these sediments and their reactivation surfaces suggest that strong winds or storms were an active agent in transportation and deposition in the Paleo Lake -Van. The dominant wind direction was perhaps from south to north as indicated by the distribution of the beach and the nearshore lake sediments.
6. The beach sediments mark the shoreline of the Paleo-Lake Van. They occur at three elevations: 1708, 1733 and 1736 m masl. (Sections-$DÖN_2$, BD_1 and KV_2, respectively). The deposits at the last two elevations may have been thought to be the products of the same shoreline if the 30 m ground pixel resolution of the ASTER DEM data is considered. On the basis of their sub-depositional environments, the paleo-shorelines may be placed at 1740 (shoreline-1) and 1710 (shoreline-2) masl (Figures 31 and 32). The age of the former is ca. ≥ 30-34 ka BP, whereas that of the latter is 20.7-20.9 ka BP as suggested by the dating of the beach or the associated lacustrine sediments more or less at the same elevations in the Karasu and Dönemeç Çayı Valleys, respectively. 1740 m maximum lake-level dictates that no lacustrine facies younger than ≥ 30-34 ka BP can be found above the elevation of 1740 m in the lake basin. Therefore, the terrace sediments at the elevations of 1754-1761 masl in the Çayarası Valley (Section-CV_1) must have been elevated to these hights by a fault zone, extending between the villages Kalecik and Değirmen as described first by Ketin (1977) (Figure 1).

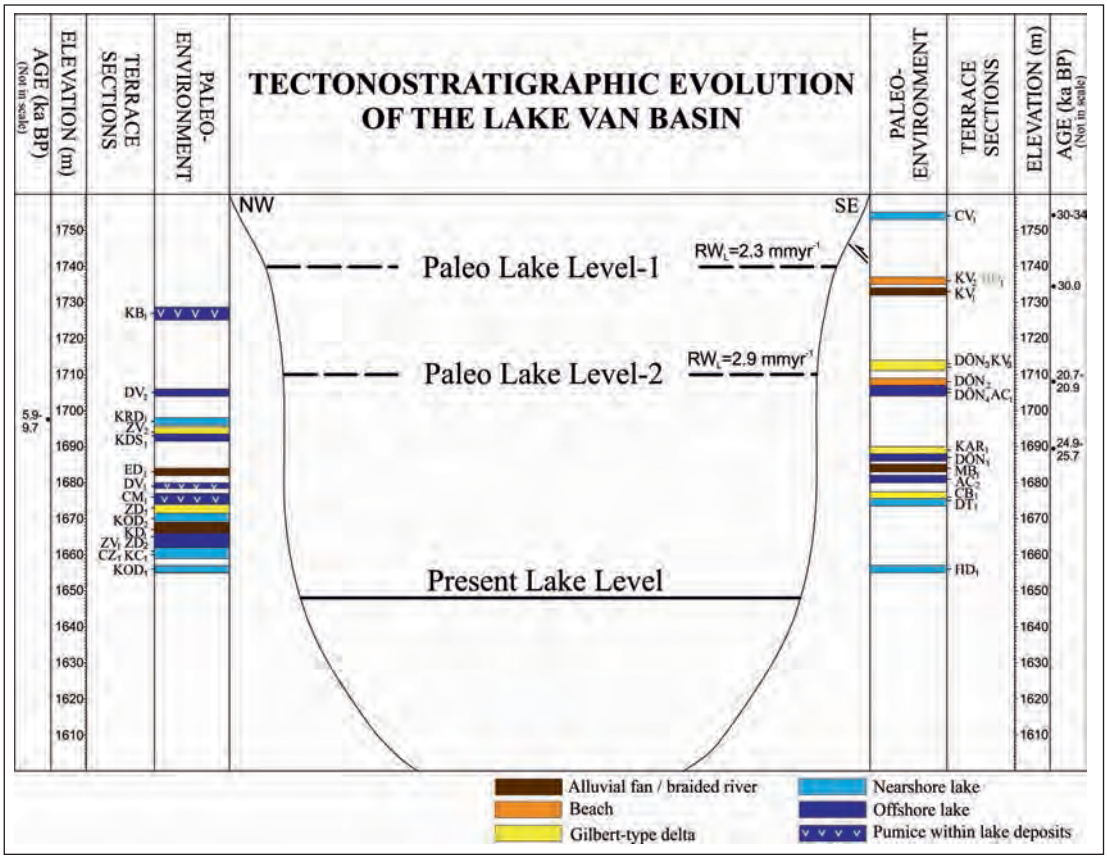

Figure 31- The scheme summarizing the lake level changes, on the basis of palae-environments of the Lake Van.

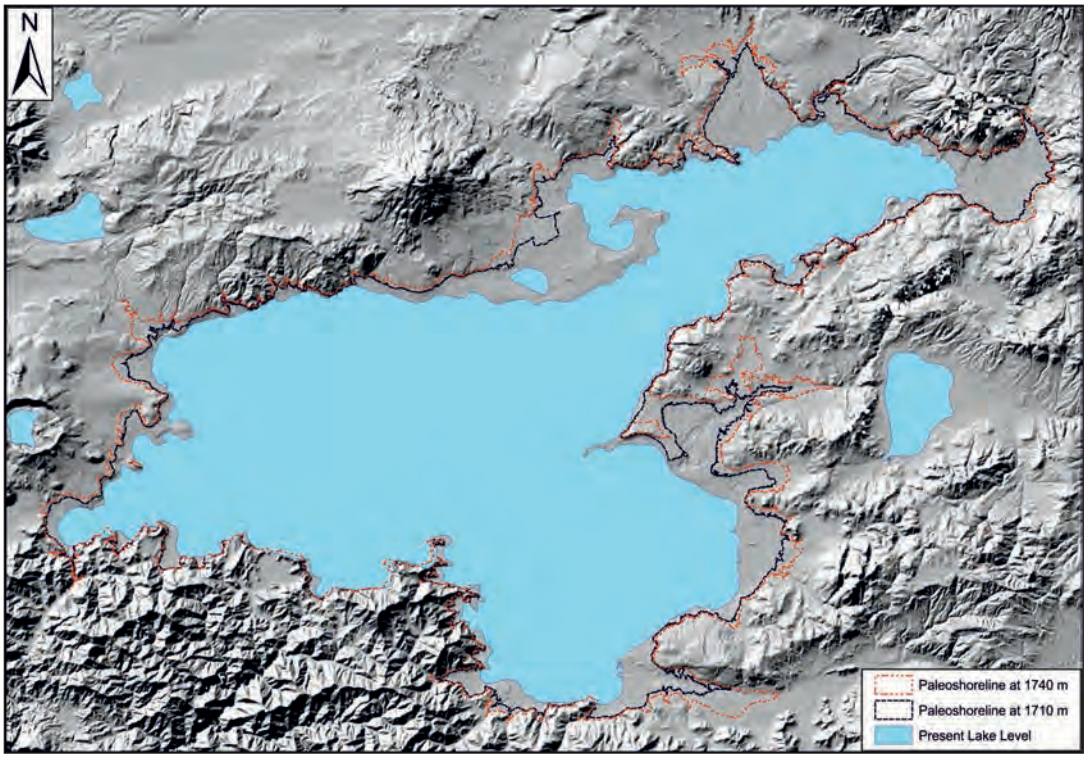

Figure 32- The map of the palaeoshoreline at 30-34 and 20.7-20.9 ka BP at 1740 and 1710 m, respectively.

7. Beside the present shoreline, the recognition of another two paleoshorelines in the Lake Van Basin suggests changes in the lake-level during the deposition of the terrace sediments examined (Figure 31). The consistent younging of the paleo-shorelines toward low elevations suggests that these changes took place as a gradual drop in lake-level, rather than by fluctuations. The lack of large-scale cyclicity in the terrace successions also supports this interpretation. The present lake-level was attained in probably three stages during the last ~30 ka BP. The lake-level dropped first from 1740 to 1710 masl from ~32 ka BP to 21 ka BP and then a further drop occurred to about 200 m below the present lake level at about 15-14 ka BP, as evidenced in sedimentary sections recovered from within the lake (Figure 32). A rise to the present level of 1647 masl occurred in the latest glacial and early Holocene. The drops were probably caused by both climate and tectonic processes, although the former may have been more effective. Particularly, the changes in the amounts of precipitation and evaporation with time must have played an important role. From the shoreline elevations and their ages, rate of the water level drop was calculated as 2.3 mm yr^{-1} for the first stage and 2.9 mm yr^{-1} for the second stage. The first and second stages of lake-level drops took place before and after the Last Glacial Maximum.

Acknowledgements

This study was supported by ITU-BAP Project No. 36595.

Received: 12.11.2014
Accepted: 18.06.2015
Published: December 2015

References

Akyüz, H. S., Zabcı, C., Sançar, T. 2011. Preliminary report on the 23 October 2011 Van earthquake, Istanbul Technical University, Istanbul, Turkey

Allen, J. R. L. 1984. Developments in Sedimentology, Sedimentary Structures. *Elsevier*, 663 p.

Ambraseys, N. N. 1988. Engineering seismology. *Earthquake Engineering and Structural Dynamics* 17, 1-105.

Blair, T. C., Mc Pherson, J. G. 1994. Alluvial fans and their natural distinction from rivers based on morphology, hydraulic processes, sedimentary processes and facies assemblages. *Journal of Sedimentary Research* 64, 450-589.

Blockley, S.P.E., Lane, C.S., Hardiman, M., Rasmussen, S.O., Seierstad, I.K., Steffensen, J.P., Svensson, A., Lotter, A.F., Turney, C.S.M., Ramsey, C.B., INTIMATE members. 2012. Synchronisation of palaeoenvironmental records over the last 60,000 years, and an extended INTIMATE1 event stratigraphy to 48,000 b2k. *Quaternary Science Reviews* 36, 1-222.

Bluck, B. J. 1967. Deposition of some Upper Old Red Sandstone conglomerate in the Clyde area: a study in the significance of bedding. *Scot. J. Geol.* 3, 139-167.

Bull, W. B. 1972. Recognation of Alluvial-Fan Deposits in the Stratigraphic Record. (Rigby, J. K., Hamblin, W. K. (Ed.). Recognation of Ancient Sedimentary Environments. *Society of Economic Paleontologists and Mineralogists*. Special Publication 16, 63-83.

Carryer, S. J. 1966. A note on the formation of alluvial fans..*New Zealand Jour. Geology and Geophysics* 9, 91-94.

Chapron, E., Ariztegui, D., Mulsow, S., Villarosa, G., Pino, M., Outes, V., Juvignie, E., Crivelli, E. 2006. Impact of the 1960 major subduction earthquake in Northern Patagonia (Chile, Argentina). *Quaternary International*. 158, 58-71.

Clifton, H. E. 1973. Marine-nonmarine facies change in middle Miocene rocks, southeastern Caliente Range, California; in Sedimentary facies changes in Tertiary rocks- California Ti'ansverse and southern Coast Ranges. *Annual Meeting AAPG-SEPM-SEG*., 55-57.

Çağatay, M.N., Öğretmen, N., Damcı, E., Stockhecke, M., Sancar, Ü., Eriş, K.K., Özeren, S., 2014. Lake level and climate records of the last 90 ka from the Northern Basin of Lake Van, eastern Turkey. *Quaternary Science Reviews* 104, 97-116.

Çukur, D., Krastel, S., Demirel-Schülter, F., Demirbağ, E., İmren, C., Niessen, F., Toker, M., PaleoVan-Working Group 2013. Sedimentary evolution of Lake Van (Eastern Turkey) reconstructed from high-resolution seismic investigations. *International Journal of Earth Sciences (Geol. Rundsch.)* 102 (2), 571-585.

Çukur, D., Krastel, S., Schmincke, H-U, Sumita, M., Winkelmann, D., Çağatay, M.N., Meydan, A.F., Damcı, E., Stockhecke, M. 2014. Seismic stratigraphic evolution of the Lake Van, eastern Turkey. *Quaternary Science Reviews* 104, 63-84.

Damcı, E., Çağatay M. N., Krastel, S, Öğretmen, N., Çukur, D., Ülgen, U.B., Erdem, Litt, T., Anselmetti F.S. Eriş,K.K., ICDP PaleoVan Scientific Party. 2012. Lake level changes of Lake Van over the Last 400 ka: Evidence from Deltas in Seismic Reflection Data and ICDP Drilling. *European Geosciences Union (EGU) General Assembly*, 22-27 April 2012, Vienna, 626.

Danulat, E., Selçuk, B. 1992. Life history and environmental conditions of the anadromous *Chalcalburnus tarichi* (Cyprinidae) endemic to the extremely alkaline Lake Van, Eastern Anatolia, Turkey. *Arch. Hydrobiol.* 126: 105-125.

Davidson Arnott, R. G. D., Greenwood, B. 1976. Beach and Nearshore Sedimentation. Davis, R. A., Ethington, R. L. (Ed.). *Soc. Econ. Paleontol. Mineral.* Special Publication 24, 149-168.

Degens, e.t., Kurtman, F. 1978. The geology of Lake Van. *Maden Tetkik ve Arama Genel Müdürlüğü Press*, 158p.

Degens, E.T., Wong, H.K., Kempe, S., Kurtman, F. 1978. A Van Gölü'nün Jeolojik Gelişimi: Bir Özet. Degens, E.T., Kurtman, F. (Ed.). The Geology of Lake Van. *Maden Tetkik ve Arama Genel Müdürlüğü*, 147-158.

Degens, E.T., Wong, H.K., Kempe, S., Kurtman, F. 1984. A Geological study of Lake Van, Eastern Turkey. *Geologische Rundschau* 73, 701-734.

Doğan, B., Karakaş, A. 2013. Geometry of co-seismic surface ruptures and tectonic meaning of 2011 Mw 7.1 Van earthquake (East Anatolian Region, Turkey). *Journal of Structural Geology* 46, 99-114.

Dorsey, R. J., Umhoefer, P. J., Renne, P. R. 1995. Rapid subsidence and stacked Gilbert-type fan deltas, Pliocene Loreto basin, Baja California Sur, Mexico. *Sedimentary Geology*. 98, 181-204.

Dunne, L. A., Hempton, M. R. 1984. Deltaic sedimentation in the Lake Hazar pull-apart basin, south-eastern Turkey, *Sedimentology* 31, 401-412.

Ekström, G., Nettles, M., Dziewo*f*ski, A.M., 2012. The global CMT project 2004–2010: Centroid-moment tensors for 13,017 earthquakes. *Physics of the Earth and Planetary Interiors* 200–201, 1-9.

Emre, Ö., Duman, T.Y., Özalp, S., Elmacı, H., Olgun, Ş., Şaroğlu, F., 2013. Açıklamalı Türkiye Diri Fay Haritası Ölçek 1:1250000 (Active Fault Map of Turkey with an Explanatory Text 1:1250000 scale), 89 pp., *Maden Tetkik ve Arama Genel Müdürlüğü*, Ankara.

Erdik, M., Kamer, Y., Demircioğlu, M., Şeşetyan, K. 2012. 23 October 2011 Van (Turkey) earthquake. *Natural Hazard* 64, 651-665.

Ergin, K., Güçlü, U., Uz, Z. 1967. Türkiye ve civarının deprem kataloğu (A Catalof of earthquakes for Turkey and surrounding area), *İstanbul Teknik Üniversitesi, Maden Fakültesi Ofset Baskı Atölyesi*, İstanbul

Erinç, S. 1953. Doğu Anadolu Coğrafyası. *İstanbul Üniversitesi Yayınları*, İstanbul.

Falk, P. D., Dorsey, R. J. 1998. Rapid development of gravelly high-density turbidity currents in marine Gilbert-type fan deltas, Loreto Basin, Baja California Sur, Mexico. 45, 331-349.

Fielding, E. J., Lundgren, P. R., Taymaz, T., Yolsal Çevikbilen, S., Owen, S. E. 2013, Fault-slip source models for the M 7.1 Van Earthquake in Turkey from SAR Interferometry, pixel offset tracking, GPS and seismic waveform analysis, *Seismological Research Letters* 84 (4), 579-593.

Gessner, F. 1957. Van Gölü, zor Limnologie des grossen Soda Sees in Ostanatolien (Türkei). *Arch. Hydrobiol.* 53, 1-22.

Gloppen, T. G., Steel, R. J. 1981. The deposits, internal structure and geometry of six alluvial fan – fan-delta bodies (Devonian, Norway) – a study in the significance of bedding sequences in conglomerates. In: *F. G: Ethridge (Ed.) Non-Marine deposits – Models for Exploration. Soc. Econ. Paleontol. Mineral.*, Spec. Publi. 31, 49-69.

Görür, N. 1992. A tectonically controlled alluvial fan which developed into a marine fan-delta at a complex triple junction: Miocene Gildirli Formation of the Adana Basin, Turkey. *Sedimentary Geology*. 81, 243-252.

Güner, Y. 1984. Nemrut yanardağının jeolojisi, jeomorfolojisi ve volkanizmasının evrimi, *Jeomorfoloji Dergisi* 12, 23-65.

Harvey, A. M., Mather, A. E., Strokes, M. 2005. Alluvial fans: geomorphology, sedimentology, dynamics – introduction. A review of alluvial-fan research *in* Harvey, A. M., Mather, A. E., Stokes, M. (Eds) Alluvial Fans Geomorphology, Sedimentology, Dynamics, *Geological Society* Special Publication 251, 1-7

Hayes, M. O. 1967. Hurricanes as geological agents, south Texas coast. *Bulletein American Association of Petroleum Geologists* 51, 937-942.

Heward, A. P., 1978. Alluvial fan and lacustrine sediments from the Stephanian A and B (La Magdalenai Cinera-Matallana and Sabero) coalfields, northern Spain. *Sedimentology* 25, 451-488.

Horasan, G., Boztepe-Güney, A. 2007. Observation and Analysis of Low-Frequency Crustal Earthquakes In Lake Van and its Vicinity, Eastern Turkey. *Journal of Seismology* 11, 1-13.

Howard, J. D. 1967. Georgia coastal region, Sapelo Island, U.S.A. Sedimentology and biology. VIII. Conclusions. *Senckenbergiana Marit* 4, 217-222.

Johnson, A. M. 1970. Physical processes in geology: San Francisco. Freeman. *Cooper and Company*, 577 p.

Kaden, H., Peeters, F., Lorke, A., Kipfer, R., Breenwald, M., Tomonaga, Y. 2005. Mixing processes in Lake Van (Turkey). *9th European Workshop on Physical Processes in Natural Waters (extended abstract)*. Lancaster, UK.

Kaden, H., Peeters, F., Lorke, A., Kipfer, R., Tomonaga, Y., Karabıyıkoğlu, M. 2010. Impact of lake level change on deep-water renewal and oxic conditions

in deep saline Lake Van, Turkey. *Water Resources Research* 46, W11508.

Kadıoğlu, M., Sen, Z., Batur, E. 1997*a*. The greatest soda-water lake in the world and how it is influenced by climatic change. *Ann. Geophysicae* 15, 1489-1497.

Kadıoğlu, M., Sen, Z., Batur, E. 1997*b*. The greatest soda-water lake in the world and how it is influenced by climatic change. *Ann. Geophysicae* 15, 1489-1497.

Kempe, S. 1977. Warvenchronologie und organische Geochemie des Van Sees, Ostrrürkei, Ph.D. thesis, *Mitt. Geol. Palaeontol. Inst. Univ. Hamburg*.

Kempe, S., Degens, E.T. 1978. Lake Van varve record: the past 10.420 years. Degens, E.T., Kurtman, F. (Ed.). Geology of Lake Van. *Maden Tetkik ve Arama Genel Müdürlüğü Yayınları*. Ankara, 56-63.

Kempe, S., Kazimierczak, J., Landmann, G., Konuk, T., Reimer, A., Lipp, A. 1991. Largest known microbialities discovered in Lake Van, Turkey. *Nature* 349, 605-608.

Kempe, S., Landmann, G., Müller, G. 2002. A floating varve chronology from the last glacial maximum terrace of Lake Van/Turkey. *Research in deserts and mountains of Africa and Central Asia* 126, 97–114.

Ketin, İ. 1977. Van Gölü ile İran sınırı arasındaki bölgede yapılan jeoloji gözlemlerinin sonuçları hakkında kısa bir açıklama. *TJK Bült*. 20, 79-85.

Kumar, N., Sanders, J. E. 1976. Characteristics of shoreface storm deposits: modern and ancient examples, *J. Sediment. Petrol*. 46, 145-162.

Kuzucuoğlu, C., Christol, L., Mouralis, D., Doğu, A.F., Akköprü, E., Fort, M., Brunsteın, D., Zorer, H., Fontugne, M., Karabıyıkoğlu, M. 2010. Formation of the Upper Pleistocene terraces of lake Van (Turkey). *Journal of Quaternary Science* 25, 1124–1137.

Kwiecien O, Stockhecke, M., Pickarski, N., Litt, T., Sturm, M., Anselmetti, F., Haug, G. 2014. Dynamics of the last four glacial terminations recorded in Lake Van, Turkey. *Quaternary Science Reviews* 104, 42-52.

Landmann, G. 1996. Van See/Türkei: Sedimentologie, Warvenchronologie und regionale Klimaentwicklung der letzten 15.000 Jahre. Doktora Tezi, *Hamburg Üniversitesi* (unpublished).

Landmann, G., Reimer, A. ve Kempe, S. 1996*a*. Climatically induced lake level changes at Lake Van, Turkey, during the Pleistocene / Holocene transition. *Global Biochemical Cycles* 10, 797-808.

Landmann, G., Reimer, A., Lemcke, G., Kempe, S. 1996*b*. Dating Late Glacial abrupt climate changes in the 14.570 yr long continuous varve record of Lake Van, Turkey. *Palaeogeography, Palaeoclimatology, Palaeoecology* 122, 107-118.

Landmann, G., Kempe, S. 2005. Annual deposition signal versus lake dynamics: Microprobe analysis of Lake Van (Turkey) sediments reveals missing varves in the period 11.2–10.2 ka BP. *Facies* 51, 143-153.

Landmann, G., Steinhauser, G., Sterba, J.H., Kempe, S., Bichler, M. 2011. Geochemical fingerprints by activation analysis of tephra layers in LakeVan sediments, Turkey. *Applied Radiation and Isotopes* 69, 929–935.

Lewis, D. W. 1980. Storm-generated graded beds and debris flow deposits with Ophiomorpha in a shallow offshore Oligocene sequence at Nelson, South Island, New Zealand, *N. Z. J. Geol. Geophys*. 23, 353-369.

Litt, T., Krastel, S., Sturm, M., Kipfer, R., Oercen, S., Heumann, G., Franz, S. O., Ulgen, U. B., Niessen, F. 2009. 'PALEOVAN', International Continental Scientific Drilling Program (ICDP): site survey results and perspectives. *Quaternary Science Reviews* 28, 1555-1567.

Litt, T., Anselmetti, F.S., Baumgarten, H., Beer, J., Çağatay, N., Cukur, D., Damci, E., Glombitza, C., Haug, G., Heumann, G., Kallmeyer, J., Kipfer, R., Krastel, S., Kwiecien, O., Meydan, A.F., Orcen, S., Pickarski, N., Randlett, M., Schmincke, H., Schubert, C.J. Sturm, M., Sumita, M., Stockhecke M.,, Tomonaga, Y., Vigliotti, L., Wonik, T. 2012. The PALEOVAN Scientific Team, 500,000 Years of Environmental History in Eastern Anatolia: The PALEOVAN Drilling Project. *Sciencetific Drilling* 14, 18.

Litt, T. Pickarski, N., Heumann, G. 2014. A 600,000 Year Long Continental Pollen Record from Lake Van, Eastern Anatolia (Turkey). *Quaternary Science Reviews*.

López-García, P., Kazmierczak J., Benzerara, K., Kempe, S., Guyot, F., Moreira, D. 2005. Bacterial diversity and carbonate precipitation in the giant microbialites from the highly alkaline Lake Van, Turkey. *Extremophiles* 9, 263-274.

Lowe, D.R. 1979. Sediment gravity flows: Their classification and some problems of aplication to natural flows and deposits, in Doyle, L. J., Pilkey, O. H. (Eds.) *Geology of continental slopes: Society of Economic Paleontologists and Mineralogits Special Publication* 27, 75-82.

Lowe, D. R. 1982. Sediment gravity flows II: depositional models with special reference to the deposits of high density turbidity currents. *Journal of Sedimentary Petrology* 52, 279-297.

Mc Calpin, J. P., Nelson, A. R. 1996. Introduction to Paleoseismology in *McCalpin, J. P. (Ed.) Paleoseismology*, Academic Press, New York, pp. 1-32

McConnico, T.S., Bassett, K.N. 2003. Quaternary Gilbert-style fan deltas and Podocarp forests along the

modern transpressional Hope fault, New Zealand. *Geological Society of America* 35, 510.

McConnico, T. S., Bassett, K. N. 2007. Gravelly Gilbert-type fan delta on the Conway Coast, New Zealand: Foreset depositional processes and clast imbrications. *Sedimentary Geology* 198, 147-166.

Moretti, M., Pieri, P., Tropeano, M. 2002. Late Pleistocene soft-sediment deformation structures interpreted as seismites in paralic deposits in the city of Bari (Apulian forelan, southern Italy). Geological Society of America, Special Paper 359.

Mouralis D., Kuzucuoğlu C., Scaillet S., Doğu A-F., Christol A., Akköprü E., Fontugne M., Zorer H., Guillou H. 2010. Les pyroclastites du sud-ouest du lac de Van (Anatolie orientale, Turquie): implications sur la paléo-hydrographie régionale. *Quaternaire* 21, 417-433.

Nemec, W. 1990. Deltas – remarks on terminology and classification. In: Coarse-grained Deltas. Colella, A. and Prior, D. B. (Ed.). International Association of Sedimentologists. *Blackwell Scientific Publications*, Special Publication 10, Oxford, 3-12.

Nemec, W., Steel, R. J. 1984. Alluvial and Coastal Conglomerates: Their signifcant features and some comments on gravelly mass-flow deposits. In: Sedimentology of Gravels and Conglomerates – Memoir 10, 1-34.

Nemec, W., Steel, R. J. 1985. Stacked, shore-attached, sheet sandstones in a Paleocene inland seway succession (Endalen Member, Spitsbergen) (abs): International Association of Sedimentologists, 6th European Regional Metting, Lleida, Spain. 321-324.

Nichols, G. 2009. Sedimentology and Stratigraphy. *Wiley-Blackwell*, 419 p.

Nilsen, T. H. 1982. Alluvial fan deposits: In: Scholle, P. A., Spearing, D. (Eds.), Sandstone depositional environments. *Mem. Am. Assoc. Pet. Geol.* 31, 49-86.

Örgülü, G., Aktar, M., Turkelli, N., Sandvol, E., Barazangi, M. 2003. Contribution to the seismotectonics of eastern Turkey from moderate and small size events. *Geophysical Research Letters* 30, 8040.

Picard, M. D., High, L. R. 1972. Recognition of ancient sedimentary environments. Rigby, J. K., Hamblin, W. K. (Ed.). *Soc. Econ. Paleontologists Mineralogists Special Publication* 16, 108-145.

Picard, M. D., High, L. R. 1981. Physical stratigraphy of ancient lacustrine deposits. In: Ethridge, F. G., Flores, R. M., Recent and ancient nonmarine depositional environments: Models for exploration. *Society of Economic Paleontologists and Mineralogists*, Special Publication 31, 233-259.

Reimer, A., Landmann, G., Kempe, S. 2009. Lake Van, Eastern Anatolia, hydrochemistry and history. *Aquat. Geochem.*15, 195-222.

Postma, G. 1990. Depositional achitecture and facies of river and fal deltas: a synthesi, in: Colella, A., Prior, D.B. (Eds.), Coarse Grained Deltas, *Int. Assoc. Sedimento.,* Spec. Publ. 10, 13-27

Rust, B. R. 1972. Structure and Process in a braided river, *Sedimentology* 18, 221-245.

Reineck, H. E., Singh, I. B. 1975. Depositional Sedimentary Environments. *Springer Verlag*, 439 .

Schnellmann, M., Anselmetti, F. S., Giardini, D., McKenzie, J. A., Ward, S. N. 2002. Prehistoric earthquake history revealed by lacustrine slump deposits. *Geology* 30, 1131-1134.

Schnellmann, M., Anselmetti, F. S., Giardini, D., McKenzie, J. A., Ward, S. N. 2005. Mass movement-induced fold-and-thrust belt structures in unconsolidated sediments in Lake Lucerne (Switzerland). *Sedimentology* 52, 271-289.

Seilacher, A. 1969. Fault-graded beds interpreted as seismites. *Sedimentology* 13, 155-159.

Sly, P. G. (1978). Sedimentary Processes in Lakes. In: Lerman, A. (Ed.) *Lakes*, Springer New York**:** 65-89.

Sohn, Y. K. 2000. Depositional Processes of Submarine Debris Flows in the Miocene Fan Deltas, Pohang Basin, SE Korea with Special Reference to Flow Transformation. *Journal of Sedimentary Research* 70, 491-503.

Steel, R. J. 1974. New Red Sandstone floodplain and piedmont sedimentation in the Hebridean Province. *J. Sedim. Petrol.* 44, 336-357.

Steel, R. J., Wilson, A. C. 1975. Sedimentation and tectonism (?Permo-Triassic) on the margin of the North Minch Basin,. *J. Geol. Soc. London* 131, 183-202.

Stockhecke, M. Anselmetti, F.S., Meydan, A.F. Odermatt, D., Sturm, M. 2012. The annual particle cycle in Lake Van (Turkey). *Palaeogeography, Palaeoclimatology, Palaeoecology* 333-334, 148–159..

Stockhecke, M., Anselmetti, F.S., Sturm, M. 2014. Past seismic activity in Eastern Anatolia recorded over several glacial/interglacial cycles in the sediments of Lake Van. *Quaternary Science Reviews*.

Stockhecke, M., Kwiecien, O., Vigliotti, L., Anselmetti, F.S. Beer, J., Çağatay, M.N., Channell, J.E.T,. Kipfer, R., Lachner, J., Litt, T., Pickarski, N., Sturm, M. 2014. Chronostratigraphy of the 600,000 year old continental record of Lake Van (Turkey). *Quaternary Science Reviews*. 104, 8-17.

Stockhecke, M., Sturm M., Brunner, I., Schmincke, H.-U., Sumita, M., Kwiecien, O., Çukur, D., Anselmetti, F.S. 2014. Sedimentary evolution and

environmental history of Lake Van (Turkey) over the past 600,000 years. *Sedimentology* 61(6), 1830-1861.

Sumita, M., Schmincke, H.U. 2013*a*. Impact of volcanism on the evolution of Lake Van II: Temporal evolution of explosive volcanism of Nemrut Volcano (eastern Anatolia) during the past ca. 0.4 Ma. *Journal of Volcanology Geothermal Research* 253, 15–34.

Sumita, M., Schmincke, H.U. 2013*b*. Impact of volcanism on the evolution of Lake Van I: evolution of explosive volcanism of Nemrut Volcano (eastern Anatolia) during the past >400,000 years. *Bulletin of Volcanology 75*, 714.

Şaroğlu, F., Güner, Y. 1981. Doğu Anadolu'nun jeomorfolojik gelişimine etki eden öğeler: Jeomorfoloji, tektonik, volkanizma ilişkileri. *TJK Bülteni* 24, 39-50.

Şenel, M., Ercan, T. 2002, 1:500000 Ölçekli Türkiye Jeoloji Haritası, Van Paftası, *Maden Tetkik ve Arama Genel Müdürlüğü*, Ankara

Şengör. A.M.C., Yılmaz, Y. 1981. Tethyan evolution of Turkey: A plate tectonic approach. *Tectonophysics* 75, 181-241.

Şengör. A.M.C., Görür, N., Şaroğlu, F. 1985. Strike-slip faulting and related basin formation in zones of tectonic escape: Turkey as case study. Biddle, K.T., Christie-Blick, N. (Ed.). Strike-slip faulting and basin formation. Spec. Publ. Soc. Econ. Paleontol. *Mineral* 37, 227-264.

Şengör, A., Özeren, S., Genç, T., Zor, E. 2003. East Anatolian high plateau as a mantle supported, north-south shortened domal structure. *Geophysical Research Letters* 30, 24.

Şengör, A.M.C., Özeren, M.S., Keskin, M., Sakınç, M., Özbakır, A.D., Kayan, İ. 2008. Eastern Turkish high plateau as a small Turkic-type orogen: Implications for post-collisional crust-forming processes in Turkic-type orogens. *Earth-Science Reviews*. 90, 1–48.

Tan, O. 2004. Kafkasya, Doğu Anadolu ve Kuzeybatı İran Depremlerinin Kaynak Mekanizması Özellikleri ve Yırtılma Süreçleri, Doktora Tezi, İTÜ Fen Bilimleri Enstitüsü, İstanbul (unpublished).

Todd, S. P. 1989. Stream-driven, high-density gravelly traction carpets: possible deposits in the Trabeg Conglomerate Formation, SW Ireland and some theoretical considerations of their origin. *Sedimentology* 36, 513-530.

Toker, M., Krastel, S., Demirel-Schlueter, F., Demirbağ, E., İmren, C. 2007. Volcano-seismicity of Lake Can (Eastern Turkey): A comparative analysis of seismic reflection and three-component velocity seismogram data and new insights into Volcanic Lake Seismicity. *Earthquake Symposium Kocaeli*. 22-26 October 2007, 103-109.

Toker, M., Şengör, A. M. C. 2011. Van Gölü havzasının temel yapısal unsurları, tektonik ve sedimanter evrimi, Doğu Türkiye, *İTÜ Dergisi* 10 (4), 119-130.

Türkelli, N., Sandvol, E., Zor, E., Gök, R., Bekler, T., Al-Lazki, A., Karabulut, H., Kuleli, S., Eken, T., Gürbüz, C., Bayraktutan, S., Seber, D., Barazangi, M. 2003. Seismogenic zones in Eastern Turkey. *Geophysıcal Research Letters* 30, 8039-8042.

Utkucu, M. 2006. Implications for the water level change triggered moderate (M ? 4.0) earthquakes in Lake Van basin, Eastern Turkey. *Journal of Seismology* 10, 105-117.

Üner, S. 2014, Seismogenic structures in Quaternary lacustrine deposits of Lake Van (eastern Turkey), *Geologos* 20 (2), 79-87.

Valeton, I. 1978. A morphological and petrological study the terraces around Lake Van, Turkey. Degens, E.T. and Kurtman, F. (Ed.). Geology of Lake Van. *MTA Publications* 169, 64-80.

Van Ransbergen, P., De Batist, M., Beck, C. 1999. High-resolution seismic stratigraphy of glacial to interglacial fill of a deep glacigenic lake: Lake Le Bourget, Northwestern Alps, France. *Sediment Geol*. 128, 99-129.

Volland, S., Sturm, M., Lukas, S., Pino, M., Müller, J. 2007. Geomorphological and sedimentological evolution of a lake basin under strong volcano-tectonic influence: the seismic record of Logo Calafquen (south-central Chile). *Quaternary International*. 161, 32-45.

Wick, L., Lemcke, G., Sturm, M. 2003. Evidence of Lateglacial and Holocene climatic change and human impact in eastern Anatolia: high resolution pollen, charcoal, isotopic and geochemical records from the laminated sediments of Lake Van, Turkey. *The Holocene* 13, 665–675.

Wolff, E. W., Chappellaz, J., Blunier, T., Rasmussen, S. O., Svensson, A. 2010. Millennial–scale variability during the last glacial: The ice core record. *Quaternary Scienc. Reviews* 29, 2828–2838.

Wong, H.K., Degens, E.T. 1978. The bathymetry of Lake Van; eastern Turkey. Degens E.T., Kurtman F. (Ed.). The Geology of Lake Van. *MTA Press*. Ankara, 6-10.

Wong, H.K, Finckh, P. 1978. Shallow structures in Lake Van. Degens, E.T., Kurtman, F. (Ed.). Geology of Lake Van. *MTA Yayınları*. Ankara, 20-28.

Yılmaz, Y., Güner, Y., Şaroğlu, F. 1998. Geology of the Quaternary volcanic centres of the east Anatolia. *Journal of Volcanology and Geothermal Research* 85, 173–210.

Bull. Min. Res. Exp. (2015) 151: 47-106

Bulletin of the
Mineral Research and Exploration

http://bulletin.mta.gov.tr


BULLETIN OF THE
MINERAL RESEARCH AND EXPLORATION

CONTENTS

LATE CENOZOIC EXTENSIONAL TECTONICS IN WESTERN ANATOLIA: EXHUMATION OF THE MENDERES CORE COMPLEX AND FORMATION OF RELATED BASINS

Gürol SEYİTOĞLU[a*] and Veysel IŞIK[a]

[a] *Ankara University, Department of Geological Engineering, Tectonics Research Group, 06100 Tandoğan, Ankara*

Keywords:
Extensional Tectonics, Core Complex, Neogene, Detachment Fault, Graben

ABSTRACT

The Aegean region (Western Anatolia, Aegean Sea and Greece) is one of the areas of the earth under the effect of extensional tectonics and includes the typical features of core complexes in this type of region. The Menderes Massif in Western Anatolia was exhumed initially as an asymmetric core complex in the Early Miocene due to extension beginning in the Oligocene and then the central Menderes Massif was further exhumed as a symmetric core complex. This article discusses the exhumation mechanisms of the Menderes Massif and development of surrounding sedimentary basins in light of new findings. The proposed model successfully explains, the location of the Oligocene Kale basin, different movement directions of the Lycian nappes in northern and southern parts of the Datça-Kale Main Breakaway Fault and the top-to- the NNE directed shearing dominantly observed in the whole Menderes Massif.

1. Introduction

The Aegean region (Western Turkey, Aegean Sea and Greece) is one of the rapidly extending areas of the earth. The determination of a metamorphic core complex in the Aegean region (Lister et al., 1984), similar to that previously described in the "Basin and Range" region of North America with comparable tectonic characteristics, has created results deeply affecting tectonic perceptions of the region.

The similarity of structures, sedimentary basins, volcanism and underground sources developing under extensional tectonic regimes in two different and distant regions of the earth is noteworthy. Earth scientists working in these two different regions have encountered similar problems with mechanisms and initiation age of extensional tectonics, basin stratigraphy, and relationship of volcanism and tectonism. Currently in the Aegean region, where many national and international research groups continue to study, the search for answers to scientific problems continues.

This article comprises the viewpoint and assessment of the Ankara University Tectonics Research Group on the Cenozoic geology of Western Anatolia, located east of the Aegean region, containing underground sources in the form of borax, lignite, uranium, oil, gold and geothermal energy and where frequent destructive earthquakes are experienced. There are many research papers and tectonic hypotheses in the Aegean region making it impossible to explain each in detail and provide all related references. By drawing the reader's attention to this point, it may be appropriate for the reader to perform their own literature search.

1.1. Detachment Faults and Core Complex Formation

Metamorphic core complexes are the main tectonic features under the effect of large-scale crustal extension (Coney, 1980; Wernicke, 1981; 1985). Described for the first time in the "Basin and Range" region of North America, core complexes are known as "Cordilleran" metamorphic core complexes in the literature. Metamorphic core complexes comprise one or more tectonic slices represented

* *Corresponding author: Gürol Seyitoğlu, seyitoglu@ankara.edu.tr*

structurally from top to bottom by metamorphic and/or non-metamorphic lithologies, low angle normal fault(s) and basement rock units (Figure 1). The tectonic slices in the hanging wall block of the fault carry widespread effects of brittle deformation. Again metamorphic rocks have very low-low grades of metamorphism. Detachment faults (low angle normal faults), the main structural element of the core complex, and related ductile shear zones separate the non-metamorphic and/or low grade metamorphic rocks from crystalline (plutonic, high grade metamorphics) basement rocks. The basement units are generally Precambrian metamorphic rocks accompanied by Tertiary granitoid intrusions. In the literature movement of the detachment fault and related ductile shear zone are mentioned as compatible with Tertiary granitoid intrusions (Hetzel et al., 1995*b*; Işık et al., 2003*b*; 2004*a; b*).

Metamorphic core complexes are common extensional mechanisms in regions that have experienced thickening of continental crust in the past. Typical examples are described from different regions of the world (Cordillera, Aegean region, Himalayas, Alps). Metamorphic core complex studies in previous years have been completed on the areas of special interest of these basic concepts: (1) Metamorphic core complex models, (2) Low angle normal faulting (detachment faults) mechanics and geometry and (3) relationship between magmatism and extensional deformation (Fletcher et al., 1995).

Metamorphic core complex models: When the geometry and kinematics of regional scale extensional shear zones are considered, two different metamorphic core complexes are found. These are symmetric and asymmetric core complexes (Malavieille 1993) (Figure 2). Symmetric metamorphic core complexes are represented by two detachment faults with opposing directions and the ductile shear zones related to them. Middle and lower crustal rocks symmetrically outcrop along these zones. Contrary to symmetrical ones, exhumation of asymmetric metamorphic core complexes occur along a single detachment fault and related ductile shear zone.

Mechanics and geometry of detachment faults: Used by Armstrong (1972) to describe Tertiary-age normal faults, detachment faults control exposure of middle-lower plate rocks (Lister and Davis, 1989). According to Davis and Lister (1988) detachment faults have these basic characteristics: (1) Detachment faults bring non-metamorphic or low grade metamorphosed upper plate rocks into contact with high grade metamorphosed lower plate rocks. (2) Detachment faults separate uppermost younger rocks from older rocks below. (3) Detachment faults have regional scale. (4) Normal faults in the upper plate may link to detachment faults with different geometries. (5) Detachment faults show large displacements; this displacement may be on the scale of tens of kilometers. (6) Detachment faults are commonly ductile deformation structures and these are overlain by brittle deformation structures (Figure 3).

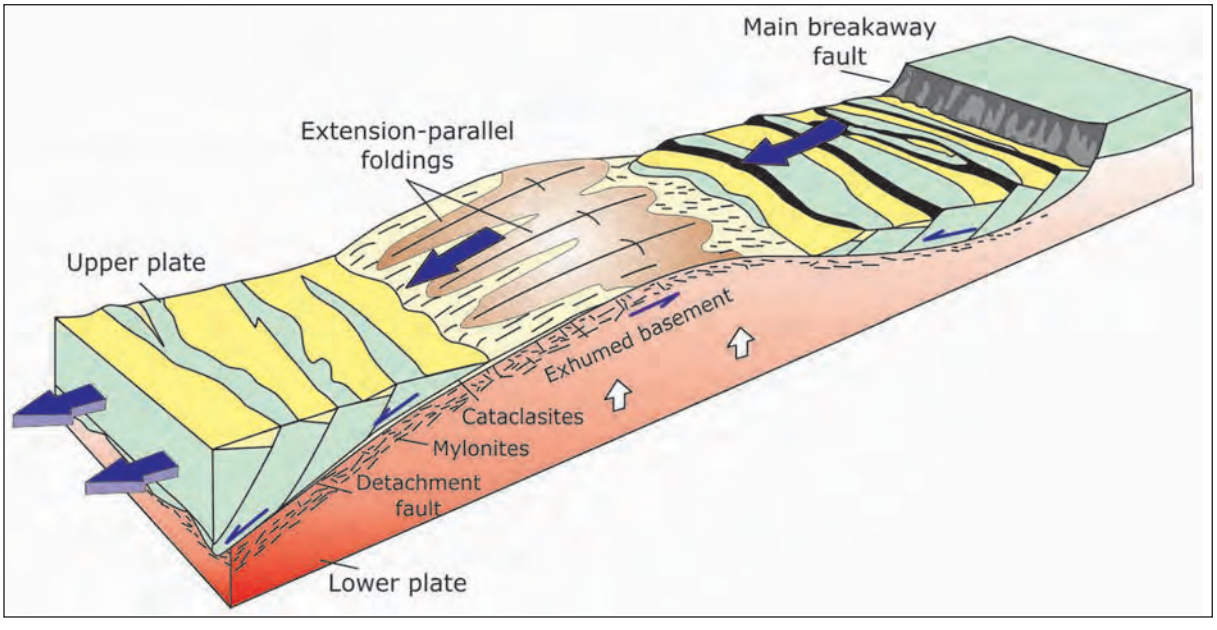

Figure 1- Typical metamorphic core complex and related structures (redrawn after Fossen 2010).

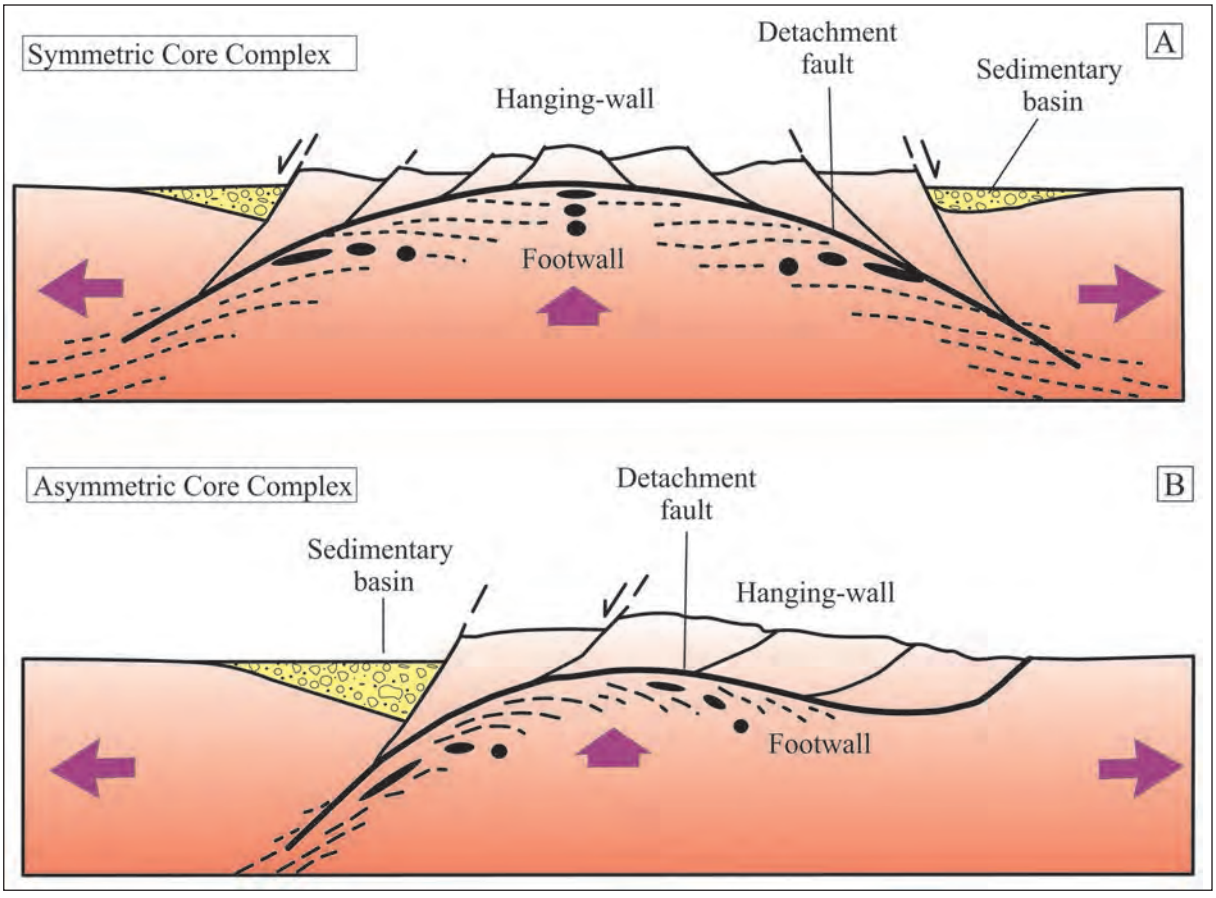

Figure 2- Metamorphic core complex models. A) Symmetric and B) asymmetric core complexes.

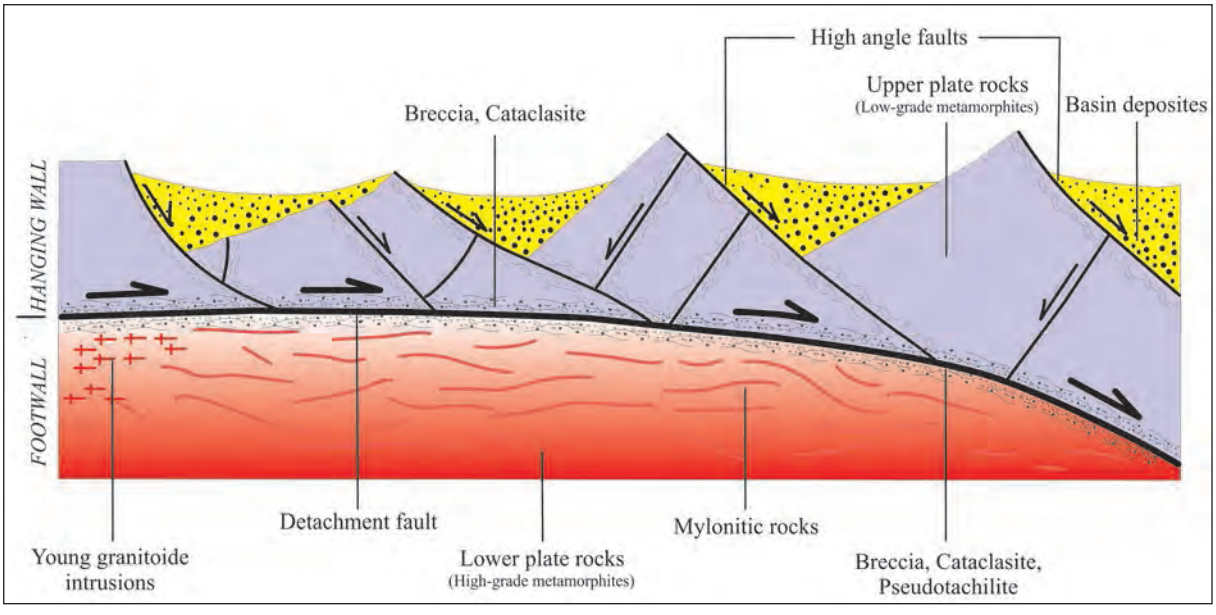

Figure 3- Cross-section of a typical detachment fault and internal structural characteristics.

While these characteristics of detachment faults are largely accepted, there is still discussion on the formation of the faulting and whether it is low-angle throughout development, in other words there is controversy over their origins. The first model of detachment faults proposed that these faults had low angles (dip lower than 30°) (Davis and Lister, 1988; Lister and Davis, 1989); however if the largest stress direction (σ_1) had a vertical direction during extension, the formation of a low-angle normal fault is not mechanically possible and thus it was reported that not every seismicity could produce such faulting. The latest developments on this topic may be seen in studies by Collettini (2011) and Prante et al. (2014).

Contrary to the "detachment faults develop with low angle" model, Buck (1988) and Wernicke and Axen (1988) recommended that detachment faults are initially high-angle normal faults and that due to doming of the footwall linked to the extensional regime, the faults become low-angle. In the flexural rotation/rolling hinge model, detachment faults in situations where the possibility of developing a sliding motion are not present, high-angle faulting develops in the hanging wall block. Thus within the system while motion continues along high-angle faults, non-active faults rotate to become low-angle. According to Buck (1988) and Wernicke and Axen (1988) the youngest faults are those with the most vertical dip.

Relationship between magmatism and extensional deformation: Many studies of metamorphic core complexes have proposed that crustal extension forms during magmatic activity and there is a genetic relationship between the two processes. According to this, rising mantle heat flow and/or mafic magma located at the bottom of the crust causes thermal softening and this initiates extension (Rehring and Reynolds, 1980; Reynolds, 1985; Gans et al., 1989; Lister and Baldwin, 1992).

Detachment faults in metamorphic core complexes typically present a "ridge and groove" structural topography (Spencer, 1982; 1984; Davis and Lister, 1988; Yin, 1991; Yin and Dunn, 1992). The undulated appearance of detachment faults and sedimentary deposition is related to (1) macroscopic geometry of banded rocks in upper and lower plates, (2) mesoscopic finite strain in upper and lower plates and (3) relative time of mylonitization. The structural characteristics representing the transition from ductile to brittle deformation in the footwall block of the detachment fault are generally related to evolution of the shear zone (Işık et al., 2003*b*). Accordingly, rocks in the ductile shear zone at middle crustal levels are carried into faulting zone in the upper section of the crust (Davis and Lister, 1988).

1.2. Extensional Tectonic Models in the Aegean Region

In the Aegean region with N-S extensional tectonics dominant, there are differing opinions on the initiation time of extension and its causes. Plate tectonic concepts were used in an attempt to explain the current structure of the Eastern Mediterranean (McKenzie, 1970) and focal mechanism solutions of earthquakes in the region were presented, forming the basis of a tectonic escape model (McKenzie, 1972; Figure 38). The tectonic escape model develops a cause-effect relationship and describes a process triggered by collision along the Bitlis Suture in Southeast Anatolia in the Middle Miocene resulting in development of the North Anatolian and East Anatolian Faults, western escape of the Anatolian plate, and concluding with the N-S extensional tectonic regime displayed in E-W grabens in Western Anatolia in the Late Miocene (Dewey and Şengör, 1979; Şengör, 1982; Şengör et al., 1985).

However, the N-S extensional tectonics in the Aegean is also explained by a back-arc extensional model. The time of subduction of the Aegean arc has key importance for back-arc extension, with the trench migrating south and southwest causing extension in the back-arc region. The initiation of subduction has been proposed as Middle Miocene (13 Ma) by Le Pichon and Angelier (1979; 1981) and as Pliocene (5 Ma) by McKenzie (1978) and Jackson and McKenzie (1988). Taking note of Cretan geology according to Meulenkamp et al. (1988) and tomographic images obtained from the subducting plate by Spakman et al. (1988), the initiation of subduction in the Aegean arc must have begun before at least 26 Ma; however for back-arc opening to form related to subduction the subducting plate must reach a certain length and accordingly the extension of the back-arc in the Aegean was stated to have begun in the Middle-Late Miocene. However, Thomson et al. (1988) have proposed that the roll-back process of the Aegean arc began to have effect in the Early Oligocene (Figure 4).

Among the reasons for acceptance of the initiation of extensional tectonics in Western Anatolia as "Late Miocene" (Şengör et al., 1985), the Late Cenozoic stratigraphy developed during lignite exploration by Turk-German cooperation in Western Anatolia played an important role (Becker-Platen, 1970;

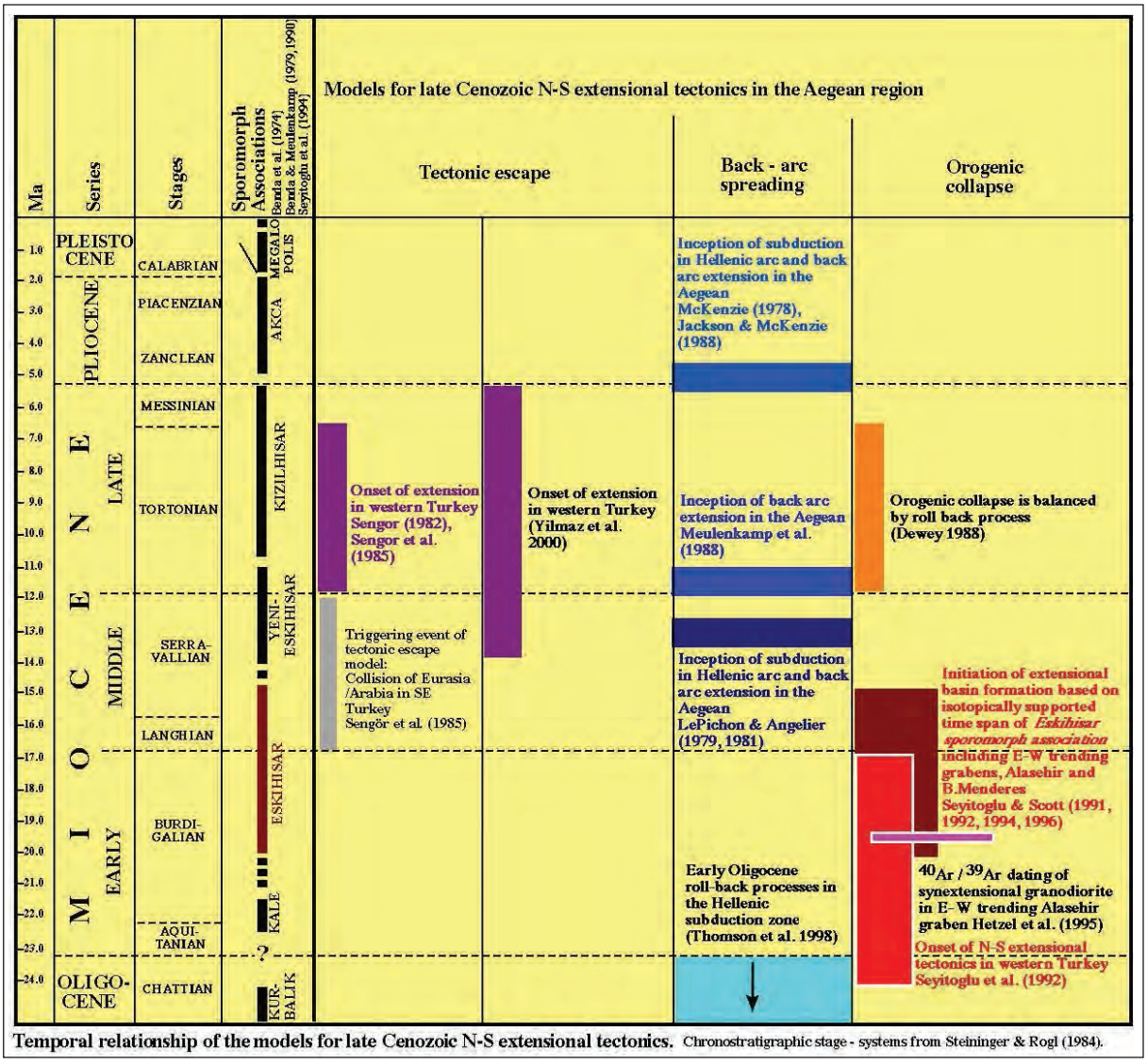

Figure 4- Temporal relationship of models proposed for Late Cenozoic N-S extensional tectonics in Western Anatolia. Chronological divisions from Steininger and Rögl (1984), age intervals of sporomorph assemblages from Benda et al. (1974), Benda and Meulenkamp (1979; 1990) and Seyitoğlu et al. (1994). The chart was adapted from Seyitoğlu and Scott (1996), by including data from Yılmaz et al. (2000) and Thomson et al. (1998).

1971). This study described the Neogene sequence in Western Anatolia as, from bottom to top, Upper Miocene Turgut member, Upper Miocene-Lower Pliocene Sekköy member, Lower Pliocene Yatağan member and Upper Pliocene-Lower Pleistocene Milet member. At the same time palynologic studies defined the sporomorph associations in Western Anatolia and related them to the above stratigraphy. According to Benda (1971) the Eskihisar sporomorph association is found between the base of the Turgut member and the lowest portion of the Sekköy member. The Yenieskihisar sporomorph association is found in the upper portion of the Sekköy member. With the possibilities presented by radiometric age dating, age dating began to be completed on volcanic rocks in Western Anatolia and the true placement of volcanic rocks and interlayered lignite levels and sporomorph associations began to be determined. From this point of view, Benda et al. (1974) represents the beginning, Benda and Meulenkamp (1979) the development and Benda and Meulenkamp (1990) the final stage. According to these studies, the age of the Eskihisar sporomorph association is determined as 20-14 Ma (Early-Middle Miocene), the age of the Yenieskihisar sporomorph association is 14-11 Ma (Middle-Late Miocene), the age of the Kızılhisar sporomorph association is 11-5 Ma (Late Miocene), the age of the Akça sporomorph

association is 5-2 Ma (Pliocene), and the Megalopolis sporomorph association is younger than 2 Ma (Pleistocene) (Benda et al., 1974; Benda and Meulenkamp, 1979; 1990) (Figure 4).

The presence of Early Miocene basins in Western Anatolia were revealed by Kaya (1981) using radiometric age dates for volcanic rocks in the region; however taking note of the NNE strike of the basins, a cross-graben model (Şengör, 1987) was proposed. According to this model, north-trending basins developed similarly to Tibet-type grabens during N-S compression in the Early Miocene and from the Late Miocene the E-W trending graben system continued to develop by cutting the north-trending basins. Sediments from the north-trending basins should be found as remnants in the E-W trending graben systems. The cross-graben model (Şengör, 1987) explains both the locations of the basins developing in the Early Miocene and the opinion that the N-S extensional tectonic regime began to develop in the Late Miocene in Western Anatolia. As a result, extensional tectonics in the Aegean continues to be linked to the tectonic escape model.

By using the establishment of the sporomorph associations age intervals, especially the position of Eskihisar sporomorph association on the west Anatolian stratigraphy, Seyitoğlu and Scott (1991) stated that "Late Miocene" timing of the initiation of basin development in Western Anatolia should change, because basin development is largely beginning in the Early Miocene and it is linked to the orogenic collapse (Seyitoğlu and Scott, 1991). Required for the cross-graben model (Şengör, 1987), as described in the short explanation of the hypothesis above, it is clear that finding Early Miocene age rocks in north-trending basins is not sufficient to refute to opinion that the cause of the N-S extension in Western Anatolia is the tectonic escape model. Here the important thing is Early Miocene age data from E-W trending basins and showing that these sediments are controlled by E-W trending faults. This data was obtained from Eskihisar sporomorph association in Hasköy, noted in brief by Becker-Platen (1970; p. 174). A field study of the sedimentary unit including the Hasköy lignites checked whether it was within the Büyük Menderes graben or not and showed the E-W graben system developed in the Latest Oligocene-Early Miocene. It was clearly stated that the tectonic escape model could not be shown as the reason for N-S extension in western Anatolia due to timing inconsistencies (Seyitoğlu and Scott, 1992*a*) (Figure 4).

In the Gördes basin, one of the north-trending basins, Early Miocene central volcanics cut both the ophiolitic basement of the Izmir-Ankara suture zone and the sedimentary sequence. This situation requires that compression due to the Izmir-Ankara suture zone end before the Early Miocene, if it is correct that the Lycian nappes in southwest Anatolia are originated from the Izmir-Ankara suture zone (Ricou et al., 1975). The Menderes Massif must be free of Lycian nappe cover before the Early Miocene due to Early Miocene basins observed at Gördes and Dalama. As a result the last Lycian nappe movements, documented as continuing until the Late Miocene in southwest Anatolia (de Graciansky 1970; Besang et al., 1977), must have developed as rootless gravity slides (Seyitoğlu et al., 1992).

It has been stated that there is a relationship between extensional tectonics, thought to begin in the Late Miocene period in Western Anatolia, and the character of volcanism with calc-alkaline volcanism dominant in the Early-Middle Miocene attributed to a compressional regime and alkaline volcanism becoming widespread in the Late Miocene related to extensional tectonics (Yılmaz, 1989; 1990; Savaşçın and Güleç, 1990; Güleç, 1991; Savaşçın, 1991). However, when the beginning of extensional tectonics in Western Anatolia was pulled back to the Latest Oligocene-Early Miocene, the volcanism in the region was reexamined and the geochemical signature of calc-alkaline volcanism developing during the extensional tectonic regime was found to be inherited from previous subduction events while in the advanced period of the continuing extensional tectonics alkaline volcanism developed with thinning of the crust. The situation of calc-alkaline volcanism at the beginning of the extensional tectonic period followed by later alkaline volcanism has also been observed in the "Basin and Range" province (Seyitoğlu et al., 1992, Seyitoğlu and Scott, 1992b).

E-W grabens in Western Anatolia contain sediments from the Early Miocene period based on palynological data (Seyitoğlu and Scott, 1992a; 1996*a*; Seyitoğlu, 1992); together with radiometric age data from volcanic rocks and palynological analyses in north-south basin fill which indicate that north-south basins began to develop in the Early Miocene (Seyitoğlu et al., 1992; Seyitoğlu and Scott, 1994; Seyitoğlu et al., 1994; Seyitoğlu, 1997; Seyitoğlu and Benda, 1998), all reveal that these two differently trending basins developed simultaneously. Noting that the tectonic escape and back-arc extension models could not explain the sedimentary

basin development in Western Anatolia due to age inconsistencies, an orogenic collapse model was proposed for the Early Miocene (Seyitoğlu, 1992; Seyitoğlu and Scott, 1996*b*). This proposal is different in terms of age from the Late Miocene orogenic collapse proposed by Dewey (1988) for the Aegean (Figure 4).

Koçyiğit et al. (1999) determined different structural and temporal relationships for extension in Western Anatolia and explained their findings with an episodic two-stage model. According to the model, extension in the region developed in two separate stages. The first event is related to orogenic collapse in the Early-Middle Miocene. The second event encompasses the Plio-Quaternary to the present day and is represented by normal faulting and graben formation. These two extensional stages are separated by a N-S crustal compressional period (Late Miocene-Early Pliocene). The two-stage graben model has been supported by a variety of later studies (Bozkurt, 2000; 2001; 2003; Sözbilir, 2002; Bozkurt and Sözbilir, 2004; Kaya et al., 2004; Beccaletto and Stenier, 2005; Bozkurt and Rojay, 2005).

Yılmaz et al. (2000) related the basis of extension in Western Anatolia to the tectonic escape model. According to the researchers the region was under the effects of a N-S compressional regime until the Early-Middle Miocene period. The Late Miocene-Early Pliocene (?) is a period of peneplanation. Then the region felt the effects of a N-S extensional regime. Similarly Gürer et al. (2009) advocated the presence of a NE-SW trending compression and E-W extensional regime in the Early-Middle Miocene. In the Pliocene-Quaternary period the basin formation in the region is explained within a N-S extensional regime related to the tectonic escape model.

1.3. Metamorphic Core Complex formation in the Aegean Region

Since the beginning of the 1980s the formation of metamorphic core complexes has been propounded to explain the exhumation of crystalline massifs in an extensional regime in the "Basin and Range" region of North America (Coney, 1980; Wernicke, 1981; Norton, 1986; Hill, 1987; Hodges et al., 1991; Malavielle, 1993). After Lister et al. (1984) proposed the formation of a metamorphic core complex similar to the regional extension in the "Basin and Range" province for the Aegean islands, many similar formations have been described in the Aegean region (Gibson, 1990; Gautier and Brun, 1994; Bozkurt and Park, 1994; Dinter et al., 1995; Jolivet et al., 1996; Vandenberg and Lister, 1996; Hetzel et al., 1995; Okay and Satır, 2000; Işık et al., 2001; Gessner et al., 2001). These are the core complexes of Menderes, Kazdağ, Rhodope, Cyclades and Crete (Işık et al., 2004) (Figure 5).

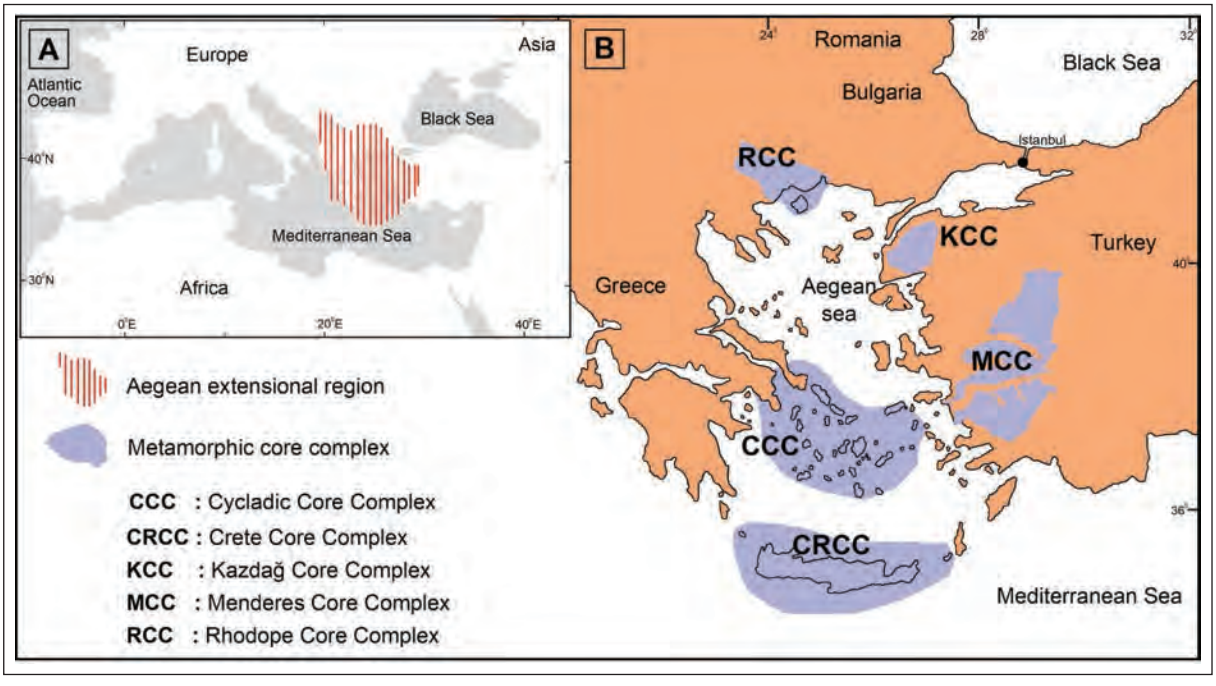

Figure 5- A) Map showing the location of Aegean extensional province. B) Metamorphic core complex formations in the Aegean region (Western Turkey, Aegean Sea, Greece) (adapted from Işık et al., 2003; 2004).

2. Menderes Core Complex

In the literature the Menderes Massif, defined as the Menderes core complex, is one of the areas with crystalline basement in the Aegean (Figure 5B). The massif is bounded to the north by the Izmir-Ankara-Erzincan zone and by the Lycian nappes to the south. While it is covered by Neogene sequences to the east, in the west it passes to units of the Cyclades massif. The Menderes Massif has a NE-SW broad dome-shaped exposure in Western Anatolia and is a complex formed of mainly metamorphic and granitic rocks.

The first geological information related to the massif was presented by Tchihatcheff (1867-1869). The first detailed geological mapping and investigation was performed by Philipson (between 1910-1915) and it was named the "Lydia-Caria massif". Philipson considered the massif a core unaffected by the Alpine orogeny and interpreted the gneisses as being Precambrian. In later years while Akyol (1924) described the massif as the "Saruhan-Menteşe massif", Ketin (1966) investigated it under the name "Western Anatolian massif". Today the widely-used nomenclature of "Menderes Massif" was used by Pajares (1944). The placement of the massif within the framework of plate tectonics and description of its evolution were completed by Şengör et al. (1984).

Since the 1950s many studies have increasingly been completed on the massif. In these studies the lithodemic nature of the units in the massif, timing of deformation and metamorphism and exhumation mechanism have all been topics of debate. Studies in the region specified the two main lithology groups that form the massif many years ago and these are widely accepted (Schuiling, 1962; Dürr, 1975; Şengör et al., 1984; Konak et al., 1987; Dora et al., 1995). However, some uncertainties still continue related to the concepts of core and cover and different opinions are common. One of these is related to the contact relationship between the two units. Some studies have determined the contact between the two units as unconformable (Çağlayan et al., 1980; Şengör et al., 1984; Konak et al., 1987; Dora et al., 1995; Candan et al., 2011). According to Şengör et al. (1984) this unconformity represents the Pan-African unconformity in the region. The character of the contact between the two units has also been defended as intrusive (Erdoğan, 1992; Bozkurt et al., 1993; 1995). Another of the uncertainties related to the units defined as core or cover is formed by their lithology, age and metamorphism. Core rocks are dominantly gneiss species and high grade metamorphic rocks. A significant portion of these gneisses are named "augen gneiss" due to their appearance. There are different interpretations of the primary rock for augen gneiss. While Schuiling (1958; 1962) determined they were originally sedimentary based on zircon morphology, Graciansky (1965) determined they were originally magmatic. Bozkurt et al. (1995) stated they were originally magmatic based on the geochemistry of the rocks. There are different opinions on the age of these gneisses. There are those who defend the gneisses as Precambrian (Şengör et al., 1984; Dora et al., 1995; Satır and Friedrichsen, 1986; Hetzel et al., 1998), in addition to those who consider them Tertiary (Bozkurt et al., 1993, 1995). Cover rocks, dominantly comprising lithologies such as schist and marble, are formed of low grade metamorphics. The limited fossil findings in these rocks are interpreted as from the interval between the Paleozoic and Tertiary (Dürr, 1978; Çağlayan et al., 1980; Şengör et al., 1984; Satır and Friedrichsen, 1986; Dora et al., 1995; Özer et al., 2001).

A variety of studies have examined the metamorphic characteristics of the massif. Just as some of these studies have interpreted that the massif was affected by a single metamorphism (Ashworth and Evirgen, 1984), some have determined characteristics of multiple metamorphism events (Schuiling, 1962; Akkök, 1983; Şengör et al., 1984; Candan, 1994; 1996; Oberhansli et al., 1997, Candan and Dora, 1998; Whitney and Bozkurt, 2002). The general view is that the character of the current metamorphism of the massif was shaped by Barrovian-type metamorphism in the Tertiary and that metamorphism developed under green schist-amphibolite facies conditions. This metamorphism is known as the "Main Menderes Metamorphism" in the literature (Şengör et al., 1984).

Since the 1990s studies in different regions of the massif have propounded the view that the massif is a core complex (Verge, 1993; Bozkurt and Park, 1993; 1994; Hetzel et al., 1995*a*, Emre and Sözbilir, 1997; Gessner et al., 2001; Işık and Tekeli, 2001; Ring et al., 2003; Seyitoğlu et al., 2004). Contrarily there are studies in the literature that do not concur that the formation is a metamorphic core complex (Okay, 2001; Erdoğan and Güngör, 2004; Westaway, 2006; Akay, 2009).

2.1. Lithological Characteristics

When we investigate the terminology of massif for the broad outcrop of the Menderes core complex in Western Anatolia, it appears to be based on metamorphic rocks with different metamorphisms and deformations and the young granitoid intrusions that cut them.

Taking note of the protolith stratigraphy of the metamorphics within this, defining them as core/Pan African basement and cover units has become a tradition. According to this, Pan-African basement is formed of Precambrian-Cambrian metasedimentary rocks and metamagmatites that have intruded them. Within this framework the basement rocks are paragneiss and schist and metamagmatite lithologies with a primary intrusive relationship to these. Cover units are Paleozoic-Mesozoic metapsammite, metapelite and metacarbonate rocks. The lower sections of the cover units are mainly represented by marble intercalated with schist and quartzite while upper sections commonly include thick marble lithologies. Within these sections it is possible to observe metabauxite levels with rudist fossils. The uppermost section is formed of pelagic marble levels (Şengör et al., 1984; Satır and Friedrichsen, 1986; Konak et al., 1987; Oberhansli et al., 1997; Candan et al.; 1998; 2011; Dora et al., 1990; 1995; 2001; Işık, 2004; Koralay et al., 2004). A variety of studies have determined the primary relationship between Pan-African basement and cover units as a regional scale unconformity (Çağlayan et al., 1980; Şengör et al., 1984; Candan et al., 2011).

Apart from metamorphics the other lithologies in the massif are local granitoid intrusions cutting the metamorphics and deformed with the metamorphics. Isotopic dating of these rocks, exposed at various scales especially in the upper and northern sections of the massif, have revealed them to be Miocene age (Hetzel et al., 1995; Delaloye and Bingöl, 2000; Işık et al., 2004*b*; Glodny and Hetzel, 2007). The intrusions are petrographically granodiorite, quartz monzonite and granite, with lesser amounts of quartz diorite and diorite. Geochemical data suggest the intrusions are generally subalkaline-peraluminum I-type (Işık et al., 2003; 2004*a, b*; Aydoğan et al., 2008; Akay, 2009).

All these lithologies were transformed at varying rates and into different types of shear zones during exhumation of the massif.

2.2. Structural Characteristics

In structural terms the Menderes Massif is a regional-scale Tertiary core complex. Within this framework, the massif represents mega, meso and micro structures developed with penetrative character in the extensional regime (Figure 6).

The megascopic structures in the Menderes Core Complex are formed of detachment faults and/or shear zones related to these (Figure 6) (Işık et al., 2003*a,b*; 2004*b*; Işık and Seyitoğlu, 2006; 2007). From south to north, these are (Figure 7): (1) Datça-Kale Main Breakaway Fault, (2) Lycian Detachment Fault, (3) Kayabükü Shear Zone, (4) Büyük Menderes Detachment fault (5) Alaşehir Detachment Fault and (6) Simav Detachment Fault. These structures are accompanied by high-angle normal faults that control the current topography of the core complex.

2.2.1. Datça-Kale Main Breakaway Fault

Datça-Kale Main Breakaway Fault is NE-SW trending normal fault zone extending from Gökova Gulf near Datça to the Denizli basin (Figure 7). It was interpreted by Seyitoğlu et al. (2004) as the fault playing a role in the initial exhumation of the Menderes core complex (see: Section 4). The Gökova graben at the southwest corner of Turkey is 150 km long and between 5 and 30 km wide. The north and south sides of the graben are bounded by faults; the south side is bounded by the Datça Fault (Kurt et al. 1999). On submarine seismic reflection profiles the Datça Fault (Kurt et al., 1999) appears to be a north-dipping listric normal fault with clear control of the sedimentary sequence on the hanging wall (Seyitoğlu et al., 2004). Investigations in the NE-SW-trending Kale basin have discovered that the basin begins with Upper Oligocene units (Hakyemez, 1989; Akgün and Sözbilir, 2001; Gürer and Yılmaz, 2002). During our investigations in the southeast section of the basin we observed the Kale-Tavas basin units are bounded by NE-SW-trending and NW-dipping normal faults. These faults are interpreted as having a genetic association with the Datça Fault located to the southwest. The footwall of the breakaway fault comprises dominant carbonate rocks of the Lycian nappes outcropping in the region and ophiolite and ophiolitic melange rocks. Basin fill is found in the hanging wall of the fault (Hakyemez, 1989; Akgün and Sözbilir, 2001; Gürer and Yılmaz, 2002).

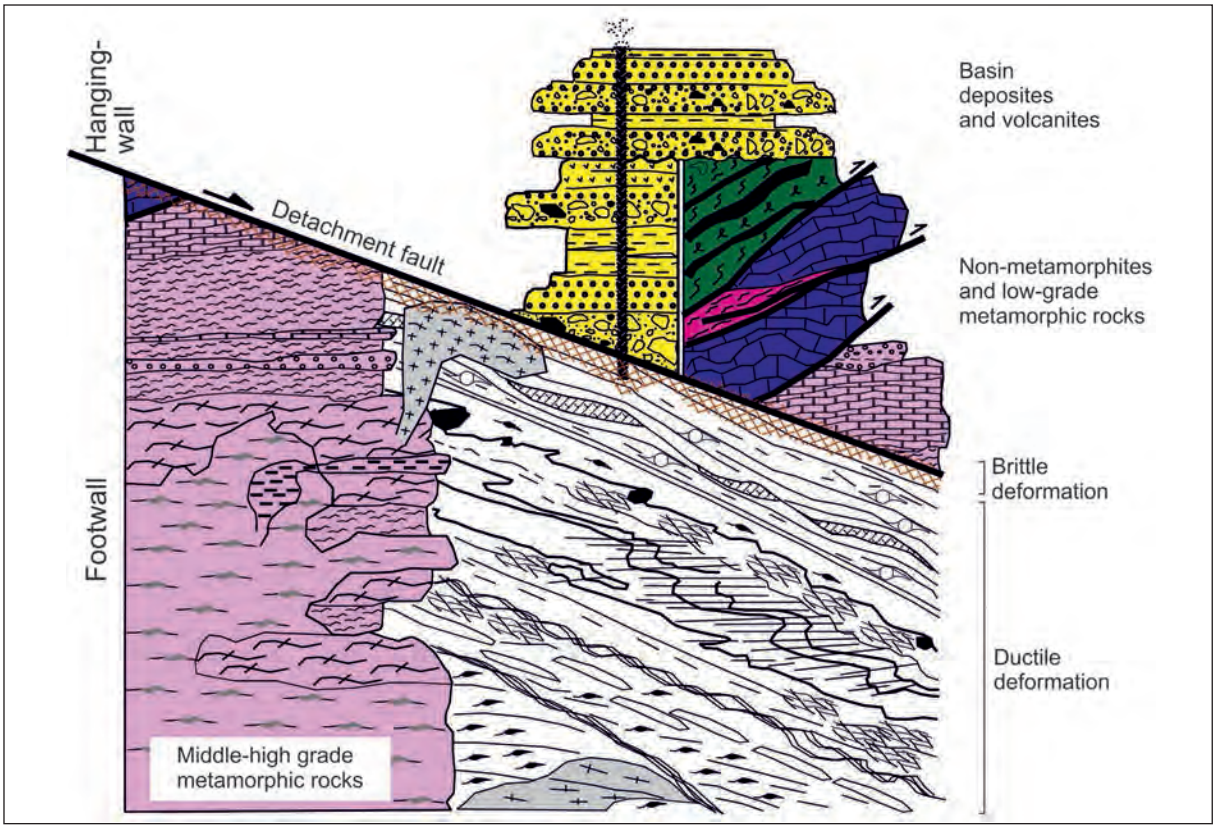

Figure 6- Cross section showing detail of a general detachment fault observed in the Menderes Metamorphic Core Complex.

2.2.2. Lycian Detachment Fault

The Lycian nappes, bordering the south and southeast of the Menderes core complex, have a special importance for the evolution of the Tethys ocean and Alpine orogeny. The Lycian nappes represent tectonic slices with different extents and tectonically overlie the relative Beydağı autochthon to the south. Basically the nappes are formed of three main units. These are; Lycian thrust slices formed of Upper Paleozoic-Tertiary aged sedimentary rocks; ophiolitic melange rocks called the Lycian melange and peridotite nappes called the Lycian ophiolite (Collins and Robertson, 1998). Though there is no full consensus related to the origin of the Lycian nappes, it is widely accepted that these tectonic slices represent the northern branch of the Neo-Tethys ocean located north of the Menderes Massif and moved from north over the massif to south (Şengör and Yılmaz, 1981; Şengör et al., 1984). It is proposed that emplacement of the nappes in the region occurred in the interval from the Upper Cretaceous to Late Miocene (Okay, 1989; Collins and Robertson, 1998; 1999). Studies in recent years which found carpholite mineral representing high pressure metamorphism at the base of the Lycian nappes (Oberhansli et al., 2001; Rimmele et al., 2003) have led to different interpretations relating to the geodynamics of the region. Rimmele et al. (2003) defined a shear zone between the Menderes Massif and the Lycian nappes. They determined three deformation events based on interpretations of the kinematics of deformation in the region. These are; (1) deformation represented by southern emplacement of the Lycian nappes; (2) main Alpine deformation and (3) deformation representing regional extension. Accordingly, the first deformation represents the transport of the Lycian nappes from the north and emplacement in the south. Later deformation represents Eocene main Alpine deformation and related metamorphism. Researchers explain northerly kinematics of this deformation as back thrusting. The deformation related to Oligo-Miocene extension is defined in the core and cover units of the Menderes Massif (Rimmele et al., 2003).

Ring et al. (2003) interpret the discontinuity between the Menderes Massif and Lycian nappes as reactivation of thrust faults forming the detachment fault. According to the researchers, the Menderes

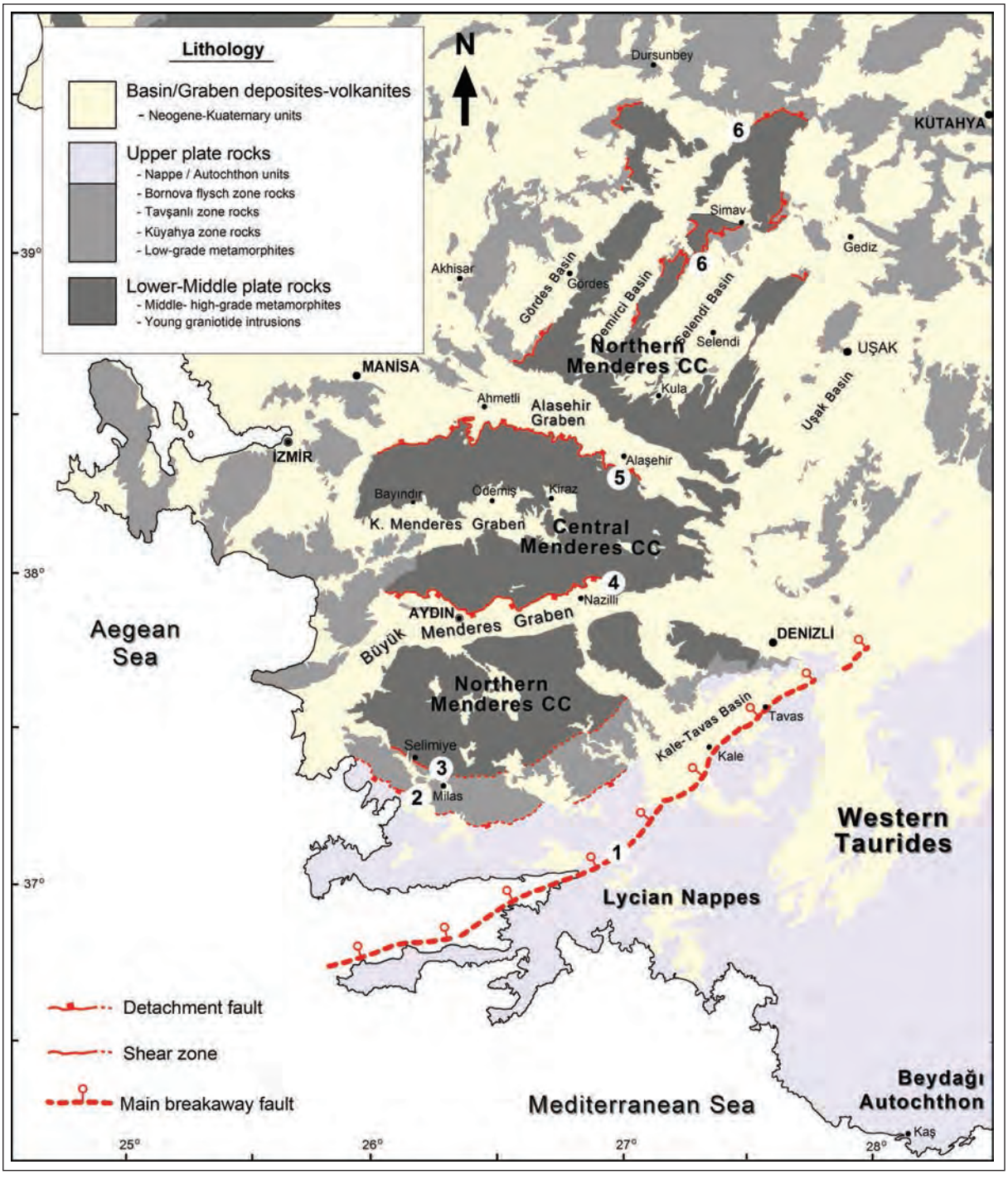

Figure 7- Detachment faults and ductile shear zones observed in the Menderes Core Complex (adapted from Işık et al. 2003, 2004). 1: Datça-Kale Main Breakaway Fault, 2: Lycian Detachment Fault, 3: Kayabükü Shear Zone, 4: Büyük Menderes Detachment fault, 5: Alaşehir Detachment Fault and 6: Simav Detachment Fault. See text for related references.

Massif is a symmetric core complex with the Lycian Detachment Fault controlling the southern section.

2.2.3. Selimiye (Kayabükü) Shear Zone

Though the Selimiye (Kayabükü) Shear zone was first described as an extensional detachment fault by Bozkurt and Park (1994), it was named the Kayabükü Shear Zone by Işık et al. (2003*a*, 2004). The extensional structures in this section have been examined in numerous studies (Bozkurt and Park, 1994; 1997*a*; 1997*b*; 1999; Bozkurt et al., 1995; Bozkurt, 2004).

The region of the Selimiye Shear Zone is important in some regards. A significant portion of the interpretations and assessments of the Menderes Massif are the result of studies in this section. The presence of the core-cover contact and character of the contact proposed within the basic stratigraphy of the massif is debatable. Many studies have interpreted the contact between the two units as the Pan-African unconformity (Şengör et al., 1984; Konak et al., 1987; Candan et al., 2011). According to Bozkurt and Park (1994), cover rocks of the Menderes Massif are separated from the core rocks by a south-dipping detachment fault with the extensional character of the contact examined in detail by later studies (Bozkurt and Park, 1997*a*; 1997*b*; Bozkurt et al., 1995; Bozkurt, 2004). The interpretation of the contact as again having intrusive character with Cenozoic-age metamagmatites representing the core rocks has been made (Bozkurt and Park, 1994). However, isotopic ages obtained from these rocks indicate the metamagmatites are Precambrian in age (Hetzel and Reischmann, 1996; Loos and Reischmann, 1999; Gessner et al., 2004).

Our field studies in the region have shown that there is no typical detachment fault between the two units and that the contact relationship has the characteristics of a ductile shear zone (Figures 7, 8). Stated differently, the contact was not affected by brittle deformation processes. The protolith rocks of the Selimiye Shear Zone comprise metamagmatite, metapsammite, metapelite and metacarbonate rocks. These rocks have been affected by upper green schist and amphibolite facies metamorphism. The multiple metamorphism features in the massif have been determined in a variety of studies (Candan and Dora, 1998; Whitney and Bozkurt, 2002; Gessner et al., 2004). Metamorphic rocks are cut by small outcrops of young granitoid intrusions.

The effects of extensional deformation are clearly observed in the rocks of the region. Our hand sample and microscopic investigations have shown widespread mylonitization in these rocks. Foliation and lineation structures are typical in mylonitic rocks. In outcrop and hand samples mylonitic foliation is represented by flattened feldspar minerals and quartz banding and mica mineral orientations. Though the development of this foliation is penetrative, it presents a heterogeneous development linked to lithology differences. Foliation planes are dominantly NW-SE trending and dip SW with dip amounts varying between 5° and 55°. These planes are found with E-W and ENE-WSW trends locally. These clear foliation planes are overprinted by secondary weak and poorly developed foliation planes. The secondary foliation has similarly oriented trend, however dips are from 30° to 70° southwest. Lineation is another typical structural component of extensional deformation. Stretching lineation is represented by lengthened minerals and mineral groups. Stretching lineation strikes NNE-SSW and NE-SW with dips SSW and SW.

Microscopic investigation has found that blastomylonite is dominant in metamorphic rocks in a wide area in the region. These rocks are accompanied by different mylonite formations. Porphyroclast composition is dominantly large feldspar grains in mylonitic rocks. Biotite, muscovite, quartz and tourmaline minerals are observed at varying sizes as porphyroclasts. Matrix composition of the rock is mainly recrystallized quartz and mica minerals. Recrystallized feldspar minerals are again observed in the matrix. In areas where crystal plasticity deformation mechanisms developed strongly, development of bands up to a centimeter thick parallel to foliation in quartz minerals is typical. In addition to band development kinking of recrystallized grains and core-shell textures are among other features of the crystal plasticity deformation mechanisms.

Mesoscopic and microscopic kinematic indicators reveal that exhumation of core rocks along the Selimiye shear zone occurred with NE oriented movement followed by SW oriented movement. Young intrusions outcropping in the region include structures representative of SW movement showing that these intrusions were affected by the late stages of extension.

Figure 8- Field view of Selimiye (Kayabükü) shear zone.

2.2.4. Büyük Menderes Detachment Fault

Büyük Menderes Detachment Fault bounds the northern side of the Büyük Menderes graben (Figure 7). This fault has also been named the Başçayır (Emre and Sözbilir, 1997) or Güney (Gessner et al., 2001*a*; Ring et al., 2003) detachment fault. With a curved geometry, the footwall of the Büyük Menderes Detachment Fault is composed of metamorphic rocks of the massif and young granitoids (Figure 9). Here the metamorphic lithologies and structural features may be correlated with the characteristics of the Selimiye shear zone. Common mylonitic orthogneiss with mylonitic paragneiss (mica gneiss, garnet mica gneiss, biotite gneiss), schist (mica schist, garnet mica schist, muscovite quartz schist, quartzitic schist, kyanite staurolite schist) and marble are contained in the footwall of the detachment fault. Mesoscopic and microscopic kinematic analysis data from mylonitic rocks have revealed two different kinematic orientations, similar to the Selimiye Shear Zone. Accordingly the footwall rocks were first affected by ductile deformation representing top-to-the NE movement linked to regional extension and then by deformation related to a top-to-the SSW movement overprinting textural features. The Büyük Menderes Detachment Fault is related to the second deformation. Hanging wall rocks are low-grade metamorphic rock masses of varying sizes and sedimentary units of the Büyük Menderes graben. Lithologies representing mylonitic gneiss are observed in local areas. The fill in the Büyük Menderes graben is dated as Early Miocene-Quaternary and consists of mainly clastics (Seyitoğlu and Scott, 1992*a*; Şen and Seyitoğlu, 2009).

There are outcrops where the detachment fault plane and slip surface are visible (Figure 10). The lithology which best preserves the plane is marble. The Büyük Menderes Detachment Fault trends NE-SW and NW-SE and dips from 10°-42°. In sections where fault striations have been preserved on the plane, the lineations are NE-SW; with a small amount NNE-SSW. The dip direction of the fault lineations is

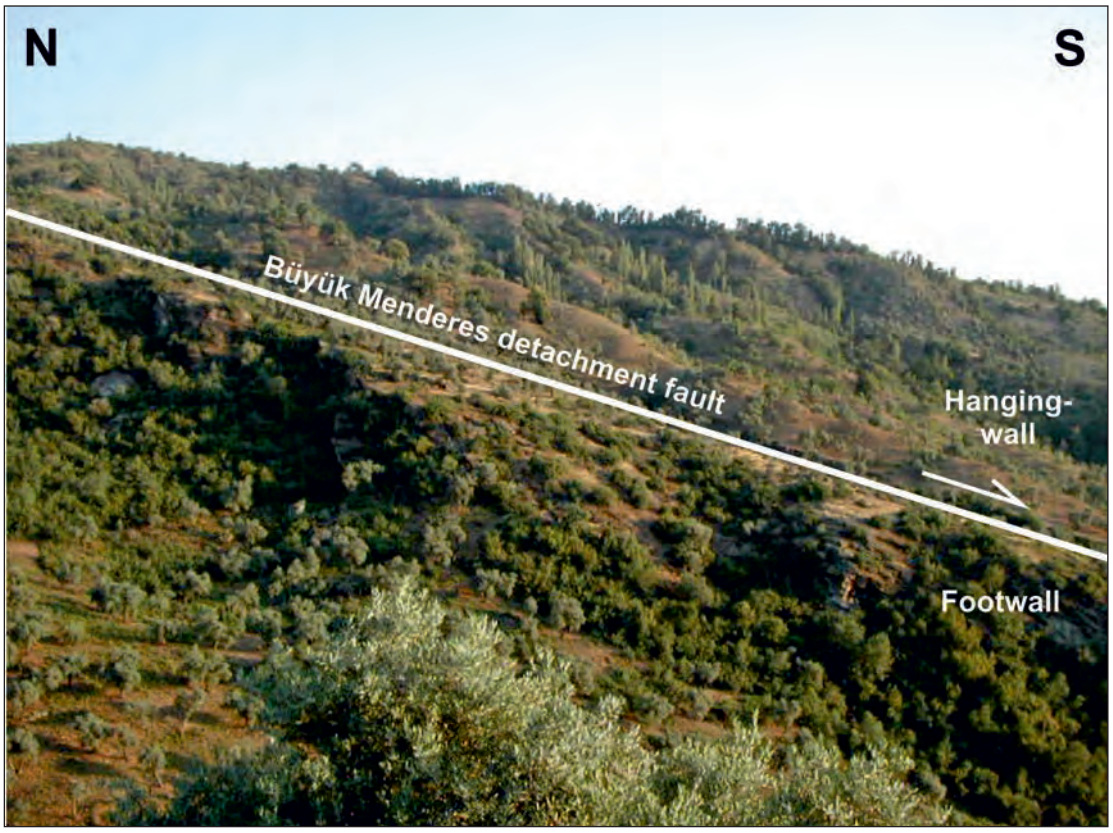

Figure 9- Appearance in the field of the Menderes Detachment Fault. See text for details.

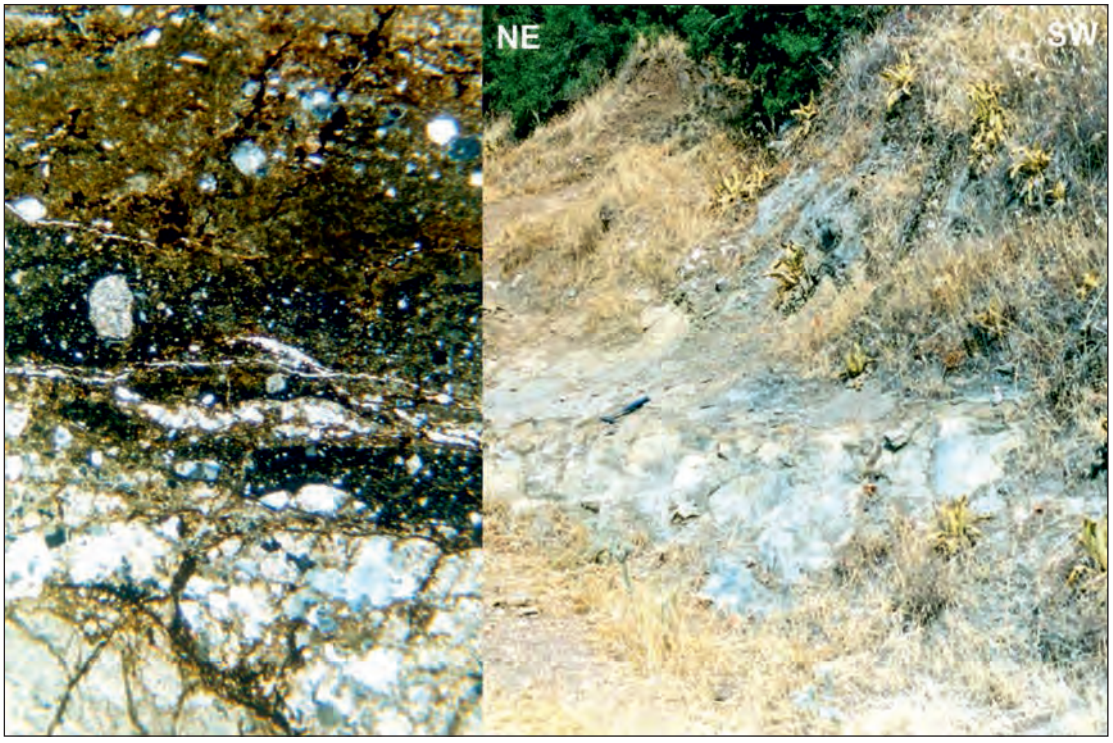

Figure 10- Appearance of brittle deformation of the hanging and foot walls of the Büyük Menderes detachment fault in the field (right). Thin section appearance of the slip plane of the detachment fault. Upper section of the photograph shows development of cataclasite on the thin section slip plane (left).

toward the SW. Along the detachment fault, rock above and below the fault plane comprises a cataclastic zone (Işık et al., 2003b) with thickness varying from 1 to 60 m. While the severity of brittle deformation is very intense in sections close to the fault plane, in areas distant from the plane this effect gradually reduces. The systematic development of the effects of brittle deformation is clearly observable, especially in the footwall. Accordingly, in sections close to the fault plane cemented (cohesive) breccia and cataclasite formations are dominant (Figure 10). The hanging wall of the fault plane has characteristic uncemented breccia and/or fault gouge.

2.2.5. Alaşehir Detachment Fault

The Alaşehir Detachment Fault is among typical detachment faults developed within the crust (Figure 11). In this regard, it has been a study topic for many research groups (Emre, 1992; Hetzel et al., 1995*a*; 1995*b*; Emre and Sözbilir, 1997; Koçyiğit et al., 1999; Gessner et al., 2001*a*; Seyitoğlu et al., 2002; Işık et al., 2003*b*; Seyitoğlu et al., 2004; Purvis and Robertson, 2005; Hetzel 2007, Öner and Dilek, 2011). The Alaşehir Detachment Fault has been described as the Allahdiyen (Emre, 1992), Karadut (Emre and Sözbilir, 1997), Çamköy (Koçyiğit et al., 1999) and Kuzey detachment fault (Gessner et al., 2001a; Ring et al., 2003) in the literature. The characteristics of the Alaşehir Detachment Fault have been determined in detail by Işık et al. (2003*b*).

The footwall of the fault is again various metamorphic rocks of the massif and syn-tectonic young granitoid intrusions (Işık et al., 2003*b*). The metamorphic rocks have similar lithological characteristics to the Selimiye Shear Zone and the footwall of the Büyük Menderes Detachment Fault. Along the detachment fault, outcrops of varying sizes of syn-tectonic intrusions are granodiorite, monzonite and granite rock types. These lithologies are accompanied by mafic inclusions in places. The main mineral composition of these rocks is feldspar, quartz and varying ratios of biotite and hornblende; secondary minerals include apatite, sphene, ilmenite and opaque minerals. Both metamorphic rocks and young intrusions show the effects of ductile and brittle deformation indicating exhumation linked to extension (Figures 12 and 13).

Ductile deformation in these rocks is characterized by widespread mylonitic formations. Apart from blastomylonite formations in metamorphic rocks, protomylonite, mylonite and ultramylonite formations are found within granitoid rocks. Typical structural elements in these rocks are mylonitic foliation and lineations, with similar textural characteristics to mylonitic foliation and lineations observed in other zones in the massif.

Along the detachment fault foliation has NE-SW orientation, with dominant dip direction to the NW. Fewer SE dip directions have been measured. Stretching lineations are typical lineation features in these rocks. They have NE-SW trend and NE dip. Kinematic data obtained along the zone (asymmetric porphyroblasts, S-C, -C' structure, oblique foliation,

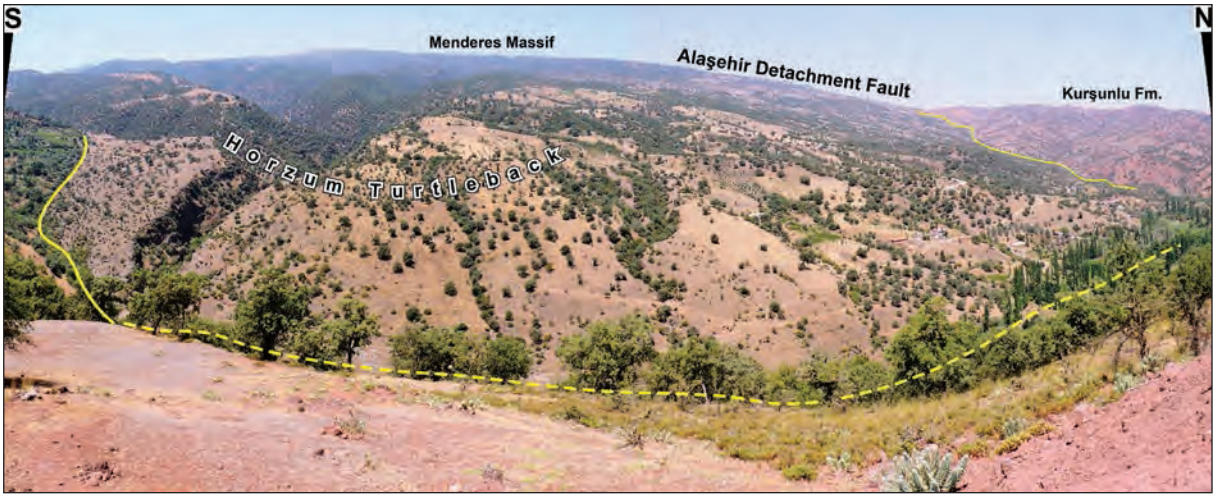

Figure 11- General appearance of the Alaşehir Detachment Fault (Kavaklıdere-Horzumkeserler road). For characteristics of the detachment fault see Işık et al. (2003b), for its role in graben development see Seyitoğlu et al. (2002) and for the "Horzum Turtleback" formation mechanism see Seyitoğlu et al. (2014).

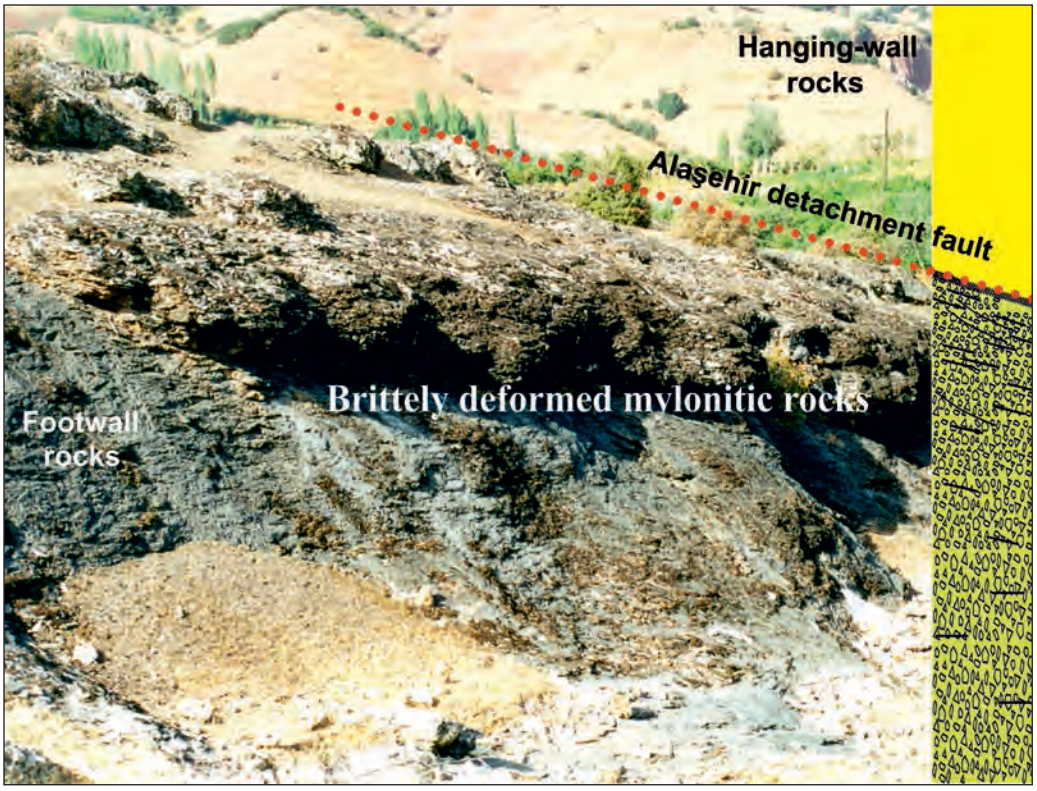

Figure 12- Appearance of brittle deformation features of the footwall of the Alaşehir Detachment Fault in the field.

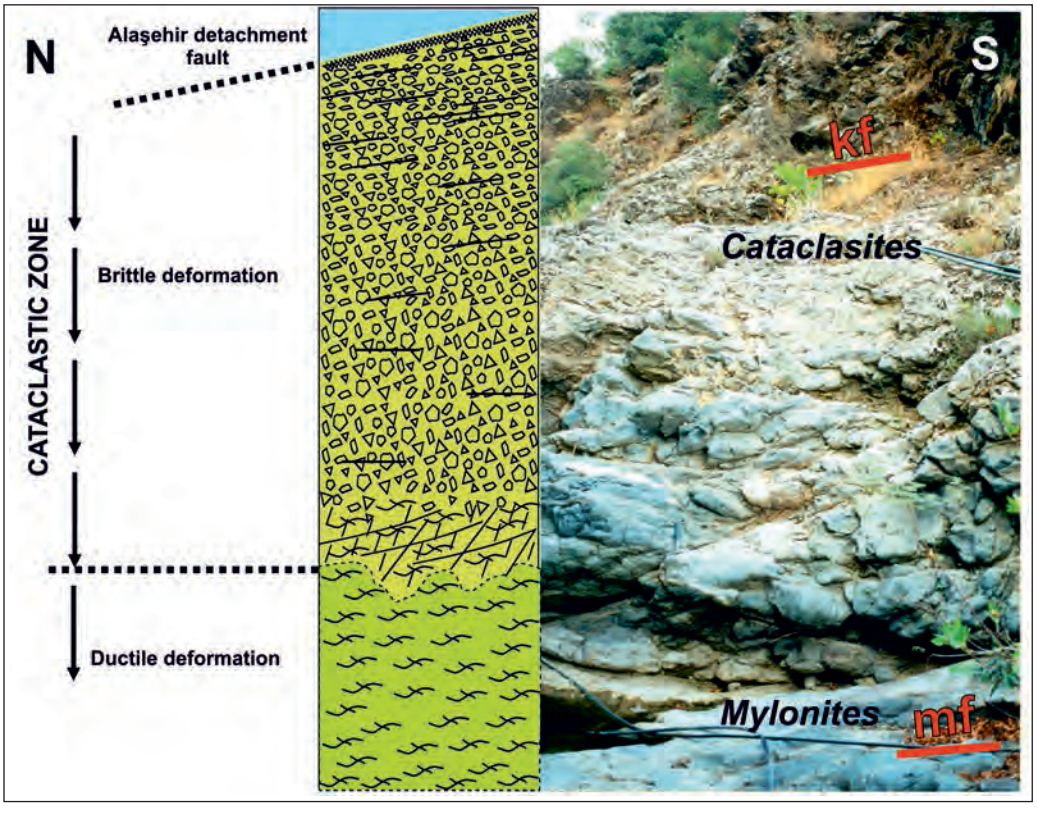

Figure 13- Appearance of ductile-brittle deformation transition on the Alaşehir Detachment Fault in the field and schematic sections of this relationship.

mica fish) indicate ductile deformation developing as a result of a top-to-the NE directed extensional regime.

In the field ductile-brittle transition is clearly observed along the Alaşehir Detachment Fault (Figure 13). Işık et al. (2003*b*) described a cataclastic zone within the detachment fault, which incorporates products of brittle deformation. The cataclastic zone is 1 to 20 m thick, and represents different brittle deformation events (Figure 12). The zone begins with systematic and non-systematic fracturing at the base, before transitioning to breccia toward the top. The textural features of the breccia levels change toward the top and a transition is seen to cataclasite-type fault rocks (Figure 12). Especially in cataclasite rocks lateral continuity is limited and rough cataclastic foliation is locally observed. Generally this foliation appears parallel to mylonitic foliation. The top of the zone is bounded by the detachment fault surface. The slip surface is locally preserved and fault striations are clear. The slip lineations are NE-SW trending and dip NE, in accordance with the stretching lineations linked to ductile deformation. This situation indicates that the Alaşehir Detachment Fault was formed by ductile and brittle stages within the same regime (Işık et al., 2003*b*).

The hanging wall of the Alaşehir Detachment Fault is mainly formed of sedimentary rocks of the Alaşehir graben. This sedimentary sequence of different formations is Early Miocene-Quaternary in age (Seyitoğlu et al., 1996*a*; Seyitoğlu et al., 2002; Şen and Seyitoğlu, 2009).

2.2.6. Simav Detachment Fault

The Simav Detachment Fault is at the very north of the Menderes core complex. The fault was first described by Işık et al. (1997) and Işık and Tekeli (2001) (Figure 14). The Simav Detachment Fault divides the moderate-high grade metamorphic rocks of the massif and young granitoid rocks in the region, from low-grade metamorphic rocks, ophiolitic melange rocks and Neogene-Quaternary sedimentary and volcanic basin sediments.

Moderate-high grade metamorphic rocks in the footwall of the fault are mainly composed of gneiss

Figure 14- General appearance of the Simav Detachment Fault in the field.

(banded gneiss, orthogneiss, biotite gneiss) and schists. Migmatitic banded gneiss outcrops in the lowest sections of the region structurally. Sequences of light- and dark-colored bands are clear, with thickness of bands from a few mm to a few cm. These metamorphics structurally transition to biotite gneiss in upper sections. Schist interlayering in the gneiss and marble, amphibolite bands and lenses at varying levels are present. Orthogneiss has similar features as those mentioned in other sections of the massif. Other lithologies in the footwall of the Simav Detachment Fault are granitoid intrusions (Eğrigöz and Koyunoba plutons). Granitoids are medium-grained, have holocrystalline granular texture in hand samples and are formed of granodiorite, granite and monzonite rock types. Occasional felsic, with lesser amounts of mafic, dikes and pegmatites are among other rocks found in the footwall.

Along the Simav Detachment Fault these rocks have been affected by differing amounts of ductile deformation, and may be compared to the Alaşehir Detachment Fault, especially. Mylonitization has affected metamorphics and granitoids by varying amounts. Mesoscopic and microscopic investigation has provided important information related to mylonitization along the Simav Detachment Fault (Işık and Tekeli, 1998; 1999; 2001; Işık, 2004; Işık et al., 2004). Mylonitic foliation and lineation are characteristic. In gneiss and schist rocks mylonitic foliation is represented by quartz banding, recrystallized quartz and mica minerals and preferential orientation of biotite, plagioclase, sometimes muscovite, sillimanite, kyanite and tourmaline porphyroblasts. In marbles foliation is visible as recrystallized calcite and/or calcite prophyroclasts with preferential stretching. In pegmatites a foliation formed by stretched recrystallized quartz and muscovite grains is typical. In granitoids mylonitic foliation is generally represented by recrystallized quartz and biotite minerals. The measured foliation planes are dominantly NW-SE striking and slope to the SW. Other sections of the foliation measurements are NE-SW striking and slope to the SE. The mean dip amount is 27°. Stretched quartz, feldspar, kyanite, tourmaline, hornblende and mica are common minerals and groups that form the mylonitic lineation (Figure 15). The lineation direction is NE-SW. The dominant dip direction of these lineations is SW, with fewer NE dips measured. In this section of the massif, there is NW-NE stretching lineation found. The dip

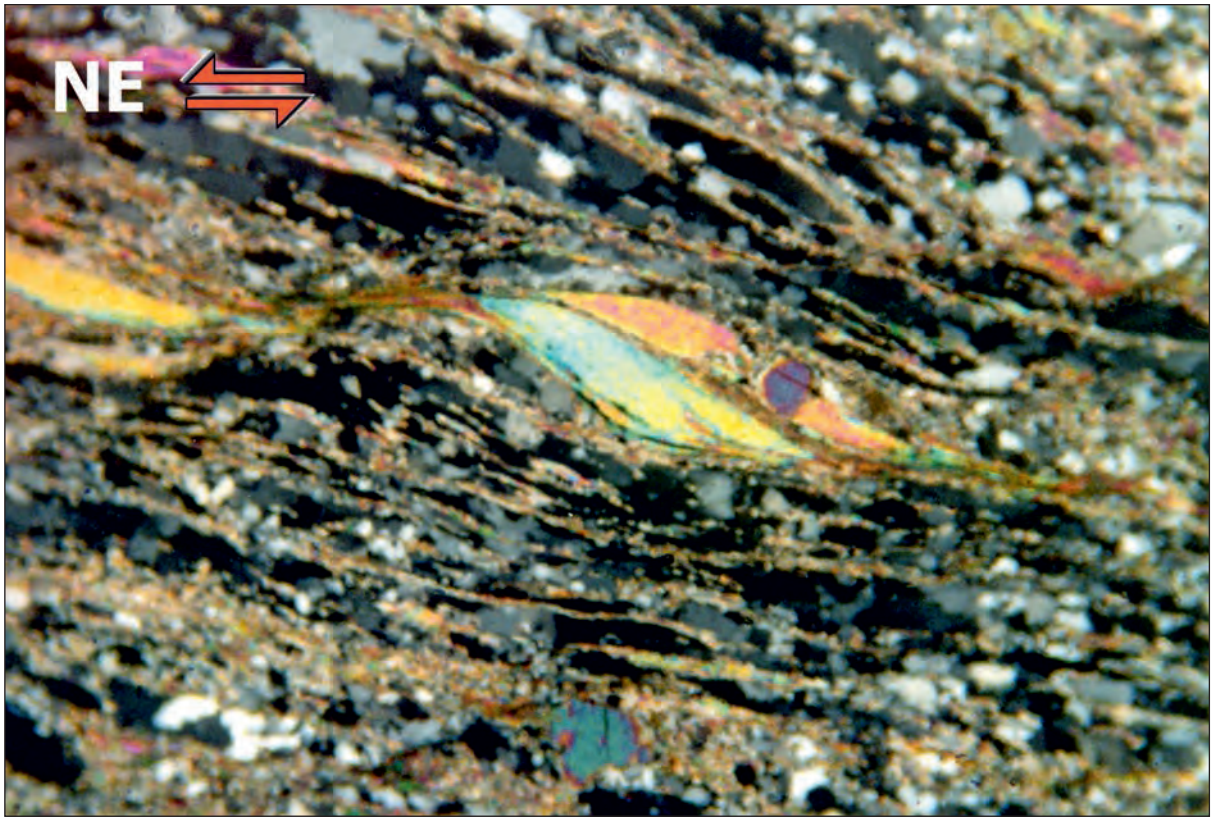

Figure 15- Typical mica fish appearance on oriented thin section. Movement direction top-to-the NE.

direction of these lineations is SW. Perpendicular to mylonitic foliation and on parallel surfaces to lineation, there are common kinematic indicators (asymmetric porphyroclasts, oblique recrystallization, mica fish, S-C and S-C' fabrics, shifted grains and V-pull apart micro textures). These indicators show the extensional tectonics forming the Simav Detachment Fault represented a top-to-the N-NE directed movement (Figures 15 and 16).

Brittle deformation structures in the Simav Detachment Fault are defined by a cataclastic zone. The apparent thickness of the zone reaches 100 meters, but typical features are observed within 30 meters. Mylonitic rocks within the cataclastic zone have fractured outcrops and hand samples, small-scale faulting, fragmentation, crushing and alteration features. In sections close to the fault plane there are high rates of crushing and milling with cataclasite and local breccia fault rocks observed with fracturing, mesoscopic faulting and breccia formation in sections slightly further from the plane.

The hanging wall of the Simav Detachment Fault within the north of the Menderes core complex is represented by metamorphic and non-metamorphic lithologies, generally formed of allochthonous rock units and Neogene-Quaternary basin sediments. Especially in low grade metamorphics and non-metamorphic rocks, the effects of varying amounts of brittle deformation are commonly observed. These rocks are characterized by high-angle faults of mappable scale with WNW-ESE and NW-SE directions. The normal component is clear on surfaces with relative movement visible. The movement direction is mainly toward the NE. However, there are a few SW dipping faults found. Some faults have clear listric geometry.

3. Neogene Basins in Western Anatolia

3.1. East-West-Trending Grabens

One of the dominant morphological features in Western Anatolia is E-W-trending grabens (Figure 7). The most comprehensive explanation of the basis of Turkey's neotectonics at time of publication, in the article by Şengör et al. (1985) the E-W grabens represented the initiation of N-S extensional tectonics in the Aegean (revolutionary structures). After Early Miocene ages were obtained from E-W graben fill (Seyitoğlu and Scott, 1992*a*; Seyitoğlu, 1992),

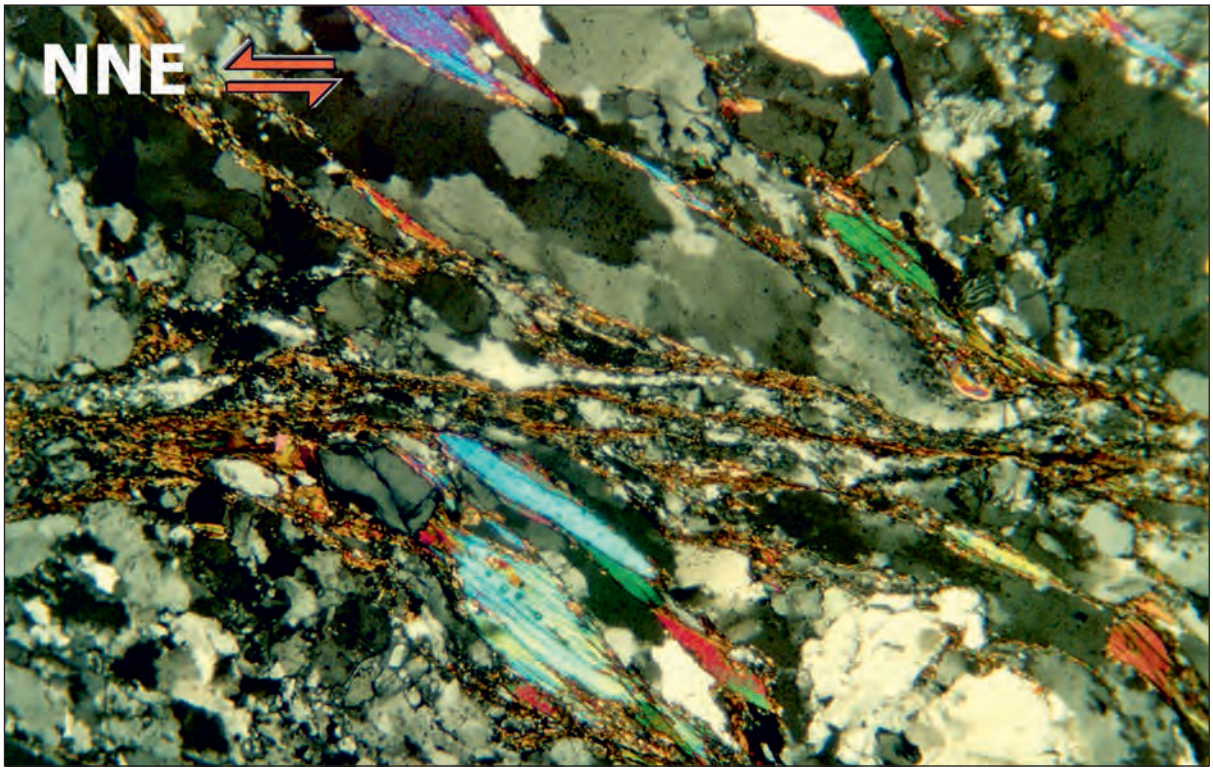

Figure 16- S-C fabric on oriented thin section. Horizontal foliation represents C-plane, diagonal foliation represents the S-plane. Movement direction is top-to the NNE.

sedimentological investigation determined whether graben fill in E-W grabens belonged to them and not pre-existing structures, a matter significantly emphasized by Cohen et al. (1995). This was because the data obtained from this fill determined the initiation time of extensional tectonics in Western Anatolia and was used to test the validity of proposed tectonic models (Seyitoğlu, 1992). If a section of the sedimentary sequence within the grabens is revealed to belong to cross grabens as proposed in the cross graben model, it would question the validity of age data obtained from the fill for initiation of E-W grabens. In a sedimentological study of both Alaşehir (Gediz) and Büyük Menderes sediments by Cohen et al. (1995), the fill in both grabens were coeval with the E-W graben system and they determined that the ages obtained from graben fill could be used for graben formation (Cohen et al., 1995; p. 637). Contrary to this, interpretation of the deepest graben fill as belonging to north-trending basins continues in some studies (Yazman, 1997; Yılmaz et al., 2000; Yılmaz and Gelişli, 2003; Gürer et al., 2009).

3.1.1. Alaşehir Graben

Grabens are generally named after the river they contain; as a result the name Gediz graben is commonly used. However, it is thought that using the name Alaşehir graben is more appropriate than Gediz graben (Seyitoğlu, 1992) because; (1) the town of Alaşehir is located within the graben while the town of Gediz is not within the graben, (2) the Gediz river does not run along the whole graben but enters in the middle of the graben at Adala, (3) the surface ruptures of the 28 March 1970 Gediz earthquake (M=7.0) developed outside the graben near the town of Gediz, and (4) Alaşehir stream, Alaşehir town and surface ruptures of the 28 March 1969 Alaşehir earthquake (M=6.1) are within the graben (Arpat and Bingöl, 1969; Ketin and Abdüsselamoğlu, 1969; Eyidoğan and Jackson, 1985).

While studies related to basin fill in the Alaşehir graben have proposed many formation names, it is not possible to observe or map some of these throughout the whole graben. In the field three different formations are clearly distinguished and their relationships to faults are observable (Figure 17). The lowest Alaşehir formation and the Kurşunlu formation above it are unconformably followed by the Sart formation and the sequence ends in current alluvial sediments (Figure 18) (Seyitoğlu et al., 2002).

The first two sedimentary sequences in the Alaşehir graben, the Alaşehir and Kurşunlu formations, are bounded by the Alaşehir Detachment Fault (Fault I). In the lower sections of the Alaşehir formation (İztan and Yazman, 1990) angular blocky conglomerates are found. The clasts are formed of mylonitic rocks. Toward the top of the unit it transitions to yellow sandstone-mudstone intercalations. Generally within 50 m toward the top the clast size rapidly reduces and angular blocky conglomerates up to 1.5 m are found within very fine-grained lacustrine sediments. The upper section of the formation passes to very well lithified laminated mudstone rich in organic material passing into sandstone and limestone with conglomerate levels observed. Grey sediments indicating underwater environmental conditions intercalate with red sediments, before passing into a unit dominated by

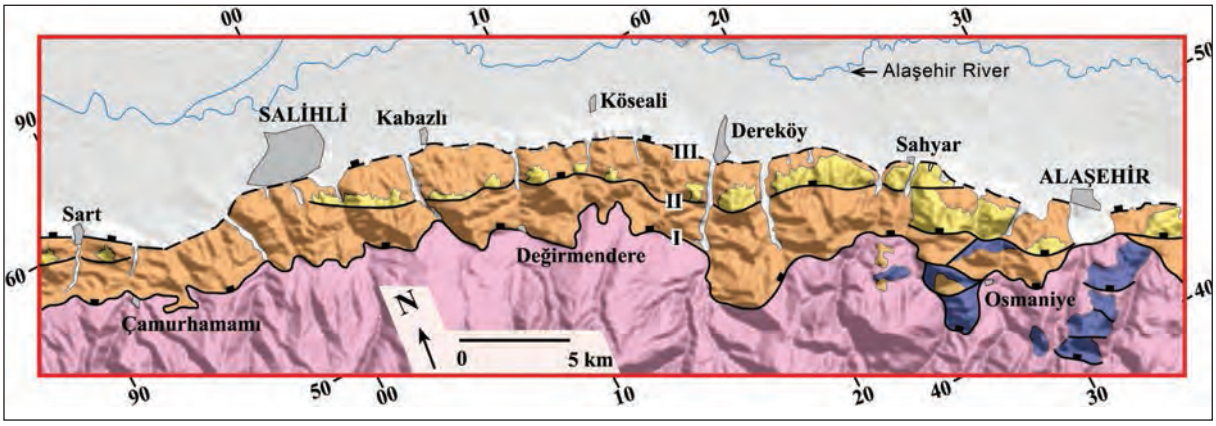

Figure 17- Geological map of the Alaşehir graben (taken from Seyitoğlu et al., 2000). Pink represents metamorphic basement, blue represents the Alaşehir formation, dark yellow-orange represents the Kurşunlu formation, light yellow represents the Sart formation and gray represents Quaternary alluvium.

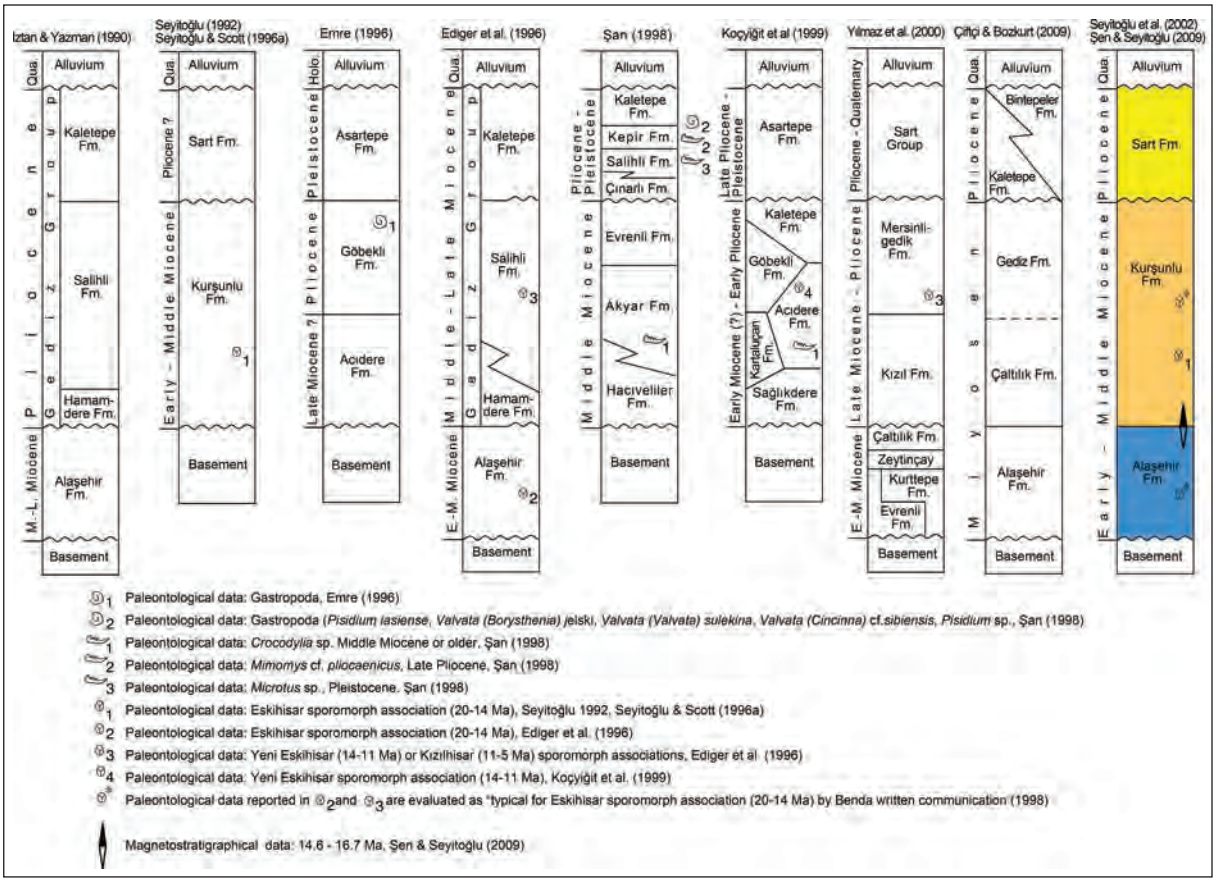

Figure 18- Stratigraphy of the Alaşehir graben (modified from Demircioğlu et al., 2010).

red color. This unit is described as the Kurşunlu formation (Seyitoğlu, 1992; Seyitoğlu and Scott, 1996*a*; Seyitoğlu et al., 2002). The Kurşunlu formation comprises angular conglomerates followed by coarse and fine sandstone in a cyclical sedimentary sequence. The typical red color of the Kurşunlu formation is seen in the lower levels while in the upper levels the color lightens to pink with gray intercalations.

The Eskihisar sporomorph association (20-14 Ma) has been defined in both the Alaşehir formation (Ediger et al., 1996) and the Kurşunlu formation (Seyitoğlu and Scott, 1996*a*). Taking note of magnetostratigraphic age data obtained from the transition between the Alaşehir and Kurşunlu formations (14.6-16.6 Ma) and the thickness of the lower Alaşehir formation, the age of initiation of the graben is determined as Early Miocene (Şen and Seyitoğlu, 2009).

The Sart formation which overlies the Alaşehir and Kurşunlu formations above an unconformity comprises light yellow, slightly consolidated conglomerates and sandstones. The name Sart formation is taken from the ancient city of Sardis (Seyitoğlu, 1992; Seyitoğlu and Scott, 1996*a*; Seyitoğlu et al., 2015*a*). The Pliocene Sart formation contains microfossils (Şan, 1998). Within the graben this formation developed on the hanging wall of Fault II (Seyitoğlu et al., 2002). Quaternary alluvium is found on the downdropped block of Fault III forming the graben plain and surface rapture from the 28 March 1969 Alaşehir earthquake developed along this fault (Arpat and Bingöl, 1969; Eyidoğan and Jackson, 1985) (Figures 17 and 18).

When studies of the tectonic evolution of Alaşehir graben are investigated, it is possible to observe traces of the "low angle vs. high angle" argument about normal faults in structural geology in assessments of the faults controlling graben formation. There are two different views on formation of the Alaşehir graben. The first group of researchers says the graben bounding faults were low-angle from the time of basin formation and these are cut by the higher-angle faults which young toward the north (Hetzel et al., 1995; Emre and Sözbilir,

1997; Sözbilir, 2001; Öner and Dilek, 2011). The second group of researchers proposes that initiation of the Alaşehir graben involved high-angle normal faults which gradually became low angle over time (Seyitoğlu and Şen, 1998; Gessner et al., 2001; Bozkurt, 2001; Seyitoğlu et al., 2002; Purvis and Robertson, 2005; Çiftçi and Bozkurt, 2009; 2010; Demircioğlu et al., 2010; Seyitoğlu et al., 2014).

According to Öner and Dilek (2011), from the first group of researchers who define the Alaşehir graben as a supradetachment basin developing on the Alaşehir Detachment Fault, at the start of basin development from the Early Miocene low-angle detachment faults were active, accompanied by scissor faults and from the Late Pliocene (3.5 Ma) high-angle faults cut the detachment fault leading to back-tilting of the sequence (Öner and Dilek, 2011). The lack of validity of this model may be shown with a few points. (1) Comparing basin fill in "rift basins" and "supradetachment basins" the clearest difference is the distance of the lacustrine depocenter from the main fault (Friedmann and Burbank, 1995). In supradetachment basins due to the giant alluvial fan deposits, lacustrine basins develop far from the basin edge whereas in rift basins due to high-angle normal faults the largest depocenter is very close to the edge of the basin and alluvial fans are of limited size (Friedmann and Burbank, 1995). When the geologic map of Öner and Dilek (2011) is examined, it is possible to observe the oldest rocks in basin fill are organic-rich mudstone and lacustrine limestone [Gerentaş fm. and Kaypaktepe fm. in Öner and Dilek, (2011)] located very close to the basin-edge fault. This feature was mentioned by Seyitoğlu et al. (2002) and the necessity of high-angle faults bordering the basin/graben initially was stated. (2) The Alaşehir Detachment Fault is one of the most dated faults on the earth. With the age dating completed to date it is possible to access relative spatial locations of the Alaşehir Detachment Fault (Seyitoğlu et al., 2014). Age dates on the Alaşehir Detachment Fault vary from 1.75±0.62 Ma to 21.70±4.50 Ma (Lips et al., 2001; Gessner et al., 2001; Catlos and Çemen, 2005; Glodny and Hetzel, 2007; Catlos et al., 2010; Buscher et al., 2013; Hetzel et al., 2013). In the supradetachment basin model of Öner and Dilek (2011), the Alaşehir Detachment Fault is cut by high-angle faults from 3.5 Ma and must cease activity. However, the age data mentioned above identified movement on the fault up to 1.75±0.62 Ma. (3) In the supradetachment basin model, the crosscutting relationships of faults in the Alaşehir graben are ordered relatively (Öner and Dilek, 2011; Figure 12c). The faults are ordered from old to young as high angle, low angle, high angle, low angle. When it is considered that the proposed model involves development of first low angle and then high angle normal faults, it appears that this situation is not observed in nature.

The second group of researchers who believe the Alaşehir graben began with high-angle faults have adapted the flexural rotation/rolling hinge model to the Alaşehir graben (Seyitoğlu et al., 2002). In the original "flexural rotation" model (Buck, 1988; Wernicke and Axen, 1988) initially high-angle normal faults reduce in angle due to isostatic rebound. New normal faults developing in the hanging wall of the first fault undertake the task of the first fault which cannot cope with the extension. This situation implies that movement should end on the rotating first fault and primary throw on faults formed pre-rotation will remain unchanged. At the end of the process, faults and related sediments young towards the center of the graben (Buck, 1988; Wernicke and Axen, 1988; Manning and Bartley, 1994; Axen and Bartley, 1997).

In the initial stages of the Alaşehir graben, the Alaşehir and Kurşunlu formations were deposited in front of high-angle faults (Fault I) in the Early Miocene. This conclusion is reached due to the proximity of the lacustrine facies to the graben edge in the mapped area of the Alaşehir formation (Seyitoğlu et al., 2002) (Figure 19). Additionally, geological maps by Cohen et al. (2005), Purvis and Robertson (2005) and Öner and Dilek (2011) include similar results. As observed in gravity data (Akçığ, 1988; Ateş et al., 1999) and seismic profiles parallel to the graben (Çiftçi and Bozkurt, 2010) in front of the towns of Alaşehir and Salihli, there are two separate sub-basins separated by possible "relay ramps" (Seyitoğlu et al., 2002). Thermochronological data from the Alaşehir graben (Gessner et al., 2001; Figure 3f) show that rocks in the footwall of Fault I were rapidly exhumed since about 5 Ma. This data supports the view that Fault II formed in the downdropped block of Fault I and while the Sart formation was being deposited ahead of this, Fault I rotated to become low angle (Figure 19).

As Fault I rotated and became low angle, different to the original "rolling hinge" model, activity continued and field data show this caused a larger amount of metamorphic basement to be exposed (Seyitoğlu et al., 2002; Figure 11). Here as a result of

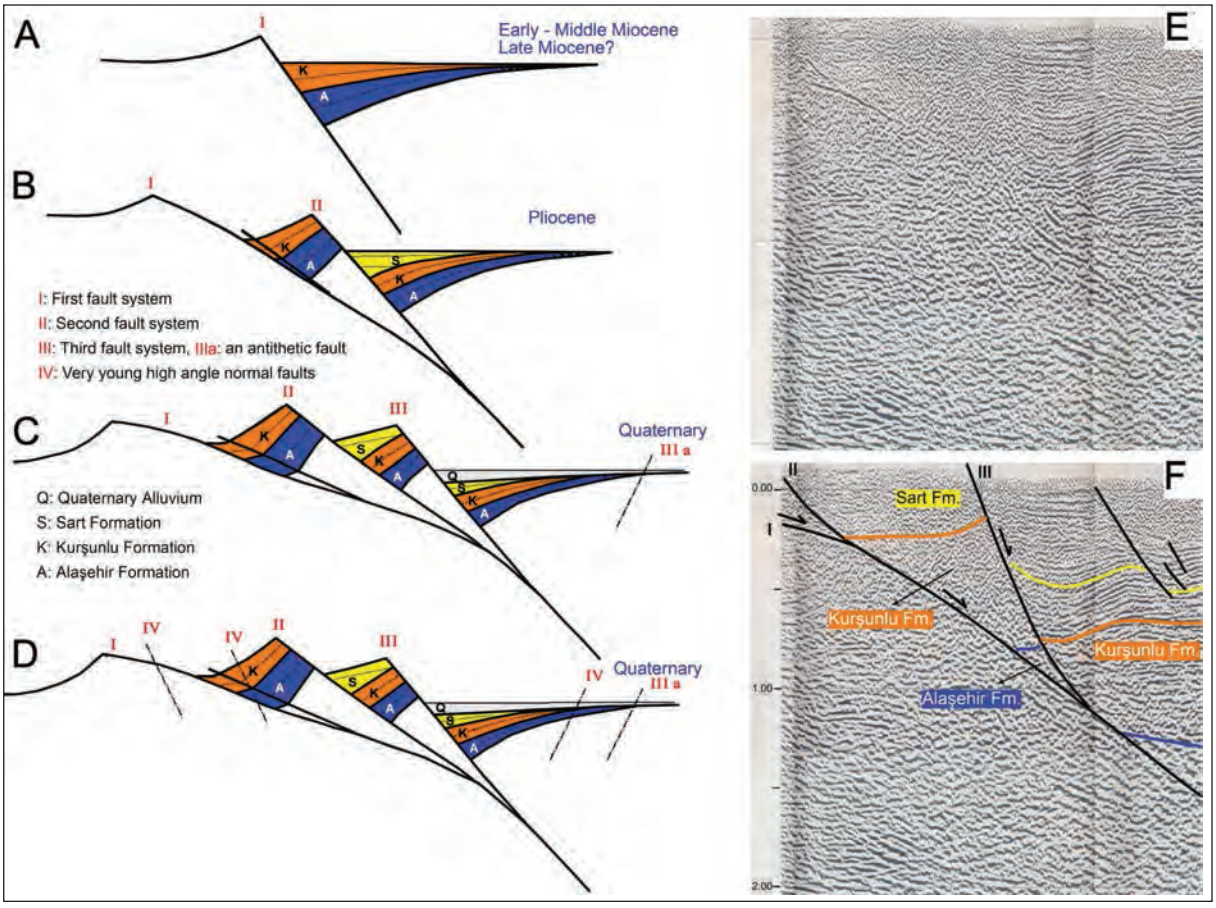

Figure 19- "Alaşehir-type rolling hinge" model for the Alaşehir graben (A-D) and seismic reflection profiles of the graben showing Fault II and Fault III merged to Fault I (E-F) (Adapted from Seyitoğlu et al., 2002; Demircioğlu et al., 2010; Seyitoğlu et al., 2014).

the low angle normal faults affecting the Kurşunlu formation with activity on these low angle normal faults occurring after deposition of the formation, it is understood that there was activity on the rotated low angle fault. Age dating (9.2±0.3 - 3.7±0.2 Ma) from the same location confirms this (Hetzel et al., 2013; Samples 10Me09 and 10Me10, Figure 3b). Preservation of activity as Fault I rotates to low angle is different to the original model. This difference is described as the "Alaşehir type rolling hinge model" (Seyitoğlu et al., 2014). This model explains (1) the extensional tectonic regime continuing from the Early Miocene to Quaternary without major disruption, (2) the large interval of dates obtained from the Alaşehir Detachment Fault (1.75±0.62 Ma to 21.70±4.50 Ma), and (3) the formation mechanism of the Horzum Turtleback (Seyitoğlu et al., 2014).

In the hanging wall of Fault II, Fault III developed and Fault I and II continued to rotate to lower angles and Quaternary alluvium was deposited on the downdropped block of Fault III. At the same time faults developing on the northern side of the Alaşehir graben made the graben symmetric. High angle faults (Fault IV) developing from the Quaternary to the present appear to cut low angle faults (Seyitoğlu et al., 2002) (Figure 19).

Faults identified on seismic reflection profiles completed by TPAO match faults mapped on the surface and named as Fault I, II and III (Demircioğlu et al., 2010). Accordingly at depth Faults II and III merge to Fault I but do not cut it (Figure 19). This finding supports the "rolling hinge" model of evolution of the Alaşehir graben. Seismic reflection profiles also illustrate the wedge geometry of the Alaşehir formation. This data shows that the Alaşehir formation was deposited simultaneous to E-W striking faults (Demircioğlu et al., 2010) and are not the product of north-trending basins as advocated by Yılmaz et al. (2000).

One of the most striking models for the evolution of the Alaşehir graben is the two-stage extensional

model. Koçyiğit et al. (1999) examined sequences in the Alaşehir graben and found folds in rocks of the Salihli group and assuming a horizontal position for the Karataş group above an angular unconformity, they determined a N-S oriented short regional compressional stage in the Late Miocene-Early Pliocene. Seyitoğlu (1999) mentioned the radiometric age dates and palynologic analyses (Seyitoğlu, 1997*b*; Seyitoğlu et al., 1997; Seyitoğlu and Benda, 1998) from the Selendi and Uşak-Güre basins immediately to the north of the Alaşehir graben along with the horizontal placement of the İnay Group with age interval in the Lower-Middle Miocene and lack of effects from regional compression as contradicting this view. Seyitoğlu et al. (2000) investigated folds in the Alaşehir graben and found they were drag folds or rollover anticlines related to normal faults showing they were folds related to extensional tectonics, given a theoretical basis in Janecke et al. (1998). Purvis and Robertson (2005) concur with this observation. Sözbilir (2002) introduced the interpretation that the folds in graben fill developed in an extensional regime and formation was related to the ramp and flat geometry of detachment faults.

3.1.2. Büyük Menderes Graben

The Büyük Menderes graben is an east-west structure where the main fault is located on the north side. The base of the graben fill is blocky conglomerate, sandstone and mudstone with lignite levels of the Hasköy formation and it is reported that the formation includes E-W trending normal growth faults (Sözbilir and Emre, 1990). The Hasköy formation was determined to have been deposited in the Middle-Late Miocene by Sözbilir and Emre (1990) and this age was supported in palynological studies by Akgün and Akyol (1999). Among our reservations about this age data are the lack of first hand correlation of the proposed age with isotopic age data, and mammal or marine biochronological ages (Seyitoğlu and Şen, 1999). The response to this debate states the lack of confidence in isotopic age data (Akyol and Akgün, 2001).

It is known that Leopold Benda's Hasköy locality is where the Eskihisar sporomorph association was recorded (Becker-Platen, 1970). Taking this information together with the new age interval for the Eskihisar sporomorph association (20-14 Ma), the age of initiation of the E-W-trending Büyük Menderes graben, and as a result the N-S extensional tectonics in the Aegean, is determined to be Early Miocene (Seyitoğlu and Scott, 1992*a*).

The Gökkırantepe formation, conformably overlying the Hasköy formation (Sözbilir and Emre, 1990), is formed of red conglomerate, sandstone and mudstone and is accepted as the second sedimentary sequence in the graben (Figure 20). The transition from the Hasköy formation to the Gökkırantepe formation was dated to 14.88 - 15.97 Ma by magnetostratigraphy (Şen and Seyitoğlu, 2009). According to a mainly sedimentological study of the Büyük Menderes graben, each of the formations is a product of the E-W graben (Cohen et al., 1995) and the initiation age of the graben is described as Early Miocene (Seyitoğlu and Scott, 1992*a*; Şen and Seyitoğlu, 2009).

The Asartepe formation in the Büyük Menderes graben unconformably overlies previous units (Sözbilir and Emre, 1990; Şen and Seyitoğlu, 2009). At the Şevketin Dağı location within the formation, micromammalian fossils with Late Pliocene-Pleistocene ages are found (Ünay et al., 1995; Ünay and De Bruijn, 1998) (Figure 21).

Gürer et al. (2009) proposed the presence of a Late Pliocene-Pleistocene sequence according to micromammalian data from between Aydın – Ortaklar in the Büyük Menderes graben. According to age data, there is a high possibility that the position of this sequence in Büyük Menderes stratigraphy is equivalent to the Asartepe formation with certain position. To confirm this it is necessary to complete careful geological mapping laterally from the Şevketin Dağı location where the Asartepe formation is observed toward Aydın. The lack of validity of the claim of inconsistency between palynological ages near Nazilli and the micromammalian ages proposed by Bozkurt (2000) has been shown by similar geological mapping (Şen and Seyitoğlu, 2009). Here while the Eskihisar sporomorph association (20-14 Ma) was recorded in the Hasköy formation, the Late Pliocene-Pleistocene micromammalian age findings are within the Asartepe formation at different stratigraphic levels (Şen and Seyitoğlu, 2009) (Figure 21).

The newest study to support the cross graben model proposed by Şengör (1987) is by Gürer et al. (2009) who propose that the Lower-Middle Miocene sedimentary sequence in the Büyük Menderes graben was deposited under a N-S compressional regime in north-trending basins (Tibet-type grabens). Based on the Late Pliocene-Pleistocene micromammalian ages obtained from the sequence between Aydın – Ortaklar in the Büyük Menderes graben, mentioned

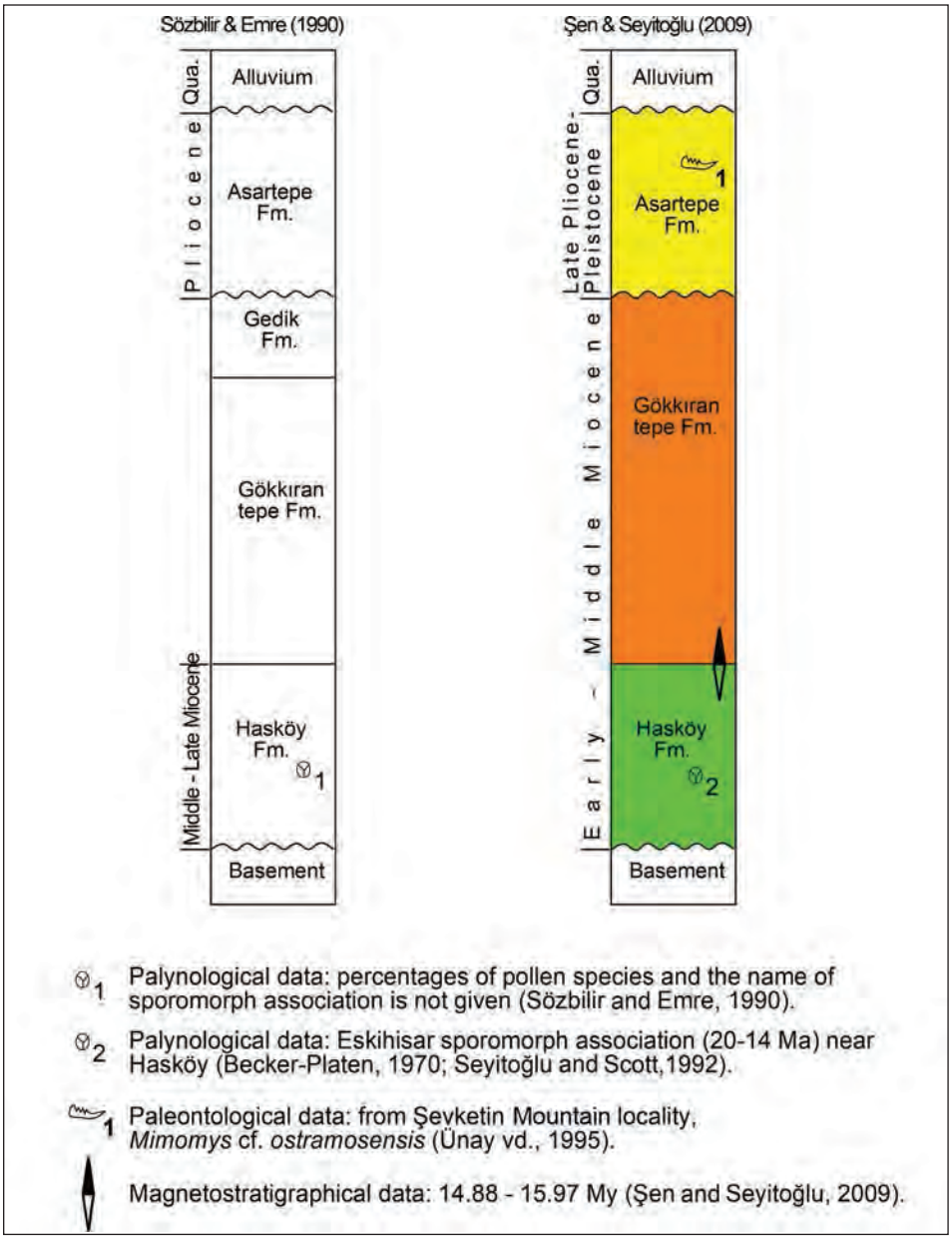

Figure 20- Generalized stratigraphy of the Büyük Menderes graben (prepared after Şen and Seyitoğlu, 2009).

above, it is advocated that the extensional regime in Western Anatolia began in this period and evidence of the compressional regime continuing to the Late Pliocene is shown by the last movement of the Lycian nappes in SW Anatolia. This model does not comply with several observations and studies in Western Anatolia. (1) Sedimentological studies of both the Alaşehir and Büyük Menderes grabens have stated that the sediments are coeval to tectonism and the age of these sediments may be used to identify the age of formation of E-W grabens (Cohen et al. 1995). The lowest sequence in the E-W grabens of Alaşehir and Büyük Menderes has been proven to have Early Miocene age by magnetostratigraphical studies (Şen and Seyitoğlu, 2009). (2) As discussed in the previous section, data from studies based on seismic reflection profiles in the Alaşehir graben show the sequence at the bottom of the graben fill (Alaşehir formation) developed simultaneously to the east-west normal fault system (Demircioğlu et al., 2010; Çiftçi and Bozkurt, 2010). In the study by Çiftçi et al. (2011) assessing seismic reflection data from the Büyük Menderes graben, seismic reflection profiles in an E-W direction showed the lowest two sequences in the

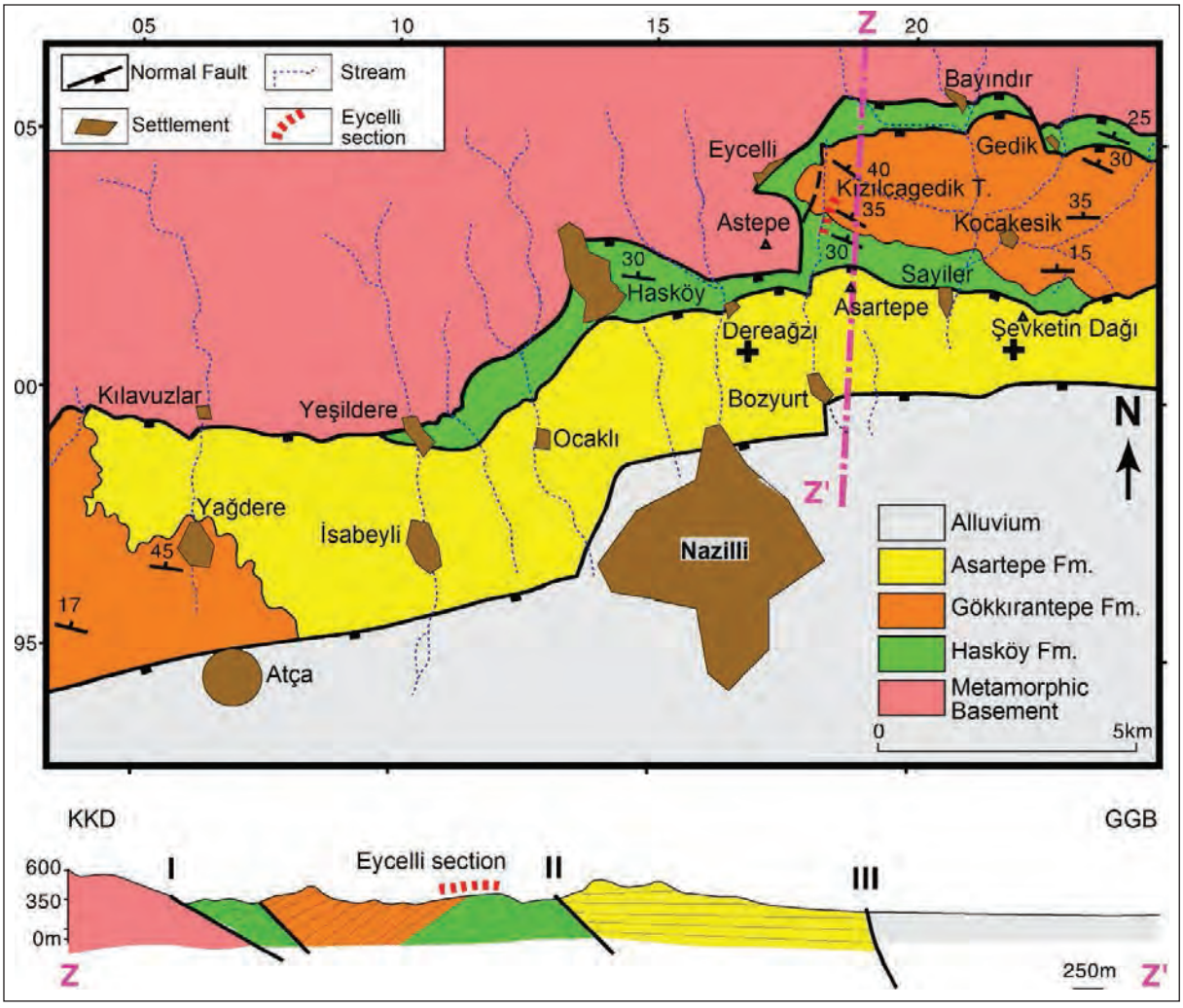

Figure 21- Geological map and cross section north of Nazilli in the Büyük Menderes graben. Dashed red line indicates location of magnetostratigraphic section (Taken from Şen and Seyitoğlu, 2009).

graben fill (equivalent to Hasköy and Gökkırantepe formations) have lens-shaped geometries, while on N-S seismic reflection profiles E-W normal faults acting as growth faults for the first two sequences. North-trending faults, observed at the surface and proposed by Gürer et al. (2009) as controlling units equivalent to the lowest unit of graben fill, the Hasköy formation, developed after deposition and are reported to be transfer faults frequently observed developing in basins with normal faults (Çiftçi et al., 2011). These findings make the proposed assessment by Gürer et al. (2009) invalid. (3) Gürer et al. (2009) used movement of the Lycian nappes to the south as data showing continuation of the compressional tectonic regime until the Late Pliocene. However, the ages of basins in the Menderes Massif (Gördes and Dalama-Kuloğulları; Seyitoğlu et al., 1992) and thermochronological ages (Gessner et al., 2001*b*) show that the massif was freed of Lycian nappe cover before the Early Miocene, requiring the last movement of Lycian nappes toward the south, thought to have been sourced at the Izmir-Ankara suture zone, to be rootless and for this crustal shortening is not required. This was stated by Seyitoğlu et al. (1992) and this opinion was supported by Collins and Robertson (2003). (4) The deformed units and reverse fault images used to support the view of Gürer et al. (2009) that the compressional tectonic regime continued to the Late Pliocene. Firstly it must be determined whether the deformation is due to slump folding. Additionally, it must not be forgotten that folds and reverse faulting in sequences above detachment faults may develop linked to the ramp-flat geometry of the detachment fault (McClay, 1989; 1990). In recent times data from within the Alaşehir graben was published in a study assessing

similar structures as products of progressive deformation (Şengör and Bozkurt, 2013). Another dimension of the topic are the regional effects of the proposed compression continuing to the Late Pliocene (Gürer et al., 2009) or short-duration compression between the Late Miocene-Pliocene (Koçyiğit et al., 1999). As discussed in an earlier section, the İnay Group, with definite Lower-Middle Miocene age based on palynology and isotopic age data in basins immediately north of the E-W trending grabens, is in a horizontal position and was not affected by the proposed regional compression (Seyitoğlu, 1999). However, compressional data published in papers to support the regional compression of Gürer et al. (2009) has been refuted. For example, the folds mentioned by Koçyiğit et al. (1999) have been shown to be drag folds or rollover anticlines (Seyitoğlu et al., 2000). The reverse fault proposed by Koçyiğit et al. (2000) in the Akşehir-Afyon graben was not found on seismic data (Kaya et al., 2014). Folds in Neogene units of Eskişehir plain in Koçyiğit (2005) were determined to be related to active strike-slip faulting (Seyitoğlu et al., 2015*b*). All these studies show the compressional regime in Western Anatolia did not continue to the Late Pliocene and there was no short-term compression between the Miocene-Pliocene.

3.1.3. Denizli Graben

The WNW-ESE-trending Denizli graben is located in the SE of the Menderes Massif. The graben is 70 km long and 50 km wide, with the southern edge of the graben forming the northern slope of the Babadağ reaching 2000 m. On these slopes the southern edge of the graben is bordered by the Babadağ Fault Zone with 45-50º north-dipping normal faults. The Buldan horst in the NW of the graben divides the graben fill in two. In the northern section of the graben, the Denizli graben with NW-SE normal faults developed in the Quaternary nearly unites with the Alaşehir graben. The southern section is linked to the Büyük Menderes graben by E-W Quaternary normal faults (Figure 22). Seismic activity in the region is very high due to the Babadağ and Pamukkale fault zones (Kaypak and Gökkaya, 2012).

Denizli graben fill is reported as Pliocene age (Taner, 1974*a*, *b*; 1975), so have attracted less attention of the studies dealing with the initiation of extensional tectonics. However, after the identification of micromammalian fossils showing Early Miocene age (Saraç, 2003), as the Denizli graben aroused more interest as it houses sedimentary

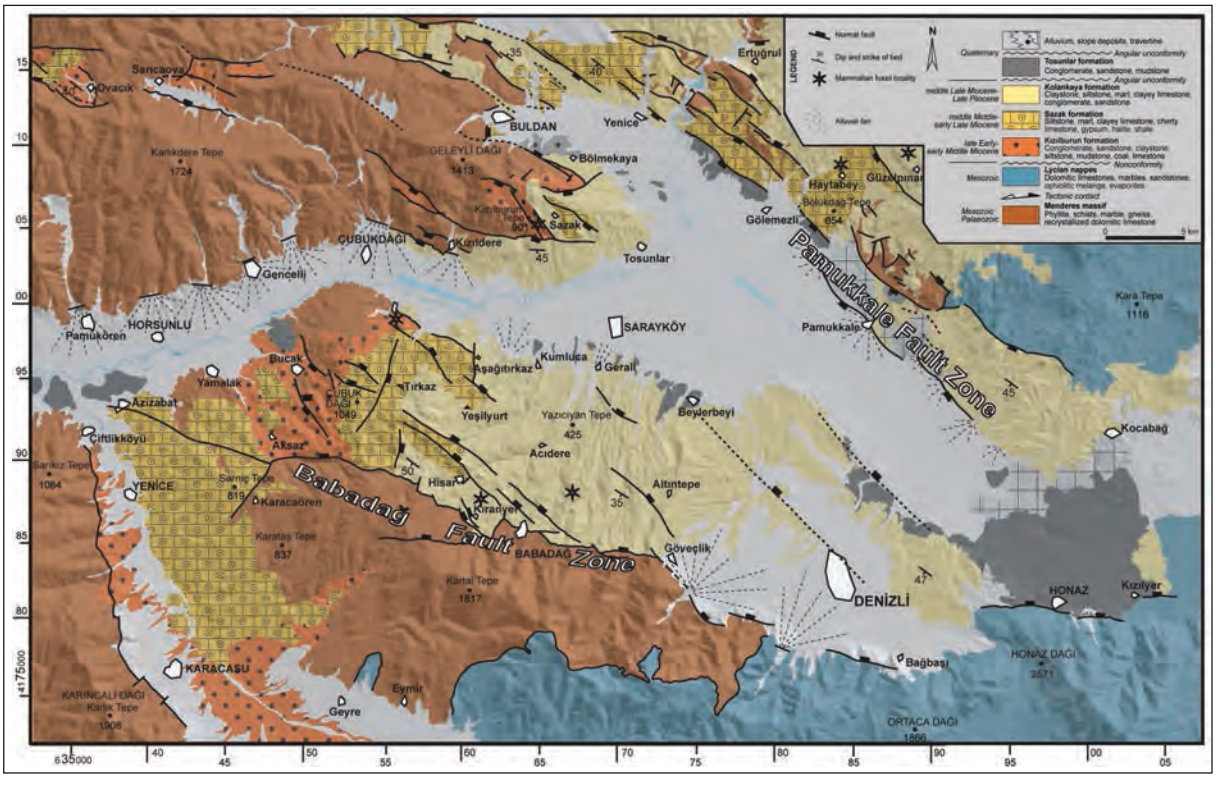

Figure 22- Geological map of the Denizli graben (Taken from Sun, 1990 and Alçiçek, 2007).

fill from a very broad time interval. Koçyiğit (2005), Westaway et al. (2005) and Kaymakçı (2006) do not accept the Lower-Middle Miocene sedimentary sequence as a product of the Denizli graben, but defend the opinion that these sediments developed outside the graben system.

According to Koçyiğit (2005) the Denizli graben developed under two stages of extensional regime separated by a compressional phase. The first extensional regime was in force from the Middle Miocene-Middle Pliocene, and then in the Latest Middle Pliocene a compressional regime reigned and from the Latest Pliocene to the present the second stage of the extensional regime developed. Westaway et al. (2005) proposed that current continental crustal extension in the Denizli region developed about 7 Ma at the beginning of the Late Miocene, revising the proposal of Westaway (1993). Kaymakçı (2006) interpreted Denizli graben fill as Upper Miocene to present sediments advocating the extension had been effective since the Late Miocene.

Alçiçek et al. (2007) revised the previously created stratigraphy (Şimşek, 1984) and geological maps (Sun, 1990) and using micromammalian findings determined the sedimentary characteristics of Denizli graben fill. The lowest level of Denizli graben fill begins with the Kızılburun formation (Figure 23). Matrix-supported coarse conglomerates

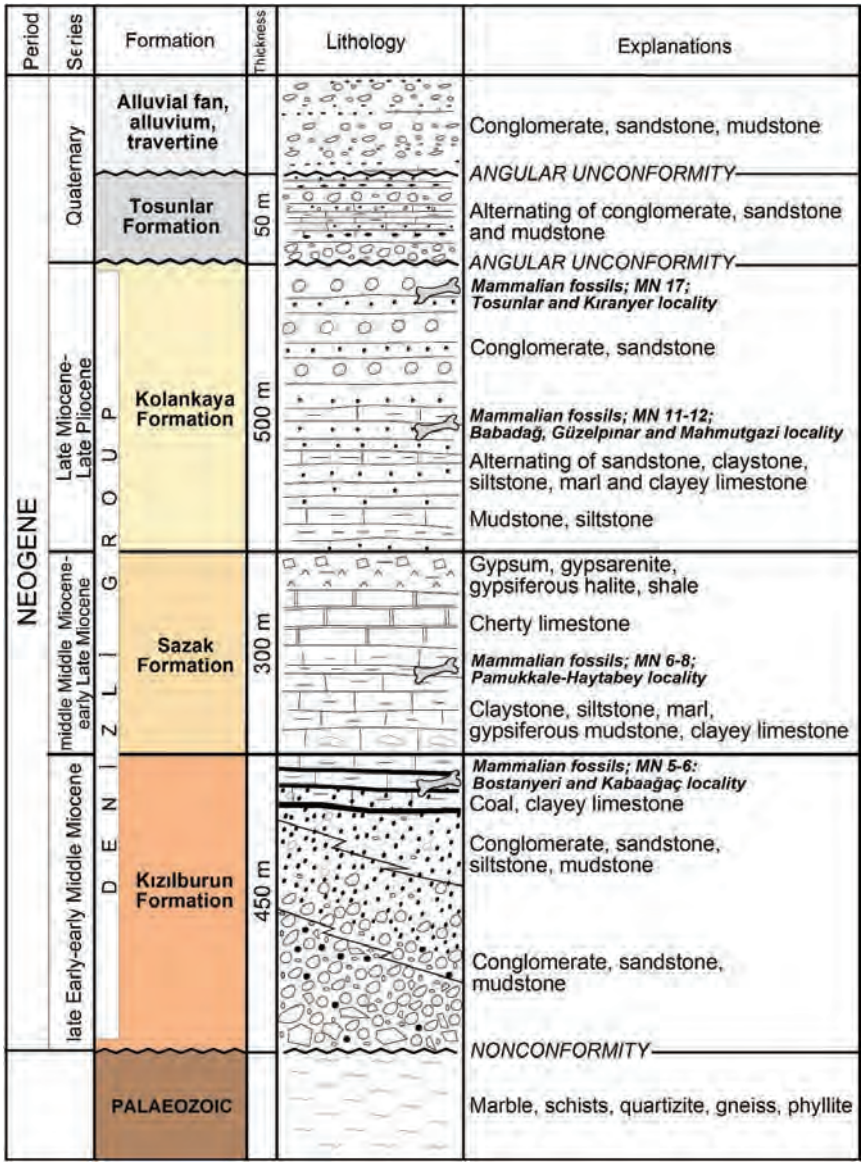

Figure 23- Generalized stratigraphy of the Denizli graben (Taken from Şimşek 1984; Alçiçek, 2007).

and red mudstone laminations pass upwards into clast-supported channel-fill conglomerates and fine-grained sediments including coal. At the localities of Bostanyeri and Kabaağaç MN5-MN6 (Late Burdigalian-Early Serravallian) fossils have been found (Saraç, 2003). The lower sections of the formation have been interpreted as proximal-medial alluvial fans while the upper sections are thought to be distal alluvial fans (Alçiçek et al., 2007).

The Sazak formation comprises limestone containing gypsum, green marl laminated siltstone-mudstone, clay limestone and fine mudstone with gypsum intercalations. Toward the top of the formation it passes into cherty limestones, gypsarenites, gypsum levels and shales. The Sazak formation includes fossils representing MN6-MN8 (Langian-Serravallian) levels (Saraç, 2003). The sequence in this formation is interpreted as lake-edge, shallow lacustrine and playa lake (Alçiçek et al., 2007).

The Kolankaya formation conformably overlies the Sazak formation and overlies the metamorphic basement at the north edge of the graben (Şimşek, 1984; Sun, 1990; Alçiçek et al., 2007). The formation, comprising laminated mudstone-siltstone, marl and clayey limestone, passes to laminated sandstones, cross-bedded conglomerates and sandstones and has been assessed as lacustrine, coastal, offshore and alluvial fan sediments (Alçiçek et al., 2007). The Kolankaya formation includes MN11-MN12 level mammalian fossils (Babadağ, Güzelpınar and Mahmutgazi locations: Sickenberg and Tobien, 1971; Saraç, 2003). Based on mammalian remains at Tosunlar and Kıranyer the Kolankaya formation was evaluated as Late Pliocene by Kaymakçı (2006).

The Tosunlar formation comprises loosely consolidated yellow-brown conglomerates, sandstone, siltstone and mudstone. It includes claystone and marl intercalations. This formation unconformably overlies previous units and is thought to be Pleistocene in age. The sequence ends with recent alluvium (Alçiçek et al., 2007) (Figure 23).

The WNW-ESE Babadağ Fault Zone bounding the Denizli graben controls sedimentation of graben fill nearly continuously deposited from the Early Miocene to the present. The relationship between the Babadağ Fault Zone and Kızılburun formation is observed in a deeply gouged valley 2 km south of Aksaz (Figure 22). Here blocky conglomerates of the Kızılburun formation overlie synthetic faults of the Babadağ Fault and it is seen that the Kızılburun formation thickens towards the Babadağ Fault with very well-developed wedge geometry (Figure 24).

Geotraverse from the Kabaağaç fossil locality to the Babadağ Fault Zone have shown clearly that though the original positions are disrupted by young normal faults, in the Early – early Middle Miocene period, the Kızılburun formation was controlled by the Babadağ Fault Zone (Figure 25).

Near Babadağ village (60588N-85191E) blocky conglomerate layers belonging to the Kolankaya formation have progressively less dip in the upper levels in the downdropped block of the Babadağ Fault Zone. This observation shows that the Babadağ Fault acted as a growth fault during deposition of the Kolankaya formation in the Late Miocene-Late Pliocene (Figure 26).

Recent activity on the Babadağ Fault Zone is clearly observed in development of alluvial fan deposits in the Quaternary (Figure 22) and seismicity (Kaypak and Gökkaya, 2012). Sarı and Şalk (2006) showed that basin fill thickened toward the Babadağ Fault Zone and had a wedge geometry using gravity data. All this data shows that the Babadağ Fault Zone played a significant role in the development of the Denizli graben from Early Miocene to Quaternary. Folds observed in the Neogene sequence in the Denizli graben and attributed to a compressional phase by Koçyiğit (2005) are the anticlines and synclines of drag folds developing on footwal or hanging wall of normal faults with an extensional origin, similar to those in the Alaşehir graben (Seyitoğlu et al., 2000).

Quaternary faults border the Buldan horst and the northern edge of the graben. A series of high-angle normal faults have created a stepped topography on the south slope of the Buldan horst and metamorphic basement together with Mio-Pliocene sequences have been uplifted. The Pamukkale Fault Zone borders the north of the Denizli graben in which travertine development and archeoseismology of Hieropolis are well known features (Altunel, 1996; Uysal et al., 2009).

3.1.4. Küçük Menderes Graben

The Küçük Menderes graben, slightly less prominent compared to the Alaşehir and Büyük Menderes grabens, has a basement of metamorphic

Figure 24- Coeval relationship between faulting on the Babadağ Fault Zone and the Kızılburun formation south of Aksaz.

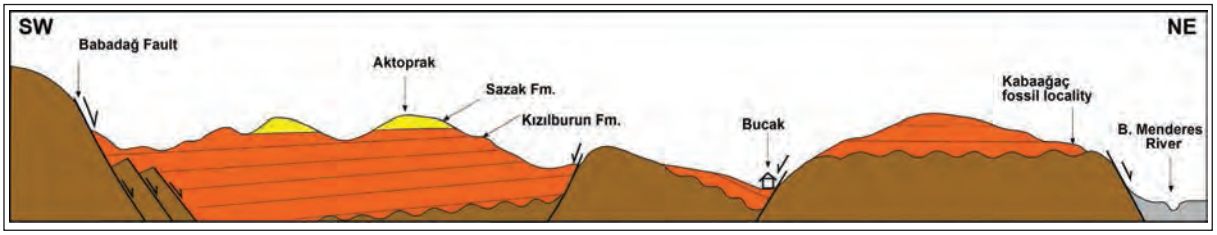

Figure 25- Scale-less cross section between Babadağ fault zone and Kabaağaç fossil locality.

Figure 26- Reduction in dip of upper layers of the Kolankaya formation, wedge geometry thickening toward the Babadağ Fault, SW of Babadağ village.

rocks namely mica gneiss, mica schists, garnet mica schist, calc-schist, quartzitic schist and marble (Seyitoğlu and Işık, 2009). Başova andesites cut the metamorphic rocks and have been dated to 14.3-14.7 Ma (Emre et al., 2006). Graben fill begins with the Suludere formation. Unconformably overlying the metamorphic basement and Başova andesites (14.3-14.7 Ma), this formation includes conglomerates, sandstone, mudstone and lacustrine limestones and is interpreted as flow-dominated alluvial fan and lacustrine sediments (Emre et al., 2006). The Aydoğdu formation unconformably overlies the Suludere formation and comprises conglomerates with light brown, reddish brown weakly lithified sandstone and mudstone intercalations. Recent alluvial sediments cover previous units (Emre et al., 2006).

At the north edge of the Küçük Menderes graben the boundary between metamorphic basement and graben fill was mapped as a reverse fault by Bozkurt and Rojay (2005), with this relationship indicating the presence of the N-S compressional phase of the two-stage extensional model. Contrary to this, Emre et al. (2006, Figure 4) mapped the same boundary as a normal fault. However, later studies by the same researchers determined that the sedimentary sequence was deposited in a compressional system in the late Middle Miocene-Early-Middle Pliocene and that normal faults developed in the Plio-Quaternary (Emre and Sözbilir, 2007). With different characteristics of the tectonic contact shown by different researchers, the north edge of the Küçük Menderes graben was carefully mapped by Seyitoğlu and Işık (2009). The results of this mapping revealed that the contact between the metamorphic basement and graben fill had characteristics of a brittle deformation zone and was bounded by an east-west-trending normal fault dipping >45° to the south. Overturned layers of the sedimentary sequence were not observed, asymmetric synclines observed on the downdropped block were interpreted as a drag fold syncline (Seyitoğlu and Işık, 2009) (Figure 27).

The Küçük Menderes graben has a unique tectonic position (Figure 28). In the north normal faults bounding the south edge of the Alaşehir graben and in the south normal faults bounding the north

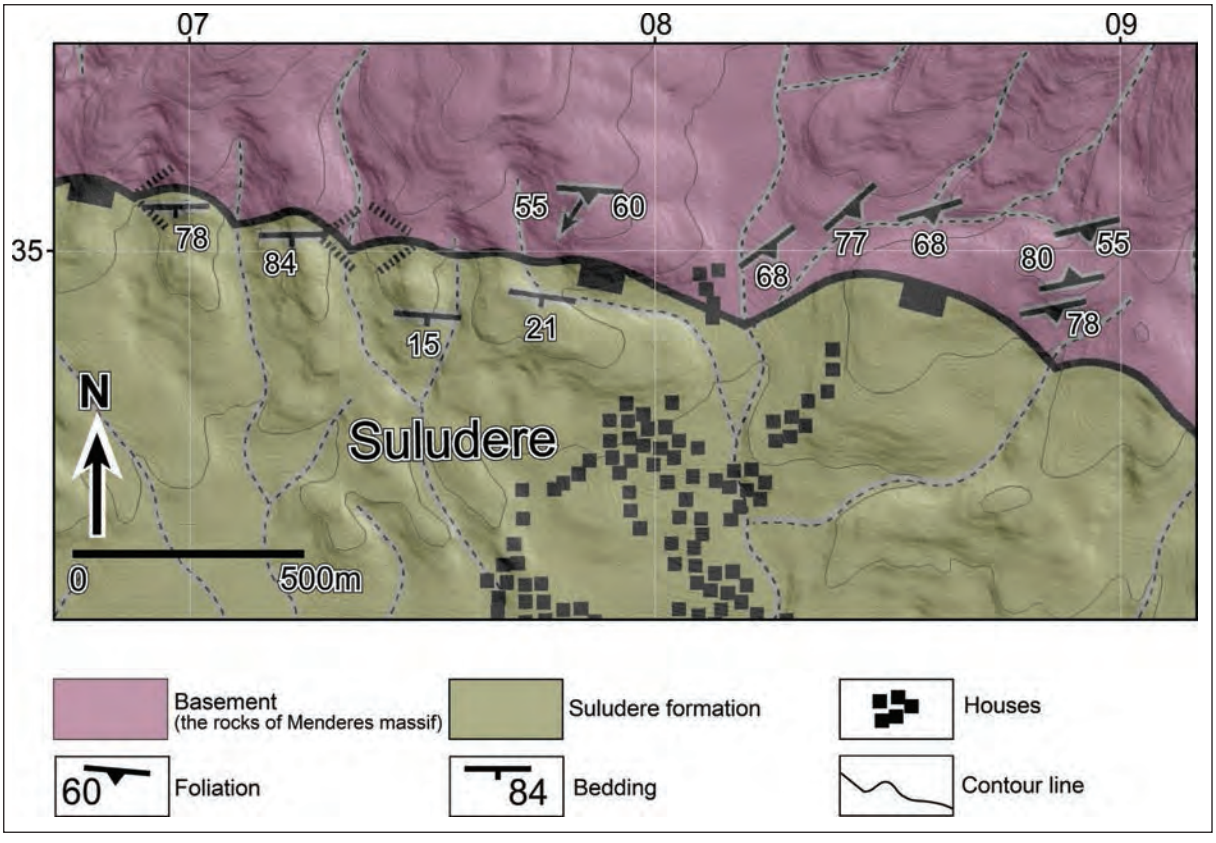

Figure 27- Geological map of the north edge of the Küçük Menderes graben near Suludere (Taken from Seyitoğlu and Işık, 2009).

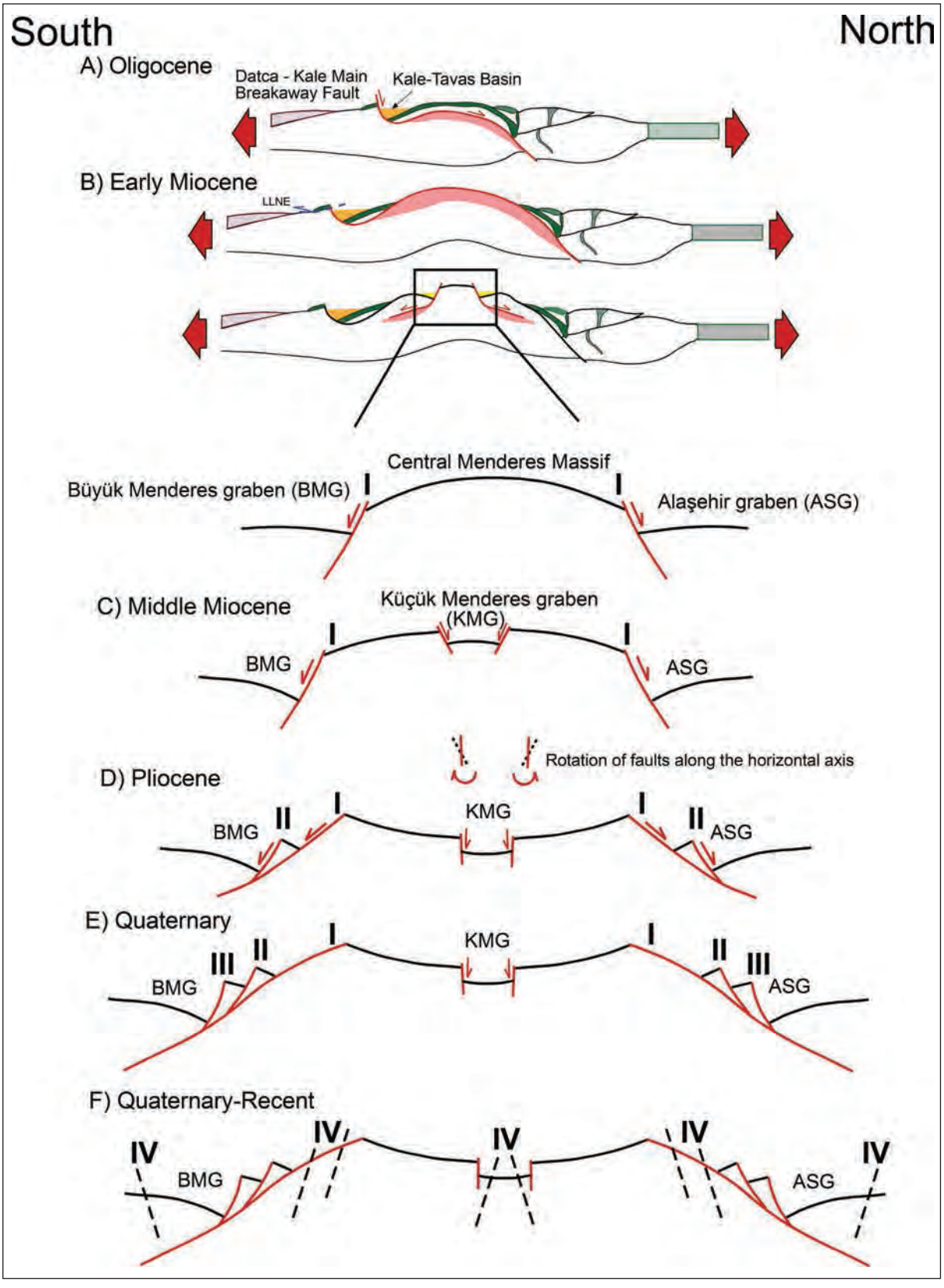

Figure 28- Unique tectonic position of the Küçük Menderes graben (Taken from Seyitoğlu and Işık, 2009).

edge of the Büyük Menderes graben have developed in accordance with the rolling hinge model and a gigantic synclinal with wave length of 45 km and width of 10 km has developed. The Küçük Menderes graben is located in the axial region of this syncline. According to kinematic analysis of folds, in the center of the fold reverse faults developed parallel to the fold axis linked to narrowing (Ramsey and Huber, 1987; Davis and Reynolds, 1996). If this basic kinematic rule is applied to the Menderes Massif between the Alaşehir and Büyük Menderes detachment faults rotating in opposite directions to each other, it may be expected that reverse faults be observed around the Küçük Menderes graben (Bozkurt and Rojay, 2005; Emre and Sözbilir, 2007). However, field studies have shown that only unusually high-angle normal faults are found north of the Küçük Menderes graben (Seyitoğlu and Işık, 2009). Possibly the high-angle faults in the Küçük Menderes graben initially were about 45º. It is thought that the current angles greater than 45º may be due to rotation of the horizontal axis. This rotation may mean results of rotation of the Alaşehir and Büyük Menderes detachment faults observed in the Pliocene of the central Menderes Massif may be related to rotation on the limbs of a large syncline developing due to the effects of an extensional tectonic regime (Seyitoğlu and Işık, 2009) (Figure 28). If compressional structures had been successfully demonstrated near the Küçük Menderes graben or even if they are in the future, it is not possible to attribute these types of structures to a regional compressional regime because the giant synclinal structure of the central Menderes Massif was created by rotational flexure of the Alaşehir and Büyük Menderes detachment faults; in other words a result of extensional tectonic processes. For this reason, it is not possible to attribute local contractions observed in the Küçük Menderes graben located in the axial region of the giant syncline to a regional compressional regime (Seyitoğlu and Işık, 2009) (Figure 28).

3.1.5. Simav Graben

The Simav graben is one of the important E-W trending grabens in Western Anatolia with a topographic difference between the south edge of the graben and the floor of 1100 m. One of the first studies in the graben is Zeschke (1954). Konak (1979) advocated that the Simav Fault is a strike slip fault active since the Early Miocene and determined that since the late Miocene 6 km of displacement has occurred based on offset metamorphic zones (Konak, 1982). The effect of this opinion may be observed on the current MTA active fault map (Emre et al., 2011). While Eyidoğan and Jackson (1985) advocated that the north and south edges of the Simav graben are bordered by faults with the northern edge currently dominant, Westaway (1990) mentioned that the main normal fault is found on the southern edge.

The nearly E-W trending and 65-70º north-dipping normal fault on the southern edge of the Simav graben is known as the "Simav Fault" in the literature, different to the Simav Detachment Fault (Seyitoğlu, 1997*a*). The Simav Fault is a high-angle fault and is post-tectonic compared to the Simav Detachment Fault (Işık, 2004). Unconsolidated blocky conglomerate and coarse sandstone is found on the hanging wall of the Simav Fault and the contact with the metamorphic basement is clearly seen. However, in the uplifted block of the Simav Fault it becomes difficult to observe the Simav Fault within basin sediments of the north-trending Demirci basin. In this situation the only criterion to separate conglomerate with blocks derived from metamorphic basement in the Demirci basin from blocky conglomerate on the downdropped block of the Simav fault is consolidation. One of the clearest morphological effects of the eastern extension of the Simav Fault is the drop of the northern section of Kıbletepe. Further east it is difficult to observe the trace of the Simav Fault in the Hacıbekir Group sediments of the Selendi basin (Seyitoğlu, 1997a). The Simav Fault is active, with focal mechanism solutions of recent earthquakes showing dominant pure normal faulting (Yolsal-Çevikbilen et al., 2014). North of the Simav Fault, the north-trending Akdere basin has semi-consolidated blocky conglomerates, coarse sandstones and white tuff units, grading up to pink conglomerates, sandstone and tuff layering covered by Naşa volcanics. According to the determination of the age of Naşa volcanics (15.8±0.3 Ma and 15.2±0.3 Ma) (Ercan et al., 1997) the sedimentary fill in the Akdere basin must be older than 15.8 Ma. The Akdere basin began to develop as a symmetric graben with activity on the eastern edge lasting longer than activity on the western edge (Seyitoğlu, 1997*a*).

3.1.6. Early Miocene-Quaternary Paleogeographic Development of East-West Grabens in the Central Menderes Massif

The paleogeographic development of the Alaşehir, Büyük Menderes, Denizli and Küçük

Menderes grabens in the interval from the Early Miocene to Quaternary is summarized in figure 29. After the first exhumation of the Menderes massif with a dome shape (see: section 4) as a result of continuing north-south extension the proto Alaşehir, Büyük Menderes, Denizli and Sarıcaova grabens began to develop in the Early Miocene (Figure 29a). Proof of sedimentation in this period in the Alaşehir, Büyük Menderes and Sarıcaova grabens comes from the Eskihisar sporomorph association (Becker-Platen, 1970; Seyitoğlu and Scott, 1992; 1996; Ediger et al., 1996). In the Denizli graben sedimentation data comes from mammalian findings from the Early Miocene at Bostanyeri and Kabaağaç localities (Saraç, 2003; Alçiçek et al., 2007). In accordance with descriptions by Gawthorpe and Hurst (1993) the remaining area between the Büyük Menderes graben and Denizli graben may be assessed as a antithetic transfer zone while the area between the Denizli graben and Alaşehir graben may be a synthetic transfer zone (Figure 29a). In the Middle Miocene the antithetic transfer zone between the Büyük Menderes and Denizli grabens was semi-parallel to the Babadağ Fault controlling the Denizli graben forming the Bozdoğan and Karacasu grabens and the proto Küçük Menderes graben formed (Figure 29b). In the Late

Figure 29- Early Miocene-Quaternary Paleogeographic Development of Alaşehir, Büyük Menderes, Denizli and Küçük Menderes grabens. Pink areas represent flexural rotation of the Alaşehir and Büyük Menderes detachment faults.

Miocene the Karacasu graben and Denizli grabens became linked (Figure 29c). In the Pliocene second faults developed in the downdropped blocks of the first faults in the Alaşehir and Büyük Menderes grabens, the first faults became low-angle in accordance with the rolling-hinge model and they began to exhume as detachment faults. The Denizli graben continued to develop under control of the Babadağ Fault (Figure 29d). In the Quaternary the third faults developed in the Alaşehir and Büyük Menderes grabens and then antithetic faults in all half-grabens activated and they became full grabens (Figure 29 e). In the interval from the Quaternary to the present, young faults and the Buldan Horst developed leaving sediments from the Denizli graben suspended above it. The Büyük Menderes graben and Denizli graben joined and the north of the Denizli graben and east of the Alaşehir graben morphologically approached each other (Figure 29f).

3.2. NE-SW-Trending Basins

North of the E-W trending Alaşehir graben the presence of parallel NE-SW trending basins attracted the attention of researchers many years ago (Kaya, 1981; Şengör, 1987). As mentioned briefly in the introduction and to be further explained in the next sections, their role within the extensional tectonics of Western Anatolia is still debated (e.g., Ersoy et al., 2011; Karaoğlu and Helvacı, 2014).

3.2.1. Gördes Basin

The first observations on the basin are in studies by Nebert (1961) and Yağmurlu (1986). Seyitoğlu et al. (1992), Seyitoğlu et al. (1994) and Seyitoğlu and Scott (1994) investigated the isotopic age dating of volcanic rocks, palynology and stratigraphy in the basin. According to these studies, in the northwest section of the basin, the basement is composed of Izmir-Ankara suture zone and Dağdere formation starts with rounded cobble conglomerate derived from the ophiolitic basement and pebble conglomerates derived from metamorphic basement interlayers before passing up into sandstone, mudstone, lignite levels (Çıtak lignite) and marls. Lignite samples from three locations in the Dağdere formation were investigated by L. Benda and Eskihisar sporomorph association (20-14 Ma) was identified (for detailed pollen list see Seyitoğlu, 1992; Seyitoğlu et al., 1994) (Figure 30).

The lower levels of the Tepeköy formation, outcropping on the south and east edges of the Gördes basin, have been uplifted by the effect of central volcanics and are observed near Azimdağı (Figure 31). After a thin conglomerate derived from ophiolites, blocky conglomerates derived from metamorphics, coarse sandstone and red lithified sandstone form the lower levels of the Tepeköy formation. The upper levels of the Tepeköy formation

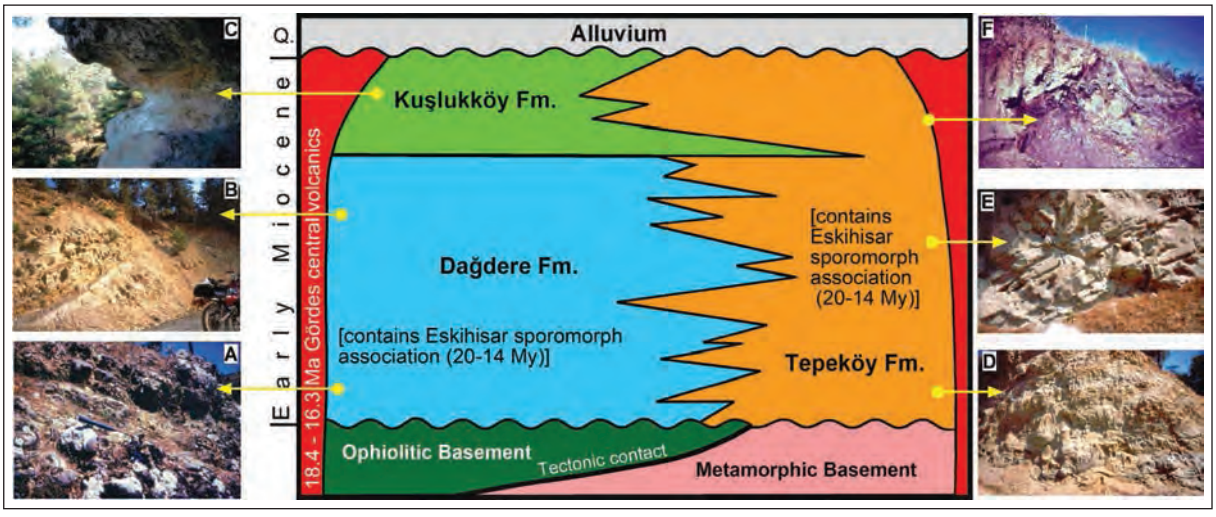

Figure 30- Stratigraphy of the Gördes basin (Taken from Seyitoğlu, 1992; Seyitoğlu and Scott, 1994). A) Conglomerate with recrystallized limestone blocks derived from ophiolitic basement which dominates the Dağdere formation. B) Upper levels of the Dağdere formations comprise fine-grained sandstone and mudstone and include lignite levels. C) The Kuşlukköy formation is distinguished by tuffs, comprising tuff, marl and limestone layers. D) Tepeköy formation includes conglomerates with blocks derived from metamorphic basement, blocks include mylonitic rocks. E) Yellow sandstone forming the upper levels of the Tepeköy formation. F) Cross cutting relationship of Gördes central volcanics and basin fill.

interfingers with the Kuşlukköy formation. Their general lithology is dark yellow sandstone and mudstones including conglomerate levels. The Tepeköy formation includes two locations with the Eskihisar sporomorph association (20-14 Ma) (Seyitoğlu, 1992; Seyitoğlu et al., 1994). The Kuşlukköy formation conformably overlies the Dağdere formation and shows lateral transition to the upper levels of the Tepeköy formation (Figure 30). The general lithology is tuff, sandstone, marl and silicified limestone intercalations. The tuff levels are the distinguishing element of the formation (Seyitoğlu and Scott, 1994). The central volcanics (18.4±0.8 Ma - 16.3±0.5 Ma) cut all basin fill and in the eastern margin of the basin a dated leucogranite dyke (24.2±0.8 Ma -21.1±1.1 Ma) provide its pebbles to the basin fill. As a result, the Gördes basin fill is broadly dated to the Early Miocene from 24 to 16 Ma (Seyitoğlu et al., 1992) (Figure 30).

Recent dating studies using new techniques for the Gördes basin have provided roughly the same results as isotopic age dating of volcanic rocks (Purvis and Robertson, 2005; Ersoy et al., 2011). Purvis and Robertson (2005) assessed the sedimentary facies of the basin fill while Ersoy et al. (2011) differentiated on the basis of formation. The Kızıldam formation at the bottom of the basin has been mapped near the basin margin faults. However, in the north of Dağdere village, the overlapped section is composed of limestones belonging to the upper levels of Dağdere formation. It is not a clastic unit of so-called Kızıldam formation. The Kızıldam formation described by Ersoy et al. (2011) has a conglomeritic unit with rounded clasts derived from ophiolitic basement and a conglomeritic unit with angular clasts derived from metamorphic basement. This situation means the Kızıldam formation is equivalent to the lower levels of the Dağdere and Tepeköy formations named in Seyitoğlu and Scott (1994) (Ersoy et al., 2011, p. 166). Contradictory to this statement, the type locality for the Kızıldam formation was chosen as the upper stratigraphic section where it interfingers with the Kuşlukköy formation (Ersoy et al., 2011). These clastic units found immediately east of Gördes are the upper sections of the Tepeköy formation, interfingering with the Kuşlukköy formation, found both above and below this formation (Seyitoğlu and Scott, 1994). However, in the general stratigraphic sequence of Ersoy et al. (2011) the Kızıldam formation is shown below the Kuşlukköy formation. The name used for the Kuşlukköy formation above the Kızıldam formation is the same as in Seyitoğlu and Scott (1994), but the descriptions are different (Ersoy et al., 2011). The contact of the original Kuşlukköy formation was drawn as the first observed tuff unit in the sequence (Seyitoğlu, 1992), in this situation the Çıtak coals remain within the Dağdere formation. However, Ersoy et al. (2011) include the Çıtak coals in the Kuşlukköy formation. According to Ersoy et al. (2011) the Kuşlukköy formation covers a large area including blocky conglomerates of the lower sections of basin fill cut and steepened by the central volcanics. The geological map in Ersoy et al. (2011, Figure 4) does not show a faulted/overlapped relationship in the southwest section of the basin. Seyitoğlu (1992) and Seyitoğlu and Scott (1994) showed that basin fill overlies metamorphic basement in the east section of the basin. These data and effects of the newly-described Kızıldam formation on the proposed regional model will be discussed later (See; Section 5.2).

3.2.2. Demirci Basin

Demirci basin sediments were examined by İnci (1984) and two sequences separated by an unconformity were determined. At the bottom of the basement fill, contrary to the original description of the Kürtköyü formation (Ercan et al., 1978), conglomerates including clasts derived from dominantly metamorphic rocks were reported to occur (İnci, 1984). Basin stratigraphy was examined by Yılmaz et al. (2000) and Early-Middle Miocene sequence and Pliocene limestones were distinguished. Ersoy et al. (2011) proposed the presence of two sequences separated by an unconformity. Here the Kürtköyü formation found in the lower section and outcropping in the north of the basin was determined to be formed of blocky conglomerate derived from metamorphic basement. It is necessary to emphasize this situation as it will be used as data in the discussion in Section 5.2 (Ersoy et al., 2011; Seyitoğlu, 1997*a*).

3.2.3. Selendi and Uşak-Güre Basins

The classic basin stratigraphy in Western Anatolia was created near Uşak by Ercan et al. (1978) and near Selendi by Ercan et al. (1983). The lower Hacıbekir Group comprises the Kürtköyü, Yeniköy and Küçükderbent formations (Figure 32). While the Kürtköyü formation is formed of conglomerates with a single source from ophiolite basement below, above schist and marble fragments are observed and are interpreted as alluvial fan deposits. The conformable

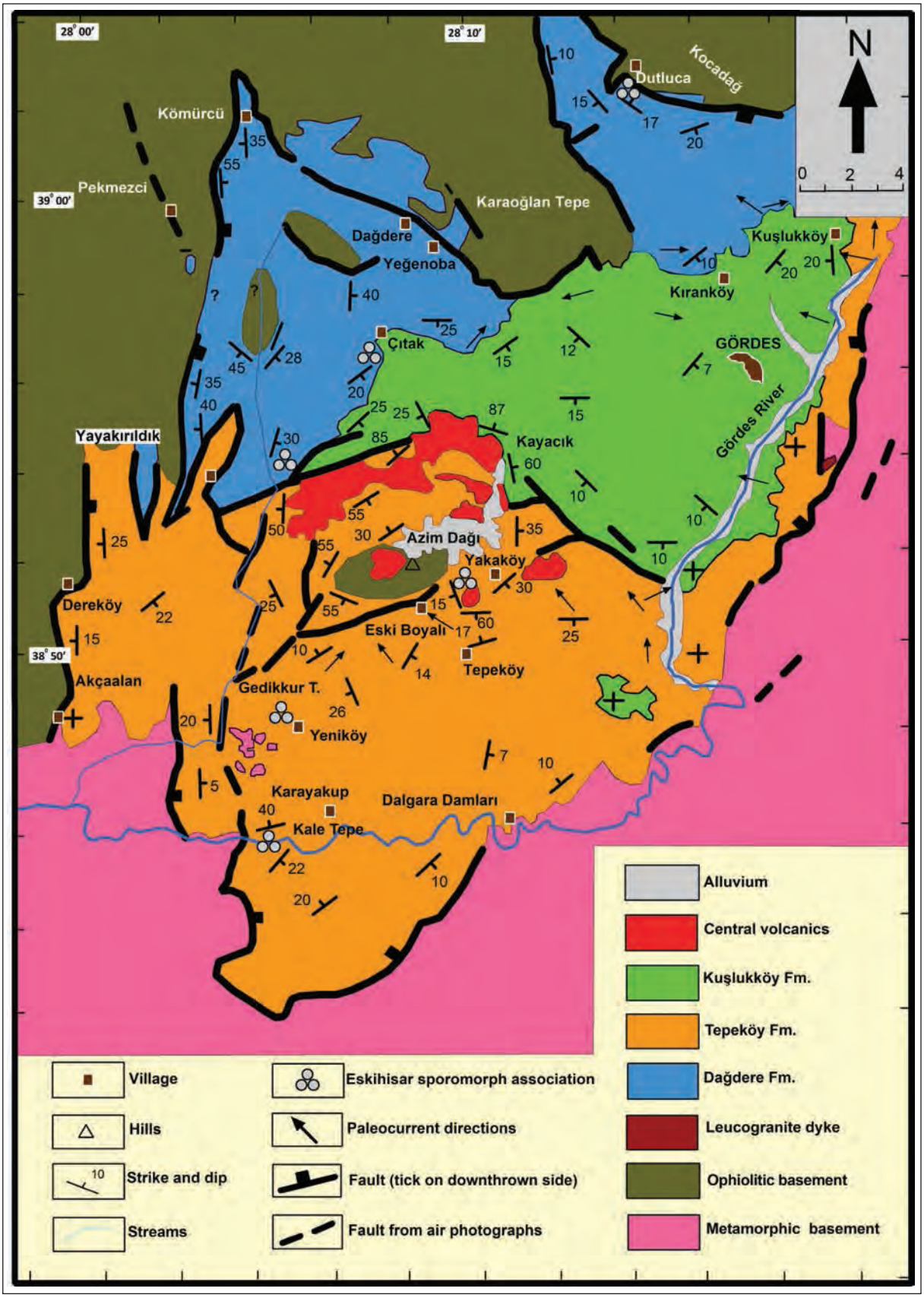

Figure 31- Geological map of the Gördes basin (Taken from Seyitoğlu, 1992; Seyitoğlu and Scott, 1994).

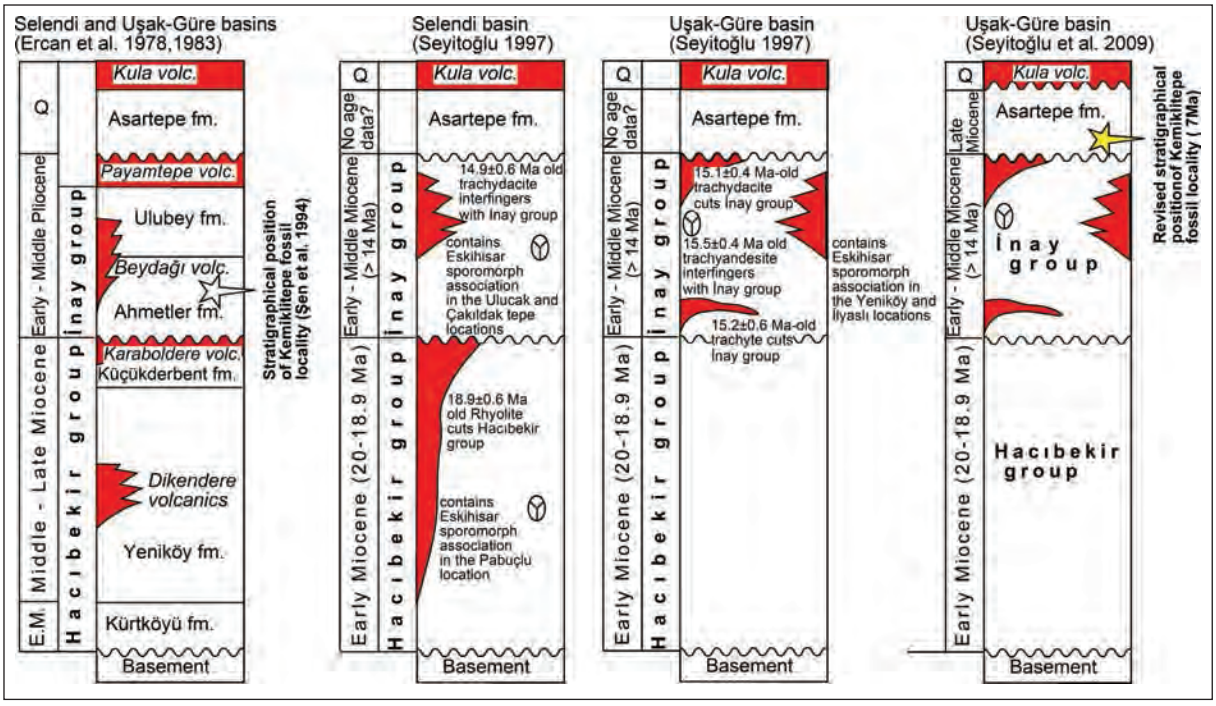

Figure 32 – Stratigraphy of the Selendi and Uşak-Güre basins and revised position of the Kemiklitepe fossil location (Taken from Seyitoğlu et al., 2009).

Yeniköy formation is formed of dark yellow-colored conglomerates, sandstone, claystone, tuffite and clayey limestone layers. Conformably overlying the Yeniköy formation, the Küçükderbent formation is composed of sandstone, claystone, tuffite and marly limestone and includes levels of organic-rich mudstone and gypsum. The İnay Group, unconformably overlying the Hacıbekir Group, is formed of the lower Ahmetler and upper Ulubey formations (Figure 32). The Ahmetler formation is divided into three members, generally formed of light-colored conglomerate, sandstone, claystone, tuffite and marls. The Ulubey formation is composed of lacustrine limestones (Ercan et al., 1978; 1983). Overlying both the Hacıbekir Group and the İnay Group unconformably, the Asartepe formation has red and orange/brown conglomerates and sandstone intercalations. This stratigraphy, along with simultaneously developing volcanic products, was named and stratigraphic positions were determined. It was reported that the Hacıbekir Group was deposited in the Early – Late Miocene, while the İnay Group formed during the Early – Late Pliocene and the Asartepe formation was assessed as Quaternary (Ercan et al., 1978; 1983).

Later studies identified the relationship between volcanic units and sedimentary units in the Uşak-Güre and Selendi basins. Isotopic age dating has been completed and palynological age dates obtained for lignite levels within the sequence (Seyitoğlu, 1997*b*; Seyitoğlu et al., 1997; Seyitoğlu and Benda, 1998).

Within the Hacıbekir Group in the Selendi basin, the Eskihisar sporomorph association (20-14 Ma) was identified, while the age of rhyolites cutting the group was determined as 18.9±0.6 Ma. Within the İnay Group, with an angular unconformity above the Hacıbekir Group, in both the Selendi and Uşak-Güre basins the Eskihisar sporomorph association has been determined. In the Selendi basin 14.9±0.6 Ma trachyandesites interfinger with the İnay Group, in the Uşak-Güre basin 15.2±0.6 Ma and 15.1±0.4 Ma trachite and trachyandesites cut the İnay Group and 15.5±0.4 Ma trachyandesite interfingers the İnay Group (Figure 32). While all of these age data show the Hacıbekir Group was deposited in the Early Miocene, they show the İnay Group formed in the early Middle Miocene. As the İnay Group includes the Eskihisar sporomorph association it cannot be younger than 14 Ma and as a result the Kemikliktepe fossil location (Şen et al., 1994) within the İnay Group and given an age of Late Miocene needs to be re-evaluated. This study once again reveals, with comprehensive data, that the E-W grabens and north-trending basins in Western Anatolia began to form

simultaneously under a N-S extensional tectonic regime (Seyitoğlu, 1997*b*).

After using the early Middle Miocene age of the İnay Group and its horizontal position to disprove (Seyitoğlu, 1999) regional compression in the proposal of a two-stage extensional model by Koçyiğit et al. (1999), discussions of the age of the İnay Group are found in a series of articles researching the regional uplift, especially. Westaway et al. (2003; 2004) investigated the uplift history of Western Anatolia by using terraces of the Gediz River covered by Kula volcanics. Using the mammalian fossil content of the Kemiklitepe fossil location, shown within the İnay Group, and magnetostratigraphy (~7 Ma) it was proposed that Gediz river erosion began after the end of deposition of the İnay Group in the Late Pliocene about 3 Ma ago (Westaway et al., 2005; Westaway et al., 2006). Uplift calculations in the region are based on this acceptance and it is proposed that as edge faults of the Uşak-Güre basin are not found, and there is a problem between the isotopic ages of the İnay Group and mammalian fossil ages, palynological ages need to be reworked (Westaway et al., 2005; 2006). Seyitoğlu et al. (2009) reviewed the stratigraphic position of the Kemiklitepe fossil location and as stated in the study first defining the age (Şen et al., 1994) determined it was not within the İnay Group, but contrarily it is in the Asartepe formation unconformably overlying the İnay Group. Additionally the Kemiklitepe fossil locality within the Asartepe formation was compared with the Karabeyli fossil location newly found in the same formation deposited in front of NE trending normal faults in the Uşak-Güre basin and it was determined that the Asartepe formation was deposited in the Late Miocene. This data confirms studies reporting the age of the İnay Group as early Middle Miocene and the isotopic age data and palynological findings (Seyitoğlu, 1997*b*; Seyitoğlu et al., 1997; Seyitoğlu and Benda, 1998) and disproves studies proposing a contradiction between mammalian fossils, and palynological and isotopic age data in Western Anatolia (Figure 32). As a result, it is necessary to reconsider studies (Westaway et al., 2003; 2004; 2005; 2006) extending the deposition of the İnay Group to the Pliocene and beginning erosion around 3 Ma, as well as all uplift models ignoring NE-trending faulting (see Seyitoğlu et al., 2009 for detail).

Other data showing the Asartepe formation deposited in the Late Miocene is found in the Selendi basin (Ersoy and Helvacı, 2007). Here the Kocakuz formation, accepted as equivalent to the Asartepe formation, is covered (Ersoy and Helvacı, 2007) by trachybasalts with ages from 8.5±0.2 Ma and 8.37±0.07 Ma (Ercan et al., 1996; Innocenti et al., 2005).

The volcanic rocks in the Selendi and Uşak-Güre basin have been dated by a more sensitive method (Ar/Ar) (Purvis et al., 2005) and obtained similar values to K-Ar results in Seyitoğlu et al. (1997). Ersoy et al. (2008) defined calcalkaline and alkaline volcanic products with two different compositions from the Early Miocene (20.03-17.87 Ma) interfingering the Hacıbekir Group and determined the presence of bimodal volcanism. The tectono-sedimentary development proposed by this study will be discussed in the latest developments section about exhumation mechanisms of the Menderes Massif (See: Section 5.2).

4. Exhumation Mechanism of the Menderes Core Complex

According to nearly all thermochronological data obtained from the Menderes Massif (Gessner et al., 2001; Ring et al., 2003), the Menderes Massif reached the surface nearly 25-20 Ma ago. Under the control of the Alaşehir and Büyük Menderes detachment faults, the central Menderes Massif appears to have been rapidly exhumed a second time since 5 Ma. Based on this data Ring et al. (2003) determined the Menderes Massif was exhumed as a symmetrical core complex between the north-dipping Simav Detachment Fault and south-dipping Lycian Detachment Fault in the Late Oligocene-Early Miocene. In the Miocene-Pliocene period the Alaşehir and Büyük Menderes detachment faults worked in accordance with the flexural rotation model in the central Menderes massif and it was determined that the symmetric core complex was uplifted once more.

Seyitoğlu et al. (2004) used previous studies and microtectonic data in the massif to propose an alternative model for the complete exhumation history of the Menderes Massif (Figure 33). Accordingly the Menderes Massif was first exhumed as an asymmetric core complex.

The main breakaway fault extends from west to east from south of the Gulf of Gökova following south of the Kale basin toward the northeast (Figure 33). This north-dipping normal fault is named the

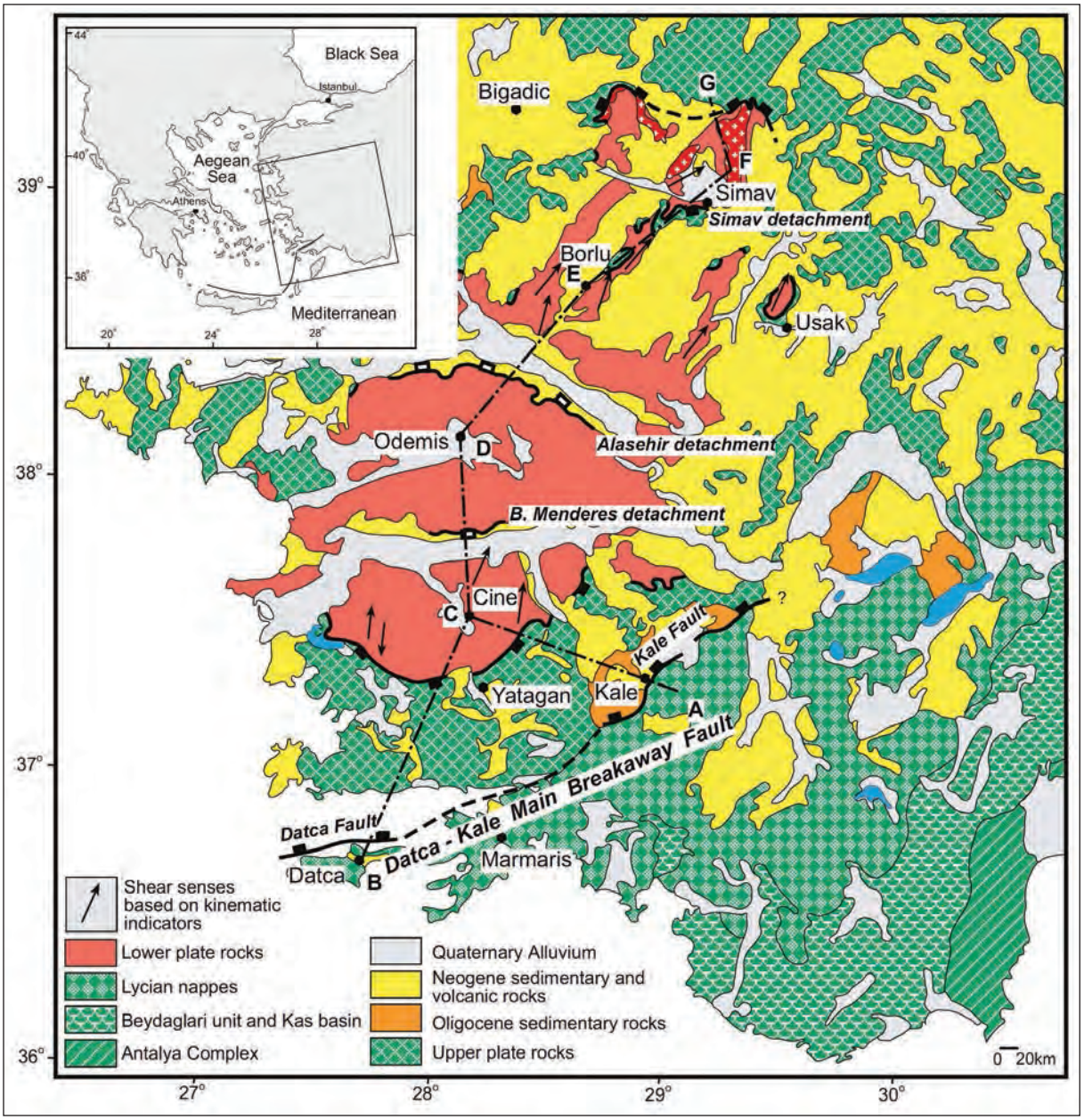

Figure 33- Menderes core complex and location of main tectonic elements in Western Anatolia (Taken from Seyitoğlu et al., 2004).

"Datça – Kale Main Breakaway Fault" (Seyitoğlu et al., 2004) and is clearly seen on submarine seismic reflection profiles in the Gulf of Gökova (Kurt et al., 1999). The north-dipping listric normal fault observed on seismic reflection profiles continues in the land toward the northeast (Çağlar and Duvarcı, 2001). A wedge geometry on the downdropped block thickening toward the main fault is clearly observed and contains a sedimentary sequence that may be said to have deposited simultaneously with faulting (Kurt et al., 1999) (Figure 34).

Though the age of this sequence was interpreted as Late Miocene-Quaternary by Kurt et al. (1999), there is no definite data on this topic. Oligocene conglomerates have been mapped north of the Gulf of Gökova (Gürer and Yılmaz, 2002) controlled by antithetics of the Datça Fault; as a result the sequence observed on the downdropped block of the Datça Fault may possibly be Oligocene (Özerdem et al., 2002). Toward the northeast the Kale basin developed in the Oligocene-Early Miocene (Dürr, 1975; Yılmaz et al., 2000; Akgün and Sözbilir, 2001) begins with coarse conglomerates derived from ophiolite

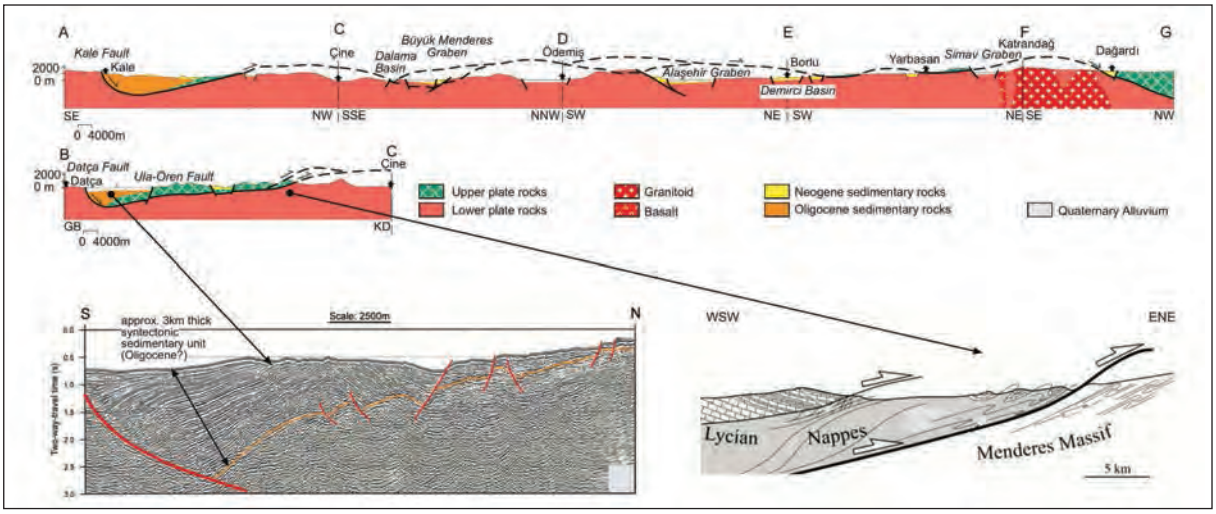

Figure 34- At top, geological cross section including the Simav Detachment Fault north of the Datça-Kale Main Breakaway Fault (Seyitoğlu et al., 2004). Lower left, reinterpretation of seismic reflection profile of the Datça Fault in the Gulf of Gökova from Kurt et al. (1999). Lower right, cross section of the region interpreted as where the Datça-Kale Main Breakaway Fault flexes and comes to the surface (Rimmele et al., 2003). See text for details.

basement and continues with conglomerates, sandstone, siltstone, shale and limestone intercalations. The coarse clastic debris flows at the base of the sedimentary sequence, fluvial deposits show paleocurrent directions from southeast to northwest and are controlled by the Kale Fault in the south of the basin (Gürer and Yılmaz, 2002). Thinning toward the top of the Kale basin, the Oligocene – Lower Miocene sequence is unconformably overlain by the Upper Miocene – Pliocene sequence. The section where the Datça-Kale Main Breakaway Fault flexes upward and reaches the surface is found 6 km north of Yatağan on the Yatağan-Çine road (Figure 35).

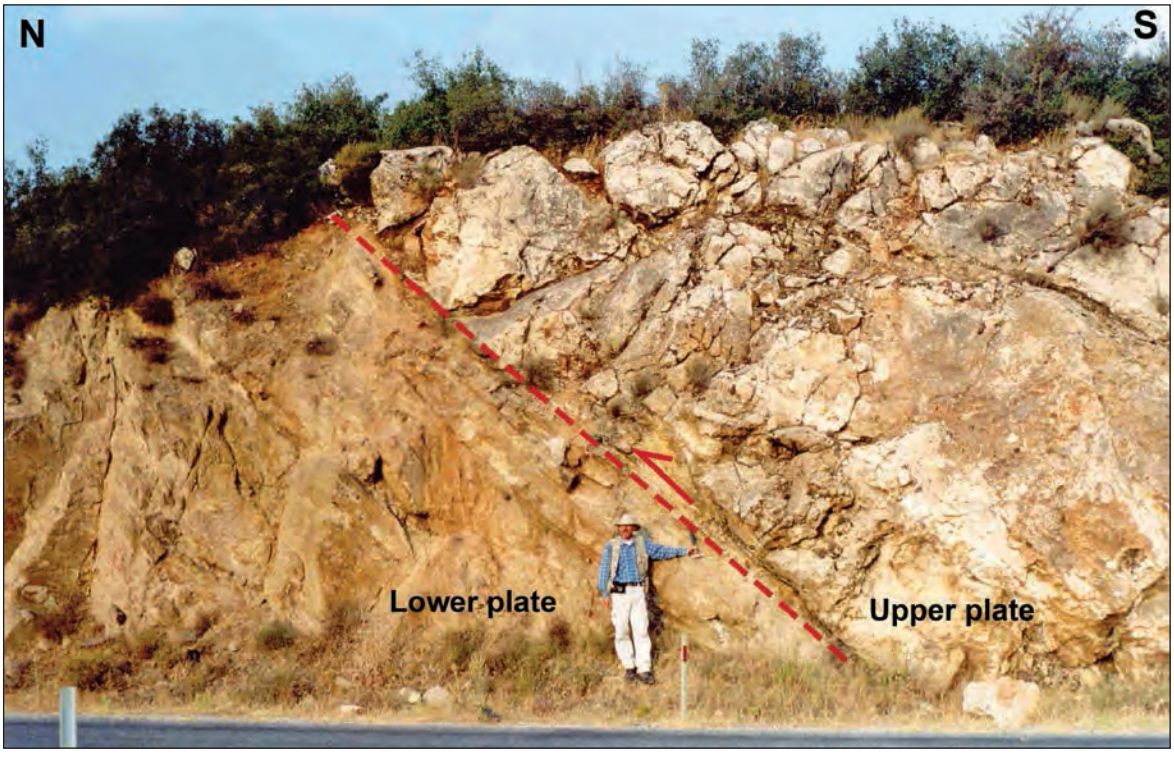

Figure 35- Section where the Datça-Kale Main Breakaway Fault flexes to reach the surface on the Yatağan –Çine road.

The footwall block is overprinted by scattered brittle structures of top-to the NNE shearing. A similar shearing direction is observed between the Lycian ophiolites and the Menderes Massif (Bozkurt and Park, 1999; Rimmele et al., 2003). It is thought that the Datça-Kale Breakaway Fault which flexes up toward the top-to the NNE shearing was formed by the main shear zone (Seyitoğlu et al., 2004) (Figure 34). According to this assessment, Gökova and Kale basin fill, Lycian ophiolites and Menderes Massif cover rocks form the upper plate above the main breakaway fault. From north of the Yatağan-Çine road to beyond Mount Simav, the whole Menderes Massif are lower plate rocks of the Datça-Kale Main Breakaway Fault and its northern continuation, the Simav Detachment Fault. Apart from this, remaining upper plate pieces from the first detachment above the massif are found currently at Dalama south of Aydın, in the southeast of the Gördes basin, in the east of the Demirci basin and south of Simav. When all data are evaluated, according to this model (Seyitoğlu et al., 2004), which is in accordance with thermochronological data, explains basin development, provides a logical explanation for the contradictory north and/or south movement within the Lycian nappes, and does not contradict geological observations, the exhumation of the Menderes Massif occurred in the following way (Figures 36 and 37).

In the Late Paleocene-Early Eocene continental collision between the Menderes-Taurus block and the Sakarya continent occurred along the Izmir-Ankara suture zone and the Lycian nappes were emplaced above the Menderes Massif causing main Menderes metamorphism in the Late Eocene (Şengör et al., 1984) (Figure 36a).

After completion of Lycian nappe emplacement, the orogeny developing as a result of collision began extension in a N-S direction. In the Oligocene at the surface the north-dipping Datça-Kale Main Breakaway Fault controlled deposition in the Gökova and Kale basins, while in the middle crust top-to-the N directed shearing occurred. This shearing is dated to 43-30 Ma in the South Menderes Massif (Hetzel and Reischmann, 1996; Lips et al., 2001; Catlos et al., 2002); however debates continue about this date (Gessner et al., 2004; Bozkurt, 2004; Erdoğan and Güngör, 2004). On the Simav shear zone, the northern continuation of the Datça-Kale Main Breakaway Fault, syntectonic intrusion of the Eğrigöz granitoid occurred at 22 Ma (Işık et al., 2003; 2004) (Figure 37a,b). This age data (Ar-Ar and apatite fission-track) generally is observed to become younger toward the north. Flexure of the Datça-Kale Main Breakaway Fault upwards began around 25 Ma according to thermochronological data. This flexure caused the development of apatite fission-track ages which young to the south in the southern Menderes Massif. Finally the flexure of the main breakaway fault brought lower plate rocks to the surface (Figures 36c and 37b) at 20 Ma as shown by thermochronological data (Gessner et al., 2001). Micro tectonic data obtained from the Menderes Massif show that post Eocene movement direction was top-to-the NNE. However, the top-to-the NNE structures in the southwest of the massif were overprinted by weaker top-to-the SSW structures (see also: Hetzel et al., 1998; Lips et al., 2001; Bozkurt, 2004). This situation may be related to the Menderes Massif having a dome shape and the main breakaway fault slipping slightly south (Seyitoğlu et al., 2004).

In the interval from the Oligocene-Early Miocene uplift of the footwall of the Datça-Kale Main Breakaway Fault caused movement of the Lycian nappes to the south due to gravity sliding and the final Lycian nappe emplacement in the Burdigalian (Seyitoğlu et al., 1992; Collins and Robertson, 1998; 2003; Seyitoğlu et al., 2004).

The dome-shaped uplift of the Menderes Massif was fragmented by the E-W Alaşehir, Büyük Menderes and Denizli grabens and north-trending basins in the Early Miocene (Seyitoğlu, 1997; Seyitoğlu et al., 2002; Şen and Seyitoğlu, 2009; Alçiçek et al., 2007). Due to the flexural rotation/rolling hinge of the Alaşehir and Büyük Menderes grabens, the central Menderes Massif was exhumed for a second time, this time as a symmetric core complex (Gessner et al., 2001; Seyitoğlu et al., 2002) (Figures 36c,d and 37c,d,e). In the Pliocene to Quaternary young grabens developed (e.g., Simav), other main grabens became symmetric and high-angle faults fragmented older structures masking the previous extensional history of the Menderes Massif (Seyitoğlu et al., 2004) (Figure 37f).

5. Discussion

5.1. Movement of the Lycian Nappes in Southwest Turkey and First Exhumation of the Menderes Massif

In Southwest Anatolia in the area between Lake Bafa and the Gulf of Gökova, movement of the Lycian nappes above the Menderes Massif was

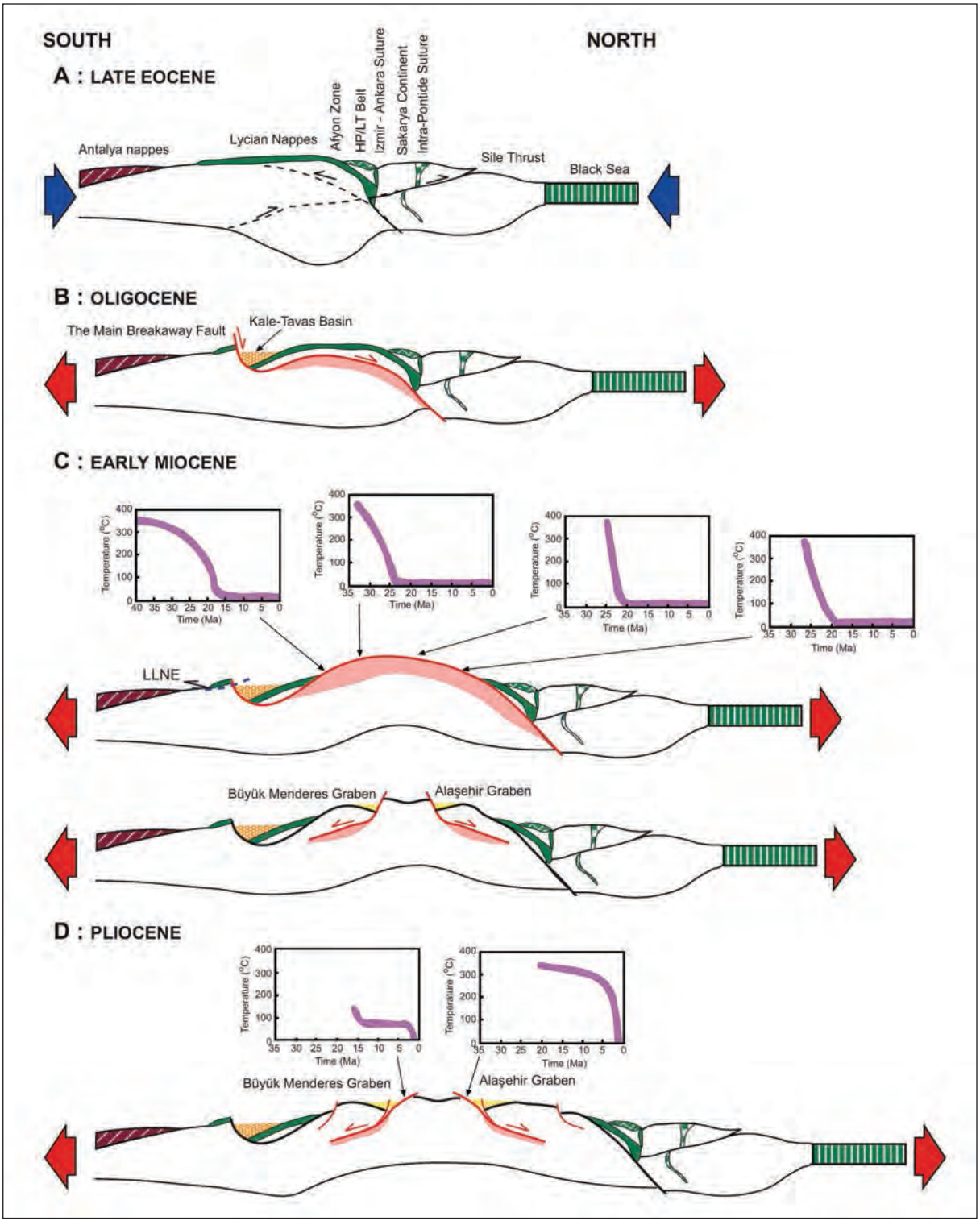

Figure 36- Two stage exhumation model of the Menderes Massif as asymmetric and symmetric core complex (Taken from Seyitoğlu et al., 2004). Thermochronologic ages belong to Gessner et al. (2001) and Ring et al. (2003). LLNE: Last Lycian Nappe Emplacement.

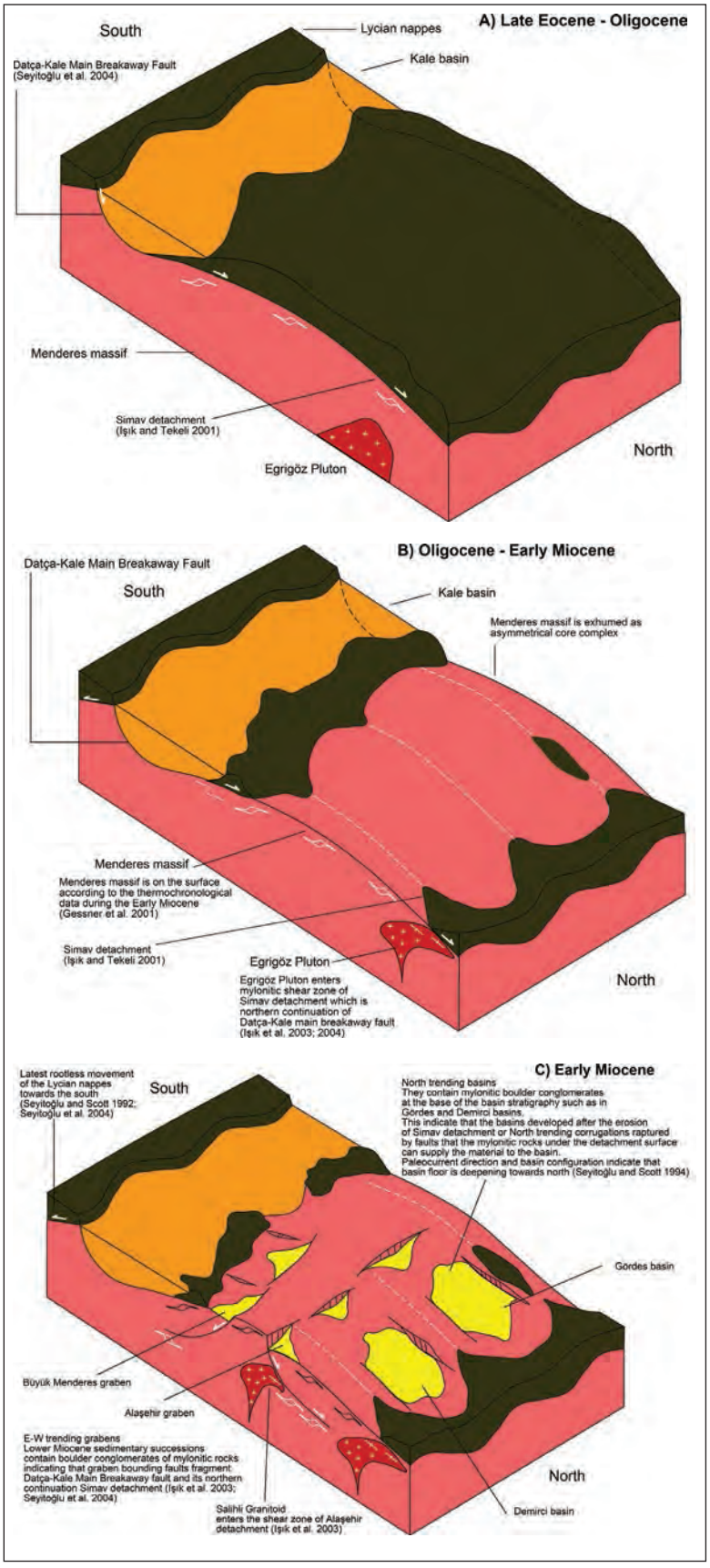

Figure 37- (A-B-C) Three-dimensional representation of exhumation of the Menderes Massif as asymmetric and symmetric core complexes.

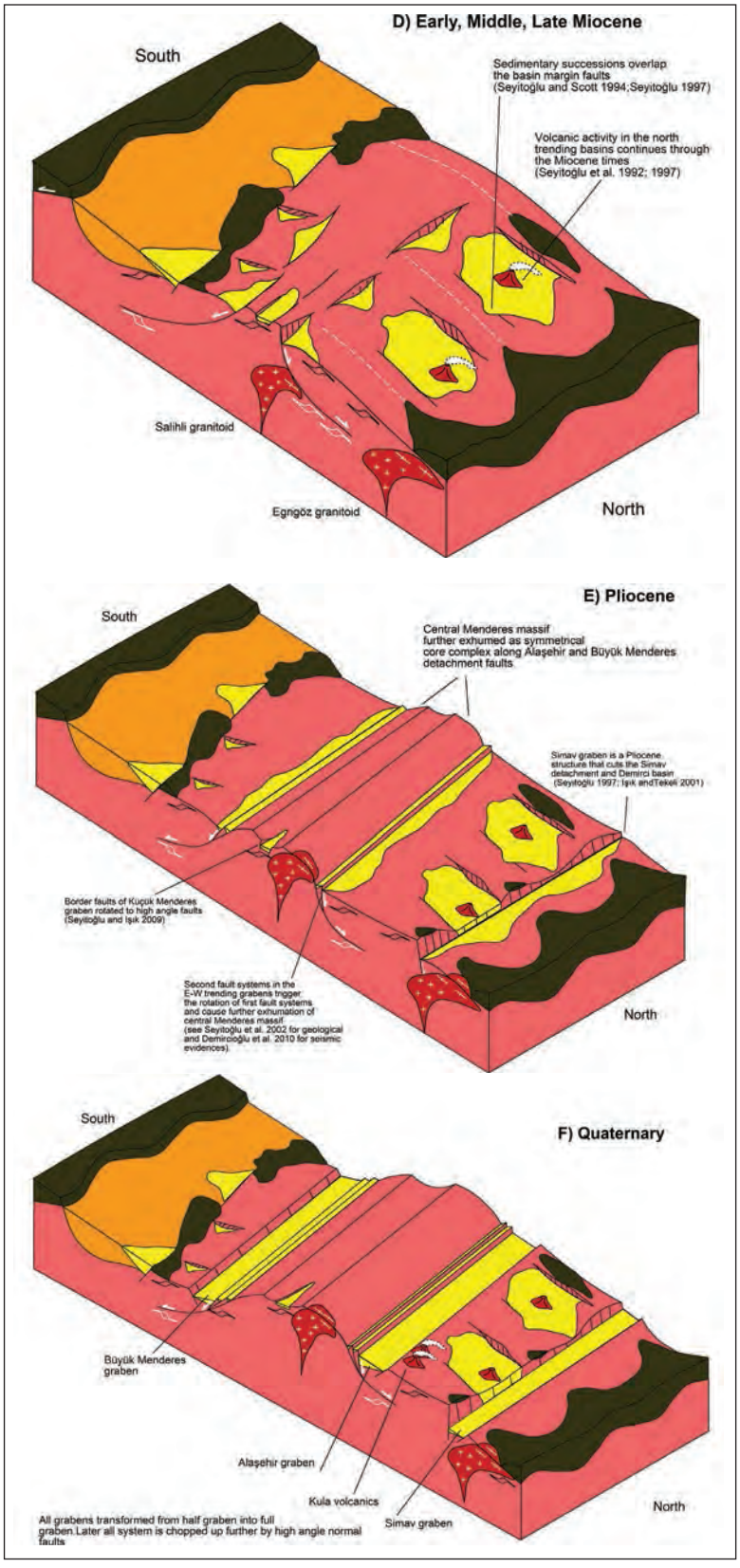

Figure 37- (D-E-F) Three-dimensional representation of exhumation of the Menderes Massif as asymmetric and symmetric core complexes.

toward the north (Bozkurt and Park, 1999; Rimmele et al., 2003). This data does not comply (Seyitoğlu et al., 2004) with the assumption that the Menderes Massif was sheared with top-to the S shearing (Ring et al., 2003) by the south-dipping Lycian Detachment Fault in the Oligocene-Early Miocene. On the other hand, the S-SE movement (Collins and Robertson, 2003) of the Lycian nappes between the Menderes Massif and Beydağları gives the impression of the contradiction about movement direction of the Lycian nappes in southwest Anatolia (van Hinsbergen, 2010). In fact the model of the first exhumation of the Menderes Massif as asymmetric (Seyitoğlu et al., 2004) provides a logical explanation of the two opposite directional movements of the Lycian nappes. In the area remaining north of the Datça-Kale Main Breakaway Fault, the movement to the north (Rimmele et al., 2003) observed for the Lycian nappes between Lake Bafa and the Gulf of Gökova is in accordance with shearing as the Datça-Kale Main Breakaway Fault reached the surface through upward flexure. The south-southeast movement of the Lycian nappes south of the Datça-Kale Main Breakaway Fault is related to the rootless gravity sliding to the south of the Lycian nappes as a result of uplift of the footwall of the main breakaway fault (Seyitoğlu et al., 2004).

5.2. Latest Developments about Exhumation Mechanisms for the Menderes Massif

On the exhumation of the Menderes Massif, van Hinsbergen (2010) proposed that as the Menderes Massif was exhumed with a top-to-the NE direction on the Simav Detachment Fault, Lycian nappes were detached above the massif toward the southeast. The element of this proposal that requires explanation is that while the movement developing on the Simav Detachment Fault in the north Menderes Massif left traces, the Lycian detachment proposed by van Hinsbergen (2010) left no trace on the massif. The dominant kinematic data from the south Menderes Massif has top-to the N direction, slightly overprinted by a top-to the S directed movement (Seyitoğlu et al., 2004). The proposal of van Hinsbergen (2010), similar to that of Ring et al. (2003), does not appear to comply with kinematic indicators in the south Menderes Massif.

A recent study investigating the complete exhumation history of the Menderes Massif (Gessner et al., 2013) proposed that the first exhumation of the massif occurred with top-to-the N directed unilateral shearing and shows it is one step closer to the asymmetric exhumation model than the symmetric exhumation model (Ring et al., 2003) by the same researchers. However, this proposal does not include any recommendations related to the necessary sedimentary basin forming in the hanging wall of the main breakaway fault (Gessner et al., 2013). In this study, Gessner et al. (2013) proposed a left directed shearing west of the Menderes Massif named the "Western Anatolian Transfer Zone". Seyitoğlu et al. (2004) stated the necessity for a transfer zone linking the main breakaway fault north of Crete proposed by Faure et al. (1991) with the Datça-Kale Main Breakaway Fault, and advocated that the Cyclades and Western Anatolia had a common extensional history (Seyitoğlu et al., 2004) (Figure 33, attached small sketch).

Recent studies encompassing only the north Menderes Massif and aiming to explain the Simav and Alaşehir detachment faults and north-trending basin development will be discussed below in terms of compliance with field observations.

The proposed model for the evolution of the northern Menderes Massif in the article by Ersoy et al. (2010) occurs in advanced stages within an extensional tectonic regime. In the Late Oligocene-Early Miocene the Simav Detachment Fault developed along with deposits of the Hacıbekir Group and bimodal volcanism above it. In the Middle Miocene, the Gediz (Alaşehir) detachment fault formed and the deposits of the İnay Group above it. On the hanging wall of the Gediz (Alaşehir) detachment fault, cross grabens bounded by oblique normal/strike slip faults developed and controlled the deposition of the İnay Group and Kocakuz (Asartepe) formation. At this stage, the noteworthy elements of the proposed model may be listed as: (a) the Gediz (Alaşehir) graben (basin) begins as a low angle detachment fault, (b) contains coeval sediments to the Middle Miocene-age İnay Group, and (c) in the Plio-Quaternary period high-angle normal faults form E-W trending symmetric Gediz (Alaşehir) and Simav grabens. The opposing opinions to the above model proposed in the article by Ersoy et al. (2010) may be summarized as follows.

(1) First exhumation of the north Menderes Massif by the Simav Detachment fault the stage where the massif is cleared of ophiolite cover (Lycian nappes) above the Simav Detachment Fault is not well reflected to the sediments of the Hacıbekir Group. The measured stratigraphic section given in Ersoy et al. (2010) has thickness of ophiolite-source

clasts as around 10 m. After such a small amount of ophiolitic material, there are conglomerates derived from rock fragments from the massif below.

The impression Ersoy et al. (2010; 2011; 2014) wish to create in their articles is the presence of the well-developed Kürtköyü formation derived from ophiolitic basement at the bottom of all north-trending basins. If this can be shown it supports deposition of the Hacıbekir Group simultaneous to the Simav Detachment Fault.

The Kürtköyü formation was first investigated in the Uşak-Güre basin in an article by Ercan et al. (1978) and was described as dominantly clastic material derived from ophiolitic basement (majority conglomerates, sandstone). However, in the Selendi basin the Kürtköyü formation is not differentiated on the geological map of the Selendi Basin in Ersoy et al. (2010) (or has such a small area that it cannot be shown on that scale of map), while the text says the conglomerate at the base of the Kürtköyü formation is metamorphic origin and emphasizes that the conglomerates in the Uşak-Güre basin mentioned in passing have ophiolitic origin. On the other hand, measured stratigraphic sections in both basins show ophiolitic-origin conglomerates. Their thickness is too thin for them to be the first detachment material considering the gigantic presence of Lycian nappes causing main metamorphism in the Menderes Massif.

In Ersoy et al. (2011) the Kürtköyü formation with proposed presence in the north of the Demirci basin is blocky conglomerate derived from metamorphic basement (according to our personal observations these blocks include mylonitic rock fragments observed below the detachment fault) which does not fit the description of the original Kürtköyü formation. This formation is more in accordance with the description of the Borlu formation by Yılmaz et al. (2000). The Borlu formation shown by Yılmaz et al. (2000) at the base of the Demirci basin, is carried to the upper sections of the sequence by Ersoy et al. (2011) (See Ersoy et al., 2011; Figure 3). Shown underneath the Yeniköy formation in the Demirci basin (Ersoy et al., 2011; Figure 9b) the Kürtköyü formation is not the original Kürtköyü formation described by Ercan et al. (1978) formed of ophiolitic-origin rock fragments.

In the Gördes basin the Tepeköy formation, coeval with the Hacıbekir Group as revealed by isotopic age dating and explained in detail in Section 3.2.1, is formed fully of mylonitic material derived from metamorphic rocks while the Dağdere formation which interfingers with it, contains material derived from dominantly ophiolitic rock (Seyitoğlu, 1992; Seyitoğlu and Scott, 1994). This observation indicates that in some areas of the massif, north-trending basins formed after being denuded of ophiolitic rock with the basins filling with clasts derived from whatever lithology was located as the basement locally. However, Ersoy et al. (2011) ignored this distinction in the Gördes basin and combined formations containing conglomerates with different composition and named them the Kızıldam formation. This formation is correlated with the Kürtköyü formation observed in other north-trending basins (Ersoy et al., 2010). When it is considered that the above explanation is incompatible with the original Kürtköyü formation in the Demirci basin, it is clear that the correlations made will create confusion in basin stratigraphy.

In the geological map of the Gördes basin presented by Ersoy et al. (2011) the conglomeratic units of the lower levels of the basin deformed by volcanics near the central volcanics are shown as the upper levels of the Kuşlukköy formation in basin stratigraphy. Apart from this the tuff levels used as a characteristic marker for the original Kuşlukköy formation definition (Seyitoğlu, 1992; Seyitoğlu and Scott, 1994) appear to not to have been taken into account by Ersoy et al. (2011). The clastic Kızıldam formation, the lower part of basin fill, overlaps ophiolitic basement on the north of Dağdere (Ersoy et al., 2011), in fact this overlapping occurred with limestone in the upper levels of the Dağdere formation (Seyitoğlu, 1992). The faulted/overlapped relationship of the Tepeköy formation, with palynological samples from lignite levels in the southwest of the Gördes basin identified to contain the Eskihisar sporomorph association, was determined to have deposited under control of high angle faults since the beginning of the Gördes basin (Seyitoğlu, 1992; Seyitoğlu and Scott, 1994); however maps for this section of the basin are not observed in the study by Ersoy et al. (2011).

In conclusion, the Hacıbekir Group or equivalent sedimentary units alleged to have been deposited above the Simav Detachment Fault do not contain significant thicknesses of sedimentary material derived from the upper plate (mainly ophiolitic rocks), with the initial sediments in some basins observed to contain mylonitic rock fragments from below the detachment fault. In the location where the

Kürtköyü formation is found in accordance with the original description (Ercan et al., 1978), there are sections with patches of ophiolitic fragments belonging to the upper plate of the Simav Detachment Fault. As a result, this casts doubt on the claim that the Hacıbekir Group was deposited simultaneously to the Simav Detachment Fault.

(2) The photograph showing the relationship between the Simav Detachment Fault and the proposed coevally deposited Hacıbekir Group (Ersoy et al., 2010; Figure 9b) does not show slipped sediments above the detachment fault but shows a buttress unconformity.

(3) In the model by Ersoy et al. (2010), it is proposed that the first stage of the Gediz (Alaşehir) basin is controlled by low angle detachment faults. The counter argument (See: Section 3.1.1) to the similar proposal by Öner and Dilek (2011) is valid for the model by Ersoy et al. (2010). Additionally the first sedimentary unit in the Alaşehir (Gediz) graben of the Alaşehir formation was deposited in the Early Miocene, which is inconsistent with the proposed Gediz (Alaşehir) graben in Ersoy et al. (2010) presented as beginning in the Middle Miocene. The Early Miocene age data (Catlos et al., 2010) obtained above the Alaşehir Detachment Fault is not explained in the Ersoy et al. (2010) model.

(4) In the last stage of the Ersoy et al. (2010) model (Plio-Quaternary), high angle faults cut the low angle Gediz (Alaşehir) detachment fault. As a result, movement is not expected on this low angle fault. However, age data above the Alaşehir Detachment Fault (Gessner et al., 2001; Buscher et al., 2013) shows activity on the Alaşehir Detachment Fault in the Plio-Quaternary period. Age data from above the Alaşehir Detachment Fault in the Early Miocene to Quaternary interval show the initial high-angle normal faults of the Alaşehir (Gediz) graben rotated and activity continued to develop in a "rolling hinge" model (Seyitoğlu et al., 2002), or in other words an "Alaşehir type - rolling hinge model" developed. Readers can reach collected age data above the Alaşehir Detachment Fault in the article by Seyitoğlu et al. (2014).

Karaoğlu and Helvacı (2012) proposed a similar model to the one discussed above by Ersoy et al. (2010). The tectono-stratigraphic sequence presented by Karaoğlu and Helvacı (2012; Figure 3) shows a physical contact between the Ahmetler and Ulubey formations and the Gediz (Alaşehir) detachment fault (Ersoy et al., 2010). Such a physical contact is not observed in the field, is not reflected in field relationships and is based on assumption. The Menderes Massif did not reach the surface in the Early Miocene near Uşak-Güre as asserted by Karaoğlu and Helvacı (2012) and it is stated that the Hacıbekir Group does not contain rock fragments from the Menderes Massif. But even in the upper levels of the Kürtköyü formation at the bottom of the Hacıbekir Group, there are metamorphic pebbles reported (Ercan et al., 1983). In the Gördes and Demirci basins, containing coeval sediments to the Hacıbekir Group, blocky conglomerates derived from the Menderes Massif are clearly observed. Similarly in the Selendi basin at Pabuçlu village metamorphic rock fragments are clearly seen in the Hacıbekir Group (Figure 38). Additionally within the Uşak-Güre basin the typical Yeniköy formation within the Hacıbekir Group observed along the Uşak-Kütahya road contains metamorphic pebbles within conglomeratic levels. At Eynehan village, the tilted Yeniköy formation is overlain above an unconformity by the İnay Group and metamorphic pebbles are clearly seen in the conglomeratic levels (Figure 39).

All of these observations show the Menderes Massif was already exhumed under the Simav Detachment Fault during sedimentation of the Yeniköy formation (Hacıbekir Group) and provided material for the Yeniköy formation. The fault shown between the Menderes Massif and the Yeniköy formation NE of Kurtçamı on the geological map presented in Karaoğlu and Helvacı (2012) does not have "detachment" features but is a moderate-angle normal fault. The cover unit of this fault is not the Merdivenlikuyu member as shown on the map, but belongs to the Asartepe formation unconformably overlying the İnay Group. The most striking relationship mapped by Karaoğlu and Helvacı (2012) is the presence of sediments belonging to the Yeniköy formation dipping toward a very low angle detachment fault near Kadiroğlu village (Karaoğlu and Helvacı, 2012). Foliation of metamorphic rocks and layering of sedimentary units above them are nearly parallel in this area with an overlapping relationship. Near to the Kadiroğlu village, İnay Group sediments have turned yellow from the heating effect of the Zahman volcanics. Moving from here, the sedimentary units colored yellow due to the heating effect may be confused with the Yeniköy formation. The true Yeniköy formation outcrops on the lower altitudes inside the valley to the east of Kadiroğlu village.

Figure 38- Metamorphic blocks in tilted blocky conglomerates of the Hacıbekir Group at Pabuçlu village in SW Selendi basin overlain above an unconformity by the nearly-horizontal İnay Group. Clear examples shown by red arrows. Length of the pickaxe is 80 cm.

The presence of metamorphic pebbles within sediments in the lower sections of the north-trending basins; in the Tepeköy formation of the Gördes basin (Seyitoğlu and Scott, 1994), in the Borlu formation of the Demirci basin (Yılmaz vd., 2000), and in the Hacıbekir Group of the Selendi and Uşak-Güre basins (Seyitoğlu, 1997) show that during deposition the Menderes Massif was already at the surface and as a result indicate that the model presented by Karaoğlu and Helvacı (2012; Figure 13) is invalid.

6. Conclusions and Recommendations

The exhumation of the Menderes Massif in the Oligocene as an asymmetric core complex caused the formation of the Oligocene Kale basin in the hanging wall of the Datça – Kale Main Breakaway Fault (Seyitoğlu et al., 2004). The observed field relationships and other observations shed doubt on the claim that the coeval sediments of Simav Detachment Fault are sediments supposedly belonging to the Hacıbekir Group observed in the north-trending basins. This situation should lead to a search for an answer to the question: if coeval sediments to the Simav Detachment Fault are not the Hacıbekir Group, what group are they? Outcropping in a very small area of the north Menderes Massif the Başlamış formation is described as an Eocene-Oligocene (?) sedimentary unit (Akdeniz, 1980) and no other Oligocene-age sedimentary outcrop is known.

Detailed kinematic analysis of the Kazdağ core complex in the Biga Peninsula has shown the first exhumation of the Kazdağ core complex was top-to-the N directed (Kurt et al., 2010). This observation allows us to speculate that the Simav Detachment Fault passed under the ophiolites of the Izmir-Ankara Suture Zone and over the Kazdağ core complex to reach Marmara. If this is true, investigation of the relationship of the Oligocene magmatism in south Marmara with the detachment is necessary and

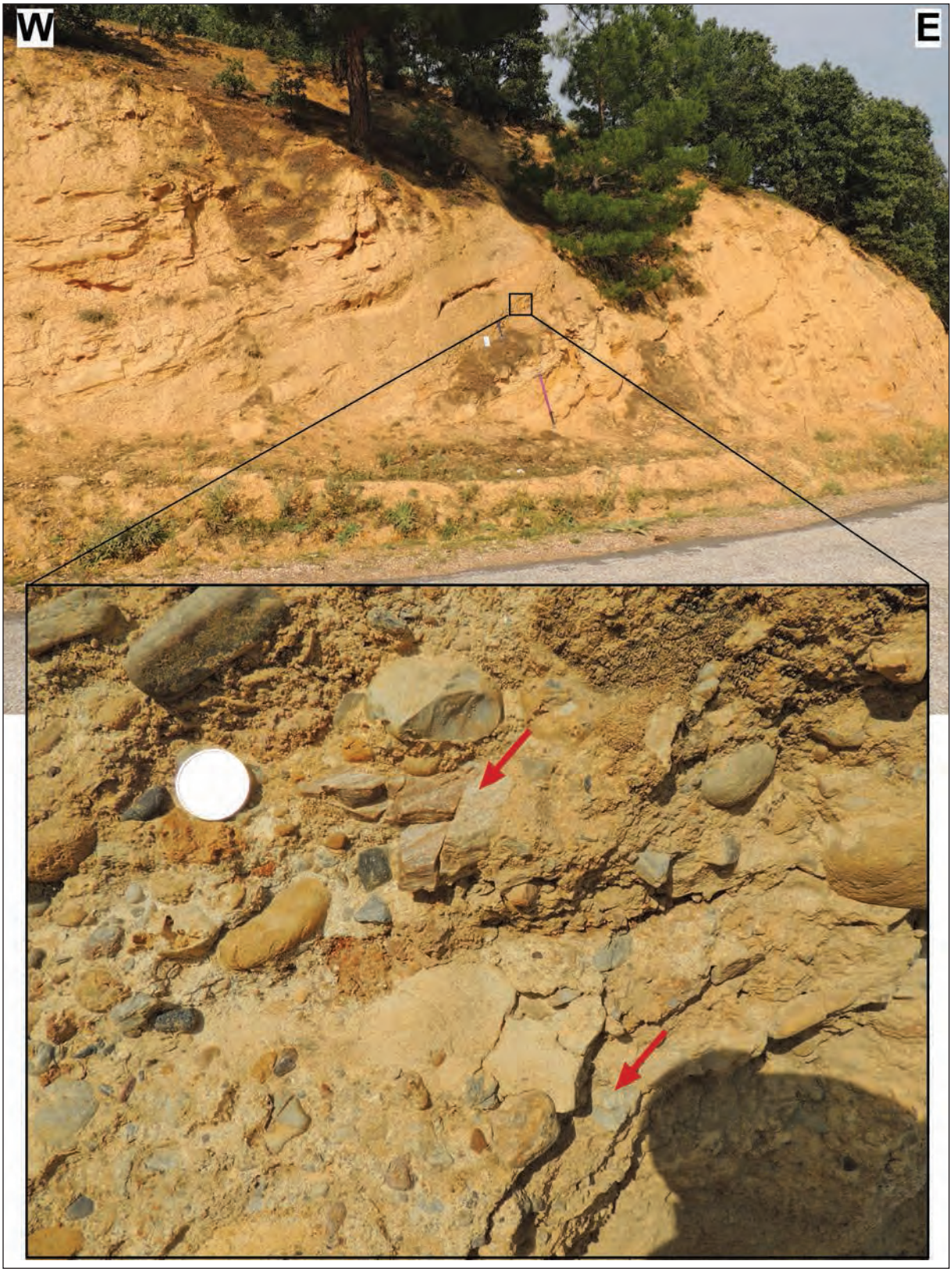

Figure 39- Metamorphic pebbles, shown by red arrows, within conglomerate levels in the tilted yellow-colored Hacıbekir Group on the Eynehan road in the Uşak-Güre basin. Length of the pickaxe is 80 cm. Scale on the close up is 25 kuruş coin.

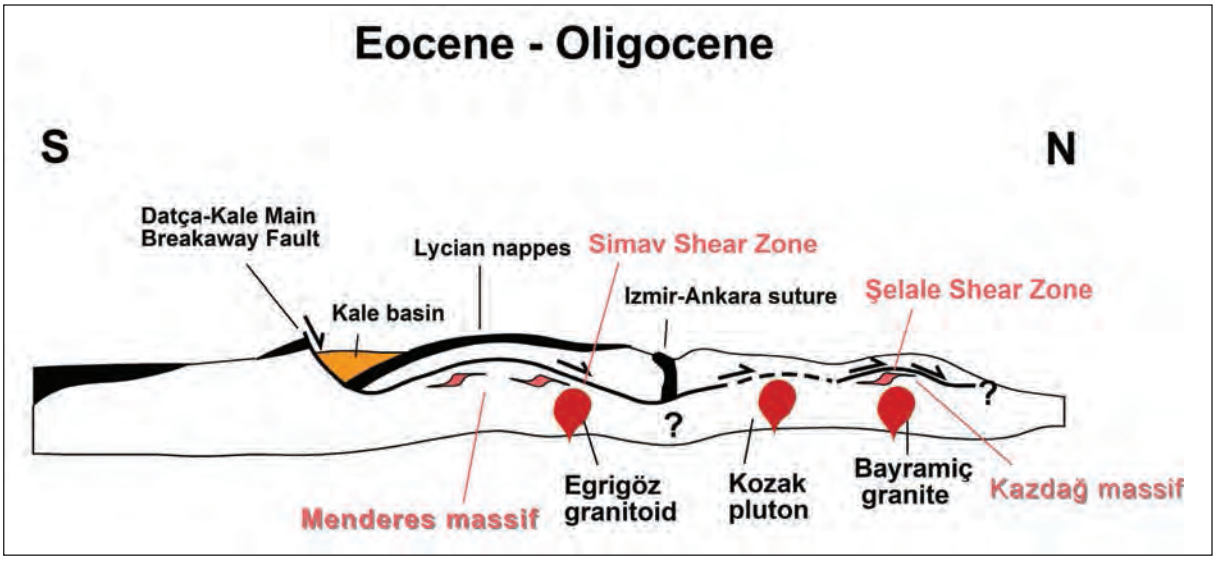

Figure 40- Sketch showing possible relationship between the Menderes core complex and the Kazdağ core complex.

possible candidates for remnants of the lower plate of the Uludağ Massif and Marmara Island granites should be reinvestigated. In this situation, the candidate for the sedimentary basin developing further north of the Simav Detachment Fault is the Eocene-Oligocene Thrace basin. If this is proven the indication that the ophiolites known as the Izmir-Ankara suture zone is a true suture zone will come under suspicion and these will have to have moved above the Simav Detachment Fault (Figure 40). Testing this hypothesis in the field, based on the data that the first detachment direction was top-to-the N in the Kazdağ core complex, will help us better understand the late Cenozoic extensional tectonics in Western Anatolia.

Acknowledgements

We gratefully remember our supervisors Barry C. Scott and Okan Tekeli for illuminating our path with their direction during our doctoral studies in Western Anatolia. We bow to the respected memories of Tuncay Ercan, Orhan Kaya, Erol Akyol, Okan Tekeli and Leopold Benda who labored on the geology of Western Anatolia and have left our presence. We thank all our colleagues working hard in Western Anatolia producing geological data and making scientific discussions possible, and Taner Ünlü who suggested this article for this special publication.

Received: 08.05.2015
Aceepted: 25.07.2015
Published: December 2015

References

Akçığ, Z. 1988. Batı Anadolu'nun yapısal sorunlarının gravite verileri ile irdelenmesi. *Türkiye Jeoloji Bülteni,* 31, 63-70.

Akdeniz, N. 1980. Başlamış Formasyonu. *Jeoloji Mühendisliği,* 10, 39-47.

Akgün, F., Akyol, E. 1999. Palynostratigraphy of the coal bearing Neogene deposits in Büyük Menderes graben, western Anatolia. *Geobios,* 32, 367-383.

Akgün, F., Sözbilir, H. 2001. A palynostratigraphic approach to the SW Anatolian molasse basin: Kale-Tavas molasse and Denizli molasse. *Geodynamica Acta,* 14, 71-93.

Akyol, E., Akgün, F. 2001. Response a Seyitoğlu G. and Sen S. 1999. 'Discussion on Akgün F. and Akyol E. 1999, Palynostratigraphy of the coal bearing Neogene deposits in Büyük Menderes graben, western Anatolia. Geobios, 32,6:915. *Geobios,* 34, 109-112.

Alçiçek, H. 2007. Denizli havzası (Sarayköy-Buldan bölgesi, GB Türkiye) Neojen çökellerinin sedimantolojik incelemesi. Doktora Tezi, Ankara Üniversitesi.

Alçiçek, H., Varol, B., Özkul, M. 2007. Sedimentary facies, depositional environments and palaeogeographic evolution of the Neogene Denizli Basin of SW Anatolia, Turkey. *Sedimentary Geology,* 202, 596-637.

Altunel, E. 1996. Pamukkale travertenlerinin morfolojik özellikleri, yaşları ve neotektonik önemleri. *Maden Tetkik ve Arama Dergisi,* 118, 47-64.

Armstrong, R.L. 1972. Low-angle (denudation) faults, hinterland of the Sevier orogenic belt, eastern Nevada and western Utah. *Geological Society of America Bulletin,* 83, 1729-1754

Arpat, E., Bingöl, E. 1969. The rift system of the Western Turkey; thoughts on its development. *Maden Tetkik ve Arama Genel Müdürlüğü Dergisi,* 73, 1-9.

Ateş, A., Kearey, P., Tufan, S. 1999. New gravity and magnetic anomaly maps of Turkey. *Geophysical Journal International,* 136, 499-502.

Axen, G.J., Bartley, J.M. 1997. Field test of rolling hinges: Existence, mechanical types and implications for extensional tectonics. *Journal of Geophysical Research,* 102, 20515-20537.

Becker-Platen, J.D. 1970. Lithostratigraphisce Untersuchungen im Kanozoikum Südwest- Anatoliens (Türkei). *Beihefte zum geologischen Jahrbuch* 97.

Becker-Platen, J.D. 1971. Stratigraphic division of the Neogene and oldest Pleistocene in Southwest Anatolia.*Newsletters on Stratigraphy,* 1-3, 19-22.

Benda, L. 1971. Principles of the palynologic subdivision of the Turkish Neogene. *Newsletters on Stratigraphy* 1-3, 23-26.

Benda, L., Innocenti, F., Mazzuoli, R., Radicati, F., Steffens, P. 1974. Stratigraphic and radiometric data of the Neogene in Northwest Turkey. *Zeitschrift der Deutschen Geologischen Gesellschaft* 125, 183-193.

Benda, L., Meulenkamp, J.E. 1979. Biostratigraphic correlations in the Eastern Mediterranean Neogene. 5. Calibration of sporomorph associations, marine microfossils and mammal zones, marine and continental stages and the radiometric scale. *Annales Geologiques Des Pays Helleniques* (hors ser.) 1, 61-70.

Benda, L., Meulenkamp, J.E. 1990. Biostratigraphic correlations in the Eastern Mediterranean Neogene.9.Sporomorph associations and event stratigraphy of the Eastern Mediterranean. *Newsletters on Stratigraphy,* 23, 1-10.

Besang, C., Eckhardt, F.J., Harre, W., Kreuzer, H., Müller, P. 1977. Radiometrische altersbestimmungen an neogenen eruptivgesteinen der Türkei. *Geologisches Jahrbuch,* B25, 3-36.

Bozkurt, E. 2000. Timing of extension on the Büyük Menderes Graben, western Turkey, and its tectonic implications. Bozkurt, E., Winchester, J.A. & Piper, J.D.A. (eds) Tectonics and Magmatism in Turkey and the Surrounding Area. *Geological Society of London. Special Publication,* 173, 385-403.

Bozkurt, E. 2003. Origin of NNE-trending basins in Western Turkey. *Geodinamica Acta,* 16, 61-81.

Bozkurt, E. 2004. Granitoid rocks of the southern Menderes Massif (southwestern Turkey): field evidence for Tertiary magmatism in an extensional shear zone. *International Journal of Earth Sciences,* 93, 52–71.

Bozkurt, E, Park, R.G. 1993. Menderes Massif: A Cordilleran type metamorphic core complex in western Turkey. EUG VII, Strasbourg, *Terra Abstracts* v.5, p.255.

Bozkurt, E., Park, R.G. 1994. Southern Menderes Massif: an incipient metamorphic core complex in western Anatolia, Turkey. *Journal of the Geological Society London*, 151, 213-216.

Bozkurt, E., Winchester, J.A., Park, R.G. 1995. Geochemistery and tectonic significance of augen gneisses from the southern Menderes massif (west Turkey). *Geological Magazine,* 132, 287-301.

Bozkurt, E., Park, R.G. 1997*a*. Evolution of a mid-Tertiary extensional shear zone in the southern Menderes massif, western Turkey. *Bulletin de la Societe Geologique de France,* 168, 1, 3-14.

Bozkurt, E., Park, R.G. 1997*b*. Microstructures of deformed grains in the augen gneiss of southern Menderes massif, western Turkey and their tectonic significance. *International Journal of Earth Sciences,* 86, 109-119.

Bozkurt, E., Park, R.G. 1999. The structure of the Paleozoic schists in the southern Menderes Massif, western Turkey: a new aproach to the origin of the Main Menderes metamorphism and its relation to the Lycian Nappes. *Geodinamica Acta,* 12, 25-42.

Bozkurt, E., Sözbilir, H. 2004. Tectonic Evolution of the Gediz Graben: Field Evidence for an Episodic, Two-Stage Extension in Western Turkey. Geological Magazine, 141, 63–79.

Bozkurt, E., Rojay, B. 2005. Episodic, two-stage Neogene extension and short-term intervening compression in Western Turkey: field evidence from the Kiraz Basin and Bozdağ Horst. *Geodinamica Acta,* 18 299-316.

Buck, W.R. 1988. Flexural rotation of normal faults.*Tectonics,* 7, 959-973.

Buscher, J.T., Hampel, A., Hetzel, R., Dunkl, I., Glotzbach, C., Struffert, A., Akal, C,. Ratz, M. 2013. Quantifying rates of detachment faulting and erosion in the central Menderes massif (western Turkey) by thermochronology and cosmogenic 10Be. *Journal of Geological Society London,* 170, 669-683.

Candan, O., Dora, Ö.O. 1998. Menderes Masifi'nde granulit, eklojit ve mavişist kalıntıları: Pan-Afrikan ve Tersiyer metamorfik evrimine bir yaklaşım. *Türkiye Jeoloji Bülteni,* 41/1, 1-35.

Candan, O., Koralay, E., Akal, C., Kaya, O., Oberhansli, R., Dora, O.Ö., Konak, N., Chen, F. 2011. Supra-Pan-African unconformity between core and cover series of the Menderes Massif / Turkey and its geological implications. *Precambrian Research,* 184, 1-23.

Catlos, E. J., Çemen, I., Işık, V., Seyitoğlu, G. 2002. In-situ timing constraints from the Menderes Massif, western Turkey. Geological Society of America, Abstracts with Programs, 180.

Catlos, E.J., Çemen, I. 2005. Monazite ages and the evolution of the Menderes Massif, western Turkey. *International Journal of Earth Sciences,* 94, 204-217.

Catlos, E.J., Baker, C., Sorensen, S.S., Çemen, İ., Hançer, M. 2010. Geochemistry, geochronology and cathodoluminescence imagery of the Salihli and Turgutlu granites (Central Menderes Massif, western Turkey): Implications for Aegean tectonics. *Tectonophysics,* 488, 110-130.

Cohen, H.A., Dart, C.J., Akyüz, H.S., Barka, A.A. 1995. Syn-rift sedimentation and structural development of Gediz and Büyük Menderes graben, western Turkey. *Journal of the Geological Society London,* 152, 629-638.

Collettini, C. 2011. The mechanical paradox of low-angle normal faults: Current understanding and open questions. Tectonophysics, 510, 253-268.

Collins, A.S., Robertson, A.H.F. 1998. Processes of Late Cretaceous to Late Miocene episodic thrust-sheet translation in the Lycian Taurides, SW Turkey. *Journal of the Geological Society London,* 155, 759-772.

Collins, A.S., Robertson, A.H.F. 2003.Kinematic evidence for Late Mesozoic - Miocene emplacement of the Lycian allochthon over western Anatolide belt, SW Turkey.*Geological Journal,* 38, 295-310.

Coney, P.J. 1980. Cordilleran metamorphic core complexes; an overview. In: Crittenden, M.D., Coney, P.J. and Davis, G.H. (Ed.). Cordilleran Metamorphic Core Complexes. *Geological Society of America. Memoir,* 153, 7-31.

Çağlar, I., Duvarcı, E. 2001. Geoelectric structure of inland area of the Gökova rift, southwest Anatolia and its tectonic implications. *Journal of Geodynamics*, 31, 33-48.

Çağlayan, M.A., Öztürk, E.M., Öztürk, Z., Sav, H., Akat, U. 1980. Menderes masifi güneyine ait bulgular ve yapısal yorum. *Jeoloji Mühendisliği,* 10, 9-19.

Çiftçi, G., Pamukçu, O., Çoruh, C., Çopur, S., Sözbilir, H. 2011. Shallow and deep structure of a supradetachment basin based on geological, conventional deep seismic reflection sections and gravity data in the Büyük Menderes graben, western Anatolia. *Surveys in Geophysics,* 32, 271-290.

Çiftçi, N.B., Bozkurt, E. 2009. Evolution of the Miocene sedimentary fill of the Gediz Graben, SW Turkey. Sedimentary Geology, 216, 49-79.

Çiftçi, N.B., Bozkurt, E. 2010. Structural evolution of the Gediz Graben, SW Turkey.temporal and spatial variation of the graben basin. *Basin Research,* 22, 846-873.

Davis, G.H., Reynolds, S.J. 1996. Structural Geology of Rocks and Regions. John Wiley & Sons Inc., 776s.

Davis, G.A., Lister, G.S. 1988. Detachment faulting in continental extension: Perspectives from the south wetern U.S. Cordillera. Clark, S.P. Processes in continental lithospheric deformation. *Geological Society of America Special Publication,* 218, 133-159.

de Graciansky, P.C., Lorenz, C., Magne, J. 1970. Sur les étapes de la transgression du Miocene inferieur observée dans les fenetres de Göcek (sud-quest de la Turquie). *Bulletin de la Societe Geologique de France,* 12, 557-564.

Demircioğlu, D., Ecevitoğlu, B., Seyitoğlu, G. 2010. Evidence of a rolling hinge mechanism in the seismic records of hydrocarbon-bearing Alaşehir graben, western Turkey. *Petroleum Geoscience,* 16, 155-160.

Delaloye M, Bingöl, E. 2000. Granitoids from Western and Northwestern Anatolia: geochemistry and modelling of geodynamic evolution. *International Geology Review*, 42, 241-268.

Dewey, J.F. 1988. Extensional collapse of orogens. *Tectonics* 7, 1123-1139.

Dewey, J.F., Şengör, A.M.C. 1979. Aegean and surrounding regions: complex multiple and continuum tectonics in a convergent zone. *Bulletin of Geological Society of America,* 90, 84-92.

Dora, Ö.O., Kun, N., Candan, O. 1990. Metamorphic history and geotectonic evolution of the Menderes massif. I.E.S.C.A. Proceedings, 2, 102-115.

Dora, Ö.O., Candan, O., Dürr, S., Oberhansli, R. 1995. New evidence on the geotectonic evolution of the Menderes massif. I.E.S.C.A. Proceedings, 1, 53-72.

Dürr, S. 1975. Über Alter und geotektonische Stellung des Menderes-Kristallins SW-Anatolien und seine Aequivalente in der mittleren Aegaeis. Doctoral Dissertation, University Marburg Lahn.

Dürr, St., Allherr, R., Keller, J., Okrusch, M., Seidel, E. 1978. The median Aegean crystalline belt: Stratigraphy, structure, metamorphism, magmatism. In closs, H. Poeder, D.H. and Schmidt, K. (Eds), Alps, Apennines, Helienides., 455-477, Shweizerbart, Stuttgart.

Ediger, V., Batı, Z., Yazman, M. 1996. Paleopalynology of possible hydrocarbon source rocks of the Alaşehir - Turgutlu area in the Gediz graben (western Anatolia). *Turkish Association of Petroleum Geologists Bulletin,* 8, 94-112.

Emre, Ö., Duman, T.Y., Özalp, S. 2011. Kütahya (NJ 35-4) Paftası, 1:250.000 ölçekli Türkiye diri fay haritası serisi no: 10. *Maden Tetkik ve Arama Genel Müdürlüğü*, Ankara-Türkiye.

Emre, T. 1992. Gediz grabeni'nin (Salihli-Alaşehir arası) jeolojisi. 45. Türkiye Jeoloji Kurultayı Bildiri Özleri, s.60.

Emre, T. 1996. Gediz grabeni'nin jeolojisi ve tektoniği. *Turkish Journal of Earth Sciences*, 5, 171-185.

Emre, T., Sözbilir, H. 1997.Field evidence for metamorphic core complex, detachment faulting and accomodation faults in the Gediz and Büyük Menderes grabens, western Anatolia. İç: IESCA Proceedings (Ed: Ö. Pişkin, M. Ergün, M.Y. Savaşçın, G. Tarcan), s. 74-93.

Emre, T., Sözbilir, H., Gökçen, N. 2006. Neogene-Quaternary stratigraphy of Kiraz – Beydağ vicinity, Küçük Menderes graben, west Anatolia.

Maden Tetkik ve Arama Genel Müdürlüğü Dergisi, 132, 1-32.

Emre, T., Sözbilir, H. 2007. Tectonic evolution of the Kiraz basin, Küçük Menderes graben: Evidence for compression/uplift-related basin formation overprinted by extensional tectonics in west Anatolia. *Turkish Journal of Earth Sciences,* 16, 441-470.

Ercan, T., Dinçel, A., Metin, S., Türkecan, A., Günay, A. 1978. Uşak yöresindeki Neojen havzalarının jeolojisi. Bulletin of the Geological Society of Turkey, 21, 97–106.

Ercan, T., Türkecan, A., Dinçel, A., Günay, E. 1983. Kula - Selendi (Manisa) dolaylarının jeolojisi. Jeoloji Mühendisliği, 17, 3-28.

Ercan, T., Satır, M., Sevin, D., Türkecan, A. 1996. Batı Anadolu'daki Tersiyer ve Kuvaterner yaşlı volkanik kayaçlarda yeni yapılan radyometrik yaş ölçümlerinin yorumu. *Maden Tetkik ve Arama Genel Müdürlüğü Dergisi*, 119, 103-112.

Erdoğan, B., Güngör, T. 2004. The problem of the core-cover boundary of the Menderes massif and an emplacement mechanism for regionally extensive gneissic granites, western Anatolia (Turkey). *Turkish Journal of Earth Sciences,* 13, 15-36.

Ersoy, Y., Helvacı, C. 2007. Stratigraphy and geochemical features of the Early Miocene bimodal (ultrapotassic and calc-alkaline) volcanic activity within the NE-trending Selendi basin, western Anatolia, Turkey.*Turkish Journal of Earth Sciences,* 16, 117-139.

Ersoy, Y., Helvacı, C., Sözbilir, H., Erkül, F., Bozkurt, E. 2008. A geochemical approach to Neogene-Quaternary volcanic activity of western Anatolia: An example of episodic bimodal volcanism within the Selendi basin, Turkey. *Chemical Geology,* 255, 265-282.

Ersoy, Y.E., Helvacı, C., Sözbilir, H. 2010. Tectono-stratigraphic evolution of the NE-SW trending superimposed Selendi basin: Implications for late Cenozoic crustal extension in western Anatolia, Turkey. *Tectonophysics,* 488, 210-232.

Ersoy, Y.E., Helvacı, C., Palmer, M.R. 2011. Stratigraphic, structural and geochemical features of the NE-SW trending Neogene volcano-sedimentary basins in western Anatolia: Implications for associations of supra-detachment and transtensional strike-slip basin formation in extensional tectonic setting. *Journal of Asian Earth Sciences*, 41, 159-183.

Ersoy, Y.E., Çemen, İ., Helvacı, C., Billor, Z. 2014. Tectono-stratigraphy of the Neogene basins in western Turkey: Implications for tectonic evolution of the Aegean extended region. *Tectonophysics*, 635, 33-58.

Eyidoğan, H., Jackson, J. 1985. A seismological study of normal faulting in the Demirci, Alaşehir and Gediz earthquakes of 1967-70 in western Turkey: implications for the nature and geometry of deformation in the continental crust. *Geophysical Journal of the Royal Astronomical Society London,* 81, 569-607.

Faure, M., Bonneau, M., Pons, J. 1991.Ductile deformation and syntectonic granite emplacement during the late Miocene extension of the Aegea (Greece). *Bulletin de la Societe geologique de France,* 162, 3-11.

Fletcher, J. M., Bartley, J. M., Martin, M. W., Glazner, A. F., Walker, J. D. 1995. Largemagnitude continental extension: An example from the central Mojave metamorphic core complex. *Geological Society of America Bulletin,* 107/ 12, 1468-1483.

Fossen, H. 2010. Structural Geology. *Cambridge University Press*. 463p.

Friedmann, S.J., Burbank, D.W. 1995. Rift basins and supradetachment basins: intracontinental extensional end-members. *Basin Research,* 7, 109-127.

Gans, P.B., Mahood, G.A., Schermer, E.R. 1989. Syn-extensional magmatism in the Basin and Range province; a case study from the eastern Great Basin.*Geological Society of America.Special Publication* 233, 60 p.

Gawthorpe, R.L., Hurst, J.M. 1993. Transfer zones in extensional basins: their structural style and influence on drainage development and stratigraphy. *Journal of the Geological Society London* 150, 1137-1152.

Gessner, K., Piazola, S., Güngör, T., Ring, U., Kröner, A., Passchier, C.W. 2001*a*. Tectonic significance of deformation patterns in granitoid rocks of the Menderes nappes, Anatolide belt, southwest Turkey. *International Journal of Earth Sciences,* 89, 766-780.

Gessner, K., Ring, U., Johnson, C., Hetzel R., Passchier, C. W., Güngör, T. 2001*b*. An active bivergent rolling-hinge detachment system: Central Menderes metamorphic core complex in western Turkey. *Geology,* 29, 611-614.

Gesner, K., Collins, A. S., Ring, U., Güngör, T. 2004. Structural and thermal history of poly-orogenic basement: U–Pb gecohronology of granitoid rocks in the southern Menderes Massif, western Turkey. *Journal of the Geological Society London,* 161, 93–101.

Gessner, K., Gallardo, L.A., Markwitz, V., Ring, U., Thomson, S.N. 2013. What caused the denudation of the Menderes Massif: Review of crustal evolution, lithosphere structure, and dynamic topography in southwest Turkey. Gondwana Research, 24, 243-274.

Glodny, J., Hetzel, R. 2007. Precise U–Pb ages of syn-extensional Miocene intrusions in the central Menderes Massif, western Turkey. *Geological Magazine,* 144, 235-246.

Güleç, N. 1991. Crust-mantle interaction in western Turkey: Implications from Sr and Nd isotope

geochemistry of Tertiary and Quaternary volcanics. Geological Magazine 128, 417-435.

Gürer, F., Yılmaz, Y. 2002. Geology of the Ören and surrounding areas, SW Anatolia. *Turkish Journal of Earth Sciences,* 11, 1-13.

Gürer, Ö.F, Sarıca-Filoreau, N., Özburan, M., Sangu, E., Doğan, B. 2009. Progressive development of the Büyük Menderes Graben based on new data, western Turkey. *Geological Magazine,* 146, 652-673.

Hetzel, R., Passchier, C.W., Ring, U., Dora, Ö.O. 1995*a*. Bivergent extension in orogenic belts: The Menderes massif (southwestern Turkey). Geology, 23, 455-458.

Hetzel, R., Ring, U., Akal, C., Troesch, M. 1995*b*. Miocene NNE-directed extensional unroofing in the Menderes massif, southwestern Turkey. *Journal of Geological Society London*, 152, 639-654.

Hetzel, R., Reischmann, T. 1996. Intrusion age of Pan-African augen gneisses in the southern Menderes massif and the age of cooling after Alpine ductile extensional deformation. *Geological Magazine*, 133, 565-572.

Hetzel, R., Romer, R.L., Candan, O., Passchier, C.W. 1998. Geology of the Bozdağ area, central Menderes massif, SW Turkey: Pan-African basement and Alpine deformation. Geologische Rundschau, 87, 394-406.

Hetzel, R., Zwigmann, H., Mulch, A., Gessner, K., Akal, C., Hampel, A., Güngör, T., Petschick, R., Mikes, T., Wedin, F. 2013. Spatiotemporal evolution of brittle normal faulting and fluid infiltration in detachment fault systems: a case study from Menderes massif, western Turkey. *Tectonics,* 32, 1-13.

Innocenti, F., Agostini, S., Di Vincenzo, G., Doglioni, C., Manetti, P., Savaşçın, M.Y., Tonarini, S. 2005. Neogene and Quaternary volcanism in Western Anatolia: Magma sources and geodynamic evolution. *Marine Geology,* 221, 397-421.

Işık, V., Tekeli, O., Çemen, İ. 1997. Mylonitic fabric development along a detachment surface in northern Menderes massif, western Anatolia, Turkey. Geol Soc Am., Annual Meeting, Abstracts with programs 29, A-220.

Işık, V., Tekeli, O. 1998. Structure of Lower Plate Rocks in Metamorphic Core Complex; Northern Menderes massif, Western Turkey. 3th Int. Turkish Geology Sym., METU, Ankara, Turkey, p. 268.

Işık, V., Tekeli, O. 1999. Microstructure of deformed grains in the granitic mylonites of lower plate: northern Menderes massif, western Turkey. EUG 10, J. Conference Abstracts, 4 (1), 730.

Işık, V., Tekeli, O. 2001. Late orogenic crustal extension in the northern Menderes massif (western Turkey): Evidences for metamorphic core complex formation. *International Journal of Earth Sciences,* 89, 757-765.

Işık, V., Seyitoğlu, G., Çemen, İ. 2003*a*. Extensional structures of the Menderes core complex, western Turkey. GSA, Annual Meeting Abstracts with Programs, Seattle, USA, v.35, p.27-28.

Işık, V., Seyitoğlu, G., Çemen, İ. 2003*b*. Ductile-brittle transition along the Alasehir shear zone and its structural relationship with the Simav detachment, Menderes massif, western Turkey. *Tectonophysics,* 374, 1-18.

Işık, V., Gürsu, S., Göncüoğlu, C., Seyitoğlu, G. 2004*a*. Deformational and geochemical features of syn-tectonic Koyunoba and Egrigöz granitoids, western Turkey. Chatzipetros, A.A., Pavlides, S.B. (Ed.), 5th International Symposium on Eastern Mediterranean Geology, Thessaloniki, Greece, 3, pp. 1143–1146.

Işık, V., Tekeli, O., Seyitoğlu, G. 2004*b*. The $^{40}Ar/^{39}Ar$ age of extensional ductile deformation and granitoid intrusions in the northern Menderes core complex: Implications for the initiation of extensional tectonics in western Turkey. *Journal of Asian Earth Science,* 23, 555-566.

Işık, V., Seyitoğlu, G. 2006. Menderes metamorfik çekirdek kompleksinde sıyrılma fayları ve ilişkili makaslama zonları, Batı Anadolu. 59. Türkiye Jeoloji Kurultayı Bildiri Özleri, s. 21-24

Işık, V., Seyitoğlu, G. 2007. Menderes Masifinin Geç Senozoyikte Asimetrik ve Simetrik Çekirdek Kompleksi Olarak Yüzeyleme ve Parçalanma Tarihçesi. Menderes Masifi Kolokyumu, Genişletilmiş Bildiri Özleri Kitabı, 88-97.

Işık, V., Seyitoğlu, G. 2010. Cenozoic Exhumation and Sedimentary Basin formation in the Menderes Massif, Western Turkey. Tectonic Crossroads: Evolving Orogens of Eurasia-Africa-Arabia. Abstracts with Programs (36-1), p.70.

İnci, U. 1984. Demirci ve Burhaniye bitümlü şeyllerinin stratigrafisi ve organik özellikleri. Türkiye Jeoloji Kongresi Bülteni, 5, 27-40.

İztan, H., Yazman, M. 1990. Geology and hydrocarbon potential of the Alaşehir (Manisa) area, western Turkey.Proceedings to International Earth Sciences Congress on Aegean regions, İzmir, 327-338.

Jackson, J.A., McKenzie, D. 1988. The relationship between plate motions and seismic moment tensors and rates of active deformation in the Mediterranean and Middle East. *Geophysical Journal,* 93, 45-73.

Janecke, U.S., Vandenburg, J.C., Blankenau, J.J. 1998.Geometry, mechanisms and significance of extensional folds from examples in the Rocky Mountain Basin and Range province, USA. *Journal of Structural Geology,* 20, 841-856.

Jolivet, L., Faccenna, C., D'agostina, N., Fournier, M., Worrall, D. 1999. The kinematics of back-arc basins, examples from the Tyrrhenian, Aegean and Japan Seas.Mac Niocaill, C., Ryan, P.D. (Ed.).

Continental Tectonics. *Journal of the Geological Society London Special Publication,* 164, 21-53.

Jolivet, L., Faccenna, C. 2000. Mediterranean extension and the Africa–Eurasia collision.*Tectonics,* 19, 1095-1106.

Jolivet, J., Faccenna, C., Huet, B., Labrousse, L., Le Pourhiet, L., Lacombe, O., Lecomte, E., Burov, E., Denèle, Y., Brun, JP., Philippon, M., Paul, P., Salaün, G., Karabulut, H., Piromallo, C., Monié, P., Gueydan, F., Okay, A.I., Oberhänsli, R., Pourteau, A., Augier R., Gadenne, L., Driussi, O. 2013. Aegean tectonics: Strain localisation, slab tearing and trench retreat. *Tectonophysics,* 597–598, 1-33.

Karaoğlu, Ö., Helvacı, C. 2012. Structural evolution of the Uşak-Güre supradetachment basin during Miocene extensional denudation in western Turkey. Journal of the Geological Society London, 169, 627-642.

Kaya, O. 1981. Miocene reference section for the coastal parts of west Anatolia.*Newsletters on Stratigraphy,* 10, 164-191.

Kaya, S., Esat, K., Ecevitoğlu, B., Işık, V., Kaypak, B., Uyar Aldaş, G., Can, A.Z., Baksı, E.E., Akkaya, İ. Seyitoğlu, G. 2014. Afyon-Akşehir grabeni batı kenarının tektonik özellikleri üzerine jeolojik ve jeofizik gözlemler: İki evreli genişleme modeli hakkındaki tartışmalara bir katkı. *Yerbilimleri,* 35, 1-16.

Kaymakçı, N. 2006. Kinematic development and paleostress analysis of the Denizli Basin (Western Turkey): implications of spatial varition of relative paleostress magnitudes and orientations. *Journal of Asian Earth Sciences,* 27, 207-222.

Kaypak, B., Gökkaya, G. 2012. 3-D imaging of the upper crust beneath the Denizli geothermal region by local earthquake tomography, western Turkey. *Journal of Volcanology and Geothermal Research,* 211, 47-60.

Ketin, İ., Abdüsselamoğlu, Ş. 1969. 23 Mart 1969 Demirci ve 28 Mart 1969 Alaşehir-Sarıgöl depremleri hakkında makro-sismik gözlemler. *Maden Mecmuası,* 4, 21-26.

Koçyiğit, A., Yusufoğlu, H., Bozkurt, E. 1999. Evidence from the Gediz graben for episodic two-stage extension in western Turkey. *Journal of the Geological Society London*, 156, 605-616.

Koçyiğit, A., Ünay, E., Saraç, G. 2000. Episodic graben formation and extensional neotectonic regime in west central Anatolia and the Isparta Angle: a case study in the Akşehir-Afyon graben, Turkey. İç: Tectonics and Magmatism in Turkey and the Surrounding Area (Ed: E. Bozkurt, J.A. Winchester, J.D.A. Piper), Geological Society London, Special Publications 173, s. 405-421.

Konak, N. 1979. Simav grabeni ve getirdiği kentleşme sorunları. Türkiye Jeoloji Mühendisliği 1. Bilimsel ve Teknik Kongresi Bildirileri, 157-164.

Konak, N. 1982. Simav dolayının jeolojisi ve metamorfik kayaçlarının evrimi. *İ.Ü.M.F. Yerbilimleri Dergisi*, 3, 313-337.

Konak, N., Akdeniz, N., Öztürk, E.M. 1987. Geology of the south of Menderes massif, correlation of Variscan and pre-Variscan events of the Alpine Mediterrenean Mountain Belt (Guide book for the field exursion along western Anatolia, Turkey) IFCP Project No. 5, 42-53.

Koralay, E., Dora, O.Ö., Chen, F., Satır, M., Candan, O. 2004. Geochemistry and geochronology of orthogneisses in the Derbent (Alaşehir) area, Eastern part of the Ödemiş-Kiraz submassif, Menderes Massif: Pan-African magmatic activity. *Turkish Journal of Earth Sciences*, 13, 37-61.

Kurt, H., Demirbağ, E., Kuşçu, İ. 1999. Investigation of submarine active tectonism in the Gulf of Gökova, southwest Anatolia-southeast Aegean sea, by multi-channel seismic reflection data. *Tectonophysics,* 305, 477-496.

Kurt, F.S., Işık, V., Seyitoğlu, G. 2010. Alternative Cenozoic exhumation history of the Kazdağ core complex. Tectonic Cross Roads: Evolving Orogens of Eurasia-Africa-Arabia. Abstracts with Programs (36-3), METU Ankara, s.70.

Le Pichon, X., Angelier, J. 1979. The Hellenic arc and trench system: a key to the neotectonic evolution of the eastern Mediterranean area. *Tectonophysics,* 69, 1-42.

Le Pichon, X., Angelier, J. 1981. The Aegean Sea. *Philosophical Transactions of the Royal Society London,* A300, 357-372.

Lips, A.L.W., Cassard, D., Sözbilir, H., Yılmaz, H. 2001. Multistage exhumation of the Menderes Massif, western Anatolia (Turkey). *International Journal of Earth Sciences,* 89, 781-792.

Lister, G.S., Banga, G., Feensta, A. 1984. Metamorphic core complexes of Cordilleran type in the Cyclades, Aegean Sea, Greece. *Geology*, 12, 221-225.

Lister, G.S., Davis, G.A. 1989. The origin of metamorphic core complexes and detachment faults formed during Tertiary continental extension in the northern Colorado River region, U.S.A. *Journal of Structural Geology,* 11, 65-94.

Lister, G.S., Baldwin, S.L. 1992. Plutonism and the origin of metamorphic core complexes. *Geology*, 21, 607-610.

Loos, S., Reischmann, T. 1999. The evolution of the southern Menderes massif in SW Turkey as revealed by zircon dating. *Journal of Geological Society London,* 156, 1021-1030.

Malavieille, J. 1993. Late orogenic extension in mountain belts: insights from the Basin and Range and the Late Paleozoic Variscan belt. *Tectonics,* 12, 1115-1130.

Manning, A.H., Bartley, J.M. 1994. Postmylonitic deformation in the Raft River metamorphic core

complex, northwestern Utah: Evidence of a rolling hinge. *Tectonics,* 13, 596-612.

McClay, K.R. 1989. Physical models of structural styles during extension. İç: Extensional tectonics and stratigraphy of the north Atlantic margins (Ed: A.J. Tankard, H.R. Balkwill). AAPG Memoir 46, s. 95-110.

McClay, K.R. 1990. Deformation mechanics in analogue models of extensional fault systems. İç: Deformation Mechanisms, Rheology and Tectonics (Ed: R.J. Knipe, E.H. Rutter). Geological Society Special Publication 54, s. 445-453.

McKenzie, D.P. 1970. Plate tectonics of the Mediterranean region. *Nature,* 226, 239-243.

McKenzie, D.P. 1972. Active tectonics of the Mediterranean region. *Geophysical Journal of Royal Astronomical Society,* 30, 109-185.

McKenzie, D. 1978. Active tectonics of the Alpine - Himalayan belt: The Aegean sea and surrounding regions. *Geophysical Journal of Royal Astronomical Society,* 55, 217-254.

Mercier J.L. 1981. Extensional-compressional tectonics associated with the Aegean arc: comparison with the Andean Cordillera of south Peru-north Bolivia. *Phil. Trans. Royal Society London,* A 300, 337-355.

Meulenkamp, J.E., Wortel, M.J.R., van Wamel, W.A., Spakman, W., Hoogerduyn Strating, E. 1988. On the Hellenic subduction zone and the geodynamic evolution of Crete since the late middle Miocene. *Tectonophysics,* 146, 203-215.

Nebert, K. 1961. Gördes bölgesindeki Neojen volkanizması hakkında bilgiler. *Maden Tetkik ve Arama Genel Müdürlüğü Dergisi*, 57, 50-54.

Oberhansli, R., Partzsch, J., Candan, O., Çetinkaplan, M. 2001. First occurrence of Fe-Mg-carpholite documenting a high-pressure metamorphism in metasediments of the Lycian Nappes, SW Turkey. *International Journal of Earth Sciences,* 89, 867–873.

Okay, A.I. 1989. Geology of the Menderes Massif and the Lycian Nappes south of Denizli, western Taurides. *Miner. Res. Explor. Bull.*, 109, 37–51.

Öner, Z., Dilek, Y. 2011. Supradetachment basin evolution during continental extension: The Aegean province of western Anatolia, Turkey. *Geological Society of America Bulletin,* 123, 2115-2141.

Özerdem, C., Çemen, İ., Işık, V. 2002. The conglomerate member of the Gökçeören formation, Ören basin, western Turkey: its age, sedimentology, and tectonic significance. Geological Society of America, Abstracts with Programs, 250.

Pamir, H.N., Erentöz, C. 1974. 1/500.000 ölçekli Türkiye Jeoloji Haritası Denizli Paftası İzahnamesi. *Maden Tetkik ve Arama Genel Müdürlüğü Yayını*, 83 s.

Phillipson, A. 1915. Reisen und Forschungen in Westlichen Kleinasien. Pet. Mitt. Erg. M., 167, 173, 177, 180 Cotha.

Purvis, M., Robertson, A.H.F. 2005. Sedimentation of the Neogene - Recent Alaşehir (Gediz) continental graben system used to test alternative tectonic models for western (Aegean) Turkey. *Sedimentary Geology,* 173, 373-408.

Prante, M.R., Evans, J.P., Janecke, S.U., Steely, A. 2014. Evidence for paleoseismic slip on a continental low-angle normal fault: Tectonic pseudotachylyte from the west Salton detachment fault, CA, USA. *Earth and Planetary Science Letters*, 387, 170-183.

Ramsay, J.G., Huber, M.I. 1987. The techniques of modern structural geology (Volume 2: Folds and Fractures). Academic Press London, 700s.

Ricou, L.E., Argyriadis, I., Marcoux, J. 1975. L'Axe calceire du Taurus un alignement de fenetres arabo-africans sous des nappes radiolaritiques, ophiolitiques et metamorphiques. *Bulletin de la Societe Geologique de France*, 17, 1024-1044.

Reynolds, S.J. 1985. Geology of the South Mountains, central Arizona. *Arizona Bureau of Geology and Mineral Tecnollogy, Geological Survey Bulletin* 195, 61 p.

Reynolds, S.J., Rehring, W.A. 1980. Mid-Tertiary plutonism and mylonitization, South Mountains, central Arizona. *Geological Society of America. Memoir* 153, 159-175.

Rimmele, G., Jolivet, L., Oberhansli, R., Goffe, B., 2003. Deformation history of the high-pressure Lycian Nappes and implications for tectonic evolution of SW Turkey. *Tectonics,* 22, 1007-

Ring, U., Johnson, C., Hetzel, R., Gessner, K. 2003. Tectonic denudation of a Late Cretaceous-Tertiary collisional belt-regionally symmetric cooling patterns and their relation to extensional faults in the Anatolide belt of western Turkey. *Geological Magazine*, 140, 1-21.

Ring, U., Collins, A.S. 2005. U–Pb SIMS dating of synkinematic granites: timing of core-complex formation in the northern Anatolide belt of western Turkey. *Journal of the Geological Society London,* 162, 289–298.

Saraç, G. 2003. Türkiye Omurgalı Fosil Yatakları. *Maden Tetkik ve Arama Genel Müdürlüğü Rapor* No: 10609, 208s. Ankara (unpublished).

Sarı, C., Şalk, M. 2006. Sediment thicknesses of the western Anatolia graben structures determined by 2D and 3D analysis using gravity data. *Journal of Asian Earth Sciences,* 26, 39–48.

Sarıca, N. 2000. The Plio-Pleistocene age of Büyük Menderes and Gediz grabens and their tectonic significance on N-S extensional tectonics in west Anatolia: mammalian evidence from the continental deposits. *Geological Journal,* 35, 1-24.

Savaşçın, M.Y. 1991. Magmatic activities of Cenozoic compressional and extensional tectonic regimes in western Anatolia. Proceedings of International

Earth Sciences Congress on Aegean Regions, İzmir Turkey, s. 420-434.

Savaşçın, M.Y., Güleç, N. 1990. Neogene volcanism of western Anatolia-Field excursion B3.International Earth Sciences Congress on Aegean Regions, İzmir Turkey.

Seyitoğlu, G. 1992. Late Cenozoic Crustal Extension, Basin formation and Volcanism in West Turkey. PhD Thesis, University of Leicester, England, UK.

Seyitoğlu, G. 1997*a*. The Simav graben: An example of young E-W trending structures in the Late Cenozoic extensional system of western Turkey. *Turkish Journal of Earth Sciences,* 6, 135-141.

Seyitoğlu, G. 1997*b*. Late Cenozoic tectono-sedimentary development of Selendi and Uşak-Güre basins: a contribution to the discussion on the development of east-west and north- trending basins in western Turkey. *Geological Magazine,* 134, 163-175.

Seyitoğlu, G. 1999. Discussion on evidence from the Gediz Graben for episodic two-stage extension in western Turkey. *Journal of the Geological Society London* 156, 1240.

Seyitoğlu, G., Scott, B.C. 1991. Late Cenozoic crustal extension and basin formation in west Turkey. *Geological Magazine,* 128, 155-166.

Seyitoğlu, G., Scott, B.C. 1992*a*. The age of the Büyük Menderes graben (west Turkey) and its tectonic implications.*Geological Magazine,* 129, 239-242.

Seyitoğlu, G., Scott, B.C. 1992*b*. Late Cenozoic volcanic evolution of the NE Aegean region. *Journal of Volcanology and Geothermal Research,* 54, 157-176.

Seyitoğlu, G., Scott, B.C., Rundle, C.C. 1992. Timing of Cenozoic extensional tectonics in west Turkey. *Journal of the Geological Society London,* 149, 533-38.

Seyitoğlu, G., Scott, B.C. 1994. Late Cenozoic basin development in west Turkey. Gördes basin: tectonics and sedimentation. *Geological Magazine,* 131, 631-637.

Seyitoğlu, G., Benda, L., Scott, B.C. 1994. Neogene palynological and isotopic age data from Gördes basin, West Turkey. *Newsletters on Stratigraphy,* 31, 133-142.

Seyitoğlu, G., Scott, B.C. 1996*a*. Age of Alaşehir graben (west Turkey) and its tectonic implications. *Geological Journal,* 31, 1-11.

Seyitoğlu, G., Scott, B.C. 1996*b*. The cause of N-S extensional tectonics in western Turkey: Tectonic escape vs. Back-arc spreading vs. Orogenic collapse. *Journal of Geodynamics,* 22, 145 - 153.

Seyitoğlu, G., Anderson, D., Nowell, G., Scott, B.C. 1997. The evolution from Miocene potassic to Quaternary sodic magmatism in western Turkey: implications for enrichment processes in the lithospheric mantle. *Journal of Volcanology and Geothermal Research,* 76, 127-147.

Seyitoğlu, G., Benda, L. 1998. Neogene palynological and isotopic age data from Selendi and Uşak-Güre basins, western Turkey: a contribution to the upper limit of Eskihisar sporomorph association. *Newsletters on Stratigraphy*, 36, 105-115.

Seyitoğlu, G., Şen, Ş. 1998. The contribution of first magnetostratigraphical data from E-W trending graben fill to the style of late Cenozoic extensional tectonics in western Turkey. Third International Turkish Geology Symposium, Abstracts 188.

Seyitoğlu, G., Şen, Ş. 1999. Discussion on "Akgün F., Akyol E. 1999. Palynostratigraphy of the coal bearing Neogene deposits in Büyük Menderes graben, Western Anatolia. Geobios, 32(3), 367-383".*Geobios,* 32, 934.

Seyitoğlu, G., Çemen, İ., Tekeli, O. 2000. Extensional folding in the Alaşehir (Gediz) graben, western Turkey. *Journal of the Geological Society London,* 157, 1097 -1100.

Seyitoğlu, G., Tekeli, O., Çemen, İ., Şen, Ş., Işık, V. 2002. The role of the flexural rotation / rolling hinge model in the tectonic evolution of the Alaşehir graben, western Turkey.*Geological Magazine,* 139, 15-26.

Seyitoğlu, G., Işık, V., Çemen, İ. 2004. Complete Tertiary exhumation history of the Menderes massif, western Turkey: an alternative working hypothesis. *Terra Nova*, 16, 358-364.

Seyitoğlu, G., Alçiçek, M.C., Işık, V., Alçiçek, H., Mayda, S., Varol, B., Yılmaz, I., Esat, K. 2009. The stratigraphical position of Kemiklitepe fossil locality (Eşme, Uşak) revised: Implications for the Late Cenozoic sedimentary basin development and extensional tectonics in western Turkey. *Neues Jahrbuch für Geologie und Palaeontologie*, 251, 1-15.

Seyitoğlu, G., Işık, V. 2009. Meaning of the Küçük Menderes Graben in the tectonic framework of the central Menderes metamorphic core complex. *Geologica Acta,* 7, 323-331.

Seyitoğlu, G., Işık, V., Esat, K. 2014. A 3D model for the formation of Turtleback surfaces: The Horzum Turtleback of Western Turkey as a case study. *Turkish Journal of Earth Sciences,* 23, 479-494.

Seyitoğlu, G., Cahill, N.D., Işık, V., Esat, K. 2015*a*. Morphotectonics of the Alaşehir graben with a special emphasis on the landscape of the ancient city of Sardis, western Turkey. İç: Landforms and Landscapes of Turkey (Ed: C. Kuzucuoglu, N. Kazancı, A. Çiner), Springer, in press.

Seyitoğlu, G., Ecevitoğlu, B., Kaypak, B., Güney, Y., Tün, M., Esat, K., Avdan, U., Temel, A., Çabuk, A., Telsiz, S., Uyar Aldaş, G. 2015*b*. Determining the main strand of the Eskişehir strike-slip fault zone using subsidiary structures and seismicity: a hypothesis tested by seismic reflection studies. *Turkish Journal of Earth Sciences*, 24, 1-20.

Sickenberg, O., Tobien, H. 1971. New Neogene and Lower Quaternary vertebrate faunas in Turkey. *Newsletters on Stratigraphy,* 1, 51-61.

Spakman, W., Wortel, M.J.R., Vlaar, N.J. 1988. The Hellenic subduction zone; a tomographic image and its geodynamic implications. *Geophysical Research Letters,* 15, 60-63.

Spencer, J.E. 1982. Origin of folding of Tertiary low-angle fault surfaces insoutheastern California and western Arizona, U. S. Geological Survey Professional Paper, Report: P 1375, pp.66.

Spencer, J. E., 1984, Role of denudation in warping and uplift of low-angle normal faults. *Geology* 12, 95-98.

Steininger, F.F., Rögl, F. 1984. Paleogeography and palinspastic reconstruction of the Neogene of the Mediterranean and Paratethys. In: The Geological Evolution of the Eastern Mediterranean (Dixon, J.E. and Robertson, A.H.F., Eds). Geological Society London, Special Publication, 17, 659-668.

Sözbilir, H. 2001. Extensional tectonics and the geometry of related macroscopic structures: field evidence from the Gediz detachment, western Turkey. *Turkish Journal of Earth Sciences,* 10, 51-67.

Sözbilir, H. 2002. Geometry and origin of folding in the Neogene sediments of the Gediz Graben, western Anatolia, Turkey. Geodinamica Acta, 15, 277-288.

Sözbilir, H., Emre, T. 1990. Neogene stratigraphy and structure of the northern rim of the Büyük Menderes graben.Proceedings to International Earth Sciences Congress on Aegean regions, İzmir, 314-322.

Sun, S. 1990. Denizli-Uşak Arasının Jeolojisi ve Linyit Olanakları. *Maden Tetkik ve Arama Genel Müdürlüğü Rapor* No: 9985, 92. Ankara (unpublished).

Şan, O. 1998. Ahmetli (Manisa) güneyinde Menderes masifi ve Tersiyer örtü kayalarının jeolojisi. Yüksek Lisans Tezi, Ankara Üniversitesi.

Şen, Ş, De Bonis, L., Dalfes, N., Geraads, D., Koufos, G. 1994. Les gisements de mammifères du Miocène supérieur de Kemiklitepe, Turquie: 1. Stratigraphie et magnétostratigraphie. İç: Les gisements de mammifères du Miocènesupérieur de Kemiklitepe, Turquie (Ed: Ş. Şen), *Bulletin du Muséum National d'Histoire Naturelle,* 4e sér.,16, sec. C, no. 1, s. 5-17.

Şen, Ş., Seyitoğlu, G. 2009. Magnetostratigraphy of early - middle Miocene deposits from E-W trending Alaşehir and Büyük Menderes grabens in western Turkey, and its tectonic implications. İç*:* Geodynamics of Collision and Collapse at the Africa – Arabia-Eurasia subduction zone. (Ed: D.J.J. van Hinsbergen, M.A. Edwards, R. Govers), *The Geological Society London, Special Publications* 311, 321–342.

Şengör, A.M.C. 1979. The North Anatolian Transform Fault: its age, offset and tectonic significance. *Journal of the Geological Society London,* 13, 269-282.

Şengör, A.M.C. 1980. Türkiye'nin Neotektoniğinin Esasları. Türkiye Jeoloji Kurumu Konferanslar Dizisi:2, Ankara, 40 s.

Şengör, A.M.C., 1982. Ege'nin neotektonik evrimini yöneten etkenler. Batı Anadolu'nun Genç Tektoniği ve Volkanizması Paneli, *Türkiye Jeoloji Kurultayı* 59-71.

Şengör, A.M.C. 1987. Cross-faults and differential stretching of hanging walls in regions of low-angle normal faulting: examples from western Turkey. İç: Continental Extensional Tectonics. (Ed: M.P. Coward,. J.F. Dewey, P.L. Hancock),*The Geological Society of London Special Publications* 28; 575-589.

Şengör, A.M.C., Yılmaz, Y. 1981. Tethyan evolution of Turkey: a plate tectonic approach. *Tectonophysics,* 75, 181– 241.

Şengör, A.M.C., Satır, M., Akkök R. 1984. Timing of tectonic events in the Menderes Massif, western Turkey: Implications for tectonic evolution and evidence for Pan-African basement in Turkey. *Tectonics,* 3, 693-707.

Şengör, A.M.C., Görür, N., Şaroğlu, F. 1985. Strike-slip deformation, basin formation and sedimentation: Strike-slip faulting and related basin formation in zones of tectonic escape: Turkey as a case study. Biddle, K.T. and Christie-Blick, N. (Ed.).Strike-slip Faulting and Basin formation.*Society of Economic Paleontologists and Mineralogist. Special Publication* 37, 277-264.

Şimşek, Ş. 1984. Denizli - Kızıldere - Tekkehamam - Tosunlar - Buldan - Yenice alanının jeolojisi ve jeotermal enerji olanakları. *Maden Tetkik ve Arama Genel Müdürlüğü Rapor* No: 7846, 85s. Ankara (unpublished).

Taner, G. 1974*a*. Denizli bölgesi Neojeni'nin paleontolojik ve stratigrafik etüdü. *Maden Tetkik ve Arama Genel Müdürlüğü Dergisi,* 82, 89-126.

Taner, G. 1974*b*. Denizli bölgesi Neojeni'nin paleontolojik ve stratigrafik etüdü. *Maden Tetkik ve Arama Genel Müdürlüğü Dergisi,* 83, 145-177.

Taner, G. 1975. Denizli bölgesi Neojeni'nin paleontolojik ve stratigrafik etüdü. *Maden Tetkik ve Arama Genel Müdürlüğü Dergisi,* 85, 45-66.

Tchihatcheff, P., 1867-1869. Asie Mineure (Description Physique) Paris.

Thomson, S.N., Stöckhert, B., Brix, M.R. 1998. Thermochronology of the high-pressure metamorphic rocks on Crete, Greece: implications for the speed of tectonic processes. *Geology,* 26, 259–262.

Ünay, E., Göktaş, F., Hakyemez, H.Y., Avşar, M., Şan, Ö. 1995. Dating of the sediments exposed at the northern part of the Büyük Menderes graben (Turkey) on the basis of Arvicolidae (Rodentia, Mammalia). *Geological Bulletin of Turkey,* 38, 75-80.

Ünay, E., De Bruijn, H. 1998. Plio-Pleistocene rodents and lagomorphs from Anatolia.*Mededelingen Nederlands Instituut voor Toegepaste Geowetenschappen TNO* 60, 431-466.

van Hinsbergen, D.J.J. 2010. A key extensional metamorphic complex reviewed and restored: The Menderes massif of western Turkey. Earth-Science Reviews, 102, 60-76.

Wernicke, B., 1981. Low-angle normal faults in the Basin and Range Province: nappe tectonics in an extending in an extending orogen. *Nature,* 291, 645-648.

Wernicke, B.P. 1985. Uniform-sense normal simple shear of the continental lithosphere. *Canadian Journal of Earth Sciences,* 22, 1, 108-125.

Wernicke, B., Axen, G.J. 1988. On the role of isostasy in the evolution of normal fault systems. *Geology,* 16, 848-851.

Westaway, R. 1990. Block rotation in western Turkey. 1.Observational evidence. *Journal of Geophysical Research* 95/B12, 19857-19884.

Westaway, R. 1993. Neogene evolution of the Denizli region of western Turkey. *Journal of Structural Geology,* 15, 37-53.

Westaway, R. 2006. Cenozoic cooling histories in the Menderes Massif, western Turkey, may be caused by erosion and flat subduction, not low-angle normal faulting. *Tectonophysics,* 412, 1-25.

Westaway, R., Pringle, M., Yurtmen, S., Demir, T., Bridland, D., Rowbotham, G., Maddy, D. 2003. Pliocene and Quaternary surface uplift of western Turkey revealed by long-term river terrace sequences. *Current Science,* 84, 1090–1101.

Westaway, R., Pringle, M., Yurtmen, S., Demir, T., Bridgland, D., Rowbotham, G., Maddy, D. 2004. Pliocene and Quaternary regional uplift in western Turkey: the Gediz river terrace staircase and the volcanism at Kula. *Tectonophysics,* 391, 121–169.

Westaway, R., Guillou, H., Yurtmen, S., Demir, T., Scaillet, S., Rowbotham, G. 2005. Constraints on the timing and regional conditions at the start of the present phase of crustal extension in western Turkey, from observations in and around the Denizli region. *Geodinamica Acta,* 18, 209-238.

Westaway, R., Guillou, H., Yurtmen, S., Beck, A., Bridgland, D., Demir, T., Scaillet, S., Rowbotham, G. 2006. Late Cenozoic uplift of western Turkey: Improved dating of the Kula Quaternary volcanic field and numerical modelling of the Gediz River terrace staircase. *Global and Planetary Change,* 51, 131–171

Yağmurlu, F. 1984. Akhisar doğusundaki kömür içeren Miyosen tortullarının stratigrafisi, depolanma ortamları ve tektonik özellikleri. *Türkiye Jeoloji Kongresi Bülteni* 5, 3-20.

Yazman, M. 1997. Western Turkey poses exploration challenges on/offshore. *The Leading Edge,* 16, 897-899.

Yılmaz, M., Gelişli, K. 2003. Stratigraphic – Structural interpretation and hydrocarbon potential of the Alaşehir Graben, Western Turkey. *Petroleum Geoscience,* 9, 277 – 282.

Yılmaz, Y. 1989. An approach to the origin of young volcanic rocks of western Turkey. İç: Tectonic Evolution of the Tethyan Region (Ed: A.M.C. Şengör), Kluwer Academic Publishers, Dordrecht, s.159-189.

Yılmaz, Y. 1990. Comparison of young volcanic associations of western and easternAnatolia formed under a compressional regime: a review. *Journal of Volcanology and Geothermal Research,* 44, 69-77.

Yılmaz, Y., Genç, S. C., Gürer, F., Bozcu, M., Yılmaz, K., Karacık, Z., Altunkaynak, S., Elmas, A., 2000. When did the western Anatolian grabens begin to develop? İç: Tectonics and Magmatism in Turkey and the Surrounding area. (Ed: Bozkurt, E., Winchester, J.A., Piper, J.D.A.). *The Geological Society London Special Publication* 173, s. 353-384.

Yolsal-Çevikbilen, S., Taymaz, T., Helvacı, C. 2014. Earthquake mechanisms in the Gulfs of Gökova, Sığacık, Kuşadası and the Simav region (western Turkey): Neotectonics, seismotectonics and geodynamic implications. *Tectonophysics,* 635, 100-124.

Yin, A. 1991. Mechanism for the formation of the domal and basinal detachment faulting : A three-dimensional analysis. *Journal of Geophysical Research,* 96, 14577-14594.

Yin, A., Dunn, J.F. 1992.Structural and stratigraphic development of the Whipple-Chemehuevi detachment fault system,, southeastern California: Implications for the geometrical evolution of domal and basinal low-angle faults. *Geological Society of America Bulletin,* 104, 659-674.

Bull. Min. Res. Exp. (2015) 151: 107-127

Bulletin of the
Mineral Research and Exploration

http://bulletin.mta.gov.tr

LATE PLEISTOCENE GLACIATIONS AND PALEOCLIMATE OF TURKEY

M. Akif SARIKAYA[a]* and Attila ÇİNER[a]

[a] *Eurasian Earth Sciences Institute, Istanbul Technical University, Maslak 34469, İstanbul*

Keywords:
Glacier, Late Pleistocene, Quaternary, Cosmogenic Surface Exposure Dating, Moraine, Paleoclimate.

ABSTRACT

Glaciers respond quickly to climatic changes and thus they are considered to be very accurate indicators of changes in atmospheric conditions. Similarly, the extent of past glaciers gives valuable insights into paleoclimatic changes. For this purpose, we reviewed the paleo-glaciated mountains where cosmogenic surface exposure dating was applied in Turkey. We also evaluated the paleoclimatic results obtained from these studies to provide a regional overview. Twenty-seven mountains in Turkey are high enough to support Quaternary valley glaciers or ice caps. The timing of glaciations was reported mainly by cosmogenic dating of moraines. We re-evaluated the dated sites and recalculated some of the published cosmogenic ages using the up-to-date production rates. The oldest geochronological records reported from the region belong to the glaciations before the globally defined Last Glacial Maximum (LGM). These glaciers developed probably during the beginning of the last glaciation (MIS 4; 71 ka ago) and stopped advancing at the end of the MIS 3 (at 29-35 ka ago). Later, glaciers expanded and reached to their most extensive locations during MIS 2 (after 29 ka ago). They reached maximum extents between 21.5 ka ago and 18.5 ka ago. This local-LGM was synchronous with the global-LGM. After the LGM, the glaciers started to retreat to less extensive positions and deposited their moraines ~16 ka ago during the Late Glacial. The Younger Dryas (~12 ka ago) advances were also reported from a limited number of mountains. Rare Early Holocene glaciations were dated to 8.5 ka in the interior regions. Late Holocene (1-4 ka ago) and Little Ice Age (between 1300-1850 AD) advances were also observed. We reconstructed the paleoclimate using glacier modeling together with paleoclimate proxy data from several regions. The results show that LGM climate was 8-11°C colder than today and moisture levels were 1.5 to 2 times in SW Turkey, somewhat similar to modern values in central parts and 30 % drier in the NE. The Late Glacial was colder by 4.5-6.4°C based on up to 50 % wetter conditions. The Early Holocene was 2.1-4.9°C colder and up to twice as wet as today, while the Late Holocene was 2.4-3°C colder and its precipitation amounts approached to similar conditions as today.

1. Introduction

Studies researching glaciers in Turkey have increased in recent years. Currently due to climatic changes our glacial assets are reducing daily and examining records of the past quantitatively will allow more reliable climatic predictions to be made for the future. As stated in the latest report by the Intergovernmental Panel on Climate Change (IPCC) on 27 September 2013, global climate change is a truth beyond doubt. According to the same report, the mean surface temperature of Earth has increased by 0.89°C since 1901 and this increase has caused a significant reduction in global snow and ice cover. Accordingly, each year global glacier volume reduce by 259 billion tons each year. The yearly ice loss from Greenland glaciers is 97 billion tons while the

* *Corresponding author: M. Akif Sarıkaya, masarikaya@itu.edu.tr*

loss in Antarctica has reached 121 billion tons (IPCC, 2013).

In Turkey the situation is no different. According to Sarıkaya (2012), the Mount Ağrı Ice Cap's surface area, the largest glacier in Turkey, has reduced by 29 % in the last 35 years (1976-2011). According to the latest study by Yavaşlı et al. (2015), the areal distribution of glaciers in Turkey had reduced in the last 41 years from 25 km^2 to 11.2 km^2. These and similar studies to date reveal the truth of climate change, but in the past how often and by how much did climate change? What was the distribution of glaciers in Turkey? What geographical and climatic relationships exist between paleo- and present glaciers? Have similar climatic changes as today happened in the past? If it is considered that past changes happened without the effect of humans, how much does natural change contribute to the climate changes today? To answer these and similar questions, it is necessary to research paleo-glacial records. This study is a review of the distribution and timing of glaciers developed during Quaternary ice ages in Turkey (Figure 1). Additionally, findings obtained about paleoclimatic conditions during these ice ages are presented.

Studies on quantitative glacial research and dating of paleo-glaciers in Turkey in recent years have shown that Turkey experienced significant glacial advances in the Late Pleistocene (126-11.6 ka) and partially in the Holocene (last 11.7 ka) (Sarıkaya et al., 2011). Previous studies were done only based on relative location and sizes (Erinç, 1951; Doğu et al., 1993; Çiner, 2003; 2004), but now can be completed in a more sensitive manner with quantitative dating studies to determine advance and retreat times of glaciers. This study brings recent studies in Turkey into a more general view and presents regional implications of glacial timing and paleoclimate.

2. Quaternary Glaciers and Ice Ages

Glaciers and climate have a direct relationship and they react very quickly to ongoing climatic changes (Oerlemans, 2001). The most reliable records of the climatic changes in the Pleistocene, called the Ice Age, come from glaciers. Climate change dominating the Quaternary (last 2.58 Ma) is the most important factor in the creation of glacial periods. Periodic changes in the orbit of Earth affect the intensity of sunlight reaching the earth and as a result Earth's climate. These changes, called Milankovitch cycles, cause glaciers to advance in cold climate conditions and retreat in relatively warmer periods.

It is thought that in the Quaternary period at least 21 glacial periods developed, each numbered by their Marine Isotope Stages (MIS). Of these glacial periods in the last 900 ka, four have reached large scales globally. These are, from the oldest to most recent, MIS 16, MIS 12, MIS 10-6-8 and MIS 4-2 glacial periods (Gibbard and Cohen, 2008).

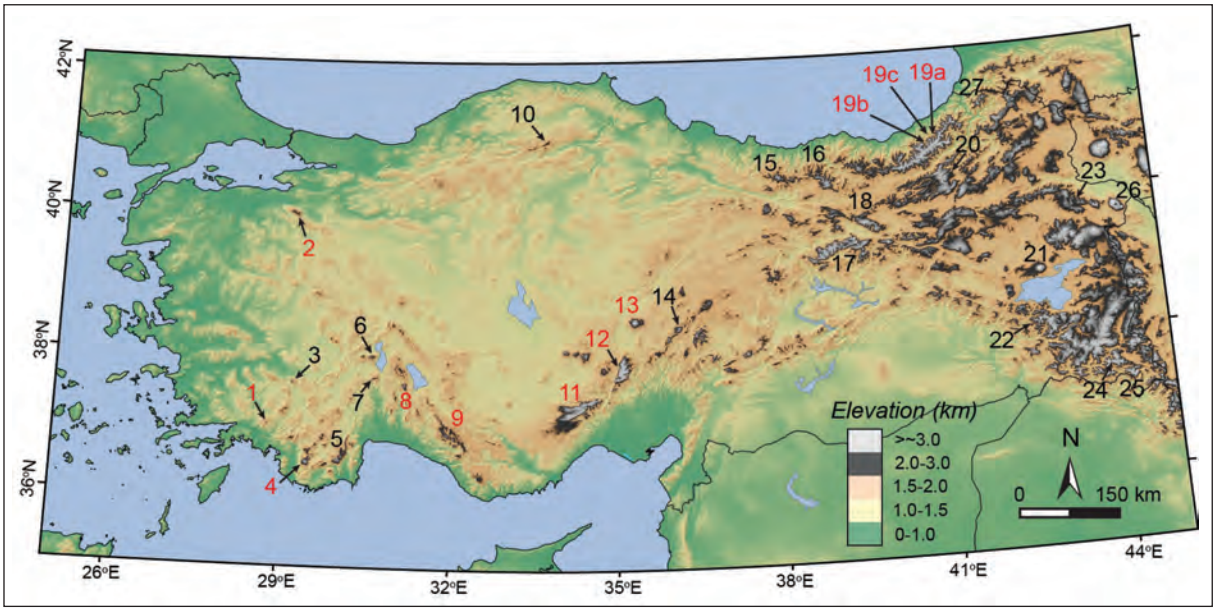

Figure 1- Distribution of glaciers in Turkey in the Late Pleistocene. Areas in red indicate cosmogenic dating areas.

In European glacial stratigraphy the MIS 16, called the Günz, ended about 610 ka ago (Termination 7) while the Mindel ice age (MIS 12) ended 424 ka ago (Termination 5). The Riss ice age (MIS 10, 8 and 6) (Penultimate glaciation) ended 130 ka ago in the period called Termination 2. The closest ice age to the present day includes MIS 4-2 and is called the Würm (or Last Ice Age) in European Alpine stratigraphy (Rose, 2007).

MIS-4 occurred between 71 ka and 57 ka (Würm I), while MIS-2 occurred from 29 ka to 14 ka ago (Würm II). Within the MIS-2 the glaciation reached maximum size from 19-23 ka (mean 21 ka) (Mix et al., 2001) which is known as the Last Glacial Maximum (LGM). During the LGM glaciers reached largest sizes in Europe, North America and many central and high latitude regions, covering one third of the continents.

We also observed the evidences of LGM, in Turkey. The traces of the latest glaciation goes back to about 14 ka years ago (Late Glacial). In this period where temperatures began to approach current conditions, some part of the world entered a rapid and short cold stadial. This period, called the Last Henrich Period (H0), is also known as the Younger Dryas (12.0-11.7 ka) named after an Alpine tundra flower Dryas octopetala. The Younger Dryas was mainly felt in northern Europe and temperatures in Greenland dropped by 12-18ºC compared to the present. The reason for this is given as large glaciers melting after the LGM disrupted oceanic currents in the North Atlantic Ocean and blocked heat transfer from equatorial regions (Alley et al., 1993). With the end of the Younger Dryas period, climatic conditions similar to the present developed and the Holocene (from 11.7 ka to the present) began (Mayewski et al., 2004).

3. Method: Cosmogenic Surface Exposure Dating

The pionering on suggest cosmogenic surface exposure dating methods to date landforms appeared in the 1950s (Davis and Schaffer, 1955), however the practical application started with advances in Accelerator Mass Spectrometry (AMS) in the 1980s (Zreda et al., 1991). This method is accepted as the beginning of a new era in Quaternary studies as due to this method any surface protected by certain conditions can be dated. For a review of this method, papers by Cerling and Craig (1994), Zreda and Phillips (2000), Gosse and Phillips (2001), Cockburn and Summerfield (2004), and Dunai (2010) are useful.

Cosmic rays that form the cosmogenic isotopes on land surface occur in the universe due to supernova explosions and radioactive radiation from the sun. These rays have a very high energy and speed and hit Earth from all directions (Dunai, 2010). The rays initially react with atmospheric elements, then reach the surface and enter reactions with lithospheric elements in rock surfaces and form new isotopes in the first 2-3 meters of the rock. These are called cosmogenic isotopes (for example: ^{10}Be, ^{14}C, ^{26}Al, ^{36}Cl, ^{41}Ca, ^{3}He, ^{21}Ne, etc.) (Dunai, 2010). If the production rate of these new isotopes within the rock is known (Schimmelpfennig et al., 2011; Marrero, 2012), and when the concentration of cosmogenic isotopes are measured, then it is possible to determine how long these rocks have been exposed at the surface. The main landforms that this method can be applied to are moraines, alluvial fans, river terraces, fault planes and volcanic surfaces.

The first applications in the literature was to glacial deposits. Moraines form as a result of glacial deposits, (Figure 2a). New surfaces are also formed by glacial erosion of bedrock (Figure 2b). These surfaces can be dated by this method. Moraines are exposed to cosmic rays from the moment the glacier starts to retreat and it is assumed that the deposited material has not been exposed to cosmic rays previously, thus the minimum age of deposition of the moraine is calculated as the beginning of glacial retreat (Zreda and Phillips, 2000). In Turkey by measurement of ^{36}Cl and ^{10}Be cosmogenic isotopes on moraines, the chronology of Quaternary glaciation has been revealed in detail and paleoclimate interpretations have been made (Akçar et al., 2007; 2008; Sarıkaya et al., 2008; 2009; Sarıkaya, 2009; Zahno et al., 2009; 2010; Zreda et al., 2011; Sarıkaya et al., 2014; Çiner et al., 2015; Akçar et al., 2015; Çiner and Sarıkaya, 2015).

4. Distribution and Chronology of Glaciers

The first studies on glaciation of Anatolia began at the end of the 1800s and beginning of the 1900s by some European voyagers (Ainsworth, 1842; Palgrave, 1872; Maunsell, 1901). Later with the contribution of Turkish researchers, glacier studies increased (Erinç, 1944; 1949*a*; 1949*b*; İzbırak, 1951; Erinç, 1951; 1952; 1953; Doğu et al., 1993; 1999). In the last 15 years the application of cosmogenic surface exposure dating to Turkish glacial deposits has given a new dimension to Quaternary studies. Moraines, previously only dated by qualitative methods such as relative relations, degree of erosion,

Figure 2- Sample collection for cosmogenic age dating: a) above blocks (Bolkar Mountains, Alagöl Valley); b) whaleback on bedrock (Aladağlar, Körmenlik Valley).

and development of soil and plant cover, began to be dated quantitatively by cosmogenic methods (Akçar et al., 2007; 2008; Sarıkaya et al., 2008; 2009; Sarıkaya, 2009; Zahno et al., 2009; 2010; Zreda et al., 2011; Sarıkaya et al., 2014; 2015; Çiner et al., 2015; Çiner and Sarıkaya, 2015).

Turkey's Late Pleistocene glaciers developed on high mountains in Anatolia; the Taurus and Eastern Black Sea Mountains, and along with individual volcanoes. According to Kurter's (1991) classification, Turkey's glacial regions can be divided in three regions. These are (1) the Taurus Mountains extending parallel to the Mediterranean coast to the southeastern most part of Turkey, (2) the Eastern Black Sea Mountains extending along Turkey's Black Sea coast and (3) scattered and isolated high mountains and volcanoes in Anatolia (Table 1). This study focuses on dating studies of old glacial deposits within Turkey which have rapidly increased in recent years. Readers may benefit from Çiner (2003; 2004), Sarıkaya et al. (2011), Sarıkaya and Tekeli (2014) and Yavaşlı et al., (2015) for studies of Turkey's current and paleo-glacial inventories.

4.1. Taurus Mountains

The Taurus Mountains contain widespread glaciers and glacial areas that can explain the paleoclimate of the Eastern Mediterranean. This mountain range can be divided into roughly three areas; (1) Western Taurus, (2) Central Taurus and (3) Eastern Taurus (Sarıkaya et al., 2011). The mean elevation of the Taurus Mountains increases from west to east. Turkey's largest current glaciers are in the Eastern Taurus, concentrated in the region close to the Turkey-Iraq-Iran border (Sarıkaya and Tekeli, 2014). However, as there are no studies on the quantitative age of glaciers in this region yet, this study will mainly focus on the Western and Central Taurus Mountains.

4.1.1. Western Taurus

In the Western Taurus, there are eight mountains with signs of Late Pleistocene glaciers. The peaks of these mountains are generally at 3000 m or a little higher. The westernmost one is Mount Sandıras (37.1ºN, 28.8ºE; 2295 m) located very close to the Mediterranean (Figure 1). Mount Sandıras presents very important information about the LGM and later glaciations with the most important evidence in the form of moraines deposited in three north-facing valleys and cirques. The largest glacier on Mount Sandıras reached a maximum length of 1.5 km from its cirque and deposited terminal moraines at an elevation of 1900 m. Sarıkaya et al. (2008) published cosmogenic ^{36}Cl surface exposure dates of nine samples belonging to four moraine ridges in two different valleys. According to re-calculations using current ^{36}Cl isotope production rates (Marrero, 2012), the most widespread glaciation appears to have begun to retreat at 22.9 ± 3.3 ka in the Kartal Lake Valley. Other moraines in the same valley show that the glacier advanced slightly and/or remained stable for several thousand years at 20.6 ± 3.1 ka. Another valley northwest of Kartal Lake Valley was found to have moraines deposited at 16.4 ± 3.2 ka and 17.2 ± 3.2 ka. The glaciers on Mount Sandıras, are smaller than in other regions. After the glaciers on Mount Sandıras reached their maximum extent at the LGM, there were some small advances and/or stabilizations in the Late Glacial period before the disappearance at the onset of Holocene.

Table 1- List of Late Pleistocene glaciers in Turkey

#	Mountain Name	Peak Elev. (m)	Lat. (DD°N)	Long. (DD°E)	LGM* Snowline (m)	Present Snowline (m)	Source
1	Sandıras Mt.	2295	37,0814	28,8380	2000	3000-3500	Sarıkaya et al. (2008)
2	Uludağ	2543	40,0706	29,2215	2400	3500	Zahno et al. (2010); Akçar et al. (2014)
3	Honaz Mt.	2571	37,6791	29,2850	2500-2600	3600	Erinç (1955; 1957); Messerli (1967)
4	Akdağ	3016	36,5439	29,5674	2518	3500	Sarıkaya et al. (2014)
5	Beydağ	3086	36,5684	30,1017	2500-2650	3600	Louis (1944); Messerli (1967)
6	Barla Mt.	2800	38,0531	30,7022	2400-2500	3750	Louis (1944); Ardos (1977)
7	Davraz Mt.	2637	37,7571	30,7317	2400-2500	3750	Louis (1944); Messerli (1967)
8	Dedegöl Mts.	2992	37,6437	31,2835	2350-2400	3300-3500	Zahno et al. (2009)
9	Geyikdağ	2850	36,8075	32,2021	2500	3400	Çiner et al. (2015)
10	Ilgaz Mt.	2587	41,0342	33,6545	?	4300	Louis (1944)
11	Bolkar Mts.	3524	37,3862	34,6087	2650	3450-3700	Çiner and Sarıkaya (2015)
12	Aladağlar	3756	37,8366	35,1453	2700	3450	Zreda et al. (2011)
13	Erciyes Mt.	3917	38,5318	35,4469	2700	3550	Sarıkaya et al. (2009)
14	Soğanlı Mts.	3075	38,4084	36,2119	2610	3550	Ege and Tonbul (2005)
15	Karagöl Mt.	3107	40,5101	38,1928	2600-2700	3500	Planhol and Bilgin (1961)
16	Karadağ	3331	40,3793	39,0710	2600-2850	3500	Gürgen (2001)
17	Mercan Mts.	3368	39,4934	39,1669	2750	3600-3700	Bilgin (1972)
18	Esence Mts.	3477	39,7836	39,7548	2750	3600-3700	Akkan and Tuncel (1993)
19a	Kavron V.	3932	40,8354	41,1614	2300-2500	3100-3200	Akçar et al. (2007)
19b	andrçenik V.	3907	40,7220	40,8924	2300-2500	3100-3200	Akçar et al. (2008)
19c	Başyayla V.	3425	40,7814	41,0104	2300-2500	3100-3200	Reber et al. (2014)
20	Mescid Mt.	3239	40,3273	41,1673	2750	3600-3700	Yalçınlar (1951)
21	Süphan Mt.	4058	38,9309	42,8326	3200	3700-4000	Kesici (2005)
22	Kavuşşahap Mts.	3503	38,2146	42,8563	?	3400	Doğu (2009)
23	Balık Lake	2804	39,7766	43,5274	?	4300	Birman (1968)
24	Buzul Mts.	4135	37,4877	44,0012	2100-2800	3600	Erinç (1952)
25	İkiyaka Mts.	3794	37,3105	44,2502	2600	3600	Bobek (1940)
26	Ağrı Mt.	5137	39,7018	44,2983	3000	4300	Sarıkaya (2012)
27	Karçal Mts.	3415	41,3472	41,9830	?	3400	Gürgen and Yeşilyurt (2012)

LGM: Last Glacial Maximum

Another glacial region in the Western Taurus is Akdağ (36.54ºN, 29.57ºE; 3016 m) (Figure 1). Located 90 km southeast of Mount Sandıras, Akdağ contains first pre-LGM glaciers dated up to today. Forty-one moraine blocks in three valleys north of Akdağ have been dated using the cosmogenic ^{36}Cl method (Sarıkaya et al., 2014) (Figures 3 and 4a,b). The glaciers attained a length of up to 6 km reaching a height of 2000 m above sea level. Before the LGM, about 35.1 ± 2.5 ka before the present, the glaciers reached an elevation of 2150 m (Sarıkaya et al., 2014). At the LGM the glaciers reached their largest extent 21.7 ± 1.2 ka before the present (height of 2050 m above sea level). Later about 15.1 ± 0.9 ka in the Late Glacial period, the glaciers retreated slightly and remained stable for a short time. Similar OSL ages (17.7 ± 4.4 ka) have been obtained by Bayrakdar (2012) for glacial deposits on Akdağ.

The Dedegöl Mountains are another glacial area about 300 km east of Mount Sandıras (37.37ºN, 31.19ºE; 2992 m) (Figure 1). The glacial sediments in this region have been dated with ^{10}Be and ^{26}Al isotopes (Zahno et al., 2009). The Muslu Valley on the eastern side of the mountains has two lateral moraines extending to an elevation of 1400 m which were dated by Zahno et al. (2009). Glaciers were determined to have developed before the LGM (>29.6 ± 1.9 ka; recalculated by Reber et al., 2014), at the LGM (21.5 ± 1.5 ka) and in the Late Glacial period (15.2 ± 1.1 ka).

The most widespread hummocky moraines in Turkey are observed in the Namaras and Susam Valleys on Geyikdağ (36.53ºN, 32.10ºE; 2877 m) (Figures 1 and 4c,d). In addition to hummocky moraines there are lateral and terminal moraines (Çiner et al., 1999; 2015). These hummocky moraines are formed on the piedmont at an elevation of 2350-2650 m as a result of melting glaciers. Thirty-four block-scale rock samples from moraines in the Namaras and Susam Valleys were dated with the cosmogenic ^{36}Cl method. The obtained ages indicate three phases of regression during the Late Pleistocene (Çiner et al., 2015). The oldest and most extensive regression was at 18.0 ± 1.1 ka, toward the end of the

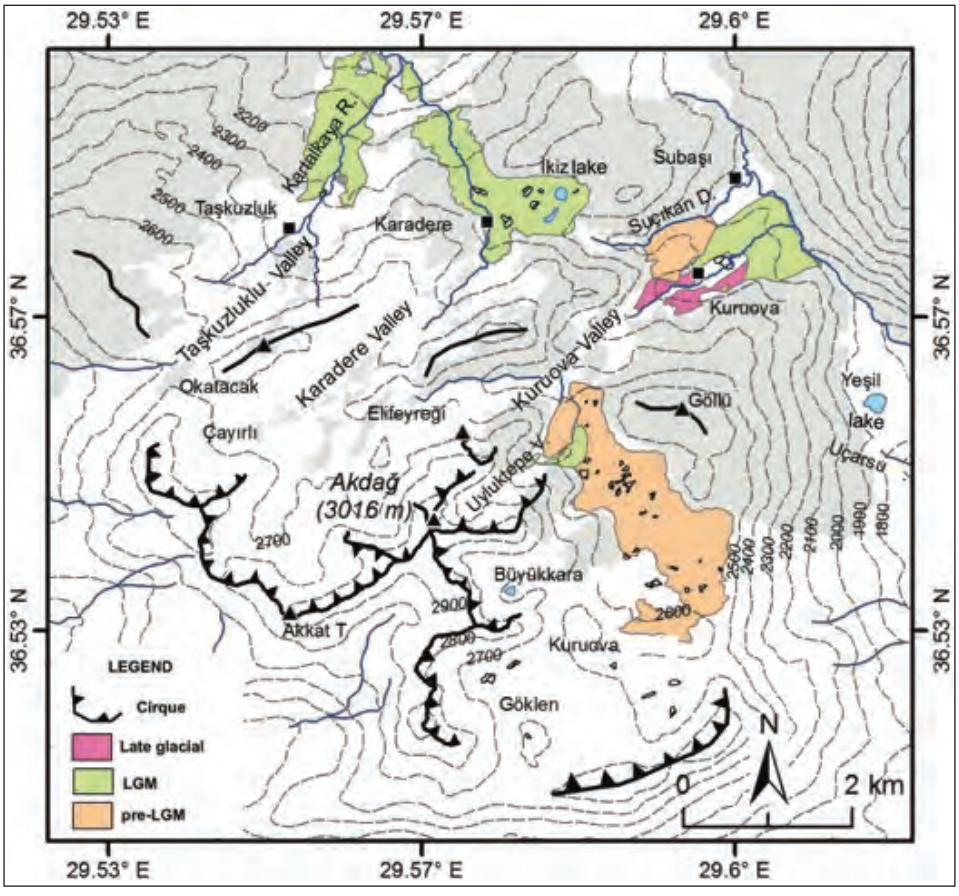

Figure 3- Akdağ glacial geomorphological and deposition map. Adapted from Sarıkaya et al. (2014).

Figure 4- a) Appearance of terminal moraine in Akdağ Taşkuzluklu Valley (scale: car); b) Terminal moraine and dried glacial lake in background in Akdağ Kuruova Valley (scale: blue hut); c) section of hummocky moraine in Geyikdağ Namaras Valley. Undifferentiated sediment layers of varying sizes from fine sand to block size. The soil and plant development on the surface of the moraine gives an idea of the age; d) Hummocky moraines in Geyikdağ Namaras Valley. The entrance to Susam Valley is seen in the background; e) Black-coloured volcanic erratics deposited on limestone bedrock in Karagöl Valley in the Bolkar Mountains (block size 2 m); f) Right and left lateral moraines in Karagöl Valley in Bolkar Mountains near Meydan Plateau (scale: incomplete hotel construction on left lateral moraine).

LGM. The Late Glacial lateral moraines were deposited at 14.0 ± 2.7 ka, while the terminal moraine in Susam Valley was formed at 13.4 ± 1.5 ka. The hummocky moraines in Susam Valley appear to have occurred along 5 km showing that the ice retreat occurred very rapidly (14.0 ± 1.3 ka). Moraines confirming the Younger Dryas in Geyikdağ were deposited near the exit of the Susam Valley about 11.6 ± 1.3 ka.

Though there are no quantitative age data, on other mountains in the Western Taurus Mountains it is possible to find evidence of Late Pleistocene glaciation in regions such as Beydağ (36.57ºN, 30.10ºE; 3086 m) (Louis, 1944; Messerli, 1967), Mount Barla (38.05ºN, 30.70ºE; 2800 m) (Ardos, 1977), Mount Honaz (37.68ºN, 29.29ºE; 2571 m) (Yalçınlar, 1954; Erinç, 1955; 1957) and Mount Davraz (37.76ºN, 30.73ºE; 2637 m) (Monod, 1977; Atalay; 1987) (Figure 1).

The snow line in the Western Taurus during the LGM varied from 2000 m to 2600 m. In other areas apart from Mount Sandıras, the LGM permanent snow line was above 2000 m (Figure 5). The reason for this is probably that in the ice ages the mountain was exposed to humid air currents due to its proximity to the Mediterranean (Doğu et al., 1993; Sarıkaya et al., 2008). In the Western Taurus Mountains the modern snow line varies from 3400 m to 3700 m. This indicates that there has been a 1100-1500 m increase in the height of the snow line since the LGM.

4.1.2. Central Taurus

The Central Taurus Mountains are in the south of Turkey and contain three glacial regions (Figure 1). These are the Bolkar Mountains, Aladağlar and Soğanlı Mountains.

The Bolkar Mountains are 200 km east of Geyikdağ (37.39ºN, 34.61ºE; 3524 m) (Figure 1). Çiner and Sarıkaya (2015) in a study of two north-facing valleys and one south-facing valley in the Bolkar Mountains using thirty ^{36}Cl samples dated terminal and lateral moraines and bedrock eroded by glaciers and erratic block samples (Figure 4e,f). The northern Karagöl and Alagöl Valleys and southern Elmalı Valley contain many lateral and terminal moraines. Accordingly, four glaciations were defined that developed before the LGM (46.0 ± 7.0 ka) (Çiner and Sarıkaya, 2015). The glaciers in the Bolkar Mountains reached their maximum size at 18.9 ± 3.3 ka. In this situation the length of the glaciers from the cirque is estimated to have reached 5.5 km. Late Glacial moraines are thought to have formed between 15.2 ± 1.6 and 12.6 ± 2.3 ka. The most recent glacial remains in the Bolkar Mountains are recorded in the Early Holocene. Holocene moraines were dated at 9.0 ± 0.9 ka in Karagöl Valley and 8.5 ± 1.8 ka in Elmalı Valley. At the exit of the Alagöl Valley, outwash plain formation ended before 8.4 ± 1.0 ka.

In Aladağlar (37.48ºN, 37.09ºE, 3575 m), there are indications of paleo-glacial activity. Zreda et al. (2011) carried out cosmogenic ^{36}Cl dating on a U-shaped glacial valley, Hacer Valley, in the east of the

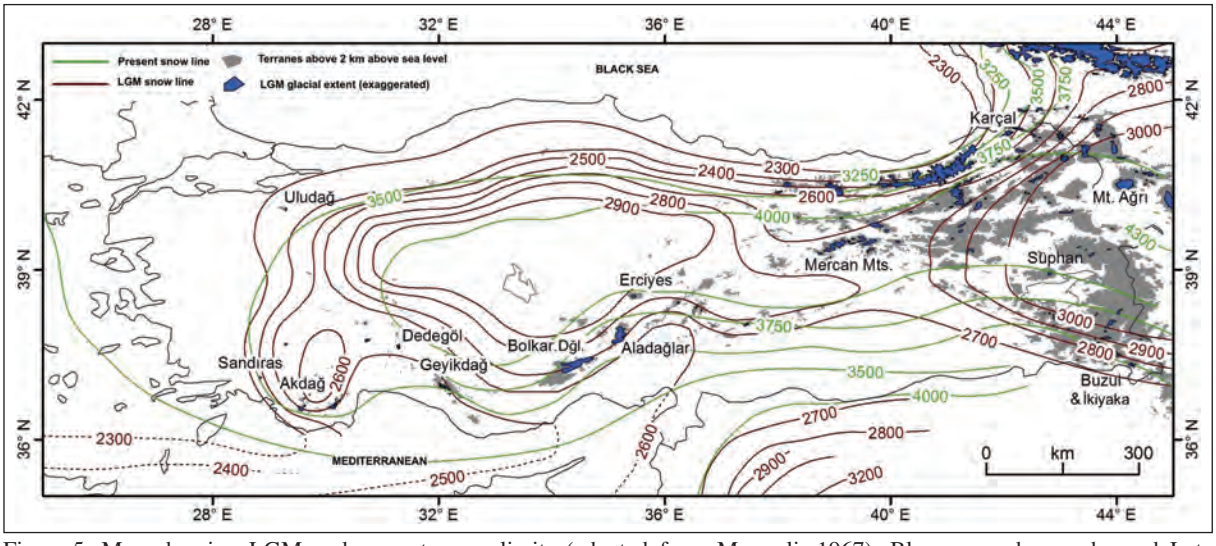

Figure 5- Map showing LGM and current snow limits (adapted from Messerli, 1967). Blue areas show enhanced Late Pleistocene glacial distribution.

Aladağlar. They revealed that at the Late Pleistocene-Holocene boundary, the glaciers retreated rapidly. Several moraine ridges were identified at an elevation of 1100 m in the Hacer Valley (valley entrance) and at Yedigöller Plateau at 3100 m elevation (Figure 6a). It is thought that there was an ice sheet completely covering the Yedigöller Plateau just below the peaks. Using new cosmogenic production rates developed by Marrero (2012), the ages of 22 samples were recalculated (Sarıkaya and Çiner, 2015). The age intervals were determined as 14.0 ± 1.5 ka for the valley floor and 11.5 ± 1.3 ka for the plateau. This shows that at the end of the Late Glacial there was a glacier extending 15 km and after the Younger Dryas there was rapid melting. Other glacial valleys in the Aladağlar indicate glaciers from much older periods. In the north and northwest sections of the Yedigöller Plateau (about 1850-2100 m) there are several valleys with terminal and lateral moraines. These contain evidence that glaciation developped in MIS 3 or MIS 4 periods based on studies in the valleys near Ecemiş Fault (Sarıkaya et al., 2015).

Mount Soğanlı is located in the Tahtalı Mountains, another glacial region of the Central Taurus. There are signs of glaciation in areas close to the peak of Mount Soğanlı (Ege and Tonbul, 2005). In the northwest of Dökülgen Valley, glacial deposits have been identified at 2250 m elevation. Hummocky moraines and terminal moraines on Mount Soğanlı have been dated relatively, indicating that there may have been effective glaciation in the Pleistocene (Ege and Tonbul, 2005).

In the Central Taurus the elevation of the snow line in the LGM varied from 2600 to 2700 m (Messerli, 1967). Currently the snow line is between 3400 and 3600 m (Figure 5). This shows that the permanent snow line has risen by 800-900 m since the LGM.

4.1.3. Southeast Taurus

Containing Turkey's largest current glaciers (Erinç, 1953; Sarıkaya and Tekeli, 2014), the Southeast Taurus Mountains contain Late Pleistocene

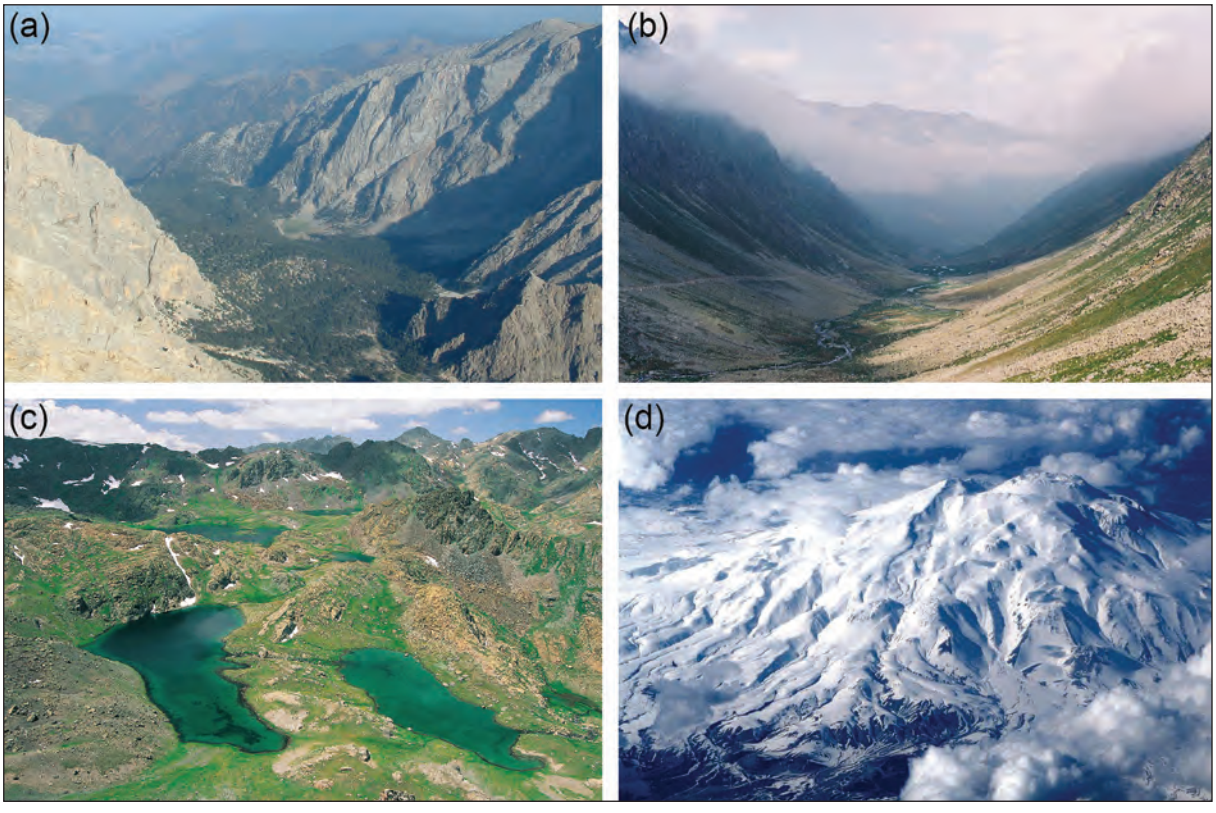

Figure 6- a) View from Aladağlar Hacer Valley to Yedigöller Plateau. Looking approximately east, with valley depth of 1500 m (Photograph: Serdar Bayarı); b) U-shaped valley caused by glacial erosion in the Kavron Valley of the Eastern Black Sea Mountains (Photograph: Naki Akçar); c) Glacial lakes in the upper portion of the Salacur Çoruh Valley. It is possible to find similar lakes on many mountains in Anatolia (Photograph: Hakan Gün, Atlas Magazine); d) Süphan Volcano 4058 m elevation (Photograph: Anonymous).

glaciers in three important areas (Figure 1). These are Mount Buzul and Mount İkiyaka within the borders of Hakkari and Kavuşşahap Mountains south of Lake Van. Studies by Bobek (1940) and Erinç (1953) found that on Mount Buzul and Mount İkiyaka, glaciers extended to an elevation of 1600 m in the Late Pleistocene (Würm) reaching lengths of 9-10 km. It is possible to see moraines belonging to these glaciers in the Zap Suyu Valley and other neighboring valleys (Erinç, 1953; Wright, 1962). To date no quantitative age data have been obtained in this region.

4.2. Eastern Black Sea Mountains

With mountain ridges running parallel to the coast of the Eastern Black Sea, they contain widespread signs of paleo-glacial activity (Figure 1). The majority of these mountains contain well-developed U-shaped glacial valleys and cirques in places close to 3000-4000 m above sea level (Figure 6b). The Eastern Black Sea Mountains rise as they move east and form a physiographic barrier between the Black Sea and the Eastern Anatolian plateau. The climate in the Eastern Black Sea Mountains is affected by mobile mid-latitude cyclones and associated frontal systems along with the high pressure system in Siberia. As a result air masses from the Black Sea produce orographic rainfall year round along the Black Sea coastal strip and the northern-facing slopes of the Eastern Black Sea Mountains (Akçar et al., 2007).

The Kaçkar Mountains, located in the highest section of the Eastern Black Sea Mountains, have had cosmogenic ^{10}Be dating completed on a typical glacial valley extending north, the Kavron Valley (Akçar et al., 2007). Accordingly moraines deposited at 27.3 ± 1.7 ka were identified in this valley, with the LGM glaciation ending at 19.8 ± 1.4 ka. Moraines belonging to the Late Glacial in the region were dated to 17.0 ± 1.1 ka, while the Younger Dryas in the region was dated to 12.8 ± 1.0 ka. Similar results were obtained for the nearby Verçenik Valley (Akçar et al., 2008). Here LGM glaciers developed at 27.5 ± 1.8 ka and ended before 20.3 ± 1.4 ka. Additionally in the Verçenik Valley moraines from 17.2 ± 1.2 ka were identified (Akçar et al., 2007). According to the latest study by Reber et al. (2014) in Başyayla Valley, glaciers developed from 57.0 ± 3.5 ka before the LGM. It has been determined that the local LGM occurred much earlier than the global LGM around 41.5 ± 2.5 ka. Additional glacial advances were identified between 32 ka and 21 ka. Lastly Late Glacial period moraines were dated to 17.0 ± 1.0 ka.

Although the elevation is low, there are terminal and hummocky moraines of Late Pleistocene age on Karadağ (40.38ºN, 39.07ºE; 3331 m) and Mount Karagöl (40.51ºN, 38.19ºE; 3107 m) in the Gümüşhane and Giresun Mountains (Çiner, 2004). Though there are large U-shaped valleys and many landforms related to glaciation in Bulut-Altıparmak and Soğanlı Mountains in the Eastern Black Sea, no quantitative data has been obtained (Gürgen, 2003). In addition to these, the Karçal Mountains (41.35ºN, 41.98ºE; 3415 m) on the Turkish-Georgian border have well-preserved glaciers, glacial landforms and rock glaciers (Gürgen and Yeşilyurt, 2012).

The current permanent snow line in the Eastern Black Sea Mountains is 3500-3550 m (Erinç, 1952) to the south and between 3100-3200 m on north-facing slopes (Figure 5). This difference is probably due to the effects of moist air coming from the Black Sea (Erinç, 1952). The LGM permanent snow line was 2600-2700 m to the south, varying between 2300-2500 m to the north.

4.3. Other Mountains in Anatolia

The Erciyes Volcano, in the Central Anatolia Volcanic Province, is another mountain that was glaciated in the Late Pleistocene (38.53ºN, 35.45ºE; 3917 m) (Figure 1). Glaciers on the north of the mountain extended to elevations of 2150 m reaching lengths of 6 km. A total of 44 samples (Sarıkaya et al., 2009) taken from two valleys, the north-facing Aksu Valley and the Üçker Valley, were dated with ^{36}Cl surface exposure dating and glacial periods at 24.4 ± 3.4 ka (LGM), 15.7 ± 1.9 ka (Late Glacial) and 10.5 ± 1.3 ka (Early Holocene) were revealed. The latest advance occurred at 4.2 ± 0.6 ka (Sarıkaya et al., 2009). The elevation of the LGM permanent snow line was calculated as 2700 m on the north slope (Sarıkaya et al., 2009), and 3000 m on the south slope (Messerli, 1967) (Figure 5). Today the permanent snow line on Erciyes is 3550 m (Sarıkaya et al., 2009). Presently there is a small glacier on the north ridge of the mountain (around 260 m long), however since 1902 there has been a horizontal melting rate of 4.2 m (Sarıkaya and Tekeli, 2014). If the melting continues at this rate, it is assumed that the Erciyes glacier will completely disappear by the year 2070 (Sarıkaya et al., 2009).

According to the first studies on Late Pleistocene glaciation on Mount Ağrı, Turkey's highest mountain, the LGM permanent snow line was around 3000 m. where an ice cap of 100 km^2 would have covered the

summit of the mountain. To date although intense moraine deposits have not been found in the valleys around the mountain, Birman (1968) mentioned some paleo-glacial traces on the mountain's south-facing slopes. Blumenthal (1958) attributed the reason for not observing moraines on Mount Ağrı to the lack of sufficient slope to produce moraines or support intense valley glaciation and volcanic activity developing later. Currently the peak of Mount Ağrı is covered by Turkey's largest ice cap. The results of a study by Sarıkaya (2011) using satellite imagery found that in 2011 the ice cap covered an area of 5.66 km^2 and determined that the area had reduced by 29% between 1976-2011. A similar study was completed by Yavaşlı et al. (2015) and the area of the ice cap was identified as 5.34 km^2 in 2013.

In the Marmara region the only glaciated mountain is Uludağ (40.04ºN, 29.13ºE; 2542 m) ski resort and according to dating studies on Kovuk Valley (Zahno et al., 2010) and the Karagöl Valley (Akçar et al., 2014) to the east, LGM glaciers developed in the ski resort valley at 24.6 ± 1.5 ka and the melting of these glaciers was completed before 18.6 ± 1.3 ka (Zahno et al., 2010). Other valleys east of Uludağ developed LGM glaciers at similar times. For example in Karagöl Valley, the LGM glaciers began to develop before 20.4 ± 1.2 ka and ended before 18.6 ± 1.2 ka. In Kovuk Valley the last melting of LGM glaciers occurred at 18.1 ± 1.7 ka before the present. On Uludağ the Late Glacial period moraines are encountered at 15 ka. The only Younger Dryas moraines in the region are from 11.6 ± 0.7 ka located within the ski resort.

Another volcanic mountain in the eastern Turkey, Mount Süphan (38.56ºN, 42.50ºE; 4058 m) had an ice cap in the LGM period and it is estimated that the ice descended to 2650-2700 m on the north side of the mountain and 2950-3000 m on the south side (Kesici, 2005) (Figure 6d). These observations, indicating 1.5-2 km long glaciers, have not been quantitatively studied. On Mount Süphan the LGM permanent snow line was 3100 m, while the current permanent snow line is around 4000 m (Figure 5).

Traces of glaciation are found on many individual mountains in Anatolia (Figures 1 and 6d). One of these is the Mercan Mountains (39.49ºN, 39.17ºE; 3368 m) located to the south of Erzincan. Detailed mapping in this region by Bilgin (1972) identified that the region was covered with an intense glacial network and the glaciers descended to 1650 m elevation (Atalay, 1987). The Esence Mountains (39.78ºN, 39.75ºE) at 3477 m elevation had well-developed Late Pleistocene glaciers. Lateral moraines formed by valley glaciers reaching 9 km length from the cirques (Yalçınlar, 1951; Atalay, 1987). It is thought that the LGM permanent snow line was around 2750 m (Figure 5). Lastly in other regions in Anatolia, like Mount Ilgaz (41.03ºN, 33.65ºE; 2587 m) (Louis, 1944) and Lake Balık (39.78ºN, 43.53ºE; 2804 m) (Birman, 1968), there are indications on the Late Pleistocene glacial presence.

5. Interpretation and Discussion

Cosmogenic isotope application in recent years in Turkey have produced significant developments in the glacial chronology of Turkey in the Late Pleistocene. Data currently obtained allow the possibility to gain a general view of the distribution and timing of Anatolian glaciers (Figure 7).

When all studies since the year 2000 are reviewed, sampling was completed generally on blocks forming moraines, bedrock eroded by glaciers, erratic blocks and outwash plain deposits and to date a total of 365 samples appear to have been collected (Table 2). These studies generally focus on the Taurus and Eastern Black Sea Mountains and in a total of 27 glacial regions 9 have been dated (Table 3). All these studies have been completed by our group and the Swiss-based study group led by Dr. Naki Akçar. Generally, studies have used ^{36}Cl, ^{10}Be and ^{26}Al isotopes with a total of 48 samples excluded from the calculations for various reasons. Among these reasons are primary isotopes in blocks yielding true ages are much older, or presenting younger ages due to the effect of erosion or overturning. Generally mean ages were calculated from geomorphologic surfaces with multiple samples in these studies and in summary it was revealed that glaciers were active in five separate time slices in the Late Pleistocene. These are pre-LGM, LGM, Late Glacial, Younger Dryas and Holocene period glaciations (Figure 7).

The majority of the paleo-glacial formations in Turkey began to develop much before the LGM (about 29-35 ka) and probably reached their maximum size by the LGM period (21 ka). Some of these began to develop much earlier than this (during MIS 4) and it is thought they partially retreated before the global LGM (at the end of MIS 3, 29 ka).

During the LGM glaciers advanced once more (21.5-18.5 ka) and reached their maximum size. This

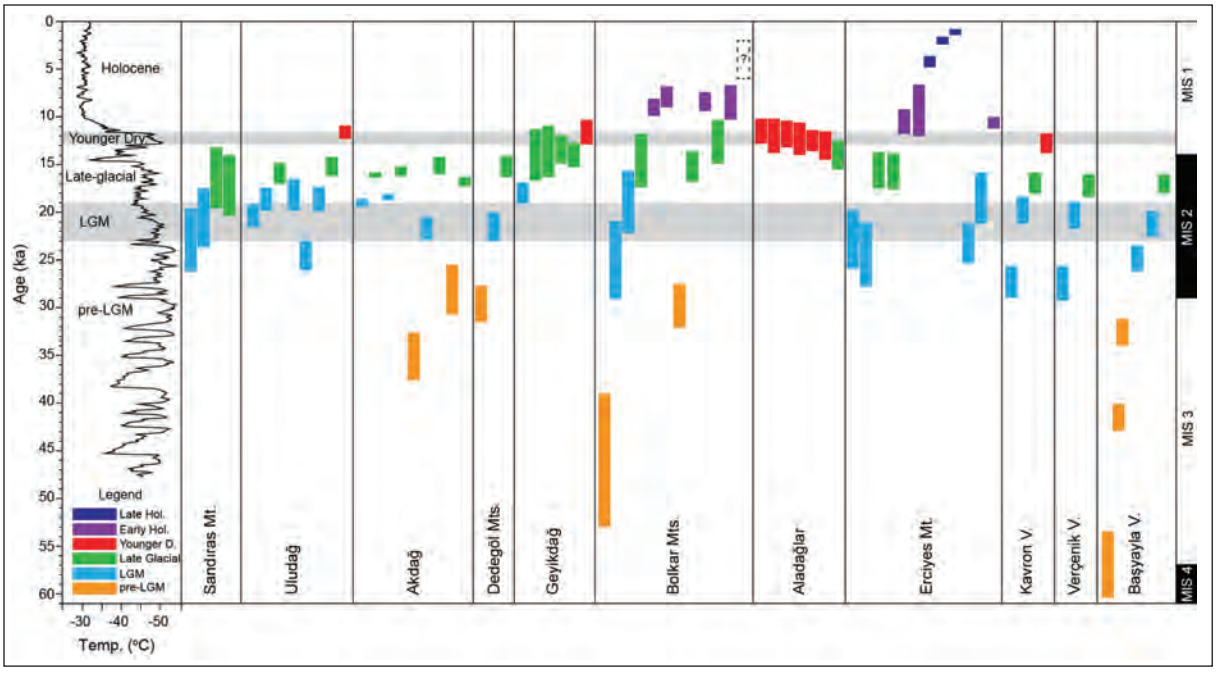

Figure 7- Correlation of glacial chronology from cosmogenic dating of mountains in Turkey. Temperatures from Greenland GISP 2 ice cores on the left (Alley, 2000), MIS series on the right. Colour coded lines give the moraine age intervals from original publications. For details see the original publications given in table 2. Horizontal grey lines show time intervals for global-LGM (Last Glacial Maximum) (19-23 ka) (Mix et al., 2001) and the Younger Dryas (11.7-12.9 ka) (Broecker et al., 2010) (Adapted from Sarıkaya and Çiner, 2015).

period was the beginning of the retreat of glaciers in Turkey. Later glaciers began to decrease in size and sometimes remained stable producing Late Glacial moraines (about 16 ka). Though shorter than the LGM and Late Glacial, in the Younger Dryas (around 12 ka) glacial advances occurred in some regions. Early Holocene glaciation developed in an extraordinary manner in the interior regions of Turkey around 8.5 ka. Lastly the precursor to current glaciers in the Late Holocene (1-4 ka) and Little Ice Age advances covered much smaller areas than paleo-glaciations and were only effective in certain regions. This paper will discuss some implications of these chronological results.

5.1. Why Are Glaciation Signs not Observed Everywhere Before The LGM?

The glacial advance in Turkey's mountains began before the global LGM. For example, the moraines in Kuruova Valley on Akdağ were dated to 35.1 ± 2.5 ka. In the upper parts of Kuruova Valley, moraines protected since before the LGM to the present have been dated to 28.1 ± 2.6 ka. The protected high topographic location of these moraines prevented their destruction by more intense glacial advances that developed in later periods.

However, in the Western Taurus on Mount Dedegöl the glacial advance was determined to have occurred 29.6 ± 1.9 ka ago (Zahno et al., 2009). Similarly in the Bolkar Mountains, a glacial advance has been revealed before the LGM (Çiner and Sarıkaya, 2015). In the Karagöl and Alagöl Valleys, the ground moraines and ground-lateral moraines were dated to 46.0 ± 7.0 ka and 29.8 ± 2.3 ka, respectively.

The glacial ages in other regions before the LGM are in agreement. Generally younger moraines are more common than old moraines from pre-LGM. This shows that the pre-LGM moraines were covered by larger and more effective LGM glaciers or were completely removed and destroyed in many areas. In all regions only four mountains were observed to have traces of glaciation from pre-LGM (Figure 7). The lack of frequent glacial traces from pre-LGM in Turkey can be explained by a broader and stronger glaciation (LGM glaciation) that developed in a later period.

Table 2- List of regions with cosmogenic age control for the Late Pleistocene. Statistics from cosmogenic samples according to isotopes, sample types and ages are given.

#	Mountain Name	Isotope	Number of samples (n=363)	Used samples (n=315)	Outliers (n=48)	Glacial ages (n=315)*	Sample types (n=363)	Source
1	Sandıras Mt.	^{36}Cl	12	10	2	LGM=6, LG=4	12 moraine blocks	Sarıkaya et al. (2008)
2	Uludağ	^{10}Be/^{26}Al	30	23	7	LGM=5, LG=12, YD=6	23 moraine blocks, 7 bedrock	Zahno et al. (2010)
2	Uludağ	^{10}Be	42	40	2	LGM=23, LG=17	41 moraine blocks, 1 bedrock	Akçar et al. (2014)
4	Akdağ	^{36}Cl	41	33	8	pre-LGM=8, LGM=18, LG=7	41 moraine blocks	Sarıkaya et al. (2014)
8	Dedegöl Mts.	^{10}Be/^{26}Al	25	19	6	pre-LGM=4, LGM=3, LG=12	6 bedrock, 19 moraine blocks	Zahno et al. (2009)
9	Geyikdağ	^{36}Cl	34	28	6	LGM=9, LG=16, YD=3	34 moraine blocks	Çiner et al. (2015)
11	Bolkar Mts.	^{36}Cl	30	22	8	pre-LGM=5, LGM=2, LG=5, EH=10	1 bedrock, 3 outwash boulder, 26 moraine blocks	Çiner and Sarıkaya (2015)
12	Aladağlar	^{36}Cl	22	22	0	LG=3, YD=19	2 bedrock, 20 moraine blocks	Zreda et al. (2011)
13	Erciyes Mt.	^{36}Cl	44	37	7	LGM=11, LG=6, EH=12, LH=8	5 outwash boulder, 39 moraine blocks	Sarıkaya et al. (2009)
19a	Kavron V.	^{10}Be	22	21	1	LGM=14, LG=5, YD=2	18 moraine blocks, 4 bedrock	Akçar et al. (2007)
19b	Verçenik V.	^{10}Be	19	19	0	LGM=4, LG=12, YD=3	10 moraine blocks, 9 bedrock	Akçar et al. (2008)
19c	Başyayla V.	^{10}Be/^{26}Al	42	41	1	pre-LGM=11, LGM=20, LG=10	41 moraine blocks, 1 bedrock	Reber et al. (2014)

Table 3- Summary of results of cosmogenic surface dating of mountains in Turkey.

#	Mountain name	Valley	Moraine	Age (ka)	Source
1	Sandıras Mt.	Karţal Lake Valley	LGM	22.9 ± 3.3	Sarıkaya et al. (2008)*
			LGM	20.6 ± 3.1	
		NW Valley	Late Glacial	16.4 ± 3.2	
			Late Glacial	17.2 ± 3.2	
2	Uludağ	Karagöl Valley	LGM	20.4 ± 1.2	Akçar et al. (2014)**
			LGM	18.6 ± 1.2	
			Late Glacial	15.9 ± 1.1	
		Kovuk Valley	LGM	18.1 ± 1.7	Zahno et al. (2010)**
		Ski Valley	LGM	24.6 ± 1.5	Zahno et al. (2010)**
			LGM	18.6 ± 1.3	
			Late Glacial	15.2 ± 1.0	
			Younger Dryas	11.6 ± 0.7	
4	Akdağ	Taşkuzluklu Valley	LGM	19.0 ± 0.4	Sarıkaya et al. (2014)
			Late Glacial	16.1 ± 0.3	
		Karadere Valley	LGM	18.4 ± 0.3	
			Late Glacial	15.7 ± 0.5	
		Lower Kuruova Valley	pre-LGM	35.1 ± 2.5	
			LGM	21.7 ± 1.2	
			Late Glacial	15.1 ± 0.9	
		Upper Kuruova Valley	pre-LGM	28.1 ± 2.6	
			Late Glacial	16.8 ± 0.5	
8	Dedegöl Mts.	Muslu Valley	pre-LGM	29.6 ± 1.9	Zahno et al. (2009)**
			LGM	21.5 ± 1.5	
			Late Glacial	15.2 ± 1.1	
9	Geyikdağ	Namaras Valley	LGM	18.0 ± 1.1	Çiner et al. (2015)
			Late Glacial	14.0 ± 2.7	
			Late Glacial	13.6 ± 2.7	
		Susam Valley	Late Glacial	13.4 ± 1.5	
			Late Glacial	14.0 ± 1.3	
			Younger Dryas	11.6 ± 1.3	
11	Bolkar Mts.	Karagöl Valley	pre-LGM	46.0 ± 7.0	Çiner and Sarıkaya (2015)
			LGM	25.0 ± 4.1	
			LGM	18.9 ± 3.3	
			Late Glacial	14.6 ± 2.8	
			Early Holocene	9.0 ± 0.9	
			Early Holocene	7.9 ± 1.1	
		Alagöl Valley	pre-LGM	29.8 ± 2.3	
			Late Glacial	15.2 ± 1.6	
			Early Holocene	8.4 ± 1.0	
		Elmalı Valley	Late Glacial	12.6 ± 2.3	
			Early Holocene	8.5 ± 1.8	
			?	4.0 ± 2.0	
12	Aladağlar	Hacer Valley	Younger Dryas	11.5 ± 1.3	Zreda et al. (2011)*
			Younger Dryas	12.0 ± 1.8	
			Younger Dryas	11.8 ± 1.4	
			Younger Dryas	12.3 ± 1.7	
			Younger Dryas	12.5 ± 1.1	
			Younger Dryas	13.0 ± 1.5	
			Late Glacial	14.0 ± 1.5	
13	Erciyes Mt.	Aksu Valley	LGM	22.8 ± 3.1	Sarıkaya et al. (2009)*
			LGM	24.4 ± 3.4	
			Late Glacial	15.6 ± 1.9	
			Late Glacial	15.7 ± 1.9	
			Early Holocene	10.5 ± 1.3	
			Early Holocene	9.3 ± 2.7	
			Late Holocene	4.2 ± 0.6	
			Late Holocene	2.0 ± 0.4	
			Late Holocene	1.1 ± 0.3	
		Üçker Valley	LGM	23.2 ± 2.1	
			LGM	18.5 ± 2.7	
			Early Holocene	10.6 ± 0.6	
19	Eastern Blacksea Mts.	19a) Kavron Valley	LGM	27.3 ± 1.7	Akçar et al. (2007)**
			LGM	19.8 ± 1.4	
			Late Glacial	17.0 ± 1.1	
			Younger Dryas	12.8 ± 1.0	
		19b) andrçenik Valley	LGM	27.5 ± 1.8	Akçar et al. (2008)**
			LGM	20.3 ± 1.4	
			Late Glacial	17.2 ± 1.2	
		19c) Başyayla Valley	pre-LGM	57.0 ± 3.5	Reber et al. (2014)
			pre-LGM	41.5 ± 1.4	
			pre-LGM	32.6 ± 1.3	
			LGM	24.8 ± 1.4	
			LGM	21.2 ± 1.3	
			Late Glacial	17.0 ± 1.0	

* Re-calculated by Sarıkaya and Çiner (2015)

** Re-calculated by Reber et al. (2014)

5.2. Widespread LGM Glaciation In Anatolia

Latest research has shown that there is good age control on local LGM glaciation on nearly all of Turkey's mountains. The chronologies we have to date show that LGM glaciation developed in Kartal Lake Valley on Mount Sandıras (17.5-26 ka; Sarıkaya et al., 2008), on Akdağ (18-23 ka; Sarıkaya et al., 2014), in Muslu Valley on Mount Dedegöl (20-23 ka; Zahno et al., 2009), in Namaras Valley on Geyikdağ (17-19 ka Çiner et al., 2015), in the Bolkar Mountains (16-29 ka; Çiner and Sarıkaya, 2015), on Erciyes Volcano (16-28 ka; Sarıkaya et al., 2009), on Uludağ (24-18 ka; Zahno et al., 2010) and in the Kaçkar Mountains (27-21 ka; Akçar et al., 2014; Reber et al., 2014). In general the LGM glacial advance began before 30 ka (initial stage of MIS 2) and reached its maximum extend before 21.5 ka. As glaciation in this period was more severe, the mountains in Turkey have more common traces of LGM glaciation compared to other periods.

The LGM dates obtained from Turkey are in accordance with LGM moraine ages from other mountains in Eastern Europe (Hughes et al., 2006; Woodward et al., 2008) and the European Alps (Hughes and Woodward, 2008). More, the dates obtained from Turkish mountains are contemporaneous with the lowest sea level during MIS 2 (120-135 m below current sea level) (Martinson et al., 1987; Yokoyama et al., 2000) and also with the ice cores, marine isotope series and global LGM (19-23 ka).

5.3. Glacial Retreat In The Late Glacial

After the LGM the glacial retreat on some mountains in Turkey continued until 18.5 ka. In this period glaciers in some regions retreated by a certain amount or remained stable for several thousands of years. Though there is little information on the amount of retreat, small valley or cirque glaciers continued to exist in upper valley systems. The duration of retreat of larger ice masses naturally took longer. For example, during the LGM on Geyikdağ the glaciers on the piedmont advanced as far as Namaras Valley. These glaciers remained under thick debris cover, slowing their reaction to changing climatic conditions (Çiner et al., 2015). As a result the glaciers on Geyikdağ began to fully retreat much later than the LGM (18.0 ± 1.0 ka). Similar situations existed for glaciers on Mount Dedegöl (14-16 ka), Akdağ (14-17 ka) and Mount Sandıras (13-20 ka).

Further east the Late Glacial retreat on Erciyes Volcano began before 14-17.5 ka. In the northeast Black Sea Mountains, in the Kavron, Verçenik and Başyayla Valleys, the Late Glacial retreat began slightly earlier compared to the mountains in the Eastern Mediterranean. This situation may be related to early warming of the Black Sea region. For example in Kavron Valley, Late Glacial moraines were deposited before 17.0 ± 1.1 ka. In Verçenik and Başyayla Valleys, dates have been determined before 17.2 ± 1.2 ka and 17.0 ± 1.0 ka, respectively.

In general the Late Glacial period on Turkey's mountains can be dated to before 16 ka. However, compared to previous advances, these glaciers were much smaller and less widely distributed.

5.4. Sparse Glaciation In The Younger Dryas

The glacial advance in the Younger Dryas (11.7-12.9 ka) (Broecker et al., 2010) has a scattered distribution in Turkey. This may be due to a lack of sufficient age data or it may be due to Younger Dryas glaciers truly developing in a sparse manner in Turkey. Glacial traces in this period are only encountered in 4 regions (Figure 7). The glacier in Hacer Valley in the east of Aladağlar is a good example of Younger Dryas glaciation. The age of a series of moraines in this 15 km valley on the mountain has been determined as the Late Pleistocene-Holocene transition (Zreda et al., 2011). However, the results of new calculations by us using current ^{36}Cl production rates have revealed that the ages of these moraines may be Younger Dryas (Sarıkaya and Çiner, 2015).

There are indications of the Younger Dryas advance on Geyikdağ. However Younger Dryas advance on other mountains in Turkey, especially in the southwest of Turkey, appears to be insufficient. The reason for the scattered distribution of Younger Dryas advance in the Taurus Mountains may be related to special climatic effects in the region.

In northeast Anatolia, Akçar et al. (2008) consider that glacial advance in the Kavron Valley very likely occurred during the Younger Dryas (12.8 ± 1.0 ka). In fact, there are traces of similar Younger Dryas glacial chronology in the mountains of southern Europe (Hughes et al., 2006). Similar Younger Dryas glacial chronologies are found in the French Maritime Alps (Federici et al., 2008), the Apennine Mountains in Italy (Giraudi and Frezzotti, 1997) and in Montenegro (Hughes and Woodward, 2008).

5.5. Rare Holocene Glaciation

In Turkey after the Late Glacial and Younger Dryas, glaciers became even smaller. When the Holocene started, glaciers were only observed on high mountains like the Bolkar Mountains and Erciyes. Samples obtained by Çiner and Sarıkaya (2015) from erratic blocks found on limestone and lateral moraines in the Karagöl Valley in the Bolkar Mountains have confirmed the presence of moraines deposited in the Early Holocene period. During the cold period in the Early Holocene on Erciyes Volcano a small glacial advance period may have been experienced. The presence of glaciers has been determined in Aksu Valley at 10.5 ± 1.3 ka and in Üçker Valley at 10.6 ± 0.6 ka on Erciyes.

Similarly in Eastern Europe, Hughes and Woodward (2008) obtained dates of 10.6 ± 0.2 ka and 9.6 ± 0.8 ka on the Durimitor Massif in Montenegro from a U-series of secondary calcite from two well-described terminal moraines. However, it is not clear yet whether the glaciers in southern and central Anatolia, along with those in Montenegro, are part of a broad region of Early Holocene glaciation or represent a limited area.

Late Holocene and Little Ice Age moraines have only been determined on Erciyes Volcano. Samples from this region have been dated to around 1-4 ka before present. In the Aksu Valley on Erciyes Volcano, terminal moraines at 3000 m elevation have been dated to 4.2 ± 0.6 ka and 1.1 ± 0.3 ka.

Similarly, Late Holocene glaciers have been described in the Apennine Mountains in Italy (around 4.3 ± 0.1 ka, 2.8 ± 0.03 ka and 1.3 ± 0.03 ka) (Giraudi, 2004), in the French Maritime Alps (Federici and Stefanini, 2001) and high cirques on Mount Olympus in Greece (Smith et al., 1997). However, fresh-looking moraines near the peaks of Erciyes Volcano and Aladağlar may possibly belong to the Little Ice Age. Late Holocene and Little Ice Age moraines have been observed also in the Kaçkar Mountains (Akçar et al., 2007; 2008).

5.6. Recent Glaciers

Though small, recent glaciers are observed on several mountains in Turkey. The most important of these is the ice cap on Mount Ağrı. The other important region of southeast Anatolia houses nearly 2/3 of active glaciers in the country (Çiner, 2003; 2004). The presence of glaciers reaching several hundreds of meter is known from the Kaçkar and Taurus Mountains. However, these glaciers are retreating and are on the brink of disappearing. The majority are covered with debris. In the Aladağlar (Gürgen et al., 2010) and Bolkar Mountains (Erinç, 1952; Çalışkan et al., 2014) several glaciers covered with debris have been determined. Before Turkey's current glaciers completely disappear emphasis should be given to scientific studies to record them.

6. Paleoclimate Interpretations From Glacial Studies

To identify climatic conditions in glacial periods, the temperature and precipitation conditions that form glaciers can be modeled. Using physical glacier models (Zweck and Huybrechts, 2005; Sarıkaya, 2009), climatic modeling of the LGM and later has been completed for a variety of regions in Turkey. For these models to work, it is necessary to know the current precipitation and temperature values and topographic conditions in the regions. Changing current climatic conditions by certain amounts creates glaciers in glacial valleys. Comparing the glacial distribution obtained from model results with glacial distribution limits observed in the field (elevations of terminal moraines, lateral moraines, etc.), an attempt could be made to estimate the climatic conditions forming glaciers.

In this context, glacier modeling analysis completed by our group (Sarıkaya et al., 2009; 2014) has shown that the largest glaciers in the LGM formed in an environment 8-11ºC colder than today (Sarıkaya et al., 2014). The precipitation conditions in that period were calculated to be 1.5-2 times higher than today for the southwestern Anatolian coast (Mount Sandıras and Akdağ), while central and interior regions (for example Erciyes) were similar to today and northern sections (Kaçkar Mountains) had 30% less precipitation than today (Sarıkaya et al., 2014).

Other proxy data obtained from Turkey and surroundings show that in the LGM the Eastern Mediterranean really had a colder climate than today (Roberts, 1983; Bar-Matthews et al., 1999; Robinson, 2006). However, there is still continuing controversy on the humidity levels in the region (Prentice et al., 1992; Rowe et al., 2012). This situation is due to inconsistency between paleobotanic evidence in the LGM indicating semi-arid climatic values with geomorphologic evidence (Roberts, 1983) belonging to relatively high paleo-lake levels. Additionally, the

almost complete disappearance of woody trees (Van Zeist et al., 1975) in the glacial period supports the opinion of a widespread cold and steppe-like climate (Elenga et al., 2000). Different scenarios have been proposed to explain these inconsistencies (Tzedakis, 2007).

Contrary to paleo-precipitation in the west of the Mediterranean region being greater than today, in the interior, north and east, the formation of drier conditions show that the paleoclimate of Turkey had a different situation in terms of atmospheric conditions, compared to today. The strengthened Siberian High, especially due to the effect of large glacial areas in higher latitudes (Scandinavian Ice Shield) and other atmospheric causes, broadening in area over the central sections of Anatolia would have prevented the frontal systems originating over the Atlantic Ocean from penetrating as far as the north and east regions of Anatolia. The subtropical high pressure belt of these systems retreating to the south, together with a more southerly trajectory (above the Mediterranean), would have moved toward the east. This situation would have caused frontal systems with more humidity and energy to meet with the cold Siberian High over the southwest of Anatolia and caused more severe precipitation episodes in this region. In cold periods jet streams and polar fronts moving to more southerly latitudes would have increased the efficacy of polar winds in Turkey and as precipitation increased in coastal areas as a result of this, the interior would have experienced less humid conditions. It is known from a variety of studies that expected climatic changes in the future (in the form of global warming) will have the opposite effect to the theory described above. Global warming will move the subtropical belt northward, thus frontal systems bringing rain to Turkey will follow a more northerly trajectory and precipitation will reduce in the south but increase in the north (Giorgi and Lionello, 2008; Şen et al., 2011; Yücel et al., 2014, Önol et al., 2014).

Model data from the Late Glacial period show that in this period mountains in the interior of Anatolia (like Erciyes) had a climate colder by about 4.5 °C to 6.4ºC and 50% more humidity (Sarıkaya et al., 2009). In the Early Holocene meanwhile, it is thought that the climate was between 2.1 °C and 4.9 °C colder than today and had up to twice the precipitation (Sarıkaya et al., 2009). In the Late Holocene period although precipitation conditions may have approached current levels, the temperature is still assumed to be between 2.4 °C and 3 °C colder than today.

Quantitative data obtained from glacial chronology over the last 15 years has changed our view of glaciers in Turkey and allowed the possibility to make very important and reliable interpretations about paleoclimate. In Turkey, with more studies than in many European countries in terms of quantitative data, the next step is to interpret the data on a broader regional scale. A better understanding of paleoclimatic conditions is a sine qua non condition to allow us to be more prepared for climate changes which are currently occurring and likely to cause significant problems in the future.

7. Conclusions

- A clear geochronology of Late Pleistocene glaciation in Turkish Mountains has been revealed by cosmogenic surface exposure dating published in recent years.
- Late Pleistocene glaciers were observed in 27 regions in Turkey. Of these to date only 9 have had cosmogenic surface exposure dating studies completed.
- Determining the lower limit for ice accumulation for Late Pleistocene glaciers, the LGM permanent snow line varied from 2000-2900 m elevation on mountains in Turkey. Due to continental conditions in central and western sections, the permanent snow line increased.
- Glaciers on mountains in Turkey generally developed in north-facing cirques or on plateaus at the peaks of mountains (generally above 3000 m). The majority of glaciers were a few km long in the form of valley or piedmont glaciers flowing to lower elevations of 1900-2200 m.
- The oldest paleo-glacial advance known developed much before the LGM in global terms (71 ka, at the beginning of MIS 4) and ended at the end of MIS 3 (29-35 ka).
- Later (29 ka) the glaciers advanced again and during MIS 2 (21.5-18.5 ka) and reached their maximum extent. In many regions these precise results, define the local-LGM for Turkish mountains and are in accordance with the global LGM.
- After the LGM, the glaciers began to retreat. This retreat commenced several thousand years later in some regions. The Late Glacial period, dated to around 16 ka, deposited moraines on many mountains in Turkey.

- The glaciers of the Younger Dryas (12 ka) have a scattered spatial distribution. As shown by undated moraines, the reason for this may be different reactions of Younger Dryas glaciers in different regions.
- The extraordinary Early Holocene glaciation (8.5 ka) is only observed in the central regions of Turkey.
- The Late Holocene (1-4 ka) and Little Ice Age glaciations, predecessors of current glaciers, rarely developed near the peaks of high-elevation mountains.
- Glacier models reveal that the LGM climate was 8-11ºC colder than today, with 1.5-2 times higher precipitation in southwest Anatolia, with similar precipitation to today in central and interior sections while the northeast was 30% drier than today.
- Glacier models belonging to later periods show that in the Late Glacial the climate was 4.5-6.4ºC colder than today and 50% more humid; in the Early Holocene it was 2.1-4.9ºC colder with twice as much precipitation while in the Late Holocene precipitation conditions approached those of today however temperature was still 2.4-3ºC colder than today.

Acknowledgements

The data and information in this paper were produced with the support of TÜBİTAK projects numbered 101Y002, 107Y069, 110Y300, 112Y139 and 114Y548 and National Science Foundation (USA) project INT-0115298. We thank all our colleagues and students who have participated and shared their experiences over a variety of field studies related to ^{36}Cl cosmogenic surface exposure dating and glacial chronology we have organized since 2001. We are grateful to Dr. Marek Zreda (Arizona University, USA) who initiated the application of cosmogenic surface dating methods to glacial deposits in Turkey. We wish to thank Dr. Naki Akçar, from Bern University (Switzerland) who has completed similar age datings in different regions and whose data and opinions we benefitted from, and reviewer Dr. Mustafa Karabıyıkoğlu.

Received: 26.03.2015
Accepted: 02.06.2015
Published: December 2015

References

Ainsworth, W.F. 1842. Travels and researches in Asia Minor, Mesopotamia. Chaldea and Armenia. J.W. Parker, London.

Akçar, N., Yavuz, V., Ivy-Ochs, S., Kubik, P.W., Vardar, M., Schluchter, C. 2007. Paleoglacial records from Kavron Valley, NE Turkey: Field and cosmogenic exposure dating evidence. *Quaternary International*, 164-165, 170-183.

Akçar, N., Yavuz, V., Ivy-Ochs, S., Kubik, P.W., Vardar, M., Schluchter, C. 2008. A case for a downwasting mountain glacier during Termination I, Vercenik valley, northeastern Turkey. J. of *Quaternary Science*, 23 (3), 273-285.

Akçar, N., Yavuz, V., Ivy-Ochs, S., Reber, R., Kubik, P.W., Zahno, C., Schlüchter, C. 2014. Glacier response to the change in atmospheric circulation in the eastern Mediterranean during the Last Glacial Maximum. Quaternary Geochronology, 19, 27-41.

Akçar, N., Vural, Y., Serdar, Y., Ivy-Ochs, S., Kubik, P., Schlüchter, C. 2015. Extensive glaciations in the Anatolian Mountains during the Last Glacial Maximum. In: Quaternary Glaciation in the Mediterranean, Editors: Philip D. Hughes and Jamie C. Woodward, Geological Society of London, Special Publications, 433.

Alley, R.B. 2000. The Younger Dryas cold interval as viewed from central Greenland. *Quaternary Science Reviews*, 19, 213-226.

Alley, R.B., Meese, D.A., Shuman, A.J., Gow, A.J., Taylor, K.C., Grootes, P.M., White, J.W.C., Ram, M., Waddington, E.D., Mayewski, P.A., Zielinski, G.A. 1993. Abrupt accumulation increase at the Younger Dryas termination in the GISP2 ice core. *Nature*, 362, 527-529.

Ardos, M. 1977. Barla Dağı civarının jeomorfolojisi ve Barla Dağı'nda Pleistosen glasyasyonu. *İstanbul Üniversitesi Coğrafya Enstitüsü Dergisi*, 20-21, 151-168.

Atalay, I.,1987. *Türkiye Jeomorfolojisine Giriş*. Ege Üniversitesi Yayınları, no:9, İzmir.

Bar-Matthews, M., Ayalon, A., Kaufman, A., Wasserburg, G.J. 1999. The Eastern Mediterranean paleoclimate as a reflection of regional events: Soreq cave, Israel. *Earth and Planetary Science Letters* 166, 85-95.

Bayrakdar, C. 2012. Akdağ Kütlesi'nde (Batı Toroslar) Karstlaşma-Buzul İlişkisinin Jeomorfolojik Analizi. İstanbul Üniversitesi, Coğrafya Bölümü, Doktora Tezi, p. 201.

Bilgin, T. 1972. Munzur Dağları Doğu Kısmının Glasiyal ve Periglasiyal Morfolojisi. İstanbul Üniversitesi Yayınları No:1757, Coğrafya Enstitüsü Yayınları No: 69.

Birman, J.H. 1968. Glacial reconnaissance in Turkey. *Geological Society of America Bulletin*, 79, 10091026.

Blumenthal, M.M. 1958. From Mount Ağrı (Ararat) to Mount Kaçkar (in German). *Bergfahrten in nordosta-*

natolsischen Glenzlanden. Die Alpen, 34, 125-137.

Bobek, H. 1940. Recent and Ice time glaciations in central Kurdish high mountains (in German). *Zeitschrift für Gletscherkunde*, 27, (1-2), 50-87.

Broecker, W.S., Denton, G.H., Edwards, R.L., Cheng, H., Alley, R.B., Putnam, A.E. 2010. Putting the Younger Dryas cold event into context. *Quaternary Science Reviews* 29, 1078-1081.

Cerling, T.E., Craig, H. 1994. Geomorphology and in-situ cosmogenic isotopes. *Annual Review of Earth and Planetary Sciences* 22, 273-317.

Cockburn, H.A.P., Summerfield, M.A. 2004. Geomorphological applications of cosmogenic isotope analysis. *Progress in Physical Geography* 28, 1-42.

Çalışkan, O., Gürgen, G., Yılmaz, E., Yeşilyurt, S. 2014. Debris-covered Glaciers During Glacial and Interglacial Periods on the Taurus Mountains (Turkey). *Procedia - Social and Behavioral Sciences*, 120, 716-721.

Çiner, A. 2003. Türkiye'nin güncel buzulları ve Geç Kuvaterner buzul çökelleri. *Türkiye Jeoloji Bülteni*, 46, 1, 55-78.

Çiner, A. 2004. Turkish glaciers and glacial deposits. In: Ehlers, J., Gibbard, P.L. (Eds.), Quaternary Glaciations: Extent and Chronology, Part I: Europe. Amsterdam, *Elsevier*, 419-429.

Çiner, A., Deynoux, M., Çörekçioğlu, E. 1999. Hummocky moraines in the Namaras and Susam valleys, Central Taurids, SW Turkey. *Quaternary Science Reviews*, 18, 4-5, 659-669.

Çiner, A., Sarıkaya, M.A. 2015. Cosmogenic ^{36}Cl Geochronology of Late Quaternary Glaciers on the Bolkar Mountains, South Central Turkey. In: Quaternary Glaciation in the Mediterranean, Editors: Philip D. Hughes and Jamie C. Woodward, *Geological Society of London, Special Publications*, 433, 1-17. http://doi.org/10.1144/SP433.3.

Çiner A., Sarıkaya, M.A., Yıldırım, C. 2015. Piedmont glaciations in the Eastern Mediterranean; insights from cosmogenic ^{36}Cl dating of hummocky moraines in southern Turkey, *Quaternary Science Reviews*, 116. 44-56. doi:/10.1016/j.quascirev.2015.03.017.

Davis, R., Schaeffer, O.A. 1955. Chlorine-36 in nature. Annals of the New York *Academy of Sciences* 62, 107-121.

Doğu, A.F., Somuncu, M., Çiçek, İ., Tuncel, H., Gürgen, G. 1993. Kaçkar Dağı'nda buzul şekilleri, yaylalar ve turizm. *Ankara Üniversitesi Türkiye Coğrafyası Araştırma ve Uygulama Merkezi Dergisi*, 157-183.

Doğu, A.F., Çiçek, İ., Gürgen, G., Tuncel H. 1999. Akdağ'ın jeomorfolojisi ve bunun beşeri faaliyetler üzerindeki etkisi (Fethiye-Muğla). Ankara Üniversitesi *Türkiye Coğrafyası Araştırma ve Uygulama Merkezi Dergisi*, 7, 95-120.

Dunai, T. 2010. Cosmogenic Nuclides Principles, Concepts and Applications in the Earth Surface Sciences. Cambridge Academic Press, 198 pp.

Ege, İ., Tonbul., S. 2005. Soğanlı Dağında Karstlaşma-Buzullaşma İlişkisi. V. Türkiye Kuvaterner Sempozyumu, *İstanbul Teknik Üniversitesi*, 2-5 Haziran 2005, İstanbul,

Elenga, H., Peyron, O., Bonnefille, R., Jolly, D., Cheddadi, R., Guiot, J., Andrieu, V., Bottema, S., Buchet, G., de Beaulieu, J.L., Hamilton, A.C., Maley, J., Marchant, R., Perez-Obiol, R., Reille, M., Riollet, G., Scott, L., Straka, H., Taylor, D., Van Campo, E., Vincens, A., Laarif, F., Jonson, H. 2000. Pollen-based biome reconstruction for southern Europe and Africa 18,000 yr BP. *Journal of Biogeography* 27, 621-634.

Erinç, S. 1944. Glazialmorphologhie Untersuchungen im Nordostanatolischen Randgebirge. *Istanbul University Geography Inst. Pub., Ph.D. dissertation Series*, 1, 56 pp.

Erinç, S. 1949*a*. Past and present glacial forms in Northeast Anatolian mountains (in German). *Geologische Rundschau* 37, 75-83.

Erinç, S. 1949*b*. Uludağ üzerinde glasiyal morfoloji araştırmaları. *Türkiye Coğrafya Dergisi, İstanbul Üniversitesi Yayınları*, 11-12, 79-94.

Erinç, S. 1951. Glasiyal ve postglasiyal safhada Erciyes Glasiyesi. *İstanbul Üniversitesi Coğrafya Enst. Dergisi*, 1 (2), 82-90.

Erinç, S. 1952. Glacial evidences of the climatic variations in Turkey: *Geografiska Annaler*, 34, 89-98.

Erinç, S. 1953. Van'dan Cilo Dağlarına. Türkiye Coğrafya Bülteni, *Ankara Üniversitesi Yayınları*, 3-4, 84-106.

Erinç, S. 1955. Honaz Dağında periglasyal şekiller (Güneybatı Toroslar). *İstanbul Üniversitesi Coğrafya Enstitüsü Dergisi*, 185-187.

Erinç, S. 1957. Honaz ve Bozdağ'da buzul izleri hakkında. *Türkiye Coğrafya Bülteni*, 8, 106-107.

Federici, P.R., Stefanini, M.C. 2001. Evidences and chronology of the Little Ice Age in the Argentera Massif Italian Maritime Alps. *Zeitschrift für Gletscherkunde und Glazialgeologie* 37, 35-48.

Federici, P.R., Granger, D.E., Pappalardo, M., Ribolini, A., Spagnolo, M., Cyr, A.J. 2008. Exposure age dating and Equilibrium Line Altitude reconstruction of an Egesen moraine in the Maritime Alps, Italy. *Boreas* 37, 245-253.

Gibbard, P.L., Cohen, K.M. 2008. Global chronostratigraphical correlation table for the last 2.7 million year, *Episodes* 31, 242-247.

Giorgi, F., Lionello, P. 2008. Climate change projections for the Mediterranean region. *Glob. Planet. Chang.*, 63:90-104

Giruadi, C. 2004. The Apennine glaciations in Italy. In: Ehlers, J. and Gibbard, P.L., (Eds.), Quaternary glaciations-extent and chronology. *Part I: Europe, Amsterdam: Elsevier*, 215-223.

Giraudi, C., Frezzotti, M. 1997. Late Pleistocene glacial events in the Central Appenines, Italy. *Quaternary Research*, 48, 280 - 290.

Gosse, J.C., Phillips, F.M. 2001. Terrestrial in situ cosmogenic nuclides: theory and application. *Quaternary Science Reviews* 20, 1475-1560.

Gürgen, G. 2003. Çapan Dağları Kuzeyinin (Rize) Glasyal Morfolojisi. *Gazi Eğitim Fakültesi Dergisi* 23, 159-175.

Gürgen, G., Yeşilyurt, S. 2012. Karçal Dağı Buzulları (Artvin). *Coğrafi Bilimler Dergisi* 10, 91-104.

Gürgen, G., Çalışkan, O., Yılmaz, E., Yeşilyurt, S. 2010. Yedigöller platosu ve Emli vadisinde (Aladağlar) döküntü örtülü buzullar, *E-Journal of New World Sciences Academy*, NEWSSA, (www.newwsa.com), 5, 98-116.

Hughes, P.D., Woodward, J.C., Gibbard, P.L. 2006. Late Pleistocene glaciers and climate in the Mediterranean region. *Global and Planetary Change*, 46, 83 - 98.

Hughes, P.D., Woodward, J.C. 2008. Timing of glaciation in the Mediterranean mountains during the last cold stage. Journal of Quaternary Science, 23 (6-7), 575-588.

IPCC, 2013. Climate Change 2013: Synthesis Report, In: team, C.w., Pachauri, R.K., Reisinger, A. (Eds.), Contribution of working groups I, II and III to the fourth assessment report of the Intergovernmental Panel on Climate Change, Geneva, Switzerland.

İzbırak, R. 1951. Cilo Dağı ve Hakkari ile Van Gölü çevrelerinde coğrafya araştırmaları, *Ankara Üniversitesi Dil Tarih Coğrafya Fakültesi yayınları*, 67 (4), 149.

Kesici, O. 2005. Küresel ısınma çerçevesinde Süphan ve Cilo dağlarında buzul morfolojisi araştırmaları. TÜBİTAK proje raporu No: 101Y131.

Kurter, A. 1991. Glaciers of Middle East and Africa - Glaciers of Turkey, In: Williams, R.S., Ferrigno, J.G. (eds), Satellite Image Atlas of the World. USGS Professional Paper, 1386-G-1, 1-30.

Louis, H.L. 1944. Evidence for Pleistocene glaciation in Anatolia (in German). *Geologische Rundschau*, 34 (7-8), 447-481.

Marrero, S. 2012. Calibration of Cosmogenic Chlorine-36, Earth, Environmental Science. *New Mexico Institute of Mining and Technology*, Socorro, New Mexico, 365.

Martinson, D. G., Pisias, N.G., Hays, J.D., Imbrie, J., Moore, T.C., Shackleton, N.J. 1987. Age, dating and orbital theory of the Ice Ages: development of a high resolution 0–300,000 year chronostratigraphy. *Quaternary Researc*h, 27, 1-29.

Maunsell, F.R. 1901. Central. The Geographical Journal 18 (2), 121-141.

Mayewski, P.A., Rohling, E.E., Stager, J.C., Karlén, W., Maasch, K.A., Meeker, L.D., Meyerson, E.A., Gasse, F., van Kreveld, S., Holmgren, K., Lee-Thorp, J., Rosqvist, G., Rack, F., Staubwasser, M., Schneider, R.R., Steig, E.J. 2004. Holocene climate variability. *Quaternary Research,* 62, 243-255.

Messerli, B. 1967. Die eiszeitliche und die gegenwartige Vergletscherung in Mittelmeerraum. *Geographica Helvetica*, 22, 105-228.

Mix, A., Bard, A., Schneider, R. 2001. Environmental processes of the ice age, land, oceans, glaciers (EPILOG). *Quaternary Science Reviews*, 20, 627-657.

Monod, O. 1977. Geological research in the Western Taurides south of Beyşehir, Turkey (in French). *Unpublished thesis, University of Paris*, 442 p.

Oerlemans, J. 2001. Glaciers and Climate Change. Sweets and Zeitlinger BV, Lisse.

Önol, B., Bozkurt, D., Turuncoglu, U., Sen, O.L., Dalfes, H.N. 2014, Evaluation of the 21st century RCM simulations driven by multiple GCMs over the Eastern Mediterranean-Black Sea region. *Climate Dynamics*, 42:1949-1965, DOI 10.1007/s00382-013-1966-7.

Palgrave, W.G. 1872. Vestiges of the glacial period in northeastern Anatolia. *Nature*, 5, 444-445.

Prentice, I.C., Guiot, J., Harrison, S.P. 1992. Mediterranean vegetation, lake levels and paleoclimate at the Last Glacial Maximum. *Nature* 360, 658-660.

Reber, R., Akçar, N., Yesilyurt, S., Yavuz, V., Tikhomirov, D., Kubik, P.W., Schlüchter, C. 2014. Glacier advances in northeastern Turkey before and during the global Last Glacial Maximum. *Quaternary Science Reviews*, 101, 177-192.

Roberts, N. 1983. Age, Paleoenvironments and climatic significance of the Late Pleistocene Konya Lake, Turkey. *Quaternary Research,* 19, 154-171.

Robinson, S.A., Black, S., Sellwood, B.W., Valdes, P.J. 2006. A review of palaeoclimates and palaeoenvironments in the Levant and Eastern Mediterranean from 25,000 to 5000 years BP: setting the environmental background for the evolution of human civilisation. *Quaternary Science Reviews,* 25, 1517-1541.

Rose, J. 2007. The use of time units in *Quaternary Science Reviews*, *Quaternary Science Reviews* 26, 1193.

Rowe, P.J., Mason, J.E., Andrews, J.E., Marca, A.D., Thomas, L., Van Calsteren, P., Jex, C.N., Vonhof, H.B., Al-Omari, S. 2012. Speleothem isotopic evidence of winter rainfall variability in northeast Turkey between 77 and 6 ka. *Quaternary Science Reviews,* 45, 60-72.

Sarıkaya, M.A. 2009. Late Quaternary glaciation and paleoclimate of Turkey inferred from cosmogenic ^{36}Cl dating of moraines and glacier modeling. Ph.D. Thesis, *University of Arizona*, Tucson, AZ, USA, 303 pp.

Sarıkaya, M.A. 2012. Recession of the ice cap on Mount Ağrı (Ararat), Turkey, from 1976 to 2011 and its climatic significance. *Journal of Asian Earth Sciences,* 46, 190-194.

Sarıkaya, M.A., Zreda, M., Çiner, A., Zweck, C. 2008. Cold and wet Last Glacial Maximum on Mount Sandı-

ras, SW Turkey, inferred from cosmogenic dating and glacier modeling. *Quaternary Science Reviews*, 27, 7-8, 769-780.

Sarıkaya, M.A., Zreda, M., Çiner, A. 2009. Glaciations and paleoclimate of Mount Erciyes, central Turkey, since the Last Glacial Maximum, inferred from ^{36}Cl cosmogenic dating and glacier modeling. *Quaternary Science Reviews*, 28, 23-24, 2326-2341.

Sarıkaya, M.A., Çiner, A., Zreda, M. 2011. Quaternary glaciations of Turkey, In: Ehlers, J., Gibbard, P.L., Hughes, P.D. (Eds.), Quaternary glaciations-Extent and chronology, A closer Look. *Elsevier*, Amsterdam, 393-403.

Sarıkaya, M.A., Çiner, A., Haybat, H., Zreda, M. 2014. An early advance of glaciers on Mount Akdağ, SW Turkey, before the global Last Glacial Maximum; insights from cosmogenic nuclides and glacier modeling. *Quaternary Science Reviews*, 88, 96-109.

Sarıkaya, M.A., Tekeli, A.E. 2014. Satellite inventory of glaciers in Turkey, In: Global Land Ice Measurements from Space, Kargel, J.S., Leonard, G.J., Bishop, M.P., Kääb, A. and Raup, B. (Eds.), Praxis-Springer (Publisher), Berlin Heidelberg, 876 pp. ISBN: 978-3-540-79817-0. 465-480.

Sarıkaya, M.A., Yıldırım, C., Çiner, A. 2015. Late Quaternary alluvial fans of Emli Valley in the Ecemiş Fault Zone, south central Turkey: Insights from cosmogenic nuclides. *Geomorphology*, 228, 512-525.

Sarıkaya, M.A, Çiner, A. 2015. The Late Quaternary glaciations in the Eastern Mediterranean, In: Quaternary Glaciation in the Mediterranean, Editors: Philip D. Hughes and Jamie C. Woodward, Geological Society of London, Special Publications, 433, http://doi.org/10.1144/SP433.3.

Schimmelpfennig, I., Benedetti, L., Garreta, V., Pik, R., Blard, P.H., Burnard, P., Bourles, D., Finkel, R., Ammon, K., Dunai, T. 2011. Calibration of cosmogenic Cl-36 production rates from Ca and K spallation in lava flows from Mt. Etna (38 degrees N, Italy) and Payun Matru (36 degrees S, Argentina). *Geochimica Et Cosmochimica Acta,* 75, 2611-2632.

Şen, O.L., Ünal, A., Bozkurt, D., Kindap, T. 2011. Temporal Changes in Euphrates and Tigris Discharges and Teleconnections, *Environmental Research Letters*, 6, 024012, doi:10.1088/1748-9326/6/2/024012.

Smith, G.W., Nance, R.D., Genes, A.N. 1997. Quaternary glacial history of Mount Olympus. *Geological Society of America Bulletin*, 109, 809-824.

Tzedakis, P.C. 2007. Seven ambiguities in the Mediterranean palaeoenvironmental narrative. *Quaternary Science Reviews,* 26, 2042-2066.

van Zeist, W., Woldring, H., Stapert, D. 1975. Late Quaternary vegetation and climate of southwestern Turkey. *Palaeohistoria,* 7, 53-143.

Woodward, J.C., Hamlin, R.H.B., Macklin, M.G., Hughes, P.D., Lewin, J. 2008. Pleistocene catchment dynamics in the Mediterranean: glaciation, fluvial geomorphology and the slackwater sediment record. *Geomorphology*, 101 (1-2), 44-67.

Wright, H.E. 1962. Pleistocene glaciation in Kurdistan. *Eiszeitalter und Gegenwart*, 12, 131-164.

Yalçınlar, İ. 1951. Glaciations on the Soğanlı-Kaçkar mountains and Mescid Dağ (in French). *Review of the Geographical Institute of the University of Istanbul* 1-2, 50-55.

Yalçınlar, İ. 1954. On the presence of the Quaternary glacial forms on Honaz Dag-and-Boz Dag (western Turkey) (in French). Compte Rendu Sommaire de la *Société Géologique de France*, 13, 296-298.

Yavaşlı, D.D., Tucker, C.J., Melocik, K.A. 2015. Change in the glacier extent in Turkey during the Landsat Era. *Remote Sensing of Environment,* 163, 32-41.

Yokoyama, Y., Lambeck, K., De Deckker, P.P.J., Fifield, L.K. 2000. Timing of the last glacial maximum from observed sea-level minima. *Nature*, 406, 713-716.

Yücel, İ., Güventürk, A., Sen, O.L. 2014. Climate change impacts on snowmelt runoff for mountainous transboundary basins in eastern Turkey. *International Journal of Climatology*, DOI: 10.1002/joc.3974.

Zahno, C., Akçar, N., Yavuz, V., Kubik, P. W., Schlüchter, C. 2009. Surface exposure dating of Late Pleistocene glaciations at the Dedegöl Mountains (Lake Beysehir, SW Turkey). *Journal of Quaternary Science*, 24, 1016-1028.

Zahno, C., Akçar, N., Yavuz, V., Kubik, P. W., Schlüchter, C. 2010. Chronology of Late Pleistocene glacier variations at the Uludağ Mountain, NW Turkey. *Quaternary Science Reviews*, 29, 1173-1187.

Zreda, M.G., Phillips, F.M., Elmore, D., Kubik, P.W., Sharma, P., Dorn, R.I. 1991. Cosmogenic Cl-36 production rates in terrestrial rocks. *Earth and Planetary Science Letters,* 105, 94-109.

Zreda, M.G., Phillips, F.M. 2000. Cosmogenic nuclide buildup in surficial materials, Quaternary Geochronology: Methods and Applications. AGU, Washington, DC, pp. 61-76.

Zreda, M., Çiner, A., Sarıkaya, M.A., Zweck, C., Bayarı, S. 2011. Remarkably extensive early Holocene glaciation in Turkey. *Geology*, 39, 11, 1051-1054. doi: 10.1130/G32097.1.

Zweck, C., Huybrechts, P. 2005. Modeling of the northern hemisphere ice sheets during the last glacial cycle and glaciological sensitivity. *Journal of Geophysical Research*-Atmospheres 110.

Bull. Min. Res. Exp. (2015) 151: 129-147

Bulletin of the
Mineral Research and Exploration

http://bulletin.mta.gov.tr

LATE PERMIAN UNCONFORMITY AROUND ANKARA AND NEW AGE DATA ON THE BASEMENT ROCKS, ANKARA, TURKEY

Mustafa SEVİN[a]*, Mustafa DÖNMEZ[a], Gökhan ATICI[a], A. Hande ESATOĞLU VEKLİ[a], Ender SARIFAKIOĞLU[a], Serap ARIKAN[a] and Havva SOYCAN[a]

[a] *Maden Tetkik ve Arama Genel Müdürlüğü, Jeoloji Etütleri Dairesi, G Blok, 06520, Balgat, Ankara*

Keywords:
Sakarya Zone, Lower Karakaya Complex, Early Carboniferous-Permian, Autochthonous carbonate basement, Late Permian unconformity

ABSTRACT

At southwest of Gölbaşı (Ankara) there are two different sequences in tectonic contact. The one at the bottom with low-degree metamorphism is represented by phyllite, metabasite, crystallized limestone, schist and quartz porphyry veins. Above them are early Carboniferous-late Permian neritic and pelagic carbonates which are unconformably overlain by late Permian clastics and carbonates. Samples collected from neritic carbonates yielded early Carboniferous (Visian-Serpuhovian) to middle Carboniferous (Bashkirian-Moskovian) ages. These carbonates of shallow facies character are overlain by radiolarite-bearing pelagic deposits of middle Carboniferous-Permian age. Fossils from the upper most neritic carbonates gave Kubergandian-Murgabian age. This Permo-Carboniferous sequence is unconformably overlain by a sequence consisting of clastics and carbonates. Basal conglomerates and sandstones contain abundant quartz and fewer amounts of carbonated-cemented metamorphic rock fragments and they change to medium-thick bedded dolomitic limestone and limestones to the top. The age of these carbonates of shallow marine character is found Murgabian-Dorashamian. It is suggested that late Paleozoic carbonate basement was deposited in a neritic environment during early-middle Carboniferous, in a pelagic environment during middle Carboniferous-Permian and again in a neritic environment during Kubergandian-Murgabian. Following a deformation stage, it was accreted onto the Variscan basement at north and carbonate deposition took place as a result of late Permian transgression and finally some of exotic blocks within the upper Karakaya Complex were derived from this basement.

1. Introduction

In the Sakarya Zone which is one of the main tectonic units in Turkey (Figure 1a), high-degree metamorphics of pre-Liassic basement which consist of gneiss, amphibolite and marbles were affected by the Variscan orogeny and cut by Devonian and/or early Carboniferous granitoids. These rocks are known as Kazdağ massif and Çamlık granitoids in the Biga peninsula (Okay et al., 1991), Söğüt metamorphics and Sarıcakaya granitoid in Eskişehir (Göncüoğlu et al., 2000; Ustaömer et al., 2012), metamorphic Serveçay group (Aydın et al., 1995; Kozur et al., 2000) and Deliktaş and Sivrikaya granites (Nzegge et al., 2006) in central Pontides and Pulur massif and Gümüşhane granitoids in the eastern Pontides (Keskin et al., 1989; Topuz et al., 2010).

One of the most controversial issues as regards the Sakarya Zone is the geologic evolution of the Karakaya Complex of the pre-Liassic basement (Tekeli, 1981). The term of "Karakaya Complex" was first used by Bingöl (1968) for low-degree metamorphic rocks in northwest Turkey and then by Tekeli (1981) and Şengör (1984) for pre-Jurassic orogenic rocks. Tekeli (1981) described late Paleozoic-early Mesozoic rocks around Ankara and Tokat as the accretionary complex and differentiated

* *Corresponding author: Mustafa Sevin, mustafa.sevin@mta.gov.tr*

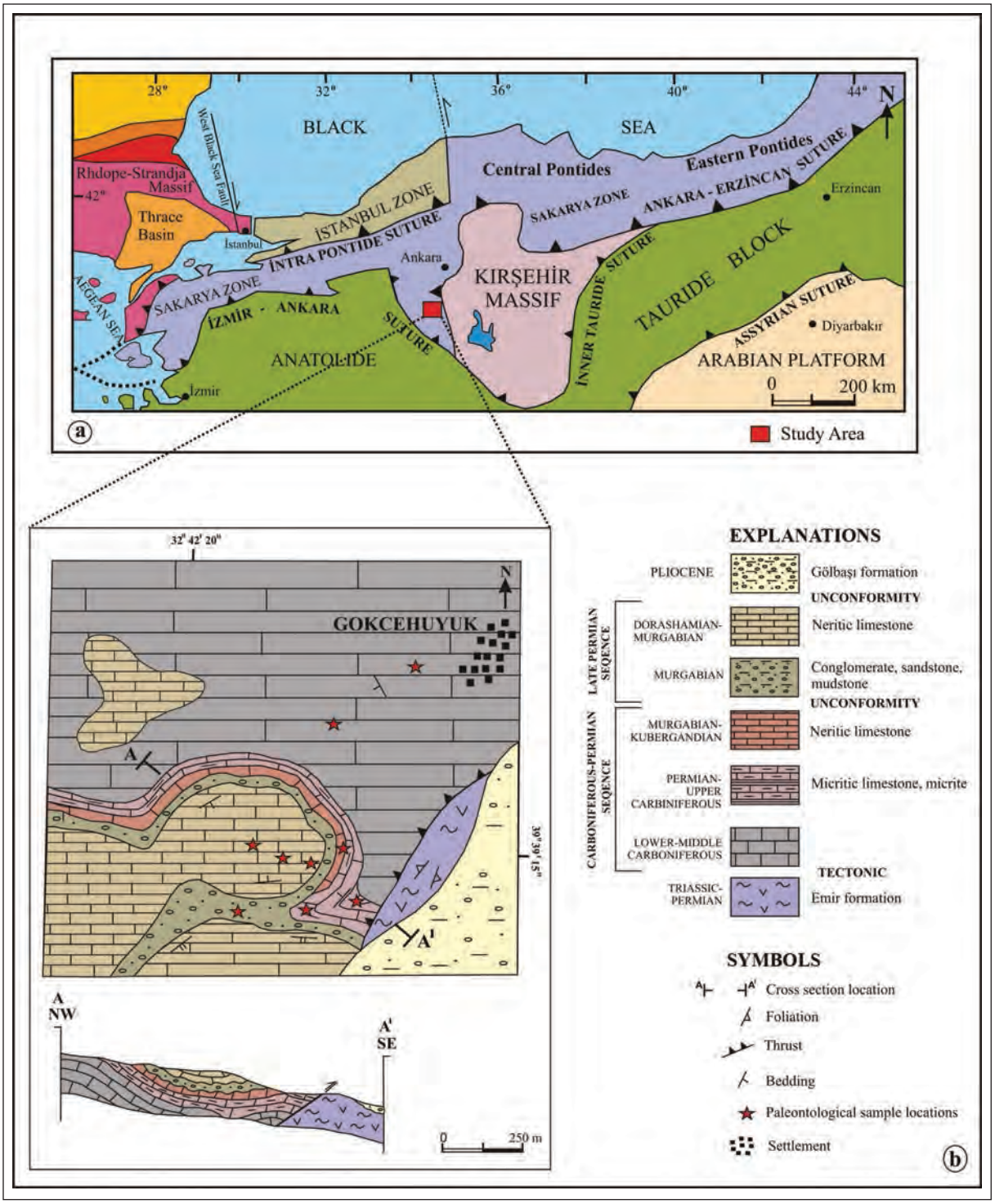

Figure 1- a) Map showing tectonic units of Turkey (Okay and Tüysüz, 1999), b) Geology map and cross section of the study area.

them as lower metamorphic series and upper blocky series. A similar differentiation was made by Okay and Göncüoğlu (2004). They differentiated extremely deformed low-degree metamorphites consisting of phyllite, metabasite and marbles at the bottom as the Lower Karakaya Complex and deformed slightly metamorphosed clastics and volcano-sedimentary rocks which also contain late Paleozoic limestone blocks as the Upper Karakaya Complex.

The Lower Karakaya Complex was studied under different names; from west to east, they are Çavdartepe formation in the Kozak region (Akyürek and Soysal, 1983), Nilüfer unit in the Biga region (Okay et al., 1991), İznik metamorphites in the Armutlu peninsula (Göncüoğlu et al., 1987), Tepeköy metamorphites at north of Eskişehir (Göncüoğlu et al., 2000), Yenişehir metamorphic group in the Yenişehir-İnegöl area (Genç and Yılmaz, 1995), Emir formation around Ankara (Akyürek et al., 1984), Gümüşoluğu and Kunduz formations in central Pontides (Yılmaz and Tüysüz, 1984), the lover Yeşilırmak group (Tüysüz, 1996; Yılmaz et al., 1997) and Turhal metamorphites (Yılmaz and Yılmaz, 2004) in the Tokat massif and Ağvanis group (Okay, 1984) and Hossa Group (Okay, 1996) in the further east. Limited fossil and radiometric data are available for these low-degree metamorphites. For this unit, fossil ages were determined; middle Triassic for conodonts from the Kozak Mountain (Kaya and Mostler, 1992), Early Triassic for conodonts around Bursa and Early Triassic for foraminifera around Ankara (Akyürek et al., 1979).

Metamorphism ages of the Lower Karakaya Complex were found as late Triassic around Bandırma and Eskişehir (Okay and Monie, 1997; Okay et al., 2002) and early Permian in the Pulur massif at east (Topuz et al., 2004*b*) (Rb-Sr for hornblende mineral and 264±3.4 Ma with $^{40}Ar/^{39}Ar$ method on albite-epidote-amphibolite sample).

Ophiolitic rocks are found as tectonic slices within these different metamorphic units at the basement which include Tozlu formation (metaophiolite) in the Biga peninsula (Duru et al., 2012), Tozman metaophiolite around Eskişehir (Göncüoğlu et al., 2000), metaophiolite around Ankara (Akyürek et al., 1984), Boğazköy metaophiolite around Bilecik (Genç and Yılmaz, 1995), Turhal metaophiolite in Tokat (Yılmaz et al., 1997) and metaultramafites within the Pulur Complex (Dokuz et al., 2015).

Arguments are not just on lithology and stratigraphy of this metamorphic basement but also on its paleogeographic setting, age and type of environment as well as relations with overlying Mesozoic units and the origin of exotic blocks within the Triassic rocks.

Although it is generally accepted that autochthonous Permo-Carboniferous carbonates do not overlie the Sakarya Zone and rather they occur as blocks within the Triassic Upper Karakaya Complex, there are also different opinions that these carbonates are derived from Gondwana (Altıner et al., 2000; Göncüoğlu et al., 2000) or Eurasia (Okay et al., 1996; Leven and Okay 1996).

Regarding the relation between basement and cover rocks, Göncüoğlu et al. (1987) suggested that early Permian limestones discordantly set on the basement. According to Saner (1977), micaschists around the Yenişehir-Geyve area gradually change to metasandstone and Permian recrystallized limestones. Akdeniz (1988) states that in the Bayburt region a Permo-Carboniferous sequence composing of clastics and carbonates to the top unconformably covers crystalline basement. Okuyucu and Göncüoğlu (2010) propounded that early Permian lagoon type carbonate rocks in south of Geyve discordantly set on the Variscan metamorphic basement. According to Yılmaz et al. (1997), around Amasya there is a late Permian unconformity above the metamorphic basement consisting of metaquartzite, phyllites and schists. The clastics of Triassic Upper Karakaya Complex contain Silurian (Alp, 1972), Early Devonian (Çapkınoğlu and Bektaş, 1999) and Permo-Carboniferous (Akyürek et al., 1982/1984) neritic limestone blocks and late Paleozoic (Devonian-Carboniferous-Permian) radiolarite and pelagic limestone blocks as well (Okay and Mostler, 1994; Okay et al., 2011).

Setting of Paleotethys is another controversial issue (Stocklin, 1977; Şengör, 1979) that is basement of Sakarya Zone is a part of Gondwana or Eurasia. It was suggested by Yılmaz (1981), Şengör and Yılmaz (1981), Şengör et al. (1984), Koçyiğit (1987), Genç and Yılmaz (1995) and Göncüoğlu et al. (2000) that Paleotethys was southerly subducted into northern margin of Gondwana and a Permo-Triassic basin was opened in the backarc region. According to Adamia et al. (1977), Tekeli (1981), Şengün (1990), Pickett et al. (1995), Pickett and Robertson (1996) and Okay (2000), Paleotethys was subducted into southern margin of Eurasia at north. The subduction of

Paleozoic-Mesozoic oceans at north and south of the Sakarya Zone during Mesozoic are another alternative (Stampfli and Borel, 2002). Two different models were proposed for occurrence of Karakaya Complex. The first is the rift model of Bingöl et al. (1975), Yılmaz (1981), Şengör and Yılmaz (1981), Şengör et al. (1984), Koçyiğit (1987), Genç and Yılmaz (1995) and Göncüoğlu et al. (2000) and another is subduction/accretion model by Tekeli (1981), Pickett et al. (1995), Pickett and Robertson (1996) and Okay (2000).

2. Stratigraphy

The studied area is located in the Sakarya Zone in the vicinity of Gökçehöyük village at southwest of Gölbaşı along the Ankara-Haymana road (Figure 1b). In the region there are two different units that are tectonically related and covered by Pliocene deposits. The Emir formation at the bottom (Figure 2; Akyürek et al., 1984) consists of extremely deformed rocks that were metamorphosed under green schist facies conditions (Lover Karakaya Complex). Above this unit is early Carboniferous-Permian neritic and pelagic carbonate sequence (Figure 2) which is unconformably overlain by Murgabian-Dorashamian sequence consisting of terrestrial clastics which change to shallow marine dolomitic limestones and limestones (Figures 1b, 2 and 3). During Lutetian basement and overlying late Permian cover were southerly transported over the İzmir-Ankara ophiolitic rocks (Figure 4a, b). MT profiles obtained from the ongoing MTA Crust Project also support this consideration (MTA 2015 project presentations).

The late Paleozoic sequence and late Permian cover under investigation are not given formation names and the unit was named as Carboniferous-

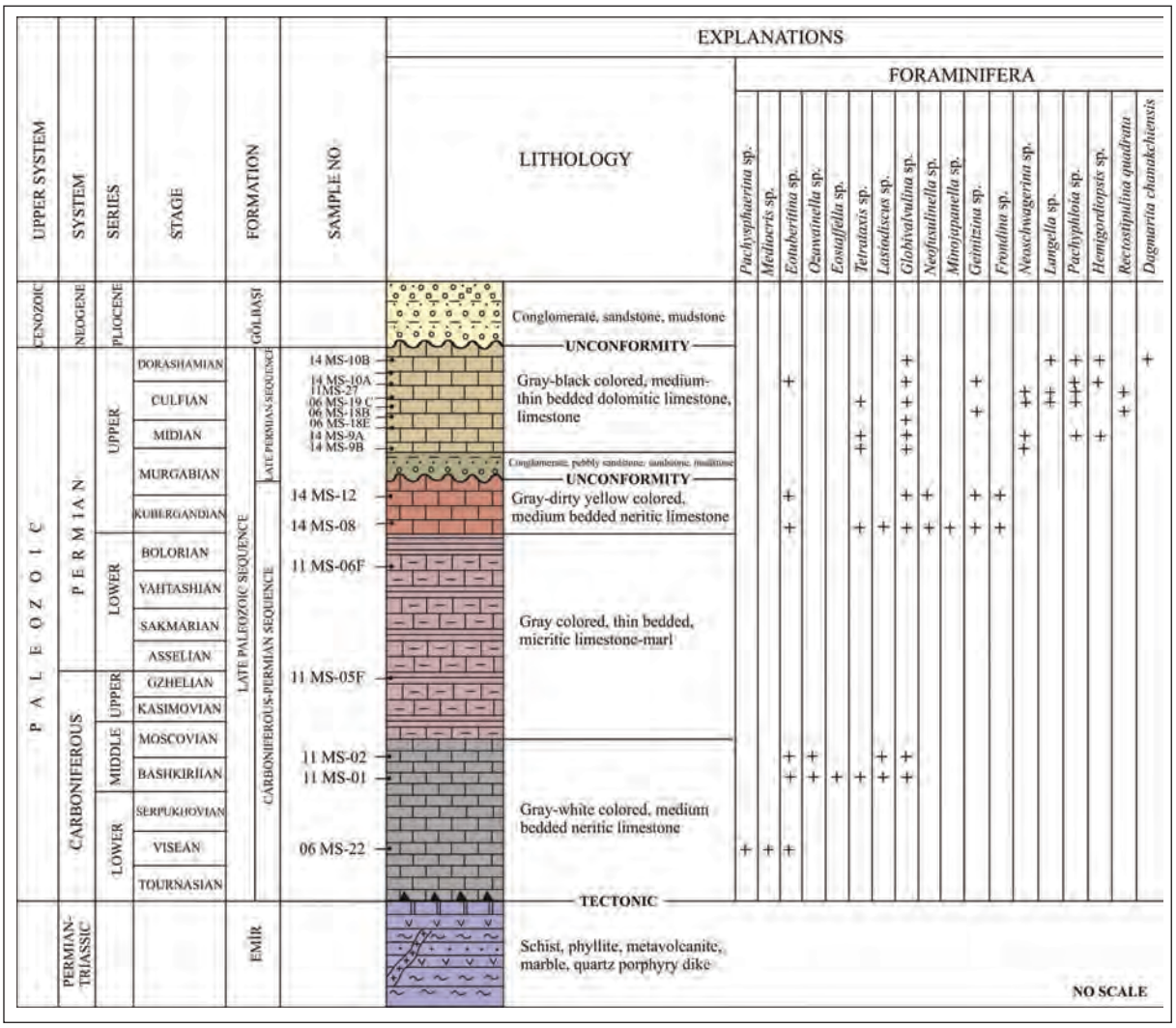

Figure 2- Generalized columnar section of the study area and foraminifera distribution of late Paleozoic sequence.

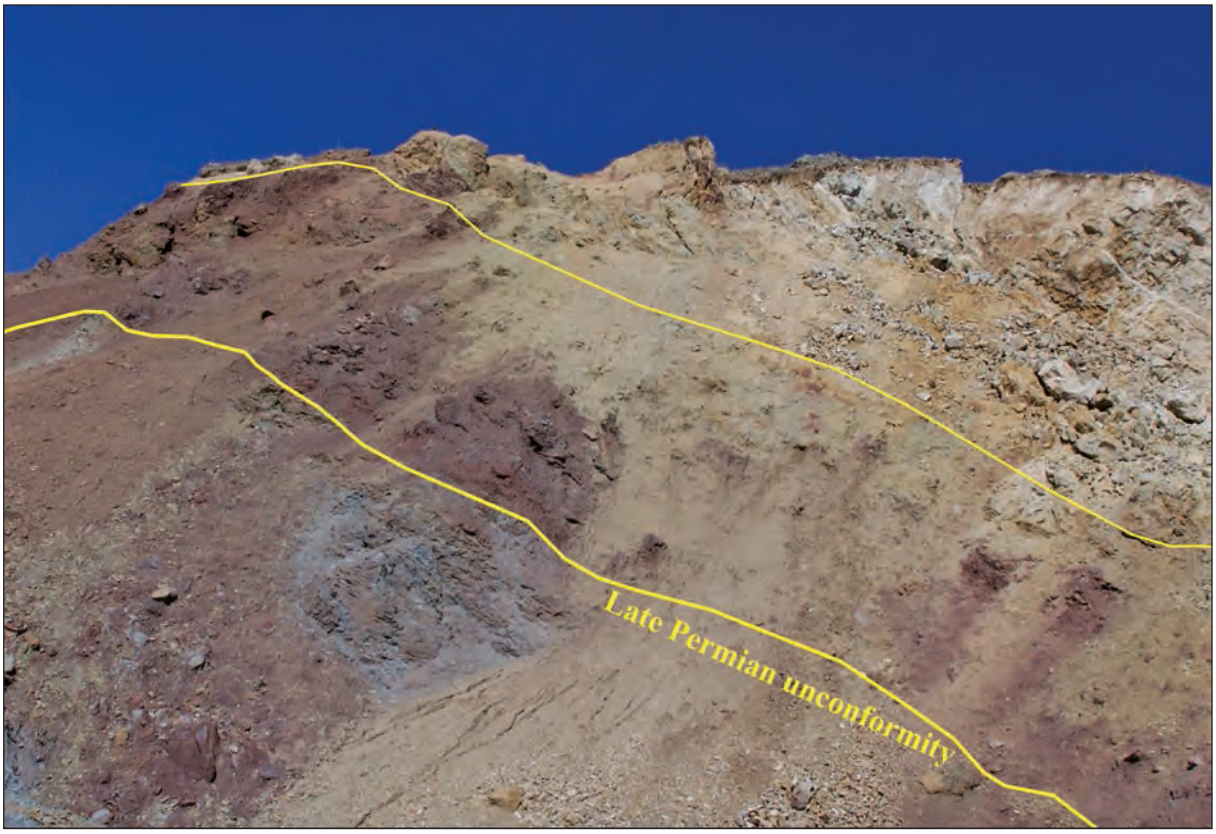

Figure 3- Late Permian unconformity; below is gray pelagic micritic limestone-marl alternation, above is reddish late Permian terrestrial clastics and beige dolomitic limestone-limestone (X: 36476488, Y: 4390205).

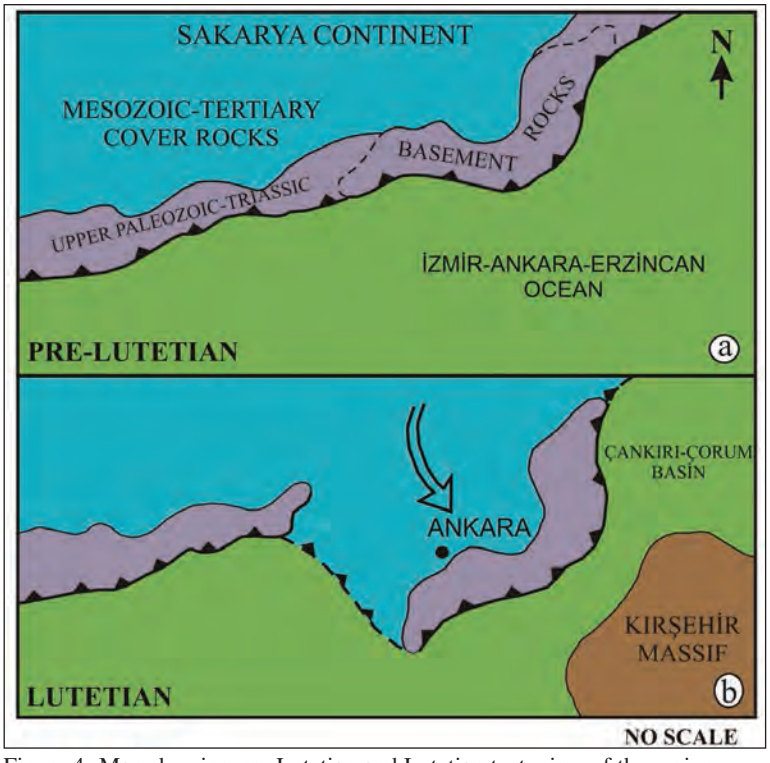

Figure 4- Map showing pre-Lutetian and Lutetian tectonism of the region.

Permian sequence and late Permian sequence. The Carboniferous-Permian carbonate sequence and unconformably overlying late Permian clastics and carbonates along the Sakarya Zone were first described in the present study.

2.1. Carboniferous-Permian sequence

Carbonates of this sequence which are in tectonic contact with underlying Emir formation are represented at the bottom by gray-white colored, thick bedded, fractured, partly crystallized neritic limestones and to the top by gray colored, thin bedded, deformed pelagic micritic limestone-marl alternation and gray colored, medium-thick bedded, neritic limestones with abundant calcite veins (Figure 2).

In samples collected from gray colored thick bedded basal limestones following fossils were determined from bottom to the top (Figure 5): *Bradyina* sp., *Pachysphaerina* sp., *Eotuberitina* sp., *Tuberitina* sp., *Mediocris* sp., *Koktjubina?* sp., *Biseriella?* sp. indicating early Carboniferous (Visian-Serpuhovian) age; *Ozawainella* sp., *Eostaffella* sp., *Tetrataxis* sp., *Lasiodiscus* sp., *Globivalvulina* sp., *Eotuberitina* sp. indicating middle Carboniferous (Bashkirian-Moskovian) and *Ozawainella* sp., *Lasiodiscus* sp., *Eotuberitina* sp., *Globivalvulina* sp., *Beresella* sp. (Figure 2, Plate I) indicating middle Carboniferous (Bashkirian-Moskovian) (TMMOB JMO, 2004).

Two samples taken from radiolarian-bearing pelagic micritic limestone (Figure 6) above the early-middle Carboniferous carbonates yield middle Carboniferous-Permian time based on radiolarite assemblage of Follicullidae Ormiston and Babcock, Albaillellidae Deflandre families.

Topmost neritic limestones that contain benthic fossils (Figure 2) yield Kubergandian-Murgabian age based on *Neofusulinella* sp., *Minojapanella* sp., *Rauserella* sp., *Parafusulina*? sp., *Kahlerina* sp., *Frondina* sp., *Geinitzina* sp., *Globivalvulina* sp.,

Figure 5- Gray colored, thick bedded early-middle Carboniferous neritic carbonates (X: 36476578, Y: 4390577).

Figure 6- Middle Carboniferous-Permian radiolarian-bearing micritic limestone-marl alternation (X: 36476400, Y: 4390180).

Hemigordius sp., *Tetrataxis* sp., *Climacammina* sp., *Lasiodiscus* sp., *Eotuberitina* sp., *Girvanella* sp., *Gymnocodium* sp., *Mizzia* sp., *Tubiphytes* sp. (Figure 2, Plate I).

Carboniferous neritic limestones in close vicinity to the study area appear to be blocks within the Triassic Elmadağ formation (Akyürek et al., 1980/1982) and Devecidağ Complex (Özcan et al., 1980); however, middle Carboniferous-Permian pelagic deposits are not mentioned in any of previous studies.

2.2. Late Permian sequence

In the Bilecik-Geyve region clastics and overlying carbonates that unconformably overlie the Carboniferous-Permian sequence are named by Saner (1977) and Eroskay (1965) as Cambazkaya formation and Derbent limestone, respectively, however the basement of sequence is thought to be transitional. In the study area, clastics are thick bedded, grayish, reddish and bluish in color and composed of conglomerate, pebbly conglomerate, sandstone and mudstone with massive appearance (Figure 7). Conglomerates are in a matrix of clay and carbonate and composed commonly of late Permian (Kubergandian-Murgabian) limestone, quartz-porphyry and lesser amount of metamorphic rock fragments of the Emir formation. Grains are 0.5-10 cm in size, partly rounded and tightly compacted. Overlying sandstones are reddish and bluish colored, thick bedded, quartz-grained and contain no fossil. In thin section, it is composed chiefly of quartz, biotite, muscovite, plagioclase and lesser amount of chlorite, chert, metamorphic and sedimentary rock fragments and opaque minerals. Clay- and carbonate-cemented, sub-rounded, well sorted and iron-oxide coated these rocks are classified as lithic arenite. The clastics are overlain by thick bedded, algae-bearing, black colored macro fossiliferous dolomitic limestone and limestone of tens of meter thickness (Figure 8a, b). Several samples of these carbonate rocks yield late Permian age (Murgabian-Midian) based on fossil assemblage of *Neoschwagerina* sp., *Langella* sp., *Pachyphloia* sp., *Globivalvulina* sp., *Hemigordius* sp., *Dunbarula* sp., *Pseudovermiporella* sp. and late Permian age (Midian) based on *Rectostipulina quadrata* Jenny-Deshusses, *Neoschwagerina* sp., *Charliella* sp., *Paraglobivalvulina* sp., *Baisalina* sp., *Langella* sp., *Climacammina* sp., *Pachyphloia* sp., *Agathammina* sp., *Pseudovermiporella* sp. and late Permian age (Midian-Dorashamian) based on

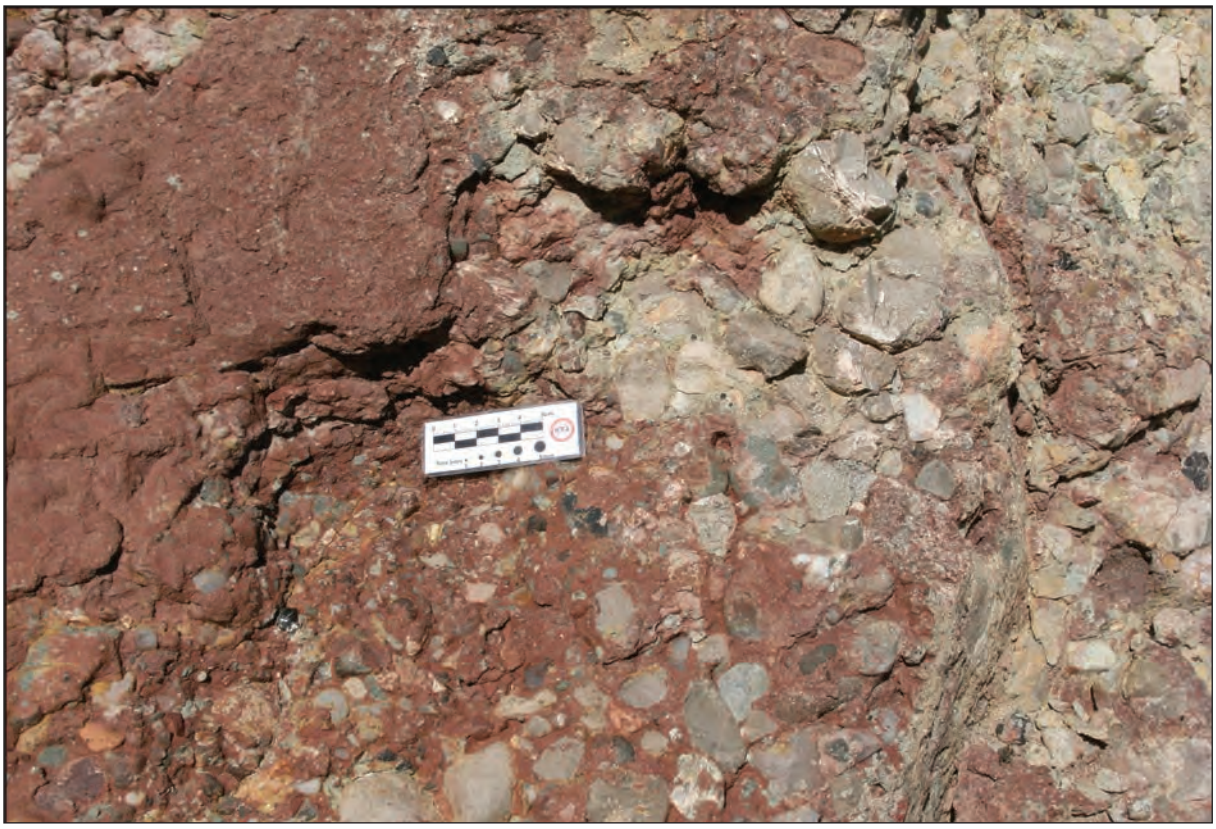

Figure 7- A view of conglomerate, sandstone, mudstone at the base of late Permian. Pebbles are mostly derived from Kubergandian-Murgabian limestone and quartz porphyry dikes (X: 36476381, Y: 4390122).

Dagmarita chanakchiensis Reitlinger, *Eotuberitina* sp., *Kamurana* sp., *Neoendothyra* sp., *Rectostipulina* sp., *Globivalvulia* sp., *Hemigordius* sp., *Reichelina*? sp., *Tubiphytes obscurus* Maslov, *Pseudovermiporella* sp. (Figure 2, Plate I) (TMMOB JMO, 2004).

As mentioned above, late Permian aged unconformable terrestrial-shallow marine (shelf-lagoon) sequence above the Carboniferous-Permian carbonate unit indicates the presence of an autochthonous carbonate sequence on the Sakarya Zone.

Early-middle Carboniferous, middle Carboniferous-Permian and late Permian (Kubergandian-Murgabian) ages obtained are the first paleontological data on autochthonous carbonates under the late Permian unconformity that were not affected by the Variscan orogeny. The middle Carboniferous-Permian radiolarite age from the sequence is also the first pelagic age data for non-blocky carbonates under the late Permian unconformity along the Sakarya Zone.

2.3. Emir Formation

Low-degree metamorphites considered within the Lower Karakaya Complex (Okay and Göncüoğlu, 2004) are described around Ankara by Akyürek et al. (1982, 1984) as clayey, sandy volcanic rocks displaying greenschist metamorphism and named as Emir formation. They are generally gray, greenish brown, grizzly colored, often folded, well foliated and intensely fractured, and therefore, do not show a regular sequence. Folding is distinct in fine-grained and thin bedded parts. Low-degree metamorphites are described as mica-chlorite-quartzschist, sericite-quartzschist, muscovite-quartzschist, graphite schist, phyllite, slate, marble and quartz porphyries cutting them. Early Triassic age data from Emir formation (Akyürek et al., 1982, 1984) which is represented solely by phyllite and graphite schist are problematic since the contact between this formation and Triassic Elmadağ formation is not apparent. Conodonts from similar rocks at south of Bursa (Kozur et al., 2000) and Kozak Mountain (Kaya and Mostler, 1992) yielded early Triassic and middle Triassic ages, respectively. On the contrary, these rocks are

Figure 8- a-b) Murgabian-Dorashamian aged brachiopod- and algae-bearing dark colored dolomitic limestone, limestone (X: 36476545, Y: 4390247).

considered as the base of blocky Triassic (Akyürek et al., 1984; Rojay and Göncüoğlu, 1997) and late Paleozoic basement (Koçyiğit et al., 1991; Altıner and Koçyiğit, 1993).

Emir formation consisting of low-degree metamorphites, starting from the Biga peninsula, can be correlated with epimetamorphites (Bingöl et al., 1975), Nilüfer unit (Okay et al., 1991), Lower Karakaya Complex (Okay and Göncüoğlu, 2004) Yenişehir Metamorphites (Genç and Yılmaz, 1995), Tepeköy Metamorphites (Göncüoğlu et al., 2000), Tokat Metamorphites (Özcan et al., 1980), Ağvanis Group (Okay, 1984). The base of unit is not recognized in the study area and it is in tectonic contact with underlying ophiolite rocks of the İzmir-

Ankara Ocean and overlying Paleozoic carbonate sequence (Figure 2).

3. Discussion

The Sakarya Zone, particularly pre-Liassic basement, has been the focus of a number of studies. The Variscan basement extends along an east-west zone. Okay and Göncüoğlu (2004) described the Karakaya Complex, which is accepted to be pre-Liassic basement, into two parts; Lower Karakaya Complex consisting of deformed, low grade metamorphites and Upper Karakaya Complex composing of clastic, volcaniclastic rocks with blocky Permian limestone. The nature of metamorphism facies and deposition and metamorphism ages of the Lower Karakaya Complex which extends from Biga peninsula to the east of Tokat are still in debate. Since late Paleozoic autochthonous carbonates above the basement are not mentioned until quite recently, Permo-Carboniferous carbonates within the Triassic Upper Karakaya Complex are considered as exotic blocks and based on their fossil fauna they are suggested to belong to Gondwana or Eurasia. In this case, setting and evolution of Paleotethys become crucial.

In the model in which Paleotethys is located at north of Tauride-Anatolides (Göncüoğlu et al., 2000), what are proposed are southerly subduction of ocean beneath Gondwana, occurrence of active continental margin and Permo-Carboniferous carbonate platform on this margin during the Carboniferous and back-arc spreading beginning from Triassic. According to Turhan et al. (2004), Permian autochthon carbonates at south of Geyve resemble both blocky Permian limestones within the Triassic units and Permian carbonates described at Taurus Mountains (Altıner et al., 2000).

However these assertions become conflicting due to following findings:

a) The absence of Variscan events at Tauride-Anatolides,

b) The fact that Triassic deposits with Permo-Carboniferous limestone blocks are found only in the Sakarya Zone in the area from Biga peninsula at west to Tokat at the east and they are contiguous to the İzmir-Ankara Suture,

c) The presence of pelagic deposits (Önder et al., 1987; Bragin et al., 2002) associated with middle Jurassic ophiolites in the Küre ophiolites that are considered as Paleotethys (Yılmaz and Tüysüz, 1984), and Late Triassic fossil ages in the İzmir-Ankara-Erzincan Zone (İAEZ) which is accepted as northern branch of Neotethys and thought to be opened in Liassic (Uğuz et al., 1999; Tekin et al., 2002), the presence of middle-late Triassic volcanic seamounts of OIB character, late Permian metamorphism age in basic rocks of oceanic crust within the Ankara mélange (Sarıfakıoğlu et al., 2011, 2014) and the presence of Devonian aged radiolarian-bearing chert slices (Okay et al., 2011) within the Triassic Orhanlar greywacke that is adjacent to the suture. Okay (2004) also previously stated that Tauride-Anatolide block and Sakarya Zone that comprises the southern margin of Pontides did not amalgamate until Tertiary.

Tekeli (1981), Pickett et al. (1995) and Okay (2000) who suggest northerly subduction of Paleotethys under the Sakarya continent and describe the Lower Karakaya Complex as a subduction accretionary complex of late Paleozoic-Triassic age. With a similar approach, Kozur (1999) proposes Triassic back-arc basin formation that was opened as a result of northerly subduction of Paleotethys beneath the Sakarya continent.

The pre-Liassic basement of the Sakarya Zone from Biga peninsula to the Eastern Black Sea is composed of metamorphic, magmatic, ophiolite and carbonate rocks of different age. This basement which was affected by the Variscan orogeny from west to eastern Black Sea is known as Kazdağ massif in the Biga peninsula, Söğüt Metamorphites in the central Sakarya region and Pulur Metamorphites at the east. As an autochthon late Paleozoic carbonate sequence above such basement, Demirözü Permo-Carboniferous in the Pulur region (Akdeniz, 1988), late Permian in the central Sakarya region (Saner, 1977) and early-late Permian (Turhan et al., 2004; Okuyucu et al., 2010) shallow marine clastics and carbonates in Geyve are mentioned. Within the Upper Karakaya Complex, exotic blocks of neritic limestones of Carboniferous age are exposed around Tokat (Özcan et al., 1980), those of Silurian and early Devonian age are in Amasya (Alp, 1972; Çapkınoğlu and Bektaş, 1999) and those of early-middle Carboniferous age are found in Ankara, Bursa and Biga peninsula (Akyürek et al., 1984; Duru et al., 2012; Kanar et al., 2013). The reason why these blocks within Triassic deposits along the Sakarya Zone are not affected by the Variscan orogeny is not

discussed in detail. We believed that these rocks are derived from Gondwana and before the upper Permian they amalgamated to the Sakarya Zone at north. Okuyucu and Göncüoğlu (2010) also noticed late Carboniferous-middle Permian neritic carbonates unconformably overlying a crystalline complex at south of Geyve. According to these authors, Fusulinid fauna in this time interval are comparable to those in south Urals, central Asia, Caspian basin, Moscow and Carnic Alps and faunal connection with Taurid-Anatolid platform was only possible after the Midian transgression.

There are two different metamorphic units in tectonic contact at pre-Liassic basement along the Sakarya Zone. The period of time these units were amalgamated is one of the main concerns of present study. They comprise Variscan basement at north composing of gneiss, amphibolite and marble cutting by Devonian-Carboniferous granitoids and low-degree metamorphites at south composing of metabasite, phyllite, marble and chert and serpantinite slices. In the central Sakarya region, Göncüoğlu et al. (2000) recognized Söğüt and Tepeköy metamorphites and a Triassic unconformity above them. In the Pulur massif, the Cenci unit representing the Variscan basement at north and the low-degree metamorphic rocks of Doğankavak unit at south are noticeable (Topuz et al., 2004*a, b*). Ar/Ar data on fengite minerals from the Doğankavak unit yielded 260 Ma and these units and tectonic contact among them are unconformably covered with Liassic deposits (Topuz et al., 2004*b*). Keskin et al. (1989) recognized Devonian-early Carboniferous carbonates and ophiolitic rock slices within the low grade metamorphites of the Pulur massif. Data particularly from the Pulur metamorphites support the idea that late Paleozoic carbonate basement in the area is amalgamated to metamorphites at the north before the Permian.

The low-degree late Permian metamorphism (Topuz et al., 2004*b*), the overlying late Permian unconformity (Yılmaz et al., 1997) and the presence of pebbles of these metamorphites at the base of late Permian (this study) are in contradiction with Early Triassic foraminifera age around Ankara (Akyürek et al., 1984) and Triassic conodont ages from Bursa and Kozak Mountain (Kaya and Mostler, 1992; Kozur et al., 2000). On the one hand, different metamorphic character of these metamorphites, their late Permian (Topuz et al., 2004b) and late Triassic metamorphism ages (Ar/Ar ages of 205-203 Ma, fengite and amphibole from eclogite: Okay and Monie, 1997; metabasites: Okay et al., 2002), geochemistry of metabasites (ocean island/plateau, Okay, 2000; Yalınız and Göncüoğlu, 2002) and the presence of Devonian, Carboniferous and Permian pelagic blocks within the Triassic units can only be explained by active continental margin character of southern Sakarya Zone during the Permo-Triassic.

As a result of this study it is proposed that Silurian-Permian neritic carbonates within the blocky Triassic along the southern margin of the Sakarya Zone represent northern margin of the Tauride-Anatolide Block rather than Eurasia and following the middle Carboniferous they were rapidly deepened, rifted and drifted northerly within the Tethyan ocean and became shallower before the upper Permian and then amalgamated to the active margin at south of Sakarya continent (Figure 9a, b, c). Following a terrestrial period in Murgabian, the region together with Carboniferous Variscan basement was transgressively overlain by late Permian neritic limestones (Figure 9d). During the Triassic period, carbonate and metamorphic exotic blocks must have been transported from rift margins to the basin which was opened on the basement by tectonism (Figure 9e).

According to Adamia et al. (1995), eastern Pontides and Transcaucasus represented the active northern margin of northern Tethys during the Paleozoic-early Cenozoic. Similarly, Okay (2011) also states that upper tectonic slices (Variscan basement) belongs to the active margin of Eurasia whereas the lower slice (Lower Karakaya Complex) belongs to the Paleotethys and amalgamated to the north during the Permo-Triassic.

New fossil data, metamorphic age and geochemical affinity of volcanics in low grade metamorphics (Lower Karakaya Complex) and similar autochthon-carbonate sequences to be found along the Sakarya Zone will greatly contribute to geodynamic evolution of the region.

4. Results

1) In the Sakarya Zone the presence of an autochthon sequence composing of late Paleozoic neritic and pelagic carbonates was described for the first time. Neritic carbonates in lower parts of the late Paleozoic sequence yielded foraminifera ages of Visian-Serpuhovian (Early Carboniferous), Bashkirian- Moskovian (middle Carboniferous),

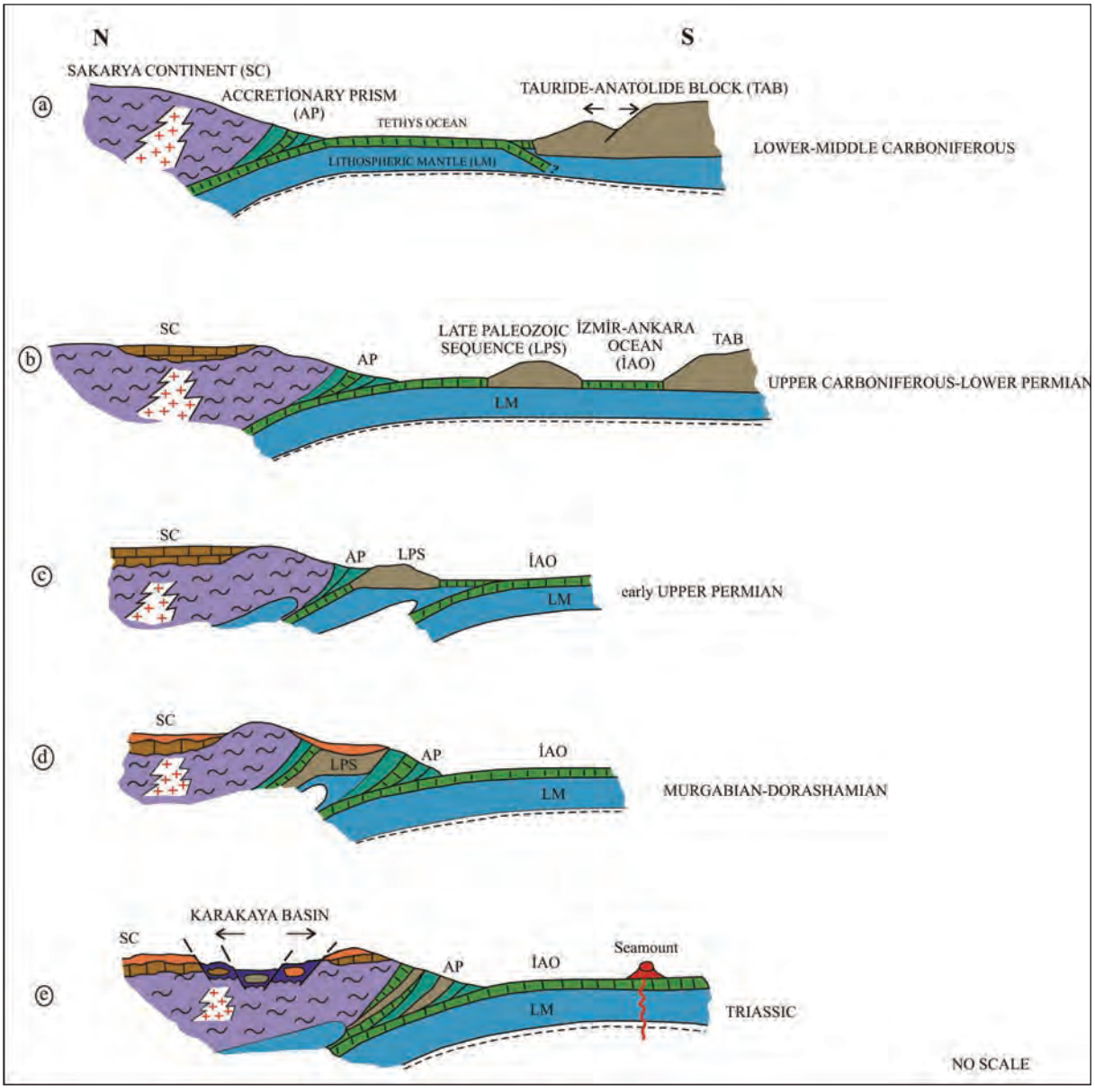

Figure 9- Schematic cross sections showing geologic evolution of the region during the early Carboniferous-Triassic interval.

radiolarites from pelagic micritic limestones comprising the upper parts yielded middle Carboniferous-Permian age and neritic carbonates topmost gave Kubergandian-Murgabian age.

2) Late Carboniferous-early Permian interval in the area is represented by pelagic deposits while carbonates on the Variscan basement along the Sakarya Zone are entirely represented by neritic carbonates.

3) In the Ankara region late Permian unconformity was recognized for the first time. The sequence unconformably overlying the basement rocks is composed of conglomerate, quartzitic sandstone, dolomitic limestones and limestone. Fossils collected from carbonates yielded Murgabian, Midian and Midian-Dorashamian stages of late Permian.

4) The presence of fossiliferous late Paleozoic carbonates indicates that basement was not affected by the Variscan orogeny that is observed along the Sakarya Zone.

5) The presence of middle Carboniferous-Permian

radiolarian-bearing pelagic carbonates within the basement rocks might show that the neritic environment was rapidly deepened and rifted.

6) The presence of rock fragments from the late Paleozoic basement and Emir formation within the late Permian conglomerates necessitates their amalgamation before the late Permian. This might indicate that Emir Formation was formed as early as Permian which is previously accepted as lower Triassic.

7) The presence of late Permian rocks of the Sakarya Zone above the Variscan basement and late Paleozoic sequence explained in this article might imply that fossiliferous late Paleozoic sequence northerly amalgamated to Eurasia margin before the late Permian and the late Paleozoic exotic blocks which are reported to occur as blocks within the Triassic units were derived from this basement which is believed to be originated from Gondwana.

8) The late Paleozoic carbonate basement, late Permian cover and the Paleozoic ophiolites among the tectonic units reported in the literature should be included to pre-Liassic basement of the Sakarya Zone.

9) As a result of Lutetian deformation, the late Permian cover and its basement have a tectonic setting above the İzmir-Ankara oceanic units at the south.

Acknowledgement

This study was conducted in the frame of field studies around Ankara during the "Project of Preparation of 1/1000.000 scaled Turkish Geological Maps" by the General Directorate of Mineral Research and Exploration (MTA). Petrographic descriptions were made by Dr. Nihal Görmüş from MAT Department of Mineral Research and Exploration. Dr. Neşat Konak, Dr. Fuat Uğuz, Dr. Erkan Ekmekçi, Assoc. Prof. Dr. Huriye Demircan and Geological Engineer Şükrü Pehlivan are acknowledged for comments that improved the manuscript.

Received: 28.01.2015
Accepted: 30.06.2015
Published: December 2015

References

Adamia, S.A., Lordkipanidze, M.B., Zakariadze, G.S. 1977. Evolution of an active continental margin as exeplified by the Alpine history of the Caucasus. *Tectonophysics* 40, 183-189.

Adamia, S.A., Bayraktutan, S., Lordkipanidze, M. 1995. Structural Correlation and Phanerozoik Evolution of the Caucasus-Eastern Pontides. Erler, A., Ercan, T., Bingöl, E., Örçen, S. (Ed). *Proceeding of an international semposium on the Geology of the Black Sea Region*, September 7-11, Ankara, Turkey, *General Directorate of Mineral Research and Exploration and Chamber of Geological Engineers*, Ankara, Turkey, 69-75.

Alp, D. 1972. Amasya yöresinin jeolojisi (Geology of the Amasya Region). *İstanbul Üniversitesi Fen Fakültesi Monografileri* 22.

Akdeniz, N. 1988. Permian and Carboniferous of Demirözü and their significance in the regional structure. *Geological Bulletin of Turkey* 3, 71-80.

Akyürek, B., Bilginer, E., Dağer, Z., Sunu, O. 1979. Hacılar (K. Çubuk-Ankara) bölgesinde Alt Triyas'ın varlığı. *Türkiye Jeoloji Kurumu Bülteni 22,2, Ankara*.

Akyürek, B., Bilginer, E., Çatal, E., Dağer, Z., Soysal, Y., Sunu, O. 1980. Eldivan-Şabanözü (Çankırı) ve Hasayaz-Çandır (Kalecik-Ankara) dolaylarının jeolojisi. *Maden Tetkik ve Arama Enstitüsü* Rapor No: 6741, Ankara (unpublished).

Akyürek, B., Bilginer, E., Akbaş, E., Hepşen, N., Pehlivan, Ş., Sunu, O., Soysal, Y., Dağer, Z., Çatal, E., Sözeri, B., Yıldırım, H., Hakyemez, Y. 1982. Ankara-Elmadağ-Kalecik dolayının jeolojisi. *Maden Tetkik ve Arama Genel Müdürlüğü* Rapor No: 7298, Ankara (unpublished).

Akyürek, B., Soysal, Y. 1983. Biga yarımadası güneyinin (Savaştepe-Kırkağaç-Bergama-Ayvalık) temel jeoloji özellikleri (Basic geological features of the region south of the Biga Peninsula, Savaştepe-Kırkağaç-Bergama-Ayvalık). *Maden Tetkik ve Arama Dergisi* 95/96, 1-13.

Akyürek, B., Bilginer, E., Akbaş, B., Hepşen, N., Pehlivan, Ş., Sunu, O., Soysal, Y., Dağer, Z., Çatal, E., Sözeri, B., Yıldırım, H., Hakyemez, Y. 1984. Ankara-Elmadağ-Kalecik dolayının temel jeolojik özellikleri (Basic geological features of the Ankara-Elmadağ-Kalecik region). *Türkiye Jeoloji Kurumu Bülteni* 20, 31-46.

Altıner. D., Koçyiğit, A. 1993. Third remark on the geology of the Karakaya basin. An Anisian megablock in northern central Anatolia; micropaleontologic, statigraphic and tectonic implications for the rifting stage of Karakaya basin, Turkey. *Revue de Paleobiologie* 12, 1-17.

Altıner, D., Özkan-Altıner, S., Koçyiğit, A. 2000. Late Permian foraminiferal biofacies belts in Turkey: paleogeographic and tectonic implication. Bozkurt, E.,

Winchester, J.A., Piper, J.A.D. (Ed). Tectonic and Magmatism in Turkey and Surrounding Area. *Geological Society, London*, Special Publication 173, 83-96.

Aydın, M., Demir, O., Özçelik, Y., Terzioğlu, N., Satır, M. 1995. A Geological Revision of İnebolu, Devrekani, Ağlı and Küre Areas: New Observations in Paleotethys-Neotethys Sedimentery Successions. Erler, A., Ercan, T., Bingöl, E., Örçen, S. (Ed). *Proceeding of an international semposium on the Geology of the Black Sea Region*, September 7-11, 1992, Ankara, Turkey, *General Directorate of Mineral Research and Exploration and Chamber of Geological Engineers*, Ankara, 33-38.

Bingöl, E. 1968. Contribution a'l' etüde geologıque de la parti centrale et sud-Est du massif de Kazdağ (Turquie). *These faculty of Science University of Nancy* (France), 189 p (unpublished).

Bingöl, E., Akyürek, B., Korkmazer, B. 1975. Biga yarımadasının jeolojisi ve Karakaya Formasyonunun bazı özellikleri (The geology of the Biga Peninsula and some features of the Karakaya Formation). *Cumhuriyetin 50. Yılı Yerbilimleri Kongresi Tebliğleri, Maden Tetkik ve Arama Enstitüsü* Dergisi, 70-77 (in Turkish with English abstract).

Bragin, N. Y., Tekin, U. K., Özçelik, Y. 2002. Middle Jurassic radiolarians from the Akgöl Formation, central Pontides, northern Turkey. *Neues Jahrbuch für Geologie und Palaontologie, Monatshefte* 2002/10, 609-628.

Çapkınoğlu, Ş., Bektaş, O. 1999. Karakaya Kompleksine ait Karasenir Formasyonu (Amasya) içindeki kireçtaşı olistolitlerinden Erken Devoniyen konodontları. *Maden Tetkik ve Arama Dergisi* 120, 159-170.

Dokuz, A., Uysal, İ., Dilek, Y., Karslı, O., Meisel, T., Kandemir, R. 2015. Geochemisry, Re-Os isotopes and highly sideropile element abundances in the Eastern Pontides (NE Turkey): Multiple episodes of melt extraction-depletion, melt-rock interaction and fertilization of the Rheic Ocean mantle. *Gondwana Research* 27, 2, 612-628.

Duru, M., Pehlivan, Ş., Okay, A.İ., Şentürk, Y., Kar, H. 2012. Biga Yarımadasının Tersiyer öncesi jeolojisi, Biga Yarımadasının genel ve ekonomik jeolojisi. *Maden Tetkik ve Arama Genel Müdürlüğü özel yayın serisi*, No: 28, 7-74 s.

Eroskay, O. 1965. Paşalar Boğazı-Gölpınar sahasının jeolojisi (Geology of Paşalar Boğazı-Gölpınar area). *İstanbul Üniversitesi Fen Fakültesi Mecmuası* B, 135-170.

Genç, Ş.C., Yılmaz, Y. 1995. Evolution of the Triassic continental margin, northwest Anatolia. *Tectonophysics* 243, 193-207.

Göncüoğlu, M.C., Erendil, M., Tekeli, O., Aksay, A., Kuşcu, İ., Ürgün, B. 1987. Geology of the Armutlu Peninsula. *IGCP Project 5, Guide Book. Field Excursion Along W-Anatolia*, 12-18.

Göncüoğlu, M.C., Turhan, N., Şentürk, K., Özcan, A., Uysal, Ş. 2000. A geotraverse across NW Turkey: tectonic units of the central Sakarya region and their tectonic evolution. Bozkurt, E., Winchester, J., Piper, J.A. (Ed). Tectonics and Magmatism in Turkey and the Surrounding Area. *Geological Society of London,* Special Puplication. 173, 139-161.

Kanar, F., Pehlivan, Ş., Kandemir, Ö., Tok, T., Çakır, K. 2013. 1/100.000 Ölçekli Türkiye Jeoloji Haritaları Serisi, *Maden Tetkik ve Arama Genel Müdürlüğü,* Bursa-H22 Paftası, No:192.

Kaya, O., Mostler, H. 1992. A Middle Triassic age for low-grade greenschist facies metamorphic sequence in Bergama (İzmir), western Turkey: The first peleontological age assignment and structural-stratigraphic implications. *Newsletter for Stratigraphy 26, 1-17.*

Keskin, İ., Korkmaz, S., Gedik, İ., Ateş, M., Gök, L. 1989. Bayburt dolayının jeolojisi. *Maden Tetkik ve Arama Genel Müdürlüğü* Rapor No: 8995, Ankara (unpublished).

Koçyiğit, A. 1987. Hasanoğlan (Ankara) yöresinin tektonostratigrafisi: Karakaya orojenik kuşağının evrimi (Tectonostratigraphy of the Hasanoğlan (Ankara) region: evolution of the Karakaya orogenic belt). *Yerbilimleri* 14, 269-294.

Koçyiğit, A., Kaymakçı, N., Rojay, B., Özcan, E., Dirik, K., Özçelik, Y. 1991. İnegöl-Bilecik- Bozüyük arasında kalan alanın jeolojik etüdü. *Orta Doğu Teknik Üniversitesi-Türkiye Petrolleri Anonim Ortaklığı* proje rapor No: 90-03-09-01-05 (unpublished).

Kozur, H. 1999. Permian development in the western Tethys. Rathanasthian, B., Rieb, S.L. (Ed). *Poceedins of the International Sympozium on Shallow Tethys* 5, 101-103.

Kozur, H., Aydın, M., Demir, O., Yakar, H., Göncüoğlu, M.C., Kuru, F. 2000. New stratigrafic and palaeographic result from the Paleozoic and early Mesozoic of the Middle Pontides (northern Turkey) in the Azdavay, Devrekani, Küre and İnebolu areas. Implications for the Carboniferous-Early Cretaceous geodynamic evolution and some related remarks to the Karakaya oceanic rift basin. *Geologica Croatia* 53, 209-268.

Leven, E.J., Okay, A.İ. 1996. Foraminifera from the exotic Permo-Carboniferous limestone blocks in the Karakaya Complex, northwest Turkey. *Rivista Italiana Paleontologiae Stratigrafia* 102, 139-174.

Nzegge, O.M., Satır, M., Siebel, W., Taubald, H. 2006. Geochemical and isotopic constrains on gnesis of the Late Paleozic Deliktaş and Sivrikaya granites from the Kastamonu granitoid belt (Central Pontides, Turkey). *N. Jb. Miner Abh.* 183, 27-40.

Okay, A.İ. 1984. The geology of the Ağvanis metamorphic rocks and neighbouring formations. *Maden Tetkik ve Arama Dergisi* 99/100, 16-36.

Okay, A.İ. 1996. Granulite facies gneisses from the Pulur region, Eastern Pontides. *Turkish Journal of Earth Sciences* 5, 55-61.

Okay, A.İ. 2000. Was the late Triassic orogeny in Turkey caused by the collision of an oceanic plateau. Bozkurt, E., Winchester, J.A., Piper, J.A.D. (Ed). Tectonics and Magmatism in Turkey and Surrounding Area. *Geological Society of London*, Special Puplications 173, 25-41.

Okay, A. İ. 2004. Türkiye'nin Jeolojisinde Paleo-Neotetis Problemi. *TMMOB Jeoloji mühendisleri Odası 57. Türkiye Jeoloji Kurultayı* Bildiri Özleri Kitabı 8-9 s., Ankara.

Okay, A. 2011. Sakarya Zonu Jura Öncesi Temelinin Metamorfik Evrimi. *TMMOB Jeoloji mühendisleri Odası 64. Türkiye Jeoloji Kurultayı* Bildiri Özleri 215-216 s., Ankara.

Okay, A.İ., Siyako. M., Bürkan, K.A. 1991. Geology and tectonic evolution of the Biga Peninsula, northwest Turkey. *Bulletin of the Technical University of İstanbul* 44, 191-256.

Okay, A.İ., Mostler, H. 1994. Carboniferious and Permian radiolarite blocks in the Karakaya Complex in northwest Turkey. *Turkish Journal of Earth Sciences* 3, 23-28.

Okay A.I., Satır, M., Maluski, H., Siyako, M., Monie., P., Mezger, R., Akyüz, S. 1996. Paleo-and Neo Tethyan events in Northwest Turkey: geological geochronological constraints. Yin, A., Harrison, M. (Ed). *Tectonics of Asia*, Cambridge University Press, pp. 420-441.

Okay, A.İ., Monie, P. 1997. Early Mesozoic subduction in the Eastern Mediterranean: evidence from Triassic eclogite in northwest Turkey. *Geology* 25, 595-598.

Okay, A.İ., Tüysüz, O. 1999. Tethyan stures of northern Turkey. Durand, B., Jolivet, L., Horvath, F., Serranne, M. (Ed). The Mediterranean Basins: Tertiary Extention Within the Alpine Orogen. *Geological Society of London*, Special Publications 156, 475-515.

Okay, A. İ., Monod, O., Monie, P. 2002. Triassic bluesschists and eclogites from northwest Turkey: vestiges of the Paleo-Tethyan subduction. *Lithos* 64, 155-178.

Okay, A.İ., Göncüoğlu, M.C. 2004. The Karakaya Complex: A review of Data and Concept. *Turkish Journal of Earth Sciences* 13, 77-96.

Okay, A.İ., Noble, P.S.Ç., Tekin, U.K. 2011. Devonian radiolarian ribbon chert from the Karakaya Complex, Northwest Turkey. *Implications for the Paleo-Tetyhan evolution, Comptes Rendus Palevol* 10, 1-10.

Okuyucu, C., Göncüoğlu, M.C. 2010. Middle-Late Aselian (Early Permian) fusulinid fauna from the post-Variscan cover in NW Anatolia (Turkey): Biostratigraphy and geological implication. *Geobios* 43, 225-240.

Önder, F., Boztuğ, D., Yılmaz, O. 1987. New paleontological data (Conodont) from the Lower Mesozoic rocks of the Göynükdağı-Kastamonu region at the Western Pontides, Turkey. *Melih Tokay Geology Semposium*, Ankara, Abstracts, 127-128 p (in Turkish).

Özcan, A., Erkan, A., Keskin, E., Oral, A., Özer, S., Sümengen, M., Tekeli, O. 1980. Kuzey Anadolu Fayı-Kırşehir Masifi arasının temel jeolojisi. *Maden Tetkik ve Arama Enstitüsü* Rapor No: 6722, Ankara (unpublished).

Pickett, E.A., Robertson, A.H.F., Dixon, J.E. 1995. The Karakaya Complex, NW Turkey: a Palaeotethyan accretionary complex. Erler, A., Ercan, T., Bingöl, E., Örçen, S. (Ed). Geology of the Black Sea Region. *Proceedings of an international semposium on the Geology of the Black Sea region*, September, 7-11, 1992, Ankara, Turkey. *Mineral Research and Exploation and Chamber of Gological Engineers*, Ankara, 11-18.

Pickett, E., Robertson, A.H.F. 1996. Formation of the Late Paleozoic-Early Mesozoic Karakaya Complex and related ophiolites in NW Turkey by Paleotethyan subduction-accretion. *Journal of the Geological Society,* London 153, 995-1009.

Rojay, B., Göncüoğlu, M.C. 1997. Tectonic setting of some pre-Liassic low grade metamorphics in northern Anatolia. *Yerbilimleri* 19, 109-118.

Saner, S. 1977. Geyve-Osmaneli Gölpazarı-Taraklı alanının jeolojisi: Eski çökelme ortamları çökelmenin evrimi. Yüksek lisans Tezi, İstanbul Üniversitesi, 312 s.

Sarıfakıoğlu, E., Sevin, M., Esirtgen, E., Duran, S., Parlak, O., Bilgiç, T., Dönmez, M., Dilek, Y. 2011. Çankırı-Çorum havzasını çevreleyen ofiyolitik kayaçların jeolojisi: Petrojenezi, tektoniği ve içerikleri. *Maden Tetkik ve Arama Genel Müdürlüğü* Rapor No: 11449, Ankara (unpublished).

Sarıfakıoğlu, E., Dilek, Y., Sevin, M. 2014. Jurassic- Paleogene intraoceanic magmatic evolution of the Ankara Melange, north-central Anatolia, Turkey. *Solid Earth* 5, 1-32.

Stampfli, G.M., Borel, G.D. 2002. A plate tectonic model for the Paleozoic and Mesozoic constrained by dynamic plate baundaries and restored synthetic oceanic isochorones: Earth Planet. *Sci. Lett.,* 169, 17-33.

Stocklin, J. 1977. Structural correlation of the Alpine ranges between Iran and Central Asia. *Mem. Ser. Soc. Geol. France*, 8, 333-353.

Şengör, A.M.C. 1979. Mid-Mesozoic closure of Permo-Triassic Tethys and its implications. *Nature* 279, 590-593.

Şengör, A.M.C. 1984. The Cimmeride Orogenic System and the Tectonics of Eurasia. *Geological Society of America*, Special Paper 195, 82 p.

Şengör, A.M.C., Yılmaz, Y. 1981. Tethyan evolution of Turkey, a plate tectonic approach. *Tectonophysics* 75, 181-241.

Şengör, A.M.C., Yılmaz, Y., Sungurlu, O. 1984. Tectonics of the Mediterranean Cimmerides: nature and evaluation of the western termination of Paleo-Tethys.

Dixon, J.E., Robertson, A.H.F. (Ed). The Geological Evolution of the Eastern Mediterranean. *Geological Society of London*, Special Publication 17, 77-112.

Şengün, M. 1990. Plate mozaic of Turkey during the Mesozoic. *International symposium on the geology of the Aegean Regions*, Abstract, 192-194 p.

Tekeli, O. 1981. Subduction complex of pre-Jurassic age, northern Anatolia. *Geology* 9, 68-72.

Tekin, U.K., Göncüoğlu, M.C., Turhan, N. 2002. First evidence of Late Carnian radiolarian fauna from the İzmir-Ankara-Sture Complex, Central Sakarya, Turkey: Implication for the opening age of the İzmir-Ankara branch of Neotethys. *Geobios* 35, 127-135.

TMMOB JMO. 2004. Jeolojik Zaman Çizelgesi. *TMMOB Jeoloji Mühendisleri Odası*, Ankara.

Topuz, G., Altherr, R., Kalt, A., Satır, M., Werner, O., Schwarz, W.H. 2004*a*. Aluminos granulites from the Pulur complex, NE Turkey: a case of partial melting, efficient melt extraction and crystallisation. *Lithos* 72, 183-207.

Topuz, G., Altherr, R., Satır, M., Schwartz, W.H. 2004*b*. Low-grade metamorhic rocks from the Pulur Complex NE Turkey: implications for the pre-Liassic evolution of the eastern Pontides. *Int. J. Earth Sci*. 93,72-91.

Topuz, G., Altherr, R., Siebel, W., Schwartz, W.H., Zack, T., Hasözbek, A., Barth, B., Satır, M., Şen, C. 2010. Carboniferous high-potassium I-type granitoid magmatism in the Eastern Pontides: The Gümüşhane pluton (NE Turkey). *Lithos* 116, 92-110.

Turhan, N., Okuyucu, C., Göncüoğlu, M.C. 2004. Autochthonous Upper permian (Midian) carbonates in the western Sakarya composite Terrane, Geyve Area, Turkey: Prelimenary Data. *Turkish Journal of Earth Sciences* 13, 215-229.

Tüysüz, O. 1996. Amasya ve çevresinin jeolojisi (Geology of the Amasya region). *Türkiye 11. Petrol Kongresi* Bildiriler Kitabı, 32-48.

Ustaömer, P.A., Ustaömer T., Robertson A.H.F., 2012. Ion Probe U-Pb Dating of the Central Sakarya Basement: A Peri-Gondwana Terrane Intruded by Late Lower Carboniferous subduction/Collision related Granitic Rocks. *Turkish Journal of Earth Sciences,* 21, 905-932.

Uğuz, M.F., Turhan, N., Bilgin, A.Z., Umut, M., Şen, A.M., Acarlar, M. 1999. Kulu (Konya), Haymana (Ankara) ve Kırıkkale dolayının jeolojisi. *Maden Tetkik ve Arama Genel Müdürlüğü* Rapor No: 10399, Ankara (unpublished).

Yalınız, M.K., Göncüoğlu, M.C. 2002. Geochemistry and petrology of "Nilüfer type" metabasic rocks of eastern Kozak Massif, NW Turkey. *1st International Symposium Faculty of Mines (İTÜ) on Earth Sciences and Engineering* 16-18 may 2002 İstanbul, Abstracts, 158.

Yılmaz, Y. 1981. Sakarya kıtası güney kenarının tektonik evrimi (Tectonic evolution of the southern margin of the Sakarya Continent). *İstanbul Yerbilimleri* 1, 33-52.

Yılmaz, Y., Tüysüz, O. 1984. Kastamonu-Boyabat-Vezirköprü-Tosya arasındaki bölgenin jeolojisi. *Maden Tetkik ve Arama Genel Müdürlüğü* Rapor No: 7838, Ankara (unpublished).

Yılmaz, Y., Serdar, H.S., Genç, C., Yiğitbaş, E., Gürer, Ö.F., Elmas, A., Yıldırım, M., Bozcu, M., Gürpınar, O. 1997 . The geology and evalution of the Tokat Massif, south-central Pontides, Turkey. *International Geology* Rewiev 39, 365-382.

Yılmaz, A., Yılmaz, H. 2004. Geology and Structural Evolution of the Tokat Massif (Eastern Pontides, Turkey). *Turkish Journal of Earth Sciences* 13, 232-247.

PLATE I

PLATE I

1, 2. *Pachysphaerina* sp., Sample No: 06MS-22

3. *Mediocris* sp., Sample No: 06MS-22,

4. *Ozawainella* sp., Sample No: 11MS-01,

5. *Eostaffella* sp.**,** Sample No: 11MS-01,

6. *Lasiodiscus* sp., Sample No: 11MS-02,

7. *Neofusulinella* sp., Sample No: 14MS-08,

8. *Minojapanella* sp., Sample No: 14MS-08,

9. *Neoschwagerina* sp., Sample No: 14MS-9B,

10. *Agathammina* sp., Sample No: 14MS-9A,

11. *Tetrataxis* sp., Sample No: 14MS-9A,

12. *Globivalvulina* sp., Sample No: 14MS-10B,

13. *Climacammina* sp., Sample No: 14MS-10A,

14, 15. *Hemigordiopsis* sp., Sample No: 14MS-9A,

16. *Dagmarita chanakchiensis* Reitlinger, Sample No: 06MS-18E,

17-18. *Pachyphloia* sp., Sample No: 11MS-27, 14MS-10A,

19, 20. *Rectostipulina quadrata* Jenny-Deshusses, Sample No: 06MS-18B, 06MS-18B,

21, 22. *Frondina permica* Sellier de Civrieux and Dessauvagie, Sample No: 14MS-12, 06MS-19C,

23. *Charliella* sp., Sample No: 11MS-27,

24. *Multidiscus* sp., Sample No: 06MS-18E

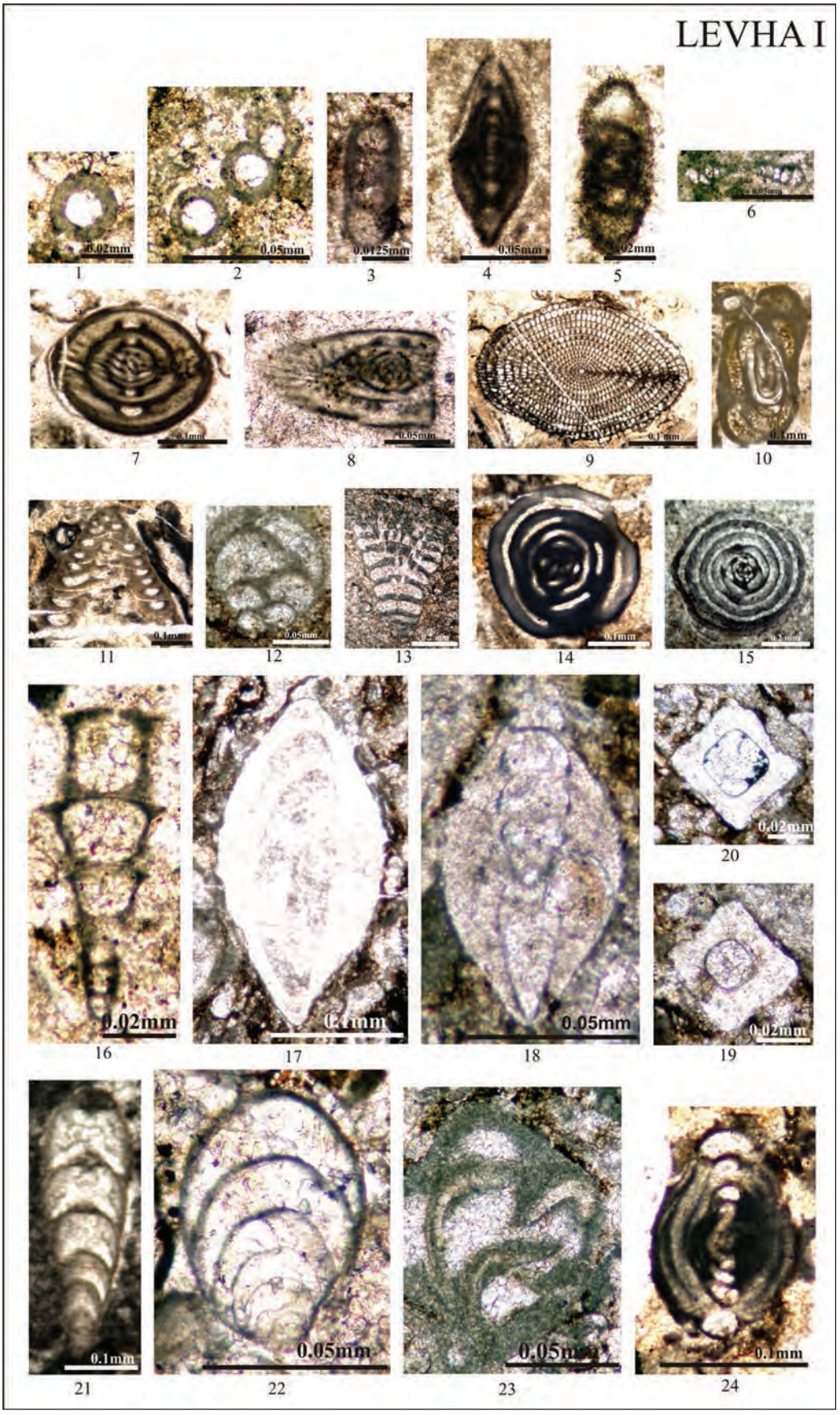
LEVHA I
0.02mm
1
0.05mm
2
0.0125mm
3
0.05mm
4
0.02mm
5
6
7
0.05mm
8
9
0.1mm
10
11
12
13
0.1mm
14
15
0.02mm
16
17
0.05mm
18
0.02mm
19
20
0.1mm
21
0.05mm
22
0.05mm
23
0.1mm
24

Bull. Min. Res. Exp. (2015) 151: 149-168

Bulletin of the
Mineral Research and Exploration

http://bulletin.mta.gov.tr

DIFFERENTIATION PROCESSES in LATE CRETACEOUS ULTRAPOTASSIC VOLCANICS AROUND AMASYA

Fatma GÜLMEZ[a]* and Ş. Can GENÇ[a]

[a] *Istanbul Technical University Geological Engineering Department, 34469 Maslak, İstanbul*

Keywords:
Late Cretaceous,
Pontides, Ultrapotassic
Magmatism, AFC.

ABSTRACT

Late Cretaceous lithologies around Amasya region are represented by Pontide fore-arc basin units which corresponds a volcanoclastic sequence. This sequence has the products of alkaline ultrapotassic magmatism accompanying calcalkaline lavas which are abundant along Pontide arc. The ultrapotassic rocks which are classified as leucitite, minette and trachyte based on their mineralogical composition, occur as dikes, stocks and rarely lava flows as to be comprised by the Late Cretaceous Volcanoclastic Succession (LCVS). Fractional crytallization accompanied by assimilation (AFC) is a low pressure processes able to differentiate ultrapotassic parental melts to various compositions in a continental margin tectonic setting.The trachytes are the youngest and the most evolved members of LCVS. Therefore we performed AFC modelling using the most primitive minette sample as starting composition and calculated the fractionation trends based on the theoretical mineralogical compositions. We also used the Triassic metapelitic basement rocks of Central Pontides as assimilant. The AFC modelling results imply that it is possible to produce trachytes by adding Central Pontide basement rocks up to 5 %, begining from the most primitive phonolitic sample of Amasya. However the differentiation of leucitite and minette is able to be explained by neither fractional nor assimilation processes.

1. Introduction

An arc environment is defined, which has developed due to the northward subduction of the Neo-Tethys Ocean, during Late Cretaceous in the geological evolution Anatolia located in the Alp-Himalaya orogenic belt (Şengör and Yılmaz, 1981; Okay and Şahintürk, 1997; Yılmaz et al., 1997; Okay and Tüysüz, 1999; Topuz et al., 2013). East-west trending island arc units, namely Pontide arc within the Pontide mountain range form the central segment of this belt that extend along Apuseni-Timok line in Balkans at the west and Sevan-Akera suture belt along the Armenian-Georgian boundary at the east (Adamia et al., 1981; Yılmaz et al., 1997; Georgiev et al., 2009; Mederer et al., 2013). The Pontide arc formation ceased by the collision of Sakarya continent and the Anatolide-Tauride platform or by the Kırşehir Blocks in early Paleocene caused by development of the İzmir-Ankara-Erzincan Suture Belt (IAESZ) (Şengör and Yılmaz, 1981; Okay and Tüysüz, 1999). Pontide arc is represented by calc-alkaline andesitic volcanics, associated pyroclastics and epiclastic units with the I-type granitic intrusions. However, in the southern parts the units of IAESZ and alkali-potassic rocks associated with forearc units are observed. The well-known locations of these alkaline potassic rocks are Ankara-Kalecik, Bayburt-Maden and Amasya-Gümüşhacıköy and the Sinop (Blumenthal, 1950; Alp, 1972). Additionally, recently discovered two outcrops in the west parts of this belt are at around Tosya and Osmancık (Genç et al., 2013). The Amasya region has critical importance due to the three different type ultrapotassic rock suites together with coeval calc alkaline andesites are

* *Corresponding author: Fatma Gülmez, gulmezf@itu.edu.tr*

present. These are identified petrographically as leucitite, minette and trachyte, and are observed in the form of dyke, stock and as lava flows within Late Cretaceous Volcanoclastic Succession together with calc alkaline andesites. This association is not typically observed in aforementioned other regions, except for the Amasya case. For example in Kalecik region, where leucititic and lamprophyric ultrapotassic rocks exhibit an interfingered appearance, but there is no outcrop showing its stratigraphical relationship between trachytic rocks and other potassic rocks. Leucititic rocks are observed in the form of stocks around Gümüşhacıköy. However, lamprophyric and trachytic rocks do not exist in this region. Considering the stratigraphical relationships and outcrop distribution, the Amasya region is the best area unique the potassic/ultrapotassic rock coexistence along the whole belt.

Ultrapotassic rocks are generated in continental rifts or under the control of the extensional tectonism following the continental collision. Its occurrence in active arc environments are limited (McKenzie, 1989; Foley, 1992; Mitchell and Bergman, 1991; Rock, 1991). The best known examples of the potassic volcanic products that accompany the calc alkaline andesitic magmatism are observed in Sunda-Banda, Kamchatka, Japanese and Mexican arcs (Yagi et al., 1975; Luhr and Kyser, 1989; Nelson, 1992). Whereas the increase of the interest and the number of studies focusing on the ultrapotassic magmatism in active subduction zones, there is still debate on which processes forms the ultrapotassic magmatism in the arc environments.

The main aim of this study is to give an example for the rare ultrapotassic magmatism which are the partial melting products of the special mantle sources, in the arc environments from the Central Pontides. The ultrapotassic rocks of the Amasya region were mapped and defined its meaning for the regional stratigraphy. Radiometric age datings, geochemical, isotope and mineral chemistry analysis have been carried out on these rocks. The data obtained from these studies were correlated with the available stratigraphic and paleontological data. Additionally, Late Cretaceous ultrapotassic rocks were classified as leucitite, minette and trachyte by their mineralogical, petrographical and geochemical characters. The petrological models were produced for its differentiation processes from leucitite/minette to trachytic rocks. In order to enlighten of their petrological evolution and crystallization processes.

2. Geology

The very comprehensive study of Alp (1972) and the detailed geological map of Rojay (1995) were used for the stratigraphical relationships of Amasya region ultrapotassic rocks with Late Cretaceous volcanic/volcanoclastic units (Figures 1-2). The Late Cretaceous unit including the ultrapotassic rocks defined collectively as the Kışlacık Group, Karatepe, Geyiközü and Fındıklı formation by previous studies. It was called as the Lokman formation by Alp (1972). The Lokman formation is known as the Everekhanları formation around Bayburt area at the east (Bektaş and Gedik, 1988; Alther et al., 2008). Besides, Kalecik and Gümüşhacıköy vicinities in west form well-known areas in which Late Cretaceous units include leucititic rocks (Bailey and McCallien, 1950; Blumenthal 1950; Çapan, 1984; Tankut et al., 1998; Tüysüz, 1995; Varol, 2013; Eyüpoğlu, 2010). In addition to this ultrapotassic belt located roughly parallel to İzmir-Ankara-Erzincan Suture; it is also necessary to note that the Hamsaros volcanics which contain Cretaceous ultrapotassic leucititic rocks around Sinop (Gedik et al., 1983; Baş, 1986; Asan et al., 2014). The volcanoclastic succession representing the Pontide forearc basin units, is called collectively as "Amasya Late Cretaceous Volcanoclastic Succession (ALCVS).

The basement of ALCVS is formed from the metamorphic rocks of the Tokat Group and overlying Liassic to Lower Cretaceous carbonates known as Vermiş, Ferhatkaya, Sarılar, Carcurum, Soğukçam and Vezirhan formations, and Bilecik Limestone (Alp, 1972; Rojay, 1995; Tüysüz, 1996). The ophiolitic material within Lower Cretaceous carbonates increase towards the Upper Cretaceous units, and turns into an "ophiolitic mélange" (Figure 2). The primary contact relationship of the mélange, which is known as Amasya formation, and ALCVS is documented as an angular unconformity (Alp, 1972; Rojay, 1995; Tüysüz, 1996).

Tüysüz (1996) reported that, the pelagic carbonate depositions began following the rift volcanism continued until Late Jurassic in the region. He also states that this sedimentation is similar to a passive continental margin deposition, and could be correlated with western part of Sakarya Continent. Rojay (1995) subdivided the carbonates (the Amasya Group) as; the Early Jurassic bioclastic carbonates, the Middle Jurassic regressive carbonates containining the Ammonitico Rosso at the bottom and the Early Cretaceous pelagic carbonates. He also argues that the

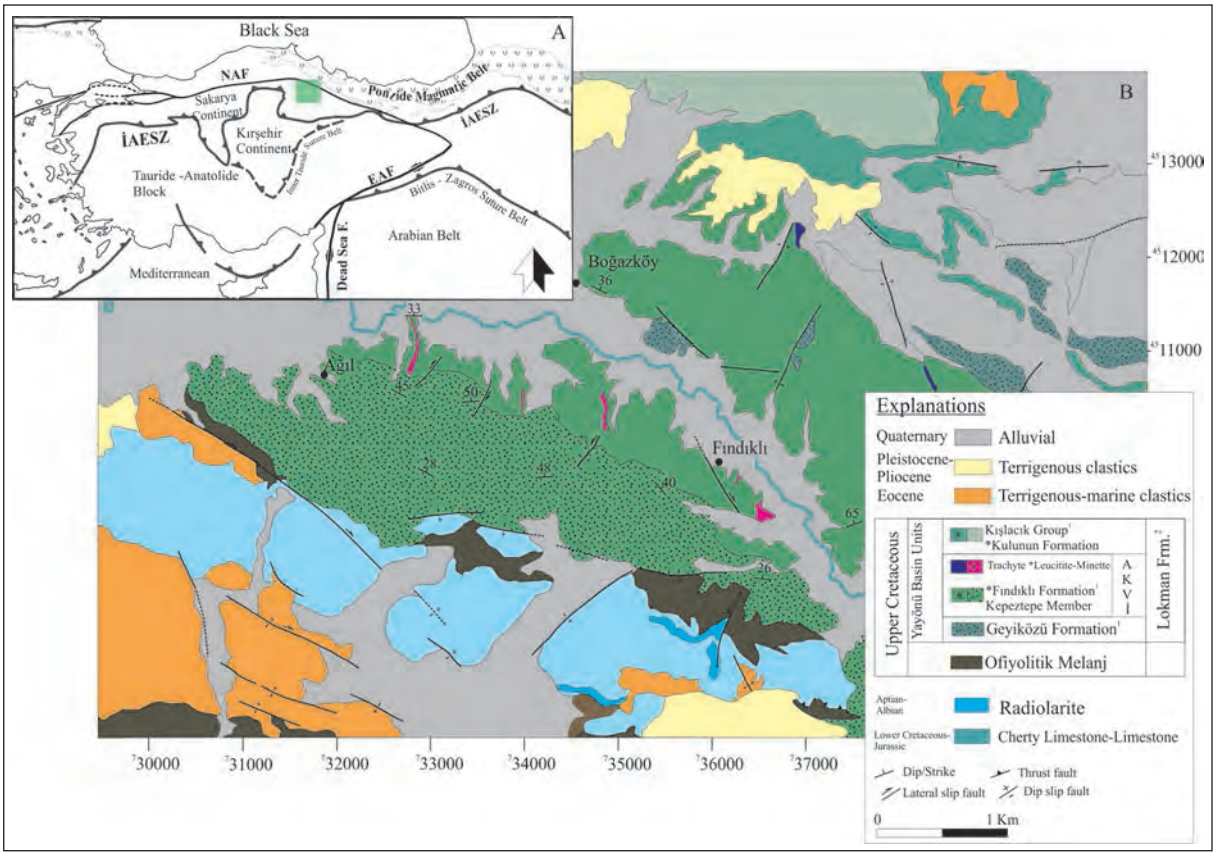

Figure 1- a) Location of the study area within general tectonic units of Anatolia (EAF: East Anatolian Fault Zone, IAESZ: Izmir-Ankara-Erzincan Suture Zone, DSF: Dead Sea Fault; Okay and Tüysüz, 1999; Ciobanu et al., 2002; Şengör et al., 2005; Sosson et al., 2010; Mederer et al., 2013) and b) Outcrops of ALCVS ultrapotassic rocks in the geological map prepared by Rojay (1995) (1: Rojay, 1995; 2: Alp, 1972).

platform, which gradually uplifted starting from Liassic, began to collapse in a deepening environment by the sudden rise of the sea level in Middle Jurassic. Rojay also emphasizes that this depositional environment was a passive continental margin, then turned into a converging plate margin in Campanian-Maastrichtian by the mélange obduction. Yılmaz et al. (1997) pointed out the limestone deposition followed by the red pelagic limestone, mudstone and radiolarite deposition during Cenomanian-Turonian period. According to these authors, this passed gradually into a wild flysch at the top by the incorporation of older limestone blocks and olistostromes, together with the blocks and slices from the ophiolitic mélange (Yılmaz et al., 1997).

ALCVS' outcrops are seen between Lapköyü at the north and Fındıklı village at south (Figure 1). It is observed that the unit begins with flysch-like sediments at the bottom, and grades into an epiclastic unit containing mostly andesitic lava pebbles. These materials are badly sorted and cemented by a mudstone, siltstone and sandstone matrix. In this paper, "volcanoclastic sediment" or "epiclastic" definition describe the non-volcanic products formed from the deposition by erosion and transportation processes (Reading, 2009). ALCVS epiclastic unit, covers all the different rock name, such as andesitic breccia, agglomerate, tuff/tuffite, pyroclastic and volcanic breccia in previous studies (Alp, 1972; Koçyiğit, 1988; Tüysüz, 1996). The "true" volcanic/pyroclastic units are beyond of this description. Field studies revealed that flysch type sediments and epiclastic units show lateral and vertical transitions. Epiclastic rocks were formed when large amounts of volcanic material is transported into the basin. Decreasing of the volcanic materials, normal flysch deposition occurred. Although the epiclastic unit is monogenetic, it also contains some leucitite and minette pebbles. In the northern areas, abundant trachyte pebbles are found to the top of the succession. Andesitic lava flows are also widespread within the volcanoclastic succession (Figure 2).

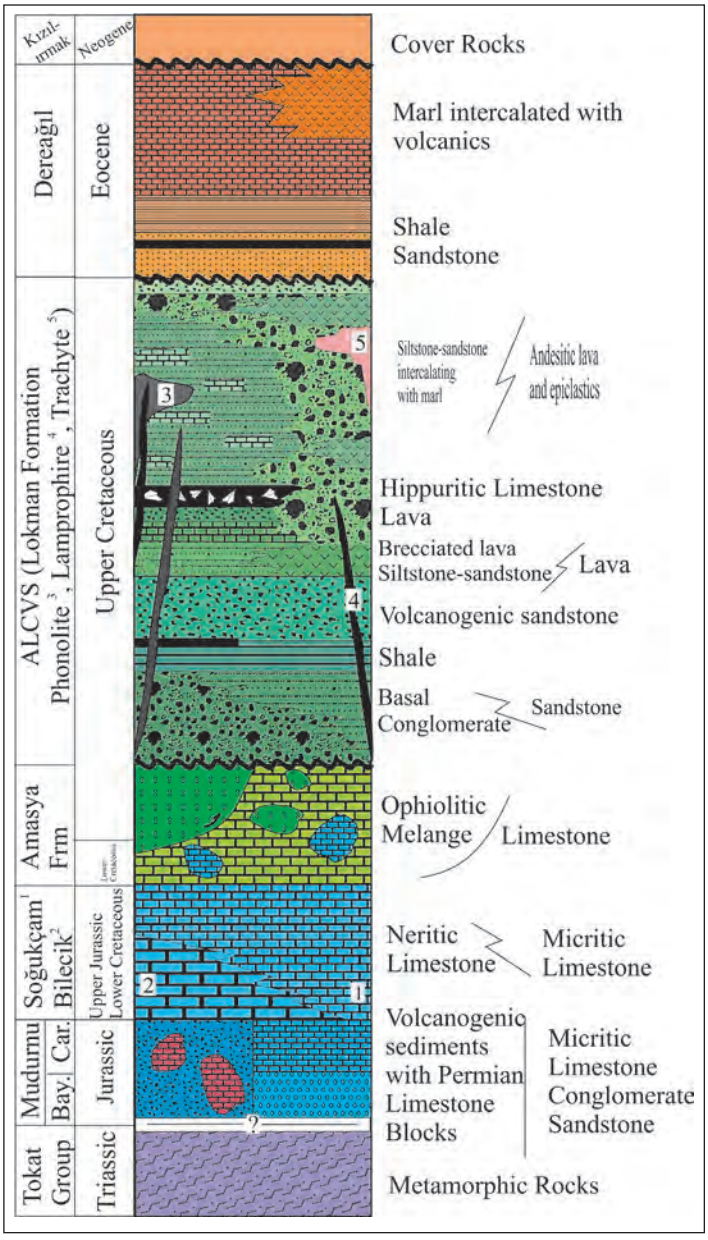

Figure 2- Stratigraphic relationship between leucitite, lamprophyre and trachytes within non-scaled, generalized stratigraphic section of Amasya and surroundings (after Alp, 1972).

There are abundant and reliable fossil findings from the ALCVS to determine its age. Alp (1972) reported the age of unit, based on macro fossils (*Actaeonella* sp., *Hippurite* sp.) rather than micro fossils as Campanian-Maastrichtian. However; Koçyiğit et al. (1988) dated units as Lower Companian-Maastrichtian in age. Asan et al (2014) carried out $^{40}Ar/^{39}Ar$ age datings from the phlogopitic micas of two shoshonitic rocks as 82.08 ± 1.13 and 81.37 ± 0.81 My. These ages are in a good agreement of the paleontological data.

3. ALCVS Magmatic Rocks

3.1. Leucitite

The outcrops of the leucitites are observed as small stocks and dikes, along Yeşilırmak valley in the south of Boğazköy (Figure 3a). These are generally yellowish to white gray colored and highly altered. These are massive and pale gray colored in relatively more fresh outcrops. Leucite crystals are dull, and pale pink-whitish in color, and embedded into the

groundmass (Figure 3b). Euhedral, bright and pink colored leucite phenocrysts, 1-2 cm in diamaters are typical. Joint sets, beddings, columnar joints or other structural features are not observed in stocks. Columnar joints developed in 1.5 m wide leucitite dike (Figure 3a). Leucitite pebbles and/or blocks are also observed within the epiclastic rocks of the ALCVS.

3.2. Minette

Minette type lamprophyres crop out in the form of NW-SE or NE-SW trending dikes, located in the south of Yeşilırmak valley and cut the epiclastics, and there are no continuations to the northern side of the valley. The northernmost of the study area, an aphyric minette dike cutting the trachyte dome is present. The width of minette dykes varies between 40 cm to 2 m. Pinkish to pale brown colors due to the feldspars and shining views because of micas are typical in hand specimens (Figure 3d). Minettes cut the epiclastic rocks and interfingered with the leucititic stock (Figure 3c). Presence of a sharp contact with leucitites has not been identified. Possibly these two rocks are transitional with each other, observed in the leucitic lamprophyre and phlogopite lamprophyre dikes of the Ankara-Kalecik area (Gülmez et al., 2014*a*).

3.3. Trachyte

Trachytes, which are the youngest ultrapotassic products of ALCVS, are observed in the form of 5 m wide, NW-SE oriented dyke around Kelışığın Hill in

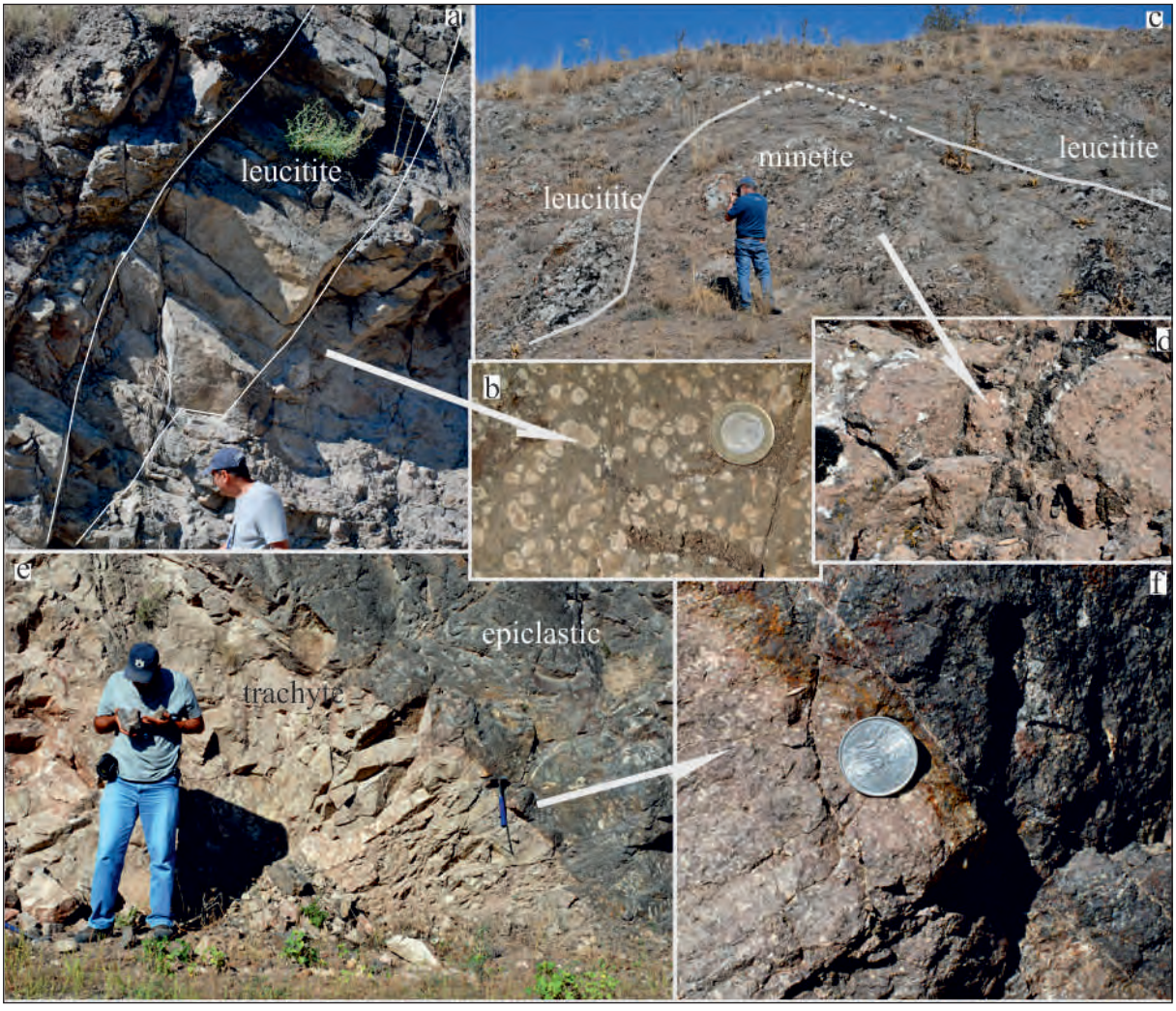

Figure 3- Outcrop views of ultrapotassic rocks a) columnar jointing forms in leucitite lava, b) leucitites in hand samples, c) general outcrop view from minette stock, d) minette in hand samples, e) the contact between trachytic dome and epiclastic units, f) the chill zone developed along the contact.

north of Yeşilırmak valley, and as a small dome around Lapköyü. Trachytic rocks are recognized with their pink color, and massive appearances (Figures 3 e-f). Coarse (upto 2 cm), euhedral prismatic feldspar phenocrystals and trachytic textures which can be observed even in hand specimens are typical for trachytes. It was observed that glassy, dark colored, partly aphyric or micro crystalline margin zone (quenching zone) at the contact of trachytic dome with epiclastic unit (Figure 3f). This zone is continuous along the contact and its width does not exceed 2-5 cm. The hypabyssal and plutonic equivalents of the unit have been documented by Alp (1972) in the NE of Amasya.

3.4. Andesites

Andesites are observed in the form of lensoidal lava flows having thicknesses not exceeding 1 m, which do not exhibit lateral continuity within epiclastic units. It alternates with the epiclastic units, and rarely cut them. They have generally massive and are gray colored on their fresh surfaces. On the alteration surfaces their colors can be reddish, brownish or greenish gray. They are also represented by the flow breccias at the bottom of the lava flows road between Boğazköy and Lapköyü. They are along the road highly altered and characterized by porphyric textures in hand samples with the relatively coarse plagioclase phenocrystals.

4. Radiochronological Findings

Radiochronological studies have been made on 1 trachytic, 1 leucitic and 2 minette type rocks in order to provide stratigraphical correlation. Sanidine and whole rock in trachytic sample, phylogopite in minettes, and leucites in leucitite were analyzed. The alteration of the mineral, the presence of another mineral or fluid inclusions, whether it exhibits compositional zoning and changes due to reactions on edges were taken as basis in the selection of minerals which are suitable for analyze. Samples were subjected to the radiation as described in the study of Dalrymple et al. (1981) in McMaster nuclear reactor in Ontario Hamilton for the production of ^{39}Ar from ^{39}K. The radiometric $^{40}Ar/^{39}Ar$ dating analyses were performed following the methods in the study of Hames et al. (2009) in the laboratories of the Auburn University (ANIMAL: Auburn Nobel Isotope Mass Analysis Laboratory). Results were evaluated by Microsoft Excel and Isoplot software (Ludwig, 2003).

Results of the analysis have been compatible with the results of previously performed stratigraphical and paleontological studies in the region. According to the results obtained from phylogopite analyses, the plateau ages determined for the minettes range between 76.78 ± 0.19 and 77.43 ± 0.15 My (Figures 4 a-b). The plateau age obtained from K-feldspars in trachyte sample is 75.83 ± 0.09 My (Figure 4c). In addition, the whole rock age determination carried out in the same sample is 70.1± 1.3 My. The plateau age could not be detected as the K amount of leucites is low because of analcimization in leucitites. Total gas age data obtained from the crystals that have spherulitic and radial K-feldspar rims, is 75.6 ± 3.7 (Figure 4d). Although there is a high error in the radiometric data obtained due to low K amount, this finding is also compatible with other findings and probably point out the crystallization age of hypocrystalline K-feldspars in groundmass.

5. Petrographical Characteristics and Classification

In the classification of volcanic units in ALCVS, studies of Le Maitre (2002) and Mitchell and Bergman (1991) were taken as basis. Accordingly; four different Late Cretaceous lithological units were defined in Amasya.

5.1. Leucitite

The general mineralogical composition of leucitites were determined as clinopyroxene+ leucite±alkali feldspar+apatite+magnetite by petrographical investigations. As secondary minerals; analcime, calcite, sericite, clay and opaque minerals were observed. Leucites are generally observed as coarse (1-3 cm in size) and in the form of idiomorphic phenocrysts. There are zones, made up of alkali feldspar, which developed as a result of the reaction with groundmass around the edges of euhedral leucites in glassy groundmass and grew radially (Figures 5 a-b). They typically exhibit isotropic behavior in crossed nicols. Leucites form the groundmass in some samples and have completely transformed into analcime (Figures 5 c-d). In studies of mineral geochemistry, the findings of fresh leucite phenocrystal or microcrystal were not encountered (Gülmez et al., 2014*b*). The mafic phase of leucitites in diopsitic composition is clinopyroxene (Figures 5 c-d). They are observed in the form of idiomorphic-hipidiomorphic, dark or pale green colored, and fissured micro/phenocrysts. Simple, penetrative or hourglass twinning, compositional zoning and

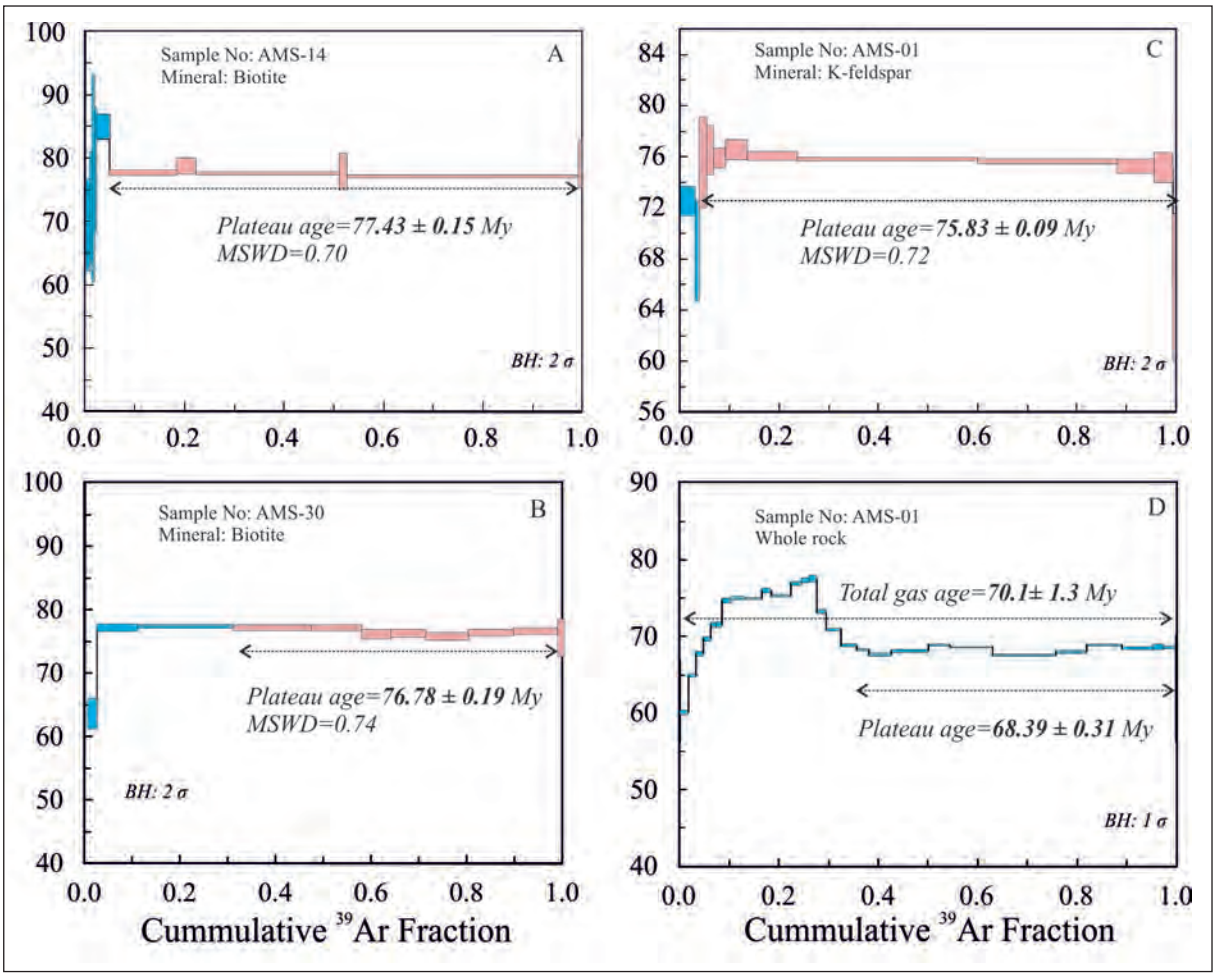

Figure 4- The age spectrum for ALCVS lavas in this study (See text and spectra for explanations, BH: Box Height, MSWD: Mean Square Weighted Distribution value).

corrosive textures, of which leucites have caused in some crystals, are widespread. They have glass and opaque minerals inclusions. Feldspar bearing leucitites are rare, and these samples do not contain feldspar as phenocrysts. Feldspar is generally observed as a cryptocrystalline matrix phase in leucitites, and causes development of spherulitic reaction textures along the rims of analcimes (Figures 5 a-b). Apatites, which are the most widespread accessory mineral of leucities are typical with their prismatic forms, and are located in groundmass as crystals or mainly as enclaves within phenocrysts.

Leucitites are generally observed both as hipocrystalline porphyric texture, characterized by the coarse leucite phenocrysts embedded in the glassy matrix. The development of devitrification texture in glassy groundmass and spherulitic texture along the rims of leucites are widespread (Figures 5 a-b). The formation of cumulate texture is also observed as a result of clustering of leucite microcrystals.

5.2. Minette

Although minette type rocks are intermingled with leucitites in outcrop scale, they differ from leucitites by lack of the leucite from the point of mineralogical composition. Their main mineralogical compositions are as follows; clinopyroxene+mica±K-feldspar+opaque mineral. As secondary minerals; calcite, clay minerals, sericite and zeolites are seen.

Mafic minerals of minettes are clinopyroxene and mica (Figures 5 e-f). Pyroxenes are the prevailing mafic mineral phase of minettes like in leucitic rocks. Although it is considered that some six-sided pseudomorphs could be olivine, the finding of fresh olivine has not been encountered. The formation of alteration related secondary calcite, zeolite and clay

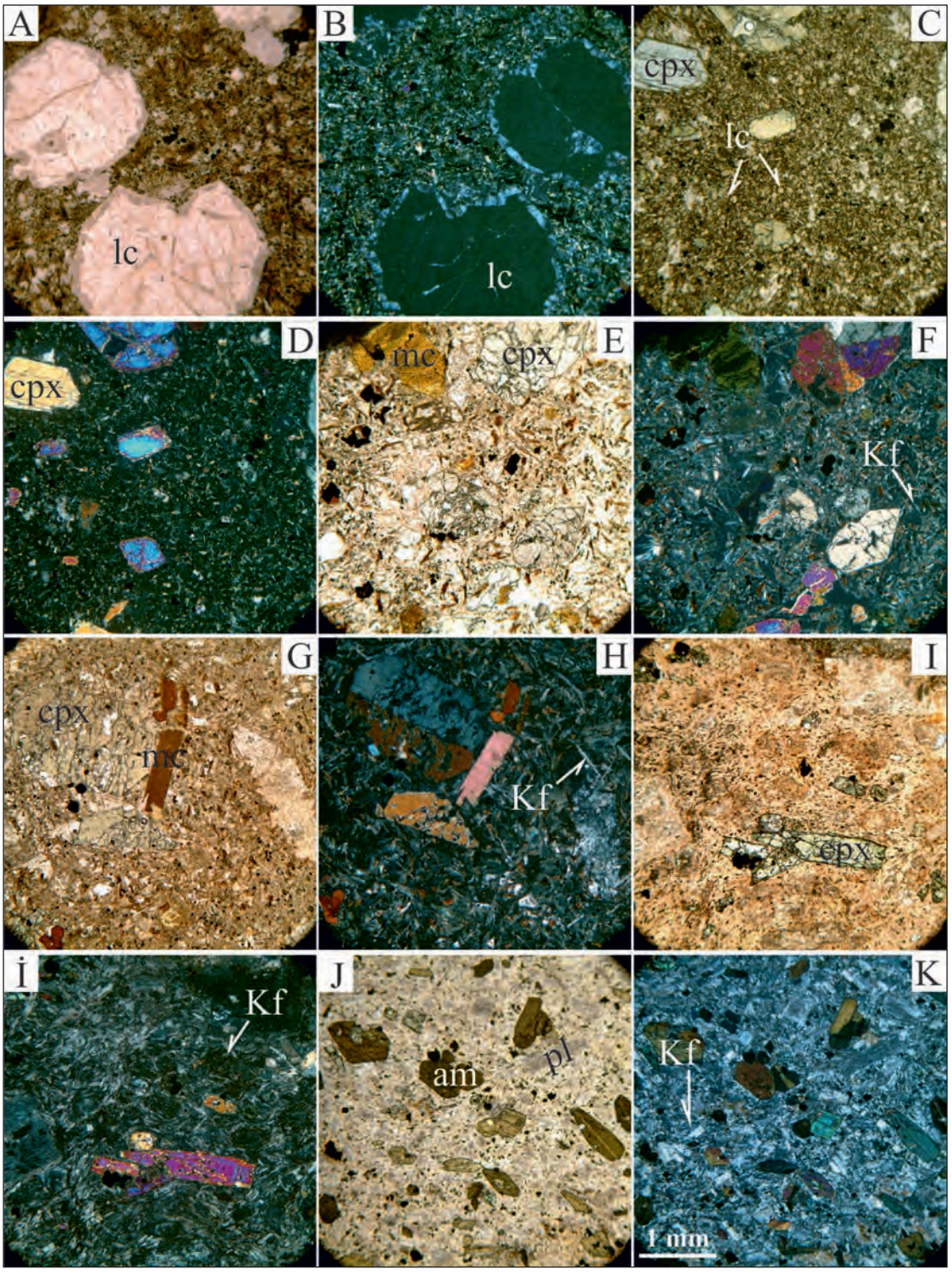

Figure 5- The thin section views of ALCVS lavas (all photos were taken by 4x magnification and the scale given in K is valid for all photos), a-b) leucite crystals under plane and cross polarized light, c-d) leucite microphenocrystals as groundmass phases, e-f) clinopyroxenes in minettes under plane and cross polarized light plane and cross polarized light, g) prismatic mica phenocrytals in minette, h) simple twinning clinopyroxene phenocrystal and Kf microliths as groundmass phases in minette sample, ı-i) trachytic texture in trachytes which contain clinopyroxene accompanies mica as mafic phase, under plane and cross polarized light, j-k) euhedral amphiboles in amphibole-bearing trachytes, altered plagioclase under plane polarized light and Kf microcrystals under cross polarized (lc: leucite, cpx: clinopyroxene, Kf: K-feldspar, pl: plagioclase, am: amphibole).

minerals are abundant in samples. Feldspars are in the form of prismatic rods, and they cause the rock to appear in pink color in hand samples (Figure 5g). They are typical with their alteration related, yellowish, simple twins and low, double refraction colors. Clinopyroxenes are similar to those of the leucitite samples, and they are represented by coarse phenocrystals or as microcrystals in groundmass. Unequilibrium textures around the rims of coarse pyroxene crystals and glass inclusions oriented closer to the outer parts of the crystals, are abundant. Zoning, simple and lamellae twinning are the other typical characteristic of pyroxenes (Figure 5f). Micas are generally phlogopite in composition (Gülmez et al., 2014*b*), and provide minettes to be easily defined in hand samples. In hand samples, they are observed as golden yellow in color. It is characterized by their perfect cleavage in one direction, strong pleochroism and parallel extinction (Figure 5g). Magmatic corrosion or alteration is not observed in phenocrysts. However, the slightly alteration and opacitized rim development is abundant in micas (in samples which are observed as pebbles in epiclastic units). Flow controlled bending and buckling of the micas are also identified in thin sections. Minettes exhibit the holocrystalline, porphyric, intergranular textures. The development of fluidal texture originating from feldspar laths can be seen in the groundmass. As some samples contain very fine grained micro/phenocrysts, they have been defined as aphyric texture.

5.3. Trachyte

Trachytic rocks in the study area can be characterized by the composition of feldspar+ plagioclase±amphibole±mica±clinopyroxene+apatite +sphene+opaque minerals. They are divided into two groups according to their mafic mineral compositions as; a) amphibole (and minor pyroxene) trachytes, and b) mica-pyroxene trachytes. As secondary minerals; calcite, sericite, chlorite and clay minerals are abundant. Sanidine is the dominant feldspar type of trachytes (Figure 5ı-k). Sanidines are observed as microliths or as prismatic phenocrysts reaching 1 cm, and they sporadically form trachytic texture (Figure 5ı-i). Amphibole inclusions are observed in sanidines. Amphiboles, which are observed as euhedral in many samples, were defined as hornblende petrographically (Figure 5j). Pyroxenes are present in the form of altered phenocrysts reaching mostly 1 mm in size or microphenocrysts within groundmass (Figure 5ı-i). Fissured and altered pyroxenes are in diopsitic composition as it was in other ultrapotassic rocks. Micas of the trachytic rocks show similarities with phlogopites in minettes in terms of yellowish, bronze colors. However; it needs for mineral chemistry study for true classification. As accessory phase, apatite crystals, which reach 1 mm size, and wedge shaped, prismatic or anhedral sphene minerals were identified.

Trachytes display idomorphic-hipidiomorphic, hipocrystalline, porphyric in texture, and trachytic (fluidal) texture development is apparent in some samples. Poikilitic texture, by which amphibole inclusions, is characteristic in feldspars.

5.4. Andesite

Andesitic rocks are generally presented by clinopyroxene+plagioclase+mica±K-feldspar+ opaque mineral assemblage. Calcite, zeolite and clay minerals as secondary minerals accompany to those primary minerals. The main feldspar type is the plagioclase. In order to determine its types optical measurements were carried out. According to extinction angle, it was determined that plagioclases are An_{45-60} in composition. Zoning and polysynthetic albite twinning is typical for the plagioclases. They are observed as altered, prismatic microphenocrystals or as microliths in the groundmass. Mica microphenocrysts, which are observed as almost fully opacitized, are in prismatic forms. Andesitic lavas are hipocrystalline, porphyric and microlithic in texture. Rarely subophitic texture which characterized by the clinopyroxene and plagioclase interfingering is also noted.

6. Whole Rock Geochemistry

Major and trace element analysis of whole rock samples of ALCVS volcanic rocks are shown in the table 1. Due to its submarine setting, the volcanic rocks have been severely affected by various alteration processes. Additionally some weathering processes which are obvious on petrographic thin sections of samples, are not unexpected after considering the age of rocks. We selected the most freshest representative 16 samples and prepared them for whole rock geochemical analysis, and then sent to ACME laboratories in Canada. Major oxides and trace elements including rare earth elements were analyzed by ICP-AES and ICP-MS, respectively. For analyses, the mixture of 200 g. powdered sample and 1.5 g. $LiBO_2$ were melted in an oven under 1050°C temperature, and the melt was then taken into 100 ml,

5% HNO_3. The solution prepared for each sample and the international standards for the calibration were also analyzed (W-2, AGV-1, GSP-2, BCR-2 and STM-1).

The SiO_2 vs. K_2O+Na_2O diagram (TAS: Total Alkali versus Silica), which the most common classification diagram for magmatic and volcanic samples with water-free oxide contents normalized to 100% are plotted on (Le Matire, 2002). We also classified ALCVS volcanic rocks on TAS diagram of Le Bas et al. (1986) (Figure 6a). However, we avoided to calculate water-free contents not to cause SiO_2 contents of the samples to increase dramatically as it would mask the silica undersaturated nature of the ALCVS ultrapotassic rocks, due to their high LOI (Loss of Ignition) values (Rock, 1991). Additionally, the readers should keep in mind TAS classification for ALCVS ultrapotassic rocks is just for an idea at first glance due to the fact that the diagram does not satisfy the requirements of the ultrapotassic and high potassium rock classification in terms of that complex mineral paragenesis and high potassium contents of ultrapotassic rocks (Conticelli et al., 2013). In this diagram, leucitic of ultrapotassic rocks plot on tephrite, tephri-phonolite fields; minettes plot on trachy-basalt, basaltic trachy-andesite, tephri-phonolite fields; andesitic rocks plot on basaltic–andesite and trachy-andesite; trachytic rocks

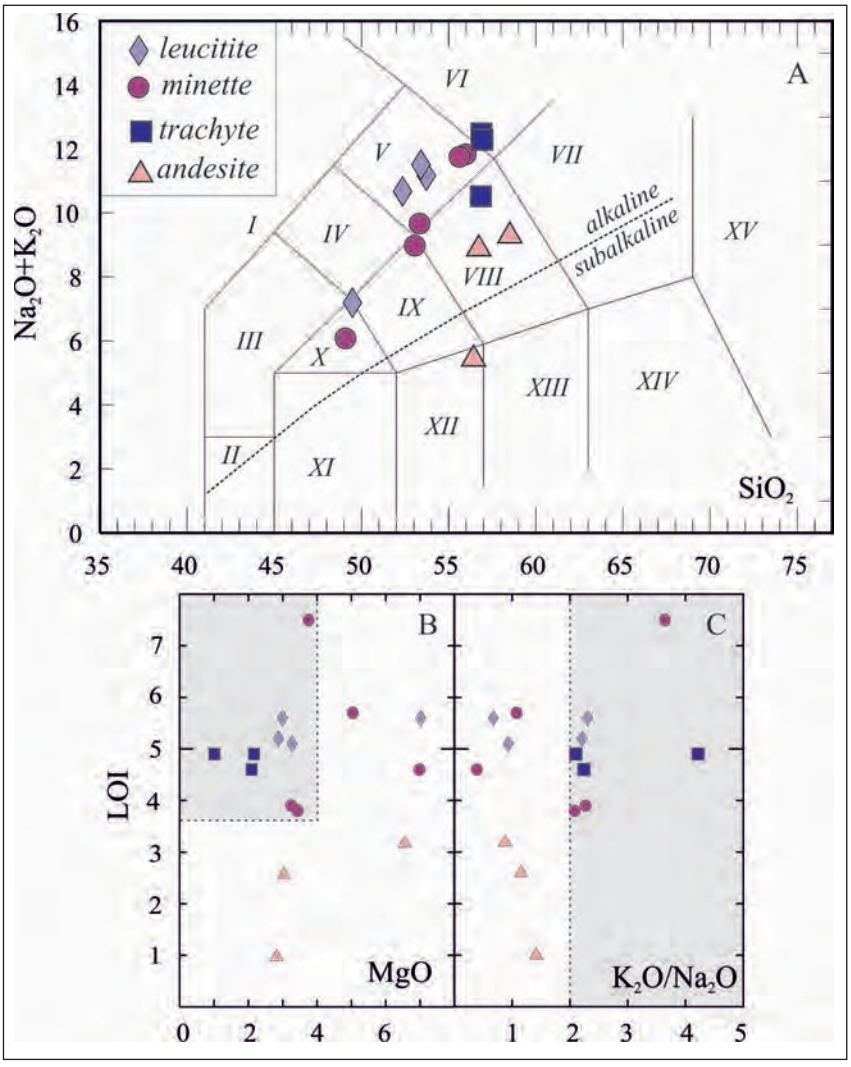

Figure 6- a) The classification of ALCVS ultrapotassic rocks on total alkaline vs. silica diagram (Le Bas, 1986), b) the variation of LOI % with K_2O/Na_2O ratio for leucitites, minettes and trachytes, c) the variation of LOI % with MgO % for leucitites, minettes and trachytes (gray colored area represents samples that yield $K_2O/Na_2O > 2$ condition).

Table 1- Whole rock major, minor and trace element analysis with calculated CIPW norms for Amasya sample.

Sample No	AMS-07	AMS-11	AMS-32	KT-34A	AMS-14	AMS-30	KT-36D	KT-33A	AMS-29	AMS-01	AMS-28	AMS-19	AMS-21	13_05
x	732040	736555	736541	733093	736640	736393	732805	733093	738157	736967	738157	738157	741380	736666
y	4511575	4510507	4510498	4512124	4510200	4510610	4512295	4512124	4511762	4513275	4511762	4511762	4510321	4512961
Rock Type	Leucitite				Minette					Trachyte			Andesite	
SiO_2	49,06	50,35	49,87	46,03	49,49	53,27	52,96	46,13	48,71	53,59	53,81	53,57	53,96	54,66
TiO_2	0,73	0,68	0,69	0,92	0,77	0,64	0,67	1,03	0,92	0,51	0,52	0,51	0,98	0,95
Al_2O_3	17,87	18,34	18,22	13,21	13,82	18,77	18,70	12,99	16,79	18,92	18,7	19,04	12,26	17,37
Fe_2O_3	7,75	6,67	6,53	10,14	7,90	6,03	6,17	10,96	7,9	4,84	4,69	4,62	7,98	6,86
MnO	0,17	0,16	0,15	0,19	0,15	0,13	0,13	0,20	0,27	0,17	0,17	0,14	0,16	0,17
MgO	3,27	2,87	2,99	7,02	5,04	3,25	3,43	6,98	3,75	2,16	2,09	1,01	6,50	2,98
CaO	4,79	4,38	4,37	9,33	8,11	2,04	2,20	10,52	4,45	2,57	3,2	5,72	9,03	5,10
Na_2O	5,18	3,26	3,25	3,99	4,03	3,44	3,63	4,11	1,9	3,79	3,58	1,9	2,76	3,98
K_2O	4,82	7,2	7,49	2,7	4,34	7,82	7,56	1,60	6,93	7,97	8,03	8,01	2,43	4,57
Cr_2O_3	<0.002	<0.002	<0.002	0,011	0,026	0,003	0,003	0,016	<0.002	<0.002	<0.002	<0.002	0,085	0,004
P_2O_5	0,84	0,47	0,46	0,49	0,38	0,37	0,37	0,54	0,5	0,17	0,18	0,16	0,27	0,39
LOI	5,1	5,2	5,6	5,6	5,7	3,9	3,8	4,6	7,5	4,9	4,6	4,9	3,2	2,6
Total	99,59	99,61	99,61	99,62	99,71	99,67	99,67	99,63	99,6	99,58	99,59	99,53	99,63	99,61
CIPW														
Quartz	0,00	0,00	0,00	0,00	0,00	0,00	0,00	0,00	0,00	0,00	0,00	0,18	6,62	1,20
Orthose	28,48	42,55	44,26	15,96	25,65	46,21	44,68	9,46	40,95	47,10	47,45	47,34	14,36	27,01
Albite	25,32	15,99	12,67	18,48	19,69	23,83	23,48	23,25	16,08	20,39	19,58	16,08	23,35	33,68
Anorthite	11,27	14,14	13,00	10,16	6,80	7,70	8,50	12,27	16,82	11,07	11,24	19,77	13,89	16,03
Leucite	0,00	0,00	0,00	0,00	0,00	0,00	0,00	0,00	0,00	0,00	0,00	0,00	0,00	0,00
Nepheline	10,03	6,28	8,03	8,28	7,81	2,86	3,92	6,25	0,00	6,33	5,80	0,00	0,00	0,00
Diopside	3,99	2,16	3,00	23,71	22,46	0,00	0,00	26,15	0,00	0,00	1,80	4,93	20,52	3,17
Wollastonite	0,00	0,00	0,00	0,00	0,00	0,00	0,00	0,00	0,00	0,00	0,00	0,00	0,00	0,00
Hypersthene	0,00	0,00	0,00	0,00	0,00	0,00	0,00	0,00	2,16	0,00	0,00	0,23	6,68	5,95
Olivine	4,41	4,31	4,24	4,55	1,50	5,67	5,99	3,69	5,03	3,77	3,06	0,00	0,00	0,00
Ilmenite	0,36	0,34	0,32	0,41	0,32	0,28	0,28	0,43	0,58	0,36	0,36	0,30	0,34	0,36
Hematite	7,75	6,67	6,53	10,14	7,90	6,03	6,17	10,96	7,90	4,84	4,69	4,62	7,98	6,86
Sphene	0,00	0,00	0,00	0,00	0,00	0,00	0,00	0,00	1,41	0,00	0,00	0,87	1,96	1,86
Perovskite	0,92	0,85	0,89	1,20	1,02	0,00	0,00	1,37	0,00	0,28	0,56	0,00	0,00	0,00
Rutile	0,00	0,00	0,00	0,00	0,00	0,49	0,52	0,00	0,04	0,16	0,00	0,00	0,00	0,00
Apatite	1,99	1,11	1,09	1,16	0,90	0,88	0,88	1,28	1,18	0,40	0,43	0,38	0,64	0,92
Sc	9	8	8	33	21	8	8	36	11	4	5	4	33	17

Table 1- (*continued*)

Co	24,3	17,5	17,3	35,4	23,4	15,5	15,6	37,7	19,5	9,1	9,2	8,9	35,9	18,7
Cs	11,9	4,7	4,1	6,5	5,7	4,2	4,1	4,0	10	18,0	17,7	1,2	0,6	5,0
Ga	16,9	19	17,7	15,6	13,1	16,7	16,1	15,8	20,8	15,5	16,1	18,5	14,5	21,7
Hf	3,1	2,9	3,2	3,2	3,6	4,1	3,9	3,4	4	3,6	4,1	4,2	3,4	5,1
Nb	10,7	15,8	14,4	8,8	9,5	18,2	17,2	8,8	14,1	13,6	13,5	14,1	7,7	16,2
Rb	134,1	279,2	279,5	61,2	89,9	217,7	207,7	99,7	173,9	191,6	199	205,4	54,9	118,8
Sr	845,5	925,2	791,1	533,2	369,9	604,1	578,5	454,9	664,3	825,2	1031,4	1677,9	700,1	889,0
Ta	0,5	0,8	0,9	0,6	0,5	0,9	1,1	0,4	0,7	0,7	0,8	0,7	0,6	0,9
Th	12,5	12,6	11,6	9,2	10,6	15,1	15,2	8,5	9,3	13,7	13,4	13,9	7,7	17,2
U	6,7	4,6	4,5	3,4	3,4	5,0	4,9	3,0	2,8	3,7	4,5	5	2,9	3,2
Zr	127,5	144,3	145	112,2	140,6	172,4	166,5	115,9	168,6	157,7	156,8	158,7	102,2	214,8
Y	21,9	20,6	20,2	24,8	20,7	19,5	20,9	27,1	26,9	21,8	22	22,9	20,7	25,0
La	40,9	39,7	38,2	33,5	37,7	41,5	39,9	33,6	41,2	44,3	42	43,9	27,0	40,9
Ce	81,5	73,8	71,8	66,5	74,1	77,9	77,2	69,8	76,3	77,8	72,9	73,4	54,7	87,9
Pr	9,19	8,58	8,46	8,21	8,12	8,24	8,14	8,90	9,22	7,93	8,03	8,13	6,35	9,60
Nd	37,3	33,4	32,8	32	30,8	29,9	30,9	39,7	35,6	28,8	31,7	31	25,0	38,0
Sm	7,44	7,21	6,53	8,32	6,58	5,87	5,86	8,90	7,77	5,67	5,87	5,95	5,32	8,13
Eu	1,83	1,77	1,85	2,14	1,72	1,57	1,57	2,30	2,16	1,63	1,74	1,71	1,44	2,16
Gd	6,29	5,8	5,64	7,42	5,80	4,83	5,02	7,91	6,62	4,87	5,14	5,11	4,89	7,10
Tb	0,92	0,81	0,8	0,97	0,84	0,75	0,77	1,21	0,99	0,79	0,79	0,77	0,77	0,97
Dy	3,87	4,16	3,95	5,26	4,13	3,79	3,57	5,42	5,21	4,13	4,37	4,15	3,77	4,93
Ho	0,89	0,82	0,76	0,8	0,82	0,78	0,80	1,05	0,97	0,83	0,8	0,78	0,82	0,84
Er	2,03	1,89	2,05	2,15	1,93	2,26	2,11	2,69	2,58	2,36	2,09	2,26	2,22	2,49
Tm	0,32	0,32	0,31	0,36	0,31	0,37	0,35	0,34	0,37	0,40	0,34	0,34	0,34	0,34
Yb	1,83	1,76	1,91	1,79	1,75	2,14	2,02	2,06	2,58	2,29	2,27	2,32	1,87	2,14
Lu	0,31	0,29	0,28	0,3	0,32	0,38	0,33	0,32	0,35	0,35	0,37	0,34	0,33	0,33
Pb	25,8	18,7	21,2	13,1	10,3	21,6	22,2	12,1	4,8	14,7	14,8	24,5	18,5	14,1
Ni	7,0	4,2	3,6	17	27,6	6,9	6,8	17,2	1,4	3,4	3,4	2,9	53,9	9,0

plot on trachy-andesite and phonolite fields. However the samples which plot on the fields of trachy-basalt, basaltic trachy-andesite and trachy-andesite, satisfy the condition of Na_2O - 2 ≤ K_2O, then they were given the names of trachy-basalt, shoshonite and latite (Le Maitre, 2002).

Except a few andesitic samples, the ALCVS volcanic rocks are in alkaline character. Leucitite and minette type rocks display similar major and trace element variations and no significant diversification on Harker-variation diagrams while trachytic rocks are silica-saturated and always represent the most enriched end members. K_2O/Na_2O values in all three rock groups, are quite variable ($0.4 < K_2O/Na_2O < 4.2$). Although leucitites, minettes and trachytes of ALCVS display the effects of alteration since they are the product of an old submarine volcanism, the lack of the marked correlation between LOI with K_2O (Figure 6 b) demonstrates that high K_2O % values have not developed due to the alteration. Beside that some of the samples with the highest MgO% (>5) and highest LOI values, have relatively low K_2O/Na_2O (< 2) ratios, are the evidences showing the migration of potassium to some extent (Figure 6c). Especially, the analcimitization was very thorough processes for leucitites, have caused loss in potassium and gain in sodium in significant amount. However, since there is no any other Na-bearing mineral phase except the analcime in leucitites, the most of Na_2O % contents of these samples could be interpreted as their primary K_2O % values. Additionally high degree carbonatization in minettes and sericitization in trachytes were very common. Although the variable effects of alteration processes on rock groups and their whole rock geochemistry, primary mineral paragenesis of ALCVS volcanic rocks suggest that leucitites, minettes and trachytes are obviously ultrapotassic in character. This is also evident by the modal mineralogical compositions estimated based on CIPW norms that have revealed that leucitites and minettes are Ne-normative (2.28-10.03%). In classical potassic rock classification diagrams of Foley et al., (1987), ALCVS leucitite, minette and trachytes plot on the area resembles Roman Province potassic rocks (Figures 7 a-b).

Leucitite, minette and trachytes display significant enrichment of Large Ion Lithophile (LIL) elements and depletion of High Field Strength (HFS) elements on N-MORB normalized multi-element diagrams (Figure 8). Negative anomalies of Nb and Ta are common for each rock groups. For comparison, one representative calcalkaline andesitic sample is also plotted on each diagram (Figure 8). The patterns of ALCVS ultrapotassic rocks on N-MORB multi-element diagrams (Figure 8a-c) are typical for subduction related rocks. They are also similar with the Enriched Mantle (EM) and with the Oceanic Island Basalts (OIB) in terms of their Ta/Yb and Th/Yb ratios (Figure 9 a), and compared with arc volcanics in terms of their Th contents with Ba/Th

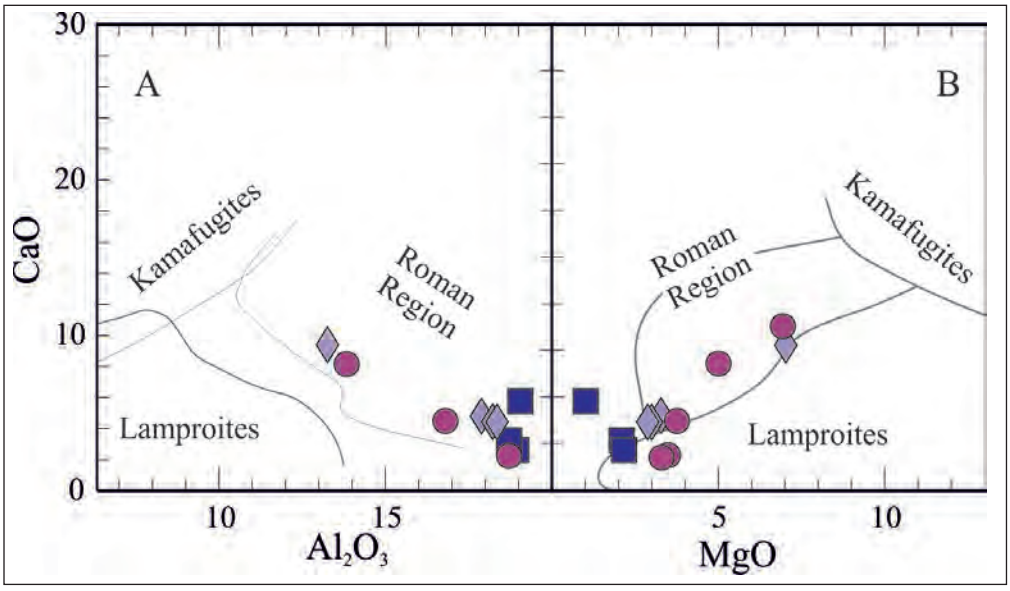

Figure 7- The display of leucitite, minette and trachyte rocks of ALCVS on the classical classification diagram of Foley et al. (1987) for ultrapotassic rocks, a) whole rock CaO % vs. Al_2O_3 % and b) whole rock CaO% vs. MgO% variation diagrams.

ratios (Figure 9 b). High Th/Yb (3.6-8), Ta/Yb (0.2-0.5) and Ba/Th (59.6-156.2) ratios and Th (7.7-17.2 ppm) values observed in all samples (including andesites), suggest a mantle source area which was modified by subduction processes. Another evidence for subduction effect to mantle source comes from negative Ti anomalies on N-MORB normalized multi-element diagrams as it strongly indicates the existence of the Ti-bearing phases such as sphene and rutile in the mantle source region (Figures 8 a-c) (Sun and McDonough, 1989). Besides, the patterns on chondrite normalized multi-element diagrams, suggest that LRE elements significantly enriched compared to HREE, and negative Eu anomaly is negligible (Eu/Eu*=0.83-0.97) (Figures 8 d-f).

7. Differentiation Processes

Trachytes, which are the youngest products of the ALCVS ultrapotassic magmatism within the Pontide forearc basin belt in terms of stratigraphical features and radiochronological data, are also the most evolved members of this magmatism based on their Mg# values (30.22-46.93) and various elemental concentrations (eq. Co: 8.9-9.2 ppm, Ni: 2.9-3.4 ppm). This is best observed on MgO% vs. major and trace element variation diagrams. Trachytes scatter on MgO% vs. SiO_2%, K_2O%, Al_2O_3%, Yb, Th, La and Rb diagrams as the most enriched end members, whereas the most depleted ones on MgO% vs. TiO2, CaO%, Fe_2O_3% and Sc, Co diagrams (Figure 10). This is probably resulted from the fractionation of various minerals. On the other hand, the studies that focus on the related Ne-normative and Qt-normative rocks that were crystallized from single melt, propose that the evolution of magma composition from silica under-saturated to saturated, could only be possible under complicated open system processes (Wilson et al., 1995; Panter et al., 1997).

Tosya region, within the Pontide forearc basin belt, is the area where ultrapotassic trachytes crop out abundantly. Tosya trachytes exhibit the primary contact relationship with metamorphic basement rocks. Trachytic dykes and stocks cut the basement rocks and replace into them differently from Amasya region. In Tosya trachytes accidental quartz originated from basement rocks, are abundant and these samples display quartz-normative composition (Genç et al., 2013).

After evaluating all of the geochemical data of Pontide forearc basin belt ultrapotassic rocks together, it is obvious the ultrapotassic melt differentiation that generate the three lithologies, was achieved by crystallization processes. This is also evident by the MgO% vs. Ta/Zr diagram. The data points of leucititic, lamprophyric and trachytic rocks (taken from Genç et al. 2013) seem to scatter along both of the trend lines resemble FC and AFC processes. The most evolved samples of Amasya trachytes represent the end member products due to the AFC processes whereas leucitites and lamprophyres present no variation on this diagram (Figure 11).

On behalf that the stratigraphical relationships between trachytes with basement rocks and other nepheline-normative ultrapotassic lithologies, with their petrographical features and the geochemical data obtained from Genç et al. (2013), assimilation accompanied during the crystallization of quartz normative trachytes. In order to examine this hypothesis, we modeled adequately AFC processes to answer the question of the degree of crustal assimilation. For this aim, we first decided the best two elements for modeling after checking the correlation coefficients for various elements of our data set and then follow the equations of DePaolo (1981). Therefore the correlation coefficient of these two elements is -0.92, we prefer Co and La. Co, as an compatible element prefer to participate in the solid mineral structure, in contrast La is an incompatible element tend to remain in melt phase. Besides, the sample 11-KT-33 is accepted as to represent the ultrapotassic primitive melt composition. We calculated the possible change of melt composition during the crystallization of hypothetical mineral paragenesis. We also compiled the partition coefficients (K_d) from GERM database. Among the hypothetical fractionation trends on Figure 12, the r_1 curve suggest the lowest crustal assimilation rate. It represents the calculated melt composition based on the $cpx_{0.35} + lc_{0.55} + ph_{0.10}$ mineral paragenesis with $D_{Co} = 3.22$ and $D_{La} = 0.020$ values. The ratio of the crustal assimilant to crystallization rate is up to 1% mostly. The r_2 melt composition is calculated according to the $cpx_{0.25} + am_{0.05} + ph_{0.25} + kf_{0.4} + plg_{0.05}$. mineral composition with $D_{Co} = 6.83$, $D_{La} = 0.022$. The assimilation rate is about 5% in case of r_2 curve of melt composition change. In terms of AFC modeling, it seems that, LCVS ultrapotassic samples tend to follow r_2 curve on La vs. Co diagram (Figure 12) as indicating that the trachytes are the possible products of accompanying assimilation during crystallization in which the rate of assimilant is 5%.

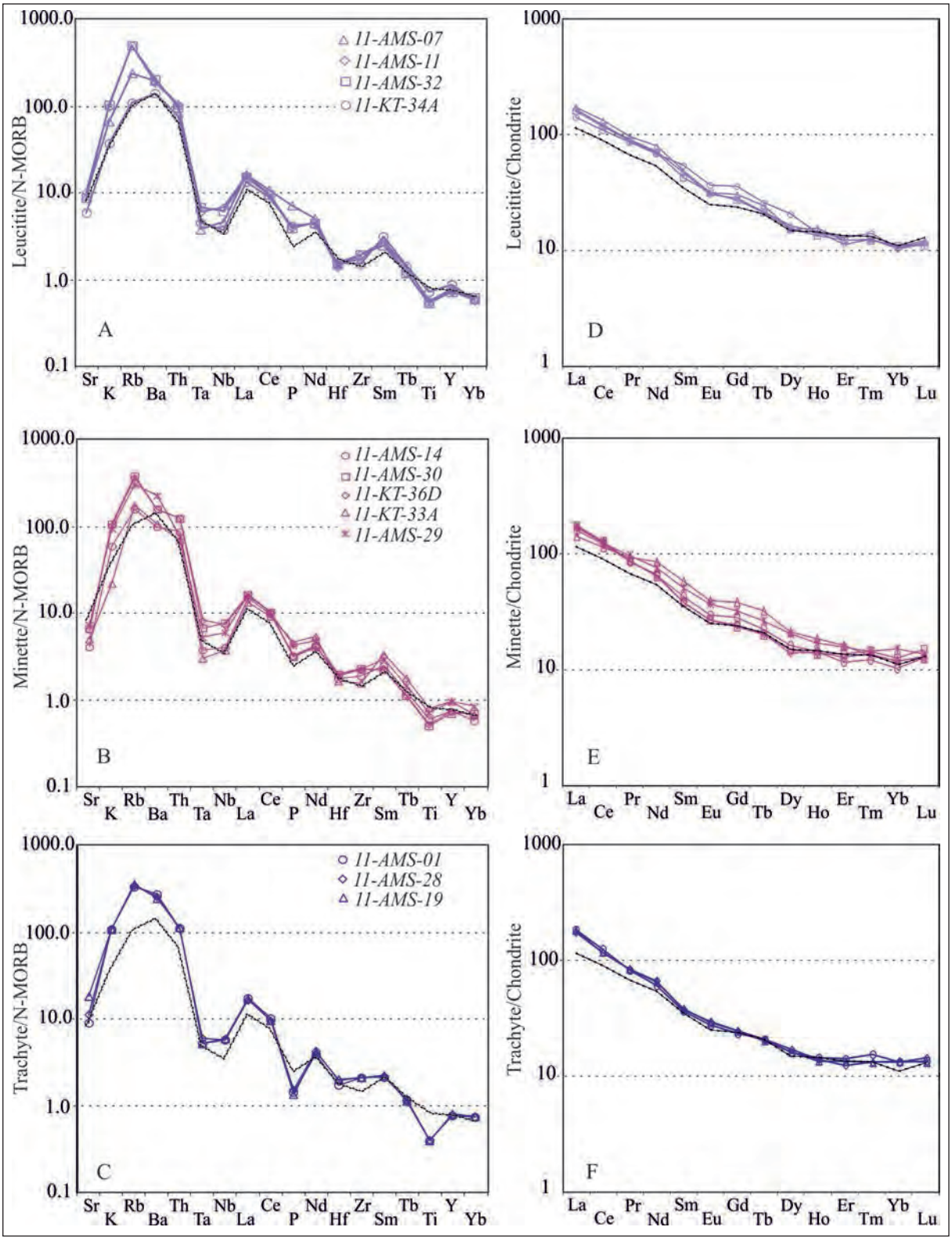

Figure 8- N-MORB and Chondrite normalized multi-element diagrams of ALCVS lava samples (explanations were given within diagrams and text). N-MORB and Chondrite values were taken from Sun and McDonough (1989).

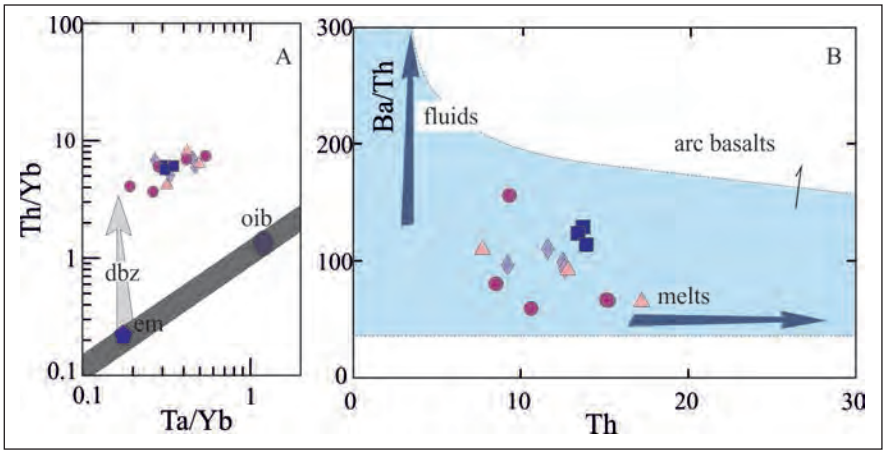

Figure 9- a) The comparison of leucitite, minette and trachyte samples with different source areas in Ta/Yb vs. Th/Yb diagram (Pearce et al., 2005); em and oib areas were taken from Sun and McDonough (1987) (em: enriched source area, oib: oceanic island basalt, dbz: subduction zone enrichment), b) the comparison of samples with arc basalts as the products of subduction modified source areas on Th (ppm) vs. Ba/Th diagram (Hawkesworth et al., 1997).

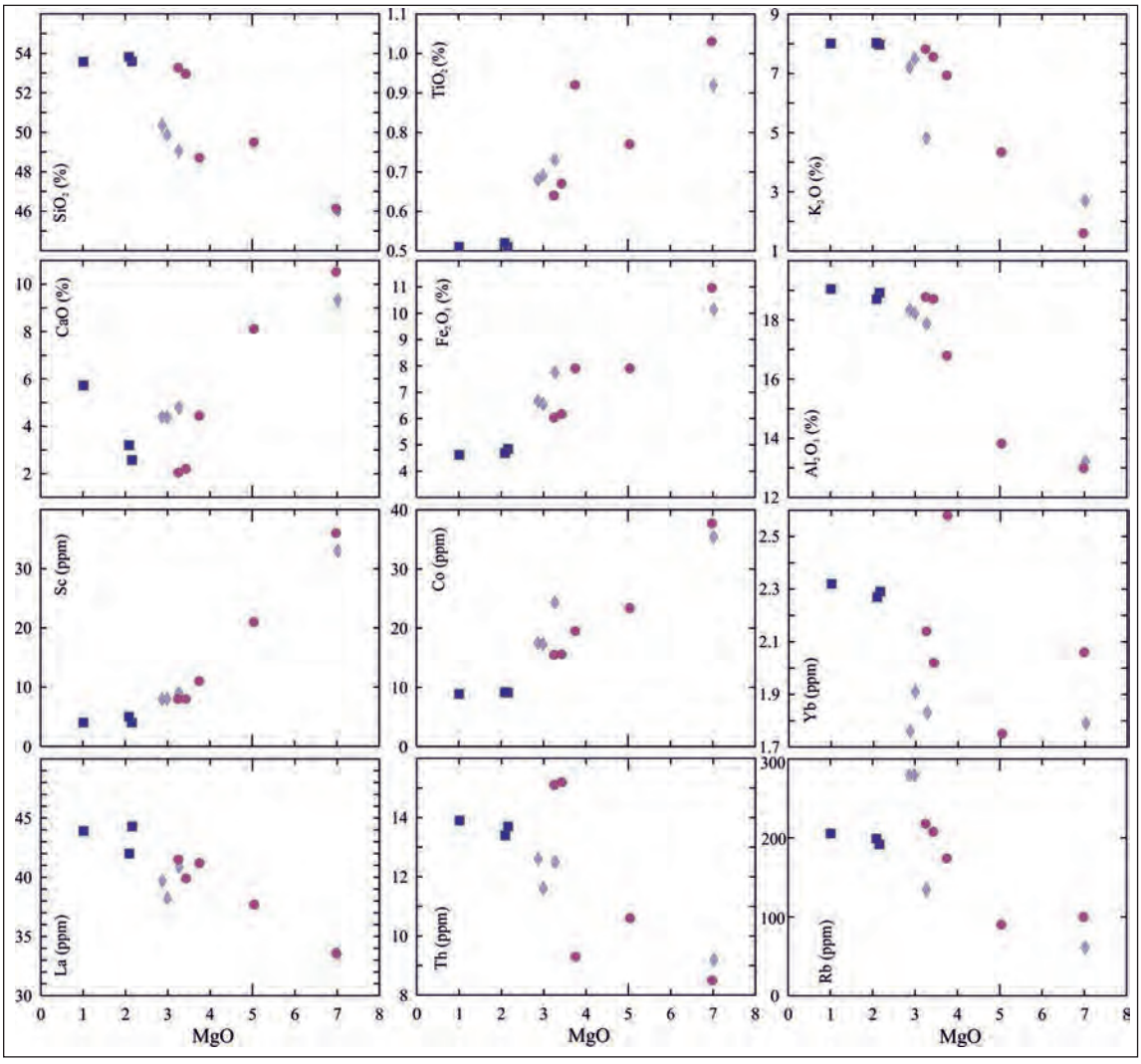

Figure 10- Some major element oxide and trace element variation diagrams MgO (%) values, for the ALCVS lavas.

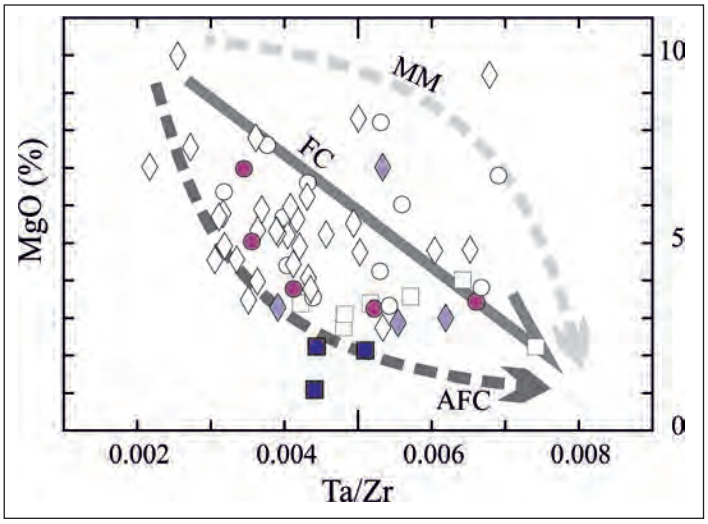

Figure 11- The distribution of samples on Ta/Zr vs. MgO diagram with the expected trend lines fractional crystallization (FC) and assimilation fractional crystallization (AFC) processes. The data for ultrapotassic rocks observed in the belt that continues westward were taken from Genç et al. (2013).

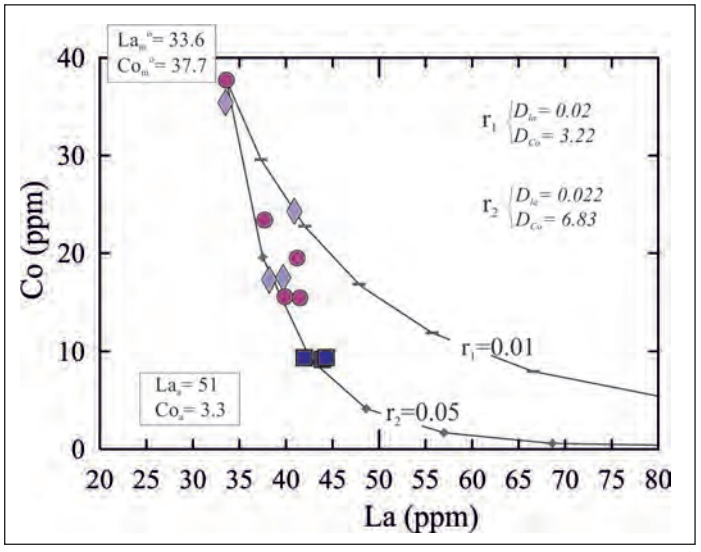

Figure 12- Co vs. La AFC modelling for ALCVS ultrapotassic rocks. See the text for explanations (m: primary melt component, a: pollutant, D: total participation coefficient).

Results

Our main results obtained from this study, are as follows:

- Late Cretaceous ultrapotassic rocks which are observed within Pontide forearc basins, comprise leucitites, minettes and trachytes. Amasya, as a part of Pontide belt, has a significance that it is a location where the all three lithologies coexist.
- Stratigraphical evidences of ALCVS suggest that the ultrapotassic volcanism and deposition of the succession were coeval and the trachytes are the youngest products of this volcanism.
- Radiochronological data is compatible with observations of local stratigraphy as the ultrapotassic volcanism occurred during Campanian time. It also confirms the trachytes are the youngest products of this volcanism.
- The ALCVS ultrapotassic rocks display

geochemical similarities with subduction zone magmatic/volcanic rocks and they associated with each other in time and space due to their common origin, despite they are represented by various lithologies.

- The nepheline normative leucitite and minette type rocks of the ALCVS is evaluated as coeval crystallization products of ultrapotassic melts due to the their field relationships and identical geochemical features (see MgO vs. major and trace element variation diagrams). The differentation between leucitites and minettes, were not controlled by fractional crystallization nor accompanying assimilation processes.
- The differentiation of quartz-normative trachytes which are the youngest products of Late Cretaceous ultrapotassic magmatism, was achieved by assimilation of %5 basement rocks during the crystallization of ultrapotassic melts.

Acknowledgement

This study is a part of the ongoing PhD thesis of Fatma GÜLMEZ (Petrological Evolution and Tectonic Implications of the Late Cretaceous (?) leucite-bearing basalts and lamprophyres of the Ankara-Erzincan Suture Belt). The PhD study was supported by TUBİTAK (Project no: 110Y088) and ITU-BAP Projects coordinated by Prof. Ş. Can GENÇ. The paper refers unpublished data belong to the project with thesis and it cites to abstracts which were presented at international meetings/conferences. We would like to thank to project teams for their contributions in field, office and laboratory studies. We appreciated Prof. Okan TÜYSÜZ as he informed us about the presence of ultrapotassic rocks in Central Pontides.

We would like to thank our TUBİTAK project team members Dr. M. F. Roden (Georgia Univ, USA) and Dr. Z. BİLLOR (Auburn University, USA) for their detailed work on the collection of representative samples for the production of radiochronological data during field studies. We also thank to Assoc. Prof. Yalçın ERSOY for his contributions to AFC modelling.

Received: 04.05.2015
Accepted: 29.05.2015
Published: December 2015

References

Adamia, S. A., Chkhotua, T., Kekelia, M., Lordkipanidze, M., Shavishvili, I., Zakariadze, G. 1981. Tectonics of the Caucasus and adjoining regions: implications for the evolution of the Tethys ocean. *Journal of Structural Geology*, 3(4), pp.437-447.

Alp, D. 1972. Amasya yöresinin jeolojisi. *İ.Ü. Fen Fakültesi Monografileri*, İstanbul, 101 p.

Altherr, R., Topuz, G., Siebel, W., Şen, C., Meyer, H. P., Satır, M., Lahaye, Y. 2008. Geochemical and Sr–Nd–Pb isotopic characteristics of Paleocene plagioleucitites from the Eastern Pontides (NE Turkey). *Lithos* 105(1), pp.149-161.

Asan, K., Kurt, H., Francis, D., Morgan, G. 2014. Petrogenesis of the Late Cretaceous K-rich rocks from the Central Pontide orogenic belt, North Turkey. *Island Arc* 23, pp.102-124.

Baş, H. 1986. Petrology and geochemistry of the Sinop volcanics. *Geological Bulletin of Turkey* 29, 143-56.

Bailey E. B. ve McCallien, W. J. (1950). The Ankara mélange and the Anatolian thrust. *Mineral Research and Exploration Institute of Turkey (MTA) Bulletin* 40, 17-21

Bektaş, O., Gedik, İ. 1988. A new formation with leucite-bearing shoshonitic volcanism in the Kop area (Everekhanları Formation) and its relationship with the evolution of the eastern Pontide arc, NE, Turkey. *Geological Society of Turkey Bulletin* 31, pp.11-19.

Blumenthal, M. M. 1950. Beitreage zur Geologie des Landschaften am Mittleren und untern Yeşilırmak (Tokat, Amasya, Havza, Erbaa, Niksar). *MTA Yayınları*, Seri D, No: 4, Ankara.

Ciobanu, C. L., Cook, N. J., Stein, H. 2002. Regional setting and geochronology of the Late Cretaceous Banatitic magmatic and metallogenetic belt. *Mineralium Deposita*, 37(6-7), pp.541-567.

Conticelli, S., Avanzinelli, R., Poli, G., Braschi, E., Giordano, G. 2013. Shift from lamproite-like to leucititic rocks: Sr–Nd–Pb isotope data from the Monte Cimino volcanic complex vs. the Vico stratovolcano, Central Italy. Chemical Geology. 353, 246-266.

Çapan, U.Z. (1984). Ankara melanjı içindeki zeolitli alkali bazaltik volkanizmanın karakteri ve yaşı hakkında. *Türkiye Jeoloji Kurumu 38. Bilimsel ve Teknik Kurultayı, Bildiri özetleri*: 121–123.

Dalrymple, G.B., Alexander, E.C., Lanphere, M.A., Kraker, G.P. 1981. Irradiation of samples for $^{40}Ar/^{39}Ar$ dating using the geological survey TRIGA reactor. *USGS Professional Paper 1176*, pp.1-55.

DePaolo, D. J. 1981. Trace element and isotopic effects of combined wallrock assimilation and fractional crystallization. *Earth and Planetary Science Letters* 53(2), pp.189-202.

Eyüboğlu, Y. 2010. Late Cretaceous high?K volcanism in the eastern Pontide orogenic belt: Implications for the geodynamic evolution of NE Turkey. *International Geology Review* 52(2-3), pp.142-186.

Foley, S. 1992. Vein-plus-wall-rock melting mechanisms in the lithosphere and the origin of potassic alkaline magmas. Lithos, 28(3), pp.435-453.

Foley, S. F., Venturelli, G., Green, D. H., Toscani, L. 1987. The ultrapotassic rocks: characteristics, classification, and constraints for petrogenetic models. *Earth-Science Reviews 24(2)*, pp.81-134.

Georgiev, S., Marchev, P., Heinrich, C. A., Von Quadt, A., Peytcheva, I., Manetti, P. 2009. Origin of nepheline-normative high-K ankaramites and the evolution of Eastern Srednogorie arc in SE Europe., 50(10), pp.1899-1933.

Gedik., A., Ercan, T., Korkmaz, S. 1983. Orta Karadeniz (Samsun-Sinop) havzası jeolojisi ve volkanik kayaçlarının petrolojisi. *Maden Tetkik ve Arama Genel Müdürlüğü Dergisi* 99, 34-51.

Genç, Ş.C., Tüysüz, O., Karacık, Z., Gülmez, F., Tüysüz, A. 2013. Ankara-Erzincan kenet kuşağı üzerinde yeralan Geç Kretase (?) yaşlı lösitli bazaltlar ile lamprofirlerin petrolojik evrimi ve tektonik anlamı. TÜBİTAK ÇAYDAG Projesi Proje No: 110Y088.

Gülmez, F., Genç, Ş.C., Tüysüz, O., Karacık, Z., Roden, M., F., Billor, M. Z., M. , Hames, W.E. 2014*a*. Geochemistry and petrogenesis of the late Cretaceous potassic-alkaline volcanic rocks from the Amasya Region (northern Turkey), EGU-2013, Vienne, *EGU General Assembly Conference Abstracts* 15, 9833p.

Gülmez, F., Genç, Ş. C., Prelevic, D. 2014*b*. Amasya ve Kalecik civarı Geç Kretase yaşlı alkali volkanik kayalarında taze lösit bulgusu, 67. *Türkiye Jeoloji Kurultayı*, 2014, Ankara, 479p.

Hames, W., Unger, D., Saunders, J., Kamenov, G. 2009. Early Yellowstone hotspot magmatism and gold metallogeny. *Journal of Volcanology and Geothermal Research*, 188(1), pp.214-224.

Hawkesworth, C. J., Turner, S. P., McDermott, F., Peate, D. W., Van Calsteren, P. 1997. U-Th isotopes in arc magmas: Implications for element transfer from the subducted crust. *Science*, 276(5312), pp.551-555.

Koçyiğit, A., Özkan, S., Rojay, B. 1988. Examples from the forearc basin remnants at the active margin of northern Neo-Tethys; development and emplacement ages of the Anatolian Nappe, Turkey. *Middle East Technical University, Ankara-Turkey* 21(1), pp.183-220.

Le Bas, M. J., Le Maitre, R. W., Streckeisen, A., Zanettin, B. 1986. A chemical classification of volcanic rocks based on the total alkali-silica diagram. *Journal of Petrology* 27(3), pp.745-750.

Le Maitre, R. W. 2002. Igneous Rocks: A Classification and Glossary of Terms: A Classification and Glossary of Terms: Recommendations of the International Union of Geological Sciences, Subcommission on the Systematics of Igneous Rocks. *Cambridge University Press UK*, 193 p.

Ludwig, K.R. 2003. User's manual for Isoplot, v. 3.0, a geochronological tool kit for Microsoft Excel. *Berkeley Geochronological Center,* Berkeley, 75 p.

Luhr, J.F., Kyser, T.K. 1989. Primary igneous analcime; Colima minettes. *American Mineralogist* 74 (1-2), pp.216-223.

McKenzie, D. 1989. Some remarks on the movement of small melt fractions in the mantle. *Earth and Planetary Science Letters* 95(1), pp.53-72.

Mederer, J., Moritz, R., Ulianov, A., Chiaradia, M. 2013. Middle Jurassic to Cenozoic evolution of arc magmatism during Neotethys subduction and arc-continent collision in the Kapan Zone, southern Armenia. *Lithos*, 177, pp. 61-78.

Mitchell, R.H., Bergman, S.C. 1991. Petrology of lamproites. *Springer NY*, 446 p.

Nelson, D.R. 1992. Isotopic characteristics of potassic rocks: evidence for the involvement of subducted sediments in magma genesis. *Lithos* 28(3), pp.403-420

Okay, A. I., Şahintürk, O. 1997. Regional and Petroleum Geology of the Black Sea and Surrounding Region. *AAPG Memoir* 68, pp.291-312.

Okay, A.I., Tüysüz, O. 1999. Tethyan sutures of northern Turkey. *Geological Society London*, Special Publications 156(1), pp.475-515.

Panter, K. S., Kyle, P. R., Smellie, J. L. 1997. Petrogenesis of a phonolite–trachyte succession at Mount Sidley, Marie Byrd Land, Antarctica., 38(9), pp.1225-1253.

Pearce, J. A., Stern, R. J., Bloomer, S. H., Fryer, P. 2005. Geochemical mapping of the Mariana arc?basin system: Implications for the nature and distribution of subduction components. *Geochemistry, Geophysics, Geosystems* 6(7), Q07006, doi:10.1029/2004GC000895

Reading, H. G. (Ed.) 2009. Sedimentary environments: processes, facies and stratigraphy. *John Wiley and Sons*, 704 p.

Rock, N. M. 1991. Lamprophyres. Blackie, *Glasgow, UK*. 285 p.

Rojay, B. 1995. Post-Triassic evolution of Central Pontides: evidence from Amasya region, northern Anatolia., 31, pp.329-350.

Sosson, M., Rolland, Y., Müller, C., Danelian, T., Melkonyan, R., Kekelia, S., Adami, S., Babazadeh, V., Kangarli, T., Avagyan, A., Galoyan, G., Mosar, J. 2010. Subductions, obduction and collision in the Lesser Caucasus (Armenia, Azerbaijan, Georgia), new insights. *Geological Society London, Special Publications*,340(1), pp.329-352.

Sun, S., McDonough, W.F. 1989. Chemical and isotopic systematics of oceanic basalts: implications for mantle composition and processes. Saunders, A.D., Norry, M.J. (Eds.),Magmatism in the ocean basins. *Geological Society Special Publication* 42, pp. 313-345

Şengör, A. M.C., Yılmaz, Y. 1981. Tethyan evolution of Turkey: a plate tectonic approach. *Tectonophysics* 75(3), pp.181-241.

Şengör, A. M. C., Tüysüz, O., İmren, C., Sakınç, M., Eyidoğan, H., Görür, N., Le Pichon, X., Rangin, C. 2005. The North Anatolian fault: A new look. *Annu. Rev. Earth Planet. Sci*.,33, pp.37-112.

Tankut, A., Dilek, Y. ve Önen, P. (1998). Petrology and geochemistry of the Neo-Tethyan volcanism as revealed in the Ankara melange, Turkey. *Journal of Volcanology and Geothermal Research*, 85(1), 265-284.

Topuz, G., Göçmengil, G., Rolland, Y., Çelik, Ö. F., Zack, T., Schmitt, A. K. 2013. Jurassic accretionary complex and ophiolite from northeast Turkey: No evidence for the Cimmerian continental ribbon. *Geology* 41(2), pp.255-258.

Tüysüz, O. 1996. Geology of Amasya and surroundings. *11th Petroleum Congress of Turkey*, Proceedings, Ankara, pp.32-48.

Tüysüz, O., Dellaloğlu, A. A. ve Terzioğlu, N. (1995). A magmatic belt within the Neo-Tethyan suture zone and its role in the tectonic evolution of northern Turkey. *Tectonophysics*, 243(1), 173-191.

Varol, E. (2013). The derivation of potassic and ultrapotassic alkaline volcanic rocks from an orogenic lithospheric mantle source: the case of the Kalecik district, Ankara, Central Anatolia, Turkey. *Neues Jahrbuch für Mineralogie-Abhandlungen*, 191(1), 55-73.

Wilson, M., Downes, H., Cebriar, J. M. 1995. Contrasting fractionation trends in coexisting continental alkaline magma series; Cantal, Massif Central, France. *Journal of Petrology* 36(6), pp.1729-1753.

Yagi, K., Ishikawa, H., Kojima, M. 1975. Petrology of a lamprophyre sheet in Tanegashima Islands, Kagoshima Prefecture, Japan. *Journal of. Japan Association of Mining, Petroleum and Economic Geologist* 70 (7), pp.213-224.

Yılmaz, Y., Tüysüz, O., Yiğitbaş, E., Genç, Ş.C. Şengör, A.M.C. 1997. Geology and tectonic evolution of the Pontides, In: A.G. Robinson (Ed.) Regional and Petroleum Geology of the Black Sea and Surrounding Region. AAPG Memoir 68, pp.183-226.

Bull. Min. Res. Exp. (2015) 151: 169-215

Bulletin of the
Mineral Research and Exploration

http://dergi.bulletin.gov.tr

GEOLOGICAL FEATURES OF NEOGENE BASINS HOSTING BORATE DEPOSITS: AN OVERVIEW OF DEPOSITS AND FUTURE FORECAST, TURKEY

Cahit HELVACI[a]*

[a] *Dokuz Eylül Üniversitesi, Jeoloji Mühendisliği Bölümü Tınaztepe Yerleşkesi, 35160 Buca/İzmir TURKEY*

Keywords:
Neogene borate basins, İzmir-Balıkesir Transfer Zon, Menderes Metamorphic Complex, Borate Deposits, Overview of Deposits, Future Forecast, West Anatolia.

ABSTRACT

The geometry, stratigraphy, tectonics and volcanic components of the borate bearing Neogene basins in western Anatolia offer some important insights into on the relationship between basin evolution, borate formation and mode of extension in western Anatolia. Some of the borate deposits in NE-SW trending basins developed along the İzmir-Balıkesir Transfer Zone (İBTZ) (e.g. Bigadiç, Sultançayır and Kestelek basins), and other deposits in the NE-SW trending basins which occur on the northern side of the Menderes Core Complex (MCC) are the Selendi and Emet basins. The Kırka borate deposit occurs further to the east and is located in a completely different geological setting and volcanostratigraphic succession. Boron is widely distributed; including in soil and water, plants and animals. The element boron does not exist freely by itself in nature, but rather it occurs in combination with oxygen and other elements in salts, commonly known as borates. Approximately 280 boron-bearing minerals have been identified, the most common being sodium, calcium and magnesium salts. Four main continental metallogenic borate provinces are recognized at a global scale. They are located in Anatolia (Turkey), California (USA), Central Andes (South America) and Tibet (Central Asia). The origin of borate deposits is related to Cenozoic volcanism, thermal spring activity, closed basins and arid climate. Borax is the major commercial source of boron, with major supplies coming from Turkey, USA and Argentina. Colemanite is the main calcium borate and large scale production is restricted to Turkey. Datolite and szaibelyite are confined to Russia and Chinese sources. Four Main borax (tincal) deposits are present in Anatolia (Kırka), California (Boron), and two in the Andes (Tincalayu and Loma Blanca). Kırka, Boron and Loma Blanca have similarities with regard to their chemical and mineralogical composition of the borate minerals. Colemanite deposits with/without probertite and hydroboracite are present in west Anatolia, Death Valley, California, and Sijes (Argentina). Quaternary borates are present in salars (Andes) and playa-lakes and salt pans (USA-Tibet). Boron is a rare element in the Earth's crust, but extraordinary concentrations can be found in limited places. The formation of borate deposits can be classified as follows: a skarn group associated with intrusives and consisting of silicates and iron oxides; a magnesium oxide group hosted by marine evaporitic sediments; and a sodium– and calcium–borate hydrates group associated with playa-lake sediments and explosive volcanic activity. Some conditions are essential for the formation of economically viable borate deposits in playa-lake volcano-sedimentary sequences: formation of playa-lake environment; concentration of boron in the playa lake, sourced from andesitic to rhyolitic volcanics, direct ash fall into the basin, or hydrothermal solutions along graben faults; thermal springs near the area of volcanism; arid to semi-arid climatic conditions; and lake water with a pH of between 8.5 and 11. A borate is defined as any compound that contains or supplies boric oxide (B_2O_3). A large number of minerals contain boric oxide, but the three that are most important from a worldwide commercial standpoint are borax, ulexite, and colemanite, which are produced in a limited number of countries. Turkey has the largest borax, ulexite and colemanite reserves in the world and all the world's countries are dependent upon the colemanite and ulexite reserves of Turkey.

* *Corresponding author: Cahit Helvacı, cahit.helvaci@deu.edu.tr*

Most of the world's commercial borate deposits are mined by open pit methods. Brines from Searles Lake, and presumably the Chinese sources, are recovered by either controlled evaporation or carbonation. Boric acid is one of the final products produced from most of the processes. Further research on the mineralogy and chemistry of borate minerals and associated minerals will the production and utilization of borate end-products. Many modern industries need industrial borate minerals, and many people use their products. In addition, boron is essential to plant life, and by extension, all life so it's hard to imagine our world without using it. Therefore, borates and their products are critical to the Sustainable Development of the world.

1. Introduction

Borate history is very ancient: derived from the Persian burah (boorak), borax was already known to the Babylonians who brought it from the Himalayas some four thousand years ago for use in the manufacture of rings, amulets, and bracelets. The Egyptians used borax in mummifying, and around 300 AD the Chinese were familiar with borax glazes, as were the Arabs three centuries later. Borax was first brought to Europe in the 13th century, presumably by Marco Polo, and since that time by traders from Tibet and Kashmir.

By the 1770s, the French had developed a source of tincal, the old name for crude borax, in Purbet Province, India, and about the same time natural boric acid (sassolite) was discovered in the hot springs in the Maremma region of Tuscany, Italy. The middle of the nineteenth century was a particularly active time for the discovery and commercial development of borate deposits. In particular, Chile started to mine the borate resources of the Salar de Ascotan in 1852 and within a few years their output accounted for a quarter of the world's annual supply of 16.000 tons. In 1856 John Veatch discovered borax in Clear Lake, Lake County, California, which led eventually to the start up of the California Borax Company in 1864 and to beginning of that states dominance of the borate industry. In Turkey modern borate mining began in 1865 when the Compagnie Industrialle des Mazures mined borates from the Aziziye Mine near Susurluk and shipped the ore back to France for processing. Demand encouraged exploitation of large-scale deposits in Turkey and the United States and overwhelmed more modest producers (Travis and Cocks, 1984).

Borates are among the most interesting of the worlds industrial minerals, first for precious metal working and later in ceramics. They form an unusually large grouping of minerals, but the number of commercially important borates is limited, and their chemistry and crystal structure are both unusual and complex. The accounts of the early exploration, mining, and processing of borates are fascinating, because their remote locations often led to unusual difficulties, and hardships in recovering the desired products. This varied from workers wading into Himalayan lakes to harvest the "floor" and then transport the borax in saddlebags on sheep across the Himalayas to the markets, to the "Dante's Inferno" of the Larderello boric acid fumaroles, to the colourful 20-mule teams of the western United States (Kistler and Helvacı, 1994; Helvacı, 2005).

The early history of borate mining in Turkey goes back to Roman times. Substantial amounts of borates have been produced in Turkey since the end of the 1800s. In 1885, a French company was operating the Sultançayırı mine in Balıkesir province. There is a record of production since 1887, which indicates that production has been continuous to the present day except for war periods. Until 1954 all recorded production came from Sultançayır, but since 1950 extensive exploration has resulted in the discovery of several important new Turkish deposits. Bigadiç deposit; Balıkesir province, has operated since 1950, and major production in the M. Kemalpaşa deposit (Kestelek), Bursa province, began in about 1952. In 1956 the Emet borate deposits, Kütahya province, were discovered accidentally by Dr. J.Gawlik whilst carrying out a survey of lignite deposits for MTA. After the discovery, the Emet deposits became the main source of colemanite in the western world. Finally, the most outstanding discovery was the Kırka borate deposit which is mainly a massive borax body, with estimated reserves several times greater than those of Boron, California (İnan, 1972; Baysal, 1972; Arda, 1969; Travis and Cocks, 1984; Dunn, 1986; Kistler and Helvacı, 1994; Helvacı, 2005). Today, however, borate mining is confined to four distinct areas in Turkey: Emet, Kırka, Bigadiç and Kestelek. Turkey is currently the largest producer of borate minerals and has the world's largest reserves. Production more than doubled in 1980 to over one million tonnes (approximately 1.500.000 tonnes) and further increases, particularly of borax from Kırka, are likely to lead to Turkey dominating the world

markets. Already Turkey is the major world producer of colemanite, much of which comes from the Emet valley (e.g. 2500 metric tons in 2011). The Eti Maden planned to expand its share in the world boron market from 36% to 39% by 2013, increasing sales to $1 billion by expanding its production facilities and product range.

Boron chemistry and reactivity are also fascinating because they form a wide variety of oxygen compounds that occur in an essentially unending variety of simple to exceedingly complex molecules. Determining their crystal structures has given rise to a separate subfield of crystallography. The boron isotopes ^{10}B and ^{11}B, varying widely in nature and their different reactivity during both physical and chemical changes means that they are an important tool in predicting many geologic and other events, again forming a specialized field in geology. Borates are defined by industry as any compound that contains or supplies boric oxide (B_2O_3). A large number of minerals contain boric oxide, but the three that are the most important from a worldwide commercial standpoint are: borax, ulexite and colemanite. These are produced in a limited number of countries dominated by the United States and Turkey, which together furnish about 90% of the world's borate supplies. Production in the United States originated in the Mojave Desert of California; borax and kernite are mined from a large deposit at Boron. Borate containing brines are pumped from Searles Lake, and a limited amount of colemanite is mined from Death Valley. There are over 40 borate deposits located along an 885 km trend in the high Andes near the common borders of Argentina, Bolivia, Chile, and Peru, of which at least 14 are currently in production. Turkish production is controlled by Eti Maden/Etibor, the national mining enterprise, which supplies most of the commercially traded ulexite and colemanite from mines in the Bigadiç and Emet districts, plus borax from the huge deposit at Kırka (Kistler and Helvacı, 1994; Helvacı and Alonso, 2000; Helvacı, 2005).

The most important worldwide borate deposits occur in western Anatolia and have been the topic of several papers which dealt with their genesis (İnan, 1972; Baysal, 1972; Helvacı, 1983; 1984; 1986; Kistler and Helvacı, 1994; Helvacı, 1995; Palmer and Helvacı, 1995; 1997; Helvacı and Orti, 1998; Helvacı and Alonso, 2000; Helvacı, 2004; 2005). They originated in Tertiary continental lacustrine basins during a period characterized by intense magmatic activity affecting western Anatolia. These borate deposits are interbedded with volcanosedimentary rocks (Floyd et al., 1998; Helvacı and Alonso, 2000). The Borate deposits and associated sedimentary rocks were deposited within playa lake environments. These borate deposits show differences between them and the associated sedimentary deposits are mainly represented by claystone, sandstone and limestone.

In this study, new stratigraphic, volcanic and tectonic observations from these basins will be presented in order to outline the main features of the borate bearing basins, and couple them with data from the other basins to produce a tectono-stratigraphic evolutionary model for borate formation within western Anatolia. Recent age data are presented here in order to determine the age of borate formation in western Anatolia. A short review of the borate deposits and future forecasts will also be outlined.

2. Geology

Western Turkey, the easternmost part of the Aegean extensional province, is one of the most famous regions in the world that have been studied in respect of both scientific and economic aspects (Helvacı and Yağmurlu, 1995; Helvacı and Alonso, 2000; Ersoy et al., 2014). The Geological history of western Anatolia is related to Alpine-contractional and subsequent-extensional tectonic activities. The region also contains many industrial raw-material deposits (borates, zeolites, clays, coal etc.) and metallic mines (Au, Ag, Pb, Zn etc.) (Helvacı and Yağmurlu, 1995). These commercial deposits are mainly related to Alpine extensional tectonics that occurred after Oligocene time. This time interval is marked by intense crustal deformation, plutonic-volcanic activity and terrestrial sedimentation; accompanied by formation of metallic deposits and industrial minerals such as gold, silver and borates. The areas located in a region that hosts both gold and boron deposits in the Neogene volcano-sedimentary rock units are the subject of this paper (Helvacı and Alonso, 2000; Yiğit, 2009).

2.1. General Characteristics of the Neogene Basins in Western Anatolia

Western Anatolia has been the focus of many geological studies of the classical extensional tectonics in this region. The NE–SW-trending Neogene volcano-sedimentary basins that characterize western Anatolia, are mainly located on the northern part of the Menderes Massif – a

progressively exhumed mid-crustal metamorphic unit that has undergone Neogene extensional tectonics in the area (Yılmaz et al., 2000; Helvacı et al., 2006; Ersoy et al., 2014). The NE–SW-trending basins are Bigadiç, Gördes, Demirci, Selendi, Emet, Güre and Uşak basins. Many studies have been carried out in these basins and different evolutionary models have been proposed by various authors for the stratigraphic and tectonic evolution of these NE–SW-trending volcanosedimentary basins. The NE–SW-trending basins were deformed by NE–SW and NW–SE-trending faulting during the late Miocene, and by E–W-trending normal faulting in the Pliocene–Quaternary. The region has been extended in a N–S-direction since at least the early Miocene, and that this extension occurred episodically in several phases. Recent studies show that there was a close relation in both space and time between the basin formation and the progressive exhumation of the Menderes Massif (Helvacı et al., 2006; Ersoy et al., 2014).

The stratigraphy, tectonics and volcanic components of the Neogene basins in western Anatolia offer some key insights into the relationship between the basin evolution and mode of extension in this intensely and chaotically deformed and extended area. With the present-day configurations, two main types of Neogene basins are recognized in the western Anatolia: (a) NE–SW and (b) ~E–W trending basins. Stratigraphy and tectonic features of the NE-SW trending basins reveal that their evolution was more complex. The E–W-trending basins are typical grabens which are still being deformed under ~N–S-extension (Ersoy et al., 2014).

The NE–SW-trending basins which occur on the northern side of the Menderes Core Complex (MCC), are the Demirci, Selendi, Uşak-Güre and Emet basins. The basins, formed on the MCC were evolved as successive supra-detachment basins and include two main sedimentary sequences: the early Miocene Hacıbekir Group and the early-middle Miocene İnay Group (Helvacı et al., 2006; Ersoy et al, 2011). There are also NE–SW-trending basins developed along the İzmir-Balıkesir Transfer Zone (İBTZ) (Kestelek, Sultançayır, Bigadiç and Gördes basins). The sedimentary infill of the basins developed on the İBTZ show distinct sequences and is controlled by mainly strike-slip and subsidiary normal faults (Helvacı et al., 2006; Ersoy et al., 2012).

2.2. Basement Units of the Neogene Basins

The Aegean–western Anatolia region is composed of several continental blocks that were originally separated by the northern branch of the Neo-Tethys marked today by the Vardar-İzmir-Ankara Suture (Figure 1; Şengör and Yılmaz, 1981). The Vardar-İzmir-Ankara Suture separated the Sakarya continent to the north and the Anatolide–Tauride block to the south and was formed by late Mesozoic northward subduction and accretion (Figure 1, Şengör and Yılmaz, 1981). The southernmost part of the region is marked by the south Aegean volcanic arc, which is formed from subduction of the African plate along the Hellenic trench (Pe-Piper and Piper, 2007).

The geology of western Anatolia is characterized by Tertiary volcano-sedimentary deposits covering a basement that includes several continental fragments and suture zones. Western Anatolia has a complex history of Late Cenozoic tectonic and magmatic activity. The basement units comprise; (1) the Menderes and Cycladic massifs, (2) the İzmir-Ankara Zone (comprising; (a) the Bornova flysch zone, (b) the Afyon zone, and (c) the Tavşanlı zone), (3) the rocks of the Sakarya Continent to the north, and (4) the Lycian Nappes to the south (Şengör and Yılmaz, 1981; Figure 1).

The region has experienced several tectonic events including subduction, obduction, continental collision and subsequent crustal thickening, extension and crustal thinning, that occurred between several continental blocks and suture zones (Figure 1). These were finally shaped by the Alpine orogeny related to Neo-Tethyan events (Şengör and Yılmaz, 1981). The main continental blocks are, from north to the south, the Sakarya zone of the Rhodope-Pontide Fragment and the Menderes Massif of the Anatolides. These two blocks are separated by the İzmir-Ankara zone that represents closure of a northward subducted Neo-Tethyan oceanic realm. The Menderes Massif is also overlain by the Lycian Nappes to the south. The İzmir-Ankara zone was formed by late Paleocene to early Eocene closure of the northern branch of the Neo-Tethys Ocean between the Sakarya continent and the Anatolide block, with the latter including the Menderes Massif and the Lycian Nappes (Şengör et al. 1984; Şengör and Yılmaz, 1981; Okay et al., 1996). The Menderes Massif is tectonically overlain by several nappes of the İzmir-Ankara Zone to the west and north, and by the Lycian nappes mainly to the south and east. In the west, the nappes are generally composed of graywackes and limestones

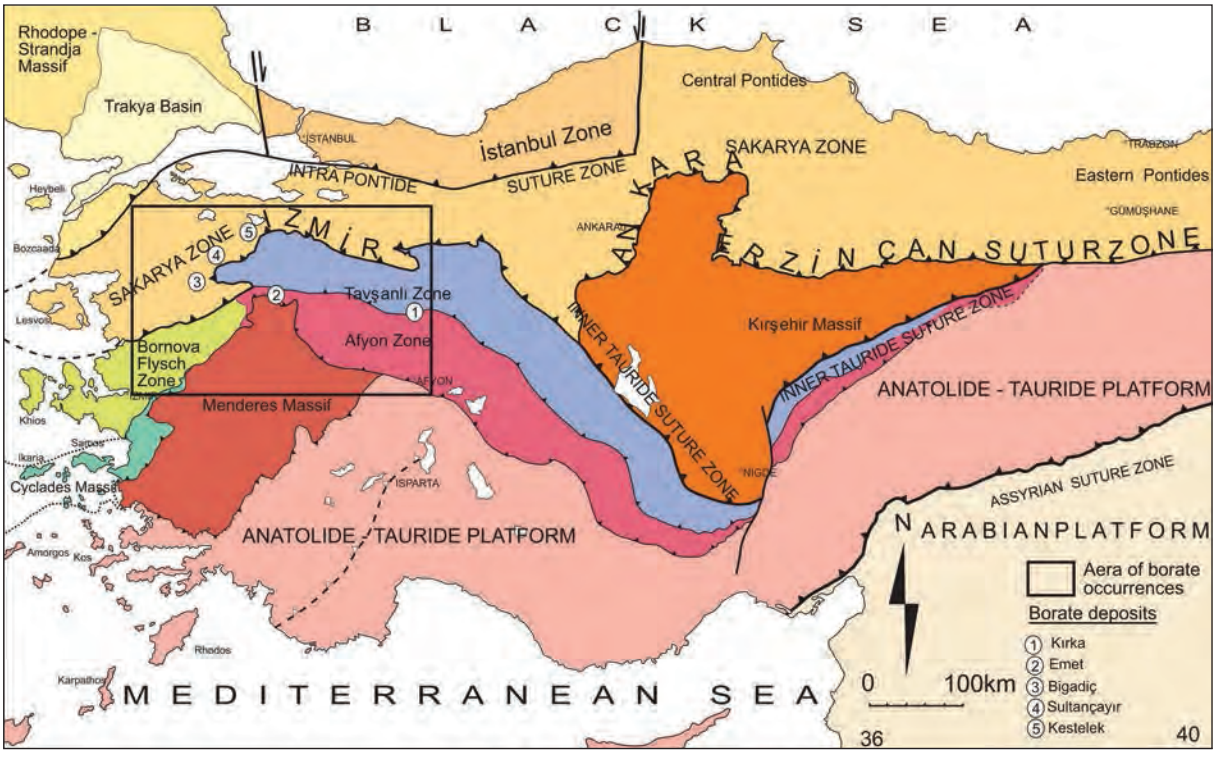

Figure 1- Tectonic map of the northeastern Mediterranean region showing the major sutures and continental blocks. Sutures are denoted by heavy lines, with the polarity of former subduction zones indicated by filled triangles. The Eocene plutonic belts in the Sakarya and Tavşanlı zones are shaded purple. The map was modified by Helvacı et al. (2014) using Şengör (1984), Okay (1989) and Okay et al. (1994, 1996).

with ophiolitic rocks of the Bornova flysch zone, while to the northeast, they are metaclastics, metabasites, and recrystallized limestones of the Afyon zone (Figure 1).

The İzmir-Ankara zone comprises the Bornova Flysch zone, the Afyon zone and the Tavşanlı Zone. The Bornova Flysch Zone comprises chaotically deformed Upper Maastrichtian – Palaeocene greywacke and shale with Mesozoic neritic limestone blocks of several kilometers in diameters (Okay et al., 1996). The Tavşanlı Zone forms a blueschist belt, representing the northward subducted passive continental margin of the Anatolide-Tauride platform (Okay et al., 1996). The Afyon zone comprises shelf-type Devonian to Palaeocene sedimentary sequence metamorphosed to greenschist facies (Okay et al., 1996).

2.3. Neogene Basins and Volcanism in Western Anatolia

Exhumation of the Menderes Massif resulted in the formation of several NE–SW-trending basins on its northern flank (the Demirci, Selendi, Güre and Emet basins), and was accompanied by strike-slip faulting and related basin formation along the İzmir-Balıkesir Transfer Zone in the west (Gördes basin; Bozkurt, 2003; Helvacı et al., 2006; Ersoy et al., 2011). The Miocene volcanic rocks occur in NE–SW-trending supra-detachment basins developed on the metamorphic rocks of the Menderes Massif (Yılmaz, 1990; Yılmaz et al., 2000; Helvacı et al., 2009; Karaoğlu et al., 2010; Ersoy et al. 2010, 2011; Ersoy et al., 2012).

The Geological evolution of western Anatolia during Neogene time is characterized by basin formation and contemporaneous wide-spread volcanic activity. The basins in the region were developed mainly in two directions: NE- and E–W-trends (Figure 2). The main NE-trending basins in the region are Bigadiç, Gördes, Demirci, Selendi and Uşak-Güre basins, while the E–W-trending basins are characterized by actively deforming grabens such as the Simav, Gediz, Büyük Menderes and Küçük Menderes grabens. The E–W-trending basins are younger in age and cut the NE-trending basins (Figure 2).

Several models have been proposed concerning the development of these basins in western Anatolia.

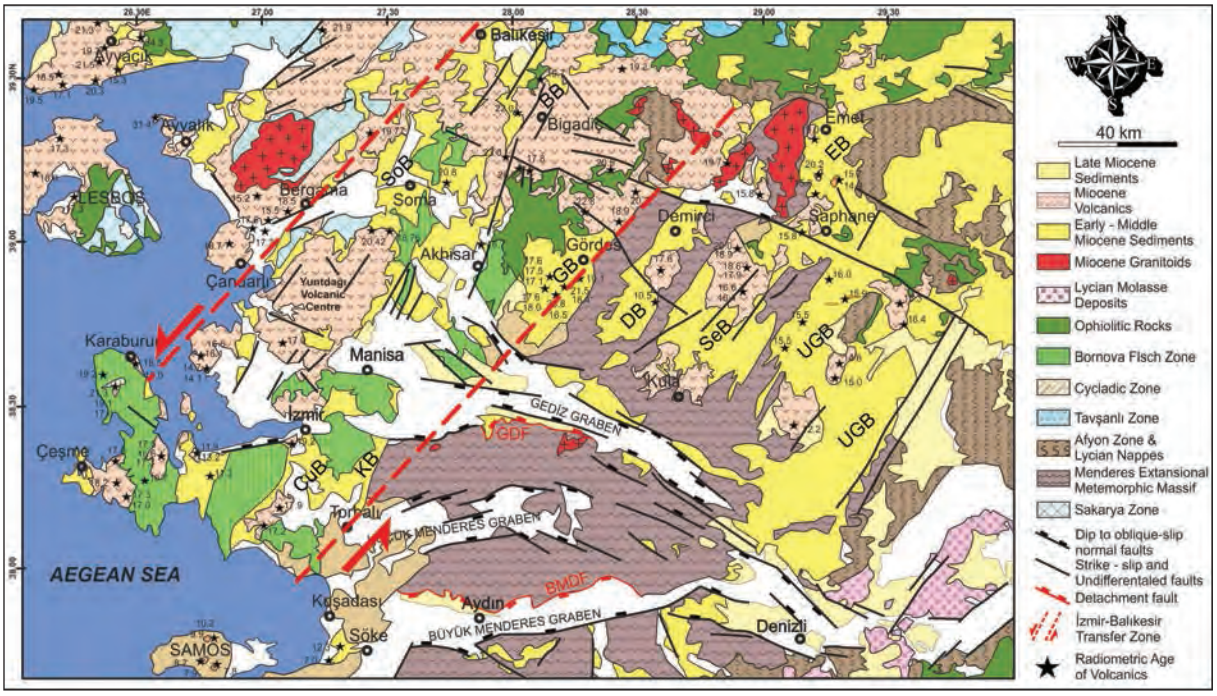

Figure 2- Geological map of the western Anatolia showing the distribution of the Neogene basins, radiometric ages of the volcanic intercalations in the Neogene sediments and major structures (modified from 1/500,000 scaled geological map of Turkey (MTA); and studies cited in the text). Abbreviations for granitoids: EyG: Eybek, KzG: Kozak, AG: Alaçamdağ, Kog, Koyunoba, EG: Eğrigöz, BG: Baklan, TG: Turgutlu and SG: Salihli granitoids. Abbreviations for basins: KB: Kocaçay Basin, BB: Bigadiç Basin; CuB: Cumaovası Basin; SoB: Soma Basin, GB: Gördes Basin, DB: Demirci Basin, SeB: Selendi Basin, UGB: Uşak–Güre Basin, EB: Emet Basin. Abbreviations for detachments: GDF: Gediz (Alaşehir) Detachment Fault, SDF: Simav Detachment Fault, BMDF: Büyük Menderes Detachment Fault (after Ersoy et al., 2014).

These are the cross-graben model, the orogenic collapse model, the two-stage episodic extension model, and the pulsed extension model (Şengör, 1987; Seyitoğlu and Scott, 1996; Purvis and Robertson, 2004). The NE-SW trending basins host the world class huge borate deposits, which are the main subject of this paper. The western Anatolian extensional basins are also rich in terms of geothermal energy resources due to their extensional tectonic setting and high heat flow (Çemen et al., 2014).

In western Anatolia, volcanic rocks from the latest Oligocene to Quaternary can be divided into two groups based on their chemical composition with temporal and spatial distribution (Yılmaz, 1990; Güleç, 1991; Seyitoğlu and Scott 1992; Ercan et. al. 1996; Seyitoğlu et al. 1997; Yılmaz et al. 2000; Aldanmaz et al. 2000). The magmatic rocks of the Late Oligocene - Early Miocene time are mainly rhyolite to basaltic andesite in composition and exhibit calc-alkaline and shoshonitic affinity. These rocks are enriched in HREE with respect to LILE and LREE, and have higher $^{87}Sr/^{86}Sr$ and lower $^{143}Nd/^{144}Nd$ isotopic composition (e.g., Bingöl et al., 1982; Güleç 1991; Aldanmaz et al. 2000). There is a time break in volcanic activity from the end of the Middle Miocene to beginning of the Late Miocene in western Anatolia (Yılmaz,1990). The volcanic rocks of mainly Late Miocene – Early Pliocene and are more basic in composition and exhibit an alkaline character. These rocks are depleted in HREE and enriched in LILE, HFSE, MREE and LREE. The volcanic rocks of the Late Miocene – Early Pliocene exhibit lower $^{87}Sr/^{86}Sr$ and higher $^{143}Nd/^{144}Nd$ isotopic ratios (Güleç,1991; Aldanmaz et al., 2000). In addition, the alkaline basaltic volcanism in the Miocene-Pliocene changed from a potassic to a sodic character (Kula volcanics: Güleç, 1991; Alıcı et al., 2002; table 2 and figure 8).

The geologic evidence indicates that the evolution of the magmatic activity in the region was related to post-collisional extensional tectonics and that the Miocene volcanic rocks in the NE–SW trending basins were emplaced during early-middle Miocene

episodic exhumation of the Menderes Massif as a core complex. The Menderes Massif was asymmetrically uplifted and collapsed, starting from the north and continuing to the south during the early to middle Miocene. The high-K calc-alkaline, shoshonitic, and ultrapotassic volcanic rock groups were produced during this interval in the region. Geochemical data show that the origin of the high-K calc-alkaline volcanics include crustal contributions to the mantle-derived magmas. While rhyolites dominated during the early Miocene, more primitive andesites are seen during the middle Miocene. At the same time, rapid increase in the amount of the ultrapotassic and shoshonitic volcanic rocks is compatible with lithospheric thinning (Ersoy et al., 2012).

In the NE-trending basins, the late Cenozoic volcanic activity is represented mainly by Early-Middle Miocene calc-alkaline moderate to felsic volcanic rocks and Plio-Quaternary alkaline volcanism. In addition to these, in the Bigadiç Basin, Early Miocene alkali basaltic volcanism has been documented (Helvacı and Erkül, 2002; Helvacı et al., 2003; Erkül et al., 2005*b*). To the east, the data show that the alkaline volcanism had already begun in the Early Miocene in the NE-trending basins, and alkaline lamproitic volcanic rocks were also introduced (Ersoy and Helvacı, 2007).

Volcanic intercalations in the NE–SW-trending Neogene volcano-sedimentary basins can be grouped as: early Miocene high-K calc-alkaline andesite, dacite and rhyolite; early-Miocene mafic volcanics; middle Miocene high-K calcalkaline andesite and dacite; middle Miocene mafic volcanics; Late Miocene mafic lavas; and Quaternary alkali basaltic volcanism.

Early-Miocene mafic volcanic units in Bigadiç basin comprise the Gölcük basalt (calc-alkaline shoshonite), which differs from the other early-Miocene mafic samples of the Selendi and Emet basins that have higher K contents (shoshonitic to ultrapotassic Kuzayır lamproite and Kestel volcanics). The early Miocene volcanism in all the NE–SW-trending basins is characterized by a bimodal volcanic association, dominated by calc-alkaline dacitic–rhyolitic members. During the early Miocene, wide-spread dacitic-rhyolitic volcanism occurred in the region (Helvacı and Erkül, 2002; Erkül et al., 2005*b*; Ersoy and Helvacı, 2007).

The middle Miocene volcanism in the region is characterized by a second-stage bimodal volcanic association, including a group of high-K calc-alkaline to andesites and dacites, and a group of shoshonitic to ultrapotassic mafic products such as lamproites, ultrapotassic shoshonites and ultrapotassic latites. These volcanic rocks interfinger with the Middle Miocene İnay Group in the Demirci, Selendi, Güre and Emet basins (Ersoy and Helvacı, 2007).

During the late Miocene a volcanic rocks group (comprising mildly alkaline basalts, K-trachybasalt and shoshonites) were produced which are characterized by the absence of the felsic magmas, and occur only in the Demirci and Selendi basin. Finally, the Quaternary is represented by the strongly alkali group of basaltic (tephrite, basanite, phonotephrite) volcanic activity emplaced on the northern flank of the Gediz graben (Kula volcanics). Overall, it is apparent that the volcanic rocks in the different basins can be correlated into distinct groups on the basis of their geochemical properties and ages of eruption (Ersoy et al., 2014).

The Neogene volcanic activity in western Anatolia was developed contemporaneously with development of NE-trending basins, giving rise to formation of thick volcano-sedimentary successions and several mineral deposits. In this respect, tectonic evolution of the Neogene basins, especially of the NE-trending ones, is a fundamental theme in studying the Neogene volcanic evolution as well as the related mineral deposits of the region. The stratigraphy of the basin fills and volcanic units are summarized in figure 3. Tectonic evolution of the NE-trending basins seems to be related to exhumation of the Menderes Massif. This episode took place in the region during the early Miocene. E–W trending grabens began to develop later. Both stages were accompanied by volcanic activity. Therefore, it is clear that tectonic shaping of the basins played a key role in the volcanic evolution and deposition of the borate and other related mineral deposits of the region.

The Miocene borate deposits of western Turkey are associated with extensive medium- to high-K calc-alkali ignimbritic volcanism and a differentiated comagmatic alkaline trachybasalt–trachydacite lava suite. Ignimbritic air-fall and reworked pumiceous clastic materials are intimately associated with the lake sediments that host the borate deposits. Local ignimbritic volcanism is considered to be the primary source of the B for the Kırka and other borate deposits. The geochemical composition of the ignimbrites associated with the borates exhibit a

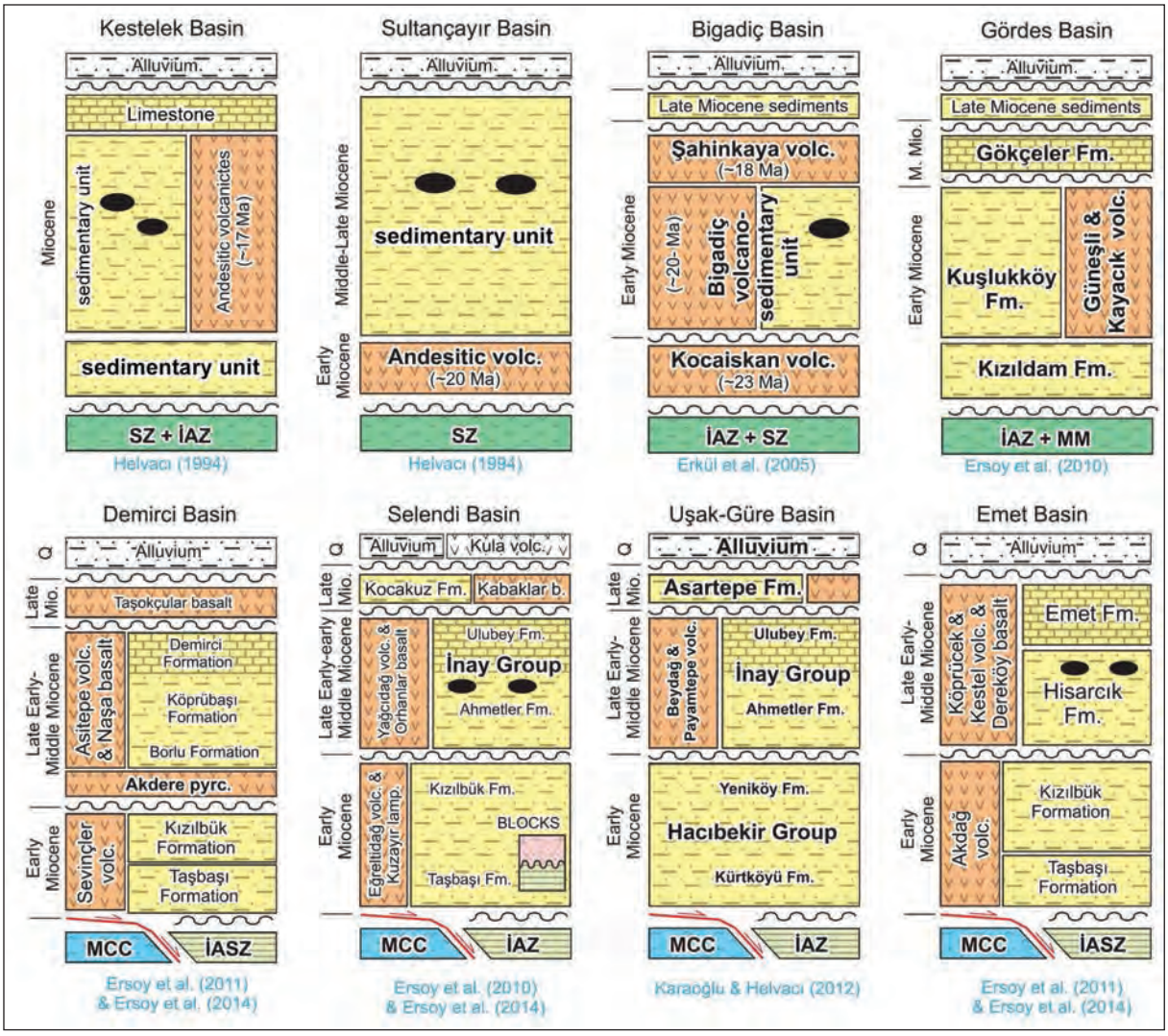

Figure 3- Stratigraphic columnar sections of the borate bearing basins in Western Anatolia. MM-metamorphic rocks of the Menderes Massif, İAZ-İzmir-Ankara zone rocks, SZ-metamorphic rocks of the Sakarya zone, MCC- Metamorphic Core Complex (modified after Ersoy et al., 2014).

number of features that might prove useful in the exploration for borates in similar volcanic domains. In particular, 'fertile' ignimbrites generally belong to a high-K calc-alkali suite, are well-evolved and fractionated (Kr/Rb is low) with a high-silica rhyolitic bulk composition, exhibit a combined high content of B, As, F, Li and Pb, with high Br/La and Br/K ratios, and a mildly fractionated REE pattern and large positive Eu anomaly (Floyd et al., 1998). Other apparent discriminants involving both compatible and incompatible elements are largely a function of different degrees of partial melting and fractionation. It is suggested that the initial source of the B and other associated elements was from LIL-rich fluids released by the progressive dehydration of altered oceanic crust and pelagic sediments in a subduction zone. The absence or presence of sediments in a segmented subduction zone may influence the variable lateral distribution of borates in active margins on a global scale. Once the crust has become enriched in B via previous or contemporary subduction-related calc-alkali magmatism, the effects of tectonic environment, climate and hydrothermal activity influence the local development of the deposits (Floyd et al., 1998).

3. Stratigraphic Correlation of Neogene Borate Bearing Basins

The stratigraphic and structural features of the Selendi, Demirci, Emet and Güre basins are compared with the adjacent Kestelek, Sultançayır, Bigadiç and Güre basins in figure 2 and 3.

The Neogene volcano-sedimentary succession in Bigadiç basin contains the Kocaiskan volcanics (23.6±0.6–23.0±2.8 Ma, table 1) that are composed of andesitic volcanics and the unconformably overlying Bigadiç volcano-sedimentary succession (Figure 3). The latter consists of borate-bearing lacustrine sediments and coeval felsic (Kayırlar, Sındırgı and Şahinkaya volcanics; 20.8±0.7–17.8±0.4 Ma K–Ar and Ar/Ar ages) and mafic (Gölcük basalt,19.7±0.4 Ma K–Ar and 20.5±0.1 Ma Ar/Ar ages) volcanic rocks (Helvacı, 1995; Helvacı and Alonso, 2000; Helvacı and Erkül, 2002; Helvacı et al., 2003; Erkül et al., 2005*a,b*). These rock units are unconformably overlain by late Miocene–Pliocene continental sediments detritus and alluvium. The radiometric ages and the stratigraphic relationships clearly indicate that the borate-bearing succession was deposited during the early Miocene and is very similar to that of Gördes basin (Figure 3).

The NE–SW-trending Gördes basin contains a similar volcanosedimentary sequence to that of Bigadiç basin. These two basins are characterized by a main early Miocene volcano-sedimentary sequence. The early Miocene volcano-sediments of Gördes basin were controlled by NE–SW-trending dextral strike- to oblique-slip and E–W-trending dip-slip normal faults. Gördes and Bigadiç basins are transtensional basins that developed during the early Miocene (Ersoy et al., 2012). The data presented here clearly show that the Demirci, Selendi, Emet and Güre basins have similar stratigraphic, geochemical and tectonic characteristics. The basin-fill of these Neogene basins are characterized by; (a) Lower Miocene Hacıbekir Group, (b) Middle Miocene İnay Group, (c) locally developed late Miocene sedimentary and basaltic volcanic rocks and (d) Quaternary sediments and basaltic volcanics, which are separated by regional-scale major unconformities (Figure 3; Ercan et al., 1978, 1983; İnci, 1984; Seyitoğlu, 1997*a,b*; Yılmaz et al., 2000; Ersoy and Helvacı, 2007; Ersoy et al., 2010). However, the Bigadiç and Gördes basins have distinct stratigraphic and tectonic features from the other NE–SW-trending basins. In that they are characterized by early Miocene volcano-sedimentary successions which were deposited along early Miocene strike-slip and related normal faults.

The NE–SW-trending Demirci, Selendi, Emet and Güre basins, which developed on the Menderes Core Complex, have similar stratigraphies that comprise two main volcano- sedimentary successions: the Lower Miocene Hacıbekir Group, and the unconformably overlying Middle Miocene İnay Group. These two groups are locally overlain by late Miocene volcanic and sedimentary units and recent sediments. The Lower Miocene Hacıbekir Group in the Demirci, Selendi, Emet and Güre basins was deposited in a supra-detachment basin formed on the Simav detachment fault (SDF). The Hacıbekir Group consists of conglomerates of the Kürtköyü formation and sandstone–mudstone alternations of the Yeniköy formation in the Demirci, Selendi and Güre basins and Taşbaşı and Kızılbük formations in the Emet basin. The İnay Group is intercalated with several syn-sedimentary andesitic to rhyolitic lava flows, dykes and associated pyroclastics in the Demirci, Selendi, Emet and Gördes basins.

In the Emet basin, the Köprücek volcanics (16.8±0.2 Ma K–Ar age; Helvacı and Alonso, 2000) crop out to the northern part of the Emet basin. The unit is composed of andesitic to rhyolitic lava flows, dykes and associated pyroclastics which interfinger with the Hisarcık formation. The thickness of the pyroclastic intercalations in the Hisarcık formation increases towards the north of the basin (Helvacı and Ersoy, 2006; Helvacı et al., 2006; Ersoy et al., 2012; figures 2 and 3). The Köprücek volcanics are overlain by the limestones of the Emet formation. In the southern part of the basin, the Hisarcık formation sediments is also conformably overlain by basaltic lava flows of the Dereköy basalt. Along the basal contact of the Dereköy basalt several pepperitic textures are developed, indicating a syn-sedimentary emplacement of the lavas. The Dereköy basalt has been dated as 15.4±0.2 and 14.9±0.3 Ma (K–Ar ages, Seyitoğlu et al., 1997; Helvacı and Alonso, 2000; table 1).

The Kırka borate deposit occurs further to the east and is located in completely different geological setting and volcanostratigraphic succession.

As far as the economic potentional of Neogene basins is concerned, a limited number of basins in western Turkey contain world class borate reserves, with mineralization present as stratabound deposits in Neogene volcano-sedimentary successions. These sediments, as well as being enriched in B, are variably enriched in Li, S, Sr and As. Potential sources for these elements include lacustrine sediments, local basement rocks and volcanism with hot spring activity. Volcanism occured throughout the sedimentary infilling of these basins, as shown by the presence of tuffaceous sediments, volcanic clasts in conglomerates, interbedded and cross cutting lavas

Table 1- Radiometric age data from the volcanic rocks associated with the borate bearing Neogene basins in western Anatolia.

Basin and Unit	Sample	Rock type	Radiometric Age (Ma), Material	References
Kestelek Basin				
	KE-1	*Trachandesitic tufff*	*17.4±0.3 (hornblend, K/Ar)*	
Sultançayır Basin				*Helvacı and Alonso, 2000*
	S-1	*Rhyolitic tuf*	*20.0 ± 0.5 (feldspar, K/Ar)*	
Bigadiç Basin				
Kocaiskan volcanics	*F-110*	*Andesite*	*23.00 ± 2.80 (biotite, K–Ar)*	
Gölcük Basalt	*F-199*	*Shoshonite*	*19.70 ± 0.40 (groundmass, Ar–Ar)*	
	F-199	*Shoshonite*	*20.50 ± 0.10 (groundmass, Ar–Ar)*	
Sındırgı volcanics	*F-194*	*Rhyolite*	*20.20 ± 0.50 (biotite, Ar–Ar)*	*Helvacı and Erkül, 2002; Helvacı et al., 2003; Erkül et al., 2005b*
	F-197	*Dacite*	*20.30 ± 0.30 (biotite, Ar–Ar)*	
Şahinkaya volcanics	*F-195*	*B. andesite*	*17.80 ± 0.40 (hornblende, K–Ar)*	
Kayırlar volcanics	*F-214*	*Latite*	*20.60 ± 0.70 (biotite, K–Ar)*	
Çamköy basalt	*B-6*	*Basalt*	*18.30 ± 0.20 (feldspar, K–Ar)*	*Helvacı, 1995*
Gördes Basin				
Kayacık volcanics	*LB-1*	*Dacite*	*16.90 ± 0.50 (biotite, K–Ar*	*Seyitoğlu et al., 1992*
	TSB	*Rhyolite*	*18.10 ± 0.50 (biotite, K–Ar)*	
	S2/5	*Rhyodacite*	*20.45 ± 0.38 (feldispat, Ar/Ar)*	*Purvis and Robertson, 2005*
	S2/11	*Acidic tuff*	*21.71 ± 0.04 (biotite, Ar/Ar)*	
Güneşli volcanics	*S2/68*	*Acidic tuff*	*17.04 ± 0.35 (biotite, Ar/Ar)*	
	861	*Rhyolite*	*18.91 ± 0.03 (sanidite, Ar/Ar)*	
Demirci Basin				
Sevinçler volcanics	*721*	*Dacite*	*19.06 ± 0.05 (plagioclase, Ar/Ar)*	*Helvacı and Ersoy, 2006; Helvacı et al., 2006; Ersoy et al., 2012*
	721	*Dacite*	*19.56 ± 0.04 (biotite, Ar/Ar)*	
Asitepe volcanics	*717*	*Andesite*	*17.58 ± 0.09 (plagioclase, Ar/Ar)*	
Naşa basalt	*ÖD-50*	*Shoshonite*	*15.80 ± 0.30 (whole rock, K–Ar)*	*Ercan et al., 1996*
Selendi Basin				
Eğreltidağ volcanics	*SE-1*	*Rhyolite*	*18.90 ± 0.60 (biotite, K–Ar)*	*Seyitoğlu et al., 1997*
	521	*Dacite*	*18.90 ± 0.10 (plagioclase, Ar/Ar)*	*Helvacı and Ersoy, 2006; Ersoy et al., 2008*
	521	*Acidic tuff*	*20.00 ± 0.20 (amphibole, Ar/Ar)*	
Kuzayır lamproiti	*518*	*Lamproite*	*17.90 ± 0.20 (groundmass, Ar/Ar)*	
	518	*Lamproite*	*18.60 ± 0.20 (phlogopite, Ar/Ar)*	
Yağcıdağ volcanics	*SE-3*	*Trachydacite*	*14.90 ± 0.60 (biotite, K–Ar)*	*Seyitoğlu et al., 1997*
	S1/3	*Acidic tuff*	*16.42 ± 0.99 (feldspar, Ar/Ar)*	*Purvis and Robertson, 2005*
	YF-2	*Dacite*	*16.43 ± 0.32 (plagioclase, Ar/Ar yaşı)*	*Helvacı and Ersoy, 2006; Helvacı et al., 2006; Ersoy et al., 2012*
Uşak–Güre Basin				
Beydağ volcanics				
Elmadağ volc. center	*U-31*	*Trachydacite*	*16.28 ± 0.05 (biotite, Ar/Ar)*	*Helvacı et al., 2009; Karaoğlu et al., 2010*
	U-68	*Pyroclastic*	*16.48 ± 0.08 (biotite, Ar/Ar)*	
İtecektepe volkanic center	*UG-63*	*Dacite*	*14.60 ± 0.30 (whole rock, K–Ar)*	*Seyitoğlu et al., 1997*
	U-159	*Dacite dike*	*15.04 ± 0.10 (biotite, Ar/Ar)*	*Helvacı et al., 2009; Karaoğlu et al., 2010*
Beydağ volkanic center	*U-161*	*Daciteik dome*	*12.15 ± 0.15 (biotite, Ar/Ar)*	
	U-2	*Dacite*	*13.10 ± 0.20 (whole rock, K–Ar)*	*Ercan et al., 1996*
Payamtepe volcanics				
Yeniköy dikes	*UG-58*	*Trachydacite*	*15.10 ± 0.40 (whole rock, K–Ar)*	*Seyitoğlu et al., 1997*
	U-153	*Trachyte*	*16.01 ± 0.08 (sanidine, Ar/Ar)*	*Helvacı et al., 2009; Karaoğlu et al., 2010*
Karabacaklar volcanics	*U-144*	*Trachyte*	*15.93 ± 0.08 (groundmass, Ar/Ar)*	
	UG-75	*Trachyte*	*15.90 ± 0.40 (whole rock, K–Ar)*	*Seyitoğlu et al., 1997*
Kıran basalt	*UG-145*	*UK Latite*	*15.50 ± 0.40 (whole rock, K–Ar)*	
Güre lamproite	*IZ-38*	*Lamproite*	*14.20 ± 0.12 (groundmass, Ar/Ar)*	*Innocenti et al., 2005*
	05GÜ02	*Lamproite*	*15.54 ± 0.33 (groundmass, Ar/Ar)*	*Preleviç et al., 2012*
Emet Basin and Gediz–Şaphane Region				
Akdağ volcanics	*E6*	*Rhyolite*	*20.20 ± 0.40 (biotite, K/Ar)*	*Seyitoğlu et al., 1997*
	E-3	*Rhyolite*	*19.00 ± 0.20 (biotite, K/Ar)*	
Köprücek volcanics	*E-1*	*Pyroclastic*	*16.80 ± 0.20 (biotite, K/Ar)*	*Helvacı and Alonso, 2000*
Dereköy basalt	*E9*	*UK latite*	*15.40 ± 0.20 (feldspar, K/Ar)*	
	E3	*UK latite*	*14.90 ± 0.60 (whole rock, K–Ar)*	*Seyitoğlu et al., 1997*
	So7-15	*UK latite*	*15.70 ± 0.50 (whole rock, K–Ar)*	*Çoban et al., 2012*
Kestel volcanics	*821*	*UK latite*	*15.91 ± 0.07 (biotite, Ar/Ar)*	*Helvacı and Ersoy, 2006; Helvacı et al., 2006; Ersoy et al., 2012*
	821	*UK latite*	*15.73 ± 0.11 (biotite, Ar/Ar)*	
Kırka Basin				
	K-2(1)	*Rhyolite*	*18.5±0.2 (biotite, K/Ar)*	*Helvacı and Alonso, 2000*
	K-2	*Rhyolitic ignimbrites*	*19.0±0.2 (biotite, K/Ar)*	
	2a-1			
	(K1-955.8m)	*Basalt*	*18.63±0.2 (New Ar/Ar data)*	
	2a-2			
	(K6-1063m)	*Trachyte*	*18.69±0.04 (New Ar/Ar data)*	*Helvacı and Yücel-Öztürk, 2013;*
	2c	*Lamproite lavas*	*16.91±0.05 (New Ar/Ar data)*	*Seghedi and Helvacı, 2014*
	2d(K-1)	*Trachyte*	*16.1±0.2 (feldspar, K/Ar)*	

and travertines from hot spring activity. Research in this area has involved mapping and sampling of the volcanic successions, K-Ar dating and detailed geochemical analysis of these lavas, as well as determination of the relationships with interfingered sediments. Data from Bigadiç, Emet and Kırka basins show that early volcanism is acidic and largely calc alkaline, although sometimes alkaline, whereas later volcanism is intermediate and exclusively alkaline. K-Ar dating of volcanic samples from the borate basins indicate that the first phase of volcanism occurred in the Early Miocene with the second phase in the Middle Miocene. Field evidence from the basins indicates that the acidic volcanism occurred prior to and during borate mineralisation whilst the intermediate alkaline volcanism occurred later. Correlation of the geochemical characteristics of the volcanic units will help us to understand the interrelationships between the formation of the borate deposit, gold mineralization, and volcanic evolution of the region.

In order to establish the role of local volcanism as a source of boron, the relationship between volcanism and associated sediments in the Emet (colemanite deposit), Bigadiç (colemanite and ulexite) and Kırka (borax deposit) basins were studied for comparison. Chemical study of volcanic rocks associated with the borate deposits of Kırka, Emet, Bigadiç, Kestelek and Sultançayır districts have been performed. The geochemical work has focussed on boron and trace elements distribution on volcanics belonging to two main stages of magmatic activity. High boron contents have been found in volcanics coming from outcrops surrounding the borate deposits. The volcanics of Lower-Middle Miocene age are mainly andesites to rhyolites of calk-alkaline affinity and show a range in B from 25 to 270 ppm. Consistently lower values (19-67 ppm) are shown by volcanites of Upper Miocene age (Helvacı, 1977; Fytikas et al., 1984; Floyd et al., 1998; Helvacı and Alonso, 2000) having shoshonitic and potassic affinities. In addition, REE have patterns typically linked to their affinity and degree of evolution, although secondary mobilization can not be exclude in order to explain some negative Ce anomalies observed. Presence of widespread secondary minerals (e.g. zeolites, calcites) supports the hypothesis of interaction with circulating shallow level water. In light of the present data the high B contents in these rocks can be explained by interaction between the volcanics and circulating boron-rich hot water. Magmatic activity may have been responsible for generating a high thermal gradient in the study area which provided the energy to drive thermal circulating water that was able to mobilize boron from sedimentary and volcanic sequences. An alternative hypothesis for generating such borate deposits is suggested by the presence in several deposits of volcanic rocks interfingered with sediments forming peperitic textures. This indicates there may have been direct contributions of volcanics and magmatic volatiles to the lacustrine basins (Erkül et al., 2006).

3.1. Bigadiç, Susurluk and Kestelek Basins

The stratigraphy of these basins was investigated by Helvacı (1983, 1995) and Erkül et al. (2005*b*). The basin-fill that lies unconformably above the basement rocks, includes Upper Cretaceous–Palaeocene Bornova Flysch Zone, Lower–Middle Eocene Başlamış formation and Oligocene detrital rocks (Erdoğan, 1990; Okay and Siyako 1991) and is represented by two distinct volcan-sedimentary associations separated by a basin-wide angular unconformity. Volcanism in the Bigadiç area is characterized by two rock units that are separated by an angular unconformity. These units are: (1) the Kocaiskan volcanics that gives K/Ar ages of 23 Ma, and (2) the Bigadiç volcano-sedimentary succession within the borate deposits that yields ages of 20.6 to 17.8 Ma (Figure 3). Both units are Early Miocene in age and are unconformably overlain by Upper Miocene-Pliocene continental deposits. The Kocaiskan volcanics are related to the first episode of volcanic activity and comprise thick volcanogenic sedimentary rocks derived from subaerial andesitic intrusions, domes, lava flows and pyroclastic-rocks.

The Kocaiskan volcanics, which are andesitic in composition, are the earliest volcanic products of the Early Miocene period, covering an area larger than 800 km^2 within the study area. The K/Ar age data indicate that the Kocaiskan unit is 23.0±2.8 Ma old, consistent with previous measurements (Table 1). The unit comprises andesitic intrusions, lavas, pyroclastic rocks and associated volcanogenic sedimentary rocks, which are unconformably overlain by the Lower Miocene Bigadiç volcano-sedimentary succession (Helvacı and Erkül, 2002; Helvacı et al., 2003; Erkül et al., 2005*b*).

The Bigadiç volcano-sedimentary succession, is a Miocene sequence comprising volcanic (e.g. Sındırgı volcanics, Gölcük basalt, Kayırlar volcanics and Şahinkaya volcanics) and lacustrine rocks (e.g. lower limestone unit, lower tuff unit, lower borate unit, upper tuff unit and upper borate unit) (Helvacı, 1995; Erkül et al., 2005*b*) (Figure 3).

The second episode of volcanic activity is represented by basaltic to rhyolitic lavas and pyroclastic rocks, accompanied by lacustrine–evaporitic sedimentation. Dacitic to rhyolitic volcanic rocks, called the Sındırgı volcanites, comprise NE-trending intrusions producing lava flows, ignimbrites, ash-fall deposits and associated volcanogenic sedimentary rocks. Other NE-trending olivine basaltic (Gölcük basalt - Early Miocene alkali basalt) and trachyandesitic (Kayırlar volcanites) intrusions and lava flows were synchronously emplaced into the lacustrine sediments. The intrusions typically display peperitic rocks along their contacts with the sedimentary rocks (Helvacı, 1995; Helvacı and Erkül, 2002; Helvacı et al., 2003; Erkül et al., 2005*b*, 2006; figure 4).

Figure 4- Peperitic texture of basaltic lava flows in lacustrine sediments, Gölcük locality, Bigadiç deposit, Turkey.

The radiometric age data reveal that the formation of the Bigadiç volcano-sedimentary succession is restricted to a period between 20.6±0.7 and 17.8±0.4 Ma. K/Ar dating of the Sındırgı volcanics yield an age of 20.2±0.5 and 19.0±0.4 Ma from rhyolites and dacites, respectively (Table 1). The total gas age corresponds to a K/Ar age of an olivine-basalt sample, namely 20.5±0.1 Ma, and an Ar/Ar age of 19.7±0.4 Ma. The K/Ar date of the NE-trending dyke of the Kayırlar volcanites is 20.6±0.7 Ma. The K/Ar dating of lavas of the Şahinkaya volcanics gave 17.8±0.4 Ma. (Helvacı and Erkül, 2002; Helvacı et al., 2003; Erkül et al., 2005*b*).

Geochemical data from the Bigadiç¸ area are also related to the extensional regime, which was characterized by bimodal volcanism related to extrusion of coeval alkaline and calc-alkaline volcanic rocks during the second volcanic episode. The formation of alkaline volcanic rocks dated as 19.70 ± 0.40 Ma can be related directly to the onset of the N–S extensional regime in western Turkey. In the Bigadiç basin widespread high-K calcalkaline andesitic to rhyolitic lava flows, domes and pyroclastic rocks are interlayered with borate-bearing lacustrine deposits (Helvacı, 1995; Helvacı and Alonso, 2000; Erkül et al., 2005*b*). The ages of the intermediate to acidic volcanism lie between 23.0 and 17.8 Ma, and interlayered high-K calcalkaline shoshonites within the basin have ages of 20.5–19.7 Ma (Helvacı, 1995; Erkül et al., 2005*b*). The volcanic unit cutting the upper borate zone in the Bigadiç Basin is assigned a late Miocene in age on the basis of its geochemical features. The geochemistry of the shoshonitic rocks in the area is similar to those of other late Miocene mafic rocks in the İzmir-Balıkesir Transfer Zone (İBTZ) (Ersoy et al., 2012; Seghedi et al., 2015).

This early-middle Miocene volcanism continues further NE (towards Susurluk-Çaltıbük; Helvacı, 1994; Helvacı and Alonso, 2000; figure 1) with widespread andesitic to rhyolitic lava flows and related pyroclastic rocks interlayered with lacustrine sediments in Sultançayır and Kestelek basins. The Miocene sequence in the Sultançayır basin consists of the following in ascending order: andesite and agglomerate; tuff; sandy conglomerate; limestone; sandy claystone containing boratiferous gypsum, bedded gypsum and tuff; and clayey limestone (Helvacı, 1994). K/Ar age dating of one tuff sample taken from the tuff unit yields an age of 20.01 Ma (Helvacı, 1994; Helvacı and Alonso, 2000).

The Miocene sequence in the Kestelek basin contains basement conglomerate and sandstones; claystone with lignite seams, marl, limestone, and tuff; agglomerates and volcanic rocks; the borate zone comprises clay, marl, limestone, tuff and borates; and limestones with thin clay and chert bands. The volcanic activity gradually increased and produced tuff, tuffite and agglomerate, and andesitic, trachytic and rhyolitic volcanic rocks that are interbedded with sediments. K/Ar age dating of one tuff sample taken from the borate zone yields an age of 17.4 Ma (Helvacı, 1994; Helvacı and Alonso, 2000) (Table 1, figures 2 and 3)

3.2. Gördes Basin

Gördes basin is confined by the Menderes Massif to the east and by ophiolitic melange units of the

Bornova flysch zone to the west (Figure 2), and has previously been studied by Nebert (1961), Yağmurlu (1984), Seyitoğlu and Scott (1994*a,b*) and Purvis and Robertson (2004, 2005). Seyitoğlu and Scott (1994*a,b*) divided the stratigraphy of Gördes basin into three main sedimentary units. The basal part of the sequence is represented by the conglomerates and sandstones of the Dağdere formation in the north and the Tepeköy formation in the south, which are overlain by the sandstone–mudstone alternation of the Kuşlukköyü formation that is also intercalated with acid tuff (Figure 3). The basin sediments are cut by dacitic–rhyolitic volcanic necks (central volcanics; Seyitoğlu and Scott, 1994*b*). The stratigraphy of Gördes basin has been revised with new field data by Ersoy et al., (2011) and the stratigraphy of the basin begins with Kızıldam formation which is conformably overlain by the Kuşlukköyü formation. The Kuşlukköyü formation interfingers with the Güneşli Volcanics and are also cut by the Kayacık Volcanics in the center of the basin (Helvacı and Ersoy, 2006; Helvacı et al., 2006; Ersoy et al., 2011). These units are unconformably overlain by the Gökçeler formation and late Miocene to Recent sediments. The Kızıldam formation crops out along the basin-bounding faults in Gördes basin.

In the eastern margin of Gördes basin, the Kızıldam formation consists of reddish-brown conglomerates of alluvial fan origin, which are mainly derived from the underlying metamorphic rocks of the Menderes Massif. Here, the Kızıldam formation unconformably overlies the metamorphic rocks and is composed of metamorphic clasts such as gneisses, schists and migmatites. In the western part of Gördes basin, the Kızıldam formation starts with well-lithified carbonate-cemented conglomerates with mainly limestone-dominated clasts derived from the rocks of the İzmir-Ankara suture zone. The type section of the Kızıldam formation is best seen around the Kızıldam village. To the center of the basin, the unit passes laterally into the Kuşlukköy formation. The Kızıldam formation is regionally correlated with the Lower Miocene Kürtköyü formation in the Demirci and Selendi basins, and is equivalent of the lower parts of the Dağdere and Tepeköy formations named by Seyitoğlu and Scott (1994*a,b*). It is also correlated with the alluvial fan facies of Purvis and Robertson (2004) (Figure 3). Seyitoğlu and Scott (1994a) obtained 24.2±0.8–21.1±1.1 Ma K–Ar ages from tourmaline leucogranite pebbles in the Kızıldam formation (Table 1). The age of the Kızıldam formation is accepted to be early Miocene on the basis of radiometric age data from the volcanic intercalations of the conformably overlying Kuşlukköy formation (Ersoy et al., 2011).

3.3. Demirci Basin

The infill of Demirci basin is cut into two sectors by the Pliocene-Quaternary Simav half-graben. The northern sector was named as the Akdere basin by Seyitoğlu (1997*b*) (Figures 2 and 3). The Neogene stratigraphy of this part of Demirci basin rests on the metamorphic rocks of the Menderes Massif that were intruded by the Oligocene–Miocene Eğrigoz and Koyunoba granitoids.

The Demirci basin is composed of two main stratigraphic units separated by an angular unconformity (Figures 2 and 3). The basin-fill starts with early-middle Miocene conglomerates of the Kürtköyü formation that pass upwards into the sandstone–mudstone alternations of the Yeniköy formation. These units are unconformably overlain, in ascending order, by the Mahmutlar formation, the Demirci formation, and the Sevinçler volcanics that crop out in the northeastern part of the basin (İnci, 1984).

Yılmaz et al. (2000) revised the stratigraphy of Demirci basin and proposed that the basin-fill started with boulder conglomerates of the Borlu formation that pass into the sandstones and mudstones of the Köprübaşı formation. The Köprübaşı formation is intercalated with andesitic lavas and pyroclastics rocks of the Okcular volcanics that crop out in the western-central part of the basin. Yılmaz et al. (2000) suggest that these units are conformably overlain by the marls and shales of the Demirci formation and all these units are early-middle Miocene in age. They are unconformably overlain by the late Miocene-early Pliocene Adala formation composed of limestones cropping out around Demirci town.

The stratigraphy of the Demirci basin contains two distinct units separated by a basin-wide angular unconformity (İnci, 1984). The older one is correlated with the Hacıbekir Group in the adjacent Selendi and Uşak-Güre basins (Ercan et al., 1978, 1983), and the data indicates that the younger volcano-sedimentary unit unconformably overlies the Hacıbekir Group and can be correlated with the İnay Group in the adjacent Selendi basin. The Hacıbekir Group in Demirci basin is composed of the Kürtköyü and Yenikoy formations and the rhyolitic volcanic rocks of Sevinçler

Volcanics. The İnay Group comprises the Akdere pyroclastics, sedimentary rocks of the Borlu, Köprübaşı, and Demirci formations which are interfingered by andesitic–dacitic Asitepe Volcanics and the Naşa basalt to the north of the basin (Figure 3). The Kürtköyü formation crops out in the northern part of Demirci basin, with the largest exposures on the southern flank of the Simav half-graben and the unit is composed of reddish-brown to pale yellow boulder conglomerates (with blocks of up to 1 m), pebblestones, cobblestones and sandstones. The conglomerates are derived from the Menderes Massif metamorphics and the Eğrigöz granitoid. The Kürtköyü formation is conformably overlain by rhyolitic pyroclastic rocks and lava flows of the Sevinçler Volcanics and the Yeniköy formation (Figure 3). The Yeniköy formation is composed of yellowish sandstones and mudstones with local laminated limestone and marls, and mainly crop out in the north of Demirci basin.

In Demirci basin, the İnay Group is composed of Akdere pyroclastics, conglomerates of the Borlu formation, sandstone–siltstone alternations of the Köprübaşı formation, and shales, marls and limestones of the Demirci formation. In the northern flank of the Simav half-graben, the İnay Group consists of Akdere pyroclastics, conglomerates and sandstones of the Borlu and Köprübaşı formations, and the Naşa basalt (Figure 3). The Borlu formation of the İnay Group is composed of boulder conglomerates (mainly derived from the Menderes Massif) with sandstone intercalations of alluvial fan origin. The Köprübaşı formation is conformably overlain by the Asitepe Volcanics in the eastern margin of Demirci basin. The Naşa basalt (15.8±0.3 and 15.2±0.3 Ma K–Ar ages of Ercan et al., 1996, table 1) is composed mainly of syn-sedimentary basaltic lava flows that flowed over the sedimentary rocks of the Borlu formation. In Demirci basin, the Köprübaşı formation passes transitionally into the marls, bituminous shales and limestones (with claystone and sandstone intercalations) of the Demirci formation (İnci, 1984, figure 3), which can be correlated with the Ulubey formation in Selendi basin (Seyitoğlu, 1997*a*; Ersoy et al., 2010). The Neogene volcano-sedimentary infill of Demirci basin are very similar to those of the Selendi and Uşak-Güre basins (Figure 3).

3.4. Selendi Basin

The Neogene stratigraphy of the Selendi Basin rests on a basement consisting of both Menderes Massif and İzmir-Ankara zone rocks (Ercan et al, 1978; Seyitoğlu, 1997; Ersoy and Helvacı, 2007). Three volcano-sedimentary units constitute the Neogene stratigraphy, each one was accompanied by different volcanic activities (Ersoy and Helvacı, 2007). At the base, the Lower Miocene Hacıbekir Group tectonically overlies the Menderes Massif and unconformably overlies the İzmir-Ankara zone rocks (Figures 2 and 3). The rocks of the İzmir-Ankara Zone occur also as olistostromal blocks in the Hacıbekir Group. Two contrasting volcanic associations accompanied deposition of the Hacıbekir Group during the Early Miocene: the Eğreltidağ volcanic unit and the Kuzayır lamproite (Ersoy and Helvacı, 2007). The Middle Miocene İnay Group, unconformably overlying the Hacıbekir Group consists of conglomerates, widely exposed claystone-sandstone-marl alternation and limestones. The claystone-sandstone-mudstone horizons include several borate occurrences such as howlite and colemanite (Helvacı and Alonso, 2000). The İnay Group is also interfingered by two contrasting volcanic associations: the Yağcıdağ volcanic unit and the Orhanlar Basalt. These units are unconformably overlain by the Upper Miocene Kocakuz formation and the Kabaklar Basalt. Finally, the Plio-Quaternary sediments and volcanic units unconformably overlie the older units. The final volcanic activity is represented by the Kula volcanics (Figure 5). The stratigraphy of the basin is very similar to the Emet Basin. In particular, the İnay Group can be correlated with the borate-bearing units in the Emet Basin. The Yağcıdağ volcanic unit can also be correlated with the Beydağ volcanics in the Uşak-Güre Basin that include gold mineralization (Kışladağ gold deposit) (Helvacı and Ersoy, 2006; Helvacı et al., 2006; Ersoy and Helvacı, 2007; Ersoy et a., 2008; Helvacı, 2012).

3.5. Emet Basin

Emet basin (Akdeniz and Konak, 1979; Helvacı, 1984, 1986; figure 3), is located between the Eğrigöz granitoid intruded into the Menderes Massif metamorphic rocks to the west, and the Afyon zone metamorphic rocks to the east (Figures 1 and 2). The stratigraphy of Emet basin comprises two Neogene volcanosedimentary units separated by a regional unconformity (Figure 3). These units can be correlated with similar rocks from other basins on the basis of their age, lithology and deformational features, and they are named as the Hacıbekir and İnay groups. In this basin, the İnay Group hosts the world's biggest colemanite and probertite borate deposits (Gawlik, 1956; Helvacı, 1984, 1986; Helvacı

Figure 5- The vent area of a lava flow, Kula Volcanics, Turkey (Location : 38.6332 North, 28.7650 East Altitude: 551 meters above sea).

and Orti, 1998; Helvacı and Alonso, 2000; Garcia et al., 2010).

The Hacıbekir Group consists of the Taşbaşı and Kızılbük formations and the Akdağ and Kestel volcanics (Figure 3). The Taşbaşı formation crops out to the western and southwestern parts of the Emet basin, and is made up of reddish-brown colored conglomerates with grayish sandstone intercalations deposited in alluvial fan facies. The basal contact of the unit is represented by a low-angle fault with the Menderes Massif, while the unit unconformably overlies the rocks of the İzmir-Ankara zone (Figure 3).

The Taşbaşı formation is locally interfingered with rhyolitic pyroclastic rocks of the Akdağ volcanics, and is conformably overlain by the Kızılbük formation. The age of the unit is early Miocene on the basis of radiometric age data from the volcanic rock intercalations. The Kızılbük formation crops out in a large area to the western and southwestern parts of the Emet basin, and is composed of coal-bearing yellowish sandstone–siltstone–mudstone alternations and laminated limestone of fluvio-lacustrine origin. The Kızılbük formation is interfingered with pyroclastic rocks of the Akdağ volcanics, which are composed of rhyolitic lava flows, domes, pyroclastics and epiclastics. The Akdağ volcanics have yielded 20.3±0.6 (Seyitoğlu et al., 1997) and 19.0±0.2 Ma (Helvacı and Alonso, 2000) K–Ar ages (Table 1). The Kestel volcanics emplaced in a NE–SW-direction to the southwest of the basin, and are composed of syn-sedimentary mafic lava flows. These volumetrically small volcanic rocks conformably overlie the Kızılbük formation. The age of the Kestel volcanics is stratigraphically accepted to be early Miocene.

The İnay Group in Emet basin is made up of the Hisarcık and Emet formations that interfinger with the Köprücek volcanics and the Dereköy basalt (Figure 3). The Hisarcık formation (Akdeniz and Konak, 1979) crops out in a large area in the Emet basin and is composed of conglomerates, pebblestones and sandstone intercalations. The age of the Hisarcık formation is accepted to be middle Miocene on the basis of volcanic intercalations in the İnay Group. Towards the center of the basin, the Hisarcık formation passes laterally into the Emet formation that is composed of sandstone – claystone – mudstone alternations of fluvio-lacustrine origin. The fine-grained parts of the unit, especially the mudstone –claystone levels contain large borate deposits which are mined for colemanite and probertite (Helvacı and Alonso, 2000; Helvacı and Ersoy, 2006; Helvacı et al., 2006; Ersoy et al., 2012).

The Köprücek volcanics crop out in the northern part of Emet basin. The unit is composed of andesitic to rhyolitic lava flows, dykes and associated

pyroclastics which interfinger with the Hisarcık formation. The thickness of the pyroclastic intercalations in the Hisarcık formation increases towards the north of the basin, which suggests that the Köprücek volcanics originated from this area. The Köprücek volcanics are overlain by the limestones of the Emet formation. The pyroclastic intercalations yield 16.8±0.2 Ma K–Ar age (Helvacı and Alonso, 2000; table 1). In the southern part of the basin, the Hisarcık formation is also conformably overlain by basaltic lava flows of the Dereköy basalt. Along the basal contact of the Dereköy basalt several pepperitic textures are developed, indicating a syn-sedimentary emplacement of the lavas. The Dereköy basalt has been dated as 15.4±0.2 and 14.9±0.3 Ma (K–Ar ages; Seyitoğlu et al., 1997; Helvacı and Alonso, 2000).

The Emet borate deposits were formed in two separate basins, possibly as parts of an interconnected lacustrine playa lake, in areas of volcanic activity, fed partly by thermal springs and partly by surface streams (Helvacı and Alanso 2000). All the lavas at Emet are enriched in B (≤68 ppm), Li (≤55 ppm) and As (≤205 ppm), slightly enriched in Sr (≤580 ppm), but have relatively low levels of S (≤80 ppm). The older acidic lavas contain higher B levels than the more recent intermediate alkaline lavas. The Early Miocene acidic volcanism at Emet basin has high levels of elements associated with mineralization, as well as having a close spatial and temporal relationship with the borates and it is therefore considered a likely source. Possible mechanisms by which volcanism might supply B, S, Sr, As and Li to the basin sediments include the leaching of volcanic rocks by hot meteoric waters, the direct deposition of ash into the lake sediments, or the degassing of magmas. Thermal springs associated with local volcanic activity are thought to be the possible source of the borates (Helvacı, 1977; Helvacı, 1984; Helvacı and Alonso, 2000).

The volcanic activity in the Emet basin, which is thought to be the source of the borate deposition, via the thermal springs, also have similar characteristics to with the Middle Miocene volcanic activity in the Uşak-Güre basins. The geological data clearly show that the Emet basin can be correlated with the Selendi and Uşak-Güre basins. These basins, most probably, were interconnected depocenters throughout the Middle Miocene (Ercan et al 1978; Seyitoğlu 1997; Ersoy and Helvacı 2007;).

3.6. Uşak and Güre Basins

The stratigraphy of the Uşak-Güre basin is similar to that of the Selendi Basin. The Uşak and Güre basins accumulated a thick fluvio-lacustrine fill in which three distinct volcanic centers (Elmadağ, İtecektepe and Beydağı) and their deposits can overlap with each other and with the sediments produced by the background sedimentation. The three large complex volcanoes providing a complex mixed siliciclastic and volcaniclastic basin infill in the respective basins where volcanism took place. All three volcanic centres display a complex succession of effusive and explosive volcanism and their reworked deposits, with abundant evidence of magma–water interaction with the lacustrine water-saturated sediment (Figures 2 and 3). All three volcanic centres then experienced a phase of volcano growth and degradation between 17 and 15 Ma ago, most likely related to a combination of tectonic movements on NE–SW-trending basement faults (Helvacı et al., 2009; Karaoğlu et al., 2010; Table 1).

The Lower Miocene Hacıbekir Group is unconformably overlain by the Middle Miocene İnay Group that contain the Middle Miocene latitic volcanics (Beydağ volcanics). The Beydağ volcanics hosted to the biggest porphyry gold deposits (Kışladağ gold deposits) in western Turkey (Helvacı, 2012). The Kışladağ gold deposit was developed in the Middle Miocene latitic Beydağ volcanic rocks (Ercan et al. 1978; Helvacı et al., 2009; Karaoğlu et al., 2010). The Beydağ volcanics interfinger with the Middle Miocene lacustrine sediments including, in ascending order, basal conglomerates, sandstone-siltstone alternation, siltstone-mudstone alternation with marls, tuff horizons and limestones (İnay Group, Ercan et al. 1978; Seyitoğlu 1997; Ersoy and Helvacı, 2007; Helvacı et al., 2009).

3.7. Kırka Basin

The Miocene sequence of the Kırka Basin, rest unconformably on a basement including Paleozoic metamorphics, Mesozoic mélange units and Eocene sediments and consists of volcanic rocks and tuffs, lower limestone with marl and tuff interbeds, borate zone, upper claystone; upper limestone containing tuff and marl with chert bands; and basalt (Arda, 1969; İnan et al. 1973; Helvacı, 1977; Gök et al. 1980; Sunder, 1980; Palmer and Helvacı, 1995). The stratigraphy and mineralogy of the Kırka borate deposit was revealed by (İnan et al., 1973; Helvacı, 1977; Palmer and Helvacı, 1995; Floyd et al., 1998; Helvacı and Alonso, 2000; Helvacı and Orti, 2004; Garcia-Veigas et al., 2011).

Large rhyolitic ignimbrite occurrences are closely connected to the Early Miocene initiation of extensional processes in central-west Anatolia along

the Tavşanlı-Afyon zones (Floyd et al., 1998) (Figures 1 and 6). Field correlations, petrographical, geochemical and geochronological data lead to a substantial reinterpretation of the ignimbrites surrounding Kırka area, known for its world-class borate deposits, as representing the climatic event of a caldera collapse, unknown up to now and newly named the "Kırka-Phrigian caldera". The caldera, which is roughly oval (24 km x 15 km) in shape, is one of the largest in Turkey and is thought to have been formed in a single stage collapse event, at ~19 Ma that generated huge volume extracaldera outflow ignimbrites (Floyd et al., 1998; Seghedi and Helvacı, 2014).

Intracaldera post-collapse sedimentation and volcanism (at ~ 18 Ma) was controlled through subsidence-related faults with generation of a series of volcanic structures (mainly domes) showing a large compositional range from saturated silicic rhyolites and crystal-rich trachytes to undersaturated lamproites (Figure 6, table 1). The volcanic rock succession provides a direct picture of the state of the magmatic system at the time of eruptions that generated caldera and post-caldera structures and offer an excellent example of silicic magma generation and associated potassic and ultrapotassic intermediate-mafic rocks in a post-collisional extensional setting (Seghedi and Helvacı, 2014).

The Kırka area, a newly discovered caldera area, is situated in the northernmost part of the Miocene Eskişehir–Afyon volcanic aea (EAV), as recently delineated by Ersoy and Palmer (2013). It is well known for its borate deposits, the largest in the world (e.g., İnan et al., 1973; Helvacı, 1977; Kistler and Helvacı, 1994; Helvacı and Alonso, 2000; Helvacı, 2005; Helvacı et al., 2012; García-Veigas and

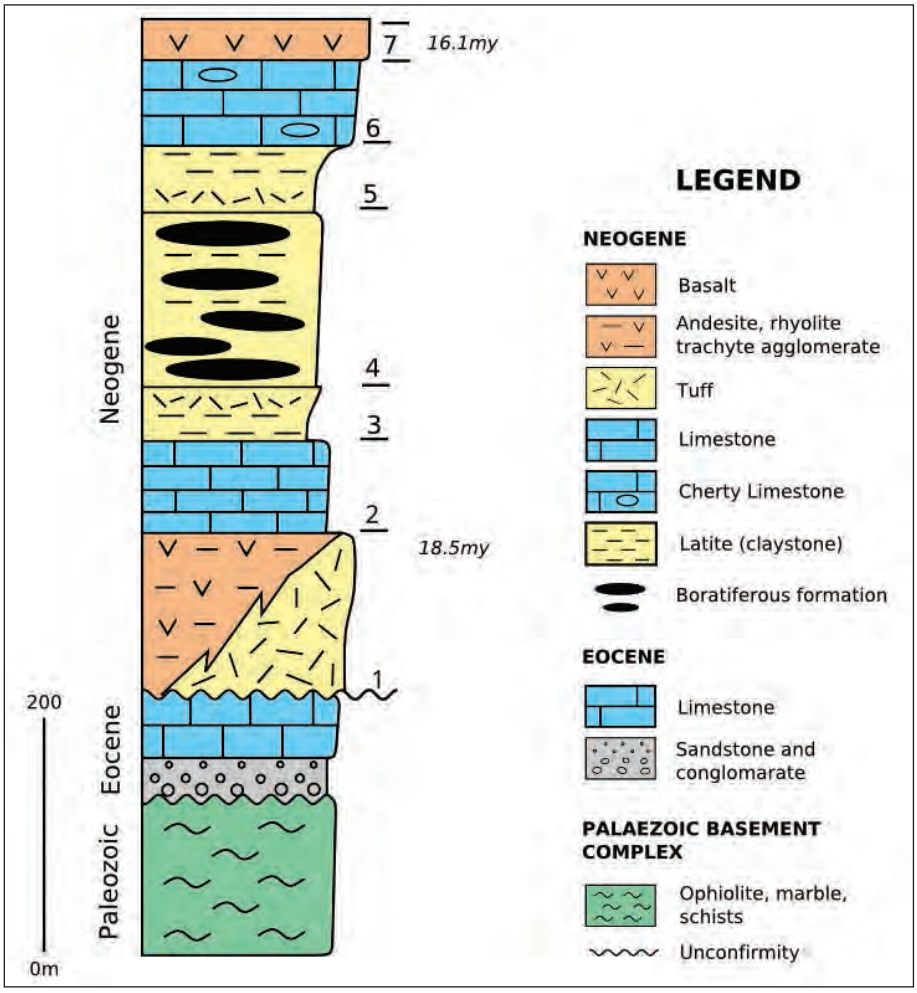

Figure 6- Stratigraphic columnar section of the Kırka borate deposit. Neogene rock units: 1: Tuffs, 2: Lower limestone, 3: Lower clay, marl and tuff, 4: Borate unit, 5: Upper clay, tuff, marl and coal bands, 6: Upper cherty limestone, 7: Basalt (after Inan et al. 1973, Helvacı 1977 and Sunder 1980).

Helvacı, 2013). It was recognized that the borates formed in closed system environments and were connected with thick calc-alkaline volcano-sedimentary successions associated with marls, mudstones, limestones and sandstones; however the caldera system was not recognized before now (Seghedi and Helvacı, 2014).

The most extensive volcanic deposits related to caldera formations are represented by ignimbrites distributed all around the caldera (Floyd et al., 1998). However, the most well-preserved outflow pyroclastic deposits are dominantly distributed toward the south of caldera (Floyd et al., 1998). The base of the volcanic sequence seems to be exposed at the structural margin of the caldera and sometimes associated with lag breccias. The field observations allowed an estimate of the exposed thickness of 160-200 m that includes the caldera-forming ignimbrites (Floyd et al., 1998). The slightly to moderately welded ignimbrite facies is less well-represented toward east, north and west outside of caldera and always associated with thick fall-out deposits. The ignimbrites are also associated with fall-out deposits. The trachyte domes largely developed as two main structures elongated N-S at the northern margin of caldera (10-15 /7 km) and cover the caldera-related ignimbrites and associated deposits, the rhyolite domes, as well the basement deposits. The northern slopes of both the trachytic tuff deposits and lamproitic lava flows are covered by Late Miocene limestones. The reconstruction of intra-caldera deposits are based on the outcrop exposures and drillings (Seghedi and Helvacı, 2014).

4. Depositional Model, Formation and Mineralogy of Borate Deposits

Although boron is one of the rarer and more unevenly distributed elements in the Earth's crust, there are extraordinary concentrations of boron on an industrial scale in some localized areas (Figure 7). Borate minerals are formed in various environments and in very different conditions. Over 250 minerals are known to contain boron, and they are found in various geological environments (Figure 8 and table 2). The most important economic deposits are very closely related to Tertiary volcanic activity in orogenic belts. They are situated close to converging plate margins; characterized by andesitic-rhyolitic magmas; arid or semi-arid climates; and non-marine evaporite environments. Turkish, United States, South American and many other commercial borate deposits are non-marine evaporites associated with volcanic activity (Ozol, 1977; Jackson and McKenzie, 1984; Floyd et al., 1998; Helvacı, 2005).

Boron is the fifth element of the periodic table and is the only electron-deficient nonmetallic element. Thus, boron has a high affinity for oxygen, forming strong covalent boron-oxygen bonds in compounds known as borates. Because it is strongly fractionated into melts and aqueous fluids, processes that led to formation of continental crust such as partial melting and emission of volatiles, also concentrated boron, resulting in enrichment by 4-8 orders of magnitude from <0.1 ppm in primitive mantle to 17 ppm in average continental crust, and to several wt% in

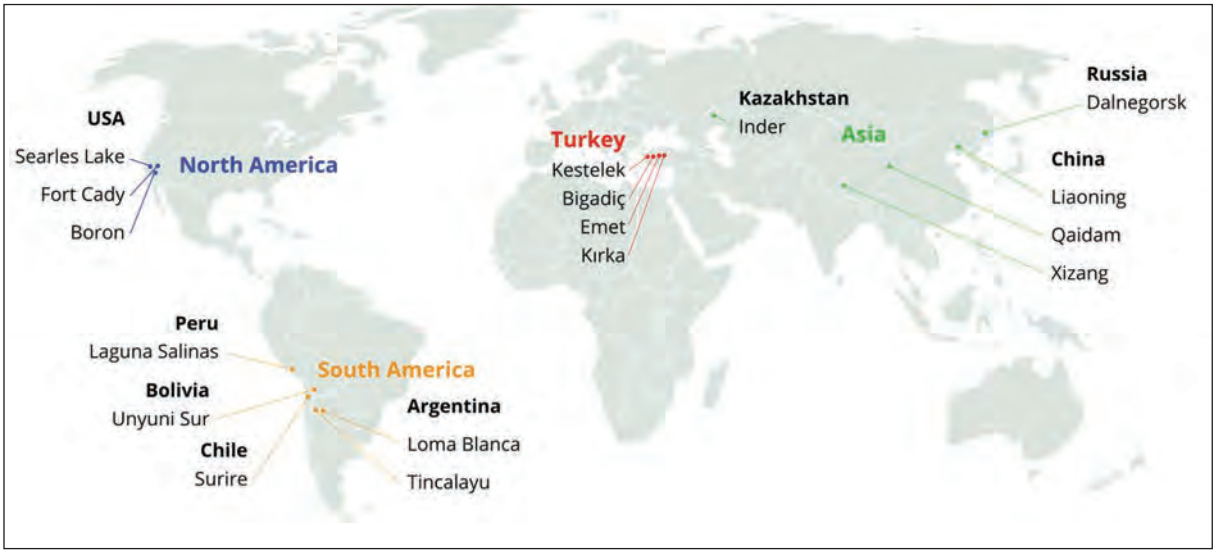

Figure 7- World major borate mines.

Table 2- Borate mineral, formulation and chemical composition.

	Structural formula	Empirical formula	Oxid like formula
Ca-borates			
Priceite	$Ca_2(B_5O_7(OH)_5).H_2O$	$Ca_4B_{10}O_{19}.7H_2O$	$4CaO5B_2O_3.7H_2O$
Colemanite	$Ca(B_3O_4(OH)_3).H_2O$	$Ca_2B_6O_{11}.5H_2O$	$2CaO3B_2O_3.5H_2O$
Meyerhofferite	$Ca(B_3O_3(OH)_5).H_2O$	$Ca_2B_6O_{11}.7H_2O$	$2CaO3B_2O_3.7H_2O$
Inyoite	$Ca(B_3O_3(OH)_5).4H_2O$	$Ca_2B_6O_{11}.13H_2O$	$2CaO3B_2O_3.13H_2O$
Ca-Na-Borates			
Probertite	$NaCa(B_5O_7(OH)_4).3H_2O$	$NaCaB_5O_9.5H_2O$	$Na_2O2CaO5B_2O_3.10H_2O$
Ulexite	$NaCa(B_5O_6(OH)_6).5H_2O$	$NaCaB_5O_9.8H_2O$	$Na_2O2CaO5B_2O_3.16H_2O$
Na-Borates			
Kernite	$Na_2(B_4O_6(OH)_2).3H_2O$	$Na_2B_4O_7.4H_2O$	$Na_2O2B_2O_3.4H_2O$
Tincalconite	$Na_2(B_4O_5(OH)_4).3H_20$	$Na_2B_4O_7.5H_2O$	$Na_2O2B_2O_3.5H_2O$
Borax	$Na_2(B_4O_5(OH)_4).8H_20$	$Na_2B_4O_7.10H_2O$	$Na_2O2B_2O_3.10H_2O$
Mg-Borates			
Szaibelyite	$Mg(BO_2(OH))$	$Mg_2B_2O_5.2H_2O$	$2MgOB_2O_3.2H_2O$
Pinnoite	$Mg(B_2O(OH)_6)$	$MgB_2O_4.3H_2O$	$MgOB_2O_3.3H_2O$
Mcasllisterite	$Mg(B_6O_7(OH)_6)_2.9H_2O$	$Mg_2B_{12}O_{20}.15H_2O$	$2MgO6B_2O_3.15H_2O$
Hungchaoite	$Mg(B_4O_5(OH)_4).7H2O$	$MgB_4O_7.9H_2O$	$MgO2B_2O_3.9H_2O$
Kurnakovite	$Mg(B_3O_3(OH)_5).5H_2O$	$Mg_2B_6O_{11}.15H_2O$	$2MgO3B_2O_3.15H_2O$
Inderite	$Mg(B_3O_3(OH)_5).5H_2O$	$Mg_2B_6O_{11}.15H_2O$	$2MgO3B_2O_3.15H_2O$
Mg-Na Borates			
Aristarainite	$Na_2Mg(B_6O_8(OH)_4)_2.4H_2O$	$Na_2MgB_{12}O_{20}.8H_2O$	$Na_2OMgO6B_2O_3.8H_2O$
Rivadavite	$Na_6Mg(B_6O_7(OH)_6)_4.10H_2O$	$Na_6MgB_{24}O_{40}.22H_2O$	$3Na_2OMgO12B_2O_3.22H_2O$
Mg-Ca Borates			
Hydroboracite	$CaMg(B_6O_8(OH)_6).3H_2O$	$CaMgB_6O_{11}.6H_2O$	$CaOMgO3B_2O_3.3H_2O$
Inderborite	$CaMg(B_3O_3(OH)_5)_2.6H_2O$	$CaMgB_6O_{11}.11H_2O$	$CaOMgO3B_2O_311.H_2O$
Mg-K-Borates			
Kaliborite	$KHMg_2(B_{12}O_{16}(OH)_{10}).4H_2O$	$K_2Mg_4B_{24}O_{41}.19H_2O$	$K_2O4MgO12B_2O_3.19H_2O$
Sr-Borates			
Veatchite-A	$Sr_2(B_{11}O_{16}(OH)_5).H_2O$	$Sr_4B_{22}O_{37}.7H_2O$	$4SrO11B_2O_3.7H_2O$
Tunellite	$Sr(B_6O_9(OH)_2).3H2O$	$SrB_6O_{10}.4.H_2O$	$SrO3B_2O_3.4H_2O$
Borosilicates			
Bakerite	$Ca_4B_4(BO_4)(SiO_4)_3(OH)_3.H_2O$	$Ca_8B_{10}Si_6O_{35}.5H_2O$	$8CaO5B_2O_36SiO_2.5H_2O$
Howlite	$Ca_2B_5SiO_9(OH)_5$	$Ca_2SiHB_5O_{12}.2H_2O$	$4CaO5B_2O_32SiO_2.5H_2O$
Searlesite	$NaBSi_2O_5(OH)_2$	$NaBSi_2O_6.H_2O$	$Na_2OB_2O_34SiO_2.2H_2O$
Boroarseniates			
Cahnite	$Ca_2B(AsO_4)(OH)_4$	$Ca_2AsBO_6.2H_2O$	$4CaOB_2O_3As_2O_5.4H_2O$
Teruggite	$Ca_4MgAs_2B_{12}O_{22}(OH)_{12}.12H_2O$	$Ca_4MgAs_2B_{12}O_{28}.18H_2O$	$4CaOMgO6B_2O_3As_2O_5.18H_2O$
Borophosphates			
Luneburgite	$Mg_3B_2(PO_4)_2(OH)_6.5H_2O$	$Mg_3P_2B_2O_{11}.8H_2O$	$3MgOP_2O_5B_2O_3.8H_2O$
Borosulfates			
Fontarnauite	$Na_2Sr(SO_4)(B_4O_6(OH)_2).3H_2O$	$Na_2SrSB_4O_{11}.4H_2O$	$Na_2OSrOSO_32B_2O_3.4H_2O$

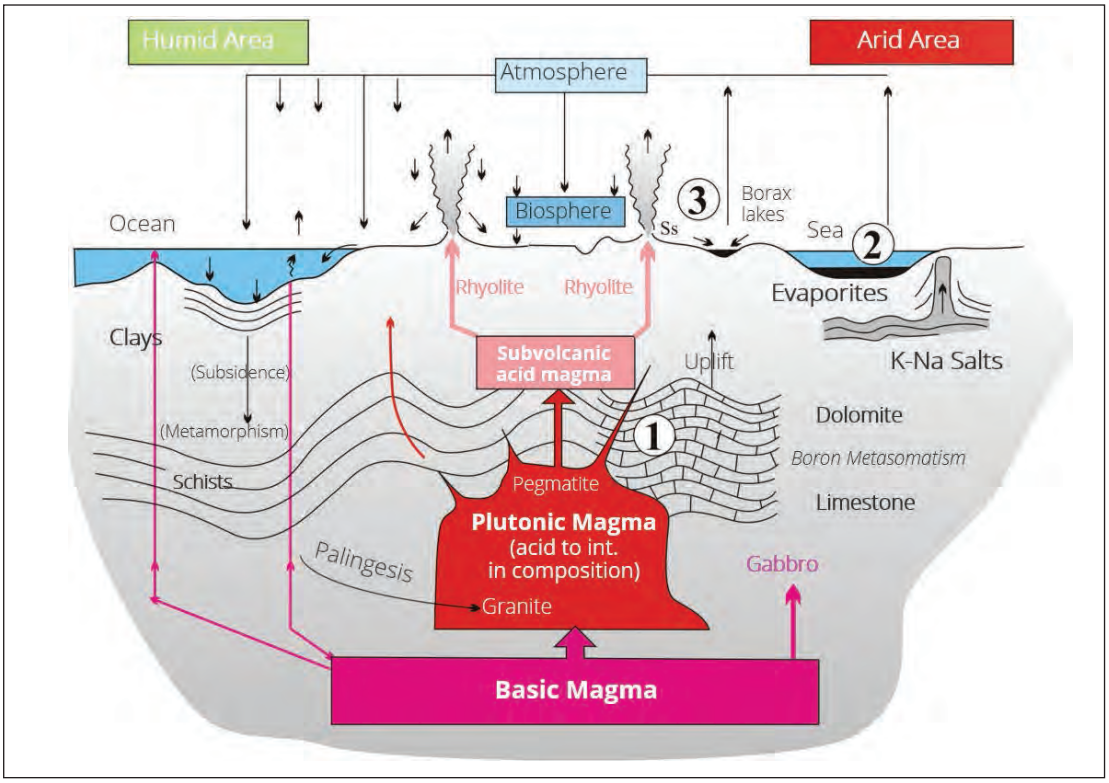

Figure 8- Scheme for the cycle of boron. 1 Skarn Deposits; 2. Marine Deposits; 3. Playa-lake Deposits (Modified after Watanabe, 1964).

pegmatites and evaporites. Major borate deposits throughout the world are found in tectonically active extensional regions associated with collisional plate boundaries (Ozol, 1977; Floyd et al., 1998; Helvacı, 2005). Most of the commercial borate deposits in the USA, South America, and Turkey are thought to be associated with continental sediments and volcanism of Neogene age. Many of the older skarn deposits also appear to be related to continental volcanic sources. Marine borate deposits are apparently the product of evaporation of seawater in a restricted basin, probably associated with a seafloor borate source, and/or progressive decanting that preferentially concentrated the borates to many times natural seawater concentrations, but these are much less abundant than non-marine borates.

Borates associated with igneous and some metamorphic rocks are thought to be an end phase of specialized magmatic segregation or leached from the intruded rocks by associated hydrothermal fluids (Figure 8).

Most of the South American deposits are associated with calcareous tuff, which occurs as a late-stage capping over the borates, and in some cases with halite and gypsum. Recent volcanic activity is indicated by basaltic to rhyolitic flows in adjacent areas, and a volcanic source for the borates is presumed. The Salar deposits of South America consist of beds and nodules of ulexite, with some borax or inyoite, associated with Holocene playa sediments, primarily mud, silt, halite, and gypsum.

Borates can be concentrated in many different ways:

- by chemical precipitation in the neighbourhood of boron-bearing springs in playa-type basins (e.g. the Boron, Searles Lake, and Billie deposits of California, and the Kırka, Sultanayır, Bigadiç, and Emet deposits in Turkey);
- by precipitation from seawater in the closing phase of a salt-forming evaporate cycle (e.g. at Stassfurt in Germany);
- by contact metasomatism with dolomite or magnesite, forming magnesium borates such as ludwigite, kotoite, and ascharite (e.g. the Teazhnoe deposits at Yakutia in Russia, and the Hol-Kol deposit in North Korea);

– by contact metasomatism with limestone, forming boron silicates such as datolite and danburite (e.g. at Ak Akhdar, Pamir, and Dalnegorskoye, Primorsky, Russia); and
– by volcanic exhalations of boric acid, i.e. sublimates (e.g. at Clear Lake, Lake County, California, at Salar de Surire, Chile, and in the Maremma area, Tuscany, Italy).

Borates constitute a group of mineral deposits of great economic interest. Several genetic types have been identified (volcanic, hydrothermal, metamorphic, sedimentary) and the most important corresponds to those deposits formed in nonmarine evaporitic settings. The formation of borate deposits can be tentatively summarized into three main groups as follows (Figure 8):

1. a skarn group associated with intrusives and consisting of silicates and iron oxides;
2. a magnesium oxide group hosted by marine evaporitic sediments; and
3. a sodium and calcium borate hydrates group associated with lacustrine (playa lake) sediments and explosive volcanic activity.

Lacustrine basins related to volcanic domains in which borates have precipitated are known in the stratigraphic record since the Oligocene, although those of Miocene age are the most economically relevant. The borate minerals in these basins were generated in saline lakes emplaced in volcanogenic (mainly pyroclastic) terrains with intense hydrothermal influence, under arid to semi-arid conditions, and in some cases at low temperatures (Figure 9). The following conditions are essential for the formation of economically viable borate deposits in playa-lake volcanosedimentary sediments (Figure 9):

1. formation of playa-lake environment;
2. concentration of boron in the playa lake, sourced from andesitic to rhyolitic volcanics, direct ash fall into the basin, or hydrothermal solutions along graben faults;
3. thermal springs near the area of volcanism;
4. arid to semi-arid climatic conditions; and
5. lake water with a pH of between 8.5 and 11.

4.1. Borate Deposits in Non-Marine Basins

Non-marine continental evaporite deposits are the major economic source of boron. The formation of large economic borate deposits requires a boron-rich source and a means of transporting and concentrating the boron in a restiricted environment. In addition to the concentrated source of the borates and a basin in

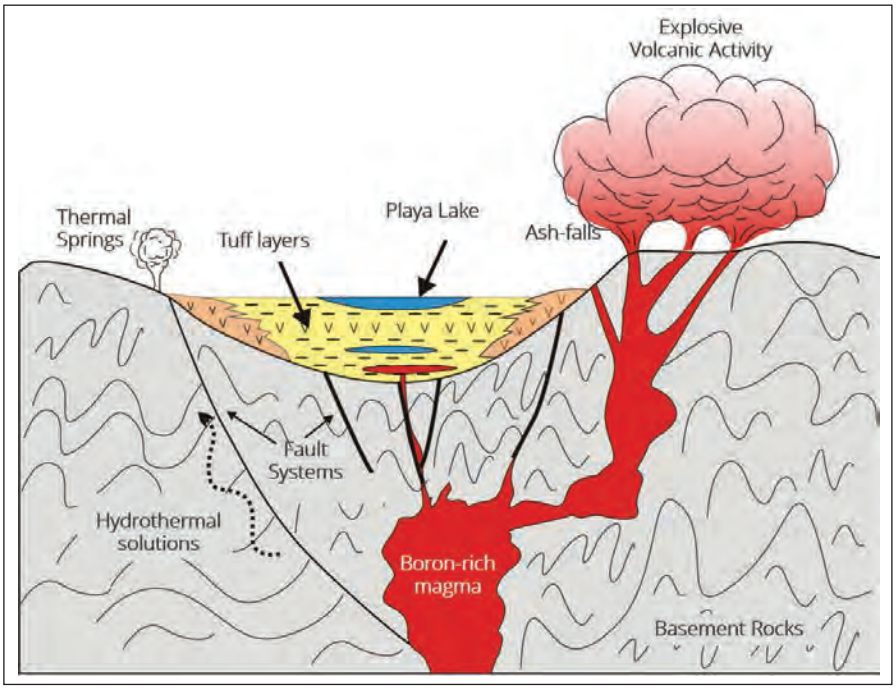

Figure 9- Generalized playa lake depositional model showing the formation of borate deposits in Neogene basins of western Anatolia, Turkey (after Helvacı, 2005).

which they can collect, an arid to semiarid climate also seems to be essential during the deposition and concentration of economic amounts of soluble borates. These soluble borates can, in the long run, be preserved only by burial; however, the lack of deposits of soluble borates older than mid-Tertiary may indicate that even burial is not able to protect borates over long periods of geological time. There are relatively a few occurrences where the element is sufficiently concentrated to be economic use. Where a degree of concentration does occur, it is usually a result of local volcanic activity (as a source of boron), a body of water such as a lake (to dissolve boron compounds), evaporative conditions (to concentrate the solution to the point of precipitation), and the deposition of a protective layer of sediment (to preserve the highly soluble borate minerals).These conditions are present in collisional tectonic settings, for which western Anatolia is a prime example, there have also been significant recent advances in the understanding of the timing of crustal metasomatic processes and collisional and extensional tectonics in this region. Therefore, the formation of borate deposits in western Anatolia is a good example for understanding and identifying boron enrichments in collision-related tectonic events in ancient mobile belts (Figure 9).

The largest borate deposits that originated as chemical precipitates are found interbedded with clays, mudstones, tuffs, limestones, and similar lacustrine sediments. There is a strong evidence that most of these deposits were closely related in time to active volcanism. Thermal springs and hydrothermal solutions associated with volcanic activity are regarded as the most likely source of the boron (Figure 9). Several South American springs in volcanically active areas are currently depositing borates, and the first borax discovered in the USA was found in the muds associated with warm springs at Clear Leak, California, in a volcanically active area. There is, however, another type of borate lake deposit, with mixed salts and/or brine containing borates in sufficient quantity of justify recovery. Searles Lake, California is as a type example of a multicomponent lake formed by evaporation of lake waters. Similarly, the Konya-Karapınar basin (Turkey) is surrounded by volcanes which have been active from the Late Miocene to recent. Active volcanism is evidenced by the discharge of thermal and mineral waters and magmatic gases. Na, B, Cl, SO_4 and CO_2 are carried into the basin by thermal and mineral waters related to this volcanism. Potentially economic deposits of borate, chlorite, sulfate and carbonate salts related to this volcanic activity are presently forming within the basin (Helvacı and Ercan, 1993).

The Italian (Tuscany) steam vents from which sassolite was recovered also represent an active volcanic source. Hydrated borates may accumulate in several ways within a non-marine basin. They may be deposited in layers in a spring apron around a borate spring, with ulexite, borax, or inyoite as the primary borate mineral. Borates may also form in a pool dominantly fed by a borate spring, with borax crystals formed in bottom muds or at the intermittently dried margins (as at Clear Lake, and at Salar de Surire, Chile). The borates found in the large South American salars, such as Uyuni and Atacama, may also have formed by leaching of surrounding rocks and subsequent evaporation (Chong, 1984).

4.2. Marine Evaporites

Borates of marine origin have been found in commercial quantities only in Europe. These are magnesium borates associated with Permian salt deposits. They were produced in Germany as a byproduct of potash mining, and in the Inder region of Kazakhstan. The Inder deposits, where the borates occur as veins in the cap of a very large salt dome complex are reported to be remobilized and concentrated from the salt during the intrusion of the salt dome itself. Some of the Chinese deposits of the Liaoning Peninsula (most likely metamorphosed Precambrian non-marine evaporites) may be of similar origin although they occur as veins in Precambrian metamorphosed limestone and magnesite (Peng and Palmer; 1995, 2002). The Inder Lake brines which are also a source of Kazakhstan production appear to be simply a sump accumulation of borates leached from the huge Inder salt dome complex. The Kara-Boğaz-Göl Lagoon borates on the east shore of the Caspian Sea would also appear to be leached from marine brines (Figure 8).

4.3. Magmatic Sources (Skarn Deposits)

Pegmatites and contact metamorphic rocks contain assemblages of various boron-containing minerals such as datolite, ludwigite, paigeite, and tourmaline (Figure 8, table 2). These represent concentrations of boron that relate more or less directly to the crystallization of intrusive granitic magma. Granites average about 10 ppm boron with a few exceptions ranging up to 300 ppm. The conditions of high temperature, 300 to 400°C and fluids under high pressure at an intrusive contact also

provide the possibility that some of the boron may be extracted from the adjacent country rocks. These borate skarn deposits, some associated with iron ores and magnesium deposits of commercial grade, are mined in both eastern Russia and China.

5. Mineralogy

By at least 3.8 Ga, boron had been concentrated sufficiently to form its own minerals, which are thought to have stabilized ribose, an essential component of ribonucleic acid and a precursor to life. Boron has with two abundant isotopes, ^{10}B and ^{11}B; the former has a large capture cross-section that makes it an excellent neutron absorber. These two stable isotopes differ significantly in atomic weight so that boron isotopic compositions of minerals and rocks retain signatures from their precursors and the processes by which they formed. Boron compounds comprise a great diversity of crystal structures. Evaporites constitute the richest concentrations of boron on Earth, and thus are the main source of boron for its many applications in medicine, electronics and the nuclear industry.

Boron is extremely dispersed in nature, averaging 0.1 ppm in land-surface water, 3 ppm in the Earth's crust, and 4.6 ppm in seawater. At low levels, water soluble boron is an essential micronutrient for the growth and viability of plants; the range between insufficient and excess boron is narrow (0.25 to 15.0 ppm) and most soils are usually within this range. Borate has been found in animal tissues at about 1ppm resulting from ingestion of fruits and vegetables; it is not known to have an essential biochemical function, although it may play a role in the body's ability to use calcium. Borate is transported in plants and animals usually complexed with polyalcohols in the aqueous phase (Garrett, 1998; Helvacı, 2005).

Boron minerals commonly form in three main geological environments as skarn minerals related to intrusives, mainly silicates and iron oxides; magnesium oxides related to marine sediment; and hydrated sodium and calcium borates related to continental sediments and volcanic activity (Figure 8, table 2). Some skarn minerals are the source minerals for the Russian and Chinese production, the major ones being datolite and szaibelyite. Borax, kernite, colemanite, and ulexite are the main evaporite minerals, which provide the source for most of the world's production from Turkey, South America, and the United States (Table 3) (Palache et al., 1951; Muessig, 1959; Watanebe, 1964; Aristarian and Hulburt, 1972; Helvacı, 1978; Kistler and Helvacı, 1994; Grew and Anovita, 1996; Grew and Anovita, 1996; Helvacı, 2005; Garrett, 1998; Helvacı, 2012) .

Over 250 boron-bearing minerals have been identified, most commonly as sodium, calcium, or magnesium salts (Table 2). Borax, ulexite, colemanite and datolite are commercially significant today (Table 3). Borax or tincal, a natural sodium borate decahydrate, may be regarded as the major commercial source of boron with supplies coming from the United States, Argentian, and Turkey. The principal commerical mixed sodium-calcium borate, ulexite, is produced in Turkey and several countries in South America, whereas large-scale production of the main calcium borate, colemanite, is restricted to Turkey.

Borax is by far the most important mineral for the borate industry. It crushes freely and dissolves readily in water; its solubility and rate of solution increases with water temperature. Borax in large tonnages is present in the deposits at Boron, California (USA), Kırka, Turkey, and Tincalayu, Argentina. Kernite is present in minor amounts at Kırka and Tincalayu, but it makes up about a third of the total reserve at Boron (California), and has a higher B_2O_3 content than borax.

Colemanite is the preferred calcium-bearing borate used by the non-sodium fiberglass industry. It has low solubility in water, although it dissolves readily in acid. Some colemanite is used in Europe in chemical plants to produce boric acid because the supply from Turkey provides B_2O_3 at lowest cost. Turkey is the world's major source of high grade

Table 3- Commercial borate minerals.

Minerals	Emprical formula	B_2O_3 content (wt.%)
Colemanite	$Ca_2B_6O_{11}.5H_2O$	50.8
Ulexite	$NaCaB_5O_9.8H_2O$	43.0
Borax	$Na_2B_4O_7.10H_2O$	35.5
Kernite	$Na_2B_{14}O_7.4H_2O$	51
Pandermite	$Ca_4B_{10}O_9.7H_2O$	49.8
Hydroboracite	$CaMgB_6O_{11}.6H_2O$	50.5
Szaybelyite (ascharite)	$Mg_2B_2O_5.H_2O$	41.4
Datolite	$Ca_2B_2Si_2O_9.H_2O$	21.8

colemanite. The United States has important reserves in the Death Valley area, but only limited amounts are produced there at this time as the reserves of main deposits are running out. Colemanite is not known to occur in major deposits outside Turkey and North America, although the higher hydrate, inyoite, is mined on a limited scale in Argentina.

Ulexite is the usual borate found on or near the surface, in playa-type lakes and marshes of Recent to Quaternary age throughout the world, where it occurs as soft, often damp, masses of fibrous crystals. These "cotton balls" or "papas" are collected in major amounts in South America and China. Ulexite of Neogene age, which is mined and produced in Turkey and also occurs lesser amounts at Boron and Death Valley in the United States.

Szaybelyite (ascharite) is a major source of both Chinese and Russian borate material. It is a magnesium borate and like colemanite, has low solubility in water. Although it is less satisfactory, due to its magnesium content, substantial tonnages are utilized in eastern Europe, Russia, and Asia; it is not traded internationally as a mineral concentrate on a major scale. The Russians also produce substantial amounts of borates utilizing the skarn borosilicates, mainly datolite, with some reports of minor amounts of danburite, ludwigite, and tourmaline. Production of datolite, a silicate mineral, is confined to Russia. These minerals must first be liberated, concentrated, and then dissolved in acid to make a usable product because their natural melting points exceed those of the other minerals used in common glass furnaces.

Pandermite (priceite) was mined in Turkey and hydroboracite was mined in Russia and Argentina. Other minerals such as inyoite, howlite, meyerhofferite, and kurnakovite occur intimately associated with the major ores.

Boracite was used in Germany prior to 1945 where boracite and minor magnesium borates were recovered as a byproduct of potash mining. Axinite, suanite, kotoite, and others are listed in the literature as occuring with the Russian borosilicate ores.

Sassolite has only mineralogic interest at most occurences, for the quantity found is generally very small. In the Lardarello region of Italy, however, natural steam carries boric acid recoverable as sassolite, and for a long period prior to 1965, several thousand tons per year were produced.

6. Major Deposits

Four main metallogenic borate provinces, with exogenous deposits in continental environments, as recognized at a global scale and these metallogenic provinces contain the most important borate reserves in the world. They are Anatolia (Turkey), Western America (USA), Central Andes (South America) and Tibet-Qinghai Plateau (Central Asia) (Figure 7). The origin of borate deposits is related to Cenozoic volcanism, thermal spring activity, closed basins and arid climate. With the exception of Tibet-Qinghai Plateau, a collisional plateau, the other provinces were generated in a tectonic framework of non-collisional continental plateaus by plate subduction (Figures 10, 11 and 12).

Anatolia, Tibet-Qinghai Plateau and California are located in the northern hemisphere and the Andes in the southern hemisphere. The age of the borates is Cenozoic, principally, Miocene and Quaternary. Miocene borate deposits are present in Anatolia (ca. 18-14 Ma) (Figure 10), California (ca. 22-6 Ma) (Figure 11) and the Andes (ca. 7-5 Ma) (Figure 12).

Tibet-Qinghai Plateau has only Quaternary borate deposits and Anatolia has mainly Miocene borate deposits, although there are uneconomic Quaternary occurrences as well (Figure 5).

Four major borax deposits are present in the world; Anatolia (Kırka), California (Boron), and two in the Andes (Tincalayu and Loma Blanca) (Figure 7). Kırka, Boron and Loma Blanca have similarities with regard to their chemical and mineralogical composition of the borate minerals, and sequences are Ca/Ca-Na/Na/Ca-Na/Ca (colemanite and/or inyoite//ulexite //borax//ulexite//colemanite and/or inyoite). Borate minerals are enclosed in greenish volcaniclastic lacustrine evaporatic sequences, with minor tectonic deformation (Figure 13). Tincalayu deposit looks very different, as evaporites enveloped within red beds, showing disharmonic deformation, and a lithologic sequence composed from base to top of halite/gypsum/borax/ulexite. Borax textures are different in those four main deposits with chemical fine varves (mm) in Kırka; chemical thick varves (cm) in Boron; massive (m) in Tincalayu; and disseminated evapocrystals (mm to cm) in Loma Blanca (Kistler and Helvacı, 1994; Helvacı and Alonso, 2000; Helvacı, 2005).

Colemanite deposits with or without probertite and hydroboracite are present in Anatolia (Emet), Death Valley, California (Furnace Creek Fm.), and

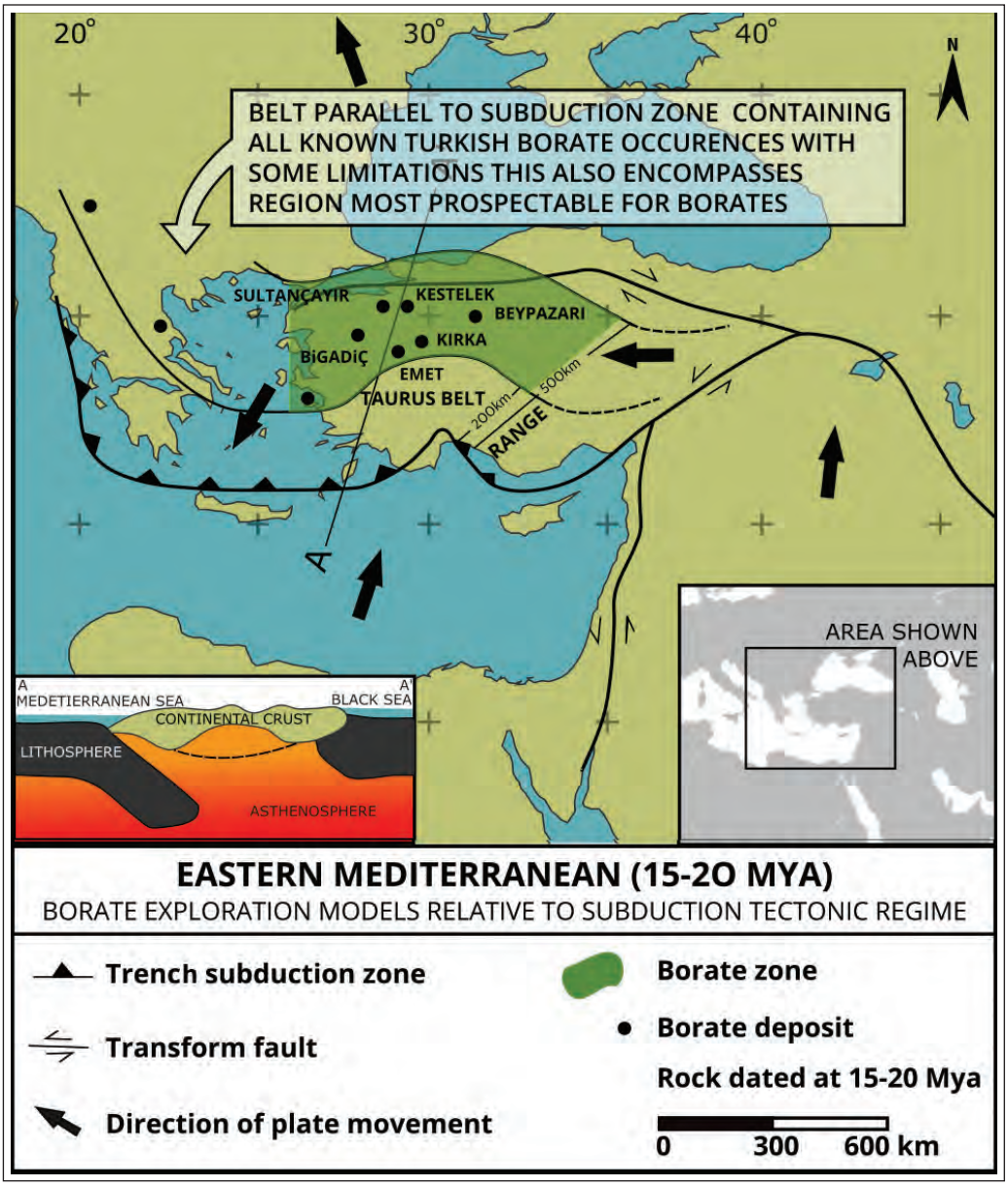

Figure 10- Known deposits and borate exploration model relative to subduction tectonic model for Eastern Mediterranean (15-20 My).

Sijes (Argentina) Quaternary borates are present in salars (Andes) and playa-lakes and salt pans (USA, Tibet-Qinghai Plateau, Central Anatolia). California and Andes have calcium and calcium- sodium borates (ulexite, borax, inyoite), as does the Tibet-Qinghai Plateau (ulexite and Mg-borates). Thermal springs and geysers, producing borate deposits, are common in the Central Andes (Kistler and Helvacı, 1994; Helvacı and Alonso, 2000; Helvacı, 2005).

6.1. Borate Deposits of Turkey

Turkish borate deposits were formed in the Tertiary lacustrine sediments during periods of volcanic activity, forming in separate or possibly interconnected lake basins under arid or semi-arid climatic conditions (Meixner, 1965; Özpeker, 1969; İnan et al., 1973; Helvacı and Firman, 1976; Helvacı, 1986, 1989, 1995; Kistler and Helvacı, 1994; Palmer and Helvacı, 1995, 1997; Helvacı and Orti, 1998; Helvacı and Alonso, 2000; Şaylı, 2003; Helvacı and Orti, 2004; Helvacı, 2005; Helvacı, 2012). Sediments in the borate lakes often show clear evidence of cyclicity, and much of the sediments in the borate basins seem to have been derived from volcanic terrain (Figures 13 and 14). In all the borate areas, intense calc-alkaline volcanic activity took place

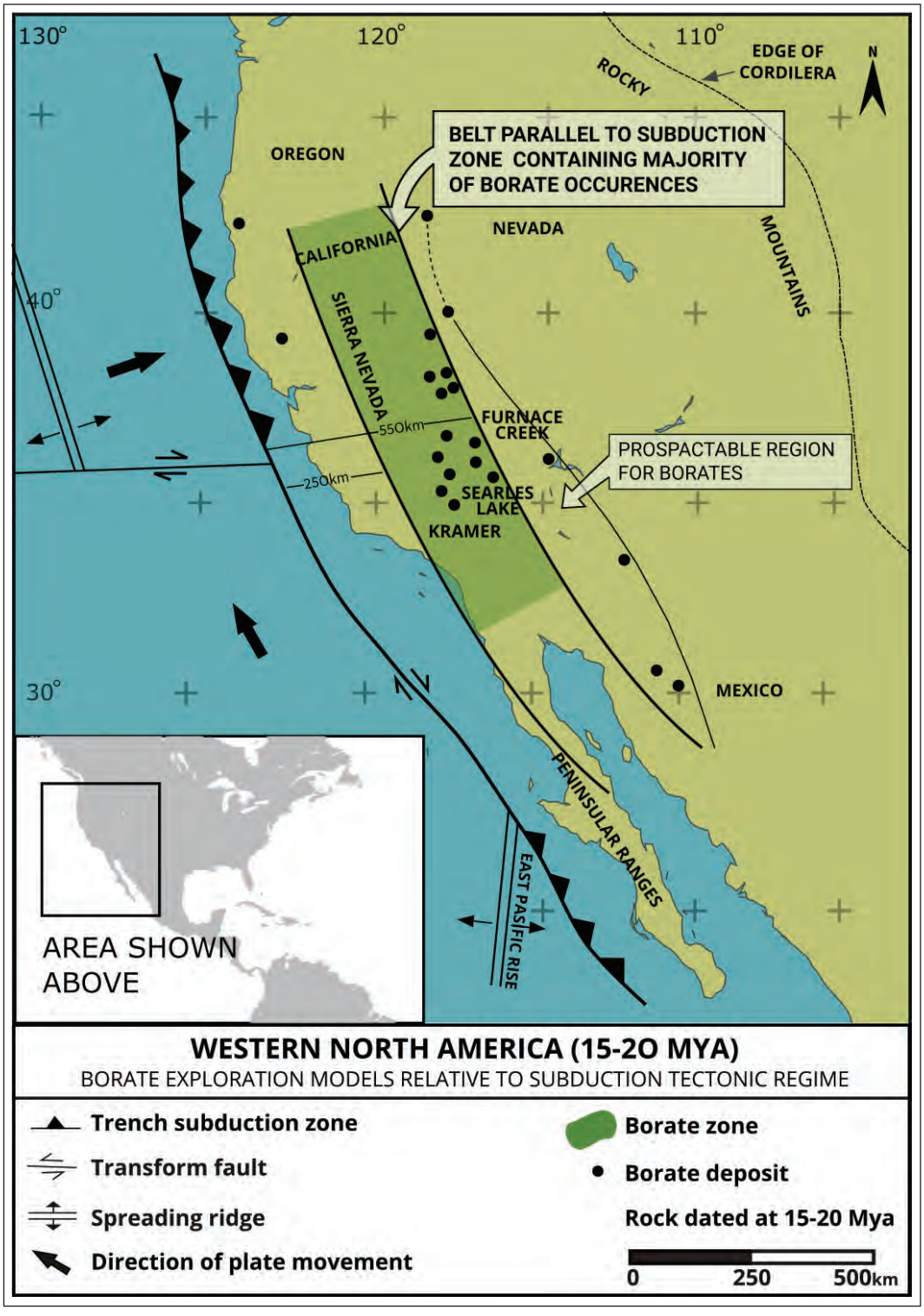

Figure 11- Borate exploration model relative to subduction tectonic model for Western North America (15-20 My).

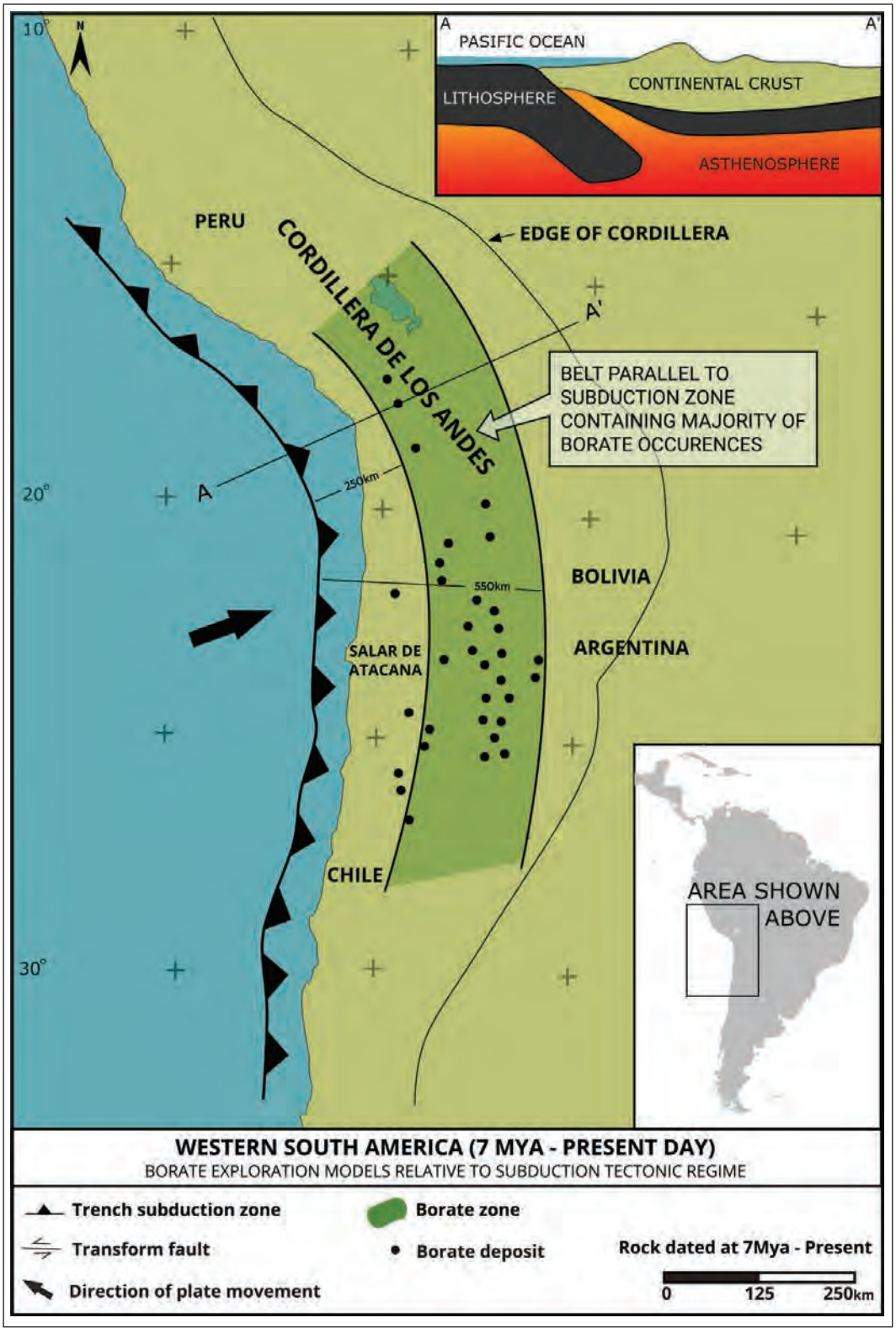

Figure 12- Borate exploration model relative to subduction tectonic model for Western South America (7 My-Present Day).

Figure 13- Volcaniclastic lacustrine evaporitic sequences associated with borate deposits, Bigadiç borate deposit, Turkey.

Figure 14- Sediments in the borate lakes showing clear evidence of cyclicity, and volcanic tuff intercalations with the sediments in the borate unit. Colemanite nodules occuring within clayey-tuffaceous matrix, Hisarcık open pit mine, Emet, Turkey.

simultaneously with the borate sedimentation. Volcanic rocks in the vicinity of the basins in which the borate deposits were formed are extensive and are represented by a calc-alkaline series of flows ranging from acidic to basic and by pyroclastic rocks which are interbedded with the sediments.

Pyroclastic and volcanic rocks of rhyolitic, dacitic, trachytic, andesitic and basaltic composition are interfingered with these lacustrine sediments (Figures 3 and 6). The existence of volcanic rocks in every borate district suggests that volcanic activity may have been necessary for the formation of borates. Thermal springs, which at present precipitates travertine, are widespread in the deposits.

Sedimentary-thickness varies from one deposit to another, probably because of deposition in a chain of interconnected lakes, and volcanosedimentary sequences exceed over 1000 m in the deposits. They are intensively dislocated by NE-SW and NW-SE-trending gravity faults (Figs. 2, 3 and 6). The extreme thickness of the borate zones at Emet, Bigadiç and Kırka indicates that there were somewhat different conditions existing at the time of the formation of these deposits. The borate deposits have the following features in common: They are restricted to lacustrine sediments deposited in a non-marine environment under arid or semi-arid climatic conditions. They were deposited in sedimentary closed basins of limited extent in regions where fresh water limestone deposition was widespread both before and after borate formation. The palaeogeographic scenario seems to have consisted of shallow lakes fed partly by hot springs and partly by streams which carried sediments from the surrounding volcanic, limestone and basement terrain (Figure 9).

Western Anatolia contains the largest borate reserves in the world and all the deposits formed during Miocene time in closed basins with abnormally high salinity and alkalinity. Neogene basins consisting of borate deposits were developed during an extensional tectonic regime in NW Turkey which was marked by NNE trending faults. All these basins were partially filled with a series of tuffaceous rocks and lavas. Boron-rich fluids are presumed to have also circulated along faults into these basins (Figure 9). The sediments deposited in the borate lakes are generally represented by tuffaceous rocks, claystones, limestones and Ca-, Na-, Mg-, Sr- borates. (Table 2). Sandstones and conglomerates occur in marginal parts of each basin. The borates are enveloped between tuff and clay-rich horizons (Figures 3, 6, 13 and 14). In the borate basins, intense calc-alkaline volcanic activity took place simultaneously with the borate sedimentation. The volcanic rocks are represented by a calc-alkaline series of flows ranging from acidic to basic and by pyroclastic rocks which are interbedded with the sediment (Figures 3 and 6).

The mineralogy of the Turkish borate deposits varies considerably and borate minerals recorded from the Turkish deposits are mainly Ca; Ca-Mg; Na and Mg borates. A rare Sr borate has been found at Kırka (Baysal, 1972; Helvacı, 1977) and Ca-As and Sr borates have been reported from the Emet district

(Helvacı and Firman, 1976 and Helvacı, 1977). The Kırka borate deposit is the only Turkish deposit is known to contain any of the minerals borax, tincalconite, kernite, inderite, inderborite and kurnakovite. Borate minerals are associated with calcite, dolomite, gypsum, celestite, realgar, orpiment and sulphur (Helvacı et al., 2012; table 2).

The known borate deposits of Turkey were formed in the NE-trending Neogene basins, and occur in 5 distinct areas (Figures 1 and 10). These are as follows: Bigadiç colemanite and ulexite deposits (Ca and Ca-Na Borate); Sultançayır pandermite deposits (Ca-type); Kestelek colemanite deposits (Ca-type); Emet colemanite deposits (Ca-type); and Kırka borax deposits (Na-type).

6.1.1. Bigadiç Deposits

Bigadiç contains the largest colemanite and ulexite deposits known in the world. The borate minerals formed in two distinct zones, lower and upper, seperated by thick tuff beds transformed during diagenesis to montmorillonite and chlorite and to zeolites. Colemanite and ulexite predominate in both borate zones, (Figures 3,15 and 16), but other borates include howlite, probertite, and hydroboracite in the lower borate zone; inyoite, meyerhofferite, priceite, terschite, hydroboracite, howlite, tunellite, and rivadavite are found in the upper borate zone (Özpeker, 1969; Helvacı, 1995; Helvacı and Orti, 1998; Yücel-Öztürk et al., 2014) (Table 2). The Bigadiç borate deposits were fed by thermal springs associated with local volcanic activity under arid climatic conditions.

6.1.2. Sultanyaçır Deposits

The borates are interbedded with gypsum, claystone, limestone, and tuff. Pandermite (priceite) is abundant, but other borates include colemanite and howlite (Table 2). Gypsum exists abundantly and calcite, zeolite, smectite, illite, and chlorite are the other associated minerals in this deposit (Orti et al., 1998; Gündoğan and Helvacı, 1993; Helvacı, 1994; Helvacı and Alonso, 2000). Howlite, which has apparently grown in the clays alternates with thin pandermite and colemanite bands. As a result of diagenetic events, some small howlite nodules are also embedded in the pandermite and colemanite noludes.

6.1.3. Kestelek Deposit

The borate zone consists of clay, marl, limestone, tuffaceous limestone, tuff, and borate. The volcanic activity produced tuff, and agglomerate, and andesitic and rhyolitic volcanics that are associated with the sediments (Helvacı, 1994; Helvacı Alonso, 2000). This sequence is capped by a unit consisting of loosely cemented conglomerate, sandstone, and limestone. The borate minerals occur interbedded with clay as nodules or masses and as thin layers of fibrous and euhedral crystals. Colemanite, ulexite, and probertite predominate, with hydroboracite

Figure 15- Colemanite nodules in varying sizes intercalated with associated sediments, Tülü open pit mine deposit, Bigadiç, Turkey.

Figure 16- Ulexite ore lenses intercalated with associated sediments, Kurtpınarı deposit, Bigadiç, Turkey.

occuring rarely. Secondary colemanite occurs as transparent and euhedral crystals in the cavities of nodules, in cracks and in vugs (Figure 17, table 2).

6.1.4. Emet Deposits

The Neogene sequence rests unconformably on Paleozoic metamorphic rocks that consist of marble, mica-schist, calc schist, and chlorite schist, and the sediments contains the borate deposits are interclated with clay, tuff, and marl containing the lensoidal borate formations (Figures 3 and 14); The unit consisting of clay, tuff and marl containing the borate deposits has abundant realgar and orpiment at some horizons indicating that arsenic and boron have a genetic relationship and volcanic origin at Emet (Table 2).

The Emet basin is one of the Neogene basins in western Turkey containing significant amounts of borate minerals, mainly colemanite. The borates are interlayered with tuff, clay, and marl with limestone occuring above and below the borate lenses. The principal borate minerals are colemanite and probertite (Figure 18), with minor ulexite, hydroboracite, and meyerhofferite. The Emet borate deposits contain many of the rare borate minerals such as veatchite-A, tunellite, teruggite, and cahnite (Helvacı and Firman, 1976; Helvacı, 1977; Helvacı, 1984; Helvacı, 1986; Helvacı and Orti, 1998; Garcia-Veigas et al., 2011).

The petrologic study of core samples from two exploratory wells in the Doğanlar sector, under optical and electron microscopy, eveals a complex mineral association in which probertite, glauberite, and halite constitute the major primary phases (without mineral precursors) precipitated in a saline lake within a volcano-sedimentary context. Other sulfates (anhydrite, gypsum, thenardite, celestite and kalistrontite), borates (colemanite, ulexite, hydroboracite, tunellite, kaliborite and aristarainite), and sulfides (arsenopyrite, realgar and orpiment) are attributed to early diagenesis. The Doğanlar deposit is the most important deposit of probertite known up to now (Garcia-Veigas et al., 2011). A new sulfate-borate mineral (fontarnauite) has been found in the deposit and the paper concerning this mineral is in press in Canadian Mineralogist (Cooper et al., in press). Montmorillonite, illite, and chlorite are the clay minerals that have been identified. Zeolites are abundant along the tuff horizons. Native sulfur, realgar, orpiment, gypsum and celestite occur in the borate zone throughout the area.

6.1.5. Kırka Deposit

The Neogene volcano-sedimentary sequence rests unconformably partly on Paleozoic metamorphics, a Mesozoic ophiolite complex, and Eocene fossiliferous limestone. The Neogene sequence consists of from bottom to top: volcanic rocks and tuffs; lower limestone with marl and tuff interbeds; borate zone; upper claystone; upper limestone containing tuff and marl with chert bands; and basalt (Figure 6). The principal mineral in the Kırka borate deposit is borax with lesser amounts of colemanite and ulexite. In addition, inyoite, meyerhofferite, tincalconite, kernite, hydroboracite, inderborite, inderite, kurnakovite, and tunnelite are found

Figure 17- Secondary colemanite crystals in the cavities of nodules, in cracks and in vugs, Kestelek, Turkey.

Figure 18- Colemanite is principal borate mineral and is interclated with green clay as nodular and elliptical lenses, Espey open pit mine, Emet, Turkey.

(Baysal, 1972; İnan et al., 1973; Helvacı, 1977; Sunder, 1980; Palmer and Helvacı, 1995; Floyd et al., 1998; Helvacı and Orti, 2004; Seghedi and Helvacı, 2014; table 2). This is the only deposit in Turkey that contains the sodium borates (borax, tincalconite, and kernite), together with inderborite, inderite, and kurnakovite. The borax body is enveloped by a thin ulexite facies, followed outward by a colemanite facies (Figure 19). The Mineral formation sequence in the Kırka deposit is Ca/Ca - Na/Na/Ca - Na/Ca (colemanite and/or inyoite / ulexite / borax / ulexite / colemanite and /or inyoite). The borate layers contain minor amounts of celestite, calcite, and dolomite, and the clay partings contain some tuff layers, quartz, biotite, and feldspar. The clay is made up of smectite-group minerals and less frequently, illite and chlorite minerals. Zeolites occur within the tuff horizons. This deposit is distinct from similar borax deposits at Boron and Tincalayu in having very little intercrystalline clay; the clay at Kırka is very pale green to white and is high in dolomitic carbonate (Figure 20). The borax crystals are fine, 10 to 20 mm, and quite uniform in size (Figure 20).

The ore body has thickness of up to 145 m, averaging 20 to 25 % B_2O_3.

6.2. Borate Deposits of USA

In 1856, J.A. Veach discovered borax in the muds associated with a mineral spring at what is now Clear Lake, in Lake County, California. Prospecting soon led to the discovery of larger deposits in the desert areas of western Nevada and southeastern California. Small-scale production began there in 1864. The first 63 years of domestic production saw several changes in both the type and location of the mineral deposits mined, but in general, production increased and the price of borax decreased as larger and better deposits were found and refinery techniques improved. The year 1927 was a benchmark in US borate history as both the large borax deposit at Boron and the Searles

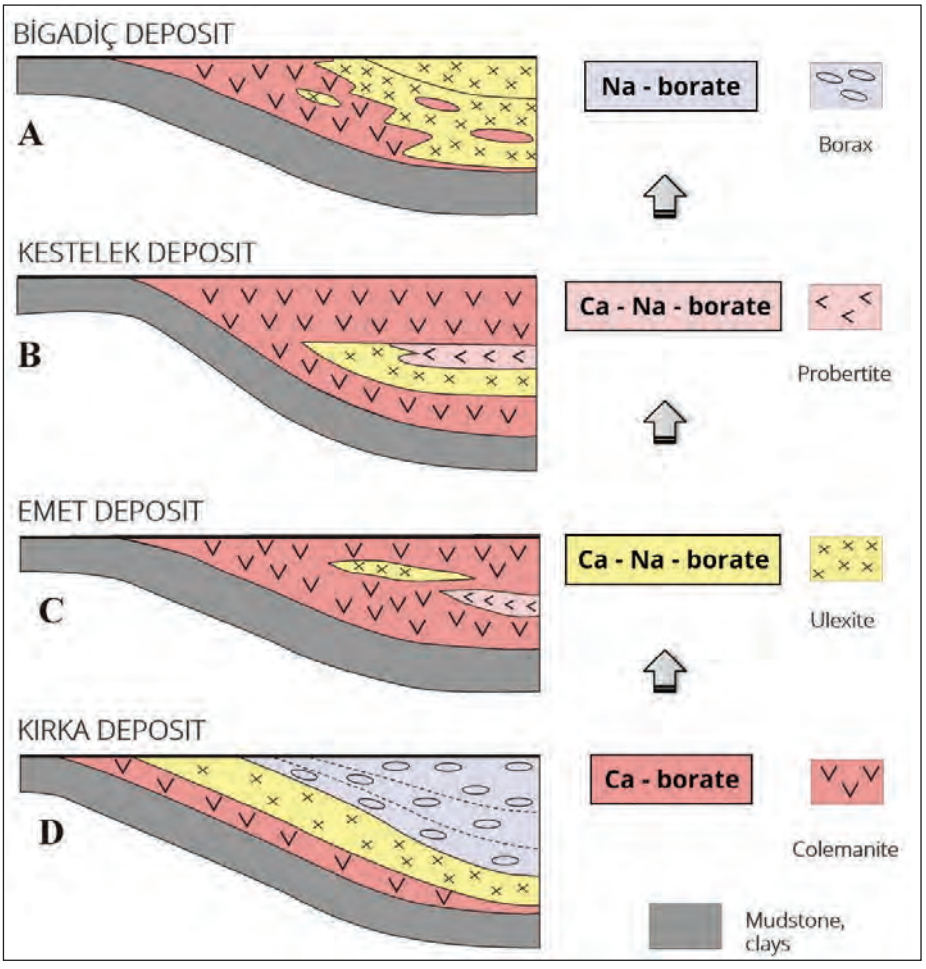

Figure 19- Sequence of boron mineral formations in Turkish borate deposits.

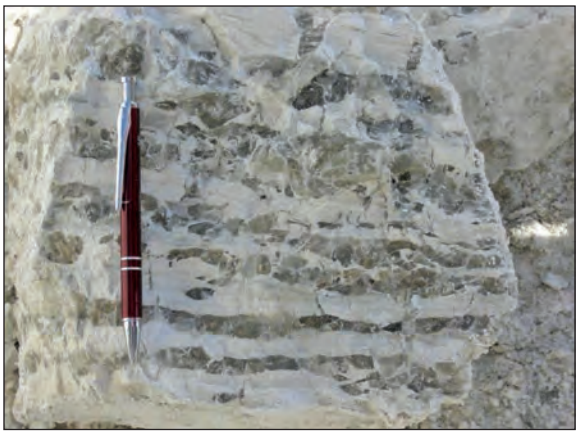

Figure 20- Borax layers and dolomitic clays alternating in Kırka borate deposit, Turkey.

Lake brines with their recoverable borax content were brought into large scale production and soon replaced most of the other domestic sources. Borates are presently produced at three locations in Southern California: Boron, Searles Lake, and, to a lesser extent, the Death Valley area (Bowser, 1965; Kistler and Helvacı, 1994;Garrett, 1998; Grew and Anovita, 1996; Helvacı, 2005; figure 11).

6.2.1. Boron, California (Kramer)

This deposit is located between the towns of Mojave and Barstow in the northwestern Mojave desert, 145 km northeast of Los Angeles. The Boron deposit consists of a lenticular mass of borax, kernite, and interbedded montmorillonite-illite clays. It is approximately 1.6 km long, 0.8 km wide, and up to 100 m thick. Outward from this central borax core, there is a facies change to ulexite and clay, which also exists above and below the borax. Colemanite facies are present as very thin lensoidal layers.

6.2.2. Saearles Lake, California

The Searles Lake playa occupies the central portion of a small desert valley midway between Death Valley and Boron, in southeastern California. The lake consists of a central salt flat, which overlies a crystalline mass of admixed salts, mainly sodium carbonates, with borax, clays and interstitial brines. The salts and brines are thought to be the end results of concentration, desiccation and decantation in a series of late Quaternary lakes which extended along the east front of the Sierra Nevada. Playa-type borax was discovered on the shores of Searles Lake as early as 1863. Small amounts of borax were produced from the playa surface until 1919, when borax along with trona and various other salts began to be recovered from brine wells sunk into the central portion of the lake, with large scale production beginning in 1927. At the present time, North American Chemicals Co. is the only company producing borates from the lake.

6.2.3. Death Valley, California

Death Valley is a long, north-trending valley near the Nevada border with Southern California. It is fault-bounded on both the east and west sides by active faults which have lowered the area near Badwater to 86 m below sea level. The valley contained several lakes during the Pleistocene and over 300 m of salts, mainly halite and gypsum, accumulated in the Badwater area at that time. Minor amounts of the playa borates, borax and ulexite, which occur with these salts, accumulated in the surface muds and seeps and were gathered in the early 1880s. The more productive playa area near Harmony, 32 km north of Badwater near the present National Park headquarters, was the source for the famous 20 Mule Team borates (1883-1897). This area of the Valley floor appers to be enriched by fluids derived from the leaching of the adjacent borate-containing Tertiary beds (Kistler and Helvacı,1994). In the late Neogene, over 2130 m of lake sediments were deposited in what is now Furnace Creek Wash, in and adjacent to the east side of Death Valley. It is these lake sediments of the Furnace Creek formation which contain the bedded borates (Tertiary colemanite-ulexite deposits) that were the main source of domestic borates from 1907 to 1927 and that are currently being mined (Figure 11). The 16 deposits that were commercially worked in the Death Valley area range in size from 181 kt to over 13.6 Mt, averaging 18 to 24 % B_2O_3. Production from the Billie underground mine operated by Newport Mineral Ventures, and from the Gerstley underground mine of US Borax located near Shoshone, California, about 50 km to the southeast of the Billie are presently almost closed down (Kistler and Helvacı, 1994).

6.2.4. South America

There are over 40 borate deposits located along an 885 km trend in the high Andes near the common borders of Argentina, Bolivia, Chile and Peru (Figure 12). This is an arid segment of the Andean tectonic-volcanic belt, characterized by compressional tectonics and many closed basins with playas or salt flats, called salars. Reserves are said to total millions of tons of B_2O_3. For many years (1852-1967), Chile

was a major producer of borates, but the industry gradually shifted to adjacent areas of Argentina. Recently, Chile has become a major borate producer again (Chong, 1984; Alonso, 1986; Alonso et al., 1988; Alonso and Viramonte, 1990; Helvacı and Alonso, 1994; Kistler and Helvacı, 1994; Helvacı and Alonso, 2000; Helvacı, 2005).

Borate spring deposits are better developed in South America than anywhere else in the world. These deposits consist of cones and aprons of ulexite and in one case borax, built up around vents from which warm to cool waters and gas are still issuing in some cases. Most deposits are associated with calcereous tufa which occurs as a late-stage capping over the borates, and sometimes with halite and gypsum as well. Recent volcanic activity is indicated by basaltic to rhyolitic flows in adjacent areas, and a volcanic source for the borates is presumed (Figure 12). The deposits currently forming are quite small, ranging from a few hundred to approximately 9 kt of borates averaging 20 % B_2O_3.

The salar deposits of South America consist of beds and nodules of ulexite with some borax or inyoite, associated with recent playa sediments, primarily mud, silt, halite, and gypsum. Springs and seeps appear to be the source of the borates. The brines of Atacama, Chile, and Uyuni, Bolivia, contain borates of possible commercial interest.

The borate deposits of Argentina are restricted to a high plateau formed in a non-collisional compressional orogen during the Late Cenozoic (Figure 10). Colemanite is the principal borate at the Monde Verde, Esperanza and Santa Rosa mines, whereas hydroboracite is the predominant borate in the Monte Amarillo deposit. The Tincalayu and Loma Blanca areas are important principally for borax occurences whereas, in salars, borax and ulexite are mainly present (Figure 12) (Kistler and Helvacı, 1994; Helvacı and Alonso, 2000). The borates are found in the Sijes formation of upper Miocene age, and there are at least six small open cut mines in the area which produce colemanite, inyoite, and hydroboracite. The borate deposits of the Pastos Grandes Depression represent the largest reserves of calcium and calcium-magnesium borates of Latin America (Figure 12, table 5). During deposition of the Sijes formation there were 3 major pulses of borate generation. The borate-bearing members of the Sijes formation are from the base to top as follows: Monte Amarillo (hydroboracite), Monte Verde (colemanite-inyoite) and Esperanza (colemanite). The Santa Rosa deposit is composed principally of colemanite and hydroboracite, with appreciable amounts of inyoite and ulexite (Helvacı and Alonso, 2000; Orti and Alonso, 2000).

The Loma Blanca borate deposit was formed in the muds of a playa-lake environment during the Late Miocene and is the fourth commercial Tertiary borax deposit in the world. This deposit consists of colemanite, inyoite, ulexite, borax, tincalconite and teruggite minerals within a mineral sequence that is a unique characteristic sequence of Argentian borate deposits (Alonso et al., 1988). Borax, tincalconite, colemanite, orpiment, native sulfur, montmorillonite, illite and chlorite have been identified in addition to the previously recorded minerals. Borax, inyoite and ulexite are the dominant minerals in the deposit. Arsenic sulfides and native sulfur are present in minor quantities, and are as widely distributed as the borates (Alonso et al., 1988).

Tincalayu is the name of a low hill located in the northwestern corner of the Hombre Muerto Salar that contains an important sodium borate deposit. The peninsula of Tincalayu which hosts the borate deposit of the same name lies in the extreme northwestern part of the Hombre Muerto Salar. The borax deposit lies within the southern part of the peninsula at an altitude of 4100 m (Helvacı and Alonso, 2000; figure 12).

There are more than 100 salars in Argentina, Chile, Bolivia, and Peru, but only about 40 contain borate facies in the chemical and detrital basin deposits (Figure 12). The dominant mineral in the salars is ulexite, and borax occurs in minor proportion (Chong, 1984). The ulexite occurs in 2 types: 1) nodules, the classic “cotton ball” called “papas” (potatoes), and 2) massive beds called “barras” by the miners of the region. The borate deposits in salars are directly related to supplies of boron-rich thermal waters. Ulexite from Chile currently enters the world market from at least five salars. About half of the total production estimated at 31 ktpy, comes from the Salar de Surire, a relatively small salar situated near the border with Bolivia. The ulexite occurs 6 to 14 cm below the surface as irregular masses and in beds that attain up to a meter in thickness and averaging perhaps 30 cm.

The source is Laguna de Salinas, Peru, which occupies a large mountain basin east of Arequipa, reached by 56 km of mountain road that crosses a mountain pass at nearly 5200 m (Figure 12). Ulexite occurs as irregular masses and lenses 25 to 130 cm

thick in fine, sandy detritus and green muds, 0.6 to 2.9 m thick, which lie below a surface layer of black to green muds with disseminated ulexite, sulfate, and halite. Very limited production of borates is reported from Bolivia. Reserves of playa borates and brines containing borates in the giant Salar de Uyuni have been known for many years, but supply and transport difficulties have hindered production (Helvacı and Alonso, 2000).

6.3. China

China produces about 27 ktpy of borate minerals and compounds from deposits in Liaoning, Xizang (Tibet), and Qinghai Provinces. The Liaoning production comes from a number of relatively small open pit and upderground mines on the Liaodong Peninsula of northeast China. There are reported to be more than 55 operations on some 112 separate deposits of which 12 contain 98 % of the reserves. The ores are magnesium borates, szaibelyite (ascharite), with ludwigite and suanite associated with magnesite, magnetite, and rare earths. The ores occur as veins in early Proterozoic (2.3 Ga) magnesian marbles of the middle Liaojitite suite. The ore bodies are closely related to, and conformable with, the Liaoji granites. Average grades are low by western standars, 5 to 18 % B_2O_3, and many of the smaller deposits are mined by labor intensive methods.

The Qinghai production comes from three playa lakes in the Tsaidam Basin of south-central China: Da Qaidam, Xiao Qaidam, and Mahai. The main borates are ulexite, pinnoite, hydroboracite, and borax. Recent reports indicate that the surface crusts of ulexite and pinnoite are mainly worked out and that most production is now from the brines. In addition, China has substantial reserves on the Tibetan Plateau where 57 lakes have been identified containing borates. These are not believed to be in large scale production at this time due to transport and supply difficulties (Kistler and Helvacı, 1994; Helvacı, 2005).

6.4. Other

There are a few data on the sources for borate production from Kazakhstan and Russia, which is estimated to be about 200 000 tpy (Ozol, 1977). For many years, the Inder (Gurvey) District of Kazakstan was considered the principal source. Borates, mainly szalbelyite and hydroboracite, occur there as veins and fracture fillings in a large Permian marine salt dome associated with gypsum, carbonate, and clay, and in the nearby brine lakes. Reserves of up to 7 Mt of 20 % B_2O_3 are reported. However, recent exchanges with Russian geoscientists indicate that 95% of the Russian supply now comes from the Bor deposit at Dalnegorsk in Primorsk near the Sea of Japan. The ore is a datolite skarn assemblage formed in Triassic limestones and siltstones intruded by a large pophyry dyke swarm. The borosilicate skarns occur over a length of 2 km and are up to 500 m wide; they have drilled ore grade material to 1000 m. Ore grade is estimated at 8 to 10 % B_2O_3 (30 to 45 % datolite). Minor production of ludwigite has been reported from small pipe-like bodies in North Korea at Khol-don (Hol-Kol) and Raitakuri, southwest of Pyongyang during the 1950s. There have been no recent reports that these deposits are currently in operation (Kistler and Helvacı, 1994). The colemanite body at Magdalena, Sonora, owned jointly by US Borax and Vitro (Mexico's major glass producer) remains on standby status pending an upturn in the market. The development of this deposit has been hampered by processing problems and the relatively high arsenic content of the ore. The occurence of low grade borates, predominantly howlite and colemanite, has been reported from the Jarandol Basin of former Yugoslavia (Figure 21). The borates here apparently lie above the commercial coal seams and are associated with zeolites, tuff, gypsum, calcite, and bitumen. A small colemanite occurrence has been noted on the Greek island of Samos just off the Turkish coast are the first borates reported from the Greek Isles (Helvacı et al., 1993). In the western part of Samos Island (Greece), a small borate lens occurs which is composed of colemanite and traces of ulexite. Layers of gypsum occur below the borates while celestite nodules and lenses occur within and above the borate body, which is hosted in Late Miocene claystone and tuffaceous layers. Hydrothermal vein deposit of borates occur in a fault zone in the northwestern part of Iran (Zencan deposit near Tebriz city).

7. Mining, Mineral Processing and Uses

7.1. Mining

The sodium borates borax (tincal) and kernite, the calcium borate colemanite, and the sodium-calcium borate ulexite make up 90% of the borates used by industry worldwide (Table 3). Most borates were extracted primarily in California and Turkey and to a lesser extent in Argentina, Bolivia, Chile, China, and Peru. Boron compounds and minerals are produced by surface and underground mining and from brine.

Figure 21- Location of borate deposits in Vardar Zone.

Commercial borate deposits in the world are mined by open pit methods (Figure 22). The world's major borate operations, the Boron mine of US Borax at Boron (Kramer), California, and the Kırka mine of Eti Maden in Turkey are huge open pit mines utilizing large trucks and shovels and front end loader methods for ore mining and overburden removal. Ores and overburden are drilled and blasted for easier handling. The boron operation uses a belt conveyor to move ore from the in-pit crusher to a coarse ore stockpile form which it is reclaimed by a bucketwheel that blends the ore before it is fed to the refinery. Kırka utilizes trucks which haul to a crusher near the refenery which is about 0.5 km from the current ore faces.

Smaller operations in Argentina, Chile, China, Turkey, and Russia use similar methods, but on a scale down-sized to the scale of the operation. Some of the South American and Chinese salar operations utilize hand labor to mine the thin salar borates, generally after stripping of overburden with a small dozer on a front end loader (Alonso and Helvacı, 1988; Helvacı, 1989; Kistler and Helvacı, 1994; Helvacı, 2005).

Borates are mined by underground methods in the Liaoning area of northeast China, at the Billie and Gerstley mines in Death Valley, California. Borate brines are recovered at Searles Lake, California, and in the Qinghai Basin of China; brines may also be utilized in the Inder region of Kazakhstan. Borate containing brines are being considered for production from several salars in South America.

7.1.1. Mineral Processing

Processing techniques are related to both the scale of the operation and the ore type, with either the upgraded or refined mineral (borax, colemanite, ulexite) or boric acid as the final product for most operations (Table 4). Borax-kernite ores (Boron, Kırka, Tincalayu) are crushed to 2,5 cm and then dissolved in hot water/recycled borate liquor. The resultant strong liquor is clarified and concentrated in large counter-current thickeners, filtered, fed to vacuum crystallizers, centrifuged, and then dried. The final product is refined borax decahydrate or pentahydrate or fused anhydrous borax, or is used as feed for boric acid production. Colemanite concentrates are used directly in specific glass melts or used as a feed for boric acid plants.

The ulexite from most of the South American salars is air dried, screened, and bagged. It is then combined with locally available sulfuric acid to produce a relatively low grade boric acid or exported as feed for boric acid plants elsewhere. The

Figure 22- Section of borate zone interbedded with clay and tuff, and limestone overburden, Espey deposit, Emet, Turkey.

magnesium borates are generally concentrated, dissolved in acid to remove the magnesium, and then converter to boric acid or sodium borates. The borosilicates of the Bor deposit in eastern Russia with their relatively low B_2O_3 grades, are crushed, and then run through a complex plants, which includes magnetic separators, heavy media separators, and flotation cells. The concentrates are then dried, leached, and calcined before being converted to boric acid or to a sodium borate.

The brines that form Searles Lake, and presumably the Chinese sources, are recovered by either controlled evaporation or carbonation. In the latter process, carbon dioxide produced from lime kilns or flue gas is bubbled through the brine to crystalize sodium bicarbonate; borax is then crystallized in vacuum crystallizers. In the "evaporation" process, a rapid, controlled coolings electively crystallizes the various salts. The remaining borate liquor is fed to tanks containing borax seed crystals which aid in the recovery of borates from the liquor. The resultant slurry is filtered, washed, redissolved, and fed to vacuum crystallizers that produce dehydrate borax products or boric acid (Kistler and Helvacı, 1994).

Boric acid is one of the final products produced from most of the processes (Table 4). The world's largest boric acid facility is located adjacent to the Boron pit and the Emet and Kırka opencast mines. Other smaller facilities around the world make use of smelter acid or other locally available acid feed-stock to produce products acceptable to their local markets.

7.2. Uses

Borate minerals have been employed in a wide range of uses for many centuries, dating from at least the 8th century when they were used primarily as a flux for assaying and refining gold and silver (Figure 23).

Borate was traded at relatively high prices for highly specialized applications into the late years of the 19th century. At that time they were being used for medicines, food preservatives, ceramic glazes, and in expanded applications as metal fluxes. Borate

Table 4- Commercial refined borate productions.

Product	**Formula**	**% B_2O_3**
Borax decahydrate	$Na_2B_4O_7\ 10H_2O$	30,5
Borax pentahydrate	$Na_2B_4O_7\ 5H_2O$	47,8
Boric acit	H_3BO_3	56,3
Borax anhydrous	B_20_3	100,0
Sodium perborate	$NaBO_3\ 4H_20$	22,0
Raw borax anhydrous	$Na_2B_2O_3$	69,2

are often defined and sold by their boric oxide or B_2O_3 content, and most statistical data are listed in tons of B_2O_3. Borax pentahydrate and boric acid are the most commonly traded commodities. Boric acid plants are operated by all of the major borate producers. Glass fiber insulation is the major end use in the United States followed by textile glass fiber and borosilicate glass, detergents, and ceramics. Detergent usage continues to be a major end use in Europe (Figure 24).

Fertilizers represented the third largest application of borates. Ceramics comprise the second largest application of borates after glass, accounting for 10% of world consumption. Borates play an important role in ceramic glazes and enamels, increasing chemical, thermal, and wear resistance. Borax and colemanite are used in ceramics primarily as fluxing agents, with borax being used in higher temperature, and colemanite in lower temperature firings. Borates were incorporated into various materials, such as cellulose insulation, textiles, and timber, to impart flame retardant properties to the materials. Boric acid is incorporated into wood flame-retardants to inhibit the transfer of combustible vapors and reduce the effective heat of combustion, resulting in reduced flame spread. The use of borates in detergents and soaps represented the fourth largest market,

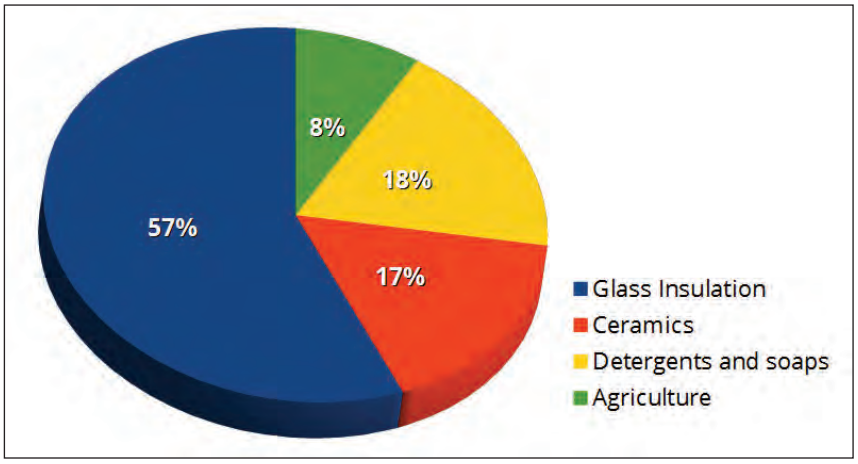

Figure 23- World borate end uses (after Helvacı, 2005).

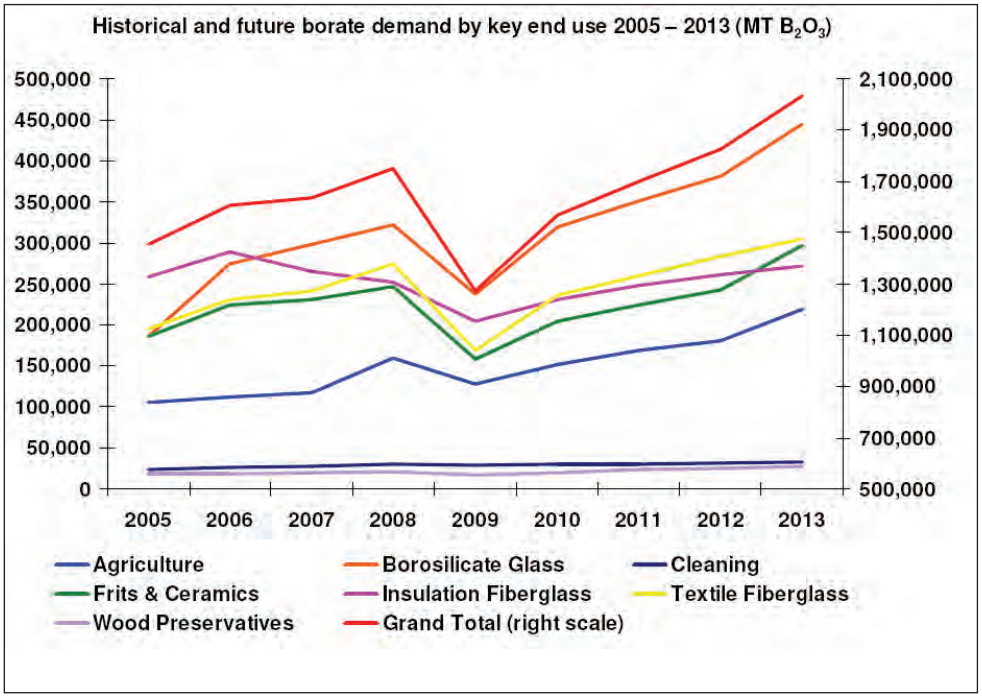

Figure 24- Present and future borate demand by key end use 2005-2013 (MT B2O3)(source: Rio Tinto).

accounting for 4% of world consumption (Kistler and Helvacı, 1994; Helvacı, 2005). Borates are incorporated into laundry detergents, soaps, and other cleaning products because they can be used as alkaline buffers, enzyme stabilizers, oxygen based bleaching agents, and water softeners. Two borates, sodium perborate and perborate tetrahydrate, are used as oxidizing bleaching agents because they contain true peroxygen bonds. The principle market for borates in 2011 was glass, representing approximately 60% of global borate consumption. Boron is used as an additive in glass to reduce thermal expansion, improve strength, chemical resistance, and durability, and provide resistance against vibration, high temperature, and thermal shock. Boron is also used as a fluxing agent, reducing the viscosity of glass during formation to improve manufacturing. Depending on the application and quality of the glass, borax, boric acid, colemanite, ulexite, and sodium borates are typically used. Ferroboron (FeB) is a binary alloy of iron with a boron content between 17.5% and 24% and is the lowest cost boron additive for steel and other ferrous metals. On average, the steel industry consumes more than 50% of the ferroboron produced annually (Eti Maden Inc., 2003). Various boron compounds are used in nuclear powerplants to control neutrons produced during nuclear fission. The isotope boron-10, in particular, possesses a high propensity for absorbing free neutrons, producing lithium and alpha particles after absorbing neutrons. Control rods composed of boron carbide are lowered into a nuclear reactor to control the fission reaction by capturing neutrons. Boric acid is used in the cooling water surrounding nuclear reactors to absorb escaping neutrons (Ceradyne Inc., 2011).

Boron minerals and their products are indispensable industrial raw materials of today. They are widely used from hygiene to health, from durable materials to space industry. Boron minerals and products used in different branches of industry, comprise major industrial utility products such as; fibreglass, medical applications and pharmaceutical materials, for safety purposes in nuclear reactors, artificial fertilizers, in photography, glass and enamel. Used in several compound forms like borax and boric acid, boron creates multi-faceted and useful components. The subject compounds provide an advantage especially in strong soldering, in welding, in reducing friction and in processes of metal purification. Borax and boric acid, with their property to diminish bacteria, to dissolve easily in water and to soften water; are extensively used in the making of soaps, cleansing agents, detergents, office products, textile colouring, protection of different materials, low resistant alloys and agricultural industry. Some boron products, because of their property as a excellent fluxing agents, are essential materials in metal purification and production of steel, atomic reactors, ignition switch fuses, lamps in electronic tools and solar batteries. Boron compounds; diborane (B_2H_6), pentaborane (B_5H_9), decaborane ($B_{10}H_{14}$) and alkali borons are foreseen as the potential jet and rocket fuels of the future (Kistler and Helvacı, 1994; Helvacı, 2005).

The principal uses of borates have not changed much in the past decade and major markets include fiberglass, insulation, textile or continuous-filament glass fibers, glass, detergents and bleaches, enamels and frits, fertilizers, and fire retardants (Figures 23 and 24). Bleaches and detergents are also the major end use; however, sales for glass and glass fibers including fiberglass, are increasing. Boron fiber-reinforced plastics continue to be utilized in quantity for aerospace frame sheathing where they combine flexibility and light weight with strength and ease of fabrication. Relatively minor uses that are expected to increase in the near future include those in fertilizers, wood preservatives, alloys and amorphous metals, fire and flame retardants, and insecticides. However, the promising field of boron-iron-silicon electrical transformers has not developed as rapidly as predicted due to various cost factors.

Miscellaneous uses include pharmaceuticals, cosmetics, anti-corrosion compounds, adhesives, abrasives, insecticides, metallurgical processes, and nuclear shielding. Research is still continuing in many areas. One of the more publicized of these is in super magnets, where borates, combined with rare earths, nickel and iron, produce an alloy that can be used to make electromagnets for computer drives, high fidelity speakers, automobile starter motors, and various household appliances.

Borates can be utilized to protect the environment by aiding in converting heavy metals in industrial waste streams into recoverable free metals and by removing impurities from polymers used in bleaching wood pulp for paper production. Borates also aid in the control of the refractive index in optical fibers for medical research where precise control is needed. Other medical applications include cancer research where the ^{10}B istope reacts with low energy neutrons to give off short range alpha particles that can be used for microsurgery in previously inoperable areas of the

brain. Current tests on boron analogues indicate they may be effective in reducing serum cholesterol and other disease-causing proteins. Borates have become a relatively modestly priced industrial mineral commodity in recent years following the development of the large deposits at Boron, and more recently, Kırka. Prices are directly related to the cost of production, of which the major cost is fuel for drying, dehydrating, and melting the refined ore into the products desired by industry. Industry prices for most products have held steady with the rate of inflation.

Borates are a lightweight commodity and are generally sold in bulk by rail carload lots, in IBC's (Intermediate Bulk Containers) or "super-sacks," and by palletized bags. Overseas shipments are made mostly in bulk from special terminals at Los Angeles, California, and from Bandırma on the Marmara Sea in Turkey, to similar terminals in the Netherlands, Belgium, and the United Kingdom, from where it is moved by barge, as well as rail and truck. Other imports to Europe arrive in Italy and Spain. Imports to the Far East are generally sold in small bag lots. Bulk imports to the United States (mainly colemanite) usually land in Charleston, SC, where there are griding facilities; this colemanite is then shipped to easter fiberglass manufacturers. There is no import duty on borates brought into the United States (Kistler and Helvacı, 1994; Helvacı, 2005).

8. Future Forecasts

Known reserves of borate minerals are large, particularly in Turkey, South America, and the United States, and production from Turkey and the United States will continue to dominate the world market. However, borates from other areas will probably take up an increasing share of the world market. This trend is already evident with boric acid from Chile reaching the Far East and Europe, and both Russia and China beginning to export (Figures 25, table 5).

Both western Europe and Japan, neither of which has local borate sources, are major markets for US and Turkish production. South America is largely self sufficient with an increasing amount in excess of their needs which is exported mainly to Europe and Japan. Russia and China both appear to be self sufficient in borates at this time, although their costs of production per ton of B_2O_3 are thought to be relatively high.

Approximately 75-80% of the world's boron reserves are located in Turkey (Engineering and Mining Journal, 2012)(Table 5). The main borate producing areas of Turkey, controlled by the state-owned mining company Eti Maden Inc., are Bigadiç (colemanite and ulexite), Emet (colemanite), Kestelek (colemanite, probertite, and ulexite), and Kırka (borax-tincal). Production of refined borates increased during the past few years owing to continued investment in new refineries and technologies. Eti Maden planned to expand its share in the world boron market from 36% to 39% by 2013, increasing sales to $1 billion by expanding its production facilities and product range. In 2009, Turkey exported 4 Mt of borates valued at $104 million (Uyanik, 2010). Consumption of borates is expected to increase, spurred by strong demand in the Asian and South American agriculture, ceramic, and glass markets. World consumption of borates was projected to reach 2.0 Mt B_2O_3 by 2014, compared with 1.5 Mt B_2O_3 in 2010 (Rio Tinto Inc., 2011; Roskill Information Services Ltd., 2010, p. 167; O'Driscoll, 2011).

The European Union (EU) added borates to a list of banned minerals, which required detergent makers to decrease their use of boron following an EU ruling that determined continuous exposure may be harmful (Lismore, 2012). Demand for boron based fertilizers was expected to rise as a result of an increase in demand for food and biofuel crops. Consumption of

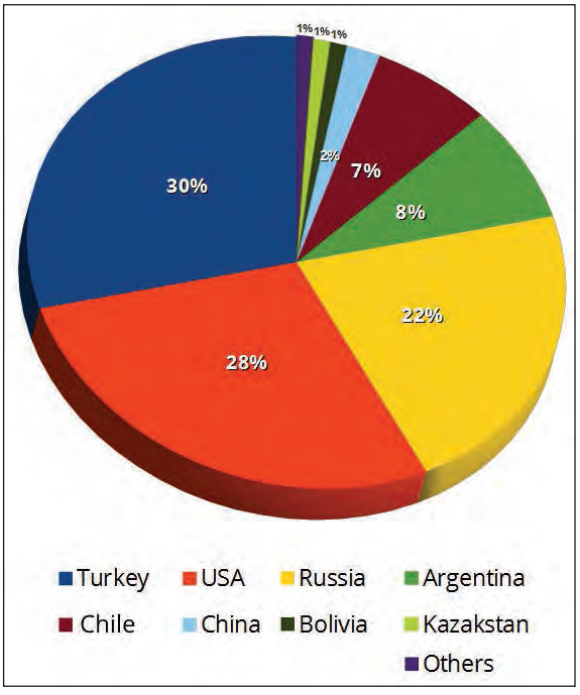

Figure 25- World borate production (Helvacı, 2005).

borates by the ceramics industry was expected to shift away from Europe to Asia, which accounted for 60% of world demand in 2011. Consumption of boron nitride is expected to increase owing to the development of high-volume production techniques coupled with the creation of new technologies. The properties intrinsic to cubic boron nitride, such as hardness (second only to diamond), high thermal conductivity, and oxidation resistance make it an ideal material in a variety of emerging applications. Hexagonal boron nitride is used in additives, ceramics, and intermetallic composites, imparting thermal shock resistance, improved machinability, and reduction of friction.

Turkey, USA, Russia, China, Kazakhstan, Italy, Argentine, Bolivia, Peru and Chile are prominent countries that produce boron minerals and products. Sassolite, borax kernite, ulexite, probertite, pandermite, colemanite, hydroboracite and szaibelyite are economically operated boron mines that have commercial importance. Borax decahydrate, borax pentahydrate, anhydrous borax, boric acid, sodium perborate tetrahydrate, sodium perborate monohydrate and anhydrous boric acid are economically significant chemical boron components. Turkey's borate deposits are the largest and highest grade (respectively 30, 29 and 25% B_2O_3) of colemanite, ulexite and borax (tincal) deposits in the world and have sufficient potential to meet the demand for many years (Table 5).

Boron consumption is directly related to the usage of glass, glass fibers, and ceramics. These materials, along with certain plastics that contain borate products, are seen as having a steady consumer demand in the construction and housewares markets well into the next century. Borates are an essential part of certain plant foods. Their use in nuclear reactor shielding and control is well documented. Other major uses, detergents, plant foods, wood preservation etc. are expected to show a slowly rising demand. Total world borate demand is expected to grow at about 3% per year in the near future, based on industry forecasts (Table 5, figure 26). Future markets are difficult to predict. Based upon recent history, the major world consumers of borates will continue to be the developed countries of North America, Europe, and Japan.

Turkish Scientific and Technical Research Institute (Tübitak- MAM), carried out a project of transforming sodium boron hydride, expected to be the most important potential hydrogen transporter of the future, into industrial production on a pilot-scale, in 2008. The discovery by a Turkish company NNT, through advanced technology of the Borpower engine- lubricant end-product, saves fuel by up to 20% in motor vehicles, expands vehicles' rectification and oil life by a factor of two.

Turkey exports 51% of its boron products to EU contries. Although the EU has recently asserted that boric acid and sodium borates have a negative effect on human reproduction, this is not supported by research in the area covered by the borate deposits and facilities, which show that boron and its products do not have a significant impact on human reproduction (Şaylı, 2003).

Table 5- The reserves and life estimates of the world's borate deposits (Helvacı, 2005).

	Know Economic Reserve (Million tons of B_2O_3)	Total Reserve (Million tons of B_2O_3)	Estimated Life of Known Reserve (year)	Estimated Life of Total Reserve (year)
TURKEY	224.000	563.000	155	389
USA	40.000	80.000	28	55
RUSSIA	40.000	60.000	28	69
CHINA	27.000	36.000	19	25
CHILE	8.000	41.000	6	28
BOLIVIA	4.000	19.000	3	13
PERU	4.000	22.000	3	15
ARGENTINA	2.000	9.000	1	6
KAZAKHSTAN	14.000	15.000	10	10
TOTAL	**363.000**	**885.000**	**253**	**610**

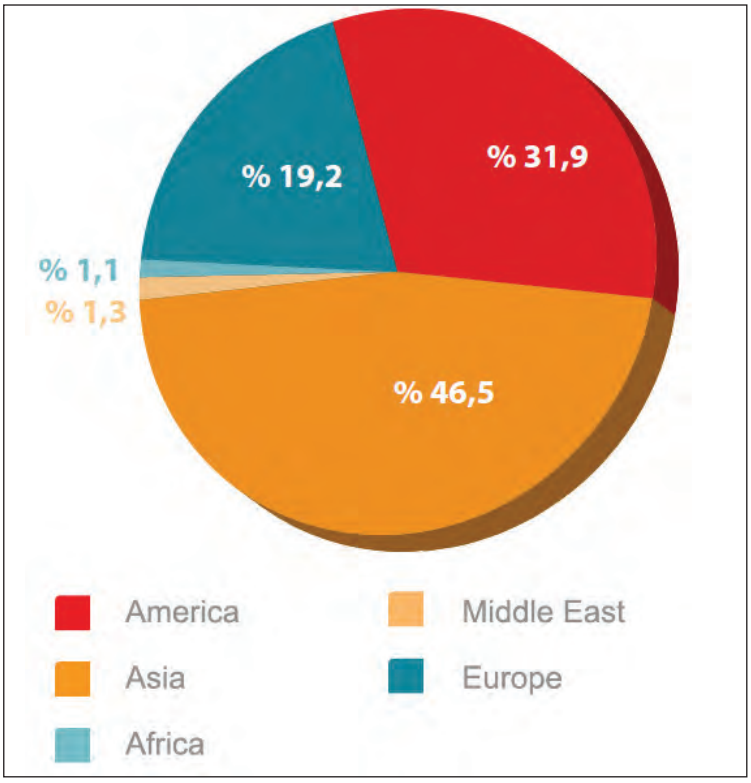

Figure 26- The World Regional Borate Consumption (%)(source: Rio Tinto).

Turkey has the largest boron mines in the world. Turkey has an important share in the world markets with borax (tincal) production in Kırka; colemanite and ulexite production in Emet, Bigadiç and Kestelek regions. Between 1980-2008, Turkey became the biggest colemanite producer in the world. Turkey's visible and potential reserves are greater than its current production. Even the most pessimistic observers are unanimous on the opinion that these borate reserves should be able to meet demands for a couple of hundred years (Figure 22, table 5). The world is dependant on Turkey with its supplies of widely used colemanite and ulexite. All countries in the world extensively using this mineral are dependant on Turkey's boron supplies. Turkey has a substantial potential in the world in terms of both the operation costs of boron mine reserves and it has grade advantages. Borate deposits in Turkey cannot be matched with any other countries in the world, with regard to reserves and grade.

As far as the National Boron Policy is concerned, after the Nationalization Act in 1979, the intensive work has been done on different borate deposits to show the value of boron mineral potential in Turkey. These natural resources, are superior to their equivalents in the world in every respect, are able to bring the country to an unrivalled position in the boron salts sector. Eti Maden Inc. and the private sector should cooperate in producing end products from boron minerals, thus follow marketing and industry oriented research policies.

It is an obligation to operate production of boron minerals towards the country's best interest, in order to hold on against world monopolies and to protect itself from their seperatist influences. In terms of mining, operation of our boron mines are at an advantage with respect to geography, transportation, energy, etc. compared to other countries (especially Latin America, USA and China) and suitable for marketing. For example, the boron deposits in South America are at an altitude of 4000 metres and those in North America are located in the middle of the desert, hence making it very difficult and problematic to operate them.

It is essential for Turkey to form a new national boron policy, so that it can appraise this natural resource with the highest return. The only way to achieve this goal is by operating boron mines towards the best interest of the country and sustaining the advantages it has. The country's resources need to be evaluated in a planned and programmed manner.

Production policy should be grounded on detailed and thorough market research. These important raw-material resources must be restructured and organized to ensure maximum return for the country's economy. In order to protect the advantages to the benefit of our country, research and technological development towards production of end-products with a high added value, should take first place in the fundamental restructuring rather than export of the raw mineral boron raw and semi-manufactured products.

As a conclusions for development of Eti Maden Inc. and Boron Salts Institute, investments and organizations are required. For the purpose of developing all kinds of industrial end-products, production, making short and long-term studies and projects, expert researchers from different fields like material, mechanical, chemistry and electric-electronic, should be employed in these institutions. This will allow closing of the gap between research and implementation and forward-looking, planned research that meets these requirements should be accelerated (Figure 27, table 5).

Today, as economic competition is becoming more intense and many studies are being made on natural resources; the existence of a massive boron reserve potential is a great opportunity for Turkey. Production and marketing of boron minerals should be directed towards end products with a high added-value, instead of raw or semi-finished products, and related investments have to be realized as soon as possible.

Boron products have a high added-value and they have a strategic role in the area they are used. Recently, boron products have been utilized in different fields of industry and shown an increase parallel to technological innovations. Rising standards of living, advancement of scientific and technological discoveries will eventually result in the demand and necessity for advanced boron compounds. Boron operation requires restructuring in a way to provide maximum return on the country's economy.

Ultimately, it is apparent that we face the responsibility and necessity to focus our policies in terms of science and nationwide, on important and strategic minerals, mainly boron. Otherwise, there is stands the possibility of coming up against unfavourable conditions as the destitute keepers of rich natural resources. The main aim here is to sustain the favourable position of our country on boron, which is a duty that relies on each and every citizen.

Acknowledgments

I am especially grateful to Eti Maden, MTA, US Borax, Borax Argentina S.A. and Industrias Quimicas Baradero and their mine managers for their generosity during fieldwork in Turkey, USA and Argentina, respectively. This study has been encouraged by a research projects supported by the Dokuz Eylül University (Project Numbers: 2005.KB.FEN.053; 2006.KB.FEN.001; 2009.KB.FEN.026; 2010.KB.FEN.009; and 0922.20.01.36) and the Scientific and Technical Research Council of

Figure 27- Eti Maden's 2023 Projection, Turkey.

Turkey (TÜBİTAK, Project No: YDAB.AG-100Y044 and ÇAYDAĞ-103Y124). Mustafa Helvacı is gratefully acknowledged for his typing and drafting assistances which significantly improved the manuscript. I would like to thank the reviews of M.R. Palmer, H.G. Dill, Y.Genç, and H.Mutlu for their constructive comments and suggestions, which have considerably improved the final version of the manuscript.

Received: 19.12.2014
Accepted: 08.02.2015
Published: December 2015

References

Akdeniz, N., Konak, N. 1979. Simav–Emet–Dursunbey–Demirci yörelerinin jeolojisi [Geology of the Simav–Emet–Dursunbey–Demirci areas]. *Maden Tetkik ve Arama Genel Müdürlüğü* Rapor No: 6547, Ankara (unpublished).

Aldanmaz, E., Pearce, J.A., Thirwall, M.F., Mitchell, J.G. 2000. Petrogenetic evolution of late Cenozoic, post-collision volcanism in western Anatolia, Turkey. *Journal of Volcanology and Geothermal Research*, 102, 67-95.

Alıcı, P., Temel, A., Gourgaud, A. 2002. Pb-Nd-Sr isotope and trace element geochemistry of Quaternary extension-related alkaline volcanism: a case study of Kula region (western Anatolia, Turkey), *Journal of Volcanology and Geothermal Research*, 115, 487-510.

Alonso, R.N. 1986. Occurrence, Stratigraphic Position and Gnesis of the Borate Deposits of the Puna Region of Argentina. PhD Thesis, *Universidad Nacional de Salta* (in Spainsh, unpublished)

Alonso, R.N, Helvacı, C. 1988. Mining and concentration of borates in Argentina. In: Aytekin, Y. (ed). Proceeding of the II International Mineral Processing Symposium, İzmir, Turkey, 551-558.

Alonso, R.N., Helvacı C., Sureda, R.J, Viramonte J.G. 1988. A new Tertiary borax deposit in the Andes. *Mineralium Deposita* 23: 299-305.

Alonso R.N.,Viramonte, J.G. 1990. Borate deposits in the Andes. In: Fontbote, L. Et al. (eds), Stratabound ore deposits in the andes, *Springer verlag*, 721-732.

Arda, T. 1969. Kırka boraks yatağı. *Maden Tetkik ve Arama Enstitüsü Endüstriyel Hammaddeler Raporu*, No. 436, Ankara (unpublished).

Aristarain, L.F., Hurlbut, C.S. Jr. 1972. Boron minarals and deposits. *Mineralogical Record*, v. 3: 165-172, 213-220.

Baysal, O. 1972. Mineralogic and Genetic Studies of the Sarıkaya (Kırka) Borate Deposits. Ph.D. Thesis. Hacettepe University, Turkey (Turkish, unpublished).

Bingöl, E., Delaloye, M., Ataman, G. 1982. Granitic intrusions in western Anatolia: a contribution to the geodynamic study of this area. *Eclogae geol. Helv.*, 75, 437-446.

Borsi, J., Ferrara, G., Innocenti, F., Mazzuoli, R. 1972. Geochronology and petrology of recent volcanics in the easthern Aegean Sea (West Anatolia and Lesvos Iceland). *Bullettin of Volcanology*, 36, 473-496.

Bowser, C.J. 1965. Geochemistry and Petrology of the Sodium Borates in the Non-marine Evaporitic Environment. Ph.D Dissertation, *University of California, Los Angeles* (unpublished).

Bozkurt, E. 2003. Origin of NE-trending basins in western Turkey. *Geodinamica Acta* 16, 61–81.

Ceradyne Inc. 2011. Boron products: Costa Mesa, CA, Ceradyne Inc. (Accessed January 5, 2011, at http://www.ceradyneboron.com/about/boron-products.aspx.).

Chong, G. 1984. Die salare in Nordchile-Geologie, Structure und Geochimie. *Geotektonische Forschungen* 67; 1-146.

Cooper, M.A., Hawthorne, F.C., Garcia-Veigas, J., Alcobé, X., Helvacı, C., Grew, E. S., Ball, N. A., (in press). Fontarnauite, $(Na,K)_2$ (Sr,Ca) (SO_4) $[B_5O_8$ (OH)] $(H_2O)_2$, a new sulfate-borate from Doğanlar (Emet), Kütahya Province, Western Anatolia, Turkey. *Candian Mineralogist*.

Çemen İ., Ersoy, E. Y., Helvacı, C., Sert, S., Alemdar, S., Billor, Z. 2014. AAPG Datapages/Search and Discovery Article #90194 2014 International Conference and Exhibition, Istanbul, Turkey, September 14-17, 2014.

Çoban, H., Karacık, Z., Ece, Ö.I. 2012. Source contamination and tectonomagmatic signals of overlapping Early to Middle Miocene orogenic magmas associated with shallow continental subduction and asthenospheric mantle ?ows in Western Anatolia: a record from Simav (Kütahya) region. *Lithos* 140–141, 119–141.

Dunn, J. F. 1986, The structural geology of the northeastern Whipple Mountains detachment fault terrane, San Bernardino County, California [M.S. thesis]: Los Angeles, California, University of Southern California, p. 172.

Engineering and Mining Journal, 2012. Industrial minerals—The boron country: *Engineering and Mining Journal* 213, no. 1, January, p. 61.

Ercan, E., Dinçel, A., Metin, S., Türkecan, A., Günay, A. 1978. Uşak yöresindeki Neojen havzalarının jeolojisi (Geology of the Neogene basins in Uşak region). *Türkiye Jeoloji Kurumu Bülteni*, 21, 97-106.

Ercan, E., Türkecan, A., Dinçel, A., Günay, A. 1983. Kula-Selendi (Manisa) dolaylarının jeolojisi [Geology of Kula-Selendi (Manisa) area]. *Geological Engineering* 17, 3–28.

Ercan, E., Satır, M., Sevin, D., Türkecan, A. 1996. Batı Anadolu'daki Tersiyer ve Kuvaterner yaşlı volkanik kayaçlarda yeni yapılan radyometrik yaş öl-

çümlerinin yorumu [Some new radiometric ages Tertiary and Quaternary volcanic rocks from West Anatolia]. *Maden Tetkik ve Arama Genel Müdürlüğü Dergisi* 119, 103–112.

Ercan, T., Satır, M., Kreuzer, H., Türkecan, A., Günay, E., Çevikbaş, A., Ateş, M., Can, B. 1985. Batı Anadolu Senozoyik volkanitlerine ait yeni kimyasal, izotopik ve radyometrik verilerin yorumu (Interpretation of new chemical, isotopic and radiometric data on Cenozoic volcanics of western Anatolia). *Türkiye Jeoloji Kurumu Bülteni*, 28, 121-136.

Erdoğan, B. 1990. Tectonic relations between İzmir–Ankara Zone and Karaburun Belt. Bull. Miner. Res. Explor. Inst. Turk. 110, 1–15.

Erkül, F., Helvacı, C., Sözbilir, H. 2005*a*. Stratigraphy and Geochronology of the Early Miocene Volcanic Units in the Bigadiç Borate Basin, Western Turkey. *Turkish Journal of Earth Science* 14, 227–253.

Erkül, F., Helvacı, C., Sözbilir, H. 2005*b*. Evidence for two episodes of volcanism in the Bigadic borate basin and tectonic implications for Western Turkey. *Geological Journal* 40, 545–570.

Erkül, F., Helvacı, C., Sözbilir, H. 2006. Olivine basalt and trachyandesite peperites formed at the subsurface/surface interface of a semi-arid lake: An example from the Early Miocene Bigadiç basin, western Turkey. *Journal of Volcanology and Geothermal Research*. 149, 240-262.

Ersoy, Y., Helvacı, C. 2007. Stratigraphy and geochemical features of the Early Miocene bimodal (ultrapotassic and calc-alkaline) volcanic activity within the NE-trending Selendi basin, western Anatolia, Turkey. *Turkish Journal of Earth Science* 16, 117 - 139.

Ersoy, E. Y., Helvacı, C., Sözbilir, H., Erkül, F., Bozkurt E. 2008. A geochemical approach to Neogene–Quaternary volcanic activity of the western Anatolia: an example of episodic bimodal volcanism within the Selendi Basin, *Chemical Geology*, 255, 1-2, 265-282.

Ersoy, E. Y. , Helvacı, C., Sözbilir, H. 2010. Tectonostratigraphic evolution of the NE-SW trending superimposed Selendi basin: Implications or late Cenozoic crustal extension in Western Anatolia, Turkey. *Tectonophysics,* 488, 1-4, 210-232.

Ersoy, E.Y., Helvacı, C., Palmer, M.R. 2011. Stratigraphic, structural and geochemical features of the NE–SW-trending Neogene volcano-sedimentary basins in western Anatolia: implications for associations of supradetachment and transtensional strike-slip basin formation in extensional tectonic setting. *J. Asian Earth Sci*. 41, 159–183.

Ersoy, E. Y., Helvacı, C., Palmer, M. R. 2012. Petrogenesis of the Neogene volcanic units in the NE–SW-trending basins in western Anatolia, Turkey. *Contrib Mineral Petrol* 163, 379–401.

Ersoy, Y.E., Helvacı, C., Uysal, İ., Palmer M.R., Karaoğlu, Ö. 2012. Petrogenesis of the Miocene volcanism along the İzmir-Balıkesir Transfer Zone in western Anatolia, Turkey: Implications for origin and evolution of potassic volcanism in post-collisional areas. *Journal of Volcanology and Geothermal Research*, 241-242, 21-38.

Ersoy, E.Y., Palmer, M.R. 2013. Eocene–Quaternary magmatic activity in the Aegean: implications for mantle metasomatism and magma genesis in an evolving orogeny. *Lithos* 180–181, 5–24.

Ersoy, E.Y., Çemen, İ., Helvacı, C., Billor, Z. 2014. Tectono-stratigraphy of the Neogene basins inWestern Turkey: Implications for tectonic evolution of the Aegean Extended Region. *Tectonophysics* 635, 33–58.

Eti Maden Inc. 2003. Pre-feasibility report summaries of boron carbide, boron nitride, ferroboron, frit and glaze, textile glass fibre, zinc borate: Ankara, Turkey, *Eti Maden Inc*., 23 p.

Floyd, P.A, Helvacı, C, Mittwede, S.K. 1998. Geochemical discrimination of volcanic rocks, associated with borate deposits: an exproation tool. *Journal of Geochemical Exploration* 60, 185-205.

Fytikas, M., Innocenti, F., Manetti, P., Mazzuoli, R., Peccerillo, A., Villari L. 1984. Tertiary to Quaternary evolution of volcanism in the Aegean region. In The Geological Evolution of the Eastern Mediterranean, Dixon JE, Robertson AHF (eds). *Geological Society of London*; Special Publications 17. 687–699.

García-Veigas, J., Ortí, F., Rosell, L., Gündoğan, I., Helvacı, C. 2010. Occurrence of a new sulphate mineral Ca 7 Na 3 K(SO 4) 9 in the Emet borate deposits, western Anatolia (Turkey). *Geological Quarterly* 54, 431-438.

García-Veigas, J., Rosell, L., Ortí, F., Gündoğan, İ., Helvacı, C. 2011. Mineralogy, diagenesis and hydrochemical evolution in a probertite–glauberite–halite saline lake (Miocene, Emet Basin, Turkey). *Chemical Geology* 280, 352–364.

García-Veigas, J., Helvacı C. 2013. Mineralogy and sedimentology of the Miocene Göcenoluk borate deposit, Kırka district, western Anatolia, Turkey. Sedimentary Geology 290, 85–96.

Garrett, D.E. 1998. Borates. Handbook of deposits, processing, properties, and use. *Academic Press, London,* 483 p.

Gawlik, J. 1956. Borate deposits of the Emet Neogene basin. *Maden Tetkik ve Arama Genel Müdürlüğü Rapor* No. 2479, Ankara (Turkish and German Text) (unpublished).

Goldschmidt, V.M. 1954. Geochemistry. *Oxford University Press,* Oxford.

Gök, S., Çakır, A., Dündar, A. 1980. Stratigraphy, petrography and tectonics of the borate-bearing Neogene in the vicinity of Kırka. *Bulletin of the Geological Congress of Turkey*, n. 2, 53-62.

Grew, E.S., Anovita, L.M. 1996. Boron. Mineralogy, petrology and geochemistry. Reviews in mineralogy,

volume 33, *Mineralogical Society of America*, Washington, D.C., 862 .

Güleç, N. 1991. Crust-mantle interaction in western Turkey: implications from Sr and Nd isotope geochemistry of Tertiary and Quaternary volcanics. *Geological Magazine* 23, 417-435.

Gündoğan, İ., Helvacı, C. 1993. Geology, mineralogy and economic potential of Sultançayır (Susurluk-Balıkesir) boratiferous gypsum basin. *Türkiye Jeoloji Kurumu Bülteni* 36, 159-172.

Helvacı, C. 1977. Geology, mineralogy and geochemistry of the borate deposits and associated rocks and the Emet Valley, Turkey. PhD Thesis, *University of Nottingham*, England (unpublished).

Helvacı C. 1978. A review of the mineralogy of the Turkish borate deposits. *Mercian Geology* 6, 257-270.

Helvacı, C. 1983. Mineralogy of the Turkish borate deposits. *Geological Engineering* 17, 37-54.

Helvacı, C. 1984. Occurence of rare borate-minerals: veatchite-A, tunellite, teruggite and cahnite in the Emet borate deposits, Turkey. *Mineralium Deposita* 19, 217-226.

Helvacı, C. 1986. Geochemistry and origin of the Emet borate deposits, western Turkey. Faculty of Engineering Bulletin, *Cumhuriyet University, Series A. Earth Sciences* 3, 49-73.

Helvacı, C. 1989. A mineralogical approach to the mining, storing and marketing problems of the Turkish borate production. *Geological Engienering* 34-35: 5-17.

Helvacı, C. 1994. Mineral assemblages and formation of the Kestelek and Sultançıyır borate deposits. *Proceedings of 29th International Geological Congress, Kyoto Part A*, 245-264.

Helvacı, C. 1995. Stratigraphy, mineralogy, and genesis of the Bigadiç borate deposits, western Turkey. *Economic Geology* 90, 1237-1260.

Helvacı, C. 2005. Borates. In : Selley R.C., Cocks, L.R.M and Plimer, I.R. (editors) Encyclopedia of Geology. *Elsevier*, vol.3, p. 510-522.

Helvacı, C. 2012. Trip to Kışladağ (Uşak) Gold Mine, Kırka and Emet Borates Deposits. Post Colloquium Field Trip Guide Book. International Earth Sciences Colloquium on the Agean Region, IESCA 2012, İzmir, Turkey, 41p.

Helvacı, C., Firman, R.J. 1976. Geological setting and mineralogy of Emet borate deposit, Turkey. Transactions/section B, *Institute of Mining and Metallurgy* 85, 142-152.

Helvacı, C., Ercan, T. 1993. Karapınar (Konya) havzasında oluşan güncel bor tuzları ve volkanizmayla ilişkileri. 46. *Türkiye Jeoloji Kurultayı 1993 Bildiri Özleri*, Sayfa 102-103.

Helvacı, C., Stamatakis, M.G., Zagouroglou, C., Kanaris, J. 1993. Borate minerals and related authigenic silicates in northeastern Mediterraean Late Miocene continental basins. *Exploration Mining Geology* 2, 171-178.

Helvacı C., Alonso, R.N. 1994. An occurrence of primary inyoite at Lagunita Playa, Northern Argentina. *Proceedings of 29th International Geological Congress, Kyoto Part A*, 299-308 Japan.

Helvacı, C., Yağmurlu, F. 1995. Geological setting and economic potential of the lignite and evaporite-bearing Neogene basins of Western Anatolia, Turkey. *Isr. J. Earth Sci., Vol. 44*, 91-105.

Helvacı, C., Orti, F. 1998. Sedimentology and diagenesis of Miocene colemanite-ulexite deposits (western Anatolia, Turkey). *Journal of Sedimentary Research 68*: 1021-1033.

Helvacı, C., Alonso, R.N. 2000. Borate deposits of Turkey and Argentina : a summary and geological comparison. *Turkish Journal of Earth Sciences* 24, 1-27.

Helvacı, C., Erkül, F. 2002. Soma ve Bigadiç arasındaki (Batı Anadolu) volkanik fasiyeslerin sedimentolojik, petrografik ve jeokimyasal veriler ışığında kökensel yorumu. *DEÜ. 0922.20.01.36 no.lu AFS Projesi,* 2002, 82 s.

Helvacı, C., Sözbilir, H., Erkül, F. 2003. Soma ve Bigadiç arasındaki (Batı Anadolu) volkanik fasiyeslerin sedimentlojik, petrografik ve jeokimyasal veriler ışığında kökensel yorumu. Türkiye Bilimsel ve Teknik Araştırma Kurumu : Proje No: YDABCAG/100Y044, Nisan 2003, İzmir, 155 s.

Helvacı, C., Ortí, F. 2004. Zoning in the Kırka borate deposit, western Turkey: primary evaporitic fractionation or diagenetic modifications? Canadian Mineralogists 42, 1179-1204.

Helvacı, C., Ersoy, E.Y. 2006. The facies characteristics and geochemical features of the volcanic rocks of the Selendi and Simav area, and their relations with the basin sedimentary rocks, western Anatolia. DEÜ. Bilimsel Araştırma Projesi No: 03.KB.FEN.058. January 2006, İzmir, 116 s.

Helvacı, C., Ersoy, Y., Erkül, F., Sözbilir, H., Bozkurt, E. 2006. Selendi Havzasının stratigrafik, petrografik, jeokimyasal ve tektonik veriler ışığında volkonosedimanter evrimi ve ekonomik potansiyeli. Türkiye Bilimsel ve Teknik Araştırma Kurumu Proje No:ÇAYDAĞ/103Y124, Aralık 2006, 134 s.

Helvacı, C., Karaoğlu, Ö., Ersoy, Y., Erkül, F., Bozkurt, E. 2009. Volcano-Tectonic evolution of the Uşak-Eşme-Banaz Basin: An approach to stratigraphic, sedimentologic and geochemical view. DEÜ. Bilimsel Araştırma Projesi No: 2005.KB.FEN.053, September 2009, İzmir, 75 s.

Helvacı, C., Orti, F., Garcia-Veigas, J., Rosell, L., Gündoğan, İ., Yücel-Öztürk, Y. 2012. NEOGENE BORATE DEPOSITS: Mineralogy, Petrology and Sedimentology; A workshop with special emphasis on the Anatolian deposits. International Earth Sciences Colloquium on the Agean Region, *IESCA 2012*, İzmir, Turkey, 64p.

Helvacı, C., Yücel-Öztürk, Y. 2013. Bor minerallerinin fluoressent yöntemiyle çalışılması. 2010 KB FEN 9, 25.03.2013.

Helvacı, C., Yücel-Öztürk, Y., Satır, M., Shang, C. K. 2014. U-Pb zircon and K-Ar geochronology reveal the emplacement and cooling history of the Late Cretaceous Beypazarı granitiod, Central Anatolia, Turkey. International Geology Review. *International Geology Review* 56, 9, 1138–1155.

İnan, K. 1972. New borate district, Eshişehir-Kırka province, Turkey. *Inst.Mining and Met.,* 8l, p.B163-l65.

İnan, K., Dunham, A.C., Esson, J. 1973. Mineralogy, chemistry and origin of Kırka borate deposit, Eskişehir Province, Turkey. Transactions/section B, *Institution of Mining and Metallurgy* 82, 114-123.

İnci, U. 1984. Neogene oil shale deposits of Demirci and Burhaniye regions. 27th International *Geological Congress, Abs vol. VII*, 13–16 (57).

Innocenti, F., Agostini, S., Di Vincenzo, G., Doglioni, C., Manetti, P., Savaşçın, M.Y., Tonarini, S. 2005. Neogene and Quaternary volcanism in Western Anatolia: magma sources and geodynamic evolution. *Marine Geology* 221, 397–421.

Jackson, J., McKenzie, D. 1984. Active tectonics of the Alpine-Himalayan Belt between western Turkey and Pakistan. *Geophysical Journal of the Royal Astronomical Society* 77, 185-264.

Karaoğlu, Ö., Helvacı, C., Ersoy, E.Y. 2010. Petrogenesis and 40 Ar/39 Ar geochronology of the volcanic rocks of the Uşak–Güre basin, western Türkiye. *Lithos* 119, 193–210.

Kistler, R.B., Helvacı, C. 1994. Boron and borates. In CARR, D.D. (ed) Industrial Minearls and Rocks. 6th edition, Society for Mining, Metallurgy and Exploration Inc., Littleton, Colarado, 171-186.

Lismore, Siobhan 2012. Borates used in detergents added to REACH list: Industrial Minerals, February 13. (Accessed September 27, 2012, at http://www.indmin.com/)

Meixner, H. 1965. Borate deposits of Turkey. Bulletin of the *Mineral research and Exploration Institute of Turkey* 125, 1-2.

Muessig, S. 1959. Primary borates in playa deposits: minerals of high hydration. *Economic Geology* 54, 495-501.

Nebert, K. 1961. Gördes (Batı Anadolu) Bölgesi'ndeki Neojen volkanizması hakkında bazı bilgiler. *Maden Tetkik ve Arama Genel Müdürlüğü Dergisi* 57, 50– 54.

O'Driscoll, Mike 2011. Rio Tinto Minerals declares force majeure on sodium borates: Industrial Minerals, January 31. (Accessed October 1, 2012, at http://www.indmin.com/.).

Okay, A.I. 1989. Tectonic units and sutures in the Pontides, northern Turkey. In: Şengör, A.M.C., (ed.), Tectonic evolution of the Tethyan region: Dordrecht, Kluwer Academic Publications, 109–115.

Okay, A.I., Siyako, M. 1991. The New Position of the İzmir-Ankara Neo-Tethyan Suture between İzmir and Balıkesir. In: Proceedings of the Ozan Sungurlu Symp., pp. 333–355.

Okay, A.I., Şengör, A.M.C., Görür, N. 1994. Kinematic history of the opening of the Black Sea and its effect on the surrounding regions: *Geology* 22, 267–270.

Okay, A.İ., Satır, M., Maluski, H., Siyako, M., Monie, P., Metzger, R., Akyüz, S. 1996. Paleo- and Neo-Tethyan events in northwestern Turkey: Geologic and geochronologic contraints. *The Tectonic Evolution of Asia*, 420- 441.

Orti, F., Helvacı, C., Rosell, L., Gündoğan, İ. 1998. Sulphate-borate relations in an evaporitic lacustrine environmet: the Sultançayır Gypsum (Miocene, Western Anatolia). *Sedimentolgy* 45, 697-710.

Ortí, F., Alonso, R.N. 2000. Gypsum-hydroboracite association in the Sijes Formation (Miocene, NW Argentina): Implications for the genesis of Mg-bearing borates. *Journal of Sedimentary Research* 70, 664–681.

Ozol, A.A. 1977. Plate Tectonics and the Process of Volcanogenic-Sedimentary Formation of Boron. *International Geology Review* 20, 692-698.

Özpeker, İ. 1969. Western Anatolian Borate Deposits and Their Genetic Studies. PhD Dissertation, *İstanbul Technical University* (Türkçe, unpublished).

Palache, C., Berman, H., Frondel, C. 1951. The system of mineralogy, 7th ed., v. 2, John Wiley & Sons, New York, 1124 .

Palmer, M.R., Helvacı, C. 1995. The boron geochemistiry of the Kırka borate deposit, western Turkey. *Geochimica et Cosmochimica Acta* 59, 3599-3605.

Palmer, M. R., Helvacı, C. 1997. The boron istope geochemistry of the Neogene borate deposits of western Turkey. *Geochemica et Cosmochimica Acta* 61, 3161-3169.

Pe-Piper, G., Piper, D.J.W. 2007. Late Miocene igneous rocks of Samos: the role of tectonism in petrogenesis in the southeastern Aegean. *Geol. Soc. Lond., Spec. Publ.* 291, 75–97.

Peng, Q.M., Palmer, M.R. 1995. The Palaeoproterozoic boron deposits in eastern Liaoning, China -a metamorphosed evaporite. *Precambrian Research* 72, 185–197.

Peng, Q.M., Palmer, M.R. 2002. The Paleoproterozoic Mg and Mg-Fe borate deposits of Liaoning and Jilin Provinces, Northeast China. *Economic Geology* 97, 93–108.

Preleviç, D., Akal, C., Foley, F., Romer, R.L., Stracke, A., van den Bogaard, P. 2012. Ultrapotassic ma?c rocks as geochemical proxies for post-collisional dynamics of orogenic lithospheric mantle: the case of southwestern Anatolia, Turkey. J. Petrol. 53, 1019–1055.

Purvis, M., Robertson, A.H.F. 2004. A pulsed extension model for the Neogene–Recent E–W-trending Alaşehir Graben and the NE–SW-trending Selendi and Gördes Basins, western Turkey, *Tectonophysics* 391, 171-201.

Purvis, M., Robertson, A.H.F. 2005. Miocene sedimentary evolution of the NE-SW-trending Selendi and Gördes Basins, Western Turkey: implications for extensional processes. *Sedimentary Geology* 174, 31-62.

Rio Tinto plc 2011. Form 20–F—Annual report for the fiscal year ended December 31, 2010: Washington, DC, Securities and Exchange Commission, March 15. (Accessed September 27, 2012, at http://www.secinfo.com/.).

Roskill Information Services Ltd. 2010. Boron—Global industry markets and outlook: London, United Kingdom, *Roskill Information Services Ltd*., 243 p.

Seghedi, I., Helvacı, C. 2014. Early Miocene Kırka-Phrigian caldera, western Anatolia - an example of large volume silicic magma generation in extensional setting. *Geophysical Research Abstracts* Vol. 16, EGU2014-5789, 2014 EGU General Assembly, Vienna, Austria, 2014.

Seghedi, I., Helvacı, C., Pécskayc Z 2015. Composite volcanoes in the south-eastern part of İzmir–Balıkesir Transfer Zone, Western Anatolia, Turkey. *Elsevier*, *Journal of Volcanology and Geothermal Research* 291, 72–85.

Seyitoğlu, G. 1997*a*. Late Cenozoic tectono-sedimentary development of the Selendi and Uşak–Güre basins: a contribution to the discussion on the development of east–west and north trending basins in Western Turkey. *Geol. Mag*. 134, 163–175.

Seyitoğlu, G. 1997*b*. The Simav graben: an example of young E–W trending structures in the late Cenozoic extensional system of Western Turkey. *Turk. J. Earth Sci*. 6, 135–141.

Seyitoğlu, G., Scott, B.C. 1991. Late Cenozoic crustal extension and basin formation in west Turkey. *Geological Magazine* 128, 155-166.

Seyitoğlu, G., Scott, B.C., Rundle, C.C. 1992. Timing of Cenozoic extensional tectonics in west Turkey. *J. Geol. Soc*. 149, 533–538.

Seyitoğlu, G., Scott, B.C. 1992. Late Cenozoic volcanic evolution of the NE Aegean region. *Journal of Volcanology and Geothermal Research* 54, 157-176.

Seyitoğlu, G., Scott, B.C. 1994*a*. Late Cenozoic basin development in west Turkey: Gördes basin tectonics and sedimentation. *Newsletter Stratigraphy* 131, 133-142.

Seyitoğlu, G., Scott, B.C. 1994*b*. Neogene palynological and isotopic age data from Gördes basin, West Turkey. *Newsletter Stratigraphy* 31, 133-142.

Seyitoğlu, G., Scott, B.C. 1996. The cause of N-S extensional tectonics in western Turkey: Tectonic escape vs. Back-arc spreading vs. Orogenic collapse. *Journal of Geodynamics* 22, 145 - 153.

Seyitoğlu, G., Anderson, D., Nowell, G., Scott, B.C. 1997. The evolution from Miocene potassic to Quaternary sodic magmatism in western Turkey: implications for enrichment processes in the lithospheric mantle. *Journal of Volcanology and Geothermal Research* 76, 127-147.

Sunder, M.S. 1980. Geochemistry of the Sarıkaya borate deposits (Kırka-Eskişehir). *Türkiye Jeoloji Kurumu Bülteni* 2, 19-34.

Şaylı, B.S. 2003. Low Frequency of Infertility Among Workers in a Borate Processing Facility, Humana Pres Inc.).

Şengör, A.M.C. 1984. The Cimmeride orogenic system and the tectonics of Eurasia: *Geological Society of America*, Special Paper, 195 p.

Şengör, A.M.C. 1987. Cross-faults and differential stretching of hanging walls in regions of low-angle normal faulting: examples from western Turkey. From Coward, M.P., Dewey, J.F., Hancock, P.L. (eds.), 1987, Continental Extensional Tectonics. *Geological Society Special Publication* 28, 575-589.

Şengör, A.M.C., Yılmaz, Y. 1981. Tethyan Evolution of Turkey: A Plate Tectonic Approach. *Tectonophysics* 75, 181-241.

Şengör, A.M.C., Satır, M., Akkök, R. 1984. The timing of tectonic events in the Menderes Massif, western Turkey: implication for tectonic evolution and evidence for Pan-African basement in Turkey. *Tectonics* 3, 693-707.

Travis, N.J., Cocks, E.J. 1984. The Tincal Trail. A history of borax. Harrap, London, 311.

Uyanik, T. 2010. Mining: Ankara, Turkey, Export promotion center of Turkey, August, 7 p. (Accessed October 1, 2012, at http://www.tcp.gov.tr/Assets/sip/san/Mining.pdf.)

Watanebe, T. 1964. Geochemical cycle and concentration of boron in the earth's crust. V.I. Verdenskii Inst. *Geochim. and Anal. Chem*. U.S.S.R. 2: 167-177.

Yağmurlu, F. 1984. Akhisar doğusunda kömür içeren Miyosen tortulların stratigrafisi, depolanma ortamları ve tektonik özellikleri. *Türkiye Jeoloji Kurumu Bülteni* 5, 3–20.

Yılmaz, Y. 1990. Comparison of young volcanic associations of western and eastern Anatolia formed under a compressional regime: a review. *Journal of Volcanology and Geothermal Research*, 44, 1-19.

Yılmaz, Y., Genç, S.C., Gürer, O.F., Bozcu, M., Yılmaz, K., Karacık, Z., Altunkaynak, Ş., Elmas, A. 2000. When did the western Anatolian grabens begin to develop? In: Bozkurt, E., Winchester, J. A. & Piper, J. D. A. (eds), Tectonics and Magmatism in Turkey and the Surrounding Area. Geological Society, London, *Special Publications* 173, 353-84.

Yiğit, O. 2009. Mineral deposits of Turkey in relation to Tethyan Metallogeny: implications for future mineral exploration, *Economic Geology*, v.104, p.19-51

Yücel-Öztürk, Y., Ay, S., Helvacı, C. 2014. Bor Minerallerinin Duraylı İzotop Jeokimyası: Bigadiç (Balıkesir) *Borat Yatağından Bir Örnek. Yerbilimleri 35* (1), 37-54.

Bull. Min. Res. Exp. (2015) 151: 217-229

Bulletin of the
Mineral Research and Exploration

http://bulletin.mta.gov.tr

VERTICAL AND HORIZANTAL ANALYSIS OF CRUSTAL STRUCTURE IN EASTERN ANATOLIA REGION

Oya PAMUKÇU[a]*, Tolga GÖNENÇ[a], Ayça YURDAKUL ÇIRMIK[a], Şevket DEMİRBAŞ[b] and Seyit TOSUN[c]

[a] *Dokuz Eylül University Engineering Faculty, Department of Geophysical Engineering Tınaztepe Campus Buca İzmir*
[b] *General Directorate of Mineral Research & Exploration (MTA), Deparment of Geophysical Research Ankara*
[c] *General Directorate of Mineral Research & Exploration (MTA), Deparment of Geophysical Research Ankara (Retired)*

Keywords:
Eastern Anatolia, gravity, derivative methods, heat flow, lithosphere.

ABSTRACT

The tectonic regime of Eastern Anatolia is determined by Arabian-Eurasian continent-continent convergence and the mechanism occurred with the convergence. North Anatolian Fault Zone (NAFZ), Eastern Anatolian Fault Zone (EAFZ), North Eastern Anatolian Faults and Bitlis Zagros Suture Zone are formed by this convergence, represent the characteristic of lithospheric structure of the region. In the scope of this study, the gravity anomalies of Eastern Anatolia were used for investigating the lithospheric structure. Firstly, second order trend analyses were applied to gravity data for examining the characteristic of the anomaly. Later, the vertical and horizontal derivatives methods were applied to the same data. Generally, the purpose of the applying derivative methods is determining the vertical and horizontal borders of the structure. Therefore, this method gives the opinion about the characteristic of the lithospheric structure of the study region. According to the results of derivative methods, the structure transitions were increased rather especially with Bitlis Zagros Suture Zone. At the last step, the gravity studies were evaluated together with the seismic activity of the region. Consequently, the geodynamical structure of the region is examined with the previous studies done in the region.

1. Introduction

In Eastern Anatolia which has major tectonic structures, with the effect of Arabian Plate's northward motion, Anatolian block and Northeastern Anatolian Block escape to west and east, respectively (Ketin, 1948; McKenzie, 1972; Barka et al., 1987). Anatolian Block is bordered by right-lateral North Anatolian Fault Zone (NAFZ) at North and the left-lateral East Anatolian Fault Zone (EAFZ) at East (Figure 1). These two faults intersect in the Karlıova triple junction (Ketin, 1966; McKenzie, 1972; Dewey, 1976; Dewey et al., 1986; Barka et al., 1987). The eastern part of Anatolian block is divided into two blocks by the left-lateral Ovacık Fault. This fault intersects NAFZ at southerneast side of Erzincan Basin. The movement of Northeastern Anatolian Block to east is complicated because the block divided into lots of minor blocks with the effect of extensional interplate deformation (Barka et al., 1987). The region between the zones (Karlıova and Erzincan Basins), where NAFZ intersect EAFZ and Northeastern Anatolian Faults, is the conjunction border of the blocks (Anatolian and Northeastern Anatolian Blocks) move in the opposite directions relatively each other (Barka et al., 1987). The major part of NAFZ located in west of Erzincan was broken by a series of earthquakes which immigrated to west and occurred between the years 1939-1967. Until today, different comments were made about the geodynamic structure of the region by examining the

* *Corresponding author: Oya Pamukçu, oya.pamukcu@deu.edu.tr*

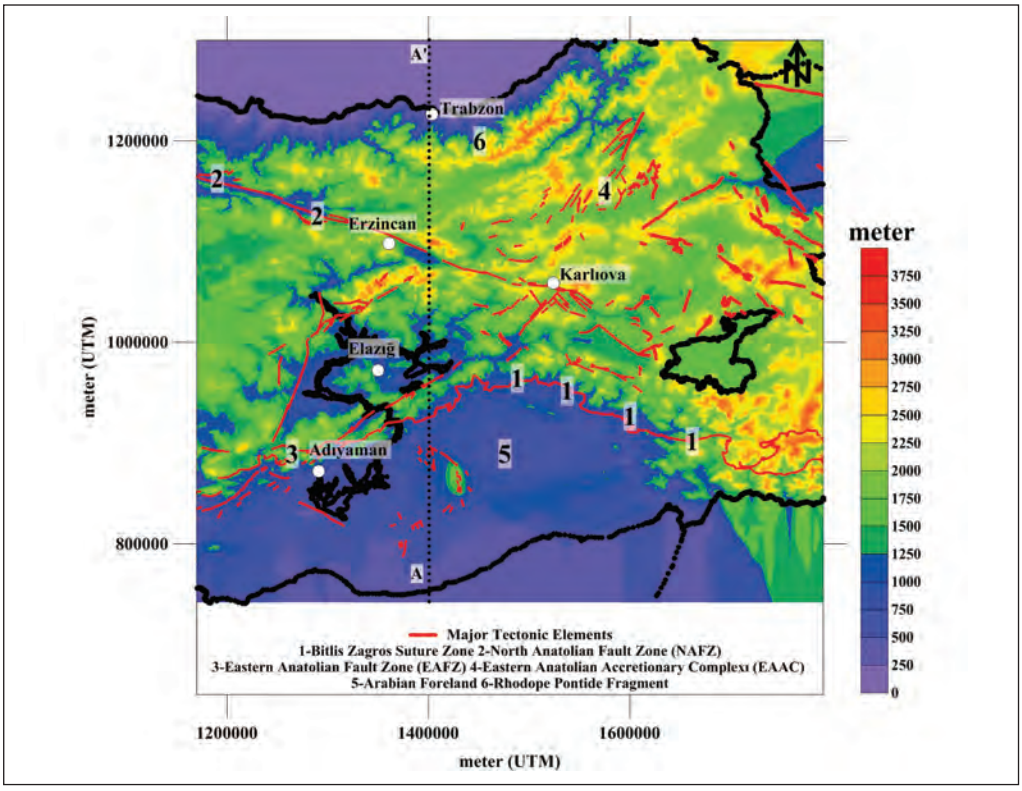

Figure 1- The topographic changes and major tectonic elements of Eastern Anatolian Region.

velocity differences on plate motions, topographic uplifts and volcanism activities and until 2003, four models were proposed (Rotstein and Kafka, 1982; McKenzie, 1972, 1976; Dewey et al., 1986; Pearce et al., 1990). In these studies generally, it was emphasized that the large-scale shortining and thickening in the crust was started by the tension of the Arabian-Anatolian Plates convergence. The new approaches were presented by the studies (Al-Lazki et al., 2003; Gök et al., 2003; Türkelli et al., 2003; Sandvol et al., 2003*a,b*; Zor et al., 2003; Şengör et al., 2003; Keskin, 2003, Pamukçu et al, 2007; Pamukçu and Akçığ, 2011; Pamukçu et al., 2014) realized after 2001 in Eastern Anatolia. In these new models, it was pointed out that the crustal thickening was not in the mentioned scale in previous studies (Rotstein and Kafka, 1982; McKenzie, 1972, 1976; Dewey et al., 1986; Pearce et al., 1990).

Pamukçu et al. (2007) determined the crustal thickness and the model of the region by using gravity data. Pamukçu and Akçığ (2011) calculated the effective elastic thickness for explaining the mechanism of the topography which compensates the crustal thickness. The Curie depths and heat flow values were obtained by using aeromagnetic data by Pamukçu et al. (2014). In the light of previous gravity and magnetic studies, in this study the estimation of the structure locations in Eastern Anatolia were done by applying the trend analysis, vertical and horizontal derivative methods (Butler, 1984; Gönenç, 2014) to the gravity data. In the last step, the results of this study were examining together with the results of the previous geophysical and geological studies.

2. Geodynamical Structure of The Study Region

As a result of the collision of Arabia with Eurasia, Neo-Tethy merged with Bitlis Ocean and closed in the late Middle Miocene in east, in the late Pliocene-Quaternary in west (Dewey et al., 1986; Robertson et al., 1991). The merging of Anatolia with Arabia along the Bitlis Zagros Suture Zone and north-south directional compression in the Late Middle Miocene obstructed the northward motion of Arabian plate (relative to African plate) up to early Pliocene (Hempton, 1987; Robertson et al., 1991; Yılmaz et al., 1993). In Eastern Anatolia the crustal thickening and high elevation (~ 2 km above the sea level) occurred between the Late Middle Miocene and the Early Pliocene (Şengör and Kidd, 1979). During these geologic time-scales, various structures were formed like as east-west directional thrust faults and extensional basins with the effect of the compression (Kelling et al., 1987; Gürsoy et al., 1992). After

ending of inter-continental collision along Bitlis Zagros Suture Zone, in the early Pliocene a new compressional and extensional tectonic regime replaced the compressional tectonic regime in Eastern Anatolia (Bozkurt, 2001). NAFZ described as inter-continental transform fault belt was occurred as the result of that activity. Subsequently, EAFZ was formed in the late Pliocene (Westaway and Arger, 1996). The compressed Anatolian Plate began its westward motion on the oceanic lithosphere of African Plate. Therefore, NAFZ and EAFZ allowed Arabian Plate to move northward faster than African Plate (Reilinger et al, 1997; Oral et al., 1995; Barka and Reilinger, 1997).

In the studies of Reilenger et al. (1997); Oral et al. (1995) and Demets et al. (1994), it was explained that while Arabian Plate velocity was 25 mm/year to N-NW, the velocity of African Plate was only 10 mm/year to N. The other important fault which controls the motion between these plates is left-lateral Dead Sea Fault Zone (DSFZ) (Bozkurt, 2001). However, Kahle et al. (1998) pointed out that the velocity of this fault was approximately 7 mm/year. This result showed that the velocity of the fault was not effective on geologic time-scales. DSFZ links the northern border of the Arabian Plate with seafloor spreading in the Red Sea. This case influences the tectonic of Cyprian Arc (Bozkurt, 2001). Consequently, DSFZ has an important role on the active tectonics of Turkey. As the results of the tectonic movements, Şengör et al., (1985) defined four different Neotectonic provinces for Turkey. These are, East Anatolian Contractional Province, North Anatolian Province, Central Anatolian 'Ova' Province and West Anatolian Extensional Province.

Until 2001 four models were presented for characterizing the collision zone in Eastern Anatolia and describing its geodynamic. The issues discussed in the light of these models are also grouped into four main categories. The opinions are like as:

– The continental subduction or delamination continue or not (Rotstein and Kafka, 1982),

– While the approximate offset along NAFZ is 2 cm/year, along EAFZ is 1cm/year. This case shows that Anatolian Block, which escapes to westward, rotates anticlockwise. It can be said that the strain, which appeared with the effect of the collision of Arabian with the Eurasia, can not be the only reason of this westward offset. Therefore, there is any lithospheric thickening on Eurasia or not (Dewey et al., 1986),

– The convergence of Arabian plate moves with the Anatolian Block which escapes as the result of right-lateral movement along NAFZ and left-lateral movement along EAFZ or not (McKenzie, 1972),

– The combinations of all process explained above occurred or not (Pearce et al., 1995).

By the help of seismological studies done in Eastern Anatolia after 2001 (Al-Lazki et al., 2003; Gök et al., 2003; Türkelli et al., 2003; Sandvol et al., 2003*a,b*; Zor et al., 2003), new opinions were presented about the model of the region (Keskin, 2003; Şengör et al., 2003)..

According to Keskin (2003), almost two-thirds of Eastern Anatolia is covered by young volcanic units ranging in age from 11 Ma to recent with the thickness approximately 1 km. This formation represents only the small part of the melt, the greater part probably locate deeper in the crust as plutonic intrusions. The Eastern Anatolian topographic uplift resembles the Tibetan plateau and was viewed as a younger version of it in many studies (Şengör and Kidd, 1979; Dewey et al., 1986). In some of these early studies pointed out that lithospheric mantle beneath Eastern Anatolia was doubled in thickness up to 300 km due to continental collision and thickening. The study of Pearce et al. (1990) about the collision-related volcanic units across the region provided a new view into the tectono-magmatic evolution of Eastern Anatolia. They recommended the delamination model which involved the detachment of the thermal boundary layer by delamination. In the study of Keskin et al. (1998) about the collision-related volcanic units on the Erzurum-Kars Plateau in the north was pointed out that the initiation of volcanism was much earlier in the north than previously thought, almost coincident with rapid uplift of the region.

The seismological studies in the region defined that an almost normal-thickness crust resides on an extremely thin mantle lithosphere or perhaps almost directly on the asthenosphere. The most remarkable point is that the areas of inferred complete lithospheric detachment almost exactly coincide with the extent of the Eastern Anatolian Accretionary Complex (Şengör et al., 2003).

Keskin (2003) explained the reasons of his model in details. According to auther the collision-related volcanic units across the author region extend from basalts to rhyolites. In lava chemistry, there is an

important difference between the Erzurum-Kars Plateau in north and Muş-Nemrut-Tendürek volcanoes in the south. Lavas of Bingol and Suphan volcanoes present transitional chemical characteristics (Pearce et al., 1990). The characteristic of volcanic products in the north around Erzurum-Kars Plateau and Mount Ararat are calc-alkaline and seem to have been occurred from an enriched mantle source including different subduction. This different subduction decreases to the south and disappears around Muş-Nemrut-Tendürek volcanoes. These lavas are alkaline and present with-in plate character. Additionally, the magma-crust interaction degree is more important in the south than in the north.

The radiometric studies defined that the volcanic activity began earlier in north than in the south and migrated to the south during the time (Keskin, 2003). Keskin (2003) criticized the previously proposed geodynamic models for Eastern Anatolian collision zone and defended that except for the slab steepening and breakoff model, there were inconsistencies in all the other models and commented as:

- The tectonic escape of micro-plates to the east and west (McKenzie, 1972) did not compensate completely for the strain triggered by the 2.5 cm/year convergence of the Arabian plate relative to Eurasia (Dewey et al., 1986);
- The subduction of Arabian plate beneath Eastern Anatolia (Rotstein and Kafka, 1982) was not supported by seismic evidence;
- The melting of normal asthenosphere by the effect of adiabatic decompression of upwelling mantle (McKenzie and Bickle, 1988) was not consistent with the seismic data;
- The continental collision and thickening of the Anatolian lithosphere (Dewey et al., 1986) were not supported by recent tomographic data;
- The hot spot activity created by a mantle plume was not consistent with the topography and fault plane solutions;
- The delamination of mantle lithosphere beneath the region (Pearce et al., 1990; Keskin et al., 1998) clarified thoroughly magma formation. Whereas, new seismic data display that there is no lithospheric mantle over a large area beneath the region. This case raises a question about whether a shallow delamination in the whole lithospheric mantle and the lower crust. Nevertheless, the shallow delamination could not be acceptable, because the existence of a mantle attached to the crust basement is needed for delamination. This case is not valid for the area underlain by the Eastern Anatolian Accretionary Complex, since these large subduction-accretion complexes do not have their own lithospheric roots as distinct from continents.
- The slab steepening and subsequently the breaking beneath a subduction-accretion complex may be the most acceptable model, consistent with the geology of the region as well as variations in magma age and chemistry across the region.

Şengör et al. (2003) discussed that oceanic area was closed in a geologic time-scale between the Late Eocene and Oligocene at the first contact of the Eastern Anatolian Accretionary Complex with Bitlis-Pötürge Massif. This complex was shortened and thickened over the oceanic lithospheric slap during the time-scale between the Late Oligecene and 13-15 Ma. This duration continued until the slap was steepened and separated from the complex approximately in 10-11 Ma. The separated slap should be vanished by sinking into the asthenosphere in the 10 Myr time-scales. The authors pointed out that the lack of deep earthquakes in region supported this opinion.

Keskin (2003) presented in the light of new geophysical data that the breakoff may be formed as shallow as 45–50 km. The disappearing of this great load and the supersession of less denser asthenosphere beneath the Eastern Anatolian Accretionary Complex was the reason of the rapid block uplift and volcanism in the region.

Örgülü et al. (2003) and Koçyiğit et al. (2001) indicated that the crustal stress field varied in the past 5 to 10 Myr. This variation corresponded with the initial of widespread volcanism in Eastern Anatolian plateau. It was pointed out that these observations were correlated with the Neo-Tethys slab breakoff beneath the region.

The slab steepening and breakoff model clarified the geochemical variations in volcanic products in the region better than the other proposed models. McKenzie and Bickle (1988) pointed out that upwelling of asthenosphere with the temperature of 1280 ºC create widespread adiabatic decompression melting at approximately 50 km. According to this model, the presence of a subduction component in the

mantle increases the melting by reducing the melting temperature. This case can represent the reason of existence of the erupted volcanic units in greater volumes in the north around the Erzurum-Kars plateau than in the south. The melting temperature are attracted to the more shallow depths by interplaying of the hot asthenosphere with the Eastern Anatolian Accretionary Complex, therefore, widespread melting are created in the crust. This view may explain the instabilities in lava chemistry and degree of magma-crust interplaying in the region (Keskin, 2003).

Keskin (2003) demonstrated that the collision type in Eastern Anatolia was not like as in Tibet and was specific character according to its crustal/lithospheric structure and plate tectonic history. Additionally, it was indicated that the slab steepening and breakoff beneath the Eastern Anatolian Accretionary Complex seemed as the great controlling mechanism for the magma genesis related with the collision in the region.

According to Şengör et al. (2003), the absence of mantle lithosphere in the Eastern Anatolian Accretionary Complex was the main question in the region. The geological evolution explained the reasons of it. The authors reported that in the early Eocene, Rhodope-Pontide arc was still active and there was no a widespread subduction-accretion complex. It was defined that the end side of the accretionary complex may contact the northern side of Bitlis-Pötürge Massif in the late Eocene and this complex was shortened and thickened over the oceanic lithospheric sliding beneath it throughout the Oligocene and additionally, the Oligocene intrusions in the Rhodope-Pontide arc may be generated by this subduction in 38.5 Ma. It was pointed out that after the East Anatolian Accretionary Complex reached to normal continental crustal thickness, the subduction was interrupted and Arabian-Eurasian convergence started to be provided by intercontinental convergence and crustal shortening from Caucasus to Northern Arabia approximately 24 Ma ago in the early Miocene and if the dip angle of slap was 45° and the velocity of convergence was 25 mm/yr, the slab would begin to break approximately at 200 km in the period between 24 Ma and 11 Ma. According to them, the breakoff would occur approximately at a depth of 50 km and 300 km north of the suture if the subducting lithosphere interrelated with the bottom of the East Anatolian Accretionary Complex. At the same time, location of initial collision-related volcanism was approximately at 75 km south of the Eastern Pontide by assuming that the plateau was shortened homogeneously along north-south and the collision-related magmatism began approximately at 200 km north of the today suture line 11 Ma ago. It was indicated that 8 Ma ago when the post-collision volcanism expanded by southward spreading, the breaking of the slap was finished.

According to them, since the slap was approximately older than 100 Ma and the thickness of the accretionary complex was approximately thinner than 45 km, the top of the complex located below the ocean level. It was represented that exposing the asthenospheric temperatures was the reason of partial melting on the bottom surface the East Anatolian Accretionary Complex. Additionally, the volcanicity of Eastern Turkey display a complex composition geochemistry ranging from andesitic-rhyolitic crustal melts to alkali olivine basalts from late Miocene to present. The volcanism most likely represents the asthenospheric rising, the adiabatic melting and the crust heating.

After the continental crust reached some thickness, the magmatism of continent-continent convergence region arised by melting of bottom part of the crust and the magmatism represented by the granites contained high potassium and the rhyolites which were the derivatives of granites on surface. On the light of plate tectonics, Alps, Appalachian Mountains, Greenville, Taurus Mountains and Himalayas are displayed as the tectonic structures occurred by lithospheric subduction or continent-continent convergence. The most prominent belts are the Bitlis Zagros Suture and Himalayas and both of them are located in Alpine-Himalayan Belt. The Bitlis Zagros Belt and Himalayas Belt occurred by the effect of Eurasian-Arabian Convergence and Eurasian-Indian Convergence, respectively.

Apart from the difficulty on evaluating the effects of lower lithosphere, the geology of continental crust is emerged by the result of the lithospheric flexure, extension and shortening. The lithospheric extension and shortening, rapidly are occurred the isothermal thinning and thickening which create the basins and mountains, respectively. Thermal discharging creates subsidence or uplift developed by sedimentation or denudation. Therefore, the most of the vertical movement caused the complexity on stratigraphic development are the result of the lithospheric deformation. Continental convergence contains the development of the floating or high field parts including subduction zones (Dewey, 1977). One of

the continental boundary or both of the boundaries may have had a long and complex terrain combination before formation of continental convergence (Coney et al., 1980). The continental convergence plate boundaries such as Alpine-Himalayan system are wide and complex zones where the relative plate displacements turned to complex and inconsistent stress. Suture belts occurred in this context developed by the thickening of the rifted boundary in the thinned continental crust accumulated again along the fore-plate. The suture zones include the crustal low velocity zones (Rybach et al., 1980). Besides, the structures in convergence systems are involved in one of the tectonic component such as plateaus, suture zones, lithospheric flexures on the fore-plate, the deformation zones on the fore-plate/ back-plate, orogenic collapse/tension zones and the structures are formed with the uplifting of topography. The tectonic components for Eastern Anatolian region were examined in details in the studies of Al-Lazki et al., 2003; Gök et al., 2003; Türkelli et al., 2003; Sandvol et al, 2003*a,b*; Zor et al., 2003, Şengör et al., 2003; Keskin, 2003; Pamukçu et al., 2007; Pamukçu and Akçığ, 2011; Pamukçu et al., 2014.

3. The Trend Analysis and Derivative Applications on Bouguer Anomalies

Butler (1984) applied 1st and 2nd order derivative methods to gravity data in his study. He mentioned that 1st order derivative was more sensitive and the results according to 2nd order derivative could be used in estimation of structure locations. Therefore, the horizontal derivative application was obtained by the methods of Blakely and Simpson (1986).

In the first step of this study, the trend analysis (Figure 3), horizontal derivative (Figure 4) and vertical derivative (Figure 5) applications were realized by using the data in the map of 500x500 m gridded Bouguer gravity anomalies (Figure 2) for the region between 37°-44° E longitudes and 37°-42° N latitudes. The values in the map of Bouguer gravity anomalies changed from 50 mGal to -210 mGal and the negative anomalies showed north-south directional extension from west to east like a fan (Figure 2).

In the obtained residual map by the results of the 2nd order trend applications, the anomaly extensions were west-east directional and the maximum and

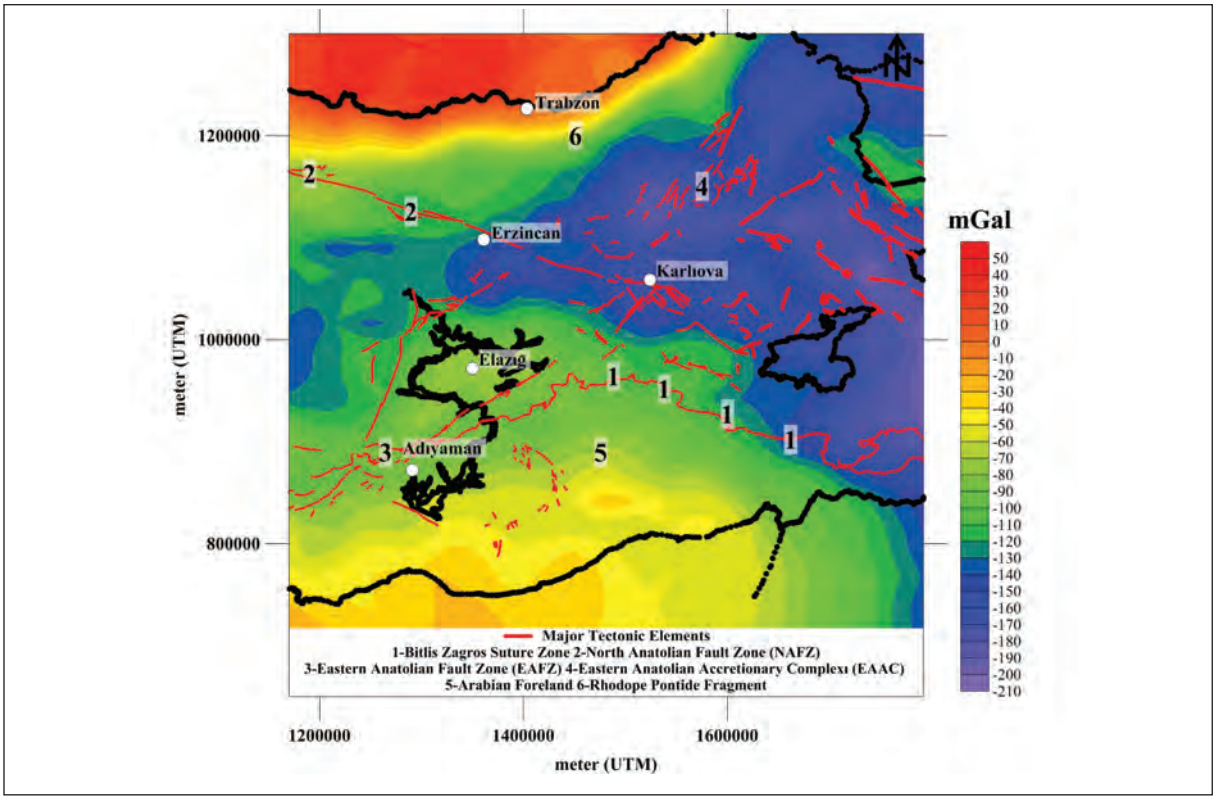

Figure 2- The Bouguer gravity anomaly map of Eastern Anatolian Region (MTA). Red lines represent the major tectonic elements of the region (Bozkurt, 2001).

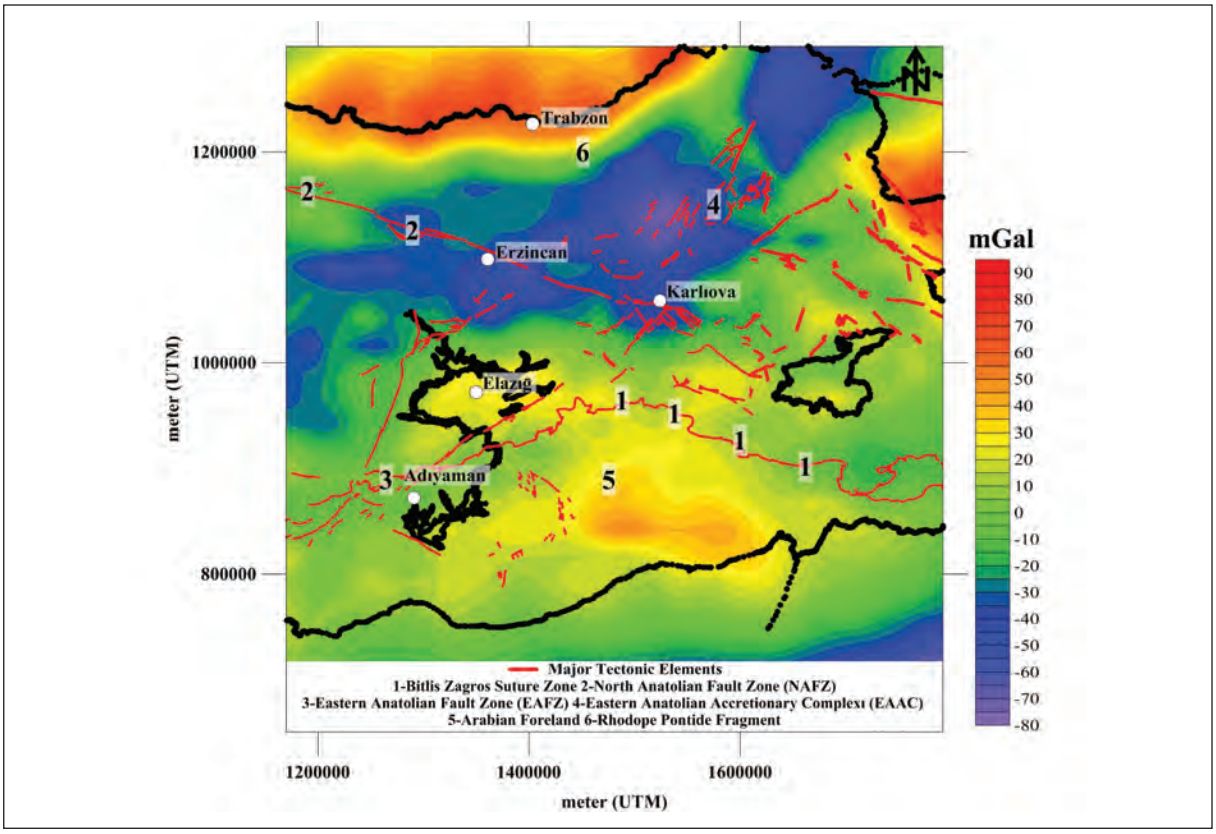

Figure 3- The gravity anomaly map obtained by eliminating 2nd order trend effect from Bouguer gravity anomaly map.

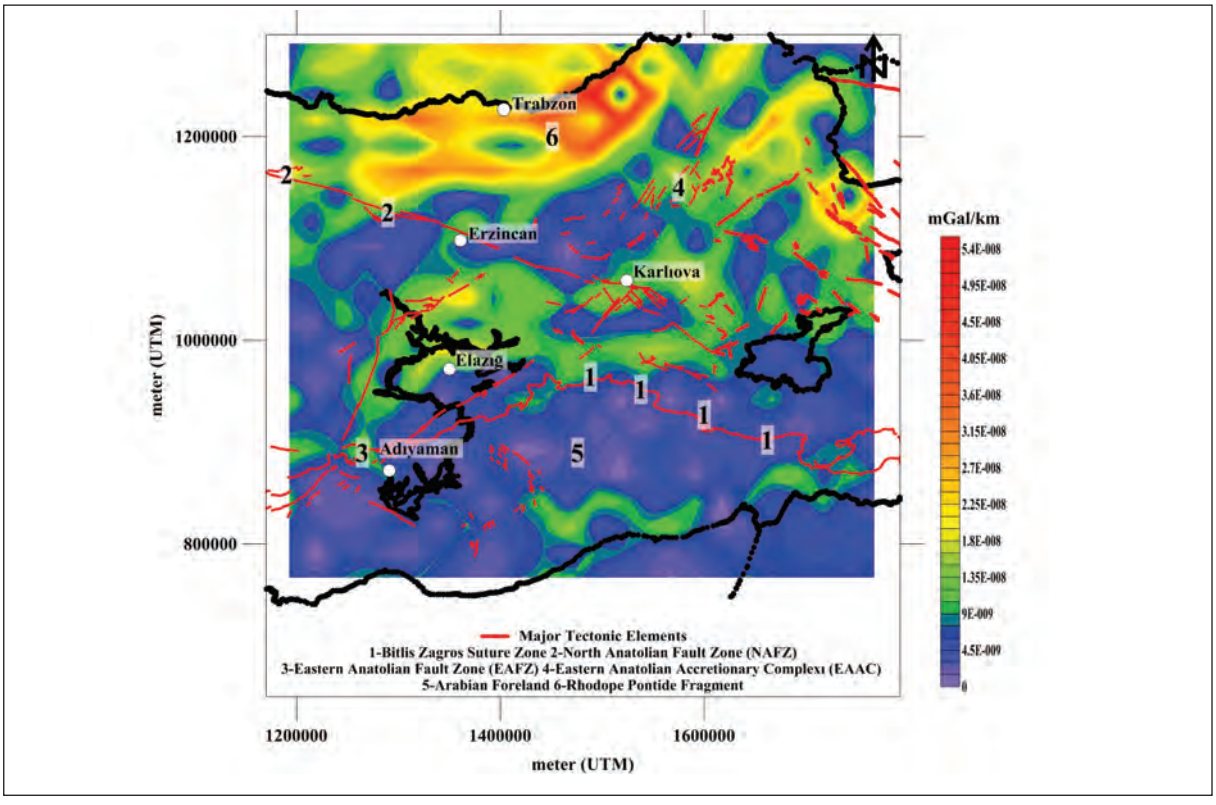

Figure 4- The map obtained by applying horizontal derivative applications on residual Bouguer anomalies shown in figure 3.

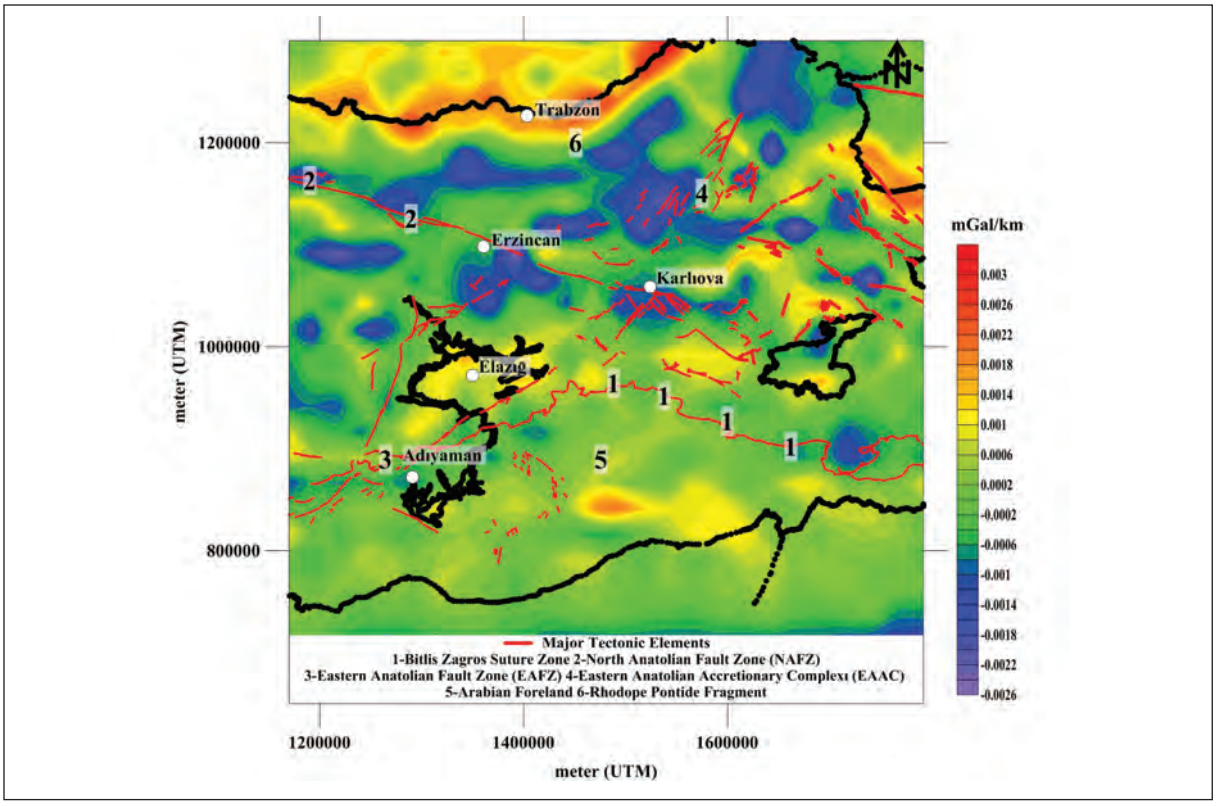

Figure 5- The map obtained by applying 1st vertical derivative application on residual Bouguer anomalies shown in figure 3.

minimum closures alternated from south to north (Figure 3). In horizontal derivative anomaly map (Figure 4), it was obtained that the borders of structures were coherence with the fracture system defined in the study and finally, the possible dominant structure locations were specified with positive anomaly closures in the vertical derivative anomaly map (Figure 5).

4. Results and Discussions

Eastern Anatolia and similar regions located in the borders of the compressional plates are large and complicated zones where the relative displacements turn to the complex and inconsistent stresses. By this scope, the research field Eastern Anatolia has too complex tectonic structures in geologic time scale. In the evaluation of the region, the marine and continental basins have significant roles. The seismological studies (Al-Lazki et al., 2003; Gök et al., 2003; Türkelli et al., 2003; Sandvol et al., 2003*a*, 2003*b*; Zor et al., 2003) realized for characterizing the compressional zone of the region and defining the geodynamics of the compression since 2003, the evolution was explained in the light of the studies and the presence of asthenospheric upwelling was determined (Şengör et al., 2003; Keskin 2003, 2007). It is expected that this upwelling causes to reduce the density of the subsurface formation with the effect of the high temperature and accordingly, brings along the reduction on values of the gravity anomalies. Therefore, the gravity anomalies of the region are examined.

In the first step of the study, the Bouguer gravity anomaly of Eastern Anatolia given in figure 3 was evaluated and 2nd order trend effect was eliminated from the anomaly. When this residual map was examined, it was seen that high amplitude gravity anomalies reached approximately 40 mGal in South of Bitlis Zagros Suture Zone, additionally in North up to Black Sea coasts the gravity anomalies presented negative values. In particular, SW-NE axial high negative amplitude anomalies which contained the Northeastern Anatolian faults were remarkable.

According to horizontal derivative results in figure 4, the possible structure boundaries were obtained as relatively high and low amplitude anomaly transitions structure and these anomaly

transitions were consistent with the extensions of NAFZ and EAFZ. Besides, it was obtained that the trends of the anomalies in horizontal derivative were SW-NE directional.

In figure 5, the negative amplitude structure borders/transition zones and positive amplitude structure locations which shown in the vertical derivative map were determined. In Figure 5, obtaining of transition zone featured structures in a wide area from North of Bitlis Zagros Suture Zone to Black Sea is a trace about the grandness of effected area of the deformation. The positive amplitude anomalies in vertical derivative method indicate the location of the structure (Gönenç, 2014). Relatively, the reduction on derivative values corresponds to the transition zone between two structures. In figure 5, the negative amplitude on vertical derivative particularly in the intersection of NAFZ and EAFZ, Karlıova and surrounding, point out the presence of a significant border there, most likely.

The subduction processes in the thermal and mechanical models (Bird et al., 1975) related with convergence zones in continental-continental compressional regions were explained by heat flows, reduction on gravity and low density zones. The high temperature degree accurring with the effect of friction on suture zones and shear stress related to the depth have importancy on thermal regimes of the shallow parts of the subduction zone. These geodynamic processes can be evaluated for Eastern Anatolia. The presence of shallow seismisity in the region (Zor et al., 2003), obtaining the effective elastic thickness thinner than crustal thickness (Pamukçu and Akçığ, 2011) and determining structure transitions throughout the Bitlis Zagros Suture Zone, NAFZ and EAFZ locations in normalized full gradient studies (Pamukçu and Akçığ, 2011) may indicate that the deformation begins just north of the suture zone. The regions with low velocities and low gravity (Figure 5), have most probably low density structure. These cases can be the results of the mechanisms of convergence duration.

For examining the seismic activity of the study area, the earthquakes (2<M<7) occurred between the years 1973-2015, obtained from Boğaziçi University, Kandilli Observatory and Earthquake Research Institute (KOERI), National Earthquake Monitoring Center were given in figure 6. These earthquakes

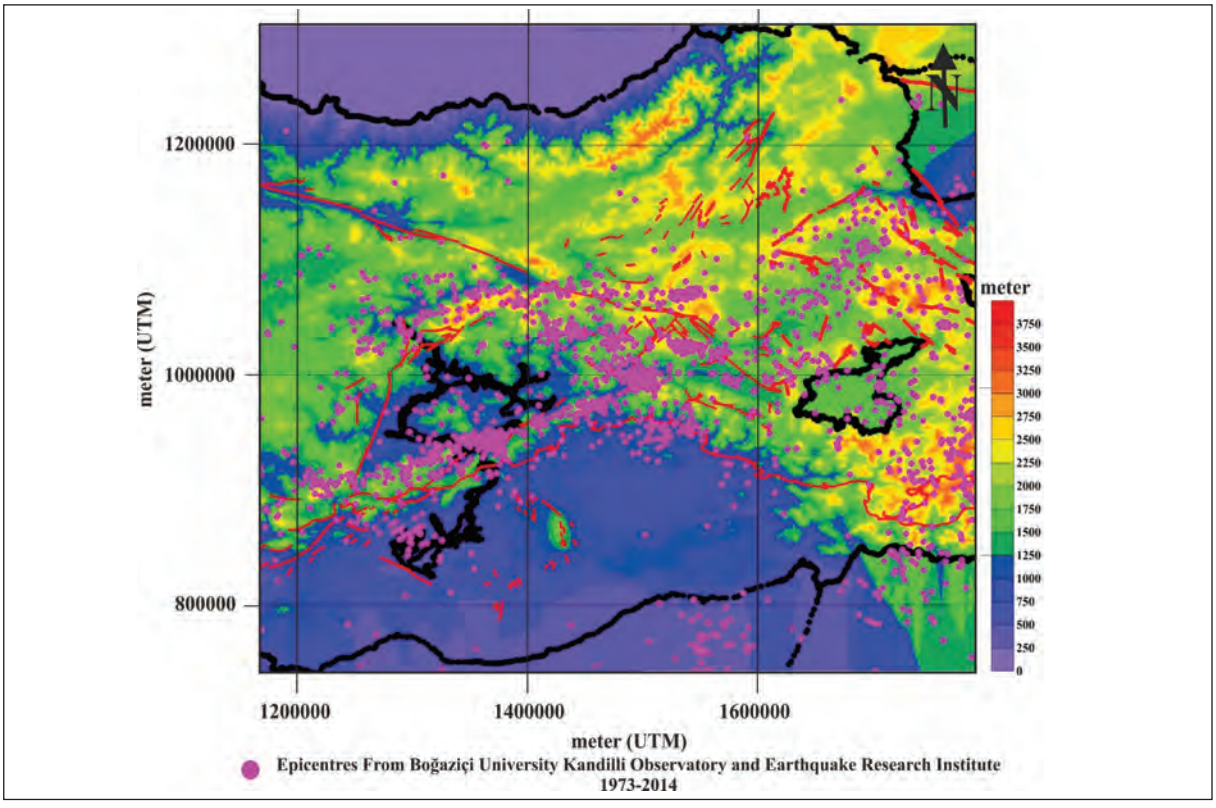

Figure 6- The earthquake epicenter distributions map of study region.

distributed as 8819 of them on NAFZ and 16548 of them on EAFZ. Therefore, it can be said that the negative amplitude structure, which was dominant in NAFZ and its surrounding shown in figure 5, may be related with less brittle and more deformed structure relative to EAFZ.

Additionally, the reasons of the negative amplitude parts obtained in figure 5 may be originated from the crustal problematic area (between the depth 20 km and 40 km) which was represented by Türkelli et al. (2003), Zor et al. (2003), Pamukçu et al. (2007), Keskin et al. (2003, 2007), Şengör et al. (2003), Pamukçu and Akçığ (2011) in figure 7.

In the area between NAFZ and EAFZ near 100000 meter latitude, the structure transition in figure 4, the negative amplitude closures in figure 5 and the regions show high seismic activity in figure 6 were determined as the area which showed decreasing crustal thickness (Pamukçu et al., 2007), decreasing S-wave velocity (Zor et al., 2003), decreasing Curie depths and increasing heat flow (Pamukçu et al., 2014). Additionally, Pamukçu et al. (2007) pointed out that in their Euler deconvolution study results, the 1400000 meter longitude was a border and the lithospheric structures may be different in west and east sides of this border.

As the last step, in figure 8, the topography (Figure 1), Bouguer gravity (Figure 2), 2nd order trend gravity (Figure 3), horizontal derivative (Figure 4), vertical derivative (Figure 5) and heat flow (Pamukçu et al., 2014) sections through 1400000 meter longitude (Figure 1, A-A¢ profile) were compared together. In the region, the latitudes between 100000 and 1200000 meter, where the topography reaches approximately 3 km (Figure 8a), Bouguer and 2nd order trend gravity anomalies present negative values (Figure 8b and Figure 8e), the region which show border features in horizontal and vertical derivatives (Figure 8d and Figure 8e) are coherent with the region which has relatively high amplitude heat flow values (Figure 8f) and indicate the borders of the flexible region which begins at 10 km depths given in figure 7. Particularly Bitlis Zagros Suture Zone, NAFZ and EAFZ present relative changes in gravity anomalies shown in figure 8b. In 2nd derivative anomalies (Figure 8d), the presence of a structure between EAFZ and NAFZ are viewed dominantly. According to the vertical derivative results (in Figure 8e), while this structure shows more

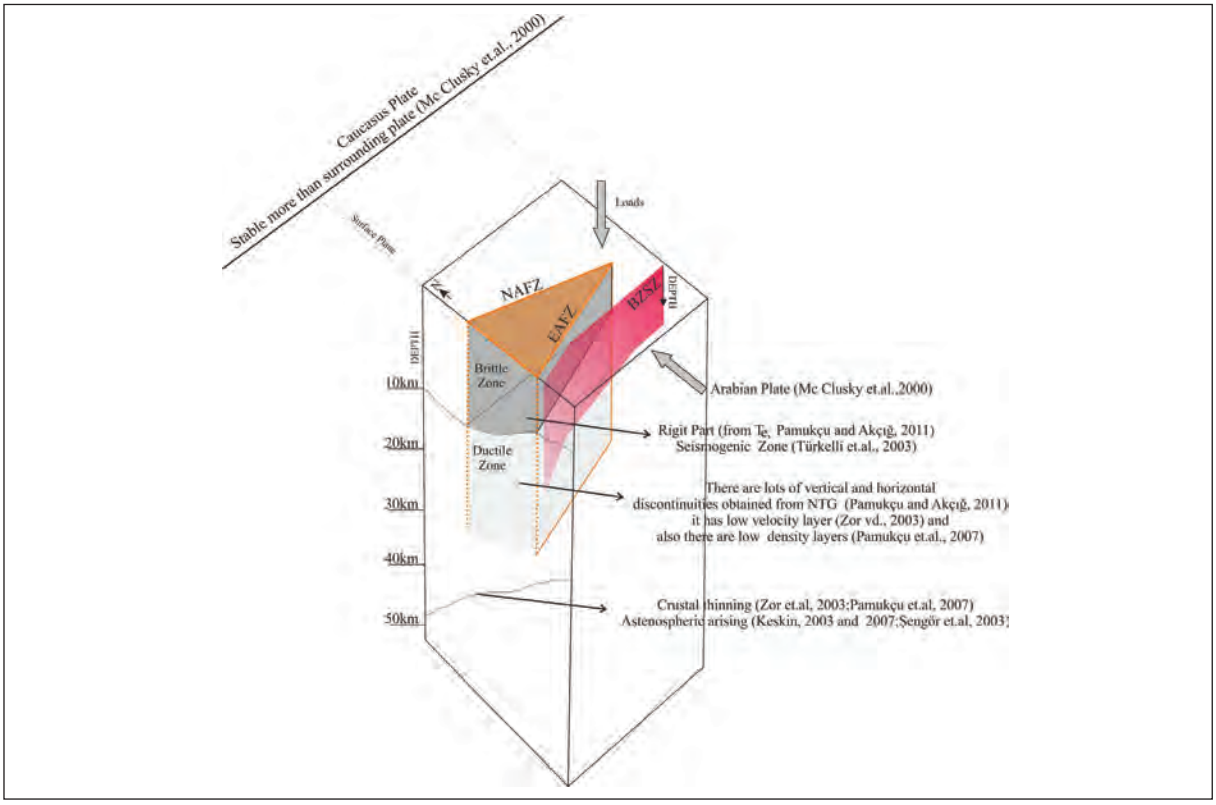

Figure 7- The schematic view of the results of the studies done for investigating the lithospheric structure of Eastern Anatolian Region (modified from Pamukçu and Akçığ 2011).

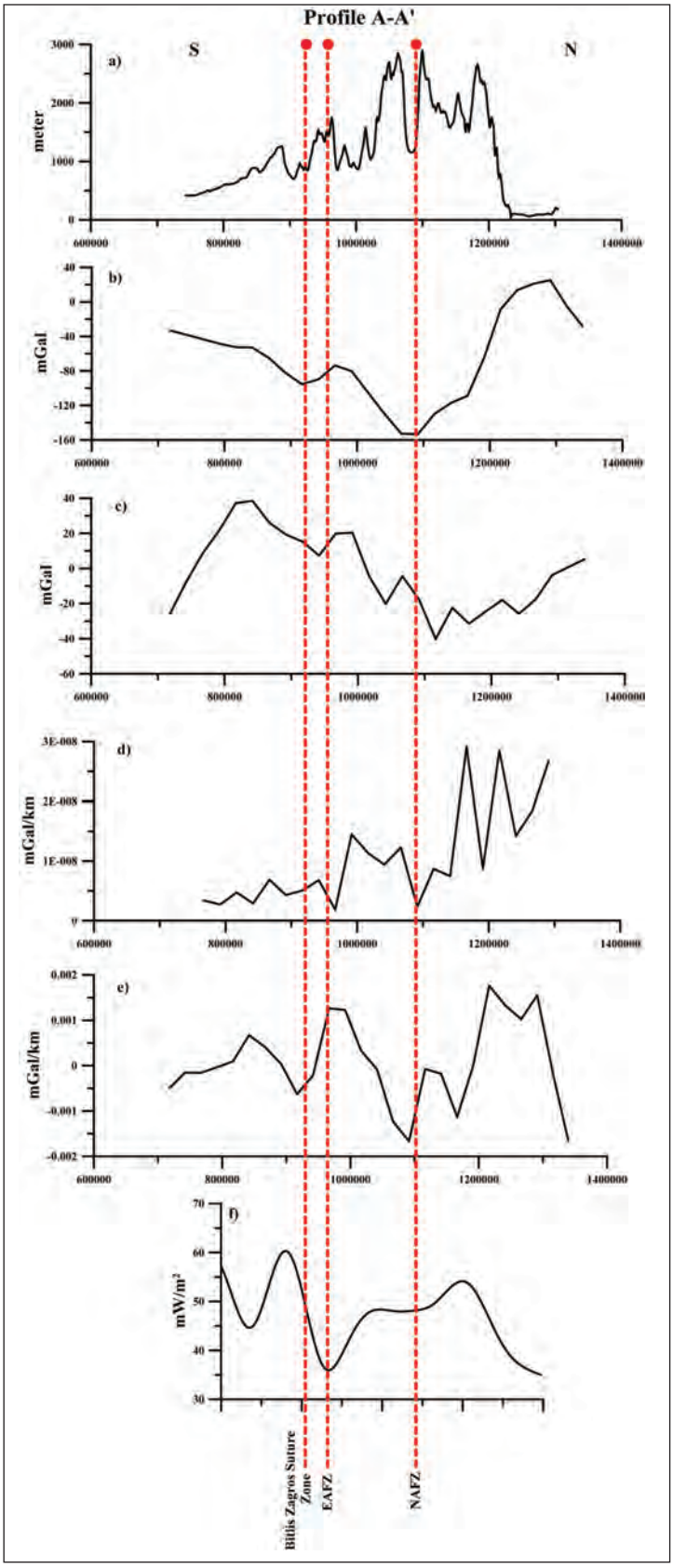

Figure 8- Between the latitudes 100000 and 1200000 meters (Figure 1, A-A' profile) a) Topographic anomaly b) Bouguer c) 2nd order trend Bouguer gravity anomaly d) horizontal and e) vertical derivative values f) heat flow values (Pamukçu et al., 2014).

compact (+mgal/km) behavior nearby EAFZ, behaves like a structure transition border (-mgal/km) toward NAFZ. Existence of amplitude of the gravity anomalies relatively low nearby NAFZ (in Figure 8b), and the heat flow values are high in the same region (in Figure 8f) indicate that the deformation is high in the region where have structure transition behavior in vertical derivative (Figure 8e). Additionally, these cases support the result which shows the earthquake focal depth distributions are less nearby NAFZ given in figure 6.

Acknowledgement

In this study, the data of TUBITAK No:101Y124 project and DEU 02.KB.FEN.084 project were used. We would like to thank the Project manager Prof. Dr. Zafer Akçığ and Assoc. Prof. Dr. Bülent Oruç, Assoc. Prof. Dr. Ali Aydın and Prof. Dr. Cahit Helvacı for their reviews.

Received: 20.02.2015
Accepted: 13.03.2015
Published: December 2015

References

Al-Lazki, A., Seber, D., Sandvol, E., Türkelli, N., Mohamad R., Barazangi, M. 2003. Tomographic Pn velocity and anisotropy structure beneath the Anatolian plateau (eastern Turkey) and the surrounding regions. *Geophysical Research Letters* 30, 24, 8043, doi: 10.1029/2003GL017391.

Barka, A.A., Toksöz, M.N., Gülen, L., Kadinsky-Cade K. 1987. Segmentation, seismicity and earthquake potential of the eastern section of the North Anatolian Fault Zone. *Yerbilimleri, Bulletin of the Earth Sciences Application and Research Centre of Hacettepe University* 14, 337-352.

Barka, A.A., Reilinger, R. 1997. Active tectonics of the Mediterranean region: deduced from GPS, neotectonic and seismicity data. *Annali di Geofisica* XI. 587-610.

Bird, P., Toksöz, M.N., Sleep, N.H. 1975. Thermal and mechanical models of continent-continent convergence zones, *Journal of Geophysical Research*, 80, 4405-4416.

Blakely R. J., Simpson R. W. 1986. Approximating edges of source bodies from magnetic or gravity anomalies. *Geophysic,* 51, 7, 1494-1498.

Bozkurt, E. 2001. Neotectonics of Turkey-a synthesis. *Geodinamica Acta* 14, 3-30.

Butler, D., K. 1984. Microgravimetric and gravity gradient techniques for subsurface cavities. *Geophysic,* 49, 1084-1096.

Coney, P.J., Jones, D.L., Monger, J.W. 1980. Cordilleran suspect terranes. *Nature* 288, 329-3.

Demets, C., Gordon, R.G., Argus, D.F., Stein, S. 1994. Effects of recent revisions to the geomagnetic reversal time scale on estimates of current plate motions. *Geophysical Research Letters* 21, 2191-2194.

Dewey, J.F. 1976. Seismicity of northern Anatolia. *Bulletin of the Seismological Society of America* 66, 843-68.

Dewey, J.F. 1977. Suture zone complexities: a review. *Tectonophysics* 40, 53-67.

Dewey, J.F., Hempton, M.R., Kidd, W.S.F., Şaroğlu F., Şengör A.M.C. 1986. Shortening of continental lithospere: the neotectonics of eastern Anatolia- a young collision zone. *Geological Society Special Publications* 19, 3-36

Gök, R., Sandvol, E., Türkelli, N. Seber, D., Barazangi, M. 2003. Sn attenuation in the Anatolian and Iranian plateau and surrounding regions. *Geophysical Research Letters* 30, 24, 8042, doi: 10.1029/2003GL018020.

Gönenç, T. 2014. Investigation of distribution of embedded shallow structures using the first order vertical derivative of gravity data. *Journal of Applied Geophysics*, 104, 44-57.

Gürsoy, H., Temiz, H., Poisson, A.M. 1992. Recent faulting in the Sivas area (Sivas Basin), Central Anatolia- Turkey. *Cumhuriyet University Bulletin of the Faculty of Engineering Serie A-Earth Sciences* 9, 1-11.

Kahle H.G., Straub, C., Reilinger, R., McClusky, S., King, R., Hurst, K., Veis, G., Kastens, K., Cross, P. 1998. The strain rate field in the eastern Mediterranean region, estimated by repeated GPS measurements. *Tectonophysics* 294, 237-252.

Kelling, G., Gökçen, S.L., Floyd, P.A., Gökçen, N.D. 1987. Neogene tectonics and plate convergence in the eastern Mediterranean: new data from southern Turkey. *Geology* 14, 425-429.

Keskin, M. 2003. Magma generation by slab steepening and breakoff beneath a subduction-accretion complex: An alternative model for collision-related volcanism in Eastern Anatolia, Turkey. *Geophysical Research Letters* 30, 24, 8046, doi: 10.1029/2003GL018019.

Keskin, M., Pearce, J.A., Mitchell, J. G. 1998. Volcanostratigraphy and geochemistry of collision-related volcanism on the Erzurum-Kars Plateau, North Eastern Turkey. *Journal of Volcanology and Geothermal Research* 85, 355-404.

Ketin, İ. 1948. Uber die tektonisch-mechanischen Folgerungen aus den grossen Anotolischen Erdbeben des letzten Dezenniums, *Geol. Rdsch.* 36, 77-83

Ketin, İ. 1966. Tectonic units of Anatolia. *Bulletin of the Mineral Research and Exploration* 66, 23-34.

Koçyiğit, A., Yılmaz, A., Adamia, S., Kuloshvili, 2001. Neotectonics of East Anatolian Plateau (Turkey) and Lesser Caucasus: implications for transition from thrusting to strike-slip faulting. *Geodinamica Acta,* 14, 177-195.

McKenzie, D. 1972. Active tectonics of the Mediterranean region. *Geophysical Journal of the Royal Astronomical Society* 30, 109-185.

McKenzie, D. 1976. The East Anatolian fault: a major structure in eastern Turkey. *Earth and Planetary Science Letters* 29, 189-193.

McKenzie, D.P., Bickle, M. J. 1988. The volume and composition of melt generated by extension of the lithosphere. *Journal of Petrology* 29, 625-679.

Oral, M.B., Reilinger, R.E., Toksöz, M.N., Kong, R.W., Barka, A.A., Kınık, İ., Lenk, O. 1995. Global positioning system offers evidence of plate motions in eastern Mediterranean. *American Geophysical Union, EOS, Transactions* 76, 9-11.

Örgülü, G., Aktar, M., Türkelli, N., Sandvol, E., Barazangi, M. 2003. Contribution to the seismotectonics of the Eastern Anatolian Plateau from moderate and small size events. *Geophysical Research Letters* 30, 24, doi:10.1029/2003GL018258.

Pamukçu, A., O., Akçığ, Z., Demirbaş, Ş., Zor, E. 2007. Investigation of crustal thickness in Eastern Anatolia using gravity, magnetic and topographic data. *Pure and Applied Geophysics 164, 11, 2345-2358*.

Pamukçu, A., O., Akçığ, Z. 2011. Isostasy of the Eastern Anatolia (Turkey) and discontinuities of its crust. *Pure and Applied Geophysics* 168, 5, 901-917.

Pamukçu, O., Akçığ, Z. Hisarlı, M., Tosun, S. 2014. Curie point depths and heat flow of Eastern Anatolia (Turkey). *Energy Sources, Part A: Recovery, Utilization, and Environmental Effects* 24, 2699-2706.

Pearce, J. A., Benger, J.F., De Long, S.E., Kidd, W.S.F, Low, P.J., Güner, Y., Şaroğlu, F., Yılmaz, Y., Moorbath, S., Mitchell, J.G. 1990. Genesis of collision volcanism in Eastern Anatolia, Turkey. *Journal of Volcanology and Geothermal Research* 44, 189-229.

Pearce, J.A., Keskin, M., Serri, G., Innocenti, F. 1995. Tectonic significance of volcanism related to arc-continent collisions. *American Geophysical Union, EOS, Transactions* 76, 602-607.

Reilinger, R.E., McClusky, S.C., Oral, M.B., King, W., Toksöz, M.N. 1997. Global Positioning, System measurements of present-day crustal movements in the Arabian-Africa-Eurasia plate collision zone. *Journal of Geophysical Research* 102, 9983-9999.

Robertson, A.H.F., Clift, P.D., Degnan P., Jones G. 1991. Palaeogeographic and paleotectonic evolution of eastern Mediteranean region. *Palaeogeography, Palaeoclimatology, Palaeoecology* 87, 289-344.

Rotstein, Y., Kafka, A.L. 1982. Seismotectonics of the southern boundary of Anatolia, eastern Mediterranean region: subduction, collision, and arc jumping. *Journal of Geophysical Research* 87, 7694-7706.

Rybach, L., Mueller, S., Mılnes, A.G., Ansorge, J., Bernoulli, D., Frly, M. 1980. The Swiss Geotraverse Basel-Chiaser-a review. *Eclogae Geologicae Helvetiae* 73, 437-62.

Sandvol, E., Türkelli, N., Barazangi, M. 2003*a*. The eastern Turkey seismic experiment: the study of a young continent- continent collision. *Geophysical Research Letters* 30, 24, 8038, doi: 10.1029/2003GL018912.

Sandvol, E., Türkelli, N., Zor, E., Gök, R., Bekler, T., Gürbüz, C., Seber, D., Barazangi, M. 2003*b*. Shear wave splitting in a young continent- continent collision: an example from eastern Turkey. *Geophysical Research Letters* 30, 24, 8041, doi: 10.1029/2003GL017390.

Şengör, A. M. C., Kidd, W.S.F. 1979. The post-collisional tectonics of the Turkish-Iranian Plateau and a comparison with Tibet. *Tectonophysics* 55, 361-376.

Şengör, A.M.C., Yılmaz, Y. 1981. Tethyan evolution of Turkey: a plate tectonic approach. *Tectonophysics* 75, 181-241.

Şengör, A.M.C., Görür, N., Şaroğlu, F. 1985. Strike-slip faulting and related basin formation in zones of tectonic escape: Turkey as a case study, in : Biddle K.T., Christie-Blick N. (Eds.), Strike-slip Faulting and Basin Formation. *Society of Economic Paleontologist Mineralogists Special Publication* 37, 227-264.

Şengör, A. M. C., Özeren, S., Genç, T., Zor, E. 2003. East Anatolian high plateau as a mantle-supported, north-south shortened domal structure. *Geophysical Research Letters* 30, 24, 8045, doi: 10.1029/2003GL017858.

Türkelli, N., Sandvol, E., Zor, E, Gök, R., Bekler,T., Al-Lazki,A., Karabulut,H., Kuleli,S., Eken,T., Gürbüz,C., Bayraktutan, S., Şeber, D., Barazangi, M. 2003. Seismogenic zones in eastern Turkey. *Geophysical Research Letters* 30, 24, 8039, doi: 10.1029/2003GL018023.

Westaway, R., Arger, J. 1996. The Gölbaşı basin, southeastern Turkey: A complex discontinuity in a major strike-slip fault zone. *Journal of Geological Society* 153 , 729-743.

Yılmaz, Y., Yiğitbaş, E., Genç, C.Ş. 1993. Ophiolitic and metamorphic assemblages of southeast Anatolia and their significance in the geological evolution of the orogenic belt. *Tectonics* 12, 1280-1297.

Zor, E., Sandvol, E., Gürbüz, C., Türkelli, N., Şeber, D., Barazangi, M. 2003. The crustal structure of the East Anatolian plateau (Turkey) from receiver functions. *Geophysical Research Letters* 30, 24, 8044, doi: 10.1029/2003GL018192.

Bull. Min. Res. Exp. (2015) 151: 231-246

Bulletin of the
Mineral Research and Exploration

http://bulletin.mta.gov.tr

ARCHAEOLOGICAL AND GEOLOGICAL CONCEPTS ON THE TOPIC OF ANCIENT MINING

Prentiss de JESUS[a] and Gonca DARDENİZ[b]*

[a] *Former Director of the American Research Institute in Turkey (ARIT) in Ankara, pdejesus@alumni.brown.edu*
[b] *Koç University Archaeology and History of Art Department, Istanbul, Turkey, gdardeniz@ku.edu.tr*

Keywords:
Ancient Metallurgy, Geology, Archaeology, Anatolia, Turkey

ABSTRACT

Geological and archaeological research on ancient mining and metallurgy are actually targeting the same goals: understanding the nature and value of a mining operation. Geologists are intent on locating and qualifying ores and minerals for future use, whereas archaeologists strive to link ores to relevant historic and prehistoric metal artifacts and activities. This article discusses research into ancient Anatolian metallurgy by underscoring the overlap between geological and archeological practices. The work of archaeologists and geologists can be mutually beneficial through a close collaboration on the collection and analysis of field data. Their accumulated and combined knowledge would accelerate the progress towards placing ancient mining activities in a chronological and meaningful context.

1. Introduction

This article attempts to outline the strategic approach that archaeologists take in studying ancient mining and metallurgy. It will be immediately discernable to geologists, for whom this article is being written, that there are striking similarities in the way an ore or resource deposit is studied. The goal of archaeologists who study the history of mining is primarily to determine how and where mining took place and to fit it into the cultural history of the past. In addition, they seek to determine the technologies applied in processing ores and how the end product, metal, is eventually used. Research does not end there. History becomes meaningful when all of societies' components –its industries, its crafts, and its social institutions– are fully understood and how they relate to each other. The production of metal played a vital role in how societies developed: their wealth, their crafts, their weapons, and their economy. None the least, metals contributed to how those societies reorganized internally into social classes and hierarchy. The rise of material wealth created an elite class separate from political and clerical leaders and established another locus of power. Metal, especially silver, became a medium of exchange and thereby ensured the future of mining. Just as the ancient miners used a handful of rudimentary methods to locate deposits present-day geologists employ modern tools and techniques to locate profitable mining possibilities. The ancient miner and the modern geologist followed paths that cross today. It is not uncommon to see current mining companies digging through ancient mining operations. What may have been an exhausted mineral deposit long ago may very well be worthwhile today because of our advanced mining technology. Economic imperatives drive the need for mining, but unfortunately today's mining operations have on occasion erased many of the ancient mining remains before they could be documented and recorded in the historical record.

Compiling a history of mining and metallurgy requires a broad view of the literature and work of many different scholars who contribute to the science

* *Corresponding author: Gonca Dardeniz, goncadardeniz@gmail.com*

and history of metals. Not only do scholars look at the metalwork and its affinities with neighboring areas or sites, but scientists are instrumental in providing valuable information on the compositions of artifacts, isotopic analysis, and geology of metallic ores. Some of the analytical techniques covered in this paper give an indication of the breadth of the different disciples involved.

General Directorate of Mineral Research and Exploration (hereafter; MTA) established in 1935 has not been on the sidelines of ancient mining research. Through its routine fieldwork it has noted many early mining operations, which has served as a guide to an historical assessment of mining in Anatolia. MTA has also sponsored fieldwork that explored ancient mining operations within the borders of Turkey (Kaptan, 1977, 1978, 1982, 1984, 2008, 2012; Başaran et al., 2012, 2010; Kartalkanat et al., 2011; Kaya et al., 2012; Pehlivan et al., 1986; de Jesus, 1977; Ryan 1960; Giles and Kuijpers, 1974). This involvement has yielded enlightening results. Valuable analyses and technical information on mining remains and ores have been produced in MTA's laboratories. MTA has been a loyal partner with other entities who share the same intense interest in the history of mining and metallurgy. Many mining artifacts are now displayed in MTA's museum for the public's enjoyment as a result of these efforts.

We have drawn the limits of this article to sketch out general concepts relating to the initial developments and characteristics of ancient mining and metallurgy in Anatolia. We will touch only lightly on mining and metallurgical developments in other areas. Relevant social and organizational impacts that mining exercised on technology and highland populations has been recently discussed by Lehner and Yener (2014). The primary goal of this paper is to demonstrate the relevance of present-day geological studies to the history of mining and metallurgy in Turkey, which we will refer to here as Anatolia.

2. Early Resource Mining

Mining has been a human activity since Palaeolithic times when early man collected stones that would best fulfill his needs, whether it was for pounding, cutting, grinding or self-defense. Flint and obsidian were eventually incorporated into the repertoire of early human groups because they could be chipped and shaped into refined tools and extremely sharp weapons. With the advent of agriculture there came a demand for specialized blades, such as microliths, used in cutting wheat stalks. Because of its superior cutting qualities Anatolian obsidian was mined and traded across a vast area of the Near East and has been found as early as 14,000 BC (Before Christ) in northern Iraq and in the Levant (Cauvin et al., 1998). Originating from such Central Anatolian deposits as Göllüdağ, obsidian cores and blades were traded as far away as the Arabian Peninsula dating to Ubaidian times (ca. 4800 BC). They are found even earlier in Mesopotamia (corresponding to present-day Iraq) and Syria at Halafian sites dating to 6000-5500 BC (Balkan-Atlı et al., 2008; Özdoğan, 2008; Healey, 2007; Wright, 1969; Châtaignier et al., 1998). Obsidian was obviously recognized as a superior material with which to make tools. The qualities of the volcanic glass offered the opportunity to fashion tools of extreme precision and beauty, as illustrated by the obsidian bifacial points found at Neolithic Çatal Höyük (Hodder 2011), some of which are now displayed in the Museum of Anatolian Civilizations in Ankara.

2.1. Copper

Man's continued curiosity with materials led him to become acquainted with metal ores such as brightly colored copper oxides and to use them for decorative beads and pigments. Use of these materials has been documented in archaeological excavations and provides a starting point for the history of metallurgy. Thanks to their familiarity with these copper oxides, prehistoric people eventually came upon native copper metal and recognized its unique characteristics. Unlike stone, it could be hammered into simple shapes, and it was more durable.

Native copper outcrops are somewhat common in Turkey, so it is not surprising that copper artifacts have been found in early Neolithic settlements, such as Çayönü Tepesi in southeastern Turkey dated from the middle of the 9th millennium BC and Aşıklı in central Turkey (Maddin et al., 1999, Shoop, 1995, Yalçın, 2000, Esin and Harmankaya, 1999). Because of its relatively high melting temperature (1085°C) native copper pieces in the early phases of the Neolithic period could not be fused, as furnaces at that time could not reach this temperature. Hence, the objects that were fashioned out of native copper were limited to the size of the copper piece found. Consequently, the earliest copper artifacts from excavations are relatively small — points, borers, beads and pendants. Only after metal craftsmen had

designed furnaces or found means of melting native copper pieces do we find larger objects, such as knives, chisels and axes. The native copper mace head from Chalcolithic Can Hasan is an exceptional piece of work dating to about 4750 BC, and its size suggests that the technology of fusing bits of native copper into one large piece had been achieved. It had been thought for a long time that the mace head was cast by the lost wax process, but this has been recently disproven by analytical study. Yalçın (2000; 1998) has shown that it was forged into a shape that accommodated a central shaft hole for the haft. Shaft hole casting would come much later. The early copper craftsman's ability to melt copper opened the door to many possibilities, not only to make tools but to fashion refined shapes that were before made of bone or wood. Over time copper became the material of preference for many objects –needles, knives, borers, fish hooks, and arrow heads, just to name a few.

2.2. Early Copper Metallurgy

Archaeologists have often maintained that the source of copper metal for many early copper artifacts found in Turkey, Syria and northern Mesopotamia came from Ergani (Tylecote, 1976; Moorey, 1999; Bamba, 1972; Hauptmann, 2000; 2007). The Neolithic site of Çayönü, mentioned above, is located only 20 km away. Although Ergani is a massive copper deposit, it is unwise to assume that all the early occurrences of native copper artifacts found in eastern Turkey came from there. As it turns out, recent studies suggest that the copper and malachite pieces found at Çayönü may have come from another source (Esin, 1995). It has also been revealed by Esin that the copper found at the Aşıklı, located 25 km southeast of Aksaray, came from a source different from the copper found at Çayönü. It is, hence, clear that there are, or were, many copper deposits scattered throughout Anatolia that contained appreciable quantities of native copper metal available at remote times in Anatolian history (Wagner and Öztunalı, 2000; de Jesus, 1980; Ryan, 1960).

Yalçın and İpek (2012) have recently explored the site of Derekütüğün in Çorum Province where native copper was mined in antiquity. Based on archaeological finds, the excavators suggest that the mine may have supplied copper to Early Bronze Age sites in the region, such as Resuloğlu, Alaca Höyük, and Eskiyapar. We must point out, however, that metal analyses have shown that not all of the metalwork from these sites was made from native copper, confirming the fact that there were also other copper sources.

Once the native copper at an outcrop was exhausted, early copper miners would have easily made the connection between the copper metal and any accociated oxides. We surmise that native copper is commonly found in context with a massive copper ore bodies, such as at Ergani. Ancient miners would have understood that the copper oxides, clearly visible by their bright blue, green and iridescent colors, were different forms of copper. The early metalworkers experimented with the ores, using different heating techniques known at the time. The discovery of smelting was the result of such efforts. Native copper is not always associated with copper ore. Substantial amounts of oxidized copper ore do not exist at Derekütüğün, so when the native copper was exhausted the mining operation there simply ceased, and the miners searched for sources elsewhere.

For the ancient smelter, extracting metal from ores was a process that involved tapping into the cosmic realm. It is generally accepted by scholars that throughout antiquity smelting was very much a ritual process that beseeched the gods to release metal from its ore. The activity of smelting was conducted by those individuals who possessed special skills and the required recipes. To arrive at a successful smelt, ritual procedures were carefully planned. The operation entailed mixing precise ore and fuel ratios, constructing efficient furnaces that could produce the temperatures required, and timing the operation accurately to extract the maximum amount of metal from the ore. The ancient smelters believed that no successful smelt would take place if the gods refused their cooperation. The smelting process was a carefully guarded ritual that constituted a portal to the secrets of the natural and occult world. Ancient smelters operated in a realm parallel to science, but it functioned on the same principles of cause and effect. For us today smelting is a technological process. For the ancient smelter it was a religious experience. Ancient metallurgy, then, was an industry that existed only by sacred authorization (Eliade 1987; 1977).

Metallurgical processes probably involved invoking the god of fire which, in the case of Mesopotamia, it was the god Gibil. Ninmug was the Mesopotamian smithing goddess and would have been invoked as metal smiths produced weapons and everyday objects whether for practical use, ritual, or

adornment. According to one Neo Assyrian text the day and month that a smelt could take place had to be selected for its favorability, and before the smelt was initiated incense was placed in front of the furnace and beer was ceremoniously poured onto the ground. Eliade (1977) informs us that even a special wood, from the styrax tree, was used to fire the smelt. This tree is indigenous to Cyprus and Turkey. The formula calls for the wood to be cut in the month of "Ab", corresponding to July-August which may correspond to the time when the sap rises in the wood and hence infusing it with a fragrant odor as well as increased combustibility. To ensure sacred propriety, the ancient text goes on to say that all the laborers involved in the smelting process had to be "purified" beforehand. The prepared smelt was referred to as an "embryo," a concept typifying the belief that the earth was female and metal was male. In the smelting process the earthen ore gave birth to metal, a male child. As a result, most forms of metal –such as weapons, tools, and vessels– were consistently considered male attributes (Eliade, 1977).

Ancient Egypt, too, had its versions of metal-related spirits. Gold was regarded as the flesh of Ra, the sun god, and Hathor, the goddess of mining and metallurgy, was often referred to as "the golden one." A temple dedicated to Hathor was found at Serabit el-Khadim in the Sinai near where turquoise mining took place. As one might expect she also carried the epithet "Lady of Turquoise." At Timna in the Negev north of Elat a shrine dedicated to Hathor was discovered and excavated in the vicinity of the copper mining operations. Again, this illustrates the close association between the goddess Hathor and metallurgical operations (Rothenberg, 1972).

We know very little about Anatolian-based mythologies, as few texts have survived that inform us about the sacred Anatolian pantheon. Yet, it is fair to speculate that gods played a vital role in the daily lives of Anatolians from the earliest of times. We are reminded by the shrines at Göbekli that, even before the Neolithic, symbols represented the mythical spirits that inhabited the world and represented an important concept to which hunter-gatherers could devote their religious tendancies (Schmidt, 2007). Although the names and mythical adventures that surrounded the Göbekli spirits are still unknown to us, for the people of that time mythical and spiritual beings encapsulated natural forces that invited their devotion. The uses of animal symbolism at Göbekli, and later at Çatal Höyük, were metaphors, or cultural codes, that conceived of the world and, in another way, revealed it. Prehistoric people had found an access to the cosmological order and supernatural forces through symbolism and ritual. Thanks to their beliefs and symbolic expression they found their spiritual place in the universe, and from that vantage point they ultimately sought to harness nature's forces. Manipulating these supernatural forces mirrored the profane technology we use today.

It is not until writing was introduced thousands of years later that we have a glimpse into the world of Anatolian mythology. The rare Yozgat tablet of the Hittite Period contains the myth of Telipinu, the god of agriculture, and mentions the existence of a "thousand gods" (Gurney, 1969). The mythological past of ancient Anatolia must have been exceedingly rich in events and concepts that touched every aspect of Anatolian life, including mining and metallurgy. We can only hope that the progress of archaeology will reveal more of this cultural heritage and fill in the blank chapters associated with this land.

While copper started as a humble native metal it had a different destiny from the precious metals such as native gold or smelted silver. From the time that craftsmen succeeded in melting copper, smelting copper ore and fashioning useful tools and weapons, it did not take long before civilization became metal-dependent. After the development of agriculture and the domestication of animals copper production constituted one of humanity's most important and durable industries.

2.3. Smelting complex ores

After the easily smelted oxides had been exhausted, miners were confronted with sulphides and complex ore bodies. The early smelters had to figure out what was required to obtain permission from the gods to release the metal from these more complex ores. Most likely through trial and error they came upon the technique of pre-roasting the ore concentrate before passing on to the smelting stage. A number of exploratory rituals and manipulations of the ore mix were no doubt attempted before a successful process was discovered. Based on archaeological evidence it appears that sometime in the Chalcolithic period in Anatolia, perhaps as early as the 5th millennium BC, that sulphide and polymetallic ores were being smelted on a routine basis. It could have been at this time that different metallurgical traditions converged and exploited their respective metals at the same site. It could be, too, that this convergence resulted in the development of

alloys. As we shall discuss below, smelters had figured out a way to produce arsenic-copper alloys for specific uses. From what we know about arsenic ores (e.g. orpiment and realgar), it is unlikely that smelters isolated arsenic as a metal. This leaves us with the notion that copper and arsenic ores were co-smelted resulting in a copper-arsenic alloy. We do not know how the copper smelter came upon arsenic nor whether co-smelting was in fact the technique used. The technology of creating copper-arsenic alloys, possibly known as early as the 5th millennium BC, remains one of the enigmas of ancient metallurgical history. Silver-copper alloys are also known, as are copper-antimony alloys, though rare. We can see from analysis of metalwork that by the end of the 4th millennium BC smelters were intentionally alloying copper with tin and producing good quality bronze (Lehner and Yener 2014: 539). It can be safely claimed that smelters in the Late Chalcolithic developed alloying and practiced it regularly to arrive at specific and anticipated results. The mining and processing of polymetallic ores should retain our interest, as it may very well represent a point at which ancient metallurgists collaborated and technologies merged, resulting in the fundamental practices that led to the sophisticated techniques evident in later periods.

2.4. Late Chalcolithic Beginnings

There is an increasing notion amongst archeaeologists that the Late Chalcolithic was an important period of incubation in the development of metallurgical techniques as well as socio-political changes that deeply affected the material life of people across a broad stretch of the ancient Near East (Sagona and Zimansky, 2009). While the developments in political organization and the exploitation of material resources was by no means uniform, it is clear that the economic fortunes of settlements was growing steadily in the Late Chalcolithic Period, which we can place at ca. 3800-3100 BC. One cannot describe the situation properly without considering Southern Mesopotamia and socio-political developments during this time. Southern Mesopotamia's urban development was fueled by a growing elite class and their desire for essential natural resources, including metals. To satisfy the demand of urban centers Mesopotamian traders reached out in different directions to obtain the metal resources they needed, principally copper, silver and gold. Later, tin would be added to this list. Some of these metals may have come from Iran, and even beyond (Nezafati et al., 2008). More relevant to our discussion here, evidence of Mesopotamian trade and contacts is visible at sites in the upper reaches of the Euphrates in Syria and farther north into eastern Anatolia where metal resources could be obtained.

The cultural impact of trading enclaves originating from Mesopotamia in the Late Uruk period will not be dealt in these pages, as the purpose of our comments here is to provide a sketch of how, where and when resources were exploited and how they are relevant to present-day geological research. It is nevertheless important to mention that Mesopotamia's trade in metals, as well as other products, traveled on a reliable path of cultural acceptance. Religious and political ideologies flowed in tandum with the trade that took place over many hundreds of years, and elements of Mesopotamian culture gradually made their way into the heart of Anatolia.

Trade was no doubt a factor in the development of the urban site of Arslantepe near Malatya and where elements of Mesopotamian culture are evident, as well at Hacınebi Tepe, Hassek Höyük and other sites situated along the Euphrates (Stein et al., 1996; Stein 2001). It has not been determined to what extent the large site of Arslantepe was involved in the metals trade, but it is likely that it was a part of the regional network that traded metals down the Euphrates to eager sites in southwest Anatolia, Syria and Mesopotamia. Archaeological surveys have revealed a number of ore deposits and polymetallic ore bodies — mainly copper but also containing silver and gold ores — that could correspond to this period of mining activity or slightly afterward (Yener and Özbal, 1987; Özbal et al., 1999; Palmieri et al., 1996). Geologists have also studied these areas (Kalender, 2011). These are good starting points for future field research aimed at establishing the origins of metal used in ancient metalwork.

The Arslantepe excavation has yielded exceptional metalwork that deserves mention, as it relates to increased production of metals and the development of metallurgical skills in the Late Chalcolithic Period. The hoard of swords and spear heads recovered in the Palace complex at Arslantepe Period VIA (dated by the excavators to ca. 3000 BC) has been celebrated as a spectacular example of smithing skills at the end of the Late Chalcolithic Period, or by other accounts, at the onset of the Early Bronze Age. In the literature the swords have been carefully described, stressing the delicate work on the handles and pummels that include silver inlay and a

superb finish of the blades. Close examination of the swords indicates that they were not intended for practical use, rather they were flat cast and are symbolic models of real swords. They were perhaps used in an emblematic fashion but were never intended for use in battle. This does not diminish their importance, as their shape and form reveal that there existed a contemporary craftsmanship that produced real swords with proper tangs, elaborate handles, silver inlay and robust hilts. These are not backwater characteristics; on the contrary, the features on the flat, symbolic swords reflect a sophisticated metallurgical tradition that must have developed earlier in the Chalcolithic period. Hence, if we accept the excavators' chronological dating of the hoard, the symbolic Arslantepe swords clearly express well-honed technologies of real, practical swords that have not yet been found anywhere in this timeframe. Given a period of time for metallurgical technology and smithing skills to develop, it is logical to assume that the metallurgical technology represented in the Arslantepe hoard began much earlier than the archaeological literature has heretofore expressed. Moreover, the coexistence of silver and arsenic-copper alloy of the swords at this time indicates an intimate relationship in the production of these metals. It appears that silver, arsenic and copper smithing techniques have converged to produce a single artifact. Gnawing questions still haunt us. The source of the silver is unknown and attempts to identify the sources of copper are still inconclusive (Di Nocera, 2010: 271). The so-called ancient workings at the metal deposits mentioned earlier have no confirmed dates. Their importance lies solely in the fact that they had been exploited in antiquity and that they are within proximity of archaeological sites.

What this means in the context of our discussion here is that much work remains before we can have a clear picture of the mines-to-metalwork process. It is not likely that excavations in settlement areas will provide the answers we are seeking. Even though some smelting may have taken place within settlements, as at Arslantepe, Hacınebi, Norşuntepe and other sites in eastern Anatolia (Hauptmann and Palmieri, 2000; 75-6; Di Nocera, 2010: 268-270; Özbal et al., 1999: 59; Zwicker, 1977: 13, ff.), their output must have been frustratingly small. At Hacınebi, for example, four smelting furnaces were discovered, but blowpipes (as opposed to bellows) were used for the forced air. This system does not suggest a large-scale operation. Experiments in crucible smelting using blowpipes have always shown to yield only small amounts of copper. To produce sizeable amounts of copper metal large and more efficient installations are called for, such as tapping furnaces, pot bellows, plenty of charcoal, and manpower for the ore preparation and smelting operation. Hence, although smelting inside settlements is known, they are conceivably designed for small outputs. The answers to our big technological questions lie in the remote areas of Anatolia where the bulk of smelting took place and where the ore deposits were mined (and here is where present-day geology can play an important role). Nearby wooded areas would have provided ample fuel, and the miners would have delivered the required manpower for ore preparation and smelting. True, full-fledged mining-processing sites are still an archaeological rarity. At present, we have the Early Bronze Age site of Göltepe-Kestel that provides us with a body of evidence pointing to the mining and processing of tin ore within a defined cultural context (Yener, 2000; Yener and Özbal, 1987, Yener and Vandiver, 1993). New reseach on the Hisarcık province of Kayseri also provided promising evidence for the Early Bronze Age tin resources of Anatolia (Yener et al., 2015). The corollary that links settlements with the relatively isolated mining sites is crucial to the understanding of the metallurgical industry in the ancient past. Was it proximity, cultural affinities, convenient trade routes, or economic necessity?

This brings us back to the heading of this section. The Late Chalcolithic Period still holds the secrets to the dynamic developments of mining, complex ore smelting, unprecedented alloying techniques, and sophisticated smithing practices as well as the trade mechanisms that allowed the industry to thrive. The challenge lies in further fieldwork that can locate these activities in the remote areas of Anatolia. It is well worth our effort to seek out those places that subsequently gave rise to the Early Bronze Age.

2.5. Early Bronze Age Metallurgy

We have embraced the concept that the Late Chalcolithic was that period in the past when great strides were made in metallurgical techniques. The emergence in the Early Bronze Age of different types of alloys, sophisticated smithing skills, abundant metal resources, and the elegant use of gold and silver presupposes that these developments owed their existence to prior initiatives in the Late Chalcolithic Period. The Early Bronze Age can be characterized as a spectacular flowering of metallurgical practices that was were long in coming. Although we find exquisite

examples of metalwork and artifacts of unique design in the Early Bronze Age, we are in no better position to indicate from where the metalworkers obtained their raw copper, silver, or gold. We have candidates, but until archaeology can provide us with reliable dates and analytical data of mine workings, the picture we sketch out for ourselves will remain lamentably hypothetical. Apart from Derekütüğün mentioned above, the only other Early Bronze Age copper mine currently known is Kozlu, discovered in the course of geological work in central Anatolia, and subsequently explored by Ergun Kaptan of MTA (Giles and Kuijpers, 1974; Kaptan, 1986). The area near the mine includes a settlement where late period artifacts were found, but a thorough exploration of the site still awaits the archaelogist's spade. While our lack of dated mining sites is frustrating, we can delight in the fact that we have abundant analyses of metalwork and many studies that enlighten us on smithing technologies in the Early Bronze Age.

Metallurgists of this period had mastered the sophisticated techniques of lost wax casting, annealing, guilding with gold and silver, multiple mold casting, shaft-hole casting, and soldering. These techniques are typical of the metalwork from Alaca, Horoztepe, Eskiyapar, Resuloğlu and other sites on the central Anatolian plateau and from Ikiztepe on the Anatolian north coast (Sagona and Zimansky, 2009; Öztürk, 1992; Yıldırım, 2006, 2010; Bilgi, 1990, 2001). In the west of Anatolia, the metalwork from Troy best represents a western metallurgical tradition that excelled in goldworking and had links with the Aegean (Tolstikov and Treister, 1996; Sazcı, 2007; Mellink, 1986). Regional metallurgical traditions appear to have existed throughout the Early Bronze Age and may reflect from where they obtained their copper and other metals, as well as their technological preferences that were traditionally attached to regional cultures. Arsenical copper seems to be common in eastern Anatolia and along the north coast. Arsenic ore outcrops are known in this region, and it has been reported that ancient galleries are associated with the arsenic deposit (orpiment and realgar) at Durağan east of Kastamonu (Özbal et al., 2000). Tin bronze tends to appear on the central Anatolian plateau, in southern Anatolia and along the Mediterranean coast. The Early Bronze Age tin mine at Kestel and/or Hisarcık could have provided tin metal for a good portion of this region (Yener and Vandiver, 1993; Yener et al., 2015). Of course arsenical copper and tin bronze artifacts crossed these regional boundaries as a result of trade and human migration.

2.6. Gold

Although gold also occurs in native metal form it was apparently not recognized for any of its qualities until the Early Bronze Age. Gold has some outstanding characteristics that other metals do not. First of all, it is very durable, and it does not oxidize or corrode like copper or iron. It can be hammered easily into very thin sheets and bent into graceful and interesting shapes. It lends itself to decorative forms, such as filigree and granulation, hence its use in jewelry. Gold was not only valued for its beauty but for its special powers. Chinese alchemists were known to have eaten small quantities of gold, which was thought to have given them long life.

The discovery of gold was probably not a complicated matter. At a very early time in human history hunter-gatherers would surely have observed shiny particles of gold collected in the bends of rivers where the natural action of the water deposited granules of heavy materials. Gold particles may have been known at a very remote time in prehistory, but they were likely viewed as no more than curiosities. The initial use of gold was dependent upon a craftsman's ability to reach gold's melting temperature of 1,064°C, and it was not until then that gold could be amalgamated into sizable pieces and shaped into decorative items. Although the higher melting temperature of copper was well known and routinely reached in the 5th millennium BC by craftsmen, present evidence suggests that they were either simply not interested in gold at that time or they did not have abundant access to it (Roberts et al., 2009: 1013-1016). Despite the existence of skilled craftsmen in Neolithic Anatolia, gold metal lingered in the shadows before it attracted any interest.

The first gold artifacts that occur in the region are outside Anatolia. A gold earring from Dhimini, Greece was recovered from Late Neolithic contexts dating to the beginning of the 5th millennium BC. Slightly later in time, a gold bead was recovered at Sitagroi III (4600-4200 BC), also in Greece. In addition to these early examples are ceramic pots gilded with gold from Varna, Bulgaria dating to ca. 4000 BC, all of which exhibit techniques that are unknown anywhere in Anatolia at this time. Stöllner et al., claim that they have excavated the oldest gold mine so far known, north of the Caucasus in Georgia. The mine shafts there indicate a mining activity lasting many centuries, and the excavators suggest a date, of "perhaps in the 2nd half of the 4th millennium B.C." (Stöllner et al., 2008). It would appear, then,

that Trans-Caucasia and southeast Europe were precursors of Anatolia in terms of gold production and technology. Archaeologists generally agree that the role of gold became associated with individuals of high status and was a symbol of their authority and power. The incentive for the production of a noble, yet impractical, metal such as gold may be related more to the social make up and hierarchy of cultures than to craftsmen's metallurgical skills. At the present time there is simply not enough known about the Chalcolithic period in Anatolia to relegate its metallurgical technologies to simple and unwarranted backwater status (Düring, 2011). While we should not claim that there is a gold producing activity in Anatolia contemporary in date to its neighbors, we can make a case for early gold production in Anatolia at some point in the Late Chalcolithic-Early Bronze Age timeframe. An early example of Anatolian gold comes from Arslantepe Level VIA in the form of a gold disc (ca. 3000 BC) (Di Nocera, 2010). This item and a spiral ring from the later "Royal" burials signal the development of a gold metallurgical industry that had likely developed previously and operated in the hinterlands of Anatolia. It is also possible that these were traded items from afar.

With the advent of the Early Bronze Age more gold artifacts in Anatolia are found, as at Troy Level II dating to ca. 2500 BC and used, as one might expect, for decoration. The keen interest in gold as late as this in Anatolia was possibly a result of the dynamic changes that took place when metallurgical traditions interacted, polymetallic ore bodies were being exploited on a large scale, population increased, and a socially-based demand for luxury goods developed in earnest (Lehner and Yener 2014: 548). Cultural developments and unequal social stratification were undoubtedly linked to the appearance of gold in currently-known Anatolian settlements. It has been convincingly pointed out that non-egalitarian communities existed in Anatolia since the Neolithic Period, but with the advent of new and precious materials that distinguished privileged classes of society from commoners there emerged a greater incentive to produce luxury items for them. In short, gold became a symbol of distinction for the growing number of elite.

The finer details relating to the initial uses of gold, its discovery, its processing, its trade and comparison with other gold-production centers will have to be addressed at another time. For the moment it is worthwhile stressing that gold production from Anatolian deposits was closely tied to the indigenous craftsmen of gold artifacts. This does not in any way suggest that Anatolia was a leader in all forms of gold craftsmanship. On the contrary, Mesopotamia seems to have led the world in splendid granulation and filigree work. The lack of resources in Mesopotamia did not prevent its craftsmen from developing a level of sophistication that exceeded all its neighbors. This is a common situation. One need only cite in passing the expertise of Egyptian shipbuilders, even though they had to import the basic material – wood. Technologies are born out of defined cultural contexts that meet the strict needs of the population. The size, quality and sophistication of an artifact are inextricably linked to its cultural foundations, hence the way an object or material is produced and how it is used. The great surge in the use of gold came around the middle of the 3rd millennium BC. Gold production must have increased considerably when one considers that amount of gold artifacts that occur at this time at Troy II, in the tombs of Alaca Höyük and elsewhere in the Near East, particularly at the Ur Royal burials (Sazcı, 2007; Arık, 1937; Zettler and Horne, 1998).

The high demand for gold resulted in dwindling primary sources. We assume that after alluvial and placer deposits could no longer provide sufficient amounts of gold metal, the early miners were obliged to seek other sources. They were quick to understand that the gold particles they had been recuperating in the rivers initially came from a higher elevation. It did not take long for them to trace the source of gold back to its primary deposit. The gold in this case would be locked up in the higher elevated host rock, commonly in amalgamated quartz. Unlike copper mining and smelting, recuperating gold was primarily a grinding and sifting process. To free gold from its gangue it is thought that miners first ground the gold-bearing quartz (hence the presence of grinding stones at mining sites) and then used a mix of water and gold ore slurry which they poured over a sifting table that imitated the actions of a flowing river. Just like nature had done before, the heavier gold particles collected in hollows and pockets of the sifting table. Such an apparatus, called a buddle, was known in Egypt dating to ca. 2000 BC (de Jesus 1980: 84). This process could be repeated as many times as possible to arrive at a concentrate of nearly pure gold particles without its gangue. Craftsmen ultimately developed refining processes using a cementation technique to refine this concentrate even more and produce gold metal of an acceptable quality (Moorey, 1999; Craddock et al., 2005). However, gold craftsmen continued to struggle with the refining process, as it

has been shown that the gold from the Royal Cemetery at Ur varied in purity between 7 and 22 carats (Fossey, 1935).

The primary and secondary sources of gold in Turkey are still in the process of being researched, but some published work has appeared in books and journals that can serve as a convenient overview (Başaran et al., 2012, 2010; Kartalkanat et al., 2011; Kaya et al., 2012; Bayburtoğlu and Yıldırım 2008, de Jesus 1980, MTA 1970).

2.7. Silver

The history of silver is generally separate from that of gold and perhaps from copper as well. Silver's development may have come about from a less noble metal: lead. As lead does not exist in native metal form, the presence of lead at an ancient site presupposes that the lead was smelted from one of its base ores, the most common being galena. The existence of lead metal is important, as it is generally thought that early silver was discovered as a result of smelting silver-bearing lead ore (Hess et al., 1998). This notion is reinforced by the fact that most lead artifacts contain silver in percentages that are higher than what one would expect from a simple lead ore. If silver came about as a result of lead smelting, in the course of time the situation conceivably became reversed; that is, lead became a by-product of silver smelting. It is consequently valid to assume that the search for evidence of ancient silver exploitation in Anatolia is linked to lead workings of some sort, either mining or smelting operations. To a lesser extent silver is associated with the occurrences of gold (Bayburtoğlu and Yıldırım, 2008). The only silver deposit systematically investigated in Anatolia is at Bolkardağ which represents not one site but several hundred stretched over 15 kms (Yener, 1986; 2000). Other sites in Anatolia have been explored and show promise of providing valuable information on lead-silver operations in the past, such as in the areas of Gümüşköy, Kütahya (Kaptan, 1984) and Niğde (Kartalkanat et al., 2011).

In the Aegean the silver-lead mines at Agios Sostis on the island of Siphnos may have been exploited as early as Early Cycladic I (3400 – 2900 BC), but details on any smelting operations are still not available. Elsewhere in the Aegean six lead-silver deposits have been located on Cycladic islands (Gale et al., 1981), but, here again, details are still needed.

The early finds of lead artifacts may help us to determine when silver might have been first produced. A confirmed example of lead comes from Yarim Tepe I in northern Mesopotamia in the form of a bracelet made from lead wire of exceptionally pure metal. Combined with other metal finds and C-14 dates the Yarım Tepe excavators state with confidence that a copper and lead metallurgy was thriving in northern Mesopotamia at the beginning of the 6th millennium BC (Merpert et al., in Yoffee et al., 1993). The afore-mentioned bracelet presupposes that somewhere lead ore was being smelted within the sphere of Anatolian lead deposits, possibly in eastern Anatolia (de Jesus 1980). Gale et al., (1981) cite other lead artifacts dating from the 5th and 4th millennium BC from Syria and Iran and suggest that lead smelting may have begun as early as the 7th millennium BC. The key question here is: how long would it have taken lead smelters to come upon silver extraction from silver-bearing lead ores?

To address that question let us review how silver is extracted. Silver is obtained in a two-step process, first by typically smelting a silver-bearing lead ore resulting in an alloy of lead and silver metal. The silver is then extracted from the alloy using a process called cupellation that oxidizes the lead (into litharge) leaving precipitated refined silver behind (Pernicka et al., 1998; Moorey, 1999; Gale et al., 1981; de Jesus (1980). Gale et al. (1981) analyzed a silver artifact from Pre-Dynastic Egypt and claim that it is an example of cupelled silver based on its lead content (0.4 %). The artifact dates from ca. 3600 BC. This would seem to be a fairly convenient date from which to consider the routine use of cupellation. It is important to note that there are no silver or lead ore deposits in Egypt, which means that the silver found there had to come from somewhere else (Nicholson and Shaw 2009: 170). Silver artifacts from the Levant fit conveniently into this timeframe, particularly those from Byblos in Lebanon (Prag 1978: 36-8), and it is tempting to see Anatolia as the principal supplier of silver at this time, perhaps coming from operations in the Bolkardağ.

Evidence for the cupellation of silver exists elsewhere. Litharge has been found at a Fatmalı-Kalecik in eastern Anatolia and also at Habuba Kabira in Syria dating to the Late Chalcolithic period (Hess et al., 1998, Lehner and Yener, 2014). The date of the "litharge cakes" from Habuba Kabıra has been set at 3300 BC (Pernicka et al., 1998). These finds indicate that silver was being extracted from argentiferous lead ore sometime around the middle of the 4th millennium BC, a conclusion we come to despite the significant lack of silver artifacts from

archaeological excavations. Recent publications reveal that Iran has significant deposits of lead-zinc-silver ore complexes that were worked in antiquity. Moreover, litharge has been recovered at a number of Iranian sites as well, indicating the practice of cupellation as early as the first half of the 4th millennium BC (Nezafati et al., 2008). Hence, when viewing the general picture for silver production, Anatolia, the Aegean, and Iran all have the capability of producing silver metal for the antique world.

Anatolia has so far produced the earliest silver artifact, or so it seems. Its first appearance comes from the Late Chalcolithic hoard (a silver ring) at Beycesultan Level XXXIV in the Lake District dated in the literature "before 4000 BC" (Mellaart, 1970 and Stronach in Lloyd and Mellart, 1962). However, this date has been challenged, based on a C-14 date from an earlier level, and it has been suggested that the date of the silver ring and its hoard should be ca. 3000-2900 BC (Prag, 1978; Kohler et al., 1961). It is the opinion of the present authors that the C-14 date is far too late for this level. Compromises are not scientific method, but if we accept a date of ca. 3500 BC for Level XXXIV because of the nature of the hoard and associated materials, it would be close in date to the cupelled silver artifact mentioned above from Pre-Dynastic Egypt and evidence of cupellation at Habuba Kabira cited above. Based on these assumptions, the practice of cupellation can be conveniently placed at the beginning or middle of the 4th millennium BC.

Decorative silver jewelry and pieces occur at the Korucutepe graves, Alişar Höyük Level 14 and somewhat later at Arslantepe Level VIA where flat swords, mentioned above, were decorated with silver inlay (Van Loon, 1973; von der Osten, 1937; Muhly, 1997; Joukowsky, 1996; Palmieri, 1981; Hauptman et al., 2002). To this we can add the silver-copper rings from the Arslantepe "Royal" tomb (Hauptmann et al., 2002). The quantity of silver and silver-copper alloys clearly represent a well-established and sophisticated silver-producing industry, operating probably somewhere in eastern Anatolia. Arslantepe's affinities with Mesopotamia in the Late Chalcolithic - Early Bronze Age indicate not only cultural exchanges and borrowings but a possible route southward of Anatolian silver prior to the establishment of Assyrian colony trade routes to central Anatolia in the 2nd millennium BC. It is worthy to mention that excavators at Hacınebi, located on the Euphrates near Syria, state that silver was possibly produced there (Özbal et al., 1999: 60). If this were the case, the silver-bearing ore could have come from farther north in the direction of Arslantepe. It is interesting that cupellation took place in a settlement and away from the argentferous deposit, which would mean transporting the ore to a habitation site for processing.

Silver was an important commodity, not only for the crafting of decorative and precious objects but it eventually became a common currency in Mesopotamia. Its use in this way assured its continued exploitation.

3. Archaeological Field Procedures

Locating mineral deposits is not always an easy process, in the present as it was in the past. Turkey is not a small country and has a varied geology and rough topography. Setting out on foot today with the expectation of finding by chance an ore deposit or an ancient mine is not a practical or methodological strategy. Successful field prospection relies on a variety of inputs, often from local inhabitants who are familiar with the terrain and geography in their area. In many remote areas of Turkey members of the local population had been shepherds who walked over vast areas of the land with their flocks and in doing so acquired an intimate knowledge of the local geography as well as its content. Plants, rocks, and structures constitute visual landmarks when shepherds navigate across an area. They become so familiar with the landscape that they are able to notice where subtle features are somehow different from the norm, whether it is a small pile of stones, an isolated depression in the soil, or a scattering of rubble. They are aware of anomalies or changes in local geographic details just as an urban dweller might see comparative changes in the urban landscape. An archeologist's or geologist's prelude to field prospection logically starts with an interview with the local inhabitants and shares with them the purpose of the field research. When local inhabitants are aware of the types of materials we are seeking the chances of locating those materials are considerably increased.

Once a site has been identified, the first step is to acquire a general layout of the site, whether it is a somewhat localized mine or simply a scatter of slag. Major topographical features and outstanding characteristics are then noted on maps and in field notes. Mapping of the site and locations of archaeological materials, ore dumps, slag remains and relevant structures are typical of the significant features that need to be recorded. Estimated tonnage

of rubble and slag are useful in classifying the magnitude of mining and metallurgical operations. To further understand the ancient mining contexts the ore, the slag dumps and the host rock are then sampled, which is a routine procedure for the mining archaeologist, just as it is for geologists. What is non-routine for the geologist is the examination and reporting of cultural material that might be present, and we are appealing here for more information of this type. Below we outline how archaeologists might handle cultural material present at a site.

3.1. Archaeological Analytical Techniques

As we have seen, analytical and sampling procedures for archaeologists follow closely what geologist do today. Characterization of an ore body, which we might refer to as ore finger-printing, is crucial in efforts to link ancient metalwork with its source. There are many other methodologies that can be used to identify a metal artifact's origin. One is isotopic analysis — especially lead isotope analysis (LIA) – that occupies a particular importance for archeology. Isotopic composition of the ore body (a form of ore finger-printing) and artifacts provides possible linkages to provenance as well as helping us to suggest certain trading patterns of goods among ancient settlements. LIA is based on measuring ^{204}Pb, ^{206}Pb, ^{207}Pb and ^{208}Pb isotopes of lead with the aid of a mass spectrometer, especially a multi collector inductively coupled plasma mass spectrometer (hereafter; MC-ICPMS) which provides high accuracy (Stos-Gale and Gale, 2009 and references cited here, Yener et al., 1995). The basic methodology of lead isotope analysis on metals involves the application of multivariate statistics and interpretation of the scientific data. In order to explain archaeological phenomenon of metallurgy through the graphs of horizontal ^{207}Pb/^{206}Pb and vertical ^{208}Pb/ ^{206}Pb and ^{206}Pb/ ^{204}Pb it is important to understand the specific choices behind these three independent ratios of lead isotope measurements in isotope geology (Gulson 1986). Lead isotope analysis can be tricky even with professional evaluation of the isotopic ratios, since different mineralogical zones with the same age may end up with the same isotopic ratios and, likewise, the mixing of ores could provide similar values.

Ancient miners could exploit an ancient mining site for a long and continuous period as well as for a brief one. To establish a chronology of an ancient mine it is extremely important to contextualize the available archaeological data. Hence, any information lacking chronological data will not be relevant to answer the questions that archaeologists eagerly seek, namely the the date of technologies relevant to ancient mining and metallurgy. C-14 dating is based on the radioactive decay rate of C-14 to estimate the age of organic based materials. This has become a routine process for archeologists to determine the antiquity of a mine when organic materials are available, such as wooden tools, mining implements, or firewood. Though rare, these materials have been found in mining galleries.

In an ideal situation, regardless of choosing one method over the other, a cumulative group of analyses should be carried out to evaluate a site. In their excavations of ancient settlements archaeologists have at their disposal a range of prospection techniques. Among these are aerial photography, resistivity measuring, and magnetic surveying. Environmental studies play an important part in archaeological reporting, including climatology, plant life, wildlife, paleobotany, osteology, dendrochronology and geography. Ethnographical studies are proving to be increasingly important in compiling a valid history and folklore of an area. For the analysis of artifacts themselves archaeological laboratories may use a variety of techniques depending on the nature of the object: carbon dating, thermoluminescence, spectroscopic analysis, isotope studies or biochemical examinations of the organic materials. Each object has its own story to tell.

The follow-on activity of any fieldwork is heavily loaded with laboratory labor. There is a vast variety of techniques available for both archaeologists and geologists. Starting from the basic optical microscopy and scanning electron microscopy (SEM), different methodologies for different research questions on ancient technologies can be applied with the aid of a wide variety of high-tech instruments, including X-Ray Diffraction (XRD), X-Ray Fluorescence (XRF), ICP-MS, Laser Ablation (LA) technologies as well as isotope studies (Begemann et al., 1989, Henderson, 2000, Hauptmann, 2007). We will not deal with these applications here. However, the interested reader can find abundant published literature on laboratory techniques used in a post-excavation stage in the works cited here (Joukowsky 1980; Bintliff (ed.) 2006; and Renfrew and Bahn, 2012).

3.2. Analysis of Artifacts

An archaeologist is exceedingly lucky to find anything in the way of archeological materials in

mining sites. As mentioned above, occasionally wood tools and implements are found, such as shovels, ladders, and other fragments (Kaptan, 2006). Ancient mining operations were not elegant. Rudimentary materials were commonly used. Large stone hammers or rocks used for crushing ores have been identified at various sites in Anatolia in addition to multi-pitted stone mortars as well as flat saddle querns (Kaptan, 2012). Hand tools made out of various types of stones (generally locally-found stones) were used to further crush ore to various particle sizes and prepare it for smelting and/or melting.

Metallurgy can be counted as a branch of pyrotechnology and is not possible without the use of hot fires and smelting or melting equipment. Mines were exploited to obtain valuable ores which could be smelted in simple crucibles or in complex installations like metallurgical furnaces. Careful examination of a site can yield fragments of crucibles and other remains related to ore processing. In rare instances, or in case of an archaeological excavation, a furnace may be uncovered. If, in the course of their fieldwork, geologists happen to come across evidence of a furnace they should bear in mind that such remains are archaeological in nature and contain valuable information on the furnace's design and technology. Much scientific data can be gathered by sampling the furnace linings and analyzing material in and around the furnace, such as slag and ore rubble. Analyses have the potential to indicate firing temperatures and firing techniques — questions that are crucial to the understanding of ancient metallurgical processes. A geologist's awareness and reporting of cultural remains could be instrumental in helping archaeologists link mining areas with archaeological settlements or other historical landmarks.

Analytical techniques and formal procedures are not the only tools that an archaeologist uses. Archaeology is a study of the history of people, but it is also a study of the material life of people. What archeologists recover from sites are implements made by hand, and the examination and evaluation of these artifacts is as much a tactile process as it is a straight forward scientific one. The touch and feel of pottery expresses information that is often difficult to capture in scientific terms. The quality of a tool, its weight in the hand, the care with which it was designed, and the wear in certain places in the course of its use convey cultural impressions that do not lend themselves to numbers. Archaeologists seek to provide a meaningful interpretation of the artifacts and sites which goes beyond just pure scientific reporting.

It was not always possible to have a mining operation and a habitation quarter at the same site. Habitation sites, or settlements, could be associated with mining operations if the latter were not too remote. The Early Bronze Age tin mining site of Kestel at Niğde and its associated settlement Göltepe, which is 2 km away from the mining operations, illustrates a classic example of a mining site-settlement relationship. In this case, archaeologists had an opportunity to date the mining operations, determine the ore processing technologies, and acquire a glimpse of the life in a mining village (Yener, 2000; Yener and Vandiver, 1993; Yener and Özbal, 1987; Kaptan, 2012). Isolated mining operations in the remote, mountainous locations in Turkey are much harder to fit into a cultural context and associate them with known settlements, which makes an integrated view of ancient mining and metallurgy challenging.

3.3. Literature Review

Follow on research entails bibliographic documentation of the site and its immediate area. As a prelude or follow-up to fieldwork one can find mention of deposits and former workings in early surveys carried out or referenced by: De Launay, 1911; Karajian, 1920; Chaput, 1936; Kovenko, 1946; de Jesus & Kaptan, 1974; and Bachman, 2008. Complementary information may be obtained from early and more recent geological reports: Simmersbach, 1904; Sharpless, 1908; Birgi, 1951; Ryan, 1960; Gümüş, 1964; MTA, 1964, 1970, 1972; and Bernard, 1970. Early travelers' accounts can also provide locations and historical accounts of ancient mines (Marco Polo in Wright, 1892; Ainsworth, 1842; Smyth, 1845; Taylor, 1868; Sayce, 1880). Classical and later accounts can also assist in the location of past mining operations (Strabo and Pliny, in Bunbury, 1879; Hamilton and Falconer, 1854-1857). An increasing amount of practical information on the flow of ancient metalwork through trade can be determined from philological studies of ancient texts, a perfect example of which is the publication on Old Assyrian copper trade in Anatolia by Dercksen (1996).

4. Conclusions

We hope we have provided in this paper some useful insights and procedures for the examination of

ancient mining sites and why cultural observations are important. The history of mining and metallurgy in Anatolia is a fascinating topic and very much-discussed in archaeological and scientific journals. Anatolia is located geographically in the middle of polarized and prolific metallurgical developments on all sides. The Balkans to the northwest, the Aegean to the west, Cyprus to the southwest, the Levant to the south, Iran to the east, and Transcaucasia to the northeast. Each of these areas had developed vibrant and innovative metallurgical technologies in antiquity. Hopefully, with more knowledge about Anatolia's mining past and MTA's continued involvement in this area of fieldwork geologists and archaeologists will be able to clarify the role of Anatolia in the development of early mining and metallurgy in the region.

Acknowledgement

We would like to thank Cahit Sönmez for his motivation for us to contribute an article to MTA bulletin. We also would like to thank the MTA Natural History Museum team Nurcan Başaran, Selma Kaya and Devrim Erşen and the museum director Dr. Gonca Nalcıoğlu. Our sincere gratitude goes to Ergun Kaptan and Professor K. Aslıhan Yener for their numerous contributions to the study of ancient metallurgy of Anatolia which deeply inspired this article.

Received: 06.06.2014
Accepted: 09.03.2015
Pulished: December 2015

References

Ainsworth, W.F. 1842. Travels and Researches in Asia Minor, Mesopotamia, Chaldea, and Armenia. 2 Vols. London.

Arık, R.Ö. 1937. Les Fouilles d'Alaca Höyük Entreprises par la Société d'Histoire Turque. *Publication de la Société d'Histoire Turque*. Série V-No. 1. Ankara.

Bachmann, H. G. 2008. Beginnings of Archaeometallurgical Research in Turkey: A Personal Retrospect. Yalçın *et al.,* (ed.). Ancient Mining in Turkey and the Eastern Mediterranean. *Atılım University*. Ankara, 3-14.

Balkan-Altı, N., Binder, D., Gratuze, B. 2008. Göllü Dağ (Central Anatolia): Obsidian Sources, Workshops and Trade. Anatolian Metal IV, Der Anschnitt, Beiheft 21. *Deutsches Bergbau-Museum*. Bochum, 203-210.

Bamba, T. 1976. Ophiolite and Related Copper Deposits of the Ergani Mining District, Southeastern Turkey. *Maden Tetkik ve Arama Genel Müdürlüğü Dergisi,* 86, 3, 36-57.

Başaran, N., Songören, T., Dilli, R., Kesgin, Ö., Kılıçdağı, R. 2012. Sivas İli Madencilik Arkeolojisi. *MTA Tabiat Tarihi Müze Müdürlüğü*. unpublished.

Başaran, N., Vurak, A., Kaya, S. Songören, T., Yalçın, Ü., Kayadibi, Ö. 2010. Amasya İli Madencilik Arkeolojisi. *MTA Tabiat Tarihi Müze Müdürlüğü*. unpublished.

Bayburoğlu, B., Yıldırım, S. 2008. Gold and Silver in Anatolia. Anatolian Metal IV, Der Anschnitt, Beiheft 21. *Deutsches Bergbau-Museum*. Bochum, 43-53.

Begemann, F., S. Schmitt-Strecker, E. Pernicka. 1989. Isotopic Composition of Pb in Early Metal Artefacts: Results, Possibilities, Limitations. In: Hauptmann, A., Pernicka, E. and Wagner, G. A. (eds.), Old World Archaeometallurgy, Der Anshnitt Beiheft 7.*Deutsches Bergbau Museum*. Bochum, 269-278.

Bernard, J.H. 1970. Mineralogy of the polymetallic ore deposit of Piraziz, vilayet Giresun, *Maden Tetkik ve Arama Genel Müdürlüğü Dergisi*, October, 16-27.

Bilgi, Ö. 1990. Metal Objects from Ikiztepe-Turkey. Beiträge zur Allgemeinen und Vergleichenden Archäologie. Bd. 9-10. 119-219.

Bilgi, Ö. 2001. Metallurgists of the Central Black Sea Region. *Task*. Istanbul.

Bintliff, J. 2006. A Companion to Archaeology. *Blackwell Publishing*. Malden, Mass./ Oxford/Carlton, Victoria.

Birgi, S.E. 1951. Notes on the influence of the Ergani Copper Mine on the development of the metal industry in the Ancient Near East, *Jahrbuch für Kleinasiatishe Forschung*, I. 337-341.

Bunbury, E.H. 1879. Ancient Geography. *John Murray*. London.

Cauvin, M. C., A. Gourgaud, B. Gratuze, N. Arnaud, G. Poupeau, J. L. Poidevin, C. Chataigner (eds.). 1998. L'obsidienne au Proche et Moyen Orient du volcan à l'outil. *BAR International Series 7238*. Oxford.

Chaput, E. 1936. Voyages d'études géologiques et géomorphogéniques en Turquie, *Mémoires de l'Institut Français d'Archéolgie de Stamboul. no. 2*, Paris.

Chataigner, C., Poidevin, J.L., Arnaud, N.O. 1998. Turkish occurrences of obsidian and use by prehistoric peoples in the Near East from 14,000 to 6000 BP, *Journal of Volcanology and Geothermal Research,* 85, 517-537.

Craddock, P. T., Cowell, M. R., Guerra, M. F. 2005. Controlling the Composition of Gold and the Invention of Gold Refining In Lydian Anatolia, in Yalçın, Ü. (eds.), Anatolian Metal III Der Anschnitt Beiheft 18. *Deutsches Bergbau-Museum*. Bochum, 67-77.

de Jesus, P. 1977. Metallurgical Practices in Early Anatolia. *Maden Tetkik ve Arama Genel Müdürlüğü Dergisi*, 87. 49-63.

de Jesus, P. 1980. The Development of Prehistoric Mining and Metallurgy in Anatolia, International Series 74. *British Archaeological Reports*. Oxford.

de Jesus, P., Kaptan, E. 1974. The Metallurgy of the Anatolians (Türkiye madencilik tarihi için bir araştırma). *Maden Tetkik ve Arama Rapor* No. 5226, Ankara (unpublished).

De Launay, L. 1911. La Géologie et les riches minérales de l'Asie. Paris.

Dercksen, Jan G. 1996. The Old Assyrian Copper Trade in Anatolia. *Brill*: Leiden.

Di Nocera, Gian Maria. 2010. Metals and Metallurgy. Their Place in the Arslantepe Society Between the End of the 4th and Beginning of the 3rd Millennium BC. in M. Frangipane (ed.) Economic Centralisation in Formative States. The Archaeological Reconstruction of the Economic System in 4th Millennium Arslantepe. *Studi di Preistoria Orientale* Volume 3. Roma. 255-274.

Düring, B. S. 2011. The Prehistory of Asia Minor. From Complex Hunter-Gatherers to Early Urban Societies. *Cambridge University Press*. Cambridge.

Eliade, M. 1977. Forgerons et Alchimistes (Smiths and Alchemists). *Flamarion*. Paris.

Eliade, M. 1987 (1957). The Sacred and the Profane. *Harcourt, Inc*. New York.

Esin, U. 1995. Early Copper Metallurgy at the Pre-Pottery Site of Aşıklı, in Readings in Prehistory Studies presented to Halet Çambel (Halet Çambel için Prehistoria Yazıları). *Graphis yayınları*. Birinci Basım: İstanbul. 61-77.

Esin, U., Harmankaya, S. 1999. Aşıklı. In Özdoğan *et al*., (eds.), Neolithic in Turkey, *Arkeoloji ve Sanat Yayınları*. Istanbul. 115-132.

Fossey, C. 1935. L'essai et affinage de l'or chez les Babyloniens, *Revue des Etudes Sémitiques*. II-VII.

Gale, N. H., Spooner, E. T. C., Potts, P. J. 1981. The Lead and Strontium Isotope Geochemistry of Metalliferous Sediments Associated with Upper Cretaceous Ophiolitic Rocks in Cyprus, Syria, and the Sultanate of Oman. *Canadian Journal of Earth Science*, 18. 1290-1302.

Giles, D.L., Kuijpers, E. 1974. Stratiform copper deposit, Northern Turkey. *Science,*186. 823-825.

Gulson, B.L. 1986. Lead isotopes in mineral exploration. *Elsevier*. Oxford.

Gümüş, A. 1964. Contribution à l'étude géologique du secteur septentrional de Kalaba Köy-Eymir Köy (région d'Edrimit) Turquie. *Maden Tetkik ve Arama Genel Müdürlüğü Publication* No. 117. Ankara.

Gurney, O. R. 1969 (1954). The Hittites. Penguin Books. *Harmondsworth*. Middlesex.

Hamilton, C.H. and Falconer, W. (Transl.). 1854-1857. The Geography of Strabo. *H.B. Bohn*. London.

Hauptmann, A. 2000. Metal Production in the Eastern Mediterranean at the transition of the 4th/3rd millennium: Case Studies from Arslantepe, in Ü. Yalçın (ed.) Anatolıan Metal I. Der Anschnitt 13. *Bergbau Museum*. Bochum. 75-82.

Hauptmann, A. 2007 (2000). The Archaeometallurgy of Copper. The Evidence from Faynan Jordan. Springer Series. Natural Sciences in Archaeology. *Springer*. Berlin, Heidelberg, New York.

Hauptmann, A., Palmieri, A. 2000. Metal Production in the Eastern Mediterranean at the transition of the 4th/3rd millennium: Case Studies from Arslantepe, in Ü. Yalçın (eds.) Anatolian Metal I. Der Anschnitt 13. *Bergbau Museum*. Bochum. 75-82.

Healey, E. 2007. Obsidian as an indicator of inter-regional contacts and exchange: three case-studies from the Halaf period. *Anatolian Studies*, 57. 171-189.

Henderson, J. 2000. The science and archaeology of materials: An investigation of inorganic materials. *Routledge*. 24-108.

Hess, K., Hauptmann, A., Wright, H., Wallon, R. 1998. Evidence of fourth millennium BC silver production at Fatmalı-Kalecik, East Anatolia. *Der Anschnitt* Beiheft 8. 57-67.

Hodder, I. 2011. The Leopard's Tale. *Thames and Hudson*. London (2006).

Joukowsky, M. S. 1980. A Complete Manual of Field Archaeology. *Prentice-Hall*. Englewood Cliffs, New Jersey.

Joukowsky, M. S. 1996. Early Turkey. *Kendall/ Hunt Publishing Company*. Dubuque, Iowa.

Kalender, L. 2011. Oxygen, carbon and sulphur isotope studies in the Keban Pb-Zn deposits, eastern Turkey: An approach on the origin of hydrothermal fluids. Journal of African Earth Sciences. Vol. 59. 341-348.

Kaptan, E. 1977. Ancient miner's shovel discovered at Anayatak Murgul Mine, Turkey. *Maden Tetkik ve Arama Genel Müdürlüğü Dergisi*, 89. 96-100.

Kaptan, E. 1978. Ancient miner's shovels and ore carrier discovered in the Espiye- Bulancar area. *Maden Tetkik ve Arama Genel Müdürlüğü Dergisi*, 91. 99-110.

Kaptan, E. 1982. New findings on the mining history of Turkey around Tokat region. *Maden Tetkik ve Arama Genel Müdürlüğü Dergisi*, 93/94. 150-162.

Kaptan, E. 1984. New Discoveries in the Mining History of Turkey in the Neighborhood of Gümüşköy, Kütahya. *Maden Tetkik ve Arama Genel Müdürlüğü Dergisi*, 97/98. 60-67.

Kaptan, E. 1986. Ancient Mining in the Tokat Province, Anatolia: New Finds. Anatolica XIII. 19-36.

Kaptan, E. 2006. Tirebolu-Harkköy Eski Maden Galerisindeki Ahşap Su Borusu. 21. *Arkeometri Sonuçları Toplantısı*.1-8.

Kaptan, E. 2008. Tirebolu-Harşit Köprübaşı Eski Maden Galerisindeki Buluntular. *Arkeometri Sonuçları Toplantısı 22*. 31-42.

Kaptan, E. 2012. Göltepe'den Özgün Bir Buluntu. In Akyol, A. A. and Özdemir, K. (eds.), Türkiye'de Arkeometrinin Ulu Çınarları. *Homer Kitabevi ve Yayıncılık Ltd. Şti*. Istanbul. 247-252.

Karajian, H.R. 1920. Mineral Resources of Armenia and Anatolia. *Armen Technical Book Co*. New York.

Kartalkanat, A., Songören, T. 2011. Niğde ve Ankara illerinde bulunan eski işletmelerin (Pb-Zn-Cu-Au-Ag-Fe) ara raporu. *Maden Tetkik ve Arama Genel Müdürlüğü Raporu*. Ankara *(*unpublished).

Kaya, S., Başaran, N. Songören, T., Kayadibi, Ö. 2012. Tokat İli Madencilik Arkeolojisi. *MTA Tabiat Tarihi Müze Müdürlüğü*. (unpublished).

Kohler, E. L. and Ralph, E. K. 1961. ë-14 Dates for Sites in the Mediterranean [Hacılar, Beycesultan, Gordion; Greece. *Anatolian Journal of Archaeology*, 65. 357-67.

Kovenko, V. 1946. Gümüşhaciköy ve Karasu Kurşun Madenleri Kuzey Kurşun Bölgesi. *Maden Tetkik ve Arama Genel Müdürlüğü Dergisi,* 36. 234-240.

Lehner, J. W., Yener, K. A. 2014. Organization and Specialization of Early Mining and Metal Technologies in Anatolia," in Roberts, B. W. and Thornton, C. P. (eds.), Archaeometallurgy in Global Perspective. *Springer*. New York. 529-557.

Lloyd, S., Mellaart, J. 1962. Beycesultan I. The Chalcolithic and Early Bronze Age Levels. *British Institute of Archaeology at Ankara*. London.

Maddin., J. D., Muhly, T., Stech, R. 1999. Early Metalworking at Çayönü. In Hauptmann, A. *et al.,* (eds.), The Beginnings of Metallurgy. Der Anschnitt, Beiheft 9. *Deutsches Bergbau-Museum*. Bochum. 37–44.

Mellaart, J. 1970. Anatolia Before c. 4000 BC., in Edwards, I. E. S. *et al.,* (eds.). Cambridge Ancient History Vol. I, Part 1, Chapter VII (*b*). *Cambridge University Press*. Cambridge. 304-26.

Mellink, M. 1986. Troy and the Trojan War. A Symposium Held at Bryn Mawr College, October 1984. *Bryn Mawr College*. Bryn Mawr.

MTA. 1964. Iron Ore Deposits of Turkey. *Maden Tetkik ve Arama Genel Müdürlüğü Publication* No. 118. Ankara.

MTA. 1970. Arsenic, Mercury, Antimony and Gold Deposits of Turkey. *Maden Tetkik ve Arama Genel Müdürlüğü Publication* No. 129. Ankara.

MTA. 1972. Lead, Copper and Zinc Deposits of Turkey. *Maden Tetkik ve Arama Genel Müdürlüğü Publication* No. 133. Ankara.

Moorey, P. R. S. 1999. Ancient Mesopotamian materials and industries: The archaeological evidence. *Eisenbrauns*: Winona Lake, Indiana.

Muhly, J. D. 1997. Artifacts of the Neolithic, Bronze and Iron Ages. In Meyers, E. M. (eds.) The

Oxford Encyclopedia of Archaeology of the Near East. *Oxford University Press*. Oxford, Vol. 4. 5-15.

Nezafati, N., Momenzadeh, M., Pernicka, E. 2008. New insights into the ancient mining and metallurgical researches in Iran. In Yalçın, Ü. *et al.,* (eds.), Ancient Mining in Turkey and the Eastern Mediterranean. *Atılım University*. Ankara. 307-328.

Nicholson, P.T., Shaw, I. 2009. Ancient Egyptian Materials and Technology. *Cambridge University Press*: Cambridge (2000).

Özbal, H. Adriaens, M. A., Bryan E. 1999. Hacinebi Metal Production and Exchange. *Paléorient,* 25 (1). 57-65.

Özbal, H., Pehlivan N., Earl, B. 2000. Durağan ve Bakır Çay Arsenik Cevherleşmelerinin Jeolojık, Mineralojik ve Kimyasal İncelenmesi. Arkeometri Sonuçları Toplantısı Vol. 16. 22-26 Mayıs. 29-40.

Özdoğan, M. 2008. Obsidian in the Context of Near Eastern Prehistory. A Conspectus on the

Status of Research, Problems and Prospects. Anatolian Metal IV, Der Anschnitt, Beiheft 21. *Deutsches Bergbau-Museum*. Bochum. 191-201.

Öztürk, J. 1992. Metal Vessels. *Museum of Anatolian Civilizations*. Prepared by Ayşe Toker. Ankara.

Palmieri, A. 1981. Excavations at Arslantepe (Malatya). *Anatolian Studies*, 31. 101-120.

Palmieri, A., Hauptmann, A., Hess, K., Sertok, K. 1996. 1995 Archaeometallurgical Campaign at Arslantepe. Arkeometri Sonuçları Toplantısı Vol. XII, Mayıs 1996. 57-63.

Pehlivan, A.N., Alpan, T. 1986. Niğde Masifi Altın-Kalay Cevherleşmesi ve Ağır Mineral Çalışmaları Ön Raporu. *Maden Tetkik ve Arama Genel Müdürlüğü Raporu*. Ankara (unpublished).

Pernicka, E., Rehren, T., Schmitt-Strecker, S. 1998. Late Uruk silver production by cupellation at Habuba Kabira, Syria. *Metallurgica Antiqua*. Der Anschnitt, Beiheft 8. 123-134.

Prag, K. 1978. Silver in the Levant in the Fourth Millennium B.C., in Moorey, P.R. S. and Parr, P. (eds.) Archaeology in the Levant: Essays for Kathleen Kenyon. Aris and Phillips Ltd. Warminster. 36-45.

Renfrew, C., Bahn, P. 2012. Archaeology. Theories, Methods, and Practice. *Thames and Hudson*. London.

Roberts, B. W., Thornton, C. P., Pigott, V. C. 2009. Development of Metallurgy in Eurasia. *Antiquity*, 83. 1012-1022.

Rothenberg, B. 1972. Were These King Solomon's Mines?. *Stein and Day Publishers*. New York.

Ryan, C.W. 1960-1957. A Guide to the Known Minerals of Turkey. *Maden Tetkik ve Arama Genel Müdürlüğü*. Ankara.

Sagona, A., Zimansky, P. 2009. Ancient Turkey. *Routledge*. New York.

Sayce, A. H. 1880. Notes from a Journey in the Troad and Lydia. *Journal of Hellenic Studies,* I. 75-93.

Sazcı, G. 2007. The Treasures of Troya. *Aygaz*. Istanbul.

Schmidt, K. 2007 (2006). A Stone Age Sanctuary in South-Eastern Anatolia. *Ex Oriente*. Berlin.

Shcoop, U. D. 1999. Aspects of Early Metal Use in Neolithic Mesopotamia. In Hauptmann, A. *et al.,* (eds.), The Beginnings of Metallurgy. Der Anschnitt, Beiheft 9. *Deutsches Bergbau-Museum*. Bochum. 31-36.

Simmersbach, B. 1904. Die mützbaren mineralischen Bodenschätze in der kleinasiatisch

Türkei. *Zeitschrift für das Berg-, Hütten-, und Salienwesen*, 52. 515-557.

Smyth, W.W. 1845. Geological features of the country round the mines of the Taurus in the pashalic of Diarbakr, described from observations made in the year 1843, *Proceedings of the Geological Society,* Vol. I. 330-340.

Stein, G. 2001. Indigenous Social Complexity at Hacınebi (Turkey) and the Organization of Uruk Colonial Contact. In Rothman (ed.) Uruk Mesopotamia & Its Neighbors. *School of American Research Press*. Santa Fe. 265-305.

Stein, G., Bernbeck, R., Coursey, C., McMahon, A., Miller, N. F., Mısır, A., Nicola, J., Pittman, H., Pollick, S., Wright, H. 1996. Uruk Colonies and Anatolian Communities: An Interim Report on the 1992-3 Excavations at Hacınebi, Turkey. American Journal of Archaeology, Vol 100, No. 2. 205-260.

Stos-Gale, Z. A., Gale, N. H. 2009. Metal provenancing using isotopes and the Oxford archeological lead isotope database, *Archeological and Anthropological Science*, 1. 195-213.

Stöllner, T., Gambaschidze, I., Hauptmann, A. 2008. The Earliest Gold Mining of the Ancient World? Research on an Early Bronze Age Gold Mine in Georgia. In Yalçın, Ü. *et al.,* (eds.), Ancient Mining in Turkey and the Eastern Mediterranean. *Atılım University*. Ankara. 271-288.

Taylor, J.G. 1868. Journal of a Tour in Armenia, Kurdistan, and Upper Mesopotamia. *Journal of the Royal Geographic Society*, 38. 281-361.

Tolstikov, V., Treister, M. 1996. The Gold of Troy. Searching for Homer's Fabled City. *Abrams, Inc. Publishers*. New York.

Tylecote, R. F. 1976. A History of Metallurgy. *The Metals Society*. London.

Van Loon, M. 1973. The Excavations at Korucutepe, Turkey, 1968-70. Preliminary Report. *Journal of Near Eastern Studies*, XXXII, 4. 357-444.

von der Osten, H.H. 1937. The Alishar Hüyük. *Oriental Institute Publications* XXVIII. Chicago.

Wagner, G. and Öztunalı, A. 2000. Prehistoric Copper Sources in Turkey. Anatolian Metal I, Der Anschnitt, Beiheft 13. *Deutsches Bergbau-Museum*. Bochum. 31-67.

Wright, G. A. 1969. Obsidian Analyses and Prehistoric Near Eastern Trade: 7000 to 3500 BC. Museum of Anthropology. *University of Michigan*. Ann Arbor.

Wright, T. 1892. The Travels of Marco Polo. *George Bell and Sons*. York / New York.

Yalçın, Ü. 2000. Anfänge der Metallverwendung in Anatolien. Anatolian Metal I, Der Anschnitt, Beiheft 13. *Deutsches Bergbau-Museum*. Bochum. 17-30.

Yalçın, Ü., İpek, Ö. 2012. Derekütüğün Tarihöncesi Maden İşletmeleri. Çorum Kazı ve Araştırmalar Sempozyumu. *İl Kültür ve Turizm Müdürlüğü*. Çorum, Vol. 2. Yayın No. 6. 11-31.

Yener, K. A., Jett, P., Adriaens, M. 1995. Silver and copper artifacts from ancient Anatolia. *Journal of Metals*, 47 (5). 70-72.

Yener, A. 1986. The Archaeometry of Silver in Anatolia: The Bolkardağ Mining District. *American Journal of Archaeology,* 90 (4). 469-472.

Yener, K. A. 2000. The Domestication of Metals. *Brill*. Leiden/ Boston/ Köln.

Yener, K. A., Kulakoğlu, F., Yazgan, E., Kontani, R. Lehner, J. W., Dardeniz, G., Öztürk, G., Johnson, M., Hacar, A. 2015. New tin mines and production sites near Kültepe in Turkey: a third-millennium BC highland production model, *Antiquity*, Vol.89, No. 345. 596-612. doi:10.15184/aqy.2015.30 .

Yener, K. A., Özbal, H. 1987. Tin in the Turkish Taurus mountains: the Bolkardağ mining district. *Antiquity* Vol. 61, No. 232. 220-26.

Yener, K. A., Vandiver, P. 1993. Tin Processing at Göltepe, an Early Bronze Age Site in Anatolia. *American Journal of Archaeology*, 97, 207-238.

Yener, K. A., Jett, P., Adriaens, M. 1995. Silver and copper artifacts from ancient Anatolia. *Journal of Metals*, 47 (5). 70-72.

Yıldırım, T. 2006. An Early Bronze Age Cemetery at Resuloğlu near Ururludağ, Çorum. A Preliminary Report of the Archaeological Work Carried Out Between the Years 2003-5. *Anatolia Antiqua* Vol. XIV. 1-14.

Yıldırım, T. 2010. Resuloğlu Kazısı ve Anadolu Arkeolojisi'ne Katkıları. Çorum Kazı ve Araştırmalar Sempozyumu. *İl Kültür ve Turizm Müdürlüğü*. Çorum, Vol. 1. Yayın No. 5. 11-28.

Yoffee, N., Jeffery J. C. (eds.). 1993. Early States in the Evolution of Mesopotamian Civilization. Soviet Excavations in Northern Iraq. *The University of Arizona Press*. Tucson and London.

Zettler, R. L., Horne, L. 1998. Treasures from the Royal Tombs of Ur. *University of Pennsylvania Museum*. Philadelphia.

Zwicker, U. 1977. Investigations On the Extractive Metallurgy of Cu/Sb/As Ore and Excavated Smelting Prtoducts from Norşuntepe (Keban) on the Upper Euphrates (3500-2800 B.C.) in Oddy (ed.) Aspects of Early Metallurgy. *Historical Metallurgy Society* and *British Museum Research Laboratory*. London. 13-26.

Bull. Min. Res. Exp. (2015) 151: 247-258

Bulletin of the
Mineral Research and Exploration

http://bulletin.mta.gov.tr

EVALUATION OF ASBESTOS EXPOSURE IN DUMANLI VILLAGE (ÇANAKKALE-TURKEY) FROM A MEDICAL GEOLOGY VIEWPOINT: AN INTER-DISCIPLINARY STUDY

Erdinç YİĞİTBAŞ[a*], Arzu MİRİCİ[b], Uğur GÖNLÜGÜR[b], Coşkun BAKAR[c], İsmail Onur TUNÇ[d], Fırat ŞENGÜN[a] and Özgür IŞIKOĞLU[a]

[a] *Çanakkale Onsekiz Mart Üniversitesi (ÇOMÜ), Mühendislik Fakültesi Jeoloji Mühendisliği Bölümü, Çanakkale*
[b] *ÇOMÜ Tıp Fakültesi, Göğüs Hastalıkları Anabilim Dalı, Çanakkale*
[c] *ÇOMÜ Tıp Fakültesi Halk Sağlığı Anabilim Dalı, Çanakkale*
[d] *Ardahan Üniversitesi, İnsani Bilimler ve Edebiyat Fakültesi, Coğrafya Bölümü, Ardahan*

Keywords:
Medical geology, Biga Peninsula, Turkey, Asbestos, Mesothelioma

ABSTRACT

Biga Peninsula has many varied and interesting medical geologic problems, as well as being rich in natural geological resources. Mainly these problems are natural radioactivity, mineral dust, metal/mineral contamination in drinking water, acid rock/mine drainage, and problems related to geothermal and drinking water. With this view exposure to asbestos was surveyed and the results of this survey were evaluated by earth scientists and medical doctors. This inter-disciplinary study was done in Dumanlı village (Çanakkale-Turkey) in the Biga Peninsula, NW Turkey. Studies have been carried out in earth sciences and the health sciences simultaneously. The asbestiform minerals around Dumanlı village are contained in sheared serpentinites which occur as tectonic slices and lenses within Çamlıca metamorphics. These tectonic slices and lenses are bounded by strike-slip faults and probably obtained their final tectonic positions in a transpressional regime during late Cretaceous-early Eocene time. Asbestiform minerals occur within stretching-shear zones in the strike-slip system. Petrographic and mineralogic indications show that the asbestiform minerals are clinochrysotile, lizardite, antigorite and actinolite. In parallel with earth science studies; verbal autopsy, pulmonary function tests and radiological examination studies were carried out. A significant correlation between asbestos exposure and radiographic pathology was identified in the region and it was understood that the duration of exposure in these cases varies from 23-80 years.

1. Introduction

In addition to the rich geological structure of the Biga Peninsula, it is an area with open potential for varied and interesting problems related to medical geology (Figure 1). The main medical geology problems may be listed as natural radioactivity, mineral dust, metal/mineral pollution of drinking water, acid rock/mine drainage, and problems related to geothermal and drinking water, etc. Though there are individual studies on these topics in the region (Örgün et al., 2007; 2008; Baba et al., 2008; Save, et al., 2009; Baba and Gündüz, 2010; Bakar et al., 2009*a*, *b*; 2010; Bundschuh, et al., 2013; Atabey, 2008; 2013; Yiğitbaş et al., 2012), as in all of Turkey, in-depth research on the topic of medical geology is required in the Biga Peninsula. Working from this perspective, asbestos exposure was investigated in a sample area in the Biga Peninsula and preliminary results were evaluated by medical and earth science experts.

Asbestos is a group of fibrous silicate minerals widely used in the past due to their insulation, electrical properties, and resistance to high voltage, chemicals and heat. Its use in more than 3000 trade

* *Corresponding author: Erdinç Yiğitbaş, erdinc.yigitbas@gmail.com*

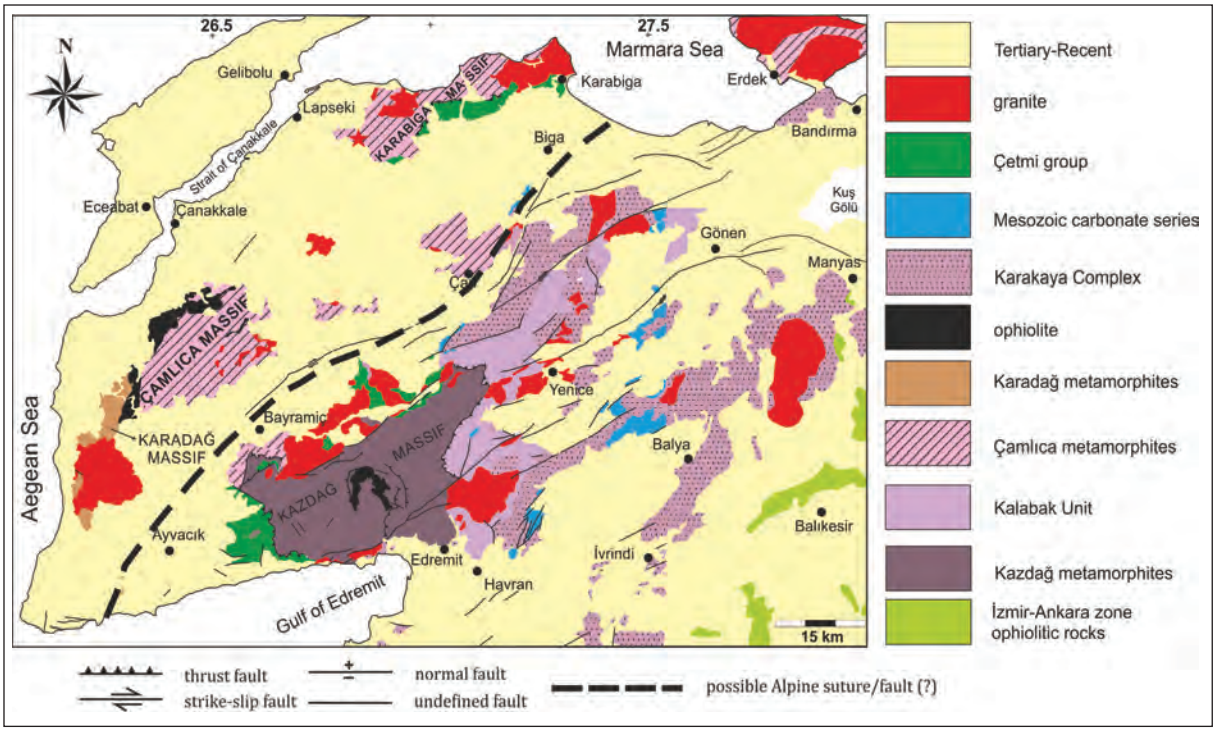

Figure 1- Simplified geological map of the Biga Peninsula (after Tunç et al. 2012). Small red colored star on the map shows the location of Dumanlı village, where this research performed.

products in sectors such as roofing materials, floor tiles, concrete pipes and textiles led to widespread distribution in areas open to the public and in the residential environment.

Asbestiform minerals used for industry may be collected into two main groups. These are 1) serpentine asbestos (chrysotile, lizardite, antigorite) and 2) amphibole asbestos (crocidolite, amosite, anthophyllite, tremolite, actinolite). The main reasons asbestiform minerals were commonly used in industry was their resistance to heat and burning, high voltage resistance, very low conductivity of heat and electricity, durability-stability in various chemicals, resistance to friction, wear and burning, and easy ability to take any form when used with a variety of materials (İrkeç, 1990 and references there in).

Chrysotile, in the serpentine group, was widely used in many industrial applications throughout the world as a trade asbestos type. It is very flexible, undulated and has high heat resistance. However it is not durable in acid environments. According to estimates more than 95% of asbestos used in trade in the United States of America was chrysotile asbestos; the majority from Canadian and Russian mines (Craighead, et al., 1982; Selikoff and Lee, 1978). When the results of many studies on the topic of asbestos to date are examined, serious negative effects on health occur due to asbestos minerals. The possibility of asbestos being related to lung diseases entered the agenda at the beginning of the 1900s. Pancoast, et al. (1918) investigated the results of asbestos and dust inhalation on the lungs nearly one hundred years ago with radiological methods. Cooke (1924) stated that a woman working for 18 years in an asbestos factory developed pulmonary fibrosis. The relationship between asbestos and malignant mesothelioma was described in a study by Wagner (1960) of mine workers in the 1960s. A short time later, exposure outside of occupation and regionally increased mesothelioma incidence was determined in a study by Newhouse and Thompson (1965) and later after Selikoff (1968) published his paper, the topic of occupational and environmental potential health problems of asbestos in countries producing asbestos began to be debated and research on the topic began to be published. Inhalation of asbestos either environmentally or occupationally causes pulmonary fibrosis (asbestosis), lung cancer, pleural or peritoneal mesothelioma and pleural changes (thickening, plaques, effusion) (Barış et al., 1979; Niklinski, et al., 2004; Doğan, 2002; Emri and Demir, 2004).

Lung and bronchial cancers are among the most common and deadly cancers in the world. According to World Health Organization data, one of the leading cancers resulting in death globally is lung cancer (WHO, 2013) and of all lung cancers it is estimated that 4-12% develop as a result of asbestos exposure (Henderson et al., 2004). Diffuse malignant mesothelioma (DMM) is a deadly tumor in mesothelial cells or mesenchymal cells under the pleura, pericardium or peritonea (Chretien et al., 1985). The relationship between DMM developing in pleura and peritoneum and asbestos exposure is clear. However apart from exposure to asbestos, idiopathic and other accepted reasons for DMM include fibrous minerals such as erionite, radiation, pleural scarring and SV 40 virus (Craighead et al., 1982).

While the prevalence of pleural mesothelioma is generally high among those exposed to asbestos the prevalence of peritoneal mesothelioma is lower. Peritoneal mesothelioma cases are mainly seen in those subject to intense exposure to asbestos. The latent period of mesothelioma caused by asbestos may be 30 years or more and exposure to low concentrations may increase latency; however death is seen within 1 year of diagnosis (Emri and Demir, 2004; Şenyiğit, et al., 2000; Lanphear and Buncher, 1992; Browne, 1994). Unlike lung cancer it has no link to cigarette intake and has be proven to develop as a result of asbestos inhalation. The results of experimental studies have shown that all types of asbestos may cause lung cancer and mesothelioma (Doğan, 2002; Suzuki and Yuen, 2002; Roggli, et al., 1993; Churg, 1988; Berman, et al., 1995; Dufresne, et al., 1995). However there is an important difference between amphibole and chrysotile asbestos in terms of potential to form malignant mesothelioma. While amphibole asbestos, such as amosite, crocidolite and tremolite, has greatest potential, chrysotile has lower potential.

Long and thin asbestos fibers are more fibrogenic than short asbestos fibers (<5 μm) as shown experimentally in both intratracheal and respiration studies (Adamson and Bowden, 1987; Lemaire, 1985; Davis and Jones, 1988; Davis, et al., 1986). In chronic respiration experiments using short chrysotile fibers in rodents, no fibrotic lesions were observed (Platek, et al., 1985). The potential for cell proliferation, damage, injury and alveolar macrophages releasing oxidants is greater with exposure to long fibers (Adamson and Bowden, 1987; Donaldson, 1989; Mossman, et al., 1989). The carcinogenicity of the asbestos fibers is affected by the diameter of the fibers. Fibers with diameter less than 0.25 μm are extremely carcinogenic (Doğan, 2002; Berman, et al., 1995).

Natural release of asbestiform minerals from source rocks occurs due to degradation and erosion processes and is concentrated by surface erosion. In seasonally dry climates fibers dry and become more susceptible to erosion. Destruction of rocks containing asbestos deposits for aims such as agriculture, mining, settlement, etc. is an important and risky anthropogenic factor increasing the rate of release of asbestos from source rocks (Derbyshire, 2005).

Turkey, among many countries with large asbestos reserves globally, has the highest prevalence of endemic pulmonary diseases related to asbestos (Karakoca, et al., 1997). The reason for this high prevalence is the high population living in rural areas and regional geologic characteristics. In Turkey mafic-ultramafic rocks and greenschists, commonly containing asbestiform minerals, are seen in virtually every outcrop. As a result the health of organisms living in areas where rocks containing asbestiform minerals outcrop may be negatively affected. Respiration of asbestos fibers in Turkey results from the use of loose rocks containing talc and asbestos, known as "white soil" by local people, as material for lime, plaster, roofing and ground stabilization (Atabey, 2009). Leading the list of wrong applications as reason for the most intense intake of asbestos by respiratory pathways, is the use of serpentinite containing asbestos in rural areas as aggregate for stabilized roads. Unfortunately this great error continues to date commonly in many regions of the country (Atabey, 2009; Yiğitbaş, et al., 2013).

Mineralogical analysis of plaster used in dwellings in rural areas has found mostly tremolite in addition to chrysotile and anthophyllite asbestos (Doğan and Emri, 2000). However in the Cappadocia region in Central Anatolia with widespread outcrops of volcanic-volcaniclastic rocks, the plaster material in houses in the rural area has been found to contain fibrous zeolite (erionite) (Baris, et al., 1987; Atabey, 2007). Experimental studies have shown that erionite has 300-800 times more carcinogenic potential compared to chrysotile and when administered intrapleurally is 100-150 times more potent than crocidolite (Carthew, et al., 1992). In fact in the Cappadocia region a variety of research showing that some important health problems result from fibrous

zeolite minerals has been completed (Barış, et al., 1987; Atabey, 2007). All this research shows that important health problems may be caused by respiration of asbestiform minerals in the natural geologic environment.

The inter-disciplinary study forming the topic of this paper was completed in Dumanlı and part of Çamyurt villages in Lapseki county of Çanakkale province in the northwest of Biga Peninsula in northwest Anatolia. After 4 cases of mesothelioma were discovered in this region in 2011 by Çanakkale Provincial Health Directorate, a study group of earth scientists from Çanakkale Onsekiz Mart University (ÇOMU) Geological Engineering Department, experts from ÇOMU Medical Faculty Chest Diseases and Public Health departments together with experts from Çanakkale Provincial Health Directorate was founded and research began. Studies continued simultaneously and in parallel in earth sciences and health sciences. Earth science studies began by obtaining a geological map to determine whether any asbestos deposits were in Dumanlı and Çamyurt villages and surrounding areas. Determined asbestos outcrops were marked on the geology maps and samples were taken. Samples were evaluated with SEM and XRD analyses after petrographic determination. The conditions and mechanism of formation of asbestos veins found was modeled within a regional tectonic framework, to determine similar formations within the region and to predict the areas for future asbestos exposure research. With this aim, in parallel to the earth science study, verbal autopsy studies to determine the causes of death in the region over the past 5 years were carried out by public health experts. Chest disease experts completed and evaluated respiratory function tests and radiological examinations of 139 people currently living in the area.

2. Geographic and Geological Setting

The Biga Peninsula is geographically bounded to the north by the Sea of Marmara and the Dardanelles, to the west by the Aegean Sea and to the South by the Gulf of Edremit. The Peninsula is linked to the Anatolian Peninsula to the east between Edremit-Akçay. The Dumanlı and Çamyurt villages in this study are in the northern part of the Biga Peninsula, which is the most northwestern part of Anatolia (Figure 1). Dumanlı and Çamyurt villages are 25 and 19 km from Lapseki, the county seat. According to data from the Turkish State Meteorology Service the climate of Çanakkale, the site of the study area, is between steppe-humid according to De Martonne's climate classification with an aridity index of 13.48 (MGM, 2014*a*). According to the Turkish State Meteorology Service Wind Atlas the study area is within the windiest region in Turkey (MGM, 2014*b*). This situation naturally causes asbestiform minerals to mix more with the air and be inhaled more by organisms.

The Biga Peninsula geologically is formed of a variety of tectonic units representing continental units of the Sakarya continent along with oceanic assemblages with different sources and very old ages (Yiğitbaş, et al., 2009; Şengün, et al., 2011; Tunç, et al., 2012).

Two metamorphic belts outcrop along a northeast-southwest trend in the Biga Peninsula. The southern belt is represented by the Kazdağ Massif, while the northern belt is represented by the Çamlıca, Karabiga and Karadağ Massifs. It has been proposed that a suture zone exists covered by thick Tertiary-Quaternary volcano-sedimentary rocks between these two different metamorphic belts. This suture zone is evaluated as the remains of the Paleotethys or Intra-Pontide Ocean (Okay, et al., 1991; 2008; Okay and Göncüoğlu, 2004; Duru, et al., 2004; 2012). Another interpretation is that the zone in the region, evaluated as an Alpine oceanic suture, is a strike-slip fault zone called the West Pontide Fault Zone (Yiğitbaş et al., 1998; Elmas and Yiğitbaş, 2001; 2005; Elmas et al., 2011).

Dumanlı village and surrounding areas, where this research was centered, was mapped in detailed fashion by the geological team (Figure 2). The village of Dumanlı is located on the Çamlıca Metamorphics, formed of mainly micaschist, gneiss and calcschist lithologies. On Figure 2 the distribution of this unit in the study area is shown by the brown color. These metamorphic rocks, especially in the north and west sections of the village, contain severely sheared serpentinite slices. On Figure 2 the serpentinite is shown by the green color. The contacts between the serpentinite slices and metamorphic rocks are close to vertical (60-90°) inclined to the northwest or southeast (Figure 3A). Horizontal or close-to-horizontal fault lines have developed on the contact faces (Figure 3B). These observations, together with the outcrop pattern of the serpentinites, show that the contact between the serpentinites and Çamlıca metamorphics formed due to the effect of right-lateral strike slip tectonics.

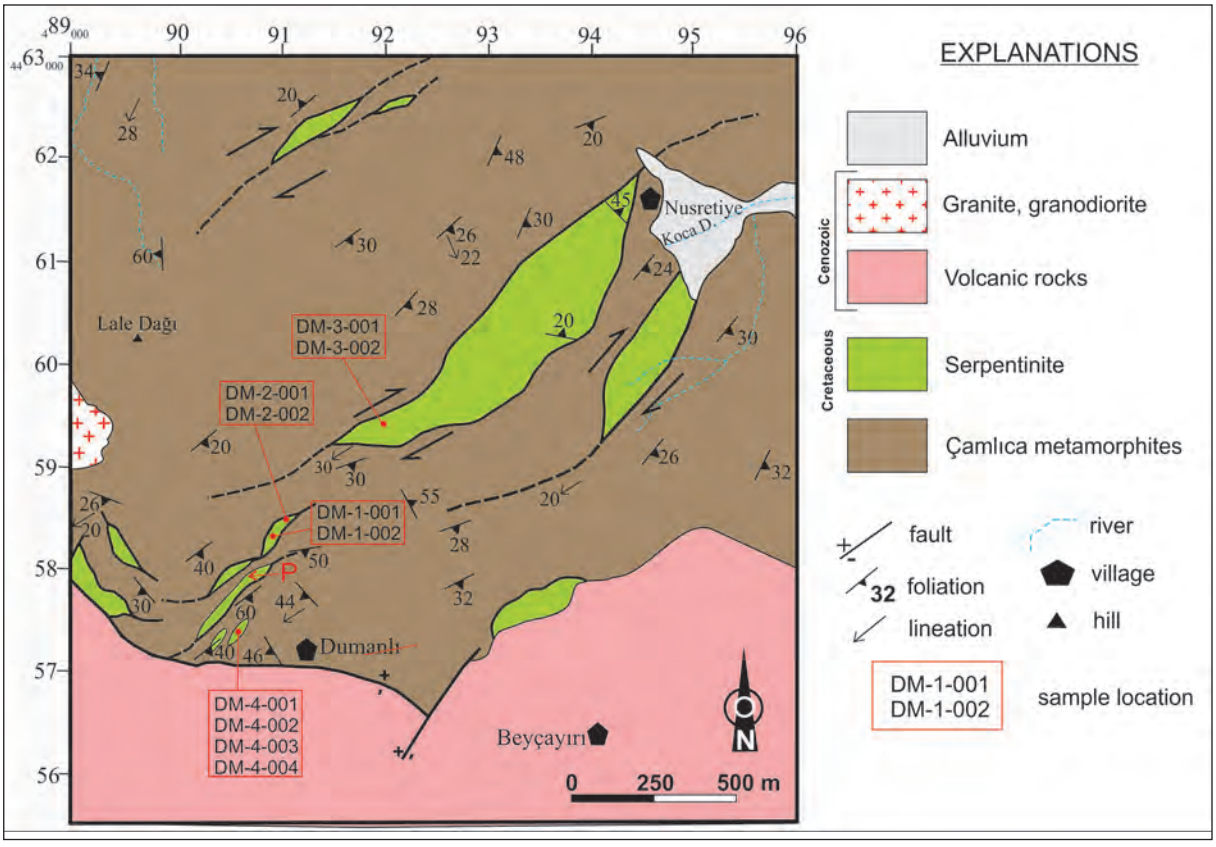

Figure 2- Geological map of Dumanlı village and surroundings. The locations of the photos in Figure 3A and 3B, are shown as "P" on the map.

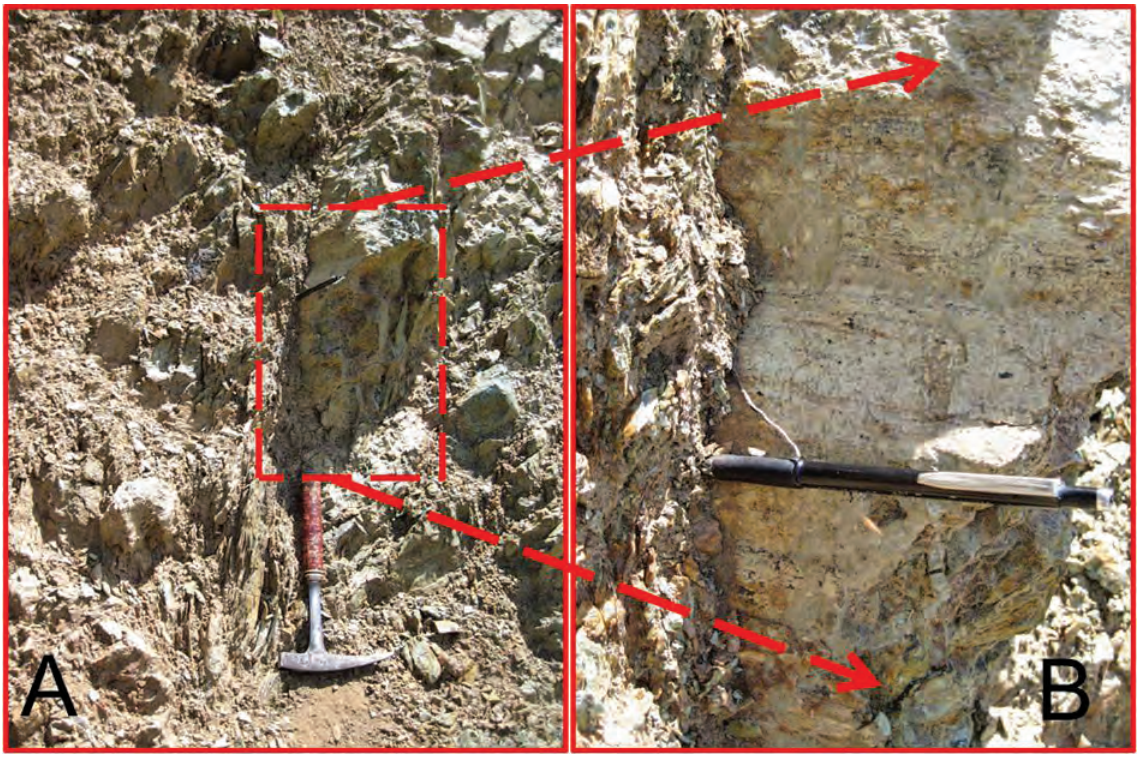

Figure 3- A) Contact relationship between the metamorphic rocks and the serpantinite lenses in the Çamlıca metamorphites. B) Close look to the contact plane.

In the mapping area the foliation in the Çamlıca metamorphics, although inclined at different angles, generally trends NE (Figure 2). The measured lineations have a dip of at most 20-30° southwest. Thus the lineation and foliation data of the metamorphic rocks, together with the contact with the contained serpentinites, show they were shaped by a right-lateral strike slip shear zone with reverse component. The asbestiform minerals developed in cracks and fractures perpendicular to the instant stress direction along the main shear zone, in T-fractures at right angles to the main shear zone in this strike-slip right-lateral shear zone (Figure 4).

In areas close to Dumanlı village there are 4 different locations where the village residents are exposed to asbestos in a variety of ways. These are locations DM-1: Tepecik (Figure 5A), DM-2: Odacıkyanı, DM-3: Kıygınaçığı and DM-4: Değirmenalanı (Figure 5B). Of these, DM-1: Tepecik and DM-4: Değirmenalanı, in particular, contain very well-developed asbestos deposits and are the closed locations to the village. DM-1: Tepecik location is about 1 km to the north of the village, while DM-4: Değirmenyanı location is 750 m west of the village. These locations were observed due to excavations for aims such as roadworks, etc. Due to the region's morphological structure and plant cover it is possible that there are other undiscovered asbestos locations.

Observations in the field have clearly shown the presence of asbestos minerals in serpentinite outcrops surrounding Dumanlı village (Figures 6A and 6B). Easily identified by the naked eye, these minerals were petrographically identified using a polarizing microscope (Figures 6C and 6D).

The presence of asbestos deposits in serpentinite outcrops in Dumanlı village and surrounding area clearly identified in the field and with a polarizing microscope were also analyzed with SEM and XRD. The SEM (Scanning Electron Microscope) and XRD (X-ray Diffractometer) results are illustrated in figures 7A and 7B. The fibrous habit, white crystals

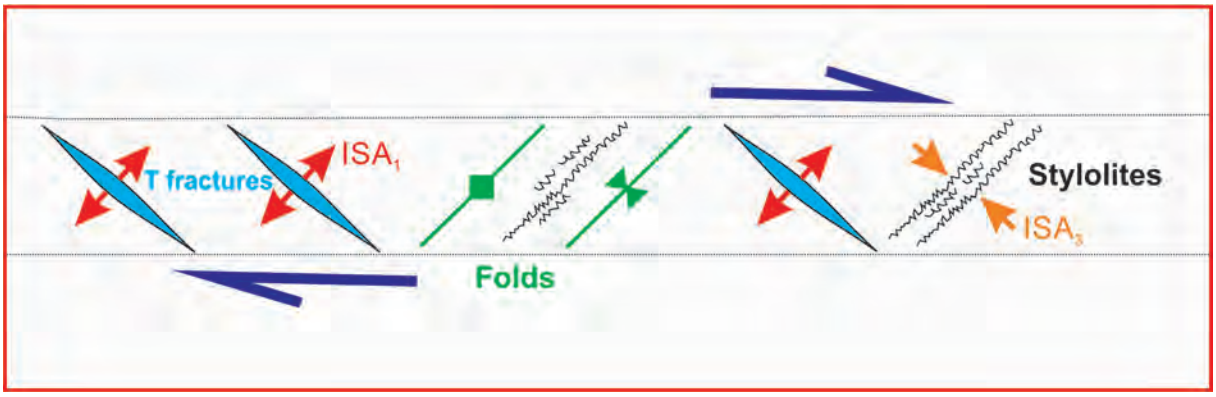

Figure 4- The model showing the T fractures, which bearing asbestiform minerals and some other important small-scale structures in a dextral strike-slip shear zone. ISA: Instanteous Stretching Axes. (For further information please see Fossen 2011).

Figure 5- A) Photos showing the DM-1 Tepecik location, located in the north of Dumanlı village and B) DM-4 Değirmenyanı location, located in the west of Dumanlı village.

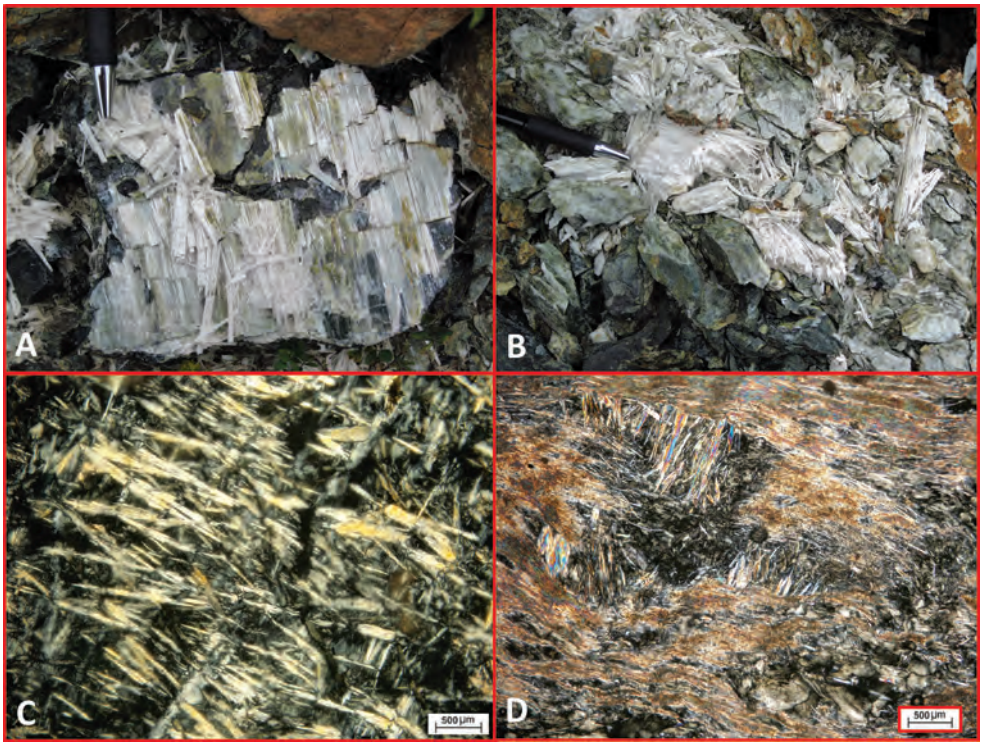

Figure 6- A,B) Asbestos fibers can be seen clearly within the serpentinites in the DM-1 Tepecik location. C,D) Micrograph photos of asbestos-bearing serpentinites, under polarized microscope. Chrysotile-asbestos minerals can be seen clearly in both two micrograph photos.

observed under SEM were determined to be antigorite ($Mg_3Si_2O_5OH_4$), lizardite $(Mg,Al)_3(Si,Fe)_2\ OH_4$ and clinochrysotile ($Mg_3Si_2O_5\ OH_4$) according to XRD results.

In the area near Çamyurt village, where one mesothelioma case was observed in 2011, no serpentinite outcrops were found. The village is located on Cenozoic volcanic-volcaniclastic rocks. As a result, just as Çamyurt village underwent detailed medical scanning similar to Dumanlı village, the volcanic rocks outcropping in the village and surrounding region were sampled and investigated. In four of the samples taken the presence of zeolite was identified under polarizing microscope (Figure 8). These were sent for SEM and XRD analysis to determine the minerals and within the volcanic/volcaniclastic rock samples hoylandite ($CaAl_2Si_7O_{18}H_2O$), Al chabazite ($NaAlSi_4O_{20}$), quartz (SiO_2) and microcline ($KAlSi_3O_8$) minerals were identified, though erionite was not found. However Çamyurt village requires more detailed investigation of both medical scanning and and the region's volcanic rocks, as a significant portion of the houses in Çamyurt village are constructed of this type of rock.

3. Medical Geology

The rocks containing asbestos outcropping at DM-1 and DM-4 locations were severely destroyed due to road works or other human requirements (Figure 5), thus just as the surficial contact of asbestiform minerals with the air increased, the grain/crystal sizes were reduced. Additionally the material taken from these locations were used as aggregate for roads in both Dumanlı village and surrounding villages, thus the asbestos was spread over a much wider area, causing an increase in the exposure area.

In parallel and simultaneous to the earth science studies in the study area a variety of studies were completed by Public Health and Chest Disease experts. At meetings the people of the village were informed and scanning was completed with a mobile microfilm device. Microfilm was taken for 133 people with macrofilm taken for 7 people. After microfilm scanning on 2nd and 3rd visits to the village, verbal autopsy was completed and respiratory function tests were carried out for the adult population. The death information in Dumanlı village between the years 2007 and 2011 was collected by

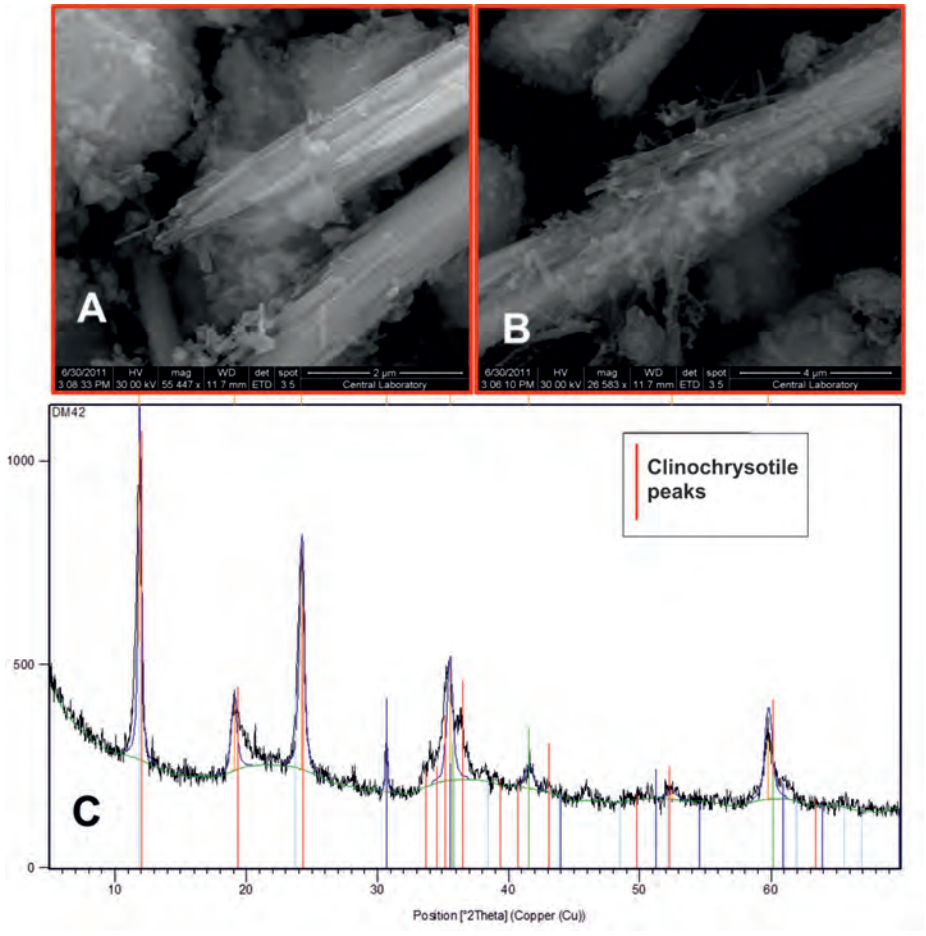

Figure 7- A and B) SEM images are showing the asbestiform crystals in the serpentinite sample. C) Clinochrysotile peaks of serpentinite sample, determined by XRD

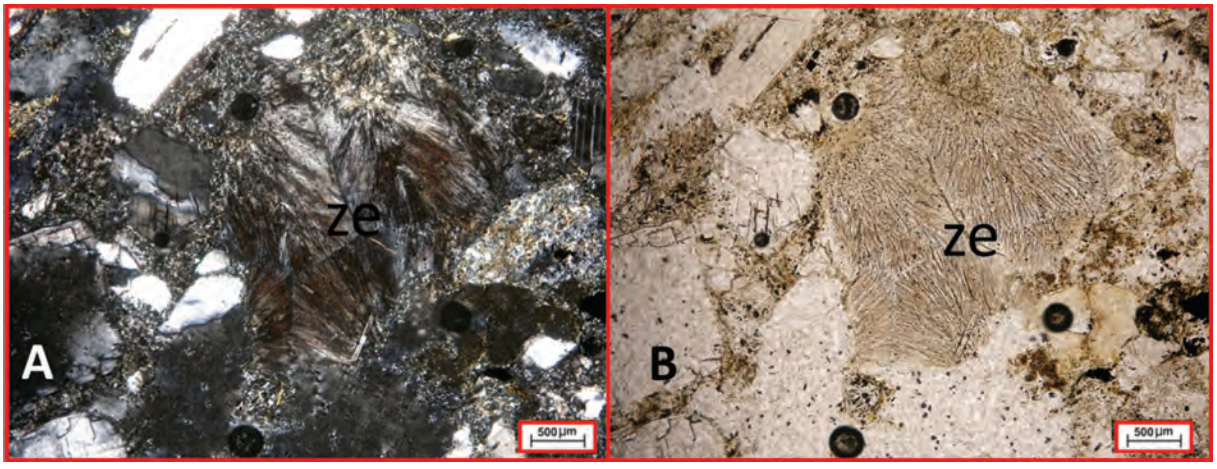

Figure 8- Micrograph photos of zeolite bearing tuffs in Çamyurt village and surroundings. A) Polarized light and B) Natural ligth images. Radial crystal agregas, which are shown as "ze" are most probably zeolite minerals.

verbal autopsy method, by public health expert C. Bakar. The verbal autopsy form, which was developed by The World Health Organization (WHO) and used in the World Health Survey (WHS) and the National Burden of Disease and Cost Effectiveness studies, used to be able to perform the verbal autopsy research (Ministry of Healt of Turkey, 2003). This form consists of mostly close-ended questions. The basic principle is to determine the cause of death based on the current disease before the person's death and their specific symptoms. Thus; sex, place of death and cause of death data of the deaths in the last five years period in Dumanlı village, is given in table 1, as a result of verbal autopsy studies.

The results indicated that the village with population of 216 (116 men and 100 women) had 9 deaths in the previous five years (2007-2011). Two of the deaths were due to lung cancer, one due to larynx cancer and one due to mesothelioma. The other four deaths were linked to other diseases. In 139 people living in the area 30 had pleural calcification, while 4 had pleural thickening. There was a significant correlation between radiological pathology and asbestos exposure found, with exposure duration varying between 23-80 years in these cases.

Table 1- The death data of the last five years (from 2007 to 2011) in Dumanlı village (Çanakkale)

AVERAGE OF AGE	**74,7±10,9 Year**
SEX	**NUMBER OF DEATHS**
Male	6
Female	**3**
PLACE OF DEATH	
At home	5
At Çanakkale Public Hospital	3
Çanakkale Onsekiz Mart University Hospital	1
CAUSE OF DEATH	
Lung cancer	2
Larynx cancer	1
Mesothelioma	1
Gastric cancer	1
Cerebrovascular diseases	1
Alzheimer and hip fracture	1
Myocardial infarction	1
Unknown	1
Total	9

4. Conclusion and Recommendations

a) Surrounding Dumanlı village, linked to Lapseki county in Çanakkale, deposits of asbestiform minerals with varying scales are found. These deposits developed along T fractures during emplacement of serpentinite lenses within Early Paleozoic Çamlıca metamorphics in the region.

b) Serpentinites containing asbestiform crystals have been used and continue to be used widely and without control for a variety of aims. It was possible to determine a positive correlation between radiological pathology and exposure to asbestos. Informing people living in areas determined to be exposed to asbestiform minerals, and those in the study area, of the harm caused by interaction with asbestos may reduce the interaction with asbestos.

c) When the mechanism and geological causes of formation of asbestiform minerals in the Biga Peninsula are investigated, it is strongly possible that other areas may face similar problems. As a result medical problems that may be caused by exposure to asbestiform minerals in the region should be carefully monitored.

d) Exposure still continues. As the material containing asbestiform minerals was used as aggregate for road works, the effective exposure area has expanded and the surface area/grain size rates have increased, increasing the asbestos concentration of exposure. To prevent the increase in effective area and severity due to using material containing asbestiform minerals for road works and similar human needs, local and central government should be informed about the topic.

e) When the geological characteristics of the region are considered in the Biga Peninsula, apart from asbestos, similar research into erionite exposure and the effects of this exposure on human and environmental health are necessary.

The types, physical and chemical characteristics of the asbestiform minerals exposed in the region

should be determined in detail and compared with the type, physical and chemical characteristics of fibers in lung tissue of people who become sick as a result of asbestos exposure.

Acknowledgement

This research was carried out with the contribution of Çanakkale Provincial Health Directorate. As a result we thank the Provincial Health Deputy Directors of the period, Dr. Şahin Kahyaoğlu and Dr. Ümmühan Kahyaoğlu. The geological maps and the tectonic model in this paper were produced during the study of the project named as TUBITAK-ÇAYDAG 110Y281.

Received: 19.09.2014
Accepted: 28.11.2014
Published: December 2015

References

Adamson, I. Y. R., Bowden, D. H. 1987. Response of mouse lungto crocidolite asbestos: II. Pulmonary fibrosis after long fibres, *The Journal of Pathology*, 152, 109–117.

Atabey, E. 2007. Aksaray-Nevşehir Arası Eriyonit Minerali İçeren Volkanik Tüflerin Dağılımı ve Akciğer Kanseri (Mezotelyoma) İlişkisi. *60 Türkiye Jeoloji Kurultayı Bildiri Özleri Kitabı*, 289-292.

Atabey, E. 2008. Doğal radyasyon kaynakları: Çanakkale ili Ayvacık ve Geyikli örneği. *Uluslararası Katılımlı Tıbbi Jeoloji Kitabı*, 85-88. YMGV Yayını ISBN:978-975-7946-33-5, Ankara.

Atabey, E. 2009. Türkiye'de asbest, eriyonit, kuvars ve diğer mineral tozları ve etkileri. *Maden Tetkik ve Arama Genel Müdürlüğü, Yerbilimleri ve Kültür Serisi*-6, 188s.

Atabey, E. 2013. Türkiye'de Doğal Radyasyon Kaynakları ve Tıbbi Jeolojik Etkileri. *Maden Tetkik ve Arama Genel Müdürlüğü, Yerbilimleri ve Kültür Serisi*-10, 158s.

Baba, A., Save, D., Sülün S., Gündüz, O., Bozcu, M., Gürdal, G., Özcan, H. 2008. Çan Kömür Havzasındaki Madencilik Faaliyetlerinin Tıbbı Jeoloji Açısından Değerlendirilmesi, *TÜBİTAK, ÇAYDAG-106Y041*.

Baba, A., Gündüz, O. 2010. Effect of alteration zones on water quality: A Case Study from Biga Peninsula, Turkey. *Archives of Environmental Contamination and Toxicology*, 58, 3, 499-513.

Bakar, C., Baba, A., Karaman, H. I. O., Şengünalp, F. 2009*a*. The neurotoxic effect of high aluminum levels in drinking water in Kirazlı area (Çanakkale, Turkey), *12th World Congress on Public Health*, 27 April- 1 May 2009, İstanbul, Turkey.

Bakar, C., Karaman, H. I. O., Baba, A., Şengünalp, F. 2009*b*. Vitamin B12 levels and neurological findings in three villages in Çanakkale region, Turkey, *12th World Congress on Public Health*, 27 April- 1 May 2009, İstanbul, Turkey.

Bakar, C., Karaman, H. I. O., Baba, A., Şengünalp, F. 2010. Effect of high Aluminium concentration in water resources on human health, Case Study: Biga Peninsula, Northwest Part of Turkey. *Archives of Environmental Contamination and Toxicology*, 58, 4, 935-944.

Barış, Y. I., Artvinli, M., Şahin A. A. 1979. Environmental mesothelioma in Turkey, *Annals of the New York Academy of Sciences*, 330, 423-432.

Barış, Y. I., Simanato, I., Artvinli, M., Pooley, F., Saracci, R., Skidmoore J., Wagner, C. 1987. Epidemiological and environmental evidence of health effect of exposure to erionite fibers: a four-year study in the Cappadocian region of Turkey. *International Journal of Cancer*, 39:10-17.

Berman, D. W., Crump, K. S., Chatfield, E. J., Davis, J. M. G., Jones, A.D. 1995. The sizes, shapes, and mineralogy of asbestos structures that induce lung tumors or mesothelioma in AF/HAN rats following inhalation. *Risk Analysis*, 15, 181-195.

Browne, K. 1994. Asbestos-related disorders. In: Parkes WR, editor. *Occupational lung disorders*. 3rd ed. Oxford: Butterworth-Heinemann, 411–504.

Bundschuh, J., Maity, J. P., Nath, B., Baba, A., Gündüz, O., Kulp, T.R., Jean, J.S., Kar, S., Tseng, Y., Bhattacharya, P., Chen C.Y. 2013. Naturally occurring arsenic in terrestrial geothermal systems of western Anatolia, Turkey: potential role in contamination of freshwater resources. *Journal of Hazardous Materials*, 262, 951-959.

Carthew P., Hill, R. J., Edwards R.E., Lee P. N. 1992. Intrapleural administration of fibers induces mesothelioma in rats in the same relative order of hazards as occurs in man after exposure. *Human and Experimental Toxicology*, 11, 530-534.

Chretien, J., Bignon, J., Hirsch, A. 1985. The Pleure in Health and Disease. Dekker, New York.

Churg, A. 1988. Chrysotile, tremolite, and malignant mesothelioma in man. *Chest*, 93, 621-628.

Cooke, W.E. 1924. Fibrosis of the lungs due to the inhalation of asbestos dust. *British Medical Journal*, 2, 147.

Craighead, J. E., Abraham, J. L., Churg, A., Green, F. H., Kleinerman, J., Pratt, P. C., Seemayer, T. A., Vallyathan, V., Weill, H. 1982. The pathology of asbestos-associated diseases of the lungs and pleural cavities: diagnostic criteria and proposed grading schema. Report of the Pneumoconiosis Committee of the College of American Pathologists and the National Institute for Occupational Safety and Health. *Archives of Pathology and Laboratory Medicine*, 06, 541–596.

Davis, J., Jones, M. A. 1988. Comparison of the pathogenicity oflong and short fibres of chrysotile asbestos in rats. *British Journal of Experimental Pathology*.

69, 717–737.

Davis, J. M. G., Addison, J., Bolton, R. E., Donaldson, K., Jones, A. D., Smith, T. 1986. The pathogenicity of long vs. short fibre samples of amosite asbestos administered to rats by inhalation and intraperitoneal injection. *British Journal of Experimental Pathology,* 67, 415–430.

Derbyshire, E. 2005. Natural Aerosolic Mineral Dusts and Human Health. *Essentials of Medical Geology Impacts of the Natural Environment on Public Health*, Edt. in chef O. Selinus, Chapter 18, 462-469.

Doğan, M. 2002. Environmental pulmonary health problems related to mineral dusts: Examples from central Anatolia, Turkey, *Environmental Geology*, 41, 571-578.

Doğan, M., Emri, S. 2000. Environmental health problems related to mineral dust in Ankara and Eskişehir, Turkey. *Yerbilimleri*, 22, 149-161.

Donaldson, K., Brown, G. M., Brown, D. M., Bolton, R. E., Davis, J.M.G. 1989. Inflammation generating potential of long and short fibre amosite asbestos samples. *British Journal of Industrial Medicine,* 46, 271–276.

Dufresne, A., Harrigan, M., Masse, S., Begin, R. 1995. Fibers in lung tissues of mesothelioma cases among miners and millers of the township of asbestos, Quebec. *American Journal of Industrial Medicine*, 27, 581-592.

Duru, M., Pehlivan, Ş., Şentürk, Y., Yavaş, F., Kar, H. 2004. New results on the lithostratigraphy of the Kazdağ Massif in northwest Turkey. *Turkish Journal of Earth Sciences*, 13, 177–186.

Duru, M., Pehlivan, Ş., Okay, A. İ., Şentürk, Y., Kar, H. 2012. Biga Yarımadası'nın Tersiyer Öncesi Jeolojisi. In: Biga Yarımadası'nın genel ve Ekonomik Jeolojisi. *Maden Tetkik ve Arama Genel Müdürlüğü, özel yayın Serisi* No.28, s.7-74.

Elmas, A., Yiğitbaş, E. 2001. Ophiolite emplacement by strike-slip tectonics between the Pontide Zone and the Sakarya Zone in northwestern Anatolia, Turkey. *International Journal of Earth Science-Geologische Rundschau*, 90, 257-269.

Elmas, A., Yiğitbaş, E. 2005. Comment on "Tectonic evolution of the Intra-Pontide sutur zone in the Armutlu Peninsula, NW Turkey" by Robertson and Ustaömer, *Tectonophysics*, 405, 213-221.

Elmas, A., Yılmaz, İ., Yiğitbaş, E., Ullrich, T. 2011. A Late Jurassic–Early Cretaceous metamorphic core complex, Strandja Massif, NW Turkey. *International Journal of Earth Science-Geologische Rundschau*, 100, 1251-1263.

Emri, S., Demir, A.U. 2004. Malignant pleural mesothelioma in Turkey, 2000-2002, *Lung Cancer*,45, 17-20.

Fossen, H. 2011. Structural Geology. Cambridge University Press, 463p.

Henderson, D. W., Rodelsperger, K., Woitowitz, H.J., Leigh, J. 2004. After Helsinki: a multidisciplinary review of the relationship between asbestos exposure and lung cancer, with emphasis on studies published during 1997-2004. *Pathology*, 36, 6, 517-550.

İrkeç, T. 1990. Asbest. *Maden Tetkik ve Arama Genel Müdürlüğü Eğitim Serisi*, No:31, Ankara.

Karakoca, Y., Emri, S., Cangir, A.K., Barış, Y.I. 1997. Environmental pleural plaques due to asbestos and fibrous zeolite exposure in Turkey. *Indoor Built Environment*, 6 100-105.

Lanphear, B. P., Buncher, C. R. 1992. Latent period for malignant mesothelioma of occupational origin. *Journal of Occupational Medicine*, 34, 718-721.

Lemaire, I. 1985. An assessment of the fibrogenic potential of veryshort 4-T30 chrysotile by intratracheal instillation in rats. *Environmental Research*, 36, 314–326.

MGM. 2014*a*. http://www.mgm.gov.tr/FILES/iklim/iklim_siniflandirmalari.pdf

MGM. 2014*b*. http://www.mgm.gov.tr/arastirma/yenilenebilir-enerji.aspx?s= ruzgaratlasi

Mossman, B. T., Hansen, K., Marsh, J., Brew, M. E., Hills, S., Bergeron, M., Petruska, J. 1989. Mechanisms of fiber-induced superoxide (O_2) release from alveolar macrophages (AM) and induction of superoxide dismutase (SOD) in the lungs of rats inhaling crocidolite. *In* Bignon, J. Peto, J. and Saracci, R. (eds). *Mineral Fibres in the NonOccupational Environment*. I.A.R.C. Publication No. 90, Lyon, France, 81–97.

Newhouse, M. L., Thompson, H. 1965. Mesothelioma of pleural and peritoneum following exposure to asbestos in the London area. *British Journal of Industrial Medicine*, 22, pp. 261-268.

Niklinski, J., Niklinska, W., Chyczewska, E., Laudanski, J., Naumnik, W., Chyczewski, L., Pluygers, E. 2004. The epidemiology of asbestos-related diseases. *Lung Cancer*, 45, 7-15.

Okay, A.I., Siyako, M., Bürkan K. A. 1991. Geology and tectonic evolution of the Biga Peninsula, northwest Turkey. *Bulletin of the Technical University of İstanbul*, 44, 191–255.

Okay, A. I., Göncüoğlu, M. C. 2004. Karakaya Complex: a review of data and concepts. *Turkish Journal of Earth Sciences*, 13, 77-95.

Okay, A. I., Bozkurt, E., Satır, M., Yiğitbaş, E., Crowley, Q.G., Shang, C.K. 2008. Defining the southern margin of Avalonia in the Pontides: geochronological data from the Late Proterozoic and Ordovician granitoids from NW Turkey. *Tectonophysics*, 461, 252-264.

Örgün, Y., Altınsoy, N., Şahin, S. Y., Güngör, Y., Gültekin, A.H., Karahan, G., Karacık, Z. 2007. Natural and anthropogenic radionuclides in rocks and beach sands from Ezine region (Çanakkale), Western Anatolia, Turkey. *Applied Radiation Isotope*, 65, 739-747.

Örgün, Y., Altınsoy, N., Şahin, S. Y., Ataksoy, B., Çelebi, N. 2008. A Study Of Indoor Radon Levels In Rural Dwellıngs Of Ezine (Çanakkale, Turkey) Usıng Solid-State Nuclear Track Detectors. *Radiation Pro-*

tection Dosimetry, 131, 379-384.

Pancoast, H. K., Miller, T. G., Landis, H.R.M. 1918. A roentgenologic study of the effects of dusts inhalation upon the lungs. *American Journal of Roentgenology*, 5, 3,129-138.

Platek, S., Groth, D., Ulrich, C., Stettler, L., Finnell, M., Stoll, M. 1985. Chronic inhalation of short asbestos fibres. *Fundamental and Applied Toxicology*, 5, 327–340.

Roggli, V.L., Pratt, P. C., Brody, A. R. 1993. Asbestos fiber type in malignant mesothelioma: an analytical scanning electron microscopic study of 94 cases. *American Journal of Industrial Medicine*, 23, 605-614.

Sağlık Bakanlığı, 2003. Başkent Üniversitesi Ulusal Hastalık Yükü ve Maliyet Etkililik Projesi: Sözel Otopsi Araştırması Ara Raporu. Sağlık Bakanlığı Refik Saydam Hıfzısıhha Merkezi Başkanlığı Hıfzısıhha Mektebi Müdürlüğü, 24 Aralık 2003, Ankara, 166s.

Save, D., Köse, O. Ö., Sülün, S., Şengünalp, F., Gündüz, O., Baba, A. 2009. The blood and hair heavy metal levels in two districts with different groundwater concentrations. *12th World Congress on Public Health*, 27 April- 1 May 2009, İstanbul, Turkey.

Selikoff, I. 1968. Occurence of pleural calcification among asbestos insulation workers. *Annals of the New York Academy of Sciences*, 132, 351-364.

Selikoff, I. J., Lee, D.H. K. 1978. Asbestos and disease. New York: Academic Press.

Suzuki, Y., Yuen, S. R. 2002. Asbestos fibers contributing to the induction of human malignant mesothelioma. *Annals of the New York Academy of Sciences*, 982, 160-176.

Şengün, F., Yiğitbaş, E., Tunç, İ. O. 2011. Geology and Tectonic Emplacement of Eclogite and Blueschists, Biga Peninsula, Northwest Turkey. *Turkish Journal of Earth Sciences*, 20, 273–285.

Şenyiğit, A., Babayiğit, C., Gökırmak, M., Topçu, F., Asan, E., Coşkunsel, M., Işık, R., Ertem, M. 2000. Incidence of malignant pleural mesothelioma due to environmental asbestos fiber exposure in the southeasth of Turkey. *Respiration*, 67, 610-614.

Tunç, İ. O., Yiğitbaş, E., Şengün, F., Wazeck, J., Hofmann, M., Linnemann, U. 2012. U-Pb Zircon Geochronology of Northern Metamorphic Massifs in the Biga Peninsula (NW Anatolia-Turkey): New data and a new approach to understand the tectonostratigraphy of the region. *Geodinamica Acta*. 25, 3-4, 202-225.

Wagner, J. C., Sleggs, C. A., Marchand, P. 1960. Diffuse pleural mesothelioma and asbestos exposure in the North Western Cape Province. *British Journal of Industrial Medicine*, 17, 260-271.

WHO, 2013. Cancer fact sheet. Facts Sheet number; 297 (January 2013). Available at http://www.who.int/mediacentre/factsheets/fs297/en/index.html Accessed: December 19, 2013.

Yiğitbaş, E., Elmas, A., Yılmaz Y. 1998. Transcurrent faulted boundary of Rhodope-Pontide continental fragment in Northwest Turkey: Western Pontide Fault. *Earthsciences Symposium of 75th The Anniversary of Turkish Republic*, Maden Tetkik ve Arama Genel Müdürlüğü, Ankara, 38.

Yiğitbaş, E., Şengün, F., Tunç, İ. O. 2009. KB Anadolu'da Mesozoyik yaşlı kaya topluluklarının dağılımı ve korelasyonu. *TÜBİTAK-ÇAYDAG Proje No.108Y232*, 118s.

Yiğitbaş, E., Mirici, A., Gönlügür, U., Bakar, C., Şengün, F., Tunç, İ.O., Kahyaoğlu, Ş., Kahyaoğlu, Ü. 2012. The effect of asbestos exposure on the Mesothelioma disease: A case study on Dumanlı Village-Lapseki-Çanakkale. *International Earth Science Colloquium on the Aegean Region 2012 (IESCA-2012)*, 1-5 October 2012 DEU, Abstracts, 191.

Yiğitbaş, E., Mirici, A., Gönlügür, U., Bakar, C., Şengün, F., Tunç, İ.O., Işıkoğlu, Ö., Kahyaoğlu, Ş., Kahyaoğlu, Ü. 2013. Biga Yarımadasının medikal jeoloji sorunlarına genel bir bakış ve bölgede asbest maruziyeti sorunu. *2.Tıbbi Jeoloji Çalıştayı Bildiriler Kitabı*, Yalçın M.G. ve Baba, A. (eds), Akdeniz Üniversitesi, 203-206.

Bull. Min. Res. Exp. (2015) 151: 259-268

Bulletin of the
Mineral Research and Exploration

http://dergi.bulletin.gov.tr

GEOLOGICAL HERITAGE AND FRAMEWORK LIST OF THE GEOSITES IN TURKEY

Nizamettin KAZANCI[a,b*], Fuat ŞAROĞLU[b] and Yaşar SULUDERE[b]

[a] *Ankara University, Faculty of Engineering, Department of Geological Engineering, 06100, Tandoğan/Ankara*
[b] *Turkish Association for Conservation of the Geological Heritage, PK 10, Maltepe/Ankara*

Keywords:
Framework List,
Geological Heritage,
Geoconservation,
Geosites in Turkey

ABSTRACT

Geosites and the special type of geosite called geological heritage are tangible materials such as rocks, fossils, minerals, sedimentary sequences, or structures about which there are results and/or documents of significant events in the geological history. A Framework List deciphers the geological events of the past without mentioning the localities or results. Ideally, there is only one Framework List for every country. The Framework List for Turkey proposed by this study includes 85 titles (frame) in 10 categories. The Stratigraphic and Volcanic-Metamorphic-Sedimentary Petrology categories are the richest for the Frameworks; however they two already contain the majority of the geosites in the JEMIRKO inventory, which contains a total of 815 geosites.

1. Introduction

Even public awareness is not so much, there have been significant changes in research and education on earth sciences since the beginning of the twenty-first century. It seems that problems in finding jobs, unemployment, and excessive disturbance of the natural environment are the leading causes of these changes. It is believed that the second half of the twentieth century will be remembered as the time interval of "heavy destruction of nature"; however, it is also a fact that it is the source of some positive developments at present. Due to the environmental problems resulting from rapid industrialization and overconsumption of natural resources after World War II, IUCN (International Union for Conservation of Nature founded in 1948) started drawing up the the Endangered Species list and the Red List (founded in 1964) as measures to be taken for environmental protection. Although UNESCO's International Convention on Conservation of Cultural and Natural Heritage adopted in 1972 and its application the World Heritage List attracted a great deal of attention, it is not possible to say that they decreased the destruction of nature. Besides, most of these measures had the aim of protecting cultural and biological properties and conserving wetlands, but ignored the earth and non-living properties. The Digne Declaration was issued with the joint signatures of 30 countries in 1991 as an uprising of earth scientists against the increasing destruction of nature. This declaration, which consists of 13 articles, can be qualified as a milestone for geological conservation. Here, it was emphasized that the inorganic part of the globe also urgently needs conservation as it is non-renewable and non-substitutable; it was underlined that some specific rocks, fossils, minerals, sedimentary sequences, geological structures, textures, and so on act as documents about the history of the earth; and the concepts of "geological site – geosite" and "geological heritage" were verbalized for the first time. It is possible to say that the Digne Declaration is a sign of earth scientists' awakening (Barettino et al., 1999 *a, b*).

* *Corresponding author: Nizamettin Kazancı, nkazanci@ankara.edu.tr*

Geosite: Natural assets such as specific assemblages of rocks, fossils, or minerals, sedimentary sequences, landforms, geological structures, and so on that reveal an event, process, or occurrence during the evolution of the Earth (Wimbledon, 1996; ProGEO Group, 1998; www.progeo.se). It is like a scientific document about the area.

Geological heritage (geo-heritage): A unique geosite whose disappearance causes the loss of information or a geological document about the relevant area. Some are under threat of extinction (Wimbledon, 1996; Kazancı, 2010).

Although the Digne Declaration has great importance for the improvement and development of studies on geological heritage and geological conservation, it is not the first attempt at the subject. The idea of protecting natural assets that have visual and scientific value can be dated back to 350 years ago, with the efforts made regarding Baumann Cave and Giant Causeway (Burek and Prosser, 2008; Doughty, 2008; Erikstad, 2008). However, these first experiences did not make a lasting impact. At the beginning of the 1970s, similar problems were expressed frequently in Turkey, but they have been forgotten in the years since then (e.g. Ketin, 1970; Arpat, 1976; Arpat and Güner, 1976; Öngür, 1976; Özdemir et al., 1986). The main attempt that resulted in the current developments was the establishment of ProGEO (European Association for the Conservation of Geological Heritage) in 1995. At about the same time, efforts to survey, record, and protect geosites were started in England (Wimbledon et al., 1995, Wimbledon, 1996). The question has been how and by whom geological heritages, of which there are a great number and many types (grouped into ten titles), would be protected (ProGeo Group, 1998). Another important discussion in the same context was held on whether or not to open these geosites to touristic visits. In the same period, the great interest in the World Heritage sites helped conservation of the sites besides causing an economic return to the local people, so that reality generated the ideas of geoparks and geotourism. The Lesbos Geopark (established by Dr N. Zourus) has a special role in that development which was started as the Museum for Fossil Trees in Crete in 1994. The museum declared itself to be a "geopark" in 2000, announced that it had created the Geoparks Network, and led the establishment of the European Geopark Network-EGN (2000) and UNESCO Global Geopark Network-GGN (2002), which are esteemed institutions today. In spite of big efforts on public awareness, concerns about the abuse of science and destruction of nature for commercial purposes will always exist (e.g. Dowling and Newsome, 2005). ProGEO, a well-matured, international non-governmental organization, publishes guidebooks and magazines to set an understanding of geological heritage and geoconservation all over the world (e.g. Wimbledon and Smith-Meyers, 2012) and issues a highly appreciated magazine (Geoheritage). The similar efforts are carried out by the Turkish Association for Conservation of the Geological Heritage, JEMİRKO (2000) (Kazancı, 2010; Kazancı et al., 2012).

Geological heritage and/or geosites are riches of a country and their existence adds value to a region. Their determination (or recognition) requires a high level of geological knowledge and expertise. It is expected that they should be researched, protected, and used for the benefit of society. In this paper, the Framework List (FL) application, which plays a role in the scientific evaluation of the geosites, is presented first and then an FL for Turkey is proposed (Figures 1 and 2).

2. Determination of Geological Heritage

As stated insistently by ProGEO, one of the considerable dangers for geosites, geological heritage, and geological conservation is the attribution of different meanings to these terms. In order to avoid deterioration, we should remain faithful to the original definitions created by ProGEO (Kazancı, 2010; www.progeo.se). The suggestion and acceptance of a geosite depend on rules. Everywhere, only people who have an education in the relevant field can make suggest a natural formation as a geosite or as geological heritage. ProGEO has described the geosites under 10 different categories or groups covering all areas of the earth sciences (ProGeo Group, 1998). These are: a) stratigraphic, b) palaeoenvironmental, c) volcanic-metamorphic-sedimentary petrology, textures and structures, events and provinces, d) mineralogical, economical, e) structural, f) geomorphologıcal features, erosional and depositional processes, landforms and landscapes, g) astroblems, h) continental or oceanic scale geological features, plate relationships, i) submarine, and j) historical and cultural geosites (www.progeo.se).

JEMİRKO has Advisory Committees, each consisting of three persons for every category. According to the method that was adopted during the

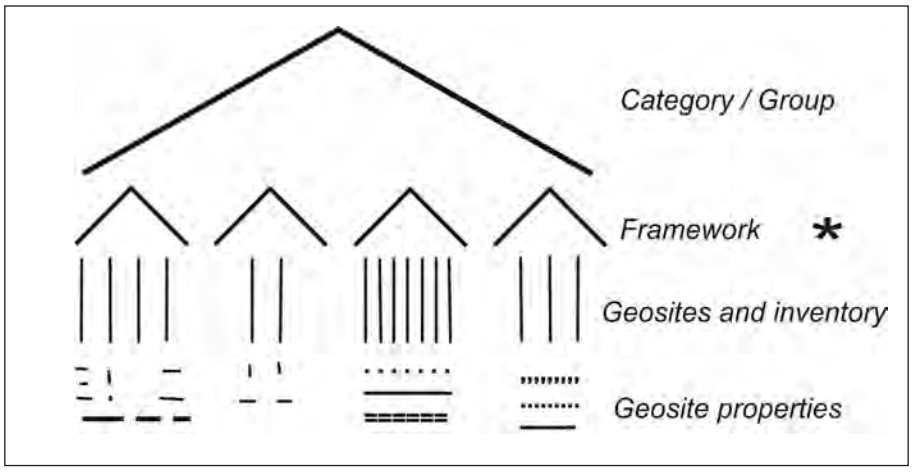

Figure 1- Schematic expression of the conceptual relations between category, frame, FL, geosite, and geosite list (inventory)* suggested by this study.

General Assembly Meeting in 2002 and approved at the meeting of ProGEO Southeastern Europe Countries Working Group (WG1) held in the same year in Turkey, the suggestions of geosite made by earth scientists using the application form are examined by the Advisory Committee of the relevant category. If necessary, members of the committee visit the site. Suggestions that are found suitable by the Advisory Committee are submitted to JEMİRKO's General Assembly. They are discussed there and eventually added to the geosite list. Suggestions that are not approved by the committee are not discussed again. Currently, there are a total of 815 geosites, some of which are in the process of approval (490), in the JEMİRKO inventory. The names and addresses of these geosites are not announced in order to protect them from plunder by collectors.

3. Geosite Framework List

As stated above, geosites are gathered under ten main groups or categories. However, this distinction is far from being informative and is not convenient for detailed analyses; it is only a rough grouping used for further steps. For example, Lake Van, Lake Beyşehir, Lake Eğirdir, Salt Lake, Lake Akşehir, Acıgöl, and Lake Eber are all under the Group f, together with canyons and rivers. The common characteristics of the different lakes is that they are all "wetlands" (a frame). It is obvious that they are considerably different from some other geosites within the same category (*Group f)*, such as the Gilindire Cave, Ballıca Cave, Çatak Canyon, of Köprülü Canyon, according to their features. Collecting the latter under another framework (canyon-valley) makes much more sense (Figure 1). Similarly, Hasandağ, Mount Erciyes, Mount Ağrı, and Karacadağ are different geosites in "*Group c*", but putting them in the framework of "stratovolcano" provides convenience in many aspects. In some cases, however, the geosites under the same category and even having similar origins can be evaluated in different frameworks (Figures 3–5).

In brief, the application of the FL is an attempt to assemble the geosites that are under the same group or category of a country list according to their common geological features (Brilha et al., 2005). The first notable benefit of this application is the fact that a large number of geosites can be classified under the same framework (encouraging the geosite description); the second one is to create an opportunity to compare geosites internationally. For instance, if there are 10 geosites in a country under the "C-T boundary framework", thanks to them the geological changes and palaeogeography of the Cretaceous–Tertiary transition can be compared with each other and also with those of different countries. Such a national and international correlation could provide new possibilities for further interpretation. In short, the FL makes it easier to conduct earth science researches and even encourages them through geosites within the same country and between different countries. So as similar studies spread over the neighbouring countries and gradually all over the world, the Frameworks and their lists (FL) should be similar at least with regard to their main categories (Figure 2). ProGEO calls on every country to create its own FL. It is important to form the FLs in a way

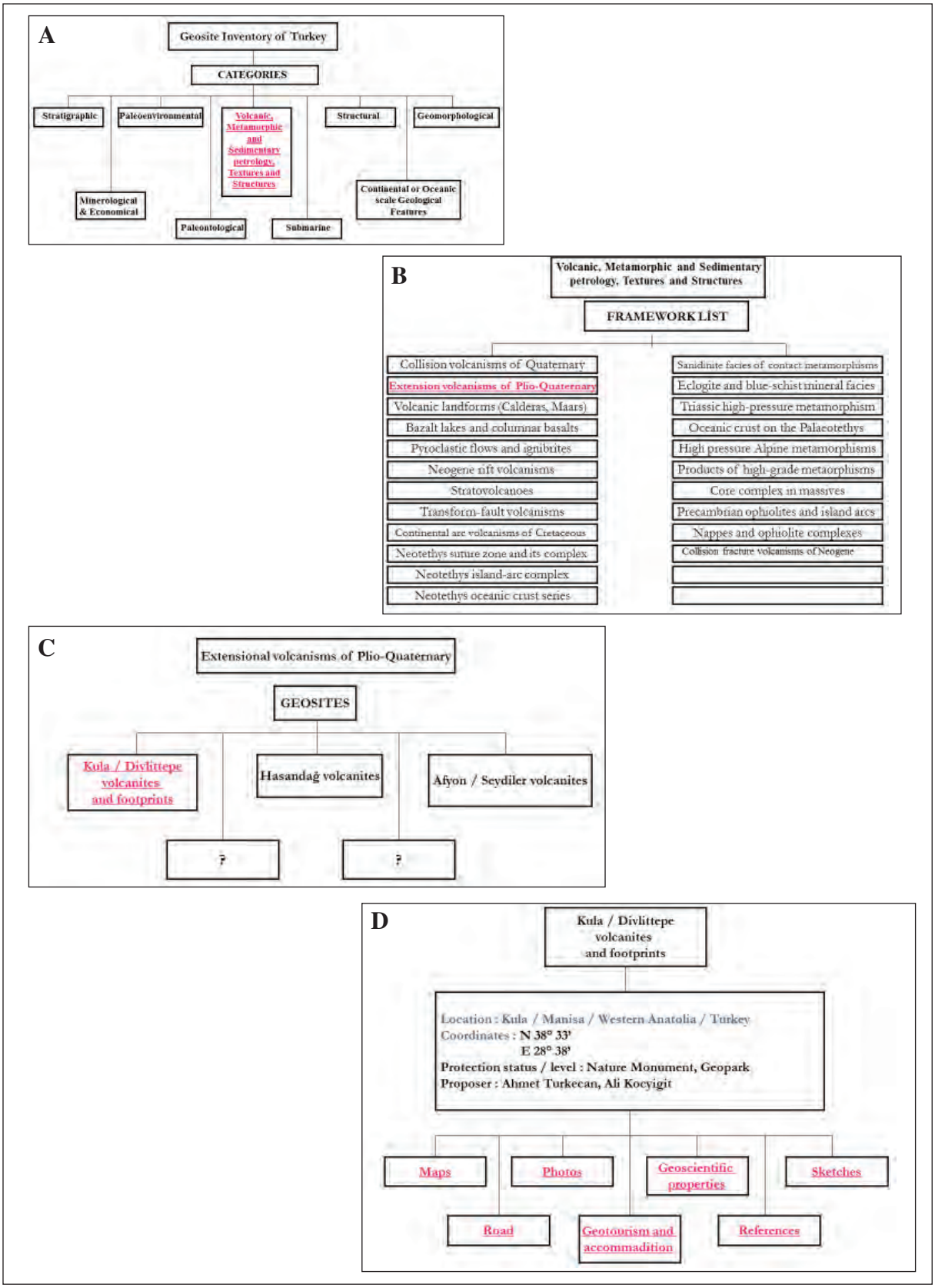

Figure 2- Applied demonstration of the definitions of category, framework list, and geosite: (a) geosite (inventory) categories and selection of one as an example (written in red), (b) the frames in the selected example category (framework list belongs to this category), (c) geosites belonging to the selected frame (written in red), (d) the information in the inventory book belonging to the selected geosites.

Figure 3- Volcanic neck cutting the Eocene units (Yozgat).

Figure 4- Lava channel on tuffs (Afyon).

Figure 5- Aygır maar and its lake (Bitlis).

based on the above-mentioned names of the geosite groups, otherwise there will be confusion again. Regardless of dimension, geographical location, and geological features, each country has only one FL. An FL is not a direct inventory, but it makes an excellent contribution to compiling an inventory (Brilha et al., 2005; De Lima et al., 2010). The extent of the FL is a sign of the geological diversity of a country; nevertheless, during the expansion of the list the main principle is to be very careful and harmonious with neighbouring countries (Theodossiu-Drandaki et al., 2004; Brilha et al., 2005). Ideally, all shareholders in earth sciences all over the country should participate in both the inventory and the FL studies.

4. Suggested Framework List

Despite the fact that the need for an FL for Turkey has been underlined before, it has not been possible to publish a written document regarding this issue (Kazancı and Şaroğlu, 2009). In this study, the following Geosite Framework List for Turkey is suggested (Table 1). The list, which is presented as 85 titles in 10 categories, resembles the "Southeastern Europe Countries Framework List", which was prepared by a wide group (Theodossiou-Drandaki et al., 2004). However, the following Geosite Framework List for Turkey is not identical to the one suggested for the Southeastern Europe Countries (the Balkans) (Theodossiou-Drandaki et al., 2004). The difference is estimated to be ca 30% (Table 1).

One of the purposes that lay behind creating the FL is to be able to choose representative geosites and geological heritage on the scale of the country, region, continent, and world in the future. For example, every country in a continent may choose the best C-T transition sedimentary sequence, and then it will be possible to determine the most typical one within the continent and finally to determine the perfect C-T sedimentary sequence of the world. If many perfect examples exist, their promotion will be continued by choosing, for example, the "Seven Wonders of the World" decennially, as is done within the implementation of World Cultural Heritage.

As mentioned in the previous paragraph, during the preparation of the proposed FL, the Balkan FL was taken into consideration. It was necessary to add a number of new titles (frameworks) because of the high geological diversity in Turkey, such as "extensional volcanism in the Plio-Quaternary", "transform fault volcanism", "local natural building stones", and so on (Table 1). The proposed List brings the following limitations (Figure 2).

The FL should be evaluated as a whole because some titles may be included in two or more categories. They are listed under the closest category so as to prevent repetitions and convergences.

Attention was paid to making the titles (Framework) focus on given subjects. In order to do so, we had to give some sub-titles in parentheses, for example, "Marine Coastal Deposits (ooids, beachrocks, terraces, sand bars)" (Table 1). The main context of that framework is that formations occurred on coastline depending on sea level changes. Such a grouping is necessary, otherwise innumerable variations may come into existence and the FL will become useless (ProGEO Group, 1998; Brilha et al., 2005).

When examining a FL, what should be considered seriously is that while geosites (and therefore the geosites inventory) are concrete, observable, and tactile objects, the framework and the FL describe the events and processes in the geological past (Figure 1). Even if there are similarities between geosites' names and frameworks, they are actually intended to describe the processes. An ideal FL should include all events and phases of the geological evolution of the country. The FL proposed here is not ideal, of course; however it should cover the principal geological events in the country, at least. To achieve it, we tried to choose individual frameworks which represent relatively wide time intervals (Table 1).

No "framework" could be formed in *Group g* (Astroblems) and *Group i* (Submarine), as there are no suggested geosites in the JEMIRKO inventory. Nevertheless, it was thought that it would be beneficial for the future to at least retain the group names. Similarly, it cannot be said that there are many geosites to be included under every title (framework) suggested here. However, the presence of the geological occurrences relevant to these titles is known from the literature. It is expected that earth scientists will contribute and overcome the deficiencies of the proposed list.

Table 1- The proposed "Geosite Framework List for Turkey"

Group a) STRATIGRAPHIC
a1) Quaternary
Marine coastal deposits (ooids, beachrocks, terraces, sand bars)
Pleistocene caliches and calcretes
a2) Phanerozoic
Late Neogene (Pliocene) marine deposits
Neogene evaporite basins
Parathetis successions
Marine and continental Miocene molasse
Complete marine cycles of Neogene
Tertiary mammalian beds
Extensive transgressions in Late Tertiary
Palaeogene basins
Paleogene bioherms
Reference stratigraphic sections of Palaeogene stages
Sedimentary and biological characteristics of time-boundaries
Late Cretaceous-Palaeocene carbonates
Late Cretaceous reefs
Mesozoic carbonate platform
Mesozoic platform deposits of Neothetis
Jurassic-Cretaceous deep marine facies
Ammonitico Rosso facies
Triassic-Jurassic carbonate successions
Late Triassic rift volcanisms related to the opening of Neothetis Ocean
Rift deposits related to the opening of Neothetis Ocean
Hersinian molasses
Marine and continental deposits of Carboniferous
Lower Palaeozoic succession of northern Gondwana
Cambrian sedimentary sequence
a3) Proterozoic
Precambrian rocks
Group b) PALAEOENVIRONMENTAL
Trace fossils
Paleokarsts
Foot prints on volcanites
Mammalia beds with hominoid and handcrafts
Fish and leaf fossils
Neogene paleosols
Neogene siliceous trees
Miocene bivalves
Large Tertiary foraminiferas
Bouma turbidite sequences
Incised valleys
Cretaceous ammonites
Devonian fishes
Euxinic environments of Early Silurian
Ordovician and Silurian Graptolites

Group c) VOLCANIC, METAMORPHIC AND SEDIMENTARY PETROLOGY, TEXTURES AND STRUCTURES, EVENTS AND PROVINCES

- Collision volcanisms of Quaternary
- Extension volcanisms of Plio-Quaternary
- Volcanic landforms (Calderas, Maars,Tuff rings)
- Bazalt flows and columnar basalts
- Pyroclastic flows and ignimbrites
- Neogene rift volcanisms
- Stratovolcanoes
- Transform-fault volcanisms
- Continental arc volcanisms of Cretaceous
- Neothetis suture zone
- Neothetis island-arc complex
- Neothetis oceanic crust series
- Sanidinite facies of contact metamorphisms
- Eclogite and blue-schist facies
- Triassic high-pressure metamorphism
- Oceanic crust on the Palaeothetis subduction zone
- High pressure Alpine metamorphisms
- Products of high-grade metamorphism
- Core complex in massives
- Precambrian ophiolites and island arcs
- Nappes and ophiolite complexes

Group d) MINERALOGICAL, ECONOMICAL

- Neogene evaporitic mineral beds (trona, borax, soelestine)
- Type localities of minerals Konyaite, Bursaite and Pandermite etc
- Lacustrine Sepiolite formations
- Metamorphic and sedimentary bauxites
- Thermal spring carbonates
- Valuable stones and gemological minerals

Group e) STRUCTURAL

- Seismically active normal and transform faults
- Tectonic creeps
- Structural landforms
- Tectonically active basins (grabens, pull-aparts)

Group f) GEOMORPHOLOGICAL FEATURES, EROSIONAL AND DEPOSITIONAL PROCESSES, LANDFORMS AND LANDSCAPES

- Recent eolian sand dunes
- Evaporite karsts
- Modern lakes, wetlands and rivers
- Modern marine coastal landforms (spits, bars, beaches, lagoons, deltas)
- Karstic landforms (obruks, sinkholes, dolins, polje, caves)
- Glacial landforms and deposits
- Canyons and valleys
- Erosional landscapes
- Volcanic landscapes

Group g) ASTROBLEMS
Group H- CONTINENTAL OR OCEANIC SCALE GEOLOGICAL FEATURES, PLATE RELATIONSHIPS Foreland trust belt of Afro-Arabian plate
Group i) SUBMARINE
Group j) HISTORICAL AND CULTURAL Antique marble and ore mines The sites where the geological terms firstly defined Local and specific building stones

5. Discussion and Conclusions

The FL presented in this study is a suggestion formed by the authors using their own experiences and comments of some eminent colleagues (Table 1). It is open to all contributions. The aim of the study (FL) is to act collaboratively with the worldwide geological community and to increase the impacts of internal researches on the literature. For example, publications that refer to titles in the FL will be followed more widely.

It should be re-emphasized that the Geosite Group (Category), Geosite FL, and Geosite Inventory are entirely different concepts, even though they are interrelated (Figure 1). Eighty-five titles (frameworks) are suggested in the present list. Most of them are found in *Groups a and c*. This means that the majority of the framework is related to stratigraphic, tectonic, and magmatic events. That is usual as the geological evolution itself occurs through these three processes. No explanation about the individual titles (frameworks) could be provided here, even in brief, as it would exceed the limits of this paper. Detailed analyses and explanations of the FLs are needed and hopefully they will be released soon by Turkish earth scientists.

One of the common results of the studies on geosites, geological heritage, the Geosite FL, and geoparks shows that all natural occurrences represent geodiversity; relevant topics and disciplines are not in competition but support each other. For instance, in the FL, all events from the Holocene to the Precambrian have to be studied by a similar methodology. The competitive atmosphere between geography and geology, geology and geophysics, hydrology and climatology, and ecology and geography seemed to be changed to a quarrel which was started once time and is still continued by some people, has not helped us to understand nature, and, moreover it has had negative effects on the development of earth sciences in the country. It is known now that walls have collapsed between disciplines and they can cooperate or learn from each other.

Another result from the geosite and FL studies is that the urgent need for geological conservation in our country has unfortunately increased to a dramatic level (Kazancı et al., 2005; 2012). Constructions, particularly larger ones, seem to be a primary threat to geosites all over the country; however, our unofficial survey showed that most of the damage has originated from the lack of public awareness of geosites. The gradually increasing interest of local administrations in geoparks and geotourism could serve geoconservation if people are informed successfully. The responsibility for this subject belongs to earth scientists.

Acknowledgements

This paper has been prepared in the light of discussions held in JEMİRKO's assemblies during the last ten years. So, it is possible to say that the proposed list is a joint product of all members. The figures were drawn by Zeynep Ataselim (AU). M.C. Göncüoğlu (METU) and Y. Güngör (İU) reviewed the paper for the journal. Attila Çiner made some linguistic improvements. The final version has been professionally proofread by PRS. The authors are grateful for all the contributions.

Received: 27.03.2015
Accepted: 11.07.2015
Published: December 2015

References

Arpat, E. 1976. İnsan ayağı iz fosilleri; yitirilen bir doğal anıt. *Yeryuvarı ve İnsan* 1/4, 65-66.

Arpat, E., Güner, Y. 1976. Ağrı buz mağarası; ender bir doğal anıt. *Yeryuvarı ve İnsan* 1/1, 95-96.

Barettino D., Vallejo M., Gallego E. (Eds).1999*a*. Towards the Balanced Management and Conservation of the Geological Heritage in the New Millenium. *ProGEO - European Association for Conversation of Geological Heritage and Sociedad Geologica de Espana*, Madrid, 459 s.

Barettino D., Wimbledon W.A.P., Gallego E. (Eds). 1999*b*. Geological Heritage: Its Conservation and Management. *ProGEO European Association for the Conservation of the Geological Heritage and Sociedad Geologica de Espana*, Madrid, 212 s.

Brilha J., Andrade C., Azerêdo A., Barriga F.J.A.S., Cachão M., Couto H., Cunha P.P., Crispim J.A., Dantas P., Duarte L.V., Freitas M.C., Granja M.H., Henriques M.H., Henriques P., Lopes L., Madeira J., Matos J.M.X., Noronha F., Pais J., Piçarra J., Ramalho M.M., Relvas J.M.R.S., Ribeiro A., Santos A., Santos V., Terrinha P. 2005. Definition of the Portuguese frameworks with international relevance as an input for the European geological heritage characterisation. *Episodes*, 28(3), pp. 177-186.

Burek, C.V., Prosser, C.D. 2008. The History of Geoconservation. *Geological Society*, Spec. Pub. 300, London, 312 s.

De Lima, F.F., Brilha, J.B., Salamuni, E. 2010. Inventorying Geological Heritage in large territories: a methodological proposal applied to Brazil. *Geoheritage* 2, 91-99.

Doughty, P. 2008. How things began: the origin of geological conservation. İç: The History of Geoconservation (Ed. Burek ve Prosser), *Geol. Soc. Spec. Pub.* 300, London, s. 7-16.

Dowling, R., Newsome, D. (eds). 2005. Geotourism. *Elsevier Pub.*, Amsterdam.

Erikstad, L. 2008. History of geoconservation in Europe. İç: The History of Geoconservation (Ed. C.V. Burek ve C.D. Prosser), *Geol. Soc. Spec. Pub.* 300, London, s. 249-256.

Kazancı, N. 2010. Jeolojik Koruma; Kavram ve Terimler. *Jeolojik Mirası Koruma Derneği yayını*, Ankara, 60 s.

Kazancı, N., Şaroğlu, F. 2009. Türkiye Jeositleri Çatı Listesi. *62. Türkiye Jeoloji Kurultayı (13-17 Nisan 2009) Bildiri Özleri Kitabı-I*, Jeoloji Mühendisleri Odası, Ankara, s. 266-267.

Kazancı, N., Şaroğlu, F., Kırman, E., Uysal, F. 2005, Basic threats on geosites and geoheritages in Turkey. *Proceedings of Second Conference on Geoheritage of Serbia*, June 2004 Belgrade, pp. 149-153, Belgrade, Serbia-Montenegro.

Kazancı, N., Şaroğlu, F., Doğan, A., Mülazımoğlu, N. 2012. Geoconservation and geoheritage in Turkey. İç: Geoheritage in Europe and its Conservation (Ed. W.A.P. Wimbledon ve S. Smith-Meyer), *ProGeo Spec. Pub*, Oslo, Norway, s. 366-377.

Ketin, İ. 1970. Türkiye'de önemli jeolojik aflörmanların korunması. Türkiye *Jeoloji Kurumu Bülteni* XI/2, s. 90-93.

Öngür, T. 1976, Doğal anıtlarin korunmasında yasal dayanaklar. *Yeryuvarı ve İnsan* 1/4, 17-23.

Özdemir, Ü., Göncüoğlu, M.C., Tütüncü, G., Tanca, N., Tümer, A. 1986. Doğal Anıtlar. Ege Univ. *Journal of Science Faculty*, Ser. B, 8, 221-230.

ProGeo Group.1998. A first attemt at a geosites framework for Europe -an lUGS initiative to support recognition of World heritage and European geodiversity. *Geologica Balcanica* 28, 5-32.

Theodossiou-Drandaki, I, R., Nakov, W.A.P., Wimbledon, W.A.P., Serjani, A., Neziraj, A., Hallaci, H., Sijaric, G., Begovic, P., Todorov, T., Tchoumatchenco, Pl., Diakantoni, A., Fassoulas, Ch., Kazancı, N., Şaroğlu, F., Doğan, A., Dimitrijevic, M., Gavrilovic D., Krstic, B., Mijovic, D. 2004. IUGS Geosites project progress - a first attempt at a common framework list for south eastern European countries. In: M. Parkes, Ed., Natural and Cultural Landscapes- the Geological foundation. *Proceedings of a Conference 9-11 September 2002*, Dublin Castle, Ireland, Royal Irish Academy, Dublin, p. 81-90.

Wimbledon, W.A.P. 1996. National site election, a stop on the road to a European Geosite List. *Geologica Balcanica* 26, 15-27.

Wimbledon, W.A.P., Benton, M.A., Berins, R.E. 1995. The development of a methodology for the selection of British geological sites for conservation. *Part I, ProGEO. Modern geology* 20, 59-202.

Wimbledon, W.A.P., Smith-Meyers, S (eds). 2012. Geoheritage in Europe and Its Conservation. *PeoGEO Spec. Pub.*, Oslo, Norway, 405 s.

Bull. Min. Res. Exp. (2015) 151: 269-283

Bulletin of the
Mineral Research and Exploration

http://bulletin.mta.gov.tr

REVIEW OF THE OCCURRENCE OF TWO NEW MINERALS IN THE EMET BORATE DEPOSIT, TURKEY: EMETITE, $Ca_7Na_3K(SO_4)_9$, and FONTARNAUITE, $Na_2Sr(SO_4)[B_5O_8(OH)](H_2O)_2$

Cahit HELVACI[a*]

[a] *Dokuz Eylül Üniversitesi, Jeoloji Mühendisliği Bölümü Tınaztepe Yerleşkesi, 35160 Buca/İzmir TURKEY*

Keywords:
Neogene borate basins, Emet borate deposit, Mineralogy, Emetite, Fontarnauite, West Anatolia.

ABSTRACT

The Emet borate deposit is situated in the middle of the known borate deposits of western Anatolia. Emet is the world biggest colemanite-probertite deposit which is located in the upper section of the volcano-sedimentary sequence of the Emet basin. Emet borate deposit is unique and has unusual mineral associations. The principal minerals in the Emet borate deposit are colemanite with minor probertite, ulexite and hydroboracite. In addition, rare species such as meyerhofferite, veatchite-A, tunellite, terrugite and cahnite occur sporadically. This is the only deposit known to contain any of the minerals veatchite-A, tunellite, teruggite and cahnite. Arsenic minerals (realgar and orpiment) are very abundant and spatially related to the borates, indicating a common genetic origin. The mineralogical record of Doğanlar boreholes is characterized by the alternation of Na-Ca borate (probertite) and Na-Ca sulphate (glauberite) units including a central halite beds. Colemanite is restricted to the base and top of the sequence in these boreholes and in the whole basin. In this part of the section the major mineral associations probertite-glauberite and halite, with several rare minerals and two new minerals (emetite and fontarnauite) were also discovered in these borehole logs. The Emet borate deposit was formed in two separate parts, possibly part of an interconnected lacustrine playa lake, in areas of volcanic activity, fed partly by thermal springs and partly by surface streams. The early colemanite, meyerhofferite, ulexite and teruggite nodules were formed directly from brines penecontemporaneously within the unconsolidated sediments below the sediment/water interface, and continued to grow as the sediments were compacted. Diagenetic alterations include the partial replacement of colemanite by veatchite-A, cahnite, hydroboracite and calcite. The new mineral, emetite, always appears as a diagenetic phase consisting of aggregates of tiny crystals that replace glauberite at the top of glauberite units. Fontarnauite is most commonly associated with probertite, glauberite and celestine in isolated colorless to light brown prismatic crystals or as clusters of crystals in core samples of these boreholes.

1. Introduction

The Geological evolution of western Anatolia during Neogene time is characterized by basin formation and contemporaneous widespread volcanic activity. The Neogene volcanic activity in western Anatolia was developed contemporaneously with development of NE trending basins, giving rise to formation of thick volcano-sedimentary successions and associated mineral deposits. In this respect, tectonic evolution of the Neogene basins is a fundamental theme in studying the Neogene volcanic evolution as well as the related mineral deposits of the region (Travis and Cocks, 1984; Fytikas et al., 1984; Ercan et al., 1985, 1996; Ersoy and Helvacı, 2007; Ersoy et al., 2011, 2012, 2014; Palmer and

* *Corresponding author: Cahit Helvacı, cahit.helvaci@deu.edu.tr*

Helvacı, 1997; Floyd et al., 1998; Helvacı, 1995; 2005).

The borate deposits of Turkey occur in western Anatolia, south of the Marmara Sea within an area roughly 300 km east-west by 150 km north-south. The main borate districts are Bigadiç, Sultançayırı, Kestelek, Emet, and Kırka (Figure l), and Turkish production supplies most of the commercially traded ulexite and colemanite from mines in the Bigadiç, Kestelek and Emet Districts, plus borax from the deposit at Kırka.

The western Anatolia borate district contains the largest borate reserves in the world (Lyday, 1982; Kistler and Smith, 1983; Helvacı, 1989; Kistler and Helvacı, 1994; Helvacı and Alonso, 2000). All the western Anatolia borate deposits were formed during the Miocene time in closed lacustrine basins with abnormally high salinity and alkalinity (Helvacı, 1986, 1989; Helvacı and Firman, 1976; Helvacı, 2005). The pre-Miocene basement of the basins is represented by the Menderes Massif, which composed of Mesozoic and Paleogene rock units and volcanics. The main borate districts of Turkey are Bigadiç, Kestelek, Sultançayır, Emet and Kırka (Helvacı, 1989, 2005; Kistler and Helvacı, 1994; Helvacı et al., 1993; Helvacı and Alonso, 2000). The important borate minerals from a worldwide commercial standpoint are borax, ulexite and colemanite. Colemanite, a very common calcium borate, is the predominant mineral in all borate districts except for Kırka. A large number of other borate minerals are found in the deposits, including pandermite, inyoite, meyerhofferite, tincalconite, kernite, hydroboracite, inderite, inderborite, kurnakovite, cahnite, terrugite, veatchite-A and tunnelite (İnan et al., 1973; Helvacı, 1977, 1978, 1983; Helvacı and Orti, 1998, 2004; Orti et al., 1998).

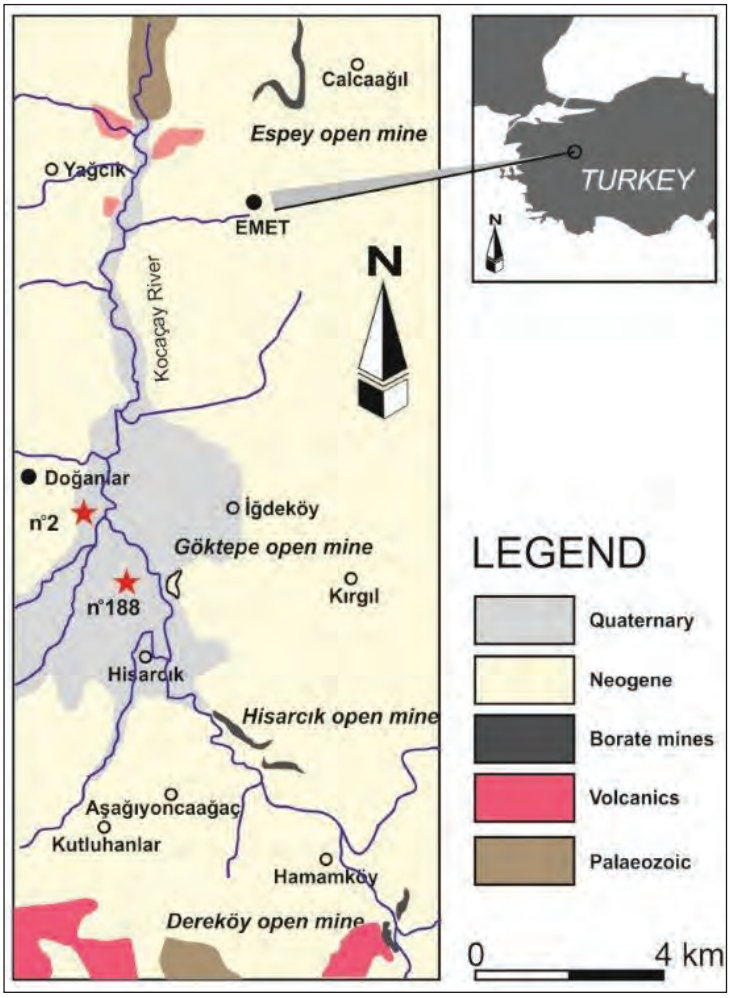

Figure 1- Location of Doğanlar boreholes and geological map of the Emet borate district showing the location of open pit mines and boreholes in western Turkey (after Helvacı, 1986).

The boron in the deposits is assumed to have been derived by leaching of the surrounding rocks by geothermal activity associated with local volcanism (Floyd et al., 1998). The borates then formed when the hydrothermal and spring waters evaporated after flowing into shallow playa lakes (Helvacı, 1995). Boron-rich fluids are presumed to have also circulated along faults into these basins (Helvacı, 1986, 2005).

The borate deposits of Turkey were formed in the lacustrine sediments of Neogene age during periods of volcanic activity. Although the sediments deposited in the borate lakes show some differences, they are generally represented by tuffaceous rocks, claystones, limestones and Ca, Na, Mg, Sr-borates. Sandstone and conglomerates occur near the base of each basin (Gawlik, 1956; Özpeker, 1969; İnan et al., 1973; Helvacı and Firman, 1976; Helvacı, 1977). Sediments in the borate lakes often show clear evidence of volcanic cyclicity. Borate minerals were deposited in a separate or possibly interconnected lake basins under arid or semi-arid climatic conditions. Pyroclastic and volcanic rocks of rhyolitic, dacitic, trachytic, andesitic and basaltic composition are intercalated with these lacustrine sediments. The existence of volcanic rocks in every borate district suggests that volcanic activity may have been necessary for the formation of borates. Much of the sediments in the borate basin seems to have been derived from volcanic terrain. Generally, the borates are enveloped between tuff and clay-rich horizons. The lithologies of the borate deposits show some differences from one to another, and they are generally interbedded with conglomerate, sandstone, tuff, claystone, marl, and limestones, and are usually enveloped by, or grade into, limestones or claystones (İnan et al., 1973; Helvacı, 1977, 1986, 2005; Sunder, 1980; Helvacı et al., 2012); and sediments often exhibit both lateral and vertical facies changes. Volcanic rocks in the vicinity of the playa lakes in which the borate deposits were formed are extensive (Floyd et al., 1998). Intense calc-alkaline volcanic activity took place simultaneously with the borate sedimentation. The volcanic rocks are generally represented by a calc-alkaline series of flows ranging from acidic to basic and by associated pyroclastic rock (Ersoy et al., 2011, 2012).

All of these sediments were generated during periods of high volcanic and hydrothermal activity. Although the mineral association of each district shows particular differences, the borates, in association with minor sulphates, are always interbedded with tuffaceous beds (Helvacı and Alonso, 2000).

The Emet borate deposits are situated in the middle of the known borate deposits of western Anatolia (Helvacı 1977, 1984, 1986, 2005). The Emet district includes Palaeozoic metamorphic rocks intruded by granite, and overlying Tertiary sediments associated with volcanic rocks (Holzer 1954; Gawlik 1956; Akkuş 1962). The principal minerals in the Emet borate deposits are colemanite with minor ulexite and hydroboracite. The deposits are mined by open-pit mining methods in the southern basin (Hisarcik and Derekoy deposits) and underground and recently open-pit mining methods in the northern basin (Espey and Killik deposits). Investigations have been carried out on various sections of the basin and samples have been collected from the open-pit, underground workings and the drill cores.

Earlier published papers by Helvacı and Firman (1976) and Helvacı (1984, 1986) indicated that the deepest part of the N-S trending Emet basin is around the Doğanlar-İğdeköy locality, where there were only weathered outcrops on both side of the Emet (Kocaçay) River. In this locality whole sequence was covered with recent Quaternary and alluvial sediments, and deep drillings were suggested to the Eti Maden Company. Concequently, in the years of 1986 and 2003 deep drilling project took place in the Doğanlar-İğdeköy locality. A number of deep boreholes intersected the thickest part of the borate zone in this area, with deepest one at about 700 meters below the surface (Figures 1, 2 and 3).

This paper is a preliminary report on the petrographic and geochemical characteristics of a new sulphate and a borate-sulphate minerals associated with lacustrine probertite-glauberite layers in these Doğanlar boreholes. These minerals are present in two boreholes recently drilled in the Emet borate district (Miocene; western Anatolia, Turkey). These boreholes were drilled with continuous rock sampling by the Eti Maden Company (Turkish Government) during 2003 for exploratory purposes in the vicinity of Doğanlar village, located seven kilometres to the south-west of Emet. The two boreholes were drilled on the Quaternary alluvium of the Kocaçay River with a distance of 1.8 km between them. Figure 1 shows the borehole sites on a simplified geological map. The main colemanite open pit mines (Espey and Hisarcık) in the area are also indicated (Figures 1 and 3). The evaporitic succession in these boreholes is mainly formed of a glauberite-

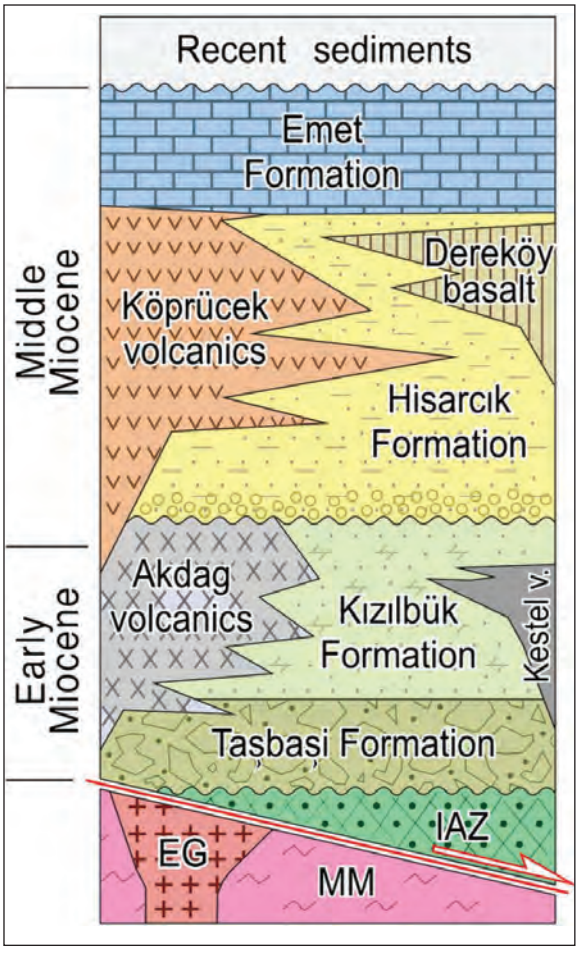

Figure 2- Generalized stratigraphic section of the Emet basin (without scale). MM: Paleozoic Menderes Metamorphic basement; EG: Eğrigöz Granitoid; IAZ: carbonates and ophiolitic rocks of Izmir-Ankara Zone; Taşbaşı formation: conglomerates; Kızılbük formation: clastic unit containing coal; Akdag, Kestel, Köprücek and Dereköy: volcanic units; Hisarcık formation: carbonates with clastic, and tuff deposits, containing borates; Emet formation: upper limestone unit (modified after Helvacı, 1984).

probertite alternation. In this part of the section the major mineral associations probertite-glauberite and halite, with several rare minerals and two new minerals (emetite and fontarnauite) were also discovered in these boreholes. They were already published elsewhere (Garcia-Vegias et al., 2010*a*, 2010*b*, 2011; Cooper et al., in press).

Emetite was found in core samples from the boreholes Kütahya-Emet no: 2 (UTM: 35S 691346 / 4350558) and no: 188 (UTM: 35S 691800 / 4348815) (called "Doğanlar boreholes") (Figure 4). We suggest the name "emetite" for the new sulphate mineral after the town of Emet. It is also noted that the fine crystal size of this new mineral hinders the appropriate chemical and crystallographic characterization required to propose it as a new mineral to the International Mineralogical Association (Garcia-Veigas et al., 2010*a*). This mineral still needs to be worked on in order to get all the data to be approved by IMM.

Fontarnauite is a new mineral found in core samples of the Doğanlar boreholes no: 2 and no: 188 drilled in the vicinity of the Doğanlar village, located seven kilometres to the southwest of the Emet town (western Anatolia, Turkey) (Figure. 1 and 4). Fontarnauite is a double salt (borate-sulphate) of sodium and strontium with minor contents of potassium and calcium. The proposed name is for deceased Dr. Ramon Fontarnau (1944-2007), Director of the Material Characterization Section of the Scientific-Technical Survey at the University of Barcelona for his effort to promote the development of scientific facilities focused on mineral characterization (Garcia-Veigas et al., 2010*b*; Cooper et al., in press).

This paper presents the short story of the two new minerals, emetite and fontarnauite (borate and borate-sulphate minerals), recently discovered in the Emet borate deposits, and attempts to define both the relationships between mineral associations, and the nature of their occurrences. The full papers of these minerals were treated elsewhere.

2. Geological Setting of Emet Basin

Emet basin (Akdeniz and Konak, 1979; Helvacı, 1984, 1986; Figure 3), is located between the Eğrigöz granitoid intruded into the Menderes Massif metamorphic rocks to the west, and the Afyon zone metamorphic rocks to the east (Figures 1, 2 and 3). The Neogene sequence rests unconformably on Paleozoic metamorphic rocks that consist of marble, mica-schist, calc schist and chlorite schist.

The borate deposits of Turkey were formed in lacustrine environments during periods of volcanic activity. The borates of the Emet area are part of the Tertiary lacustrine sediments which rest unconformablv on Palaeozoic metamorphic rocks, consisting of marble, micaschist, calc-schist and chlorite-schist (Figure 3). The sediments of the Emet district consist of predominantly lacustrine sequence. The stratigraphy of Emet basin comprises two Neogene volcanosedimentary units separated by a

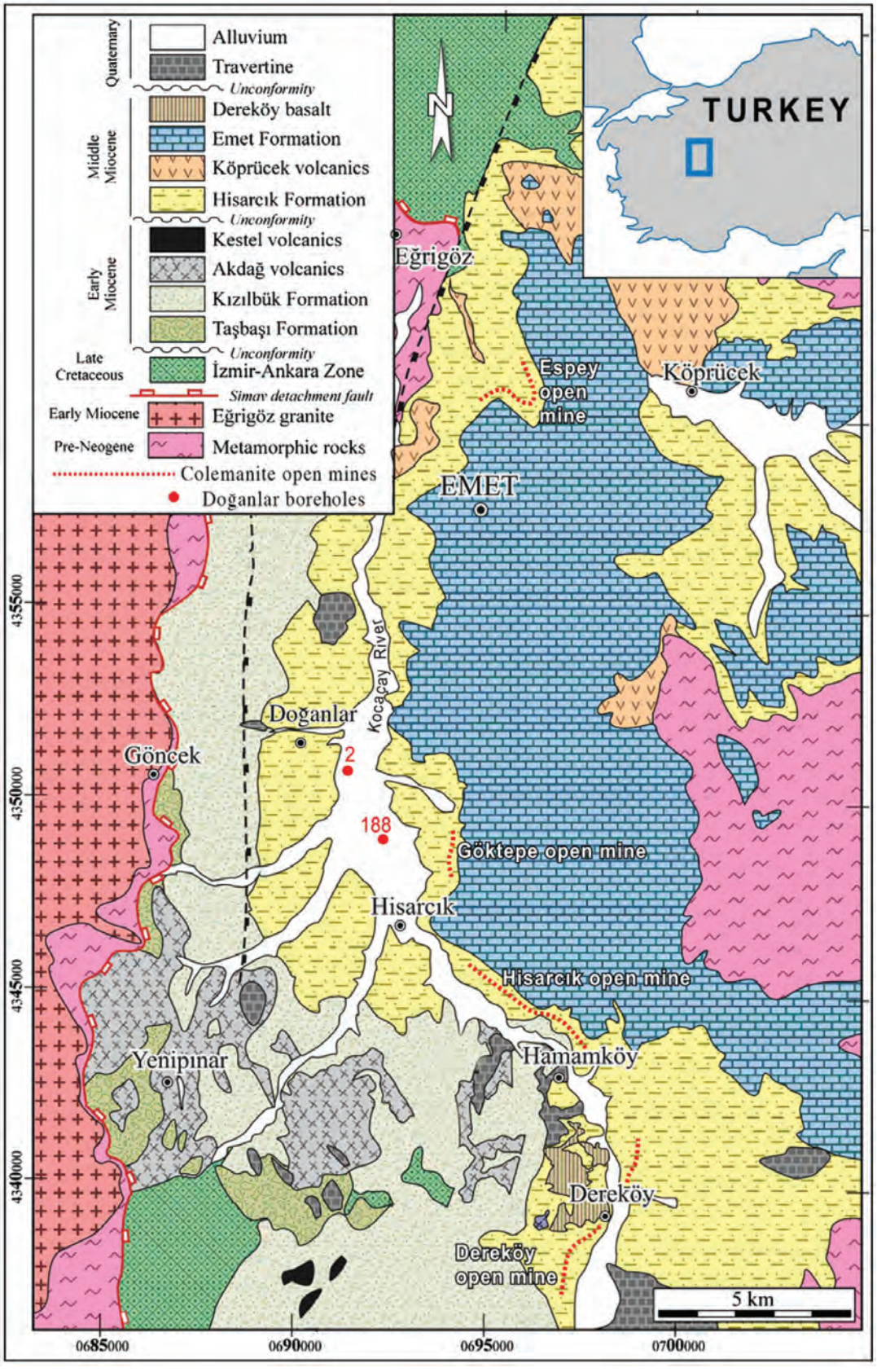

Figure 3- Geological map of the Emet borate district (modified after Helvacı, 1984) showing the location of the colemanite open pit mines and the studied boreholes.

regional unconformity (Figures 2 and 3). These units can be correlated with similar rocks from other basins on the basis of their age, lithology and deformational features, and they are named as the Hacıbekir and İnay groups. In the Emet basin, the İnay Group hosts the world's biggest colemanite and probertite borate deposits (Gawlik, 1956; Helvacı, 1984, 1986; Helvacı and Orti, 1998; Helvacı and Alonso, 2000; Garcia et al., 2011).

The Hacıbekir Group consists of the Taşbaşı and Kızılbük formations and the Akdağ and Kestel volcanics (Figures 2 and 3). The Taşbaşı formation crops out to the western and southwestern parts of the Emet basin, and is made up of reddish-brown colored conglomerates with grayish sandstone intercalations deposited in alluvial fan facies. The Taşbaşı formation is locally interfingered with rhyolitic pyroclastic rocks of the Akdağ volcanics, and is conformably overlain by the Kızılbük formation.

The age of the unit is early Miocene on the basis of radiometric age data from the volcanic rock intercalations. The Kızılbük formation crops out in a large area to the western and southwestern parts of the Emet basin, and is composed of coal-bearing yellowish sandstone–siltstone–mudstone alternations and laminated limestone of fluvio-lacustrine origin. The Kızılbük formation is interfingered with pyroclastic rocks of the Akdağ volcanics, which are composed of rhyolitic lava flows, domes, pyroclastics and epiclastics. The Akdağ volcanics have yielded 20.3±0.6 (Seyitoğlu et al., 1997) and 19.0±0.2 Ma (Helvacı and Alonso, 2000) K–Ar ages (Table 1). The Kestel volcanics emplaced in a NE–SW-direction to the southwest of the basin, and are composed of syn-sedimentary mafic lava flows. These volumetrically small volcanic rocks conformably overlie the Kızılbük Formation. The age of the Kestel volcanics is stratigraphically accepted to be early Miocene.

The İnay Group in Emet basin is made up of the Hisarcık and Emet formations that interfinger with the Köprücek volcanics and th Dereköy basalt (Figure 3). The Hisarcık formation (Akdeniz and Konak, 1979) crops out in a large area in the Emet basin and is composed of conglomerates, pebblestones and sandstone intercalations. The age of the Hisarcık formation is accepted to be middle Miocene on the basis of volcanic intercalations in the İnay Group. Towards the center of the basin, the Hisarcık formation passes laterally into the Emet formation that is composed of sandstone – claystone – mudstone - limestone alternations of fluvio-lacustrine origin. The fine-grained parts of the unit, especially the mudstone – claystone levels contain large borate deposits which are mined for colemanite and probertite (Helvacı and Alonso, 2000; Helvacı and Ersoy, 2006; Helvacı et al., 2006; Ersoy et al., 2012).

In the Emet basin, the Köprücek volcanics (16.8±0.2 Ma K–Ar age; Helvacı and Alonso, 2000) crop out to the northern part of the Emet basin. The unit is composed of andesitic to rhyolitic lava flows, dykes and associated pyroclastics which interfinger with the Hisarcık formation. The thickness of the pyroclastic intercalations in the Hisarcık formation increases towards the north of the basin, which suggests that the Köprücek volcanics originated from this area. The Köprücek volcanics are overlain by the

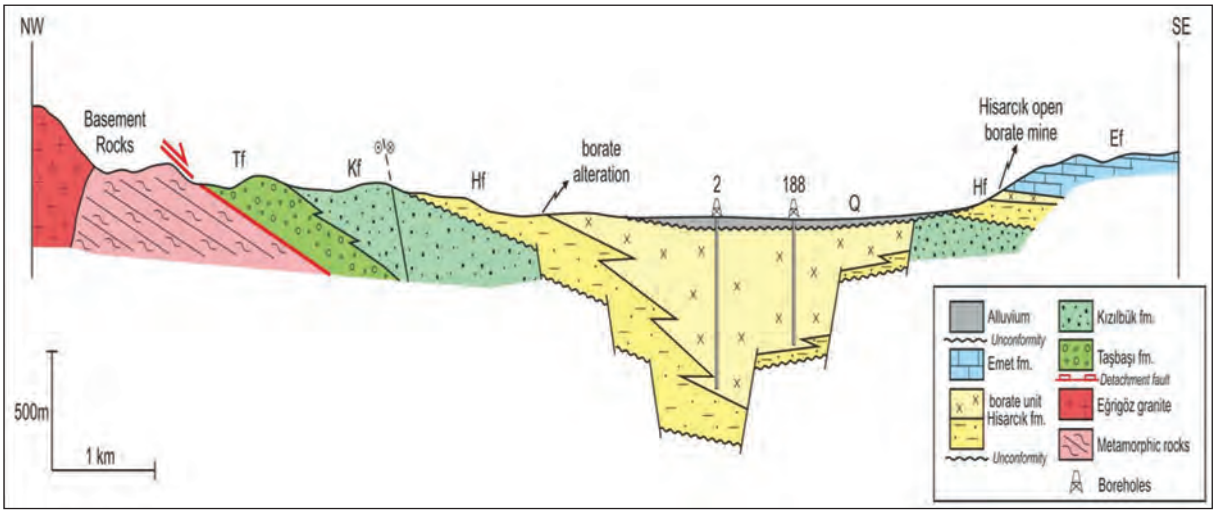

Figure 4- Cross section along the Doğanlar locality and Hisarcık opencast mine showing the deep boreholes numbers 2 and 188.

Table 1- Borates, sulphates and sulphides recognised in the Emet basin and their chemical formulas.

Borates	Ca	Colemanite	$CaB_3O_4(OH)_3\ H_2O$
		Meyerhofferite	$Ca(B_3O_3(OH)_5).H_20$
	Ca-Na	Probertite	$NaCaB_5O_7(OH)_4\ 3(H_2O)$
		Ulexite	$NaCaB_5O_6(OH)_6\ 5(H_2O)$
	K	Fontarnauite	$(Na,K)_2(Sr,Ca)SO_4[B_4O_6(OH)_2]\ 3H_2O$
		Kaliborite	$KMg_2H(B_6O_8(OH)_5)_2\ 4(H_2O)$
	Mg-Na	Aristarainite	$NaMgB_{12}O_{16}(OH)_8\ 4(H_2O)$
		Rivadavite	$Na_6Mg(B_6O_7(OH)_6)_4.10H_2O$
		Hydroboracite	$CaMg(B_3O_4(OH)_3)_2\ 3(H_2O)$
	Sr	Tunellite	$SrB_6O_9(OH_2)\ 3H_2O$
		Veatchite-A	$Sr_2(B_{11}O_{16}(OH)_5).H_2O$
	As	Cahnite	$Ca_2B(AsO_4)(OH)_4$
		Teruggite	$Ca_4MgAs_2B_{12}O_{22}(OH)_{12}.12H_2O$
Sulphates	Ca	Anhydrite	$CaSO_4$
		Gypsum	$CaSO_4\ 2H_2O$
	Ca-Na	Glauberite	$Na_2Ca(SO_4)_2$
	Na	Thenardite	$Na_2(SO_4)$
	K	Emetite	$Ca_7Na_3K(SO_4)_9$
	Sr	Celestine	$SrSO_4$
		Kalistrontite	$K_2Sr(SO_4)_2$
Sulphides	As	Arsenopyrite	FeAsS
		Orpiment	As_2S_3
		Realgar	As_4S_4

limestones of the Emet formation. The pyroclastic intercalations yield 16.8±0.2 Ma K–Ar age (Helvacı and Alonso, 2000; table 1). In the southern part of the basin, the Hisarcık formation is also conformably overlain by basaltic lava flows of the Dereköy basalt. Along the basal contact of the Dereköy basalt several pepperitic textures are developed, indicating a syn-sedimentary emplacement of the lavas. The Dereköy basalt has been dated as 15.4±0.2 and 14.9±0.3 Ma (K–Ar ages; Seyitoğlu et al., 1997; Helvacı and Alonso, 2000).

The volcanic activity in the Emet basin is thought to be the source of the borate deposition. Thermal springs associated with local volcanic activity are thought to be the possible source of the borates (Helvacı, 1977; Helvacı, 1984; Helvacı and Alonso, 2000). The older acidic lavas contain higher B levels than the more recent intermediate alkaline lavas. The Early Miocene acidic volcanism at Emet basin has high levels of elements associated with mineralization, as well as having a close spatial and temporal relationship with the borates and it is therefore considered a likely source. Possible mechanisms by which volcanism might supply B, S, Sr, As and Li to the basin sediments include the leaching of volcanic rocks by hydrothermal waters, the direct deposition of ash into the lake sediments, or the degassing of magmas (Helvacı, 2015, in this volume).

3. Mineralogy of Emet Deposit

Mineralogical studies have shown that the borate deposits in the Emet district are far more complex than previously thougt in addition to the minerals previously recorded (Özpeker 1969). The Emet basin is one of the Neogene basins in western Turkey containing significant amounts of rare borate minerals. The borates are interlayered with tuff, clay and marl with limestone occurring above and below the borate lenses. Sedimentary and early diagenetic

processes controlled the crystal growth both subaqueously and interstitially. The principal borate minerals are colemanite and probertite (Table 1; figures 5 and 6), with minor ulexite, hydroboracite and meyerhofferite. The Emet borate deposits contain many of the rare borate minerals such as veatchite-A, tunellite, teruggite, and cahnite (Helvacı and Firman, 1976; Helvacı, 1977, 1984, 1986; Helvacı and Orti, 1998; Garcia-Veigas et al., 2011). Montmorillonite, illite and chlorite are clay minerals that have been identified, and zeolites are abundant along the tuff horizons (Helvacı et al.,1993; Çolak et al., 2000).

The petrologic study of core samples from two exploratory wells in the Doğanlar sector, reveals a complex mineral association in which probertite, glauberite and halite constitute the major primary phases precipitated in a saline lake within a volcano-sedimentary context (Garcia-Veigas et al., 2011). Other sulphates (anhydrite, gypsum, thenardite, celestite and kalistrontite), borates (colemanite, ulexite, hydroboracite, tunellite, kaliborite and aristarainite) and sulphides (emetite, arsenopyrite, realgar and orpiment) are attributed to early diagenesis. The Doğanlar deposit is the most important deposit of probertite known up to now (Garcia-Veigas et al., 2011). Emetite paper is already published in an international journal (Garcia-Veigas et al., 2010*a*). A new sulphate-borate mineral (fontarnauite) has been found in the deposit (Garcia-Veigas et al., 2010*b*) (Table 2) and the paper concerning this mineral is in press in the Canadian Mineralogist (Cooper et al., in press).

The mineralogical record of Doğanlar boreholes is characterized by the alternation of Na-Ca borate (probertite) and Na-Ca sulphate (glauberite) units including a central halite beds. Colemanite is restricted to the base and top of the sequence. Kalistrontite is abundant in the sequence indicating a significant concentration of Sr in brines. Fontarnauite appears as an early diagenetic phase, replacing both probertite and glauberite, as a consequence of an anomalous chemical composition achieved by the residual brines duringevaporation in a saline lake environment with volcaniclastic contribution. Other minor minerals found in the boreholes include: borates (aristarainite, colemanite, hydroboracite, kaliborite tunellite and ulexite), sulphates (anhydrite, celestine, gypsum, kalistrontite and thenardite), and sulphides (emetite, arsenopyrite, orpiment and realgar) (Helvacı, 1984; Garcia-Veigas et al., 2011) (Figures 5 and 6; table 1).

4. Occurrence of Emetite (a new sulphate mineral): $Ca_7Na_3K(SO_4)_9$ in the Emet Borate Deposit

Emetite, a new sulphate mineral, $Ca_7Na_3K(SO_4)_9$, has been identified in two boreholes drilled in the Emet borate district. The evaporitic succession in these boreholes is mainly formed of a glauberite-probertite alternation. The chemical characterization of the mineral phases in the Doğanlar boreholes has led to the identification of a new K-bearing sulphate mineral, $Ca_7Na_3K(SO_4)_9$ named here as "emetite". The new mineral always appears as a diagenetic phase consisting of aggregates of tiny crystals that replace glauberite at the top of glauberite units. The replacement was caused by the interaction of glauberite with K-rich in terstitial brines, which are more concentrated than those from which glauberite had precipitated (Garcia-Veigas et al., 2010*a*).

This paper is to report on the petrographic and geochemical characteristics of a new sulphate mineral associated with lacustrine glauberite layers. The evaporitic succession in these boreholes is mainly formed of a glauberite-probertite alternation. Emetite was found in core samples from the boreholes Kütahya-Emet no: 2 (UTM: 35S 691346/4350558) and no: 188 (UTM: 35S 691800/4348815) (Doğanlar boreholes). This mineral is present in two boreholes recently drilled in the Emet borate district (Miocene; western Anatolia, Turkey). The name "emetite", after the town of Emet, is suggested for the new sulphate mineral (Garcia-Viagas et al., 2010*a*).

The new sulphate, $Ca_7Na_3K(SO_4)_9$, always appears as a diagenetic mineral replacing millimetre-sized crystals of glauberite. It consists of aggregates of tiny, elongated and anhedral crystals, frequently curved, which exhibit second order interference colours. They are arranged in fascicular and radial fabrics and resemble intergrowth textures (Figures 7 and 8) (Garcia-Veigas et al., 2010*a*). The aggregates form round or irregularly-shaped masses, of less than 1 mm in length, that replace the glauberite crystals from their margins, in contact with the matrix, towards the centre (Figure 7). Commonly, these masses, as well as the host glauberite crystals, are replaced by equant, euhedral crystals of anhydrite from tens of mm up to 3 mm across (Figure 8). In borehole no: 188, emetite also occurs at the top of a glauberite unit, at a depth of 312 m, where the host glauberite crystals are replaced by secondary gypsum (Figure 6). The new mineral and the anhydrite

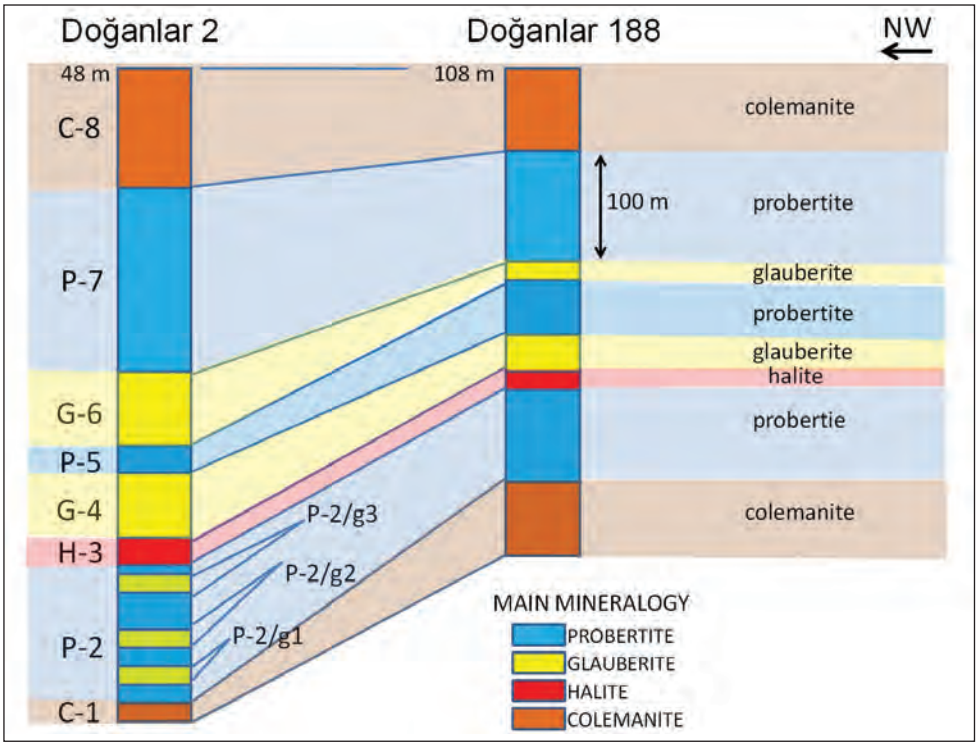

Figure 5- Lithological log correlation of the Doğanlar boreholes based on mineral associations. C-1: Basal Colemanite Unit, P-2: Lower Probertite Unit, P-2/g1: Lower-Anhydrite Subunit, P-2/g2: Intermediate Glauberite-Kalistrontite Subunit, P-2/g3: Upper Glauberite-Fontarnauite Subunit, H-3: Halite Unit, G-4: First Glauberite Unit, P-5: Intermediate Probertite Unit, G-6: Second Glauberite Unit, P-7: Upper Probertite Unit, C-8: Upper Colemanite Unit (Garcia-Veigas et al., 2011).

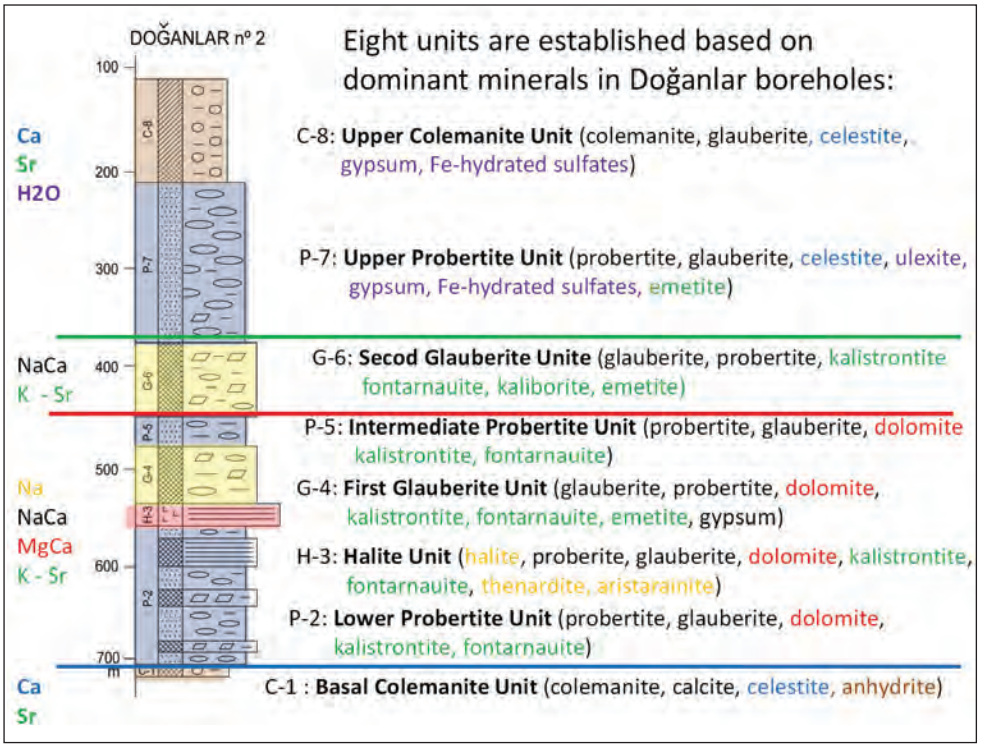

Figure 6- Schematic distribution of the evaporitic minerals with depth (borehole Doğanlar no. 2). Units as in figure 5 (Garcia-Veigas et al., 2011).

Table 2- Documents of new mineral Fontarnauite published in Mineralogical Magazine October 2014.

NEW MINERAL PROPOSALS APPROVED IN SEPTEMBER 2014 IMA No. 2009-096a	
Fontarnauite	
Kütahya-Emet 2 and 188 boreholes, near the village of Doğanlar, Kütahya Province, Western Anatolia, Turkey Mark A. Cooper, Frank C. Hawthorne, Javier Garcı´a-Veigas, Xavier Alcobe´, Cahit Helvaci, Edward S. Grew* and Neil A. Ball *E-posta: esgrew@maine.edu	
Chemical Properties of Fontarnauite	
Formula: $(Na,K)_2(Sr,Ca)(SO_4)[B_5O_8(OH)]\cdot 2H_2O$	
Crystallography of Fontarnauite	
Crystal System:	Monoclinic: P21/c; structure determined (New structure type)
Class (H-M):	2/*m* – Prismatic
Space Group:	*P*21/*b*
Space Group Setting:	*P*21/*c*
Cell Parameters:	a = 6.458(2) Å b = 22.299(7) Å c = 8.571(2) Å β = 103.05(1)°
Ratio:	a:b:c = 0.29 : 1 : 0.384
Unit Cell Volume:	V 1,202.41 Å? (Birim Hücreden hesaplanmıştır)
X-Işınları Powder Diffraction Data:	**d-spacing** **Intensity** 11.15 -100 3.395 -8 3.339 -20 3.199 -30 3.046 -10 3.025 -7 2.750 -10 2.400 -8
Type material is deposited in the collections of the Royal Ontario Museum, 100 Queens Park, Toronto, Ontario M5S 2C6, Canada, accession number M56745	
How to cite: Cooper, M.A., Hawthorne, F.C., Garcı´a-Veigas, J., Alcobe´, X., Helvaci, C., Grew, E.S. and Ball, N.A. (2014) Fontarnauite, IMA 2009-096a. CNMNC Newsletter No. 22, October 2014, page 1244; Mineralogical Magazine, 78, 1241-1248.	

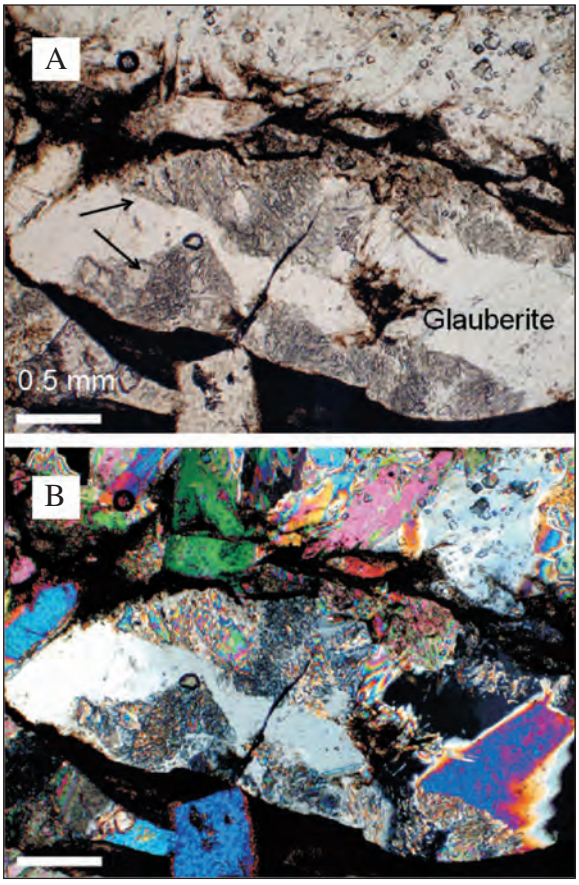

Figure 7- Glauberite crystal partially replaced by aggregates of the new sulphate mineral emetite (arrows) (A: parallel nicols, B: crossed nicols) (Garcia-Veigas et al., 2010*a*).

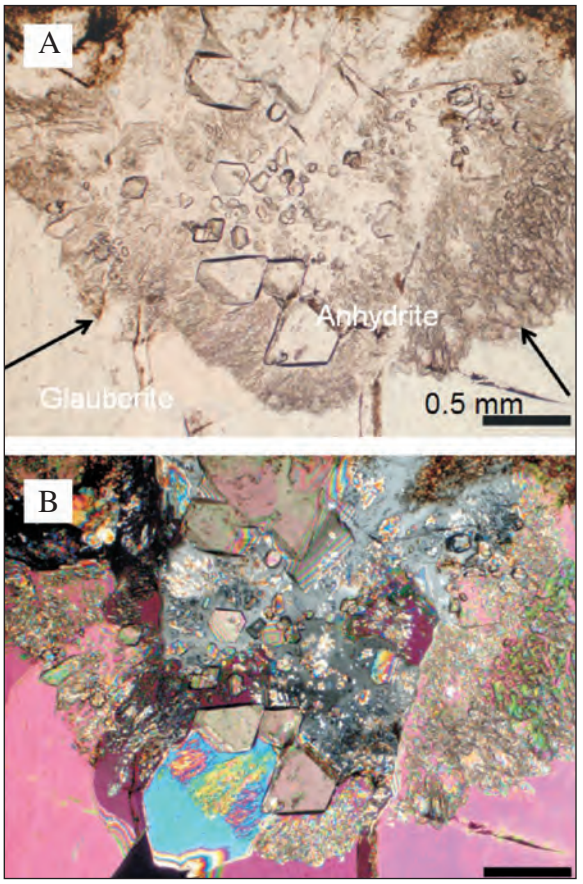

Figure 8- Round aggregate of the new sulphate mineral emetite (arrows) replacing glauberite crystals (A: parallel nicols, B: crossed nicols) (Garcia-Veigas et al., 2010*a*).

crystals have also been partly transformed to secondary gypsum, although to a lesser extent in the case of the anhydrite (Garcia-Veigas et al., 2010*a*).

5. Occurrence of fontarnauite (a new sulphate-borate mineral): $Na_2Sr(SO_4)[B_5O_8(OH)](H_2O)_2$ in the Emet borate deposit

Fontarnauite was recovered from the Kütahya-Emet 2 and 188 (Doğanlar boreholes) boreholes drilled in the Emet basin near the village of Doğanlar (García-Veigas et al. 2010*b*, 2011; Helvacı 1986, Helvacı and Orti 1998). The exploration holes were drilled during 2003 in the area to the north of the Hisarcık open cut mine in Quaternary alluvium of the Kocaçay River (Figure 4). The distance between the two boreholes is about 1.8 km. Borehole 2 is 716 m in depth; fontarnauite was observed between 530 and 581.5 m depth; borehole 188 (516 m in depth) yielded fontarnauite between 249 and 351.9 m (Garcia-Veigas et al., 2011).

Fontarnauite is most commonly associated with probertite, glauberite and celestine (Figures 9, 10 and 11). In addition, García-Veigas et al. (2010*b*) reported fontarnauite with (1) halite, (2) kaliborite replacing probertite, and (3) kalistrontite, which replaced fontarnauite in pseudomorphs after glauberite. Other minerals occurring in the boreholes, most abundantly colemanite, ulexite, dolomite, arsenopyrite, realgar and orpiment, have not been found with fontarnauite (Garcia-Veigas et al., 2011).

Fontarnauite, $Na_2Sr(SO_4)[B_5O_8(OH)](H_2O)_2$, was discovered in 2009 in cores recovered from the borate-bearing Miocene Emet basin (García-Veigas et al. 2010*b*, 2011). The mineral and its name have been approved by the International Mineralogical Association Commission on New Minerals, Nomenclature (IMA no. 2009-64a). The holotype is

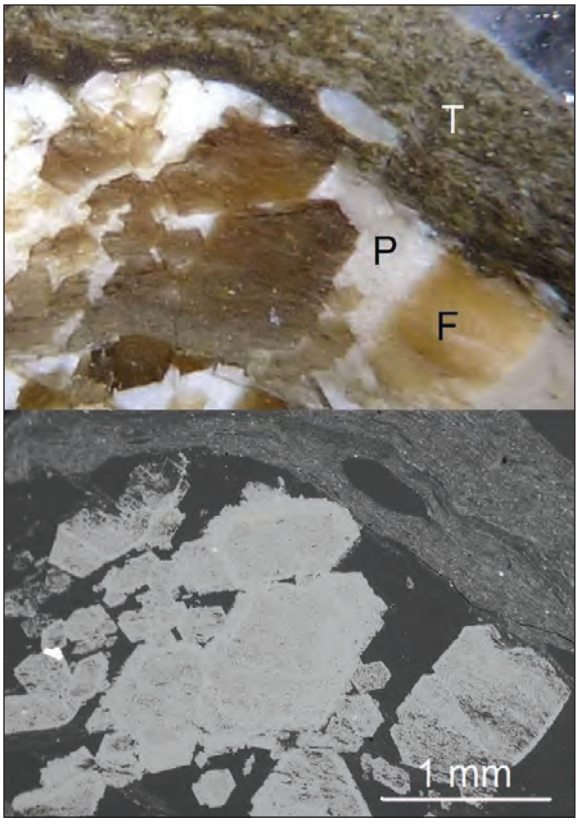

Figure 9- Optical (upper) and BSE-SEM (lower) images of a cluster of fontarnauite crystals. (F: fontarnauite, P: probertite,T: tuff). (García-Veigas et al., 2010*b*).

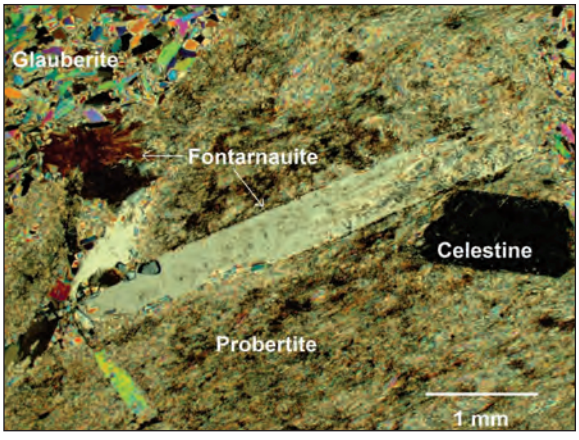

Figure 10- Prismatic fontarnauite crystals in thin section with crossed polars. Photomicrograph of prismatic fontarnauite crystals elongate along [100] (crossed polars) (García-Veigas et al., 2010*b*).

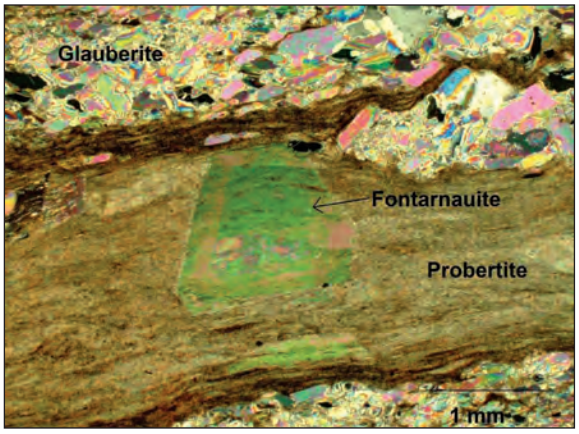

Figure 11- Photomicrograph of fontarnauite crystals with hexagonal outline formed from the {010} side pinacoid and the {011} prism (crossed polars) (after Cooper et al., in press).

deposited in the mineralogy collection of the Royal Ontario Museum, 100 Queen's Park, Toronto, Ontario M5S 2C6, Canada, accession number M56745 (Cooper et al., in pres) (Table 2).

Fontarnauite is most commonly associated with probertite, glauberite and celestine in isolated colorless to light brown prismatic crystals or as clusters of crystals less than 5 mm long (Figure 10). More often it displays pseudohexagonal sections less than 1 mm in diameter. Under microscope it shows a perfect cleavage parallel to (010) (Figure 11). It has a pearly, transparent to translucent lustre, a brittle tenacity and a white streak (Cooper et al., in press).

Fontarnauite is interpreted to be an early diagenetic phase, replacing both probertite (Figures 9, 10 and 11) and glauberite, as a consequence of the K-SO_4-enriched composition in residual brines during the evaporation in a saline lake environment to which volcaniclastic material had been added (Helvacı and Alonso, 2000; Orti et al., 1998; Garcia-Veigas et al., 2010*b*; Cooper et al., in press).

6. Conclusions

The Emet borates were formed in playa lakes, fed partly by thermal springs and partly by streams draining the catchment areas, and it may be assumed that the initial brines at all times contained an abundance of calcium and boron with minor amounts of arsenic, sulphur, strontium, magnesium and sodium. Early precipitated minerals seem to have formed within the clastic sediments. Brines were evidently rich in Ca and B in both the northern and

southern parts of the basin throughout the sequence. Both lateral and vertical changes from calcite-marls to colemanite bearing clays have been observed and a gross zoning both laterally and vertically from calcite to colemanite and back to calcite seems to be general in both areas. Ca borates, ulexite and teruggite crystallized within the sediments and did not precipitate from open water. Co-precipitation of ulexite and later diagenetic formation of tunellite occurs only rarely in the northern basin. Field and textural evidence clearly indicates the sequence Ca borate + Ca-Na borate + Sr borate.

In the southern area the sporadic occurrence of gypsum suggests that where sulphates are present the sequence is calcite + gypsum + colemanite.

Two new minerals, emetite and fontarnauite, have been discovered in the Doğanlar boreholes located in the central part of the Emet borate basin. The chemical characterization of the mineral phases in the Doğanlar boreholes has led to the identification of a new K-bearing sulphate mineral, $Ca_7Na_3K(SO_4)_9$, named as "emetite". This mineral always appears forming aggregates that partially replace the glauberite crystals at the top of the glauberite units. Fontarnauite is most commonly associated with probertite, glauberite and celestine. Fontarnauite is interpreted to be an early diagenetic phase, replacing both probertite and glauberite in the volcanostratigraphic sequence of the Emet basin.

Acknowledgments

I am especially grateful to Eti Maden Company and MTA and their managers for their generosity during fieldwork. This study has been supported by the Dokuz Eylül University and The Scientific and Technical Research Council of Turkey. Mustafa Helvacı is gratefully acknowledged for his typing and drafting assistances which improved the manuscript. I would like to thank the reviews of P. A. Schroeder and İbrahim Uysal for their constructive comments and suggestions, which have considerably improved the final version of the manuscript.

Received: 03.04.2015
Accepted: 18.06.2015
Published: December 2015

References

Akdeniz, N., Konak, N. 1979. Simav–Emet–Dursunbey–Demirci yörelerinin jeolojisi [Geology of the Simav–Emet–Dursunbey–Demirci areas]. *Maden Tetkik ve Arama Genel Müdürlüğü Rapor* No: 6547, Ankara (unpublished).

Akkuş, M.F. 1962. Geology of the Kütahya-Gediz area. *Journal of Mineral Research and Exploration Institute of Turkey*, 58: 21-30

Cooper, M.A., Hawthorne, F.C., Garcia-Veigas, J., Alcobé, X., Helvacı, C., Grew, E. S., Ball, N. A. 2014. Fontarnauite, $(Na,K)_2$ (Sr,Ca) (SO_4) $[B_5O_8$ (OH)] $(H_2O)_2$, a new sulfate-borate from Doğanlar (Emet), Kütahya Province, Western Anatolia, Turkey. *Candian Mineralogist* (baskıda).

Çolak, M., Helvacı, C., Maggeti, M. 2000. Saponite from the Emet colemanite mines, Küthahya, Turkey. *Clays and Clay Miner*., 48: 409–423.

Ercan, T., Satır, M., Kreuzer, H., Türkecan, A., Günay, E., Çevikbaş, A., Ateş, M., Can, B. 1985. Batı Anadolu Senozoyik volkanitlerine ait yeni kimyasal, izotopik ve radyometrik verilerin yorumu (Interpretation of new chemical, isotopic and radiometric data on Cenozoic volcanics of western Anatolia). *Bullettin of Geological Society of Turkey,* 28, 121-136.

Ercan, E., Satır, M., Sevin, D., Türkecan, A. 1996. Batı Anadolu'daki Tersiyer ve Kuvaterner yaşlı volkanik kayaçlarda yeni yapılan radyometrik yaş ölçümlerinin yorumu [Some new radiometric ages Tertiary and Quaternary volcanic rocks from West Anatolia]. *Mineral Research Exploration Bulletin* (Turkey) 119, 103–112.

Ersoy, Y., Helvacı, C. 2007. Stratigraphy and geochemical features of the Early Miocene bimodal (ultrapotassic and calc-alkaline) volcanic activity within the NE-trending Selendi basin, western Anatolia, Turkey. *Turkish Journal of Earth Science*, 16, 117 - 139.

Ersoy, E.Y., Helvacı, C., Palmer, M.R. 2011. Stratigraphic, structural and geochemical features of the NE–SW-trending Neogene volcano-sedimentary basins in western Anatolia: implications for associations of supradetachment and transtensional strike-slip basin formation in extensional tectonic setting. J. *Asian Earth Sci*. 41, 159–183.

Ersoy, E. Y., Helvacı, C., Palmer, M. R. 2012. Petrogenesis of the Neogene volcanic units in the NE–SW-trending basins in western Anatolia, Turkey. *Contrib Mineral Petrol* (2012) 163:379–401.

Ersoy E.Y., Çemen, İ., Helvacı, C., Billor, Z. 2014. Tectono-stratigraphy of the Neogene basins inWestern Turkey: Implications for tectonic evolution of the Aegean Extended Region. *Tectonophysics* 635 (2014) 33–58.

Floyd, P.A, Helvacı, C, Mittwede S.K. 1998. Geochemical discrimination of volcanic rocks, associated with borate deposits: an exploration tool. *Journal of Geochemical Exploration* 60: 185-205.

Fytikas M, Innocenti F, Manetti P, Mazzuoli R, Peccerillo A, Villari L. 1984. Tertiary to Quaternary evolution of volcanism in the Aegean region. In The Geological Evolution of the Eastern Mediterranean, Dixon JE, Robertson AHF (eds). Special Publications 17. *Geological Society*: London; 687–699.

García-Veigas, J., Ortí, F., Rosell, L., Gündoğan, I., Helvacı, C. 2010*a*. Occurrence of a new sulphate mineral Ca_7Na_3 $K(SO_4)_9$ in the Emet borate deposits, western Anatolia (Turkey). *Geological Quarterly* 54, 431-438.

Garcia-Veigas, J., Rosell, L., Alcob, X.,Subias, I., Orti, F., Gündoğan, İ. and Helvacı, C. 2010*b*. Fontarnauite, a new sulphate-borate mineral from the Emet bo rate district (Tur key). Macla, 13: 97–98.

García-Veigas, J. , Rosell, L., Ortí , F., Gündoğan, İ., Helvacı, C. 2011. Mineralogy, diagenesis and hydrochemical evolution in a probertite–glauberite–halite saline lake (Miocene, Emet Basin, Turkey). *Chemical Geology* 280, 352–364.

Gawlik, J. 1956. Borate deposits of the Emet Neogene basin. *Mineral Research and Exploration Institute of Turkey* Report No. 2479, Ankara (Turkish and German Text) (unpublished).

Helvacı, C. 1977. Geolgy, mineralogy and geochemistry of the borate deposits and associated rocks and the Emet Valley, Turkey. PhD Thesis, University of Nottingham, England (unpublished).

Helvacı, C. 1978. A review of the mineralogy of the Turkish borate deposits. *Mercian Geology* 6: 257-270.

Helvacı, C. 1983. Mineralogy of the Turkish borate deposits. *Geological Engineering* 17, 37-54.

Helvacı, C. 1984. Occurence of rare borate-minerals: veatchite-A, tunellite, teruggite and cahnite in the Emet borate deposits, Turkey. *Mineralium Deposita* 19: 217-226.

Helvacı, C. 1986. Geochemistry and origin of the Emet borate deposits, western Turkey. Faculty of Engineering Bulletin, Cumhuriyet University, Series A. *Earth Sciences* 3: 49-73.

Helvacı, C. 1989. A mineralogical approach to the mining, storing and marketing problems of the Turkish borate production. *Geological Engineering* 34-35, 5-17.

Helvacı, C. 1995. Stratigraphy, mineralogy, and genesis of the Bigadiç borate deposits, western Turkey. *Economic Geolgy* 90: 1237-1260.

Helvacı, C. 2005. Borates. In : Selley R.C., Cocks, L.R.M and Plimer, I.R. (editors) Encyclopedia of Geology. *Elsevier*, December 2004, vol.3, p. 510-522.

Helvacı, C. 2015. Geological faetures of Neogene basins hosting borate deposits: An overview of deposits and future forecast, Turkey. *Bulletin of the Mineral Research and Exploration* (in press).

Helvacı, C., Firman, R.J. 1976. Geological setting and mineralogy of Emet borate deposit, Turkey. Transactions/section B, *Institute of Mining and Meatllurgy* 85: 142-152.

Helvacı, C., Stamatakis, M.G., Zagouroglou, C., Kanaris, J. 1993. Borate minerals and related authigenic silicates in northeastern Mediterraean Late Miocene continental basins. *Exploration Mining Geology* 2: 171-178.

Helvacı, C., Orti, F. 1998. Sedimentology and diagenesis of Miocene colemanite-ulexite deposits (Western Anatolia, Turkey), *Journal of Sedimentary Research* 68: 1021- 1033.

Helvacı, C., Alonso, R.N. 2000. Borate deposits of Turkey and Argentina : a summary and geological comparison. *Turkish Journal of earth Sciences* (Turkish J. Earth Sci.) vol. 24: 1-27.

Helvacı, C., Ortí, F. 2004. Zoning in the Kırka borate deposit, western Turkey: primary evaporitic fractionation or diagenetic modifications?. *Canadian Mineralogists* 42, 1179-1204.

Helvacı, C., Ersoy, E.Y. 2006. The facies characteristics and geochemical featuresof the volcanic rocks of the Selendi and Simav area, and their relations with the basin sedimentary rocks, western Anatolia. DEÜ. Bilimsel Araştırma Projesi No: 03.KB.FEN.058. January 2006, İzmir, 116 s.

Helvacı, C., Ersoy, Y., Erkül, F., Sözbilir, H., Bozkurt, E. 2006. Selendi Havzasının stratigrafik, petrografik, jeokimyasal ve tektonik veriler ışığında volkonosedimanter evrimi ve ekonomik potansiyeli. Türkiye Bilimsel ve Teknik Araştırma Kurumu Proje No: ÇAYDAĞ/103Y124, Aralık 2006, 134 s.

Helvacı, C., Orti, F., Garcia-Veigas, J., Rosell, L., Gündoğan, İ., Yücel-Öztürk, Y. 2012. NEOGENE BORATE DEPOSITS: Mineralogy, Petrology and Sedimentology; A workshop with special emphasis on the Anatolian deposits. International Earth Sciences Colloquium on the Agean Region, IESCA 2012, İzmir, Turkey, 64p.

Holzer, H. 1954. Geological report of the Beyce-54/4 and Simav-71/2 area. *Mineral Research and Exploration Institute of Turkey* Report. no. 2366, Ankara (unpublished).

İnan, K., Dunham, A.C., Esson, J. 1973. Mineralogy, chemistry and origin of Kırka borate deposit, Eskişehir Province, Turkey. Transactions/section B, *Institution of Mining and Metallurgy* 82: 114-123.

Kistler, R.B., Smith, W.C. 1983. Boron and borates. In: LEFONDS,S.J. (ed), Industrial Mineral and Rocks. 5th Edition, *Society of Mining Engineers of AIME*, 533-560.

Kistler, R.B., Helvacı, C. 1994. Boron and borates. In: CARR, D.D. (ed) Industrial Minerals and Rocks. 6th Edition, Society for Mining, Metallurgy and Exploration Inc., Littleton, Colorado, 171-186.

Lyday, P.A. 1982. Boron: Minerals Yearbook 1980, U.S. Bureau of Mines, 1: p 3

Orti, F., Helvacı, C., Rosell, L., Gündoğan, İ. 1998. Sulphate-borate relations in an evaporitic lacustrine environmet: the Sultançayır Gypsum (Miocene, Western Anatolia). *Sedimentolgy* 45: 697-710.

Özpeker, İ. 1969. Western Anatolian Borate Deposits and Their Genetic Studies. PhD Dissertation, İstanbul Technical University (in Turkish, unpublished).

Palmer, M. R., Helvacı, C. 1997. The boron istope geochemistry of the Neogene borate deposits of western Turkey. *Geochemica et Cosmochimica Acta* 61: 3161-3169.

Seyitoğlu, G., Anderson, D., Nowell, G., Scott, B.C. 1997. The evolution from Miocene potassic to Quaternary sodic magmatism in western Turkey: implications for enrichment processes in the lithospheric mantle. *Journal of Volcanology and Geothermal Research,* 76, 127-147.

Sunder, M.S. 1980. Geochemistry of the Sarıkaya borate deposits (Kırka-Eskişehir). *Bulletin of the Geological Society of Turkey* 2: 19-34.

Travis, N.J., Cocks, E.J. 1984. The Tincal Trail. A history of borax. Harrap, London, 311.

BULLETIN OF THE MINERAL RESEARCH AND EXPLORATION

Foreign Edition 2015 151

CONTENTS

LOCATION OF MANAGEMENT
Redaksiyon Kurulu Başkanlığı
Maden Tetkik ve Arama Genel Müdürlüğü
Genel Müdürlük Binası (A Block)
Üniversiteler Mah. Dumlupınar Bulvarı No:139
06800 Çankaya/ANKARA/TURKEY
e-mail: redaksiyon@mta.gov.tr

Foreign edition of Bull. Min. Res. Exp. is indexed and abstracted in Thompson Reuters Isı master List, Georef, Geological Abstracts, Mineralogic abstracts and SCOPUS database, Turkish edition is indexed and abstracted in ULAKBIM database.

The Bulletin of the Mineral Research and Exploration is published in two issues in a year. Each bulletin is printed in Turkish and English languages as two separate issues.
The English and Turkish issues of the "Bulletin of the Mineral Research and Exploration" can be obtained from "BDT Department" with charge, either directly or ordered by adding postage fee from the correspondence address.
E-Mail: bdt@mta.gov.tr

The section of "notes to the authors", format, copyright and other information can be obtained from www.mta.gov.tr as PDF files.

Printed Date : 17.12.2015
Printing House: Kuban Matbaacılık Yayıncılık - İvedik Organize San. Matbaacılık Sit. 1514 Sk. No: 20 Tel 0312 395 20 70 Faks: 0312 395 37 23 www.kubanbatbaa.com
Periodical

ISSN: 0026-4563

EDITORIAL

The General Directorate of Mineral Research and Exploration (MTA) was founded 80 years ago by the directives of Atatürk in 22nd of June 1935, and is an organization, which continues its studies as one of the milestones to be a modern country of Turkey.

MTA, which started to work by the words of Atatürk; *"We gave the mission of exploration of yet the other unknown treasures of the country one by one to MTA. They will work. We hope happily surprises"*, plays an important role in the development strategy of the Republic of Turkey. Both its mission and vision rests on the principle of exploration of natural resources of the country based on geological researches, and to give acceleration to industrialization by finding them.

Today's MTA continues its studies under the main topics such as; fundamental geological surveys, the exploration and research of mineral and energy resources, geophysical surveys, drilling, laboratory studies, feasibility surveys and scientific documentation. MTA, which closely follows modern scientific and technological developments and continues its investigations under the light of these developments, is the institution of geological survey of Turkey.

As well as the scientific and technical activities of MTA, the publishing facilities related to earth sciences are also important. Bulletin of the Mineral Research and Exploration, which is a part of these publishing activities, has been a scientific journal accepted both as nationally and internationally on earth sciences since 1936.

Articles that cover results, data and assessments related to scientific and technical investigations in several branches of earth sciences take place in the Bulletin of the Mineral Research and Exploration. It is published twice a year both in English and in Turkish languages, and is also served in the web site of the Journal. All issues that have been published from past to recent (1936-2015) are available in ".pdf" format as full text. The Bulletin of the Mineral Research and Exploration, which is subjected to the period of peer review process, is published in color with its good quality printing material, and it is delivered to more than 1000 libraries by the national and international distribution and change process.

This issue is dedicated to the 80th anniversary of MTA. Researchers who were made on important contributions to earth science of Turkey were invited to submit their valuable researches by editorial board and to create this issue. We wish to thank the authors of the articles for accepting our invitation and submitting and revising their manuscripts and thank the reviewers for their comprehensive and thorough reviews.

We believe that the Bulletin of the Mineral Research and Exploration will continue its life time many more 80 years with MTA.

ACKNOWLEDGEMENT

We gratitude to the following reviewers for their valuable contributions to the Bulletin of The Mineral Research and Exploration in 2015. Besides, we would like to thank to M.Bahadır ŞAHİN, ex-chairman of Executive Editorial Board, who is appointed as Head of Geology Department for his contribution to all publications of MTA.

Akın KÜRÇER
Ali AYDIN
Ali Ekber DAYA
Alper BABA
Aral OKAY
Asuman TÜRKMENOĞLU
Bahattin ÇETİNDAĞ
Bülent ORUÇ
Candan GÖKÇEOĞLU
Cemal GÖNCÜOĞLU
Cengiz YILDIRIM
Emin ÇİFTÇİ
Ercan AKSOY
Erdin BOZKURT
Erhan TERCAN
Erhan ALTUNEL
Fuat ERKÜL
Gülten YAYLALI
Güralp ÖZKOÇ
Gürol SEYİTOĞLU
Hakan NEFESLİOĞLU
Halim MUTLU
Harald G. DILL
İbrahim UYSAL
İhsan ÇİÇEK
M. Tekin YÜRÜR
Martin PALMER
Mefail YENİYOL
Mehmet ALTUNSOY
Mehmet EROĞLU
Muhittin GÖRMÜŞ
Mustafa KARABIYIKOĞLU
Mustafa FENER
Nazire ÖZGEN ERDEM
Necati TÜYSÜZ
Okan TÜYSÜZ
Olivier MAİDET
Onur Alp YÜCEL
Osman CANDAN
Paul SCHROEDER
Pınar ŞEN
Reyhan KARA GÜLBAY
Sacit ÖZER
Saadettin KORKMAZ
Selami TOPRAK
Serdar BAYARI
Sönmez SAYILI
Şakir ŞİMŞEK
Şükrü Can GENÇ
Tanju KAYA
Timur USTAÖMER
Yalçın ERSOY
Yener EYÜPOĞLU
Yurdal GENÇ
Yıldırım GÜNGÖR
Yusuf Kağan KADIOĞLU
Zehra KARAKAŞ

BULLETIN OF THE MINERAL RESEARCH AND EXPLORATION NOTES TO THE AUTHORS

1. Aims

The main aims of the journal are

- To contribute to the providing of scientific communication on geosciences in Turkey and the international community.
- To announce and share the researches in all fields of geoscience studies in Turkey with geoscientists worldwide.
- To announce the scientific researches and practices on geoscience surveys carried out by the General Directorate of Mineral Research and Exploration (MTA) to the public.
- To use the journal as an effective media for international publication exchange by keeping the journal in high quality, scope and format.
- To contribute to the development of Turkish language as a scientific language

2. Scope

At least one of the following qualifications is required for publishing the papers in the *Bulletin of Mineral Research and Exploration*.

2.1. Research Articles

2.1.1. Original Scientific Researches

- This type of articles covers original scientific research and its results related to all aspects of disciplines in geoscience.

2.1.2. Development Researches

- The studies using new approaches and methods to solve any problems related to geosciences and/or the researches using new approaches and methods to solve any problems related to the science of engineering performed in the General Directorate of Mineral Research and Exploration.

2.1.3. Review articles

- This type of papers includes comphrehensive scholarly review articles that summarize and critically assess previous geoscience reseach with a new perspective and it also reveals a new approach.

2.2. Discussion/Reply

- This type of article is intended for discussions of papers that have already been published in the latest issue of the *Bulletin*.
- The discussion/reply type articles that criticize all or a part of a recently published article, are published in the following first issue, if it is submitted within six months after the distribution of the *Bulletin*.
- The discussions are sent to the corresponding author of the original paper to get their reply, before publication. So that, the discussion and reply articles can be published at the same time, if they can be replied within the prescribed period. Otherwise, the discussion is published alone. Re-criticising of the replies is not allowed. The authors should keep the rules of scientific ethics and discussions in their discussion/reply papers. The papers in this category should not exceed four printed pages of the journal including figures and tables etc. The format of the papers should be compatible with the "Spelling Rules" of the *Bulletin*.

2.3. Short Notes

- Short notes publishing in the *Bulletin* covers short, brief and concisely written research reports for papers including data obtained from ongoing and/or completed scientific researches and practices related to geoscience and new and/or preliminary factual findings from Turkey and worldwide.
- The short notes will follow a streamlined schedule and will normally published in the following first or second issue shortly after submission of the paper to the *Bulletin*. To meet this schedule, authors should be required to make revisions with minimal delay.
- This type of articles should not exceed four printed pages of the journal including figures, tables and an abstract.

3. Submission and Reviewing of Manuscripts

Manuscript to be submitted for publishing in the Journal must be written clearly and concisely in Turkish and/or English and it should be prepared in the *Bulletin of Mineral Research and Exploration* style guidelines. All submissions should be made online at the **http://bulletin.mta.gov.tr** website.

The authors, having no facility for online submission can submit their manuscript by post-mail to the

address given below. They should submit four copies of their manuscript including one original hard copy, and CD. The files belonging to manuscript should be clearly and separately named as "Text", "Figures" and "Tables" at the CD.

Address:
Maden Tetkik ve Arama Genel Müdürlüğü
Redaksiyon Kurulu Başkanlığı
Üniversiteler Mah. Dumlupınar Bulvarı, No: 139
06800 Çankaya-Ankara

- The manuscript submitted for reviews has not been partially or completely published previously; that it is not under consideration for publication elsewhere in any language; its publication has been approved by all co-authors.
- The rejected manuscripts are not returned back to author(s) whereas a letter of statement indicating the reason of rejection is sent to the corresponding author.
- Submitted manuscripts must follow the *Bulletin* style and format guidelines. Otherwise, the manuscript which does not follow the journals' style and format guidelines, is given back to corresponding author without any reviewing.
- Every manuscript which passes initial Editorial treatise is reviewed by at least two independent reviewers selected by the Editors. Reviewers' reports are carefully considered by the Editors before making decisions concerning publication, major or minor revision or rejection.
- The manuscript that need to be corrected with the advices of reviewer(s) is sent back to corresponding author(s) to assess and make the required corrections suggested by reviewer(s) and editors. Authors should prepare a letter of well-reasoned statement explaining which corrections are considered or not.
- The Executive editor (Editorial Board) will inform the corresponding author when the manuscript is approved for publication. Final version of text, tables and figures prepared in the *Bulletin of Mineral Research and Exploration* style and format guidelines, will need to be sent online and the corresponding author should upload all of the manuscript files following the instructions given on the screen. In the absence of online submission conditions, the corresponding author should send four copies of the final version of the manuscript including one original hard copy, and CD by post-mail. The files belonging to manuscript should be clearly and separately named as "Text", "Figures" and "Tables" at the CD.
- To be published in the *Bulletin of Mineral Research and Exploration,* the printed lenght of the manuscript should not exceed 30 printed pages of the journal including an abstract, figures and tables. The publication of longer manuscripts will be evaluated by Editorial Board if it can be published or not.

4. Publication Language and Periods

- *The Bulletin of Mineral Research and Exploration* is published at least two times per year, each issue is published both in Turkish and English. Thus, manuscripts are accepted in Turkish or English. The spelling and punctuation guidelines of Turkish Language Instution are preferred for the Turkish issue. However, technical terms related to geology are used in accordance with the decision of the Editorial Board.

5. Spelling Draft

Manuscripts should be written in word format in A4 (29.7 x 21 cm) size and double-spaced with font size Times New Roman 10-point, margins of 25 mm at the sides, top and bottom of each page. Authors should study carefully a recent issue of the *Bulletin of Mineral Research and Exploration* to ensure that their manuscript correspond in format and style.

- The formulas requiring the use of special characters and symbols must be submitted on computer.
- Initial letters of the words in sub-titles must be capital. The first degree titles in the manuscript must be numbered and left-aligned, 10 point bold Times New Roman must be used. The second degree titles must be numbered and left-aligned, they must be written with 10 point normal Times New Roman. The third degree titles must be numbered and left-aligned, they must be written with 10 point italic Times New Roman. The fourth degree titles must be left-aligned without having any number; 10 point italic Times New Roman must be used. The text must continue placing a colon after the title without paragraph returns (See:Sample article: http://bulletin.mta.gov.tr).
- Line spacing must be left after paragraphs within text.
- Paragraphs must begin with 0.5 mm indent.
- The manuscript must include the below sections respectively;
  – Title Page
  – Abstract

– Key Words
– Introduction
– Body
– Discussion
– Conclusion
– Acknowledgements
– References

5.1. Title Page and Author's Adress

The title page should include:

A short, concise and informative title

The name(s) of the author(s)

The affiliation(s) and address(es) of the author(s)

The e-mail address, telephone and fax numbers of the corresponding author

The title must be short, specific and informative and written with capital letters font size Times New Roman 10-point bold. The last name (family name) and first name of each author should be given clearly. The authors' affiliation addresses (where the actual work was done) are presented below the names and all affiliations with a lower-case superscript letter is indicated immediately after the author's name and in front of the appropriate address. Provide the full postal address of each affiliation, including the country name and, if available, the e-mail address of each author.

The author who will handle correspondance at all stages of refereeing and publication, also post-publication are to be addressed (the corresponding author) should be indicated and the telephone, FAX and e-mail address given.

Please provide a running title of not more than 50 characters for both Turkish and English issue.

5.3. Abstract

- The article must be preceded by an abstract, which must be written on a seperate page as one paragraph, preferably. Please provide an abstract of 150 to 200 words. The abstract should not contain any undefined or non-standard abbreviations and the abstract should state briefly the overall purpose of the research, the principle results and major conclusions. Please omit references, criticisms, drawings and diagrams.
- Addressing other sections and illustrations of the text or other writings must be avoided.
- The abstract must be written with 10-point normal Times New Roman and single-spaced lines.
- "Abstract" must not be given for the writings that will be located in "Short Notes" section.
- English abstract must be under the title of "Abstract".

5.4. Key Words

Immediately after the abstract, please provide up to 5 key words and with each word seperated by comma. These key words will be used for indexing purposes.

5.5. Introduction

- The introdution section should state the objectives of the work, research methods, location of the study area and provide an adequate and brief background, avoiding a detailed literature survey.
- Non-standard or un-common classifications or abbreviations should be avoided but if essential, they must be defined at their first mention and used consistently thereafter.
- When needed reminder information for facilitating the understanding of the text, this section can also be used (for example, statistical data, bringing out the formulas, experiment or application methods, and others).

5.6. Body

- In this chapter, there must be data, findings and opinions that are intended to convey the reader about the subject. The body section forms the main part of the article.
- The data used the other sections such as "Abstract", "Discussions", and "Results" is caused by this section.
- While processing subject, care must be taken not to go beyond the objective highlighted in "Introduction" section. The knowledge which do not contribute to the realization of the purpose of the article or are useless for conclusion must not be included.
- All the data used and opinions put forward in this section must prove the findings obtained from the studies or they must be based on a reference by citation.
- Guidance and methods to be followed in processing subjects vary according to the characteristics of the subjects dealt with. Various phased topic titles can be used in this section as many as necessary.

5.7. Discussions

- This section should explore the significance of the results of the work, not repeat them. This must be written as a seperate section from the results.

5.8. Conclusions

- The main conclusion of the study provided by data and findings of the research should be stated concisely and concretely in this section.
- **T**he subjects that are not mentioned sufficiently and/or unprocessed in the body section must not be included in this section.
- The conclusions can be given in the form of substances in order to emphasize the results of the research and be understandable expression.

5.9. Acknowledgements

Acknowledgement of people, grants, funds, etc should be placed in a seperate section before the reference list. While specifying contributions, the attitude diverted the original purpose of this section away is not recommended. Acknowledgments must be made according to the following examples.

- This study was carried out under the.....project.
- I/we would like to thank to …… for contributing the development of this article with his/her critiques.
- Academic and / or authority names are written for the contributions made because of ordinary task requirement.

For example:

- "Prof. Dr. İ. Enver Altınlı has led the studies".
- "The opinions and warnings of Dr. Ercüment Sirel are considered in determining the limits of İlerdiyen layer."

- The contributions made out of ordinary task requirement:

For example:

– "I would like to thank to Professor Dr. Melih Tokay who gives the opportunity to benefit from unpublished field notes"; "I would like to thank to State Hydraulic Work 5. Zone Preliminary-Plan Chief Engineer Ethem Göğer." Academic and /or task-occupational titles are indicated for this kind of contributions.

- The contributions which are made because of ordinary task requirement but do not necessitate responsibility of the contributor must be specified.

For example:

- Such sentences as "I would like to thank to our General Manager, Head of Department or Mr. /Mrs. President ……who has provided me the opportunity to research"must be used.

5.10. References

- All references cited in the text are to be present in the reference list.
- The authors must be sure about the accuracy of the references. Publication names must be written in full.
- Reference list must be written in Times New Roman, 9-point type face.
- The reference list must be alphabetized by the last names of the first author of each work.
- If an author's more than one work is mentioned, ranking must be made with respect to publication year from old to new.
- In the case that an author's more than one work in the same year is cited, lower-case alphabet letters must be used right after publication year (for example; Saklar, 2011*a, b*).
- If the same author has a publication with more than one co-author, firstly the ones having single author are ranked in chronological order, then the ones having multiple authors are ranked in chronological order.
- In the following examples, the information related to works cited is regulated in accordance with different document/work types, considering punctuation marks as well.
- If the document (periodic) is located in a periodical publication (if an article), the information about the document must be given in the following order: surnames of the author/authors, initial letters of author's/ authors' first names. Year of publication. Name of the document. Name of the publication where the document is published (in italics), volume and/ or the issue number, numbers of the first and last pages of the document.

For example:

- Pamir, H.N. 1953. Türkiye'de kurulacak bir hidrojeoloji enstitüsü hakkında rapor. *Türkiye Jeoloji Bülteni* 4, 1, 63-68.

– Barnes, F., Kaya, O. 1963. İstanbul bölgesinde bulunan Karbonifer'in genel stratigrafisi. *Maden Tetkik ve Arama Dergisi* 61,1-9.

– Robertson, A.H.F. 2002. Overview of the genesis and emplacement of Mesozoic ophiolites in the Eastern Mediterranean Tethyan region. *Lithos* 65, 1-67.

- If more than one document by the same authors is cited, firstly the ones having single name must be placed in chronological order, then the ones having two names must be listed in accordance with chronological order and second author's surname, finally the ones having multiple names must be listed in accordance with chronological order and third author's surname.

- If the document is a book, these are specified respectively: surnames of the author/authors, initial letters of author's/authors' first names. Year of publication. Name of the book (initial letters are capital). Name of the organization which has published the book (in italics), name of the publication wherethe document is published, volume and/ or the issue number, total pages of the book.

For example

– Meric, E. 1983. Foraminiferler. *Maden Tetkik ve Arama Genel Müdürlüğü Eğitim Serisi* 23, 280p.

– Einsele, G. 1992. Sedimentary Basins. *Springer-Verlag*, p 628.

- If the document is published in a book containing the writings of various authors, the usual sequence is followed for the documents in a periodic publication. Then the editor's surname andinitial letters of their name /names are written. "Ed." which is an abbreviation of the editor word is written in parentheses. Name of the book containing the document (initial letters are capital). Name of the organization which has published the book (*in italics*). Place of publication, volume number (issue number, if any) of the publication where the document is published, numbers of the first and last page of the document.

For example:

– Göncüoğlu, M.C., Turhan, N., Şentürk, K., Özcan, A., Uysal, Ş., Yalınız, K. 2000. A geotraverse across northwestern Turkey. Bozkurt, E., Winchester, J.A., Piper, J.D.A. (Ed.). Tectonics and Magmatism in Turkey and the Surrounding Area. *Geological Society of London* Special Publication 173, 139-162.

– Anderson, L. 1967. Latest information from seismic observations. Gaskell, T.F. (Ed.). The Earth's Mantle. Academic Press. London, 335-420.

- If name of a book where various authors' writings have been collected is specified, those must be indicated respectively: book'seditor/editors' surname/surnames, and initial letters of their name/names. "Ed." which is an abbreviation of the editor word must be written in parentheses. Year of Publication. Name of the book (initial letters are capital). Name of the organization which has published the book (*in italics*), total pages of the book.

For example:

– Gaskel, T.F.(Ed.)1967. The Earth's Mantle. *Academic Press*, 520p.

- If the document is an abstract published in a Proceedings Book of a scientific activity such as conference/symposium/workshop …etc. , information about the document must be given in the following order: surnames of the author/authors, initial letters of author's/authors' first names. Year of publication. Title of the abstract. Name (in italics), date and place of the meeting where the Proceedings Book is published, numbers of the first and last pages of the abstract in the Proceedings Book.

For example:

– Yılmaz, Y. 2001. Some striking features of the Anatolian geology. *4. International Turkish Geology Symposiums,* 24-28 September 2001, London, 13-14.

– Öztunalı, Ö., Yeniyol, M. 1980. Yunak (Konya) yöresi kayaçlarının petrojenezi. *Türkiye Jeoloji Kurumu 34. Bilim Teknik Kurultayı*, 1980, Ankara, 36

- If the document is unpublished documents as report, lecture notes, and so on., information about the document must be given by writing the word "unpublished" in parentheses to the end of information about the document after it is specifiedin accordance with usual order which is implemented for a document included in a periodic publication.

For example:

– Özdemir, C. Biçen, C. 1971. Erzincan ili, İliç ilçesi ve civarı demir etütleri raporu. *General Directorate of Mineral Research and Exploration Report No: 4461*, 21 p. Ankara (unpublished).

– Akyol, E. 1978. Palinoloji ders notları. *EÜ Fen Fakültesi Yerbilimleri Bölümü*, 45 p., İzmir (unpublished).

- The followings must be specified for the notes of unpublished courses, seminars, and so on: name of the document and course organizer. Place of the meeting. Name of the book, corresponding page numbers.

For example:

– Walker, G. R. Mutti, E. 1973.Turbidite facies and facies associations. Pacific Section Society for Sedimentary Geology Short Course. Annaheim. Turbitides and Deep Water Sedimantation, 119-157.

- If the document is a thesis, the following are written: surname of the author, initial letter of the author's first name. Year of Publication. Name of the thesis. Thesis type, the university where it is given, the total number of pages, the city and "unpublished" word in parentheses.

For example:

– Seymen, İ. 1982. Kaman dolayında Kırşehir Masifi'nin jeolojisi. Doçentlik Tezi, İTÜ Maden Fakültesi, 145 s.İstanbul (unpublished).

- Anonymous works must be regulated according to publishing organization.

For example:

– MTA. 1964. 1/500.000 ölçekli Türkiye Jeoloji Haritası, İstanbul Paftası. Maden Tetkik ve Arama Genel Müdürlüğü, Ankara.

- The date, after the name of the author, is not given for on-printing documents; "in press" and / or "on review" words in parenthesis must be written. The name of the article and the source of publication must be specified, volume and page number must not be given.

For example:

– Ishihara, S. The granitoid and mineralization. Economic Geology 75th Anniversary (in press).

- Organization name, web address, date of access on web address must be indicated for the information downloaded from the Internet. Turkish sources must be given directly in Turkish and they must be written with Turkish characters.

For example:

– ERD (Earthquake Research Department of Turkey). **http://www.afad.gov.tr**. March 3, 2013.

- While specifying work cited, the original language must be used; translation of the title of the article must not be done.

6. Illustrations

- All drawings, photographs, plates and tables of the article are called "illustration".

- Illustrations must be used when using them is inevitable or they facilitate the understanding of the subject.

- While selecting and arranging the illustrations' form and dimensions, page size and layout of the *Bulletin* must be considered, unnecessary loss of space must be prevented as much as possible.

- The pictures must have high quality, high resolution suitable for printing.

- The number of illustrations must be proportional to the size of the text.

- All illustrations must be sent as separate files independent from the text.

- While describing illustrations in the text, abbreviations must be avoided and descriptions must be numbered in the order they are mentioned in the text.

- Photographs and plates must be given as computer files containing EPS, TIFF, or JPEG files in 600 dpi and higher resolutions (1200 dpi is preferred) so that all details can be seen in the stage of examination of writing.

6.1. Figures

- Drawings and photos together but not the plate in the text can be evaluated as "Figure" and they must be numbered in the order they are mentioned in the text.

- The figures published in the *Bulletin of Mineral Research and Exploration* must be prepared in computing environment considering the dimensions of single-column width 7.4 cm or double-column width 15.8 cm. Figure area together with the writing at the bottom should not exceed a maximum 15.8x21.

- Figures must not be prepared in unnecessary details or care must be taken not to use a lot of space for information transfer.
- Figures must be arranged to be printed in black-and-white or colored. The figure explanations being justified in two margins must be as follows: Figure 1 -Sandıklı Town (Afyon); a) Geological map of thesouth-west, b) general columnar section of the study area (Seymen 1981), c) major neotectonic structures in Turkey (modified from Koçyiğit 1994).
- Drawings must be drawn by well-known computer programs painstakingly, neatly and cleanly.
- Using fine lines which can disappear when figures shrinks must be avoided. Symbols or letters used in all drawings must be Times New Roman and not be less than 2 mm in size when shrink.
- All the standardized icons used in the drawings must be explained preferably in the drawing or with figure caption if they are very long.
- Linear scale must be used for all drawings. Author's name, figure description, figure number must not be included into the drawing.
- Photos must have the quality and quantity that will reflect the objectives of the subject.

6.2. Plates

- Plates must be used when needed a combination of more than one photo and the publication on a special quality paper.
- Plate sizes must be equal to the size of available magazine pagespace.
- Figure numbers and linear scale must be written under each of the shapes located on the Plate.
- The original plates must be added to the final copy which will be submitted if the article is accepted.
- Figures and plates must be independently numbered. Figures must be numbered with Latin numerals and plates with Roman numerals (e.g., Figure1, Plate I).
- There must be no description text on Figures.

6.3.Tables

- Tables must be numbered consecutively in accordance with their appearence in the text.
- All tables must be prepared preferably in word format in Times New Roman fonts.
- Tables together with table top writing must not exceed 15x8 cm size.
- The table explanations being justified in two margins must be as follows:
- Table 1- Hydrogeochemical analysis results of geothermal waters in the study area.

7. Nomenclature and Abbreviations

- Non-standard and uncommon nomenclature abbreviations should be avoided in the text. But if essential, they must be described as below: In cases where unusual nomenclatures and unstandardized abbreviations are considered to be compulsory, the followed way and method must be described.
- Full stop must not be placed between the initials of words for standardized abbreviations (MER, SHW, etc.).
- Geographical directions must be abbreviated in English language as follows: N, S, E, W, NE …etc.
- The first time used abbreviations in the text are presented in parenthesis, the parenthesis is not used for subsequent uses.
- The metric system must be used as units of measure.
- Figure, plate, and table names in the article must not be abbreviated. For example, "as shown in generalized stratigraphic cross-section of the region (Figure 1……."

7.1. Stratigraphic Terminology

Stratigraphic classifications and nomenclatures must be appropriate with the rules of International Commision on Stratigraphy and/or Turkey Stratigraphy Committee. The formation names which has been accepted by International Commision on Stratigraphy and/or Turkey Stratigraphy Committee should be used in the manuscript.

7.2. Paleontologic Terminology

Fossil names in phrases must be stated according to the following examples:

- For the use authentic fossil names:
- e.g. Calcareous sandstone with *Nummulites*
- When the authentic fossil name is not used.
- e.g. nummulitic Limestone
- Other examples of use;

  e.g. The type and species of Alveolina/ Alveolina type and species

- Taxonomic ranks must be made according to following examples:

Super family: Alveolina Ehrenberg, 1939 Family: Borelidae Schmarda, 1871 Type genus: *Borelis* de Montfort, 1808 Type species: *Borelis melenoides de Montfort, 1808*; *Nautilus melo* Fitchel and Moll, 1789	*Not reference, Not stated in the Reference section*
Borelis vonderschmitti (Schweighauser, 1951) (Plate, Figure, Figure in Body Text)	*Schweighauser, 1951 not reference*
1951 *Neoalveolina vonderschmitti* Schweighauser, page 468, figure 1-4	*Cited Scweighauser (1951), stated in the Reference section.*
1974 *Borelis vonderschmitti* (Schweighauser), Hottinger, page, 67, plate 98, figure 1.7	*Cited Hottinger (1974), stated in the Reference section.*

- The names of the fossils should be stated according to the rules mentioned below:
  - For the first use of the fossil names, the type, spieces and the author names must be fully indicated

    Alveolina aragoensis Hottinger

    Alveolina cf. Aragoensis Hottinger
  - When a species is mentioned for the second time in the text:

    A.aragoensis

    A.cf.aragoensis

    A.aff.aragoensis
  - It is accepted as citiation if stated as *Alveolina aragoensis* Hottinger (1966)
- The statment of plates and figures (especially for articles of paleontology):
  - for statment of the species mentioned in the body text

Borelis vonderschmitti (Schweighauser, 1951).

(plate, figure, figure in the body text).

  - When citing from other articles

    1951 Neoalveolina vonderschmitti Schweighauser, page 468, figure 1-4, figure in body text

    1974 *Borelis vonderschmitti* (Schweighauser), Hottinger, page 67, plate 98, figure 1-7

- For the citiation in the text
- (Schweighauser, 1951, page, plate, figure, figure in the body text) (Hottinger, 1974, page, plate, figure 67, plate 98, figure 1-7, figure in the bodytext.)

8. Citations

All the citiations in the body text must be indicated by the last name of the author(s) and the year of publication, respectively. The citations in the text must be given in following formats.

- For publications written by single author:
  - It is known that fold axial plain of Devonian and Carboniferious aged units around Istanbul is NS oriented (Ketin, 1953, 1956; Altınlı, 1999).
  - Altınlı (1972, 1976) defined the general characteristics of Bilecik sandstone
- For publications written by two authors:
  - The upper parts of the unit contain Ilerdian fossils (Sirel and Gündüz, 1976; Keskin and Turhan, 1987, 1989).
- For publications written by three or more authors:

According to Caner et al. (1975) Alıcı formation reflects the fluvial conditions.

The unit disappears wedging out in the East direction (Tokay et al., 1984).

- If reference is not directly obtained but can be found in another reference, cross-reference should be given as follows:

– It is known that Lebling has mentioned the existance of Lias around Çakraz (Lebling, 1932: from Charles, 1933).

10. Reprints

The author(s) will receive 5 free reprints and two hard copies of the related issues

11. Copyright and Conditions of Publication

- It is a condition of publication that work submitted for publication must be original, previously unpublished in whole or in part.
- It is a condition of publication that the authors who send their publications to the *Bulletin of Mineral Research and Exploration* hereby accept the conditions of publication of the Bulletin in advance.
- All copyright of the accepted manuscripts belong to MTA. The author or corresponding author on behalf of all authors (for papers with multiple authors) must sign and give the agreement under the terms indicated by the Regulations of Executive Publication Committee. Upon acceptance of an article, MTA can pay royalty to the authors upon their request according to the terms under the "Regulations of Executive Publication Committe" and the "Regulations of Royalty Payment of Public Office and Institutions"

All the information and forms about the *Bulletin of Mineral Research and Explorations* can be obtained from http://bulletin.mta.gov.tr